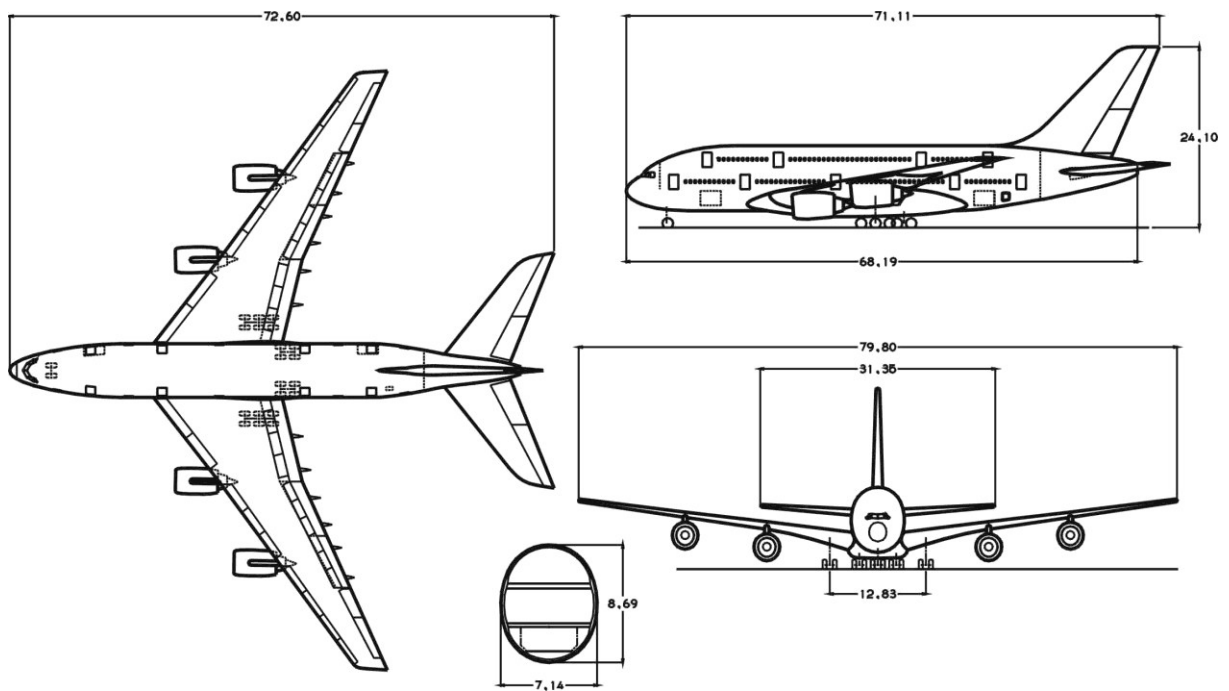




Short Course

Aircraft Design



Corporate Editor:
Deutsche Gesellschaft für Luft- und Raumfahrt Lilienthal Oberth e. V. (DGLR)

Corporate Editor:
Aircraft Design and Systems Group (AERO),
Department of Automotive and Aeronautical Engineering,
Hamburg University of Applied Sciences (HAW Hamburg)

Short Course

Aircraft Design

Estrel Hotel
Berlin, Germany, 11 – 14 September 2007

Dieter Scholz (Editor)
Hannes Ross
Erhard Rumpler
Dieter Schmitt
Dieter Scholz
Jürgen Thorbeck

September 2007

DGLR-Bericht 2007-03
ISBN: 978-3-932182-53-7 (print)
ISSN: 0178-6326

Short Course Management

Peter Brandt (Generalsekretär, DGLR)

Support Team

Christian Matalla, Aircraft Design and Systems Group (AERO)

Printing

Druckerei Thierbach

Venue

Estrel Hotel, Sonnenallee 225, D - 12057 Berlin

<https://www.estrel.com/de>

Addresses

Deutsche Gesellschaft für Luft- und Raumfahrt Lilienthal Oberth e. V.

Godesberger Allee 70, D - 53175 Bonn

<https://dglr.de>

English: Aircraft Design and Systems Group (AERO)

German: Forschungsgruppe Flugzeugentwurf und Systeme (AERO)

Berliner Tor 9, D - 20099 Hamburg

<http://AERO.ProfScholz.de>

Title Pictures

Upper picture (Airbus A380, three-view-drawing): (c) Scholz

Lower picture (Airbus A380): David Monniaux, CC BY-SA 3.0,

https://de.m.wikipedia.org/wiki/Datei:A380_dsc04393.jpg

Copyright

Each author is responsible for the copyright of pictures used in his chapter(s).

This document is protected by copyright.

The text of this document has a [CC BY-NC-ND 4.0](https://creativecommons.org/licenses/by-nc-nd/4.0/). This excludes the pictures and graphs.

Course Leader and Editor

Prof. Dr.-Ing. Dieter Scholz, MSME

- Professor at Hamburg University of Applied Sciences, Department of Automotive and Aeronautical Engineering. Teaching and research in the area of Aircraft Design, Flight Mechanics, Aircraft Systems.
- Head of the DGLR Technical Committee Manned Aircraft.
- <http://www.ProfScholz.de>

Course Instructors and Authors



Four universities – one short course

Dipl.-Ing. Hannes Ross

- Lecturer at Technical University Munich and at Bundeswehrakademie in Mannheim.
- Vice President Advanced Design & Technology EADS Military Air Systems (retired).

Professor Dipl.-Ing. Erhard Rumpler

- Professor at Munich University of Applied Sciences for aircraft design.
- http://www.fh-muenchen.de/fb03/persona/d_rumpler.pcms

Prof. Dr.-Ing. Dieter Schmitt

- Professor at Technical University Munich, Institute of Aeronautical Engineering.
- Airbus Vice President "Research & Future Projects" (retired).
- <http://www.llt.mw.tum.de>

Prof. Dr.-Ing. Dieter Scholz, MSME

(see above)

Prof. Dr.-Ing. Jürgen Thorbeck

- Professor at Technical University Berlin, Institute of Aeronautics and Astronautics, Aircraft Design and Aerostructures Group.
- Senior Manager Fleet Development Deutsche Lufthansa (retired).
- <http://www.ilr.tu-berlin.de/LB>

Target Delegates

The DGLR Short Course is arranged for graduated engineers, equivalent professionals and/or managers. It is likewise suitable for specialists in search of a broader perspective as for newcomers to the field.

Aim

The Short Course gives an insight into the procedures and the multidisciplinary interactions of aircraft conceptual design. The process of iterative synthesis and analysis in aircraft design is illustrated. A software tool for preliminary sizing is demonstrated. Methods and data to enable case studies of subsonic aircraft design are provided.

Content

The Short Course "Aircraft Design" covers following topics:

- Introduction
- Development Process
- Requirements
- Certification Standards
- Preliminary Sizing
- Fuselage Design
- Wing Design
- Empennage Design
- Landing Gear Design and Integration
- Aircraft Configurations
- Design Evaluation / DOC
- Military Aircraft Development

Learning Objectives

On completion of the Short Course, delegates will

- know aircraft design parameters and methods
- know the fundamental relationship of aircraft design parameters
- be able to size and design an aircraft to the detail as covered during the Short Course
- have a capability to structure aircraft design activities systematically and efficiently.

Short Course Schedule

The Short Course is integrated into the *First CEAS European Air and Space Conference*. The plenary sessions of the congress are included into the short course schedule.

Monday, 10.09.2007 Opening Ceremony

Tuesday, 11.09.07 **Short Course, Day 1**

08:30 - 09:30	Congress	Space Agencies	
09:40 - 11:00	Short Course	Introduction, Development Process	D. Schmitt
11:20 - 12:40	Short Course	Requirements, Certification Standards	D. Schmitt
14:00 - 15:00	Congress	A380	
15:10 - 16:30	Short Course	Preliminary Sizing	D. Scholz
16:50 - 18:10	Short Course	Preliminary Sizing	D. Scholz

Wednesday, 12.09.07 **Short Course, Day 2**

08:30 - 09:30	Congress	ATM	
09:40 - 11:00	Short Course	Fuselage Design	E. Rumpler
11:20 - 12:40	Short Course	Wing Design	D. Scholz
14:00 - 15:00	Congress	Bologna Process	
15:10 - 16:30	Short Course	Landing Gear Design	E. Rumpler
16:50 - 18:10	Short Course	Empenage Design	D. Scholz

Thursday, 13.09.07 **Short Course, Day 3**

08:30 - 09:30	Congress	Technology	
09:40 - 11:00	Short Course	Aircraft Configuration	E. Rumpler
11:20 - 12:40	Short Course	Aircraft Configuration	E. Rumpler
14:00 - 15:00	Congress	Aeronautics	
15:10 - 16:30	Short Course	Aircraft Assessment	J. Thorbeck
16:50 - 18:10	Short Course	Aircraft Assessment	J. Thorbeck

Friday, 14.09.07 **Short Course, Day 4**

08:30 - 09:50	Short Course	Military Aircraft Development	H. Ross
10:10 - 11:20	Short Course	Military Aircraft Development	H. Ross
12:20 - 13:40	Short Course	Military Aircraft Development	H. Ross
14:00 - 15:20	Short Course	Military Aircraft Development	H. Ross



1st CEAS Air & Space Conference – CEAS 2007

10-13 September 2007, Berlin, Germany



[Homepage](#) (Wayback Machine)



[CEAS 2007 DVD](#) (Wayback Machine)

Authors and Lecture Notes

D. Schmitt:

Lecture Notes: "Introduction, Aircraft Development, Certifications, Configurations"

D. Scholz:

Lecture Notes: "Preliminary Sizing"

E. Rumpler:

Lecture Notes: "Fuselage Design"

D. Scholz:

Lecture Notes: "Wing Design"

E. Rumpler:

Lecture Notes: "Landing Gear Design"

D. Scholz:

Lecture Notes: "Empennage Design"

E. Rumpler:

Lecture Notes: "Engine Integration"

E. Rumpler:

Lecture Notes: "Aircraft Configuration Design"

J. Thorbeck:

Lecture Notes: "From Aircraft Performance to Aircraft Assessment"

H. Ross:

Lecture Notes: "Military Aircraft Development"

The total notes of this short course consist of 465 pages.

Table of Contents

1	Introduction
1.1	Air Transport System
1.2	Air Vehicle Classification
2	Aircraft Development
2.1	Aircraft Development Cycle
2.2	Market Requirements
2.3	Design Problematic in Engineering
2.4	Design Methodology
3	Certification
4	Configurations
4.1	Actual Configurations
4.2	Unconventional Configurations
5	Preliminary Sizing
5.1	Landing Distance
5.2	Take-off Distance
5.3	Climb Rate during 2 nd Segment
5.4	Lift-to-Drag Ratio with Extended Landing Gear and Extended Flaps
5.5	Climb Rate during Missed Approach
5.6	Cruise
5.6.1	Thrust-to-Weight Ratio
5.6.2	Wing Loading
5.7	Lift-to-Drag Ratio during Cruise
5.8	Matching Chart
5.9	Maximum Take-Off Mass
5.9.1	Relative Operating Empty Mass
5.9.2	Relative Fuel Mass
5.10	Take-off Thrust and Wing Area
6	Fuselage Design
	design methodology
	cabin layout
	airworthiness
	design loads
	structural technology
	cutouts
	passenger doors
	inboard profile

- 7 Wing Design**
 - 7.1 Wing Parameters
 - 7.2 Basic Principle and Design Equations
 - 7.3 Flight and Operational Characteristics
 - 7.4 Ailerons and Spoilers
 - 7.5 Example: The Wing of the Airbus A310

- 8 Landing Gear Design**
 - gear arrangement
 - airworthiness
 - design loads
 - energy dissipation
 - retract kinematics
 - brakes, wheels
 - gear configurations

- 9 Empennage General Design**
 - 9.1 Functions of Empennages
 - Trim
 - Stability
 - Control
 - 9.2 Shapes of the Empennage
 - 9.3 Design Rules
 - 9.4 Design According to Tail Volume
 - 9.5 Elevator and Rudder

- 10 Engine Integration**
 - standard turbofan engines
 - engine attachment points
 - engine pylon
 - load transfer
 - ground clearance
 - turboprop engines
 - innovative concepts

- 11 Aircraft Configuration Design**
 - 11.1 Configuration Design Process
 - design methodology
 - structural components integration
 - CG travel
 - zero-lift drag
 - airworthiness
 - design loads
 - structural concept
 - 11.2 Configuration Design Problems
 - 11.2.1 160 – 200 Seat Medium Transport
 - 11.2.2 30 Seat Regional Transport

- 11.3 Special Configurations
- 11.4 Conclusions

12 From Aircraft Performance to Aircraft Assessment

- 12.1 Objectives of the Lecture
- 12.2 Preface for a Simple Approach to DOC
- 12.3 Operational Cost Structure
- 12.4 A Simplified DOC Model
 - 12.4.1 DOC Notations
 - 12.4.2 Fuel Demand
 - 12.4.3 Average Aircraft Weight
 - 12.4.4 Payload Range Diagram
 - 12.4.5 Unit Cost
 - 12.4.6 JAVA DOC Applet
- 12.5 Aircraft Family Economics
- 12.6 Presentation of DOC Calculation Results
- 12.7 Total Quality Assessment

13 Military Aircraft Development

- 13.1 Development Scenario/Environment
- 13.2 Requirements
- 13.3 Development Process and Tools
- 13.4 Technologies
 - 13.4.1 Composites
 - 13.4.2 Ejection Systems and Pilot "g" Protection
 - 13.4.3 Unstable Configurations and Digital Flight Controls
 - 13.4.4 Thrust Vectoring
 - 13.4.4.1 X-31 Enhanced Fighter Manoeuvrability (EFM) Program
 - 13.4.4.2 The VECTOR Program
 - 13.4.5 Aircraft Signature
- 13.5 Unmanned Systems
- 13.6 Future Aspects

References (from Chapters 5, 7, 9)

Appendix

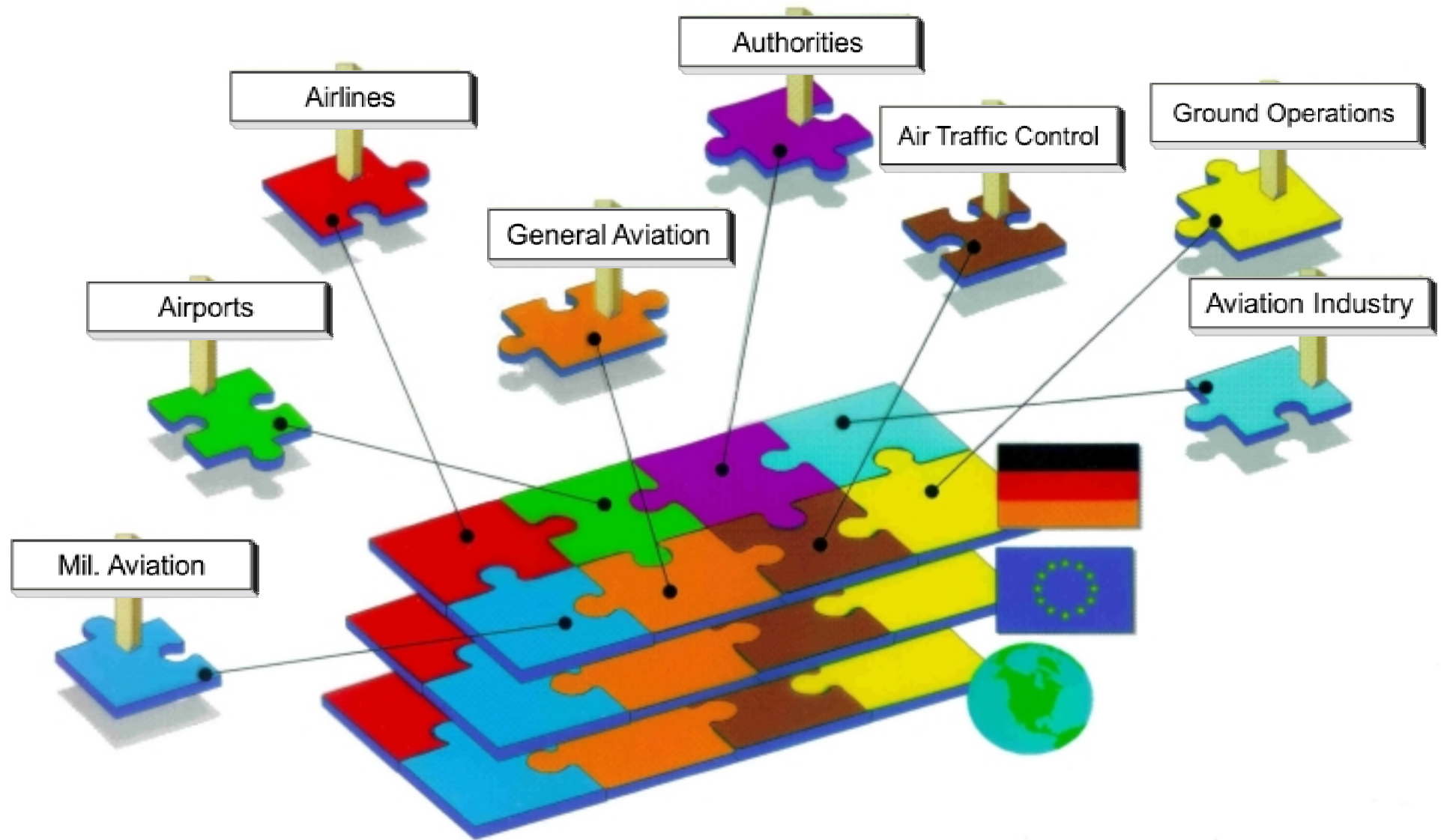
Dieter Schmitt

Chapter 1

Introduction

1.1 Air Transport System

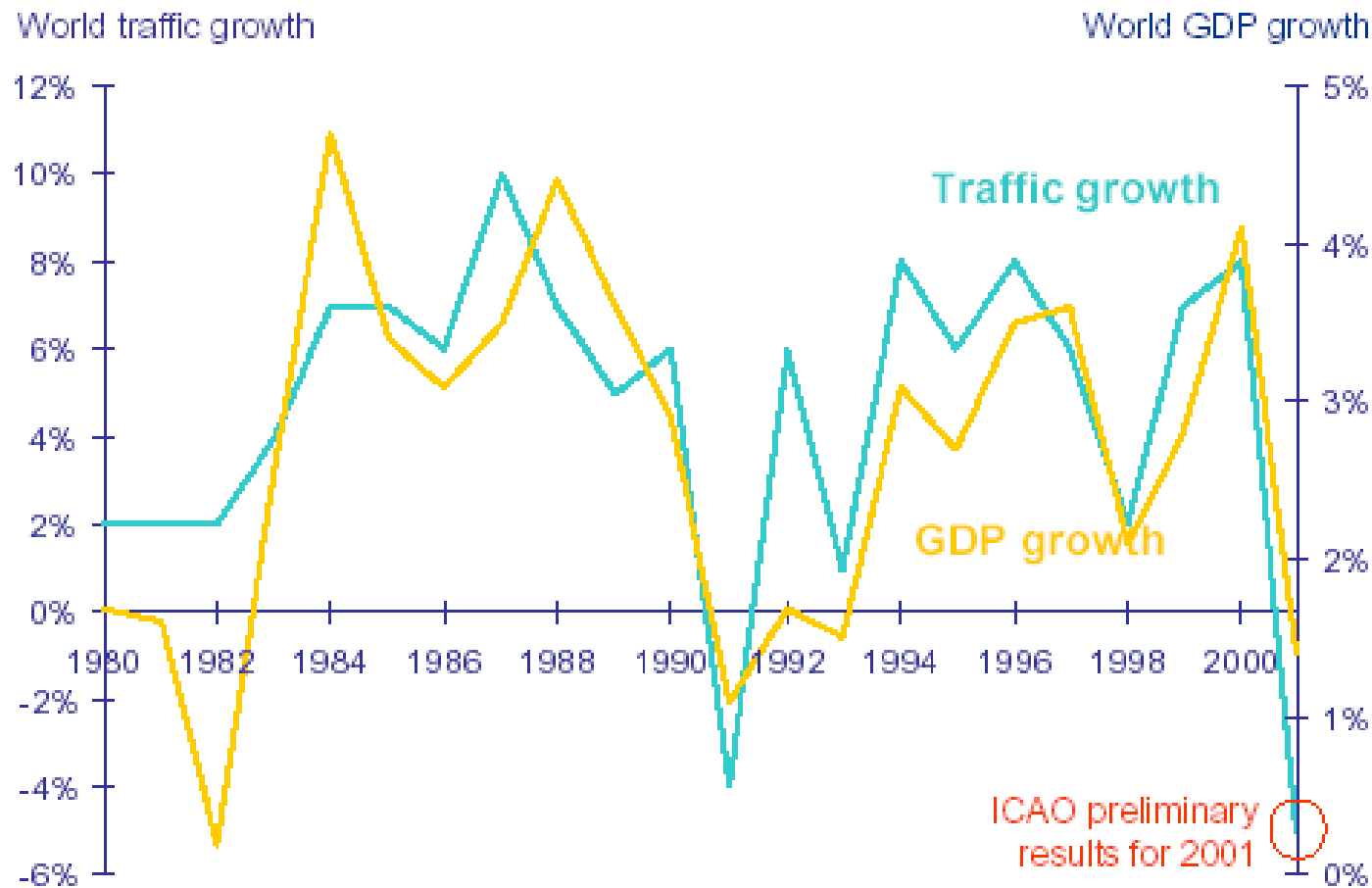
Air Transport System



Air Transport System

- ↑ The Transport system is a traditional and essential activity of national interest for each state/government and this is especially true for air transport, as this happens mainly internationally
- ↑ Transport recognizes a privilege compared to other domains of the economy:
 - 📖 Economic Reasons:
 - Export-oriented industries need proper means of transport for goods.
 - Production areas need fast, cheap and reliable ways of transport .
 - 📖 National Reasons:
 - Demonstration of power/ sovereignty, ☾ Air supremacy
 - National Air fleet ☾ Reserve für transport needs during war
 - Prestige ☾ national „flag carrier“ (Air France, Iberia, Air India, Alitalia, British Airways, ...).
- ↑ Due to the internationality of air transport on one side and the air supremacy of the states on the other side a lot of contact points and common interests exist between state/government and air transport!

Revenue Passengermiles versus GDP

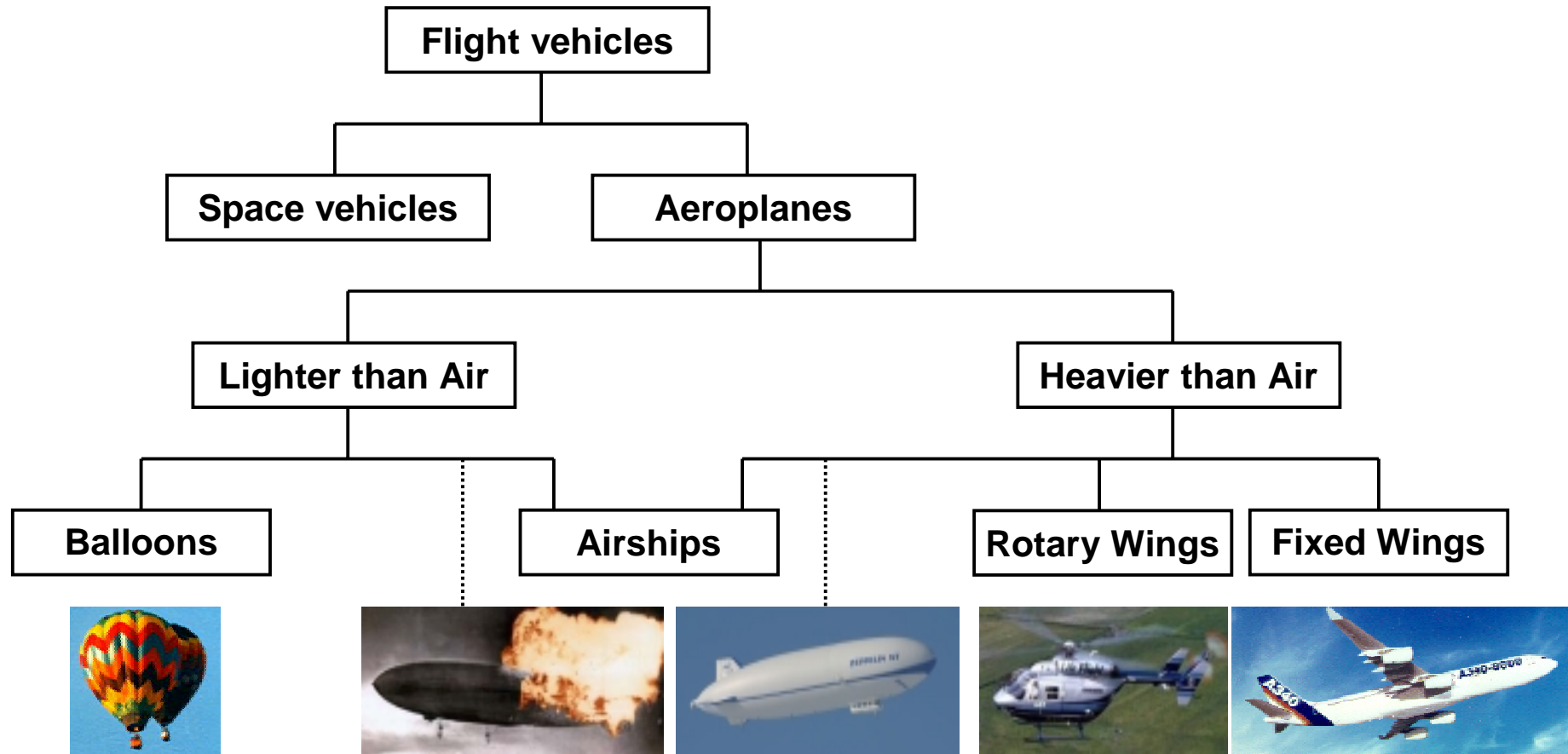


**The yearly growth rate of air transport is closely linked to
World Gross Domestic Product (GDP)**

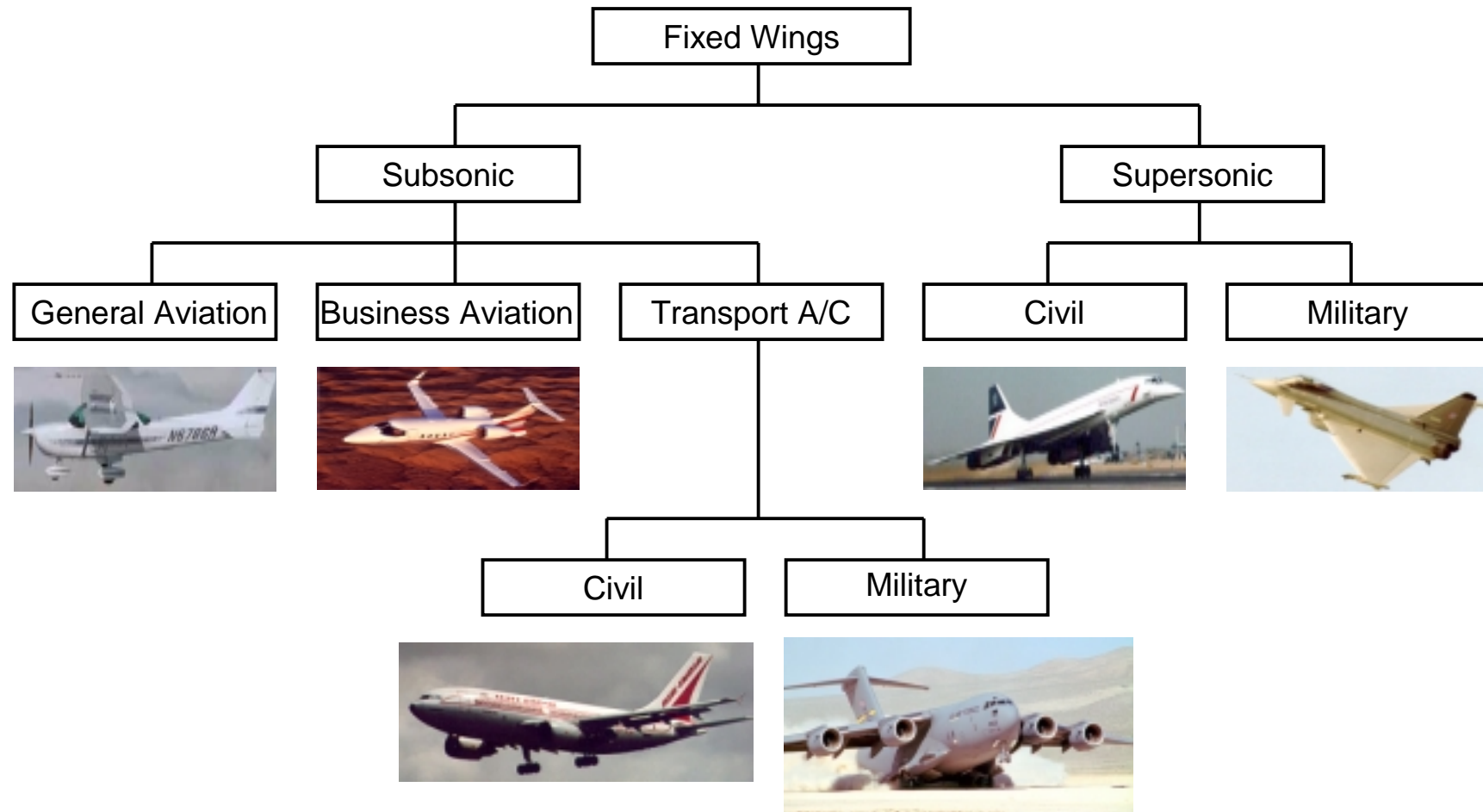
Source: GMF 2002, Airbus Global Markt Forecast 2001-2020

1.2 Air Vehicle Classification

Classification of Flight Vehicles



Classification of Fixed Wing Vehicles



Classification of Aeroplanes

Per legislation:

„Aircraft, helicopter, airships, power glider, balloons, parachute, flight models, ..

Per transport authority:

Civil or military flight vehicles

Per transport object:

Aircraft for transport of passengers, freight or mail

Per distance:

Short, medium or long -range aircraft;

Regional , Interregional, Continental or Intercontinental aircraft

Per transport carrier:

Aircraft for scheduled, charter or low cost transport

Per technical aspects:

weight category, number of engines, landing means, speed domain, configuration or structural layout

Dieter Schmitt

Chapter 2

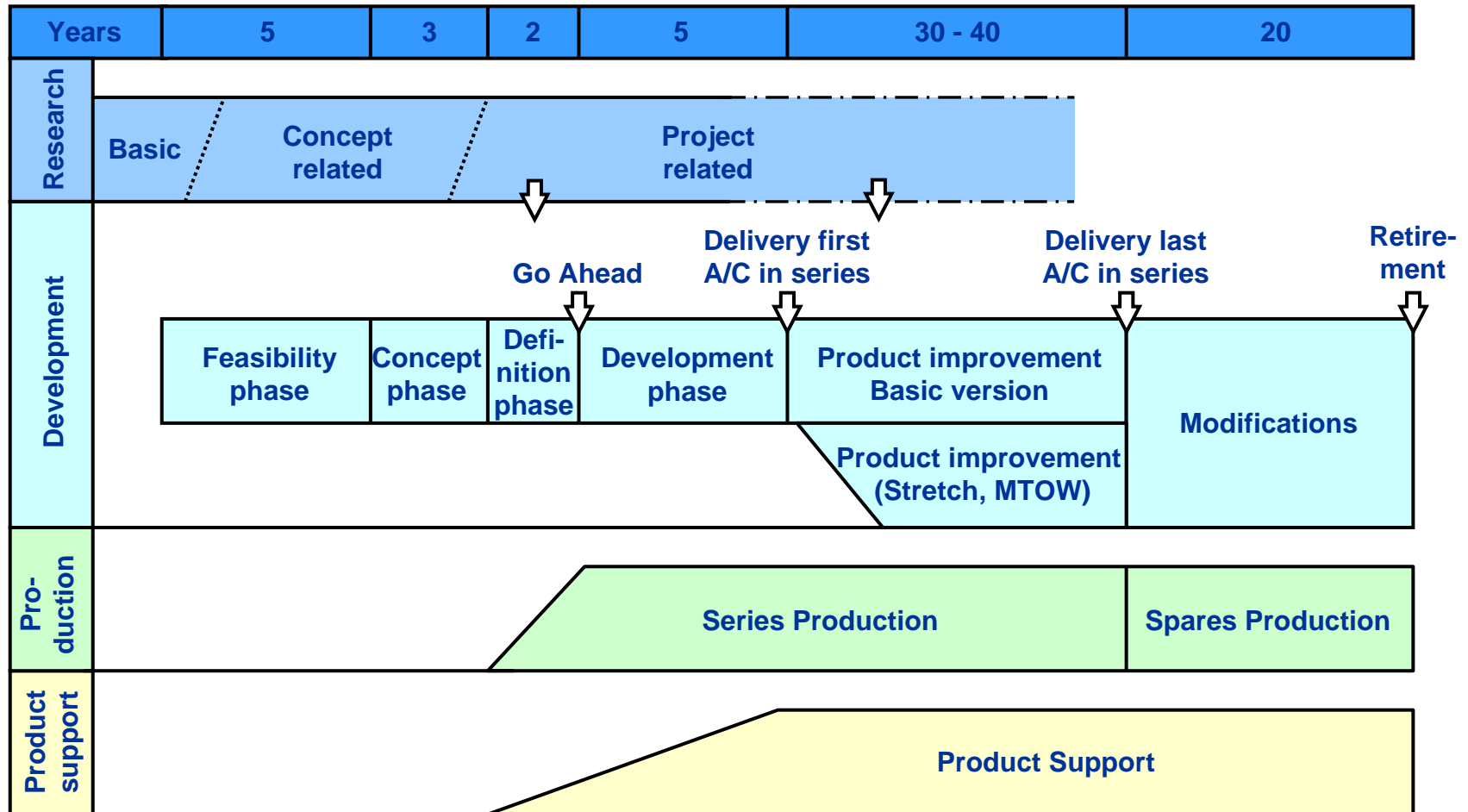
Aircraft Development

2.1 Aircraft Development Cycle

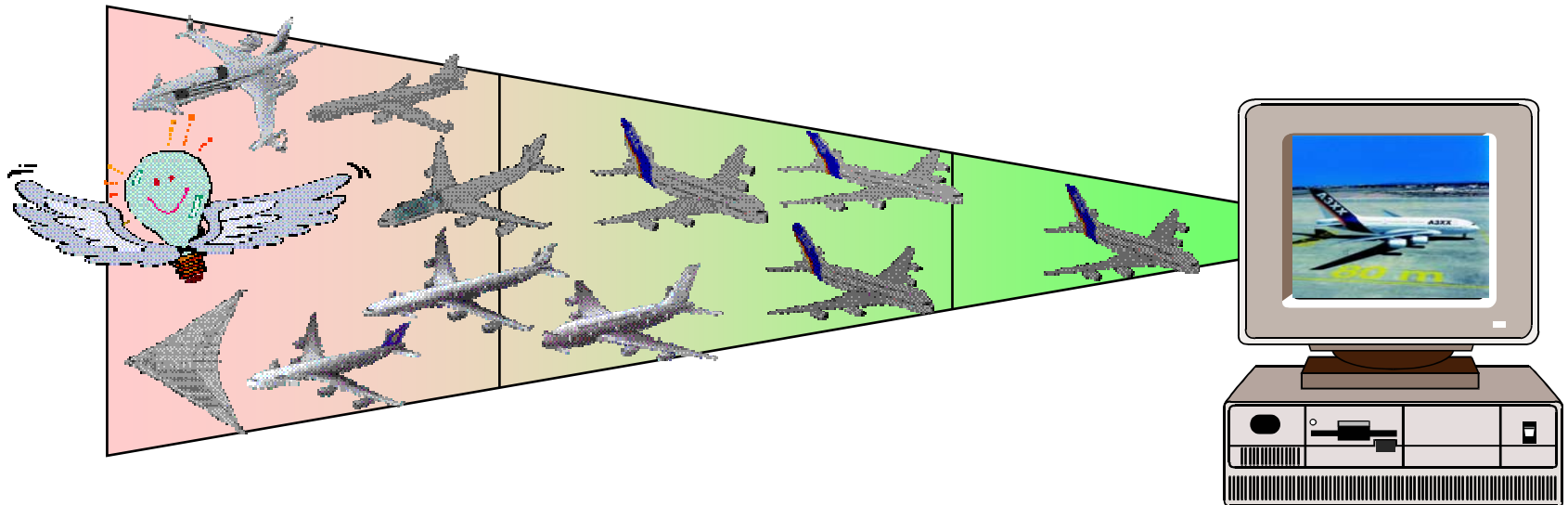
Introduction

- In the „good old days“ a group of „specialists“ (a/c design, aerodynamics, structures, production, systems, ...) could sit around a table to define the „new aircraft concept“. The project leader (chief engineer) was very experienced and was pushing his „project team“ to a new and innovative configuration.
- Market requirements were not so important as long as each new aircraft had considerable advantage in speed, range, comfort or cost against the existing competitive aircraft. Technology was the driver!
- With fuel prices staying fairly constant, benefits from new technologies being at higher cost and risk, the cost issue became the dominant element for the development of new aircraft.
- The GATT issue – introduced by the American industry against their upcoming European competition – started in Europe a rethinking about the aircraft definition and development process.
- „Concurrent Engineering“ and „Process Analysis“ are the most popular words for the new „management generation“.

Typical life cycle of a civil program



From first idea to definition



definition of a “marketable”
aircraft which is attractive to
customer for contract signature
“VR -model”
hardware model

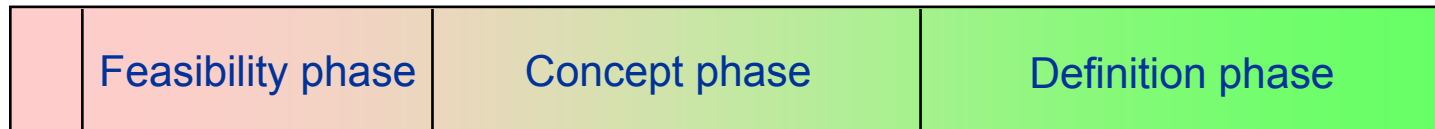
M0 M1

M3

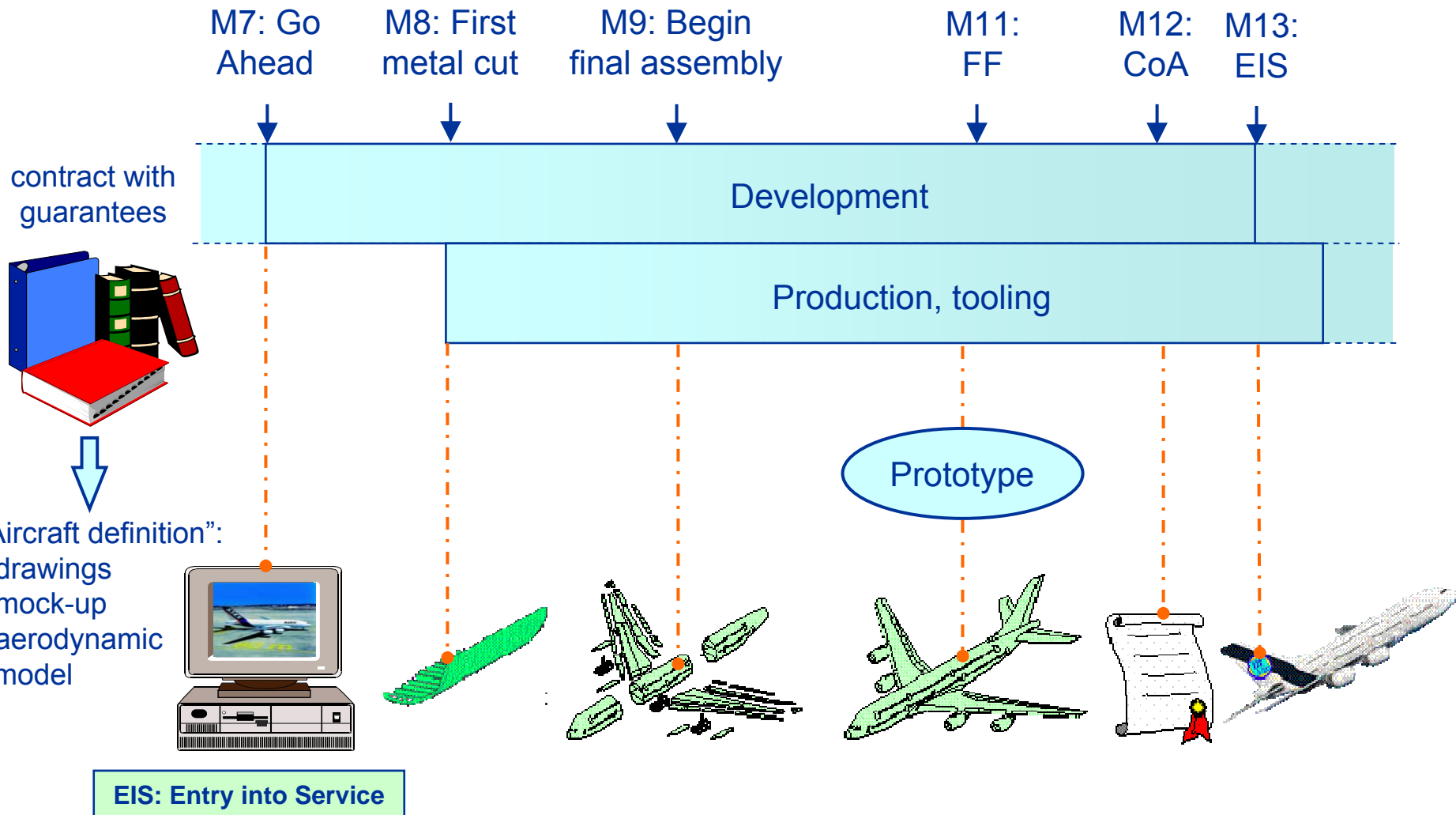
M5

2 years

M7

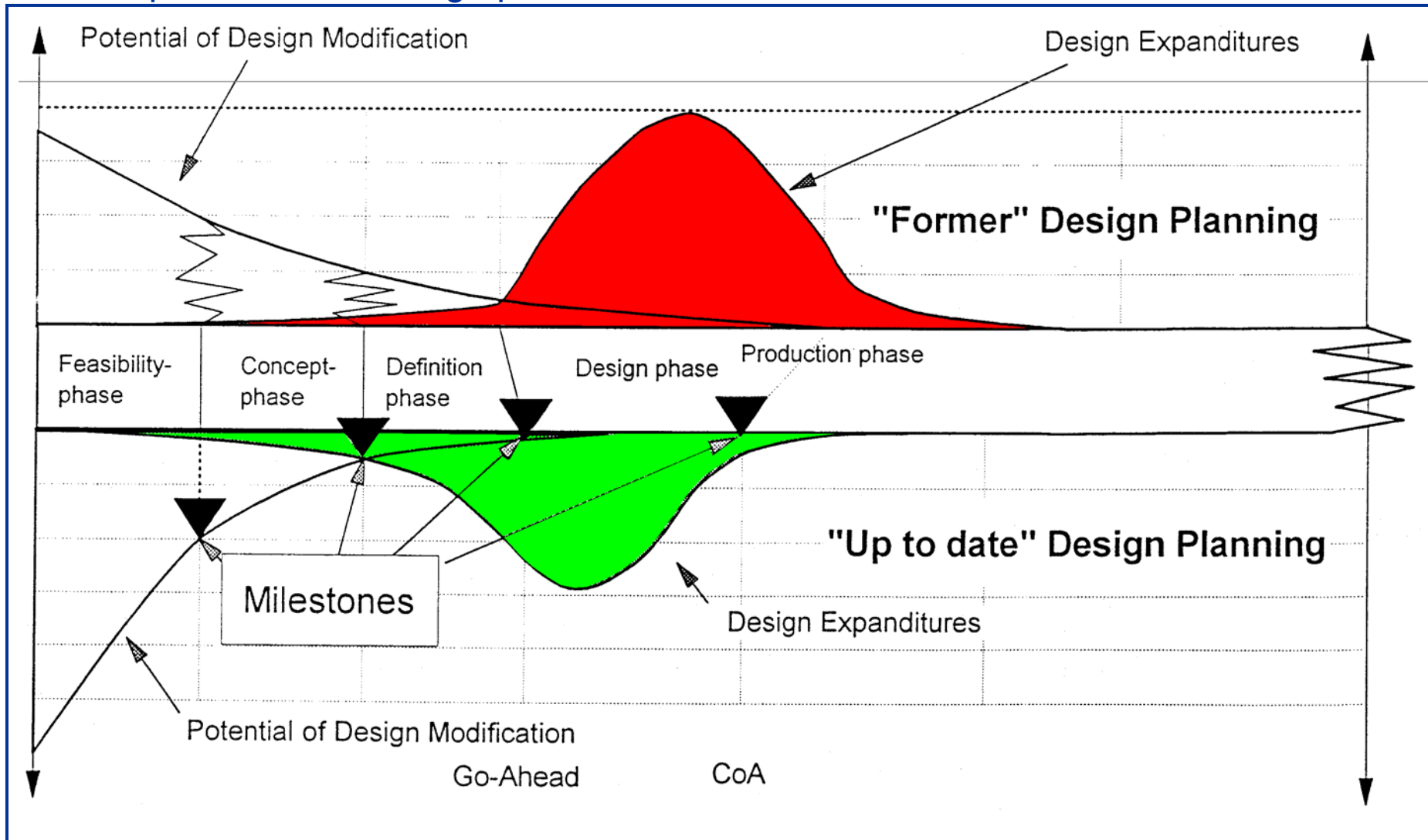


From Go Ahead to EIS



Process of core business: product definition

Goal: optimisation of design phases

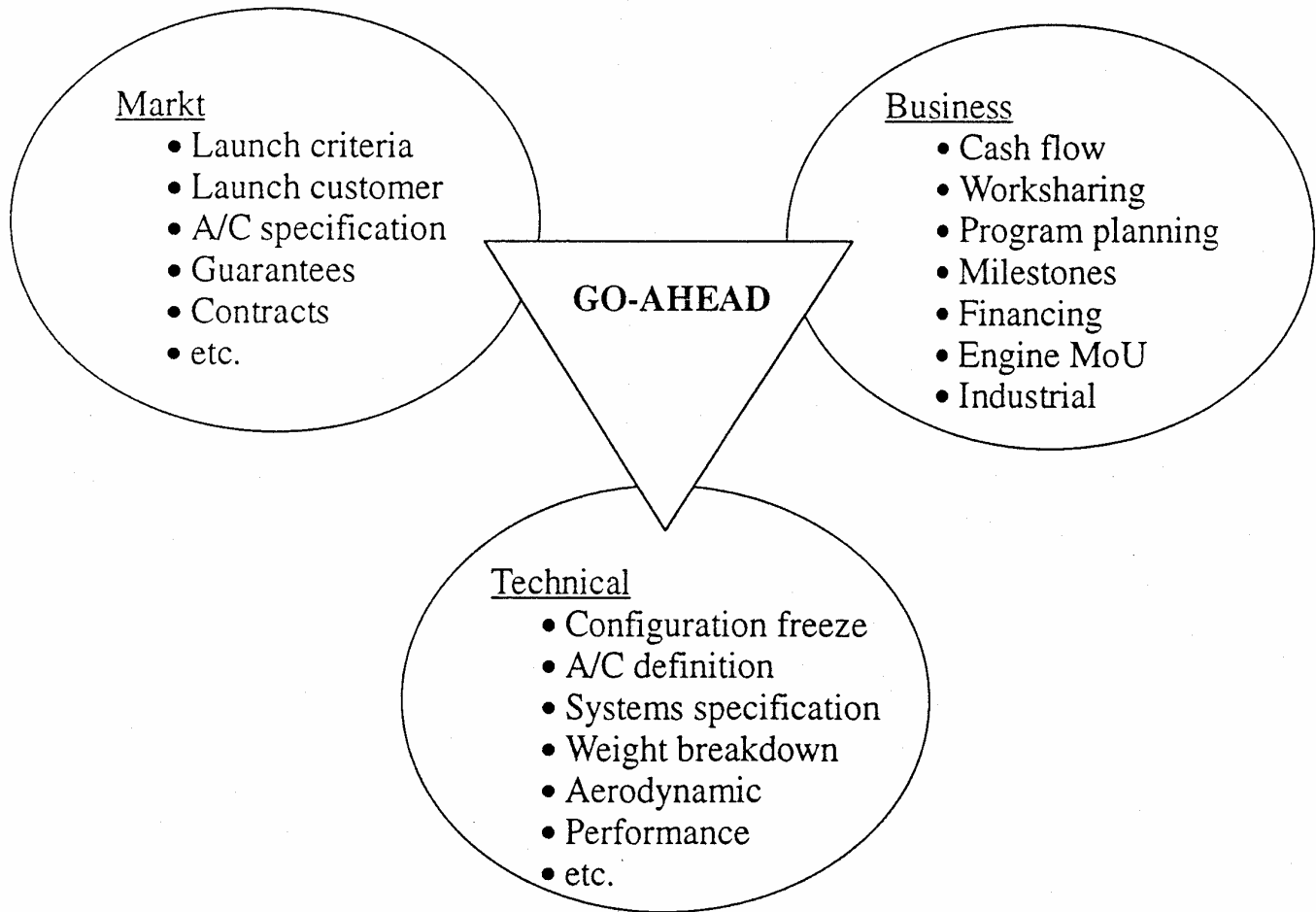


CoA: Certification of A/C

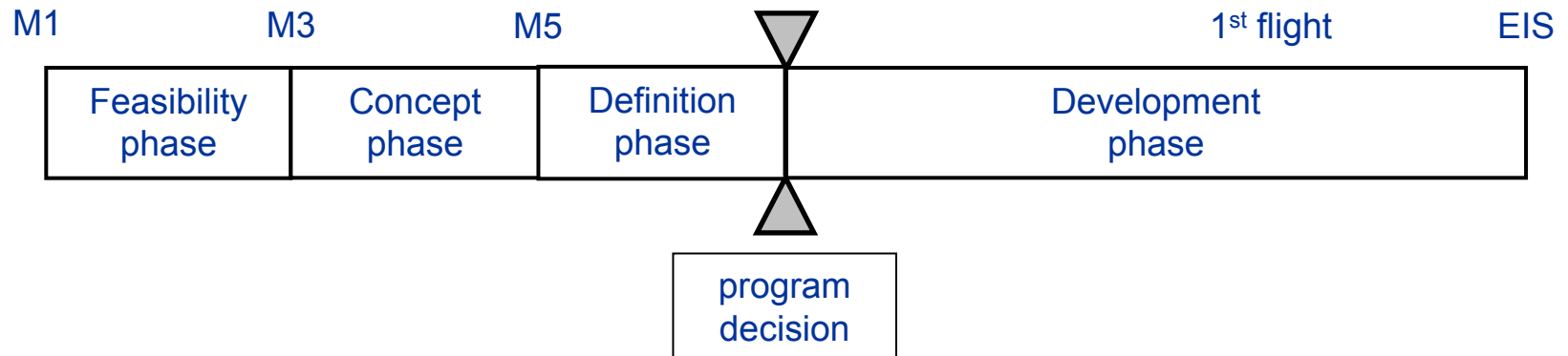
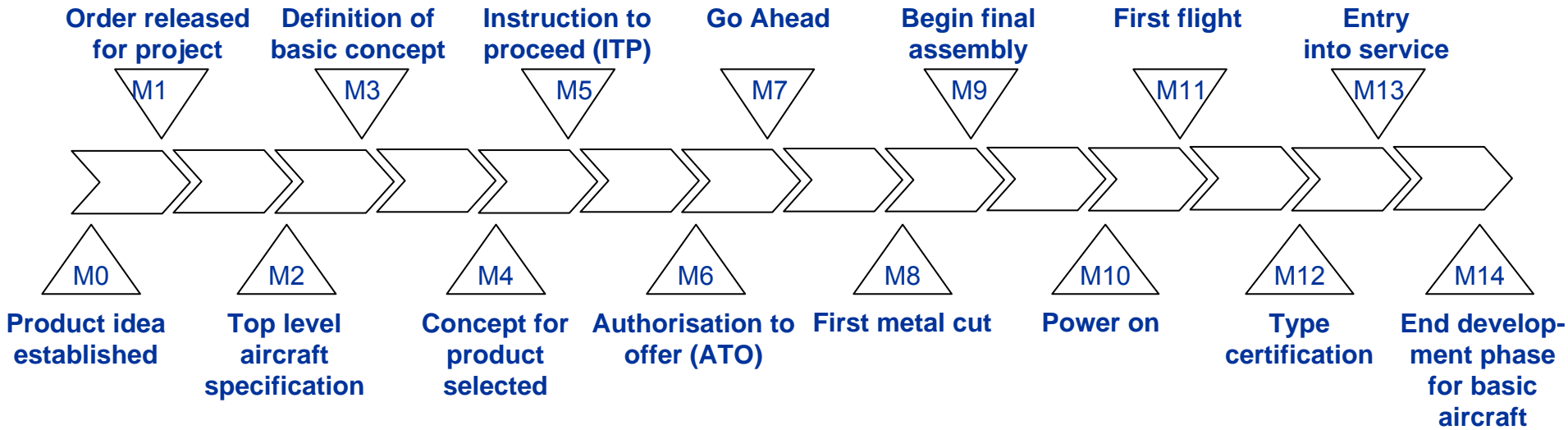
A/C development plan for Go-Ahead

FIELDS OF ACTIVITIES

Dependences by GO-AHEAD



"ACE" milestone structure



Process “*product definition*”

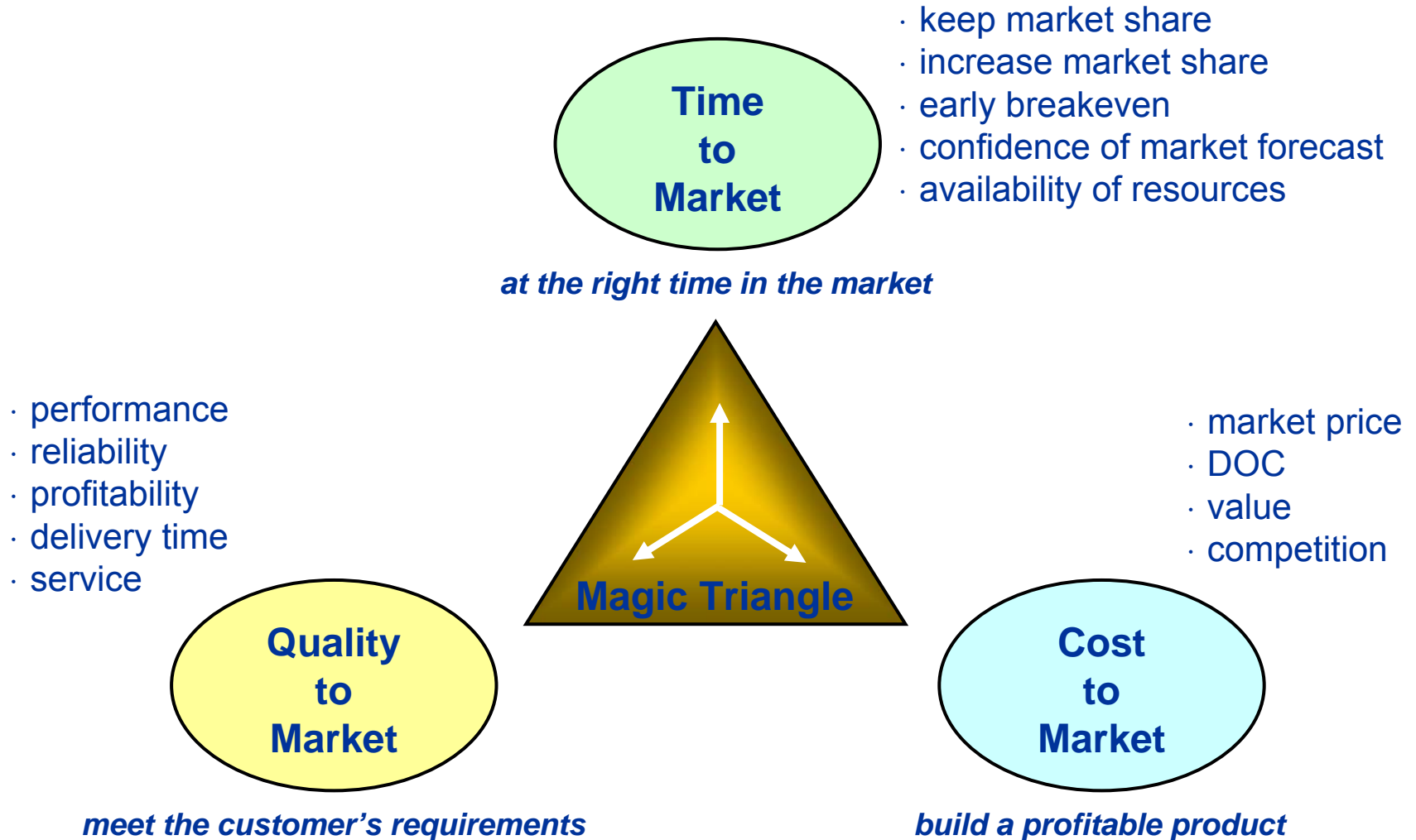
This process is completely different to all other product processes of the aircraft!

Why?

The target is not clearly fixed! – engineering wise

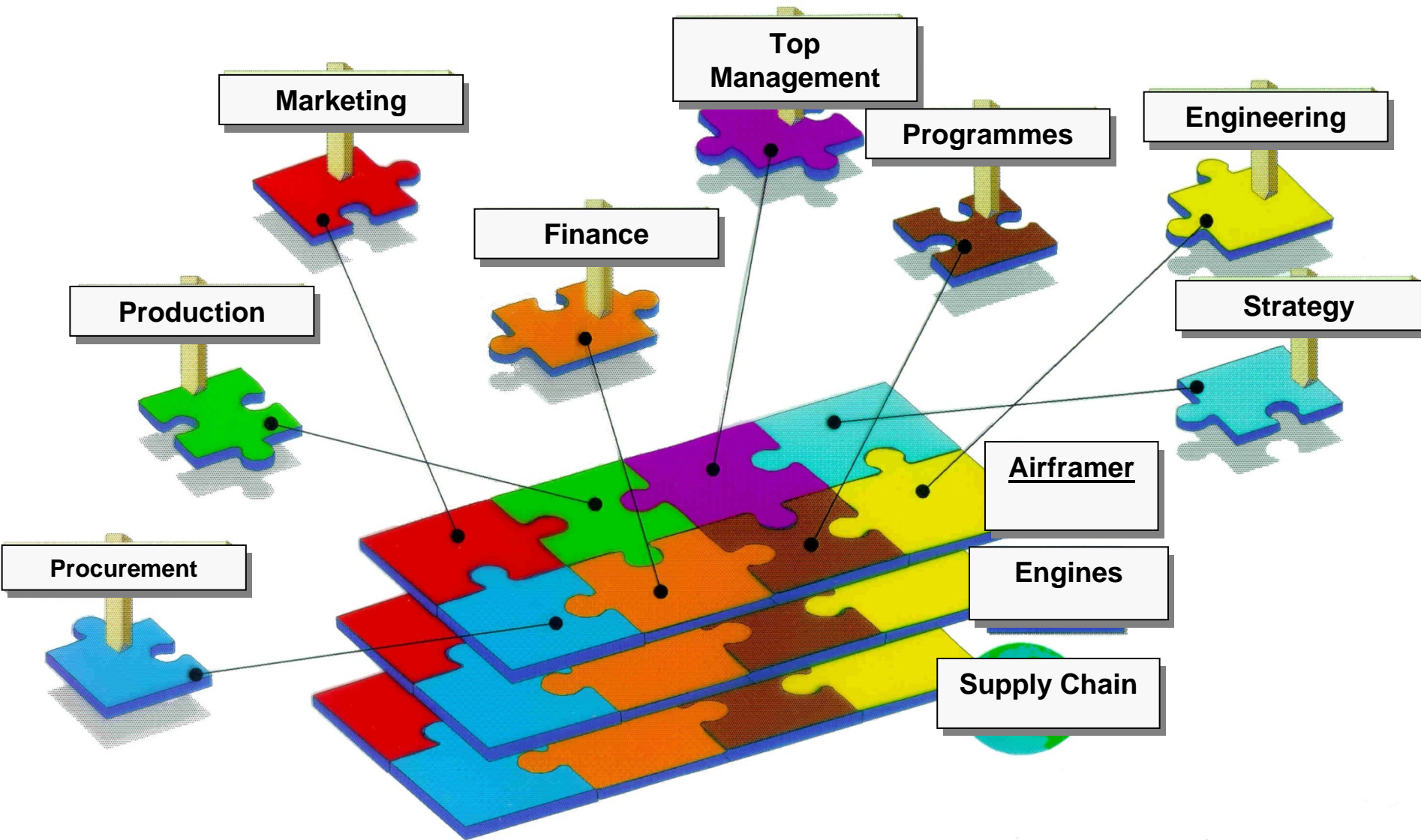
- define an aircraft configuration which is „marketable“
- there is no clear „market specification“
- the payload -range capability is about fixed
- the technology level should be high but cost efficient for the user
- the competition will not wait for your final „product definition“
- your „product proposal“ has to show a „significant“ market benefit relative to existing products
- the schedule to achieve „Go Ahead“ is defined, but will depend on market situation
- the management normally is reluctant to spend the necessary money in advance.

Time – Cost – Quality



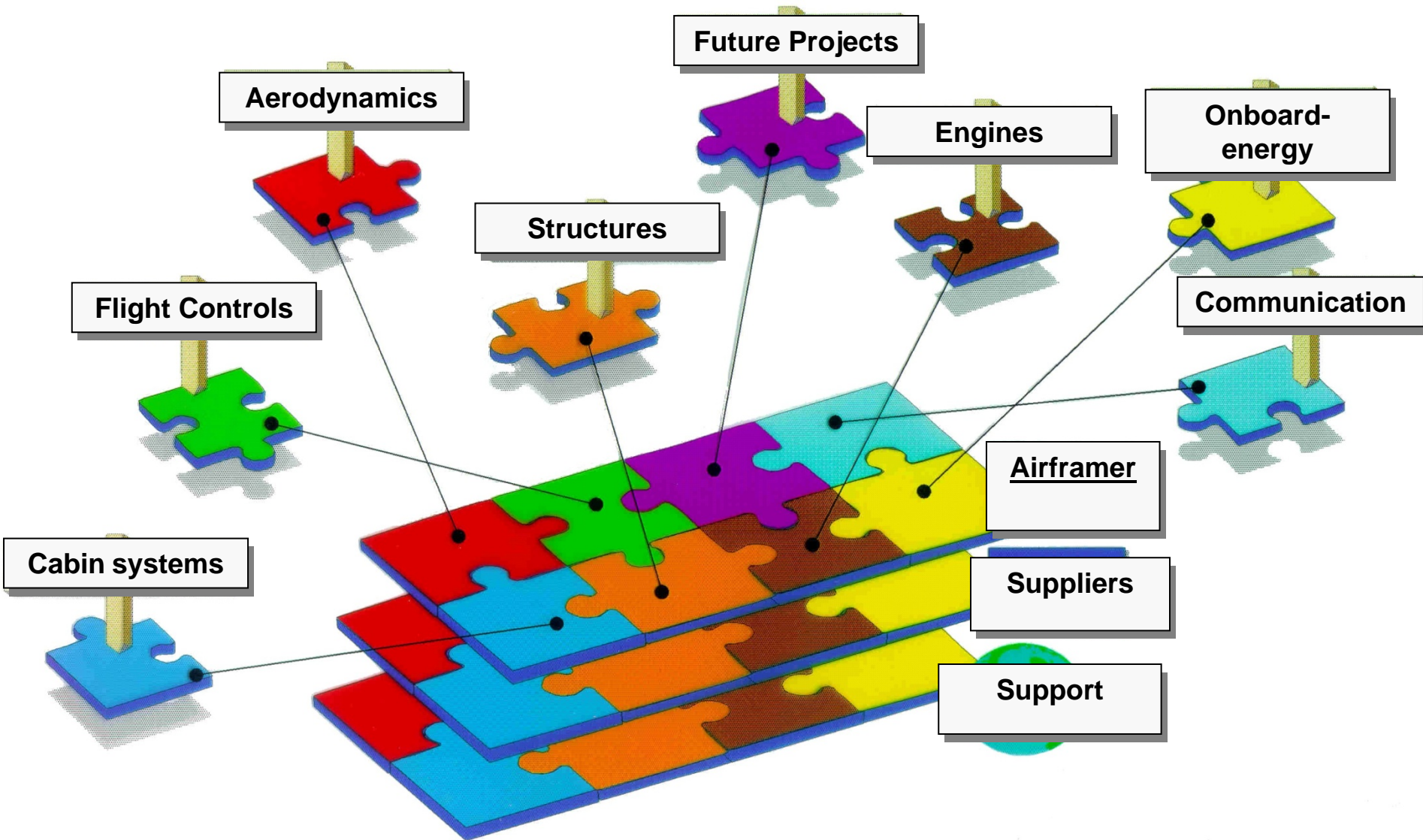
An optimum of all three areas cannot be achieved!

Aviation Industry

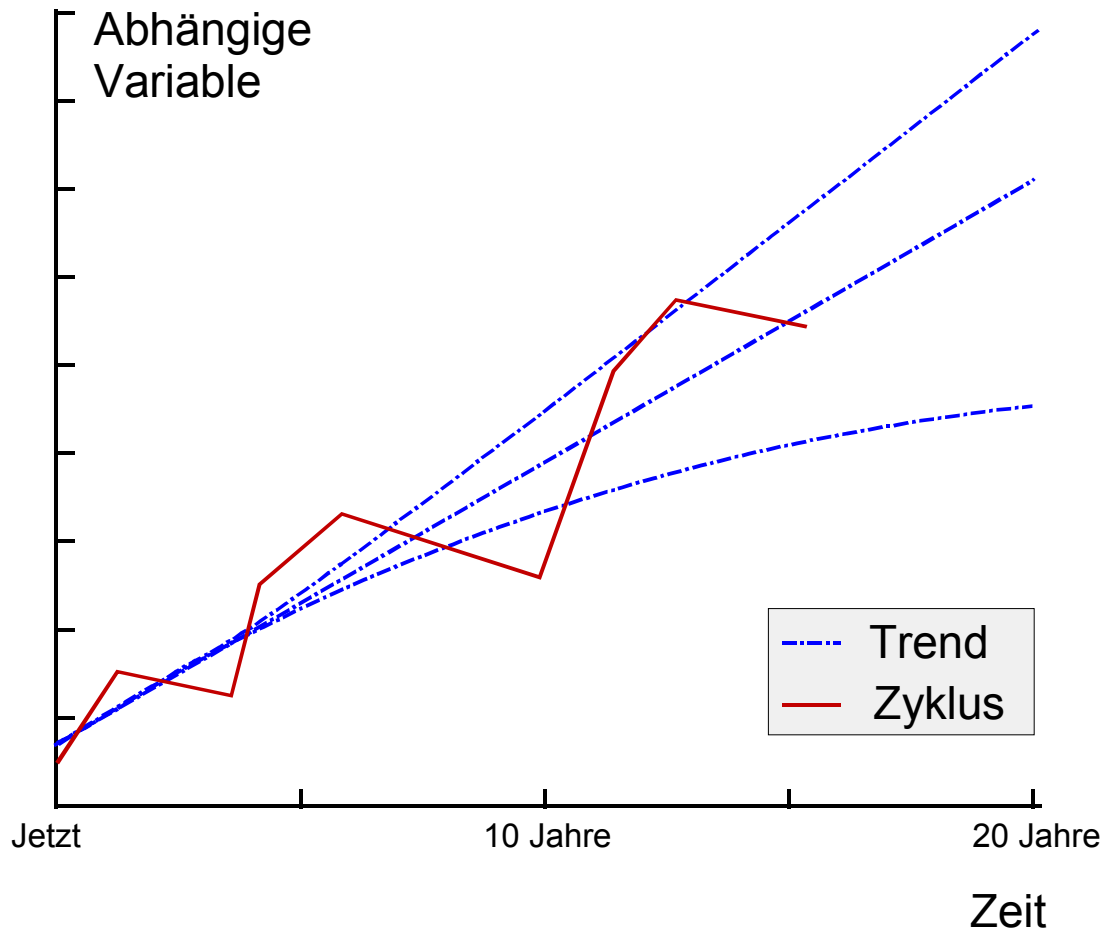


2.2 Market Requirements

Engineering (3rd level)



Trends und Cycles



Longterm trends

- Investment-Analysis
- Evaluation of new products
- Company- and markettargets
- Certification and politics
- Industrial Environment

Shortterm-cycles

- Productionrates
- Financial planning
- Support
- „What if..“ - Tests

Marketforecast

↑ There exist no unique and generally valid method for marketforecast

↑ Experience has proven a combination of different methods like

- „Top-down“ – approach
- „Bottom-up“ – approach

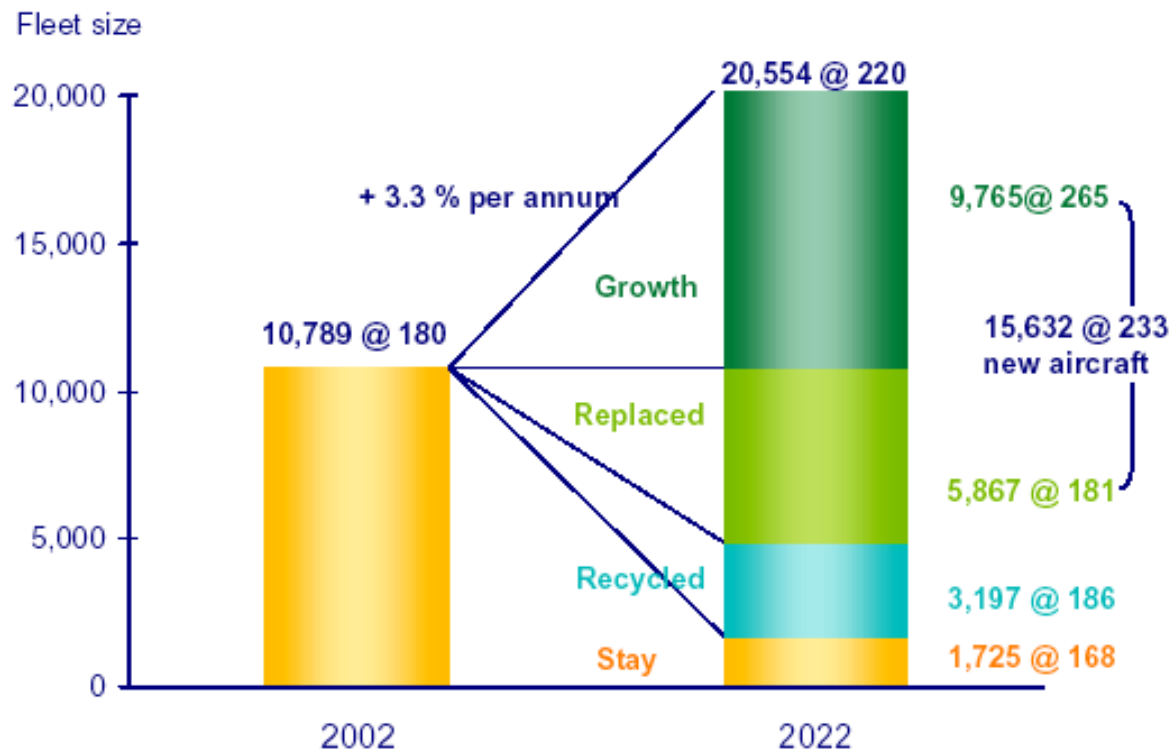
↑ In addition scenario technics have been used to capture parameters like

- Environmental aspects and future environmental fees
- Capacity constraints at airports and in densely populated areas
- fuel price developments/ alternative fuels
- alternative transport and competing communication means

Aircraft Growth and Replacement

In 2022 about 20.554 aircraft will be in service. This will be achieved by:

- 15.632 new aircraft (average size: 233 seats)
- 3.197 recycled and modified aircraft (average size: 186 seats)



Quelle: Airbus Global Market Forecast 2003

Characteristics of the Product „Air Travel“

- ⤴ The product „Air travel“ is an abstract and immaterial Service performance.
- ⤴ The passenger can not see or touch the product before buying.
- ⤴ The passenger books the flight hoping to receive a proper performance.
- ⤴ The passenger has in case of product deficits no chance for change or refusal.
- ⤴ The seller (airline, agent) has no real security for his product in case the buyer will refuse to pay the price; he therefore insists on advanced payment.
- ⤴ Producing and consuming the service performance „air travel“ are happening simultaneously. A production for stock or keeping the value of not sold performance is impossible.
- ⤴ An empty or not sold seat is a lost and later not recoverable production unit.
- ⤴ The seller needs for covering his service cost a high load factor.
- ⤴ Basic performance for the product „air travel“ is the transport of a person from his departure to his destination. In addition to this transport task there may be services before, during and after the flight.
- ⤴ Additional services will become important competing parameters besides the flight plan (departure time, routing, frequency).

Quelle: Pompl „Luftverkehr“

Passenger Requirements

Leisure traveller



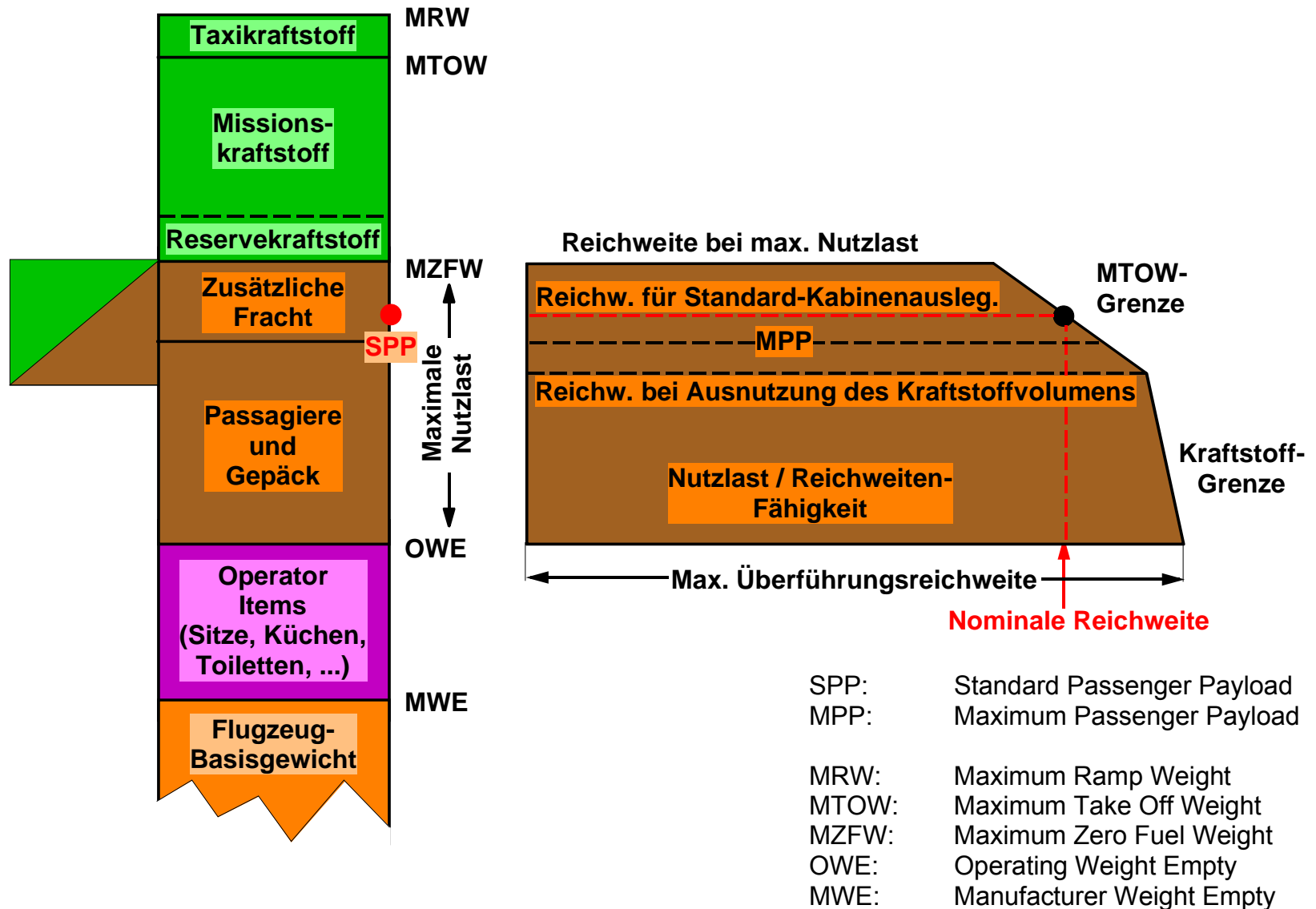
- ↑ Ticket price of prime importance
- ↑ Check-In up to 3 hours before departure are acceptable
- ↑ Flight is part of the holiday adventure
- ↑ A lot of bulky baggage (surfboard, bicycle, ..)
- ↑ On-board audio, video entertainment and computer-games
- ↑ Comfort could be much better, but .. (you get what you pay!)

Business traveller



- ↑ Ticket price is of secondary order
- ↑ Quick Check-In mandatory
- ↑ „not usable“ time during travel should be avoided
- ↑ Sufficient hand luggage
- ↑ On-Board-communication is needed
- ↑ Comfort and On-board service are very important

Payload/Range – Capability and Related Weights



2.3 Design Problematic in Engineering

Conditions for a Successful Aircraft Development

- ↑ Good market chances / good timing
- ↑ Analysis and Evaluation of competition
- ↑ Secured finance support
- ↑ Existing structures / organisations for marketing, development and production Consortium
- ↑ Worldwide Sales organization including *Product Support*
- ↑ Technical and industrial „Know-how“ / Technical innovation / proven technologies
- ↑ Timely availability of a suitable powerplant
- ↑ Definition of a long-term product strategy
- ↑ Contracts / MoU with partners and subcontractors

Design Ambiguity

Each aircraft design is facing generally the following problems:

Continuous development of
existing basis model

New development

conventional technology

Integration of new technologies

Low development cost/
higher operating cost

Higher acquisition cost/
lower operating cost

Use of existing powerplants
and systems

Introduction of new engines
and systems

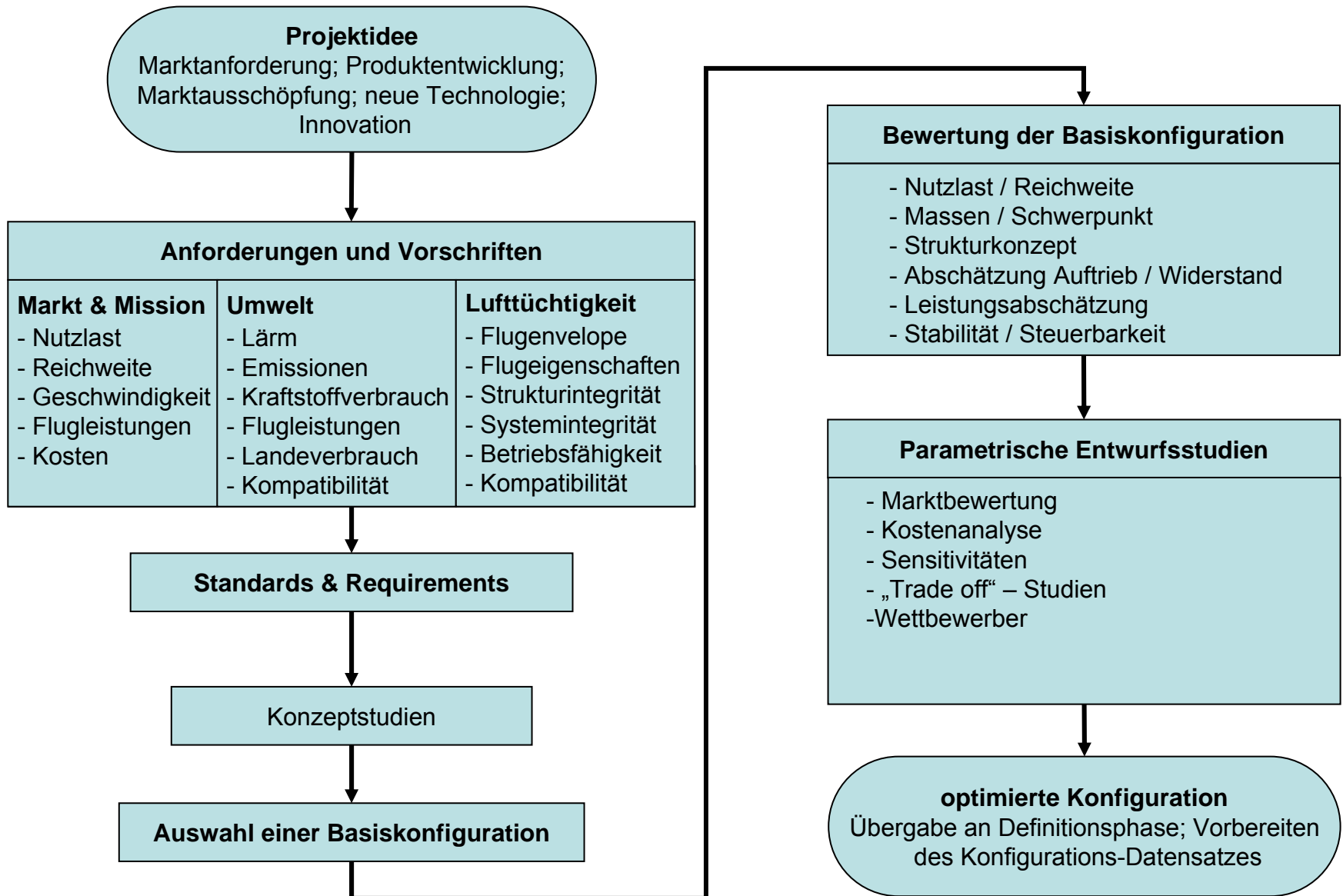
conservative marketing strategy

aggressive marketing strategy

conservative planning of
production units

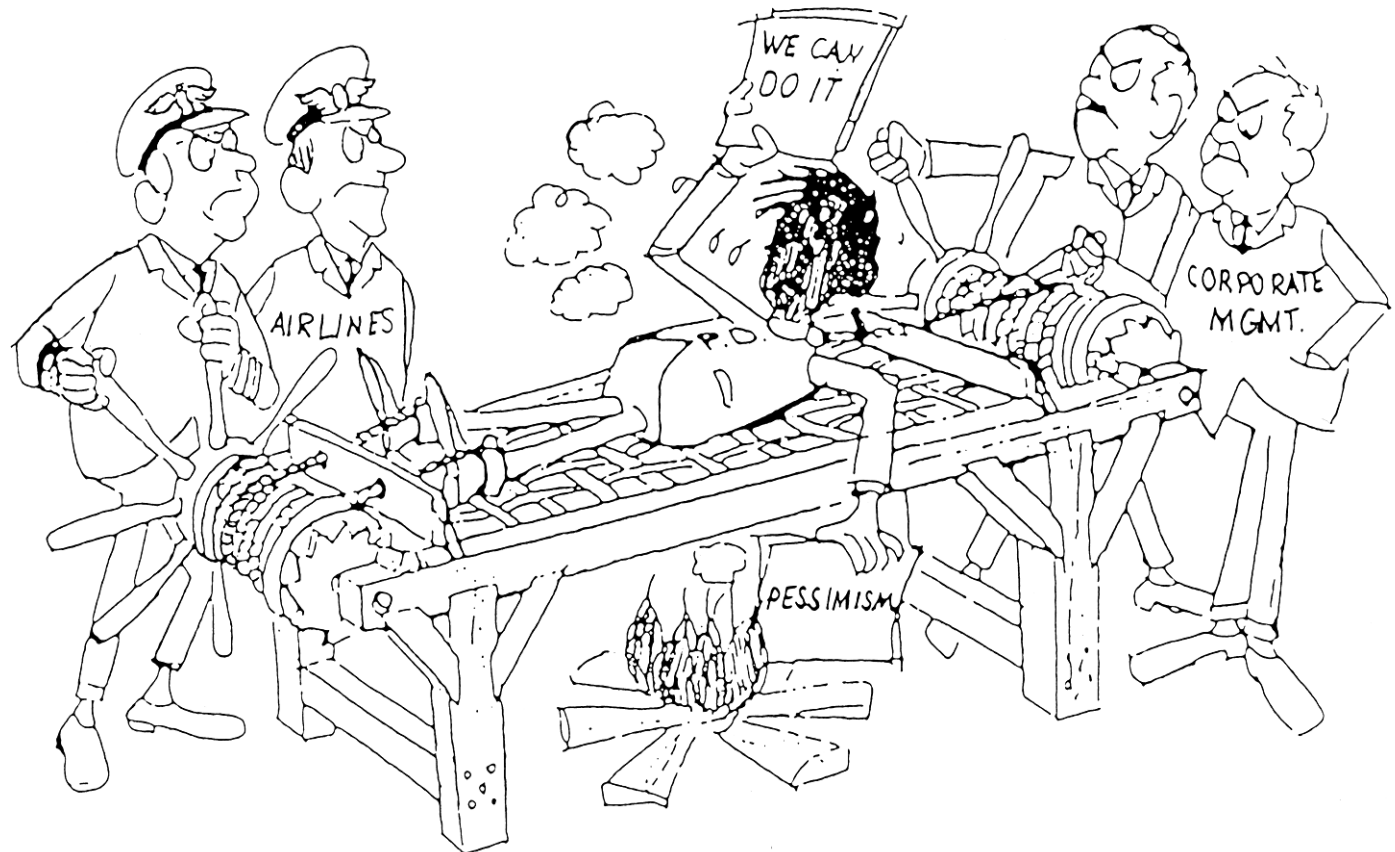
optimistic growth rates and
market assumptions

Design Requirements / Evaluation



Design Ambiguity

„The design engineer is forced from the airlines to provide optimum performance guaranties, which are ambitious and include a certain risk and at the same time, his mangement forces him to avoid any risks“



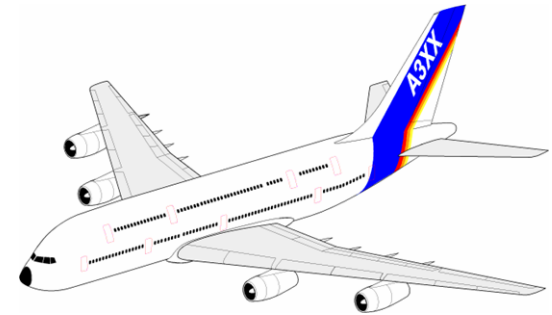
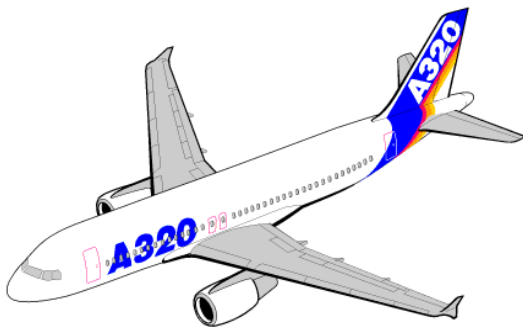
Design Goals (1)

Target is an aircraft design concept, which

- ↑ fulfils the set objectives/market requirements (payload, range, performance etc.)
- ↑ provides an advantage in DOC of „x“ percent relative to the competition,
- ↑ completes the own product family concept.

Respecting framework conditions like:

- ↑ existing propulsion systems,
- ↑ Take-off and landing requirements/performances,
- ↑ further range and payload development capabilities,
- ↑ maximum commonality to the other family members.



Design Goals (2)

- ↑ Flying higher and therefore faster
- ↑ Minimizing aircraft structural weight
- ↑ maximizing specific range (flight distance per fuel unit)
- ↑ Using aerodynamically „clean“ geometries
(ex.: swept wings for speeds beyond Mach 0,65)
- ↑ Identifying optimum value for wing loading
- ↑ Push wing aspect ratio to maximum/optimal value
- ↑ Select light and reliable systems

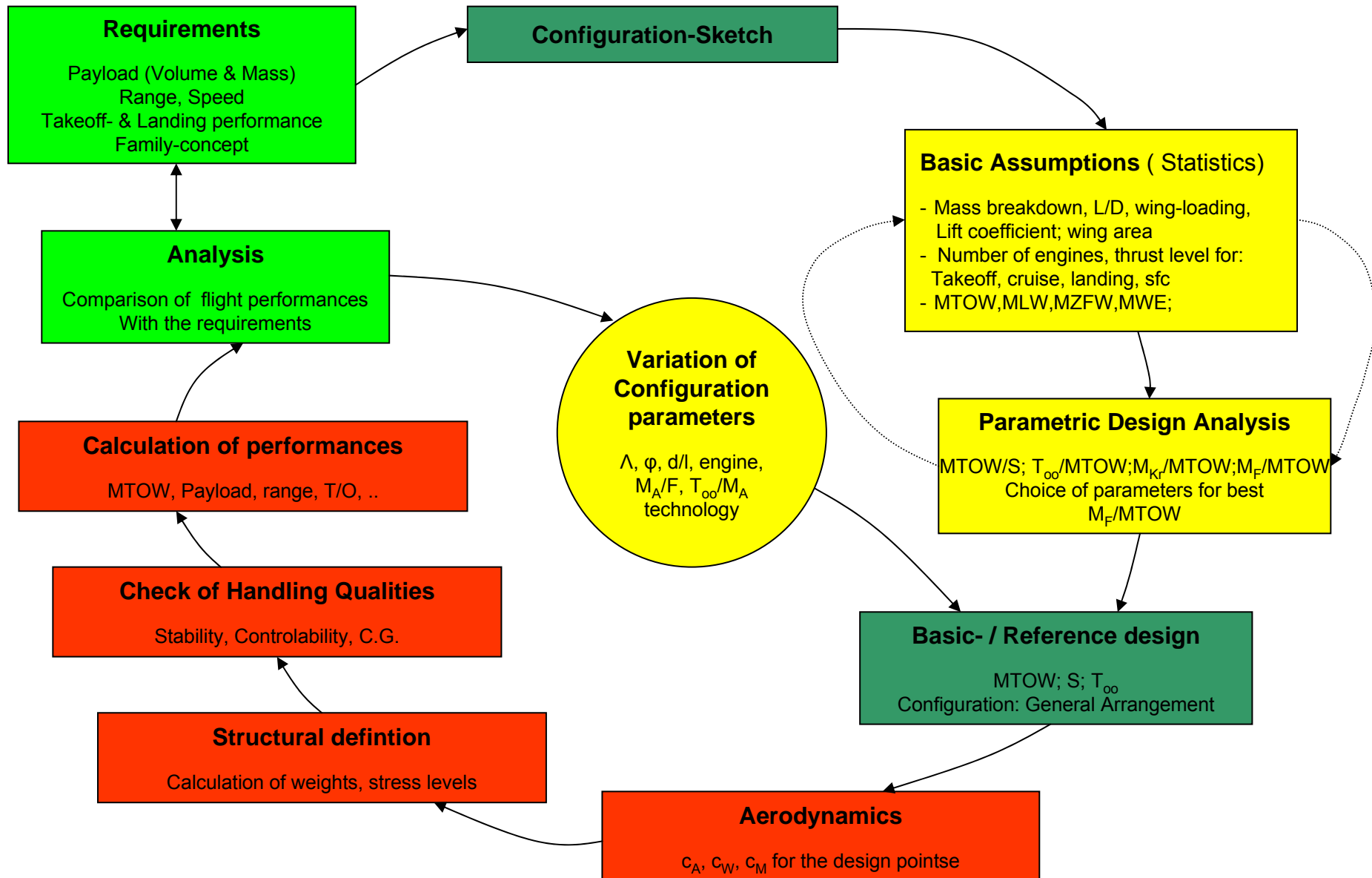
These considerations are strongly interdependent
and are often difficult to optimize.

Ex.: higher aspect ratio higher wing weight
(at same wing surface!)

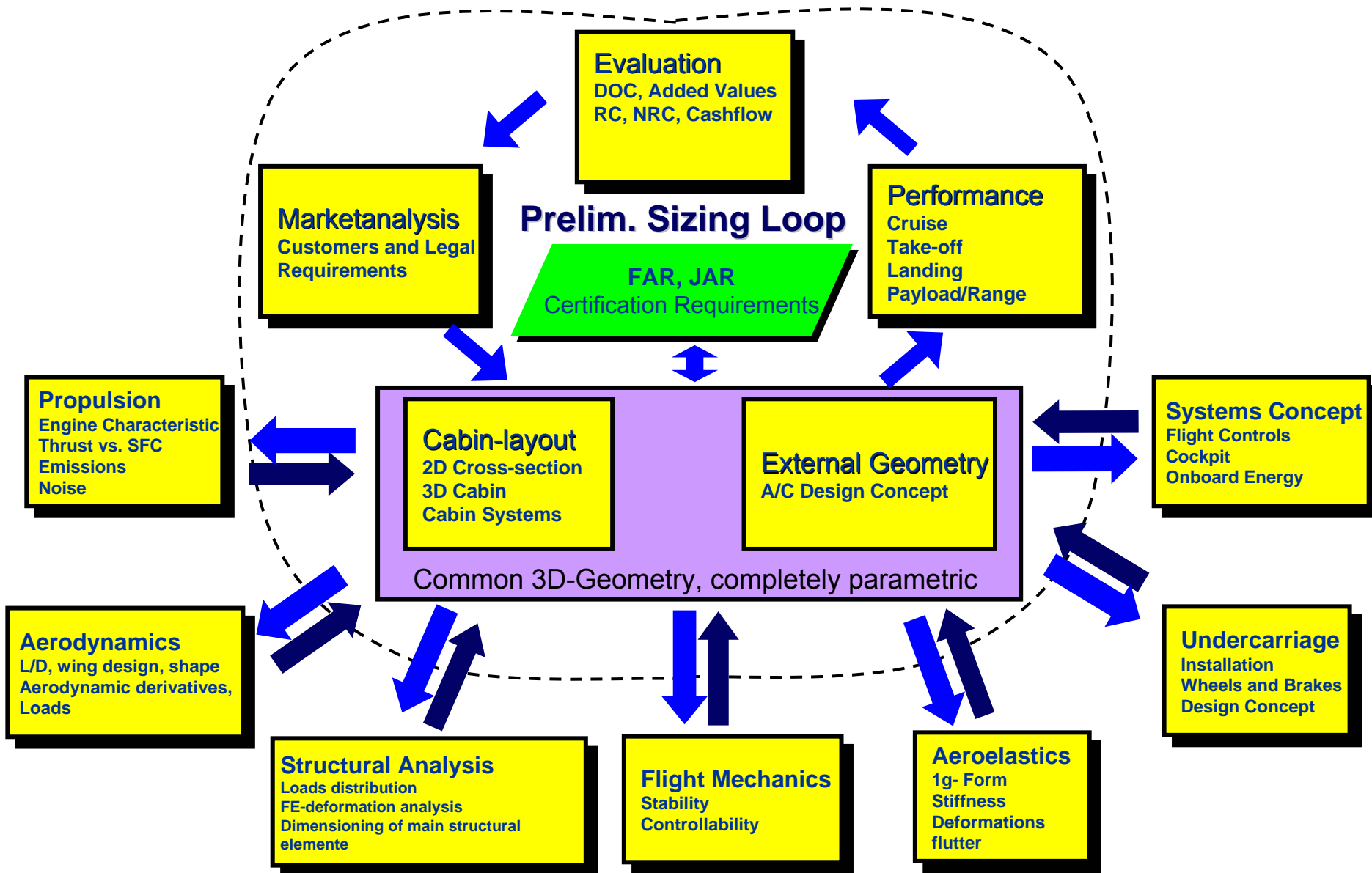
Design is an Art to search for an optimum Compromise!

2.4 Design Methodology

Definition of Reference Configuration



A/C Design Cycles



- 1.) Design Requirements & Objectives
- 2.) Definition of Airworthiness standard
- 3.) First Design sketches – Data derived from former a/c Database or previous models
- 4.) Parametric design analysis – systematic variation of main design parameters
- 5.) Definition of a reference configuration / Baseline concept including technology standard
3-View-Drawing, Aerodynamics, Weight assumptions, Flight envelope,
... *Data Basis of Design*

6.) Parametric variations of Future-project or Design/Competence centres

- Definition of cabin and payload – classes, door concept, freight, ...
- Based on geometry – definition of aerodynamic data for loads and flight mechanics
- Estimation of loads; Preliminary estimation of necessary structural dimensions for spars, frames, covers ...
- Flight mechanical estimation of stability and controllability Sizing of tail planes and fixation of necessary centre-of-gravity range
- Specification of main systems (Undercarriage, engine, environmental system, onboard-energy systems, ...)

7.) Evaluation of all flight performances (take-off, cruise, landing)

8.) Comparison with requirements, discussion of alternatives, variation of parameters

9.) Comparison with competition and critical evaluation of own design

10.) Definition of a new/improved (alternative) Reference configuration

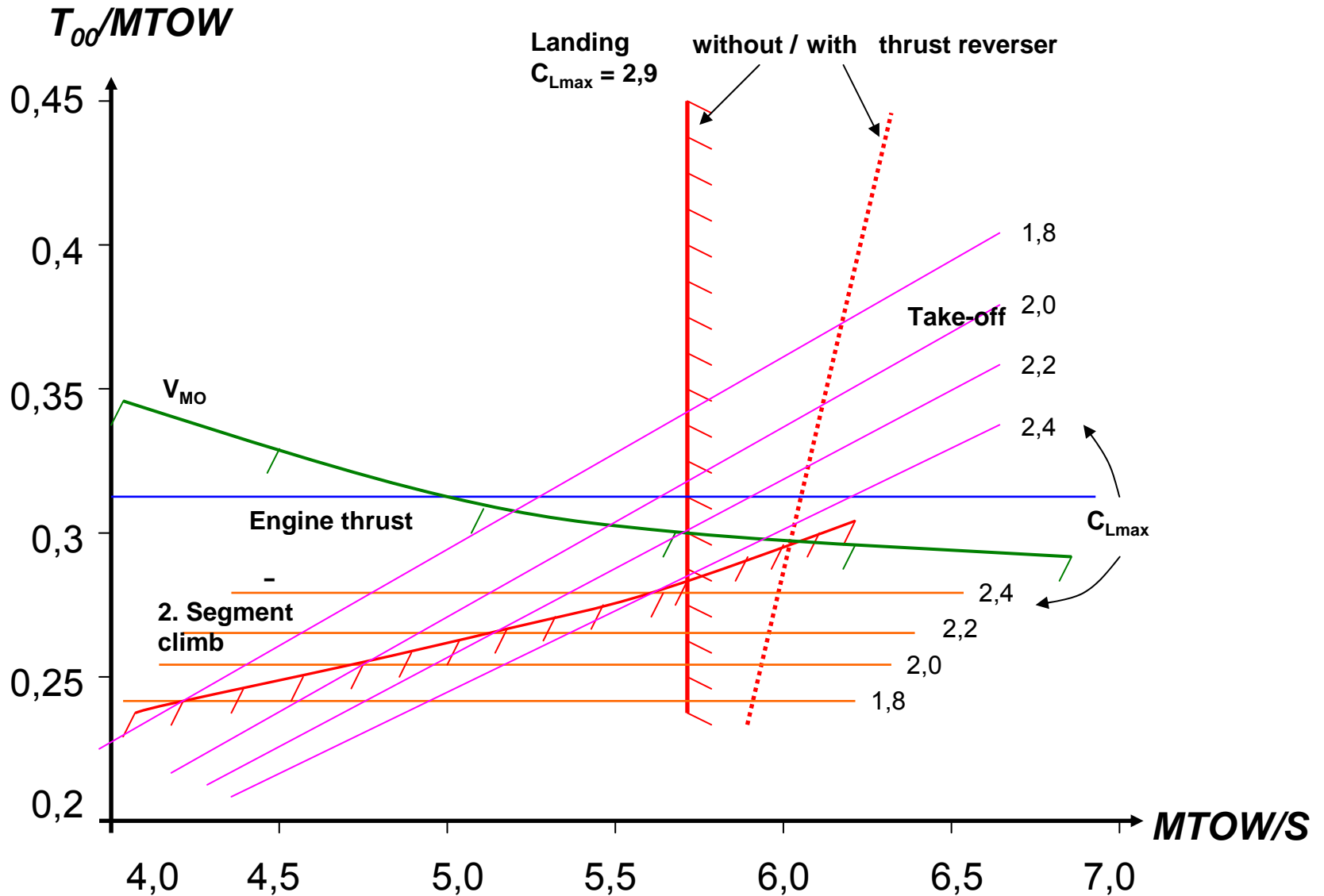
Example of Design Requirements and -goals

Capacity:	80 Seats in One-Class-Configuration; 32'' pitch
Range:	1000 nm with full number of passengers
Freight:	96'' palettes; 20 000 lbs freight for 1000 nm
Stretch potential:	up to 110 seats with 32'' pitch
Speeds:	$M = 0.76$; $V_{MO} = 320$ kts CAS; $M_{MO} = 0.8$
Initial Cruise Altitude:	ICA = 35 000 ft (ISA + 10°, 500 ft/min)
Take-off istance:	1) 5500 ft at 2000 ft elevation, ISA + 15°, MTOW 2) Denver at ISA + 28°, MTOW
Approach speed:	125 kts at ISA +20°
OEI-altitude:	16 000 ft at ISA +10°
Noise:	ICAO Annex 16 Vol.I, Stage III -3 dB (Stage IV)
Emissions:	relativ to todays ICAO-requirements CO 20%; UHC 15%; NO _x 35%; Rauch 35%
Certification:	JAR 25 + Amendments up to 66

Technology Standard - Example

Nr.	Technology items	Status	Potential / Risk	Remarks	Recommend. for baseline
I	Aerodynamics				
I.1	Winglets	Standard	No advantage for new A/C	-	No
I.2	Natural laminar flow wing	Technologyprogramm at TRL5	8-10% drag reduction	big impact on Config.: F,φ	Yes
II	Structure				
II.1	Welded fuselage	Tech.Prog.: at TRL 6 on x.x	~ 10 ^{kg} /m fuselagelength	Investment for production ↗	Yes
II.2	CFRP - wing	Tech.Prog.: TRL 5	~ 12% MWE ↘	Big Influence on Config.: material	Yes
III	Controls / Loads				
III.1	Manoeuvre load con.	...			
III.2	FBW	...			
IV	Systems				
V	Propulsion				
VI	Canard-Config.				

Parametric Design Analysis



Basic Design Requirements

1. Payload Capacity

passenger capacity
cabin standard
freight capacity

2. Range

SPP (standard passenger
payload)
max. payload
max. range

3. Speed

V_{MO} , M_{MO}
 V_{Cr}

4. Weight Definition

pax + baggage
MWE, OWE
max. fuel
MTOW, MZFW, MLW

5. Field Performance

take-off distance
landing distance
approach speed
ACN

6. En-Route Performance

OEI ceiling
max. operating altitude
ICA (initial cruise altitude)

7. Cross Section

SA, TA, MA
seat abreast
cargo compartment

8. Doors

evacuation
boarding

9. Interiors

seat layout
lavatories
galleys
stowage

10. Noise

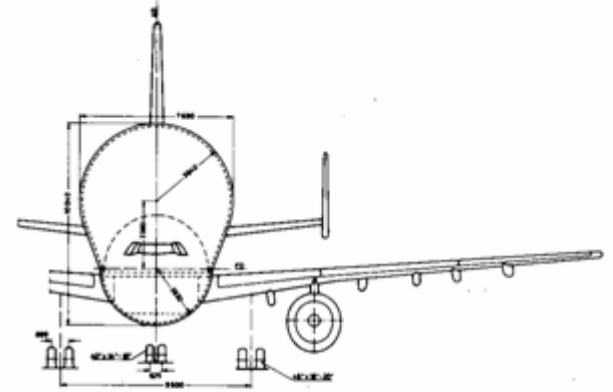
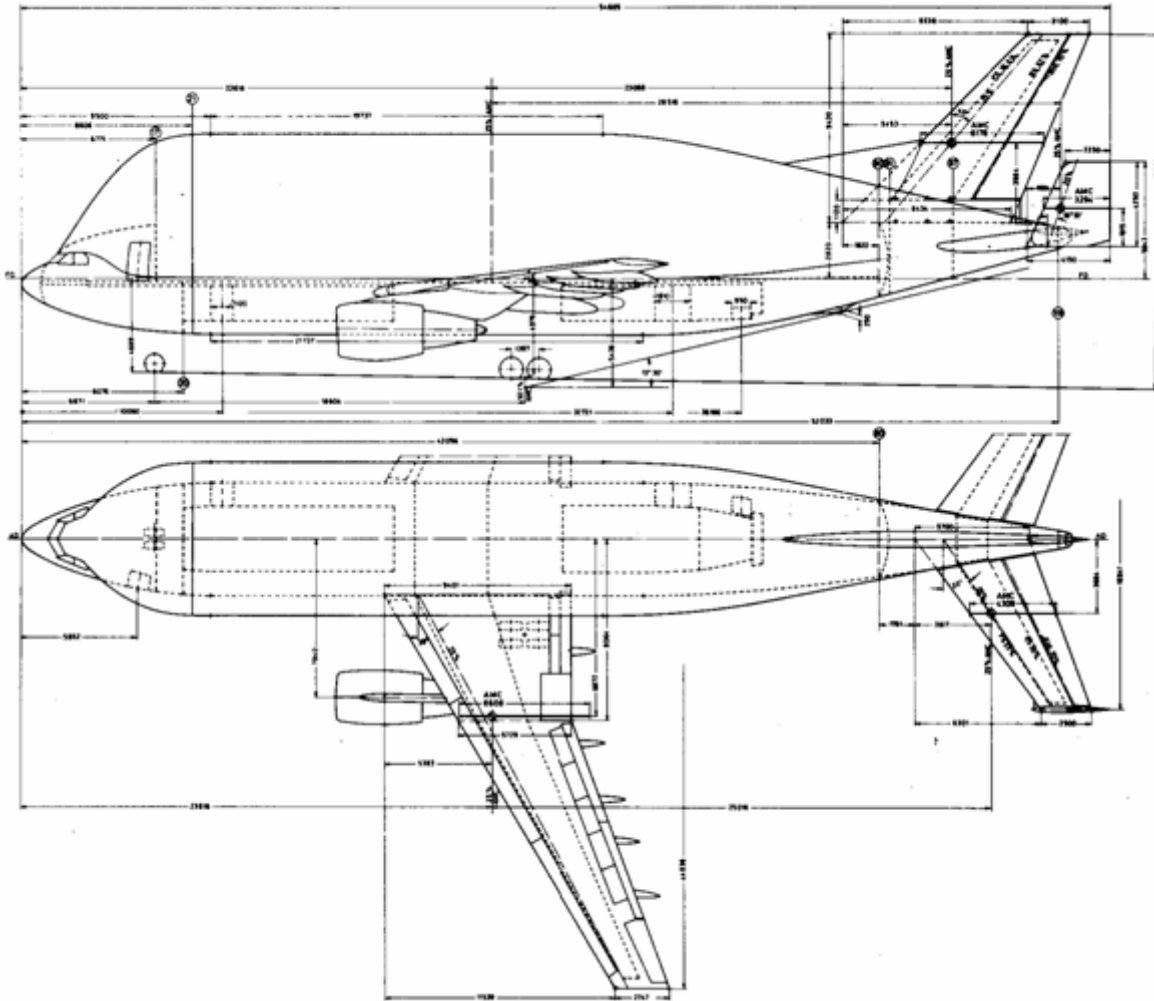
external (ICAO An. 16)
internal

11. Pollution

emission index

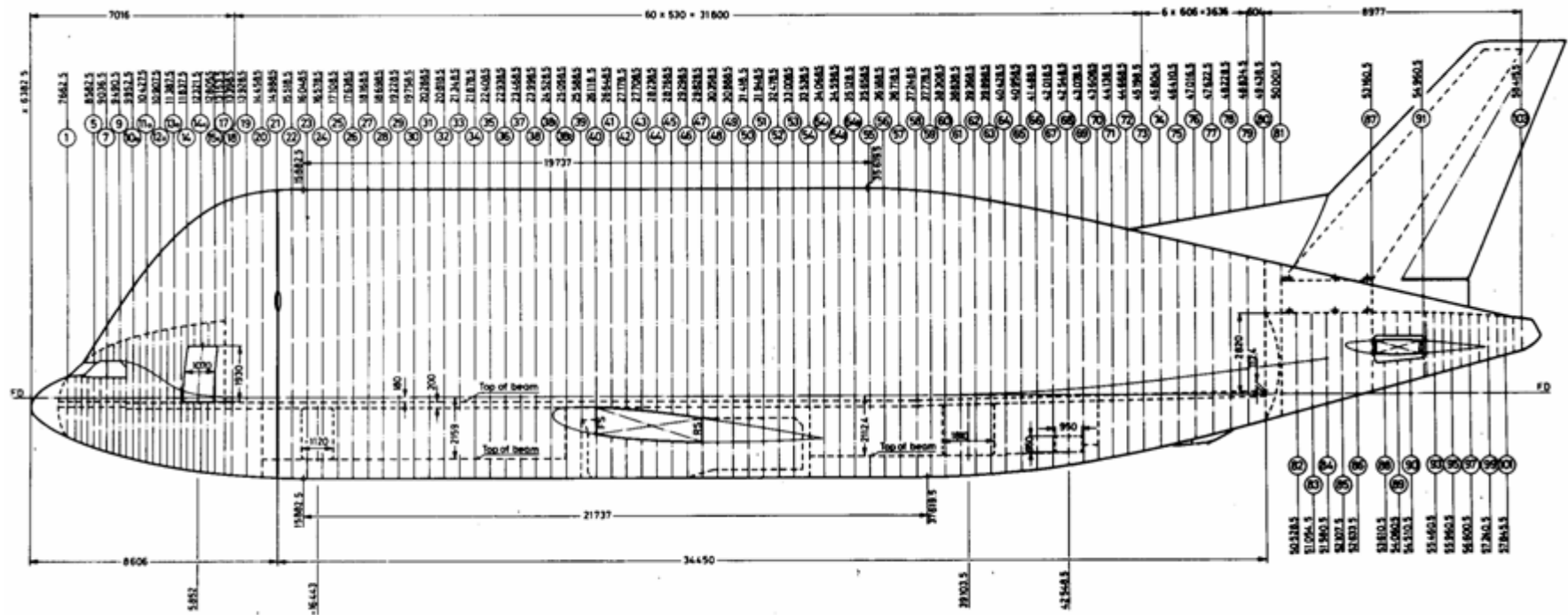
12. Fatigue Life

life cycles
life hours



	Wing	Tailplane	Fus. Rudder	Auxil. fin
Area (m ² /sq ft)	260/2800	68.5/745	54.3/584	13.5/145
Aspect ratio	7.732	4.129	1.634	1.338
Taper ratio	0.37	0.439	0.3676	0.542
T _c ratio %	10.5	10	11	8
1/s (chord span)	28°	33°	40°	16° 32'
Volum. coeffic.	—	1.012	0.707	0.033

Fuselage Concept



Dieter Schmitt

Chapter 3

Certification

Definition of aircraft safety (Airworthiness):

„The acceptable safety standard of an aircraft,

- designed and built in accordance with the relevant requirements,
- operated in the specified environment and within the quantified and defined boundaries as well as
- maintained in agreement with the specified procedures from the authorities

Technical Requirements

JAR-1	Definitions and Abbreviations	FAR-1	Definitions and Abbreviations
JAR-21	Certification Procedures for Aircraft, and Related Products & Parts	FAR-21	Certification Procedures for Products and Parts
JAR-22	Sailplanes and Powered Sailplanes		
JAR-23	Normal, Utility, Aerobatic and Commuter Category Aeroplanes	FAR-23	Airworthiness Standards: Normal, Utility, Acrobatic, and Commuter Category Airplanes
JAR-25	Large Aeroplanes	FAR-25	Airworthiness Standards: Transport Category Airplanes
JAR-26	Retroaktive Lufttüchtigkeitsforderungen		
JAR-36	Fluglärm	FAR-36	Noise Standards: Aircraft Type and Airworthiness Certification
JAR-147	Ausbildungsstellen für Instandhaltungspersonal	FAR-147	Aviation Maintenance Technician Schools
JAR-27	Small Rotorcraft	FAR-27	Airworthiness Standards: Normal Category Rotorcraft
JAR-29	Large Rotorcraft	FAR-29	Airworthiness Standards: Transport Category Rotorcraft
JAR-E	Engines	FAR-33	Airworthiness Standards: Aircraft Engines
JAR-P	Propellers	FAR-35	Airworthiness Standards: Propellers
JAR-APU	Auxiliary Power Units		
JAR-TSO	Joint Technical Standard Orders		
JAR-AWO	All Weather Operations		
JAR-VLA	Very Light Aeroplane	FAR-103	Ultralight Vehicles
JAR-145	Approved Maintenance Organisations	FAR-145	Repair Stations
JAR-OPS Part 1	Commercial Air Transportation (Aeroplanes)	FAR-121	Certification and Operations: Domestic, Flag, and Supplemental Air Carriers and commercial Operators of Large Aircraft
JAR-FCL	Lizenzierung von Flugpersonal	FAR-61	Certification: Pilots and Flight Instructors
JAR-OPS Part 3	Commercial Air Transportation (Helicopters)	FAR-127	Certification and Operations of Scheduled Air Carriers with Helicopters

JAR-25 Large Aeroplanes

Section 1 – Requirements:

- Subpart A – General
- Subpart B – Flight
- Subpart C – Structure
- Subpart D – Design and Construction
- Subpart E – Powerplant
- Subpart F – Equipment
- Subpart G – Operating Limitations and Information
- Subpart J – Gas Turbine Auxiliary Power Unit Installation

Section 2 – Acceptable Means of Compliance & Interpretations (ACJ)

Section 3 – Advisory Material (AMJ)

Definition of Safety



Accident of an An-124 directly after Takeoff.
3 out of 4 engines failed probably due to
missing anti-freezing agent in fuel.

- Absolute safety does not exist!
- Each technical and biological system can fail.
- Each technical and biological system consists of a compromise between several contradicting requirements with respect to safety and efficiency.

Source: DFG Sicherheit im Luftverkehr

Security: The New Challenge

New challenge for the air transport system is the aspect: **Security**

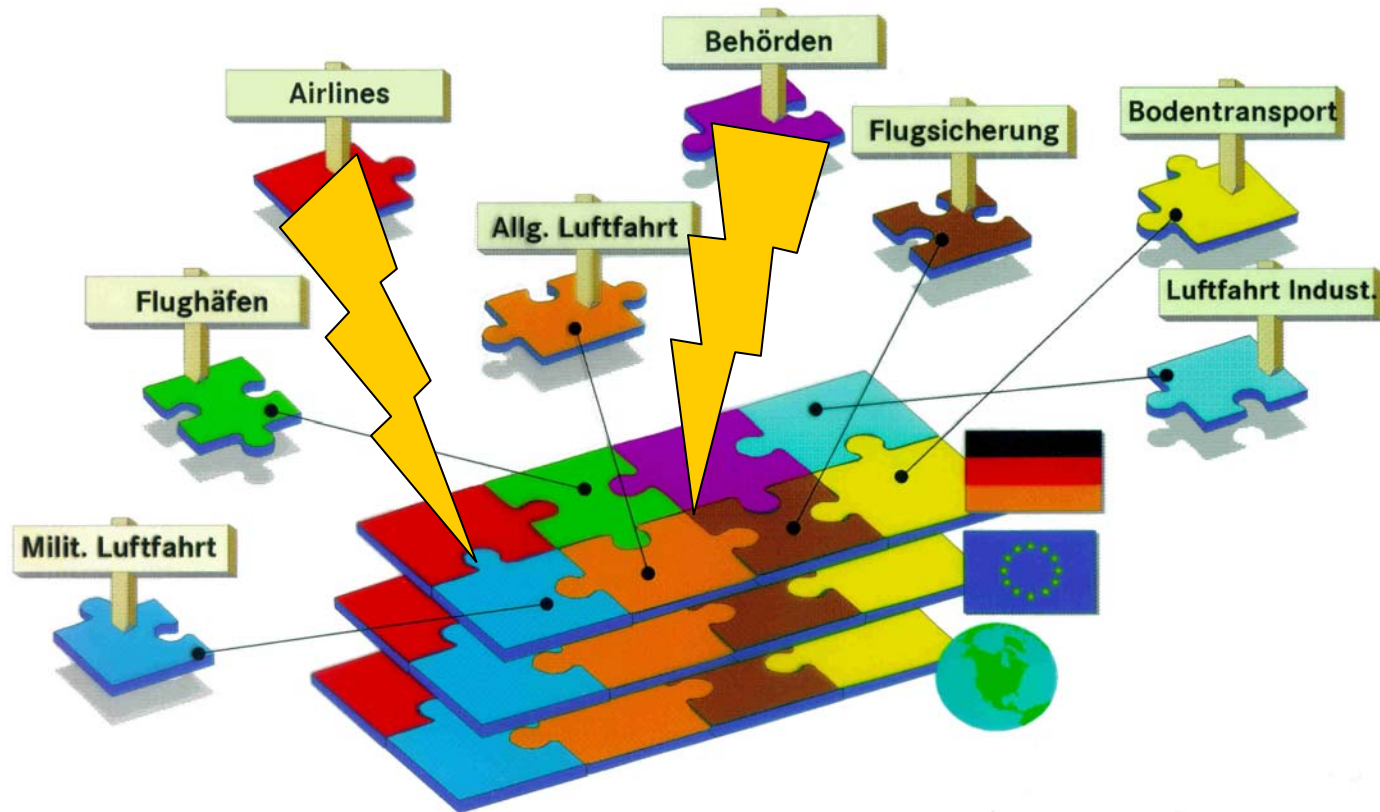
Terrorists are using aircraft esp. long-range A/C with a lot of fuel in a suicidal way as „flying bombs“ and no longer for extortion of political friends or achieving political goals (ex. asylum).



Counter measurements:

- ↑ Intensified control of passengers
- ↑ Locking and reinforcing of cockpit doors
- ↑ Use of „Air-Marshalls“
- ↑ Intensified control of personal in security critical areas

Fragility of the Air Transport System



Insurance:

Cancellation of policy against war and terror with airlines

Airlines:

Drastic reduction in passenger numbers leading to enormous financial difficulties

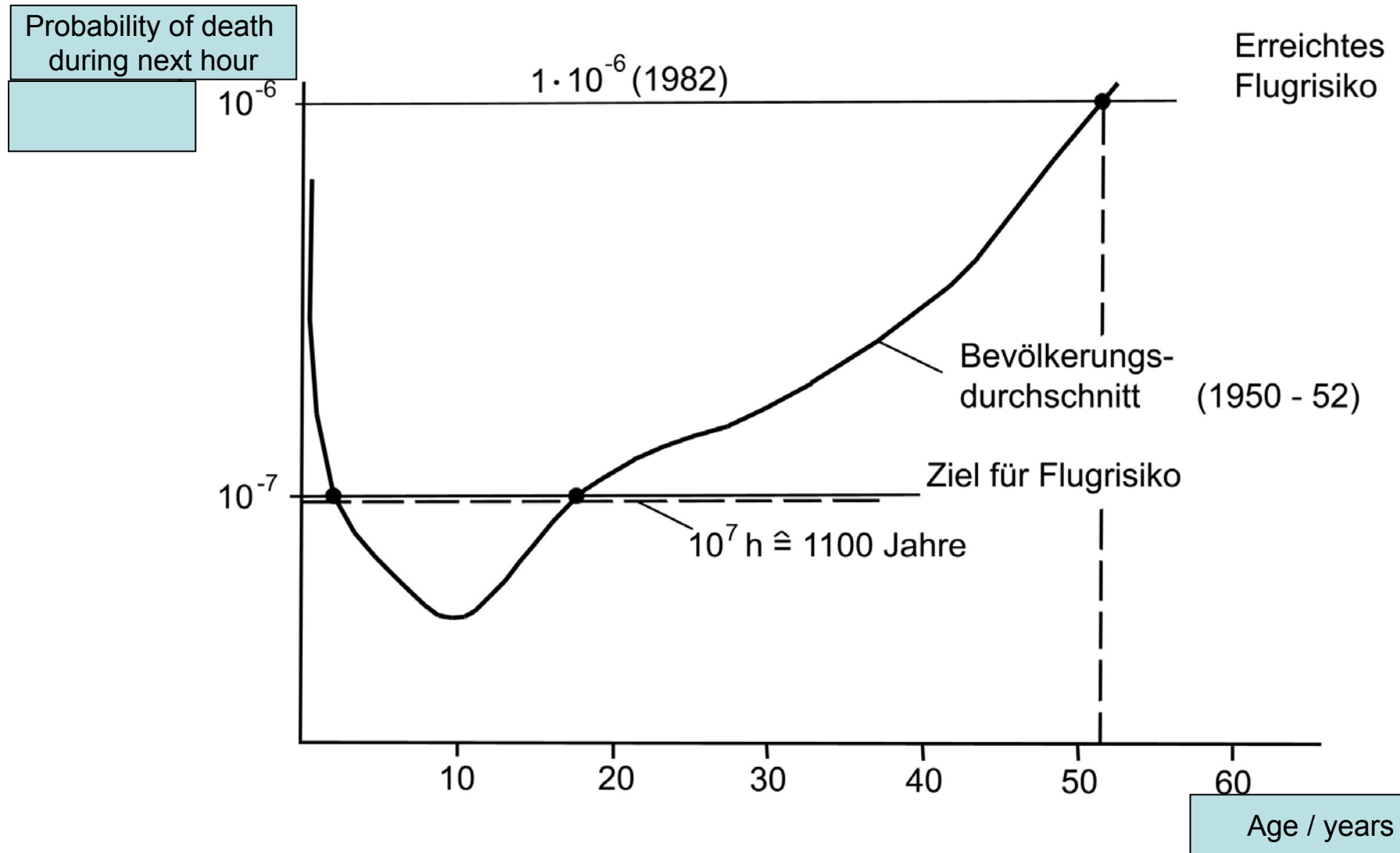
Authorities:

Closure of airspace – Aircraft stay on ground immediately

Relation between Probability and Consequence

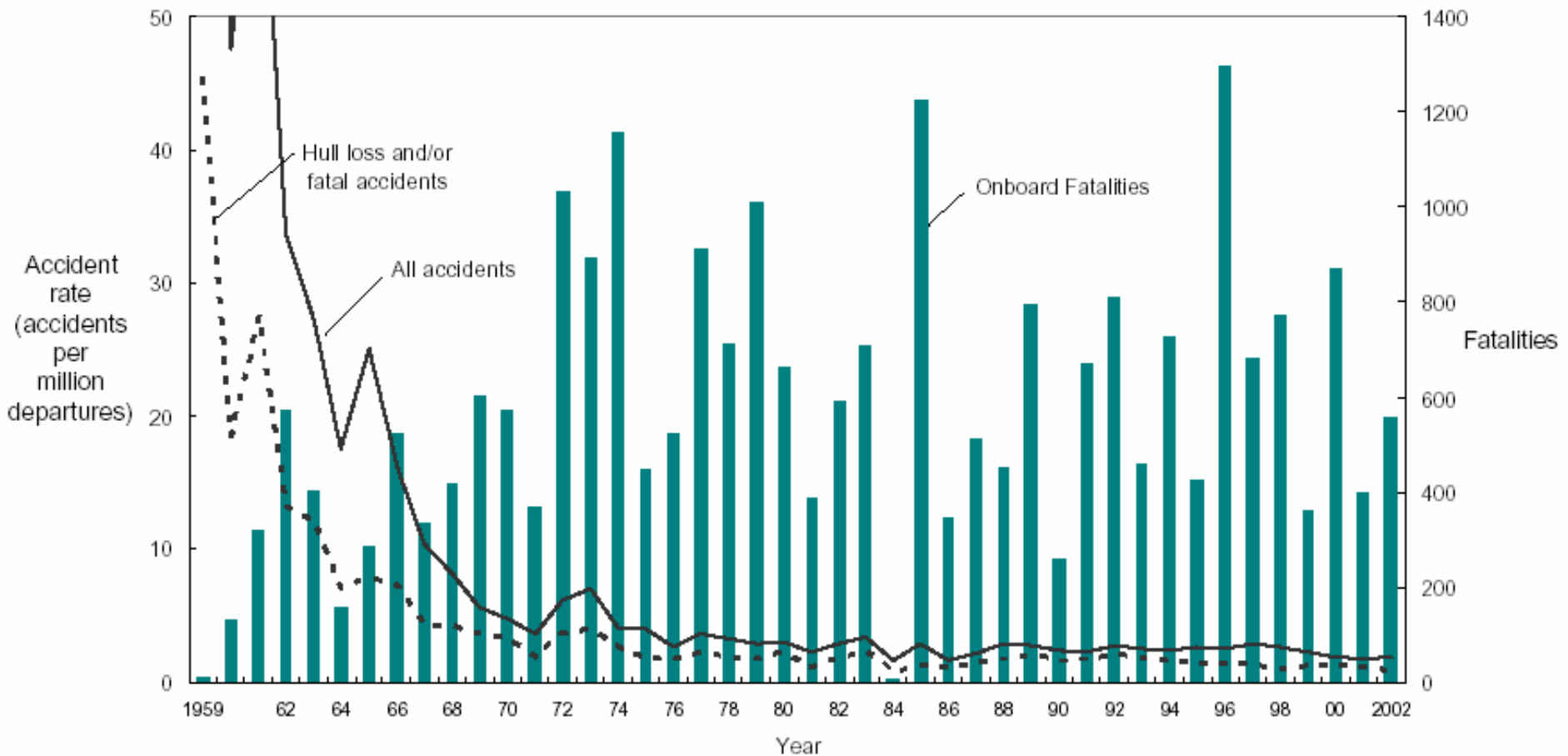
Probability of one event per flight										
	10 ⁻¹	10 ⁻²	10 ⁻³	10 ⁻⁴	10 ⁻⁵	10 ⁻⁶	10 ⁻⁷	10 ⁻⁸	10 ⁻⁹	10 ⁻¹⁰
Probability	often		Moderate/probable		Less probable		Unlikely		Very unlikely	
Effect	Small				Large		Risky		catastrophic	
Description	Happens probably often during the life of an aircraft		Happens probably not often during the operation, but can happen several times during the life of an aircraft		Happens probably not during operation, but can happen during the whole life of individual aircraft kann aber über die gesamte Lebensdauer einzelner Fluggeräte mehrfach auftreten		Unlikely over the whole lifetime of an aircraft but can be possible (not completely excluded)		So unlikely , that it has not to be considered as possible	

Risk of Death for Humans During Lifetime



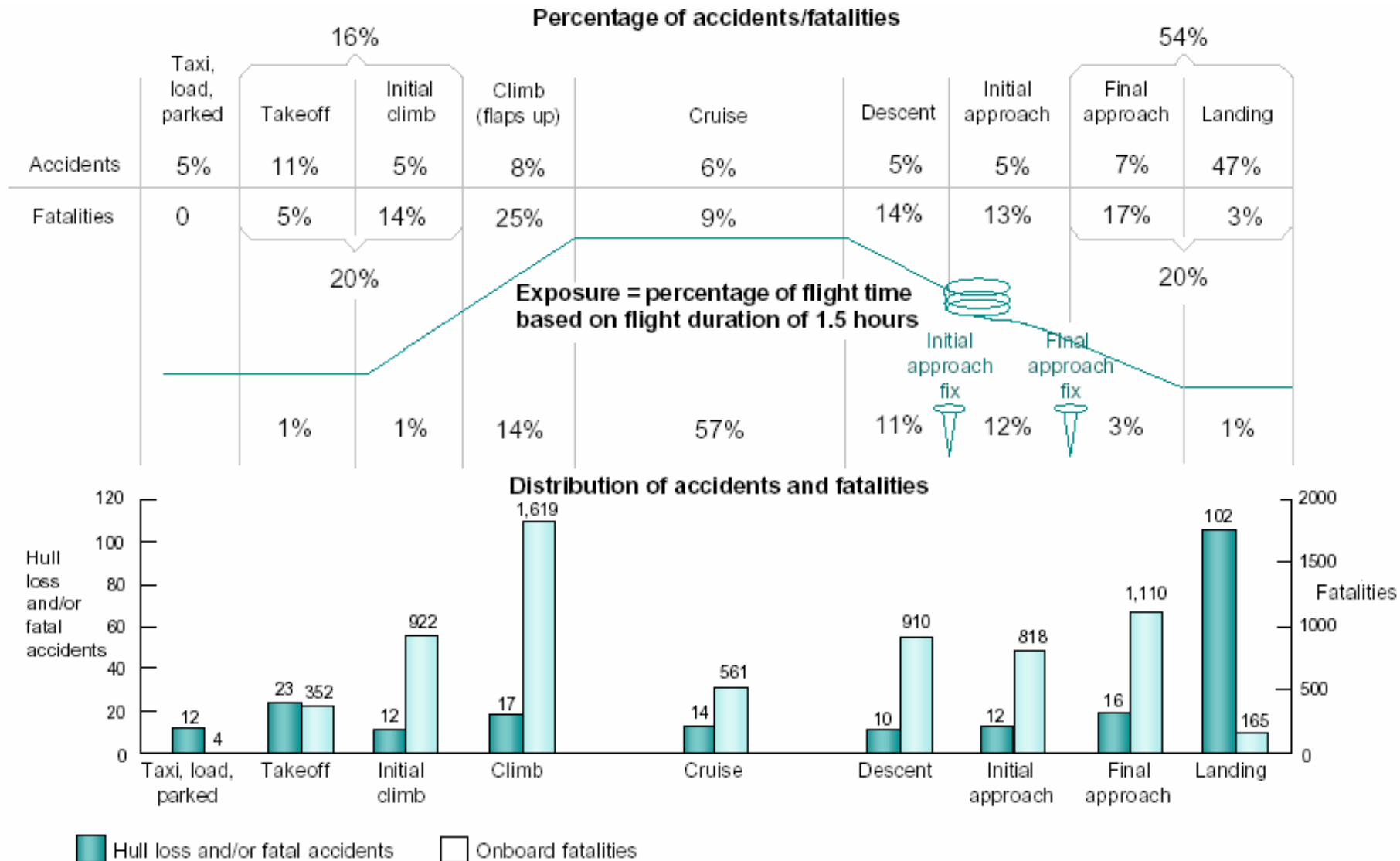
Source: DFG Sicherheit im Luftverkehr

Accidents and Fatalities in World Air Transport (1959-2002)



Source: Boeing Commercial Jet Airplane Accidents

Accidents per Flight Mission Worldwide (1993-2002)



Source: Boeing Commercial Jet Airplane Accidents

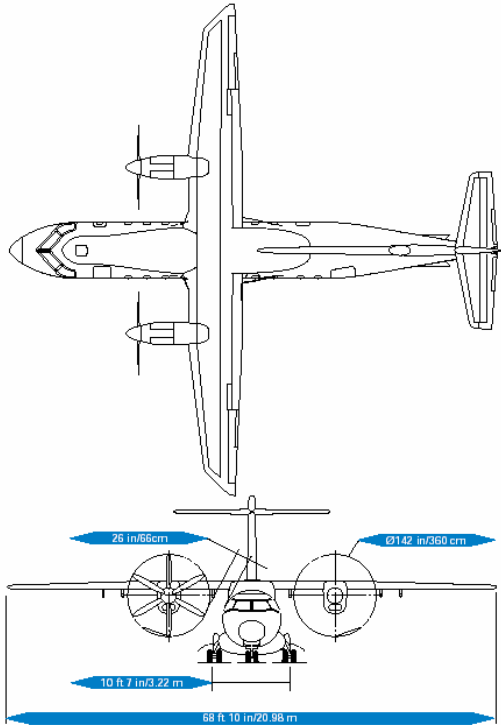
Dieter Schmitt

Chapter 4

Configurations

4.1 Actual Configurations

Actual Configurations – *Regional Aircraft*



Max. take-off weight

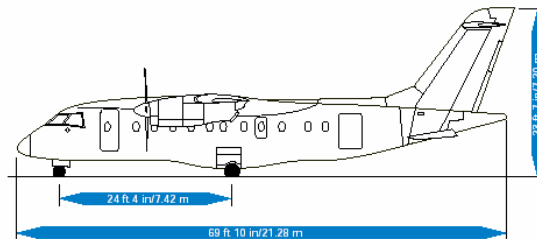
Max. landing weight

Max. zero fuel weight

Operating weight empty

Max. structural payload

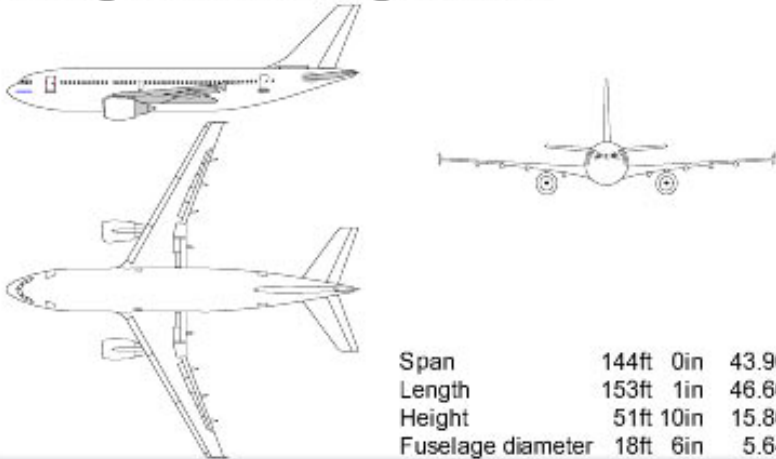
lb	kg
30,843	13,990
29,167	13,230
27,800	12,610
19,665	8,920
8,135	3,690



Actual Configurations – *Short- and Medium-range Aircraft*



A310 general arrangements



Span	144ft 0in	43.90m
Length	153ft 1in	46.66m
Height	51ft 10in	15.80m
Fuselage diameter	18ft 6in	5.64m

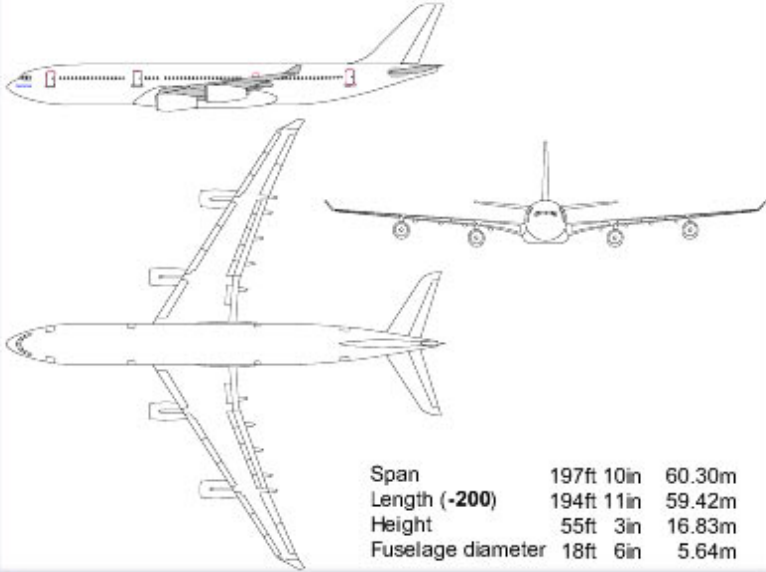
Airbus A310

©airbus.com

Actual Configurations – Long-range Aircraft



A340 general arrangements

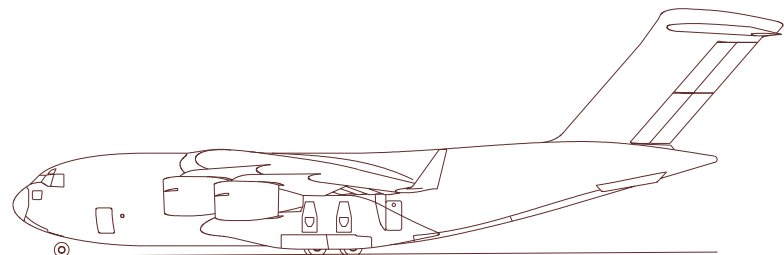
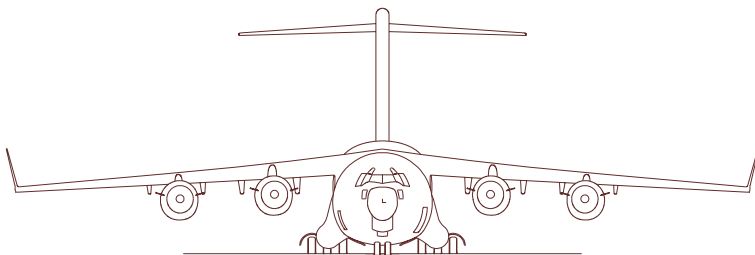
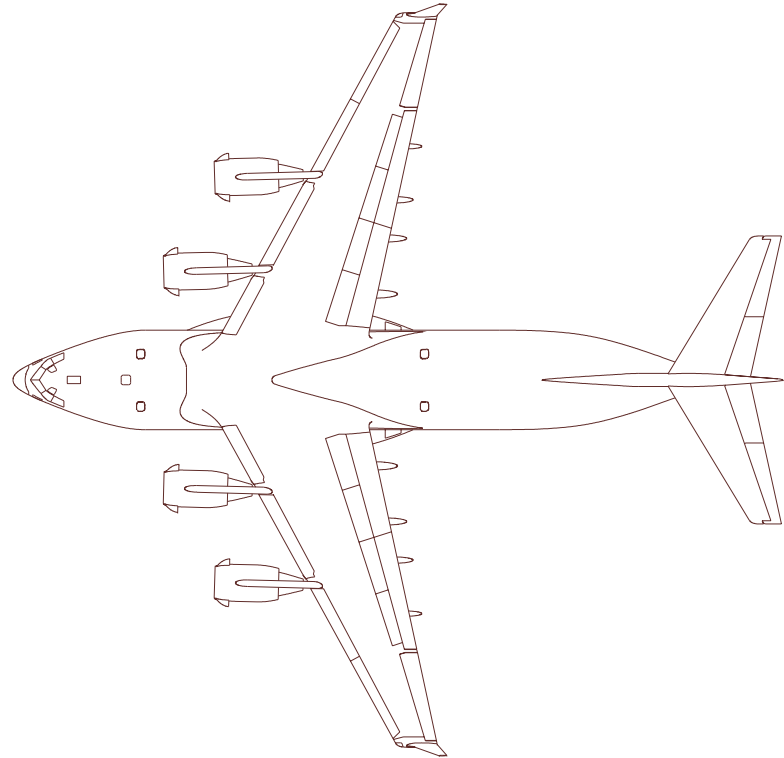


Span	197ft 10in	60.30m
Length (-200)	194ft 11in	59.42m
Height	55ft 3in	16.83m
Fuselage diameter	18ft 6in	5.64m

Airbus A340-200

©airbus.com

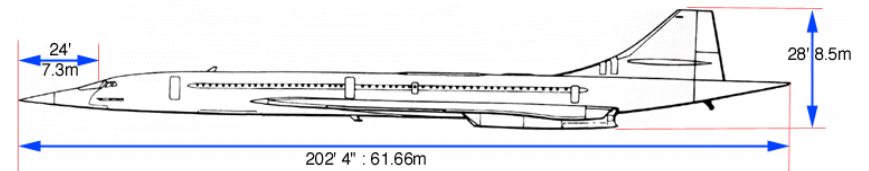
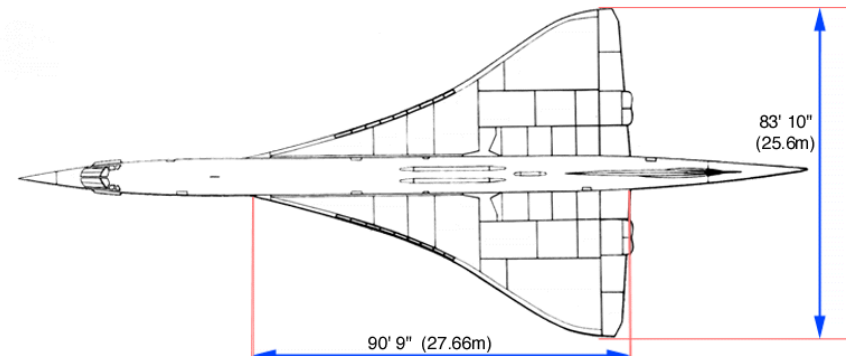
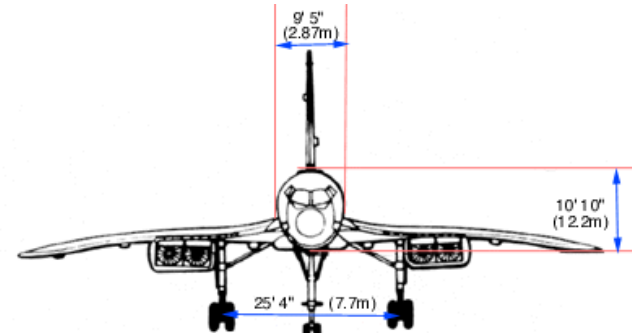
Actual Configurations – *Military-Transport Aircraft*



Boeing C17 Globemaster III

Actual Configurations – Supersonic Transport Aircraft

Aerospatiale / British Aerospace – Concorde



4.2 Unconventional Configurations

Unconventional Configurations – *Joint Wing*



AERODYNAMIC

Reduction of induced Drag



❶ AERODYNAMICS

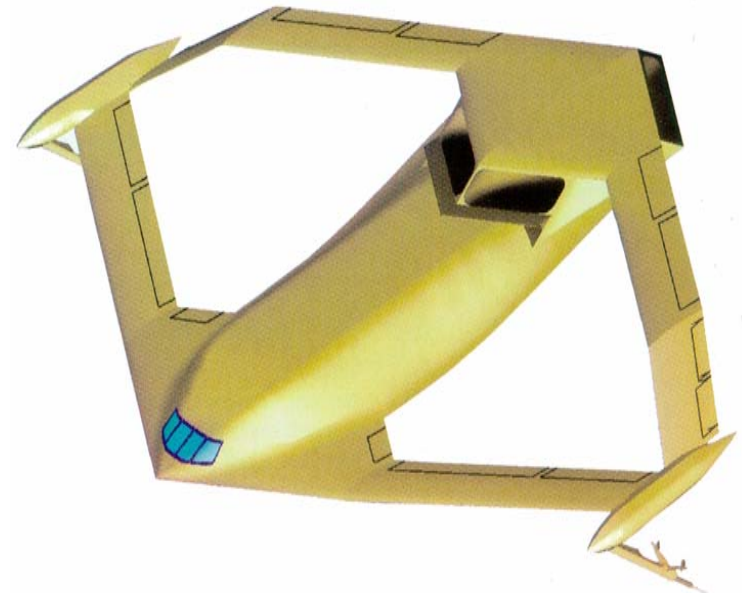
Downwash at Aft-wing

❶ reduced stability

❶ wing-tip design

❶ Weights

installation U/C



Flugrevue June 1997

Unconventional Configurations – 3-Surface-Aircraft



AERODYNAMICS

Reduction of tail-download

Trim-Drag-Advantage



WEIGHTS

Reducing Wing loading



AERODYNAMICS

Downwash at main wing



reduced stability



WEIGHTS

Canard –Installation

Canard Position ?

P

Source: Airbus

Unconventional Configurations – *Low Noise Aircraft*



EXTERNAL NOISE

Fan-Inlet-Noise and
Jet-Noise shielded

📌 **CENTER OF GRAVITY**
Unfavorable wing position

📌 **MAINTENANCE**

📌 **WEIGHT**
Engine-Installation

Unconventional Configurations – *Oblique Wing*

AERODYNAMICS

Reduction of wetted areas

WEIGHT

Good load distribution in span



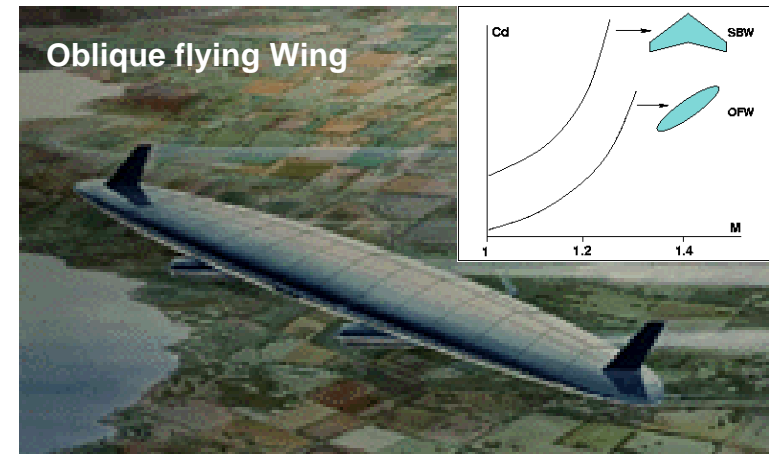
CERTIFICATION

Evacuation

Multiple Instabilities

WEIGHT

Flat structures for cabin pressure



*Significant performance potential
but multiple instabilities and
operational problems*

Hydrogen Powered Aircraft - CRYOPLANE



EMISSIONS

No CO₂, less NO_x
but contrails ?



WEIGHT

less fuel weight



INFRASTRUCTURE

Critical refuelling concept



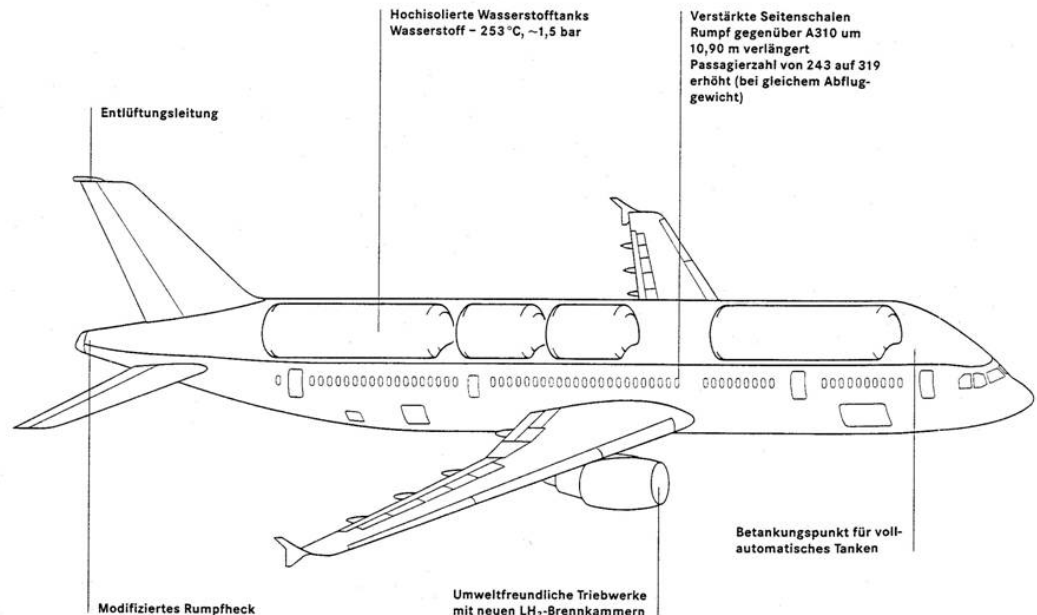
AERODYNAMICS

High fuel volume



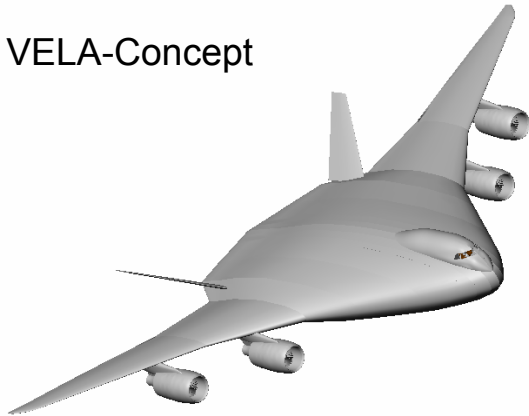
WEIGHT

Difficult tank insulation



Unconventional Configurations – *BLENDED WING_BODY*

VELA-Concept



AERODYNAMICS

Reduction of wetted surfaces



WEIGHT

Better payload distribution in span



CERTIFICATION

Evacuation



STABILITY

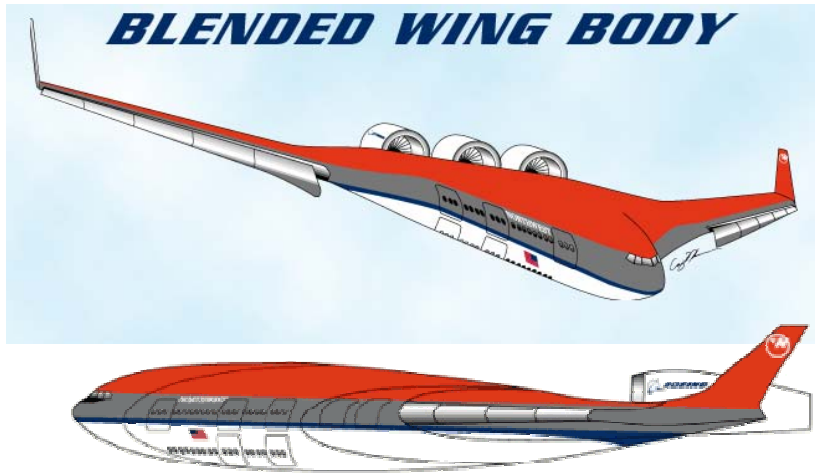


reduced longitudinal stab.

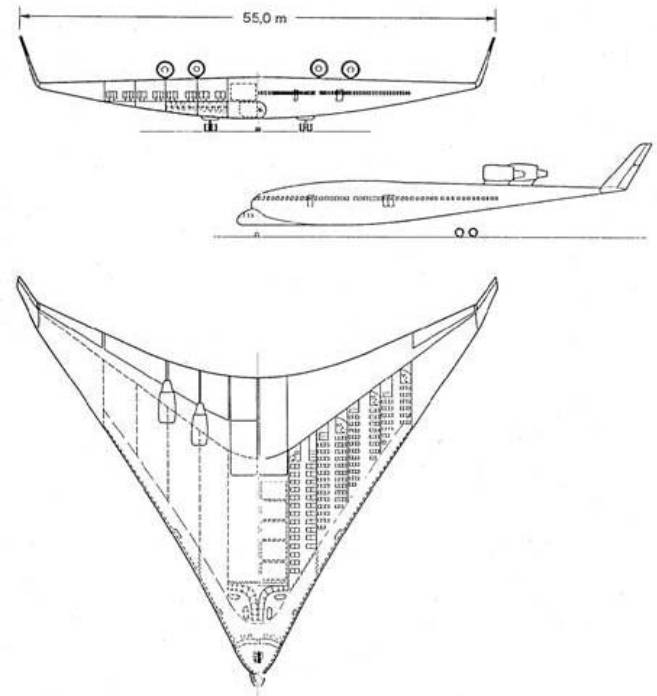


WEIGHT

Payload pressurization

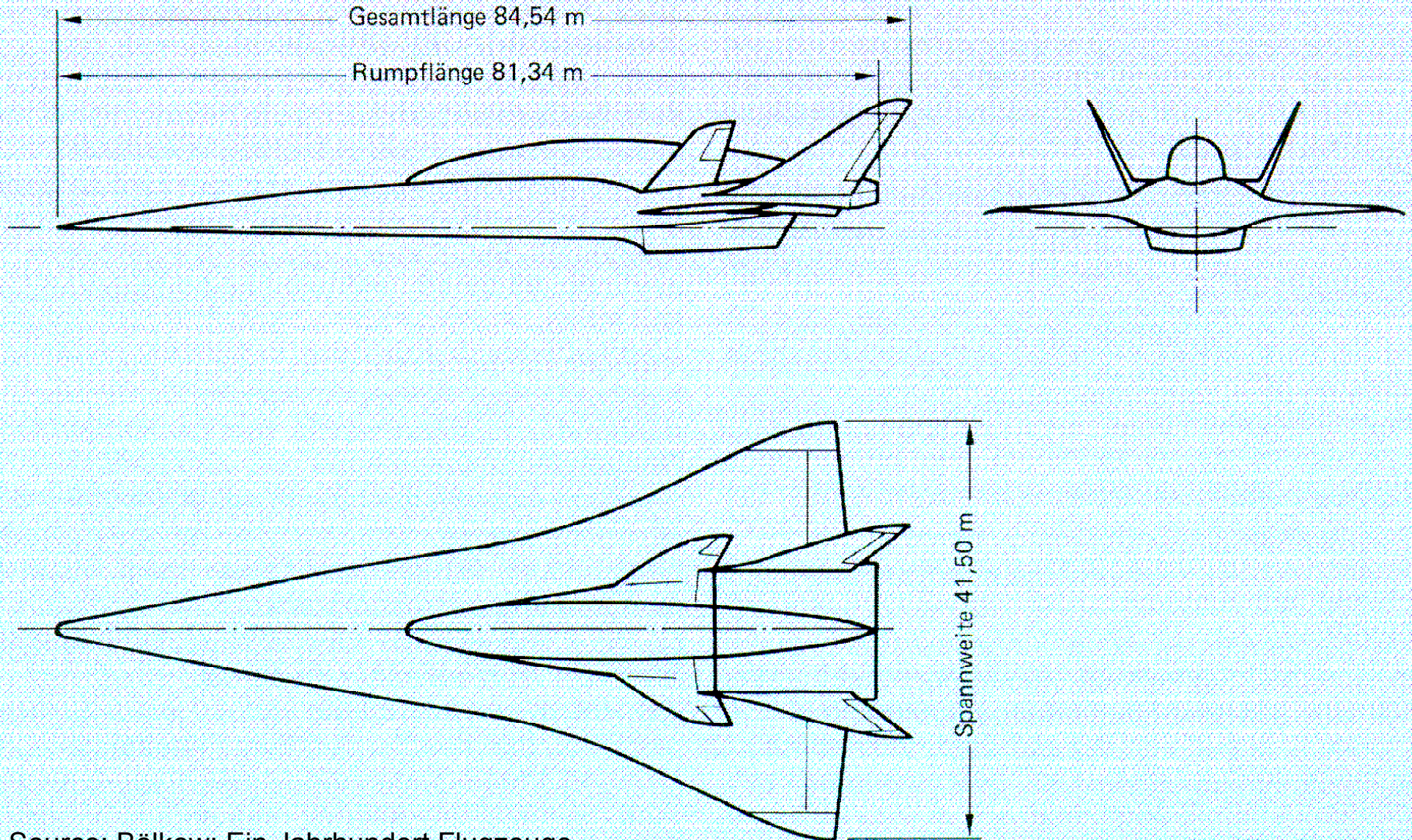


Boeing Concept



Nurflügelprojekt MBB-Entwurf III für Fluggäste und Fracht. Eine nach Prof. Hertel (1950) „gedrungene Form kleiner Flügelstreckung“ (Entwurf: Ralf Volkhausen MBB Hamburg)

Unconventional Configurations – *Hypersonic Vehicle SÄNGER*



Source: Bölkow: Ein Jahrhundert Flugzeuge

Dieter Scholz

Chapter 5

Preliminary Sizing

5 Preliminary Sizing

The preliminary sizing of an aircraft is carried out by taking into account requirements and constraints (see Section 1). A process for preliminary sizing proposed by **Loftin 1980** is shown in **Fig. 5.1** and detailed in this section. The procedure refers to the preliminary sizing of jets that have to be certified to CS-25 or FAR Part 25. The procedure could in general also be applied to other aircraft categories as there are

- very light jets certified to CS-23/FAR Part 23
- propeller aircraft certified to CS-25/FAR Part 25
- propeller aircraft certified to CS-23/FAR Part 23
- propeller aircraft certified to CS-VLA
- ...

if the respective special features and regulations are taken into account. For propeller-type aircraft the engine thrust T must be replaced by engine power P in **Fig. 5.1**. Many changes in the equations result from this modification.

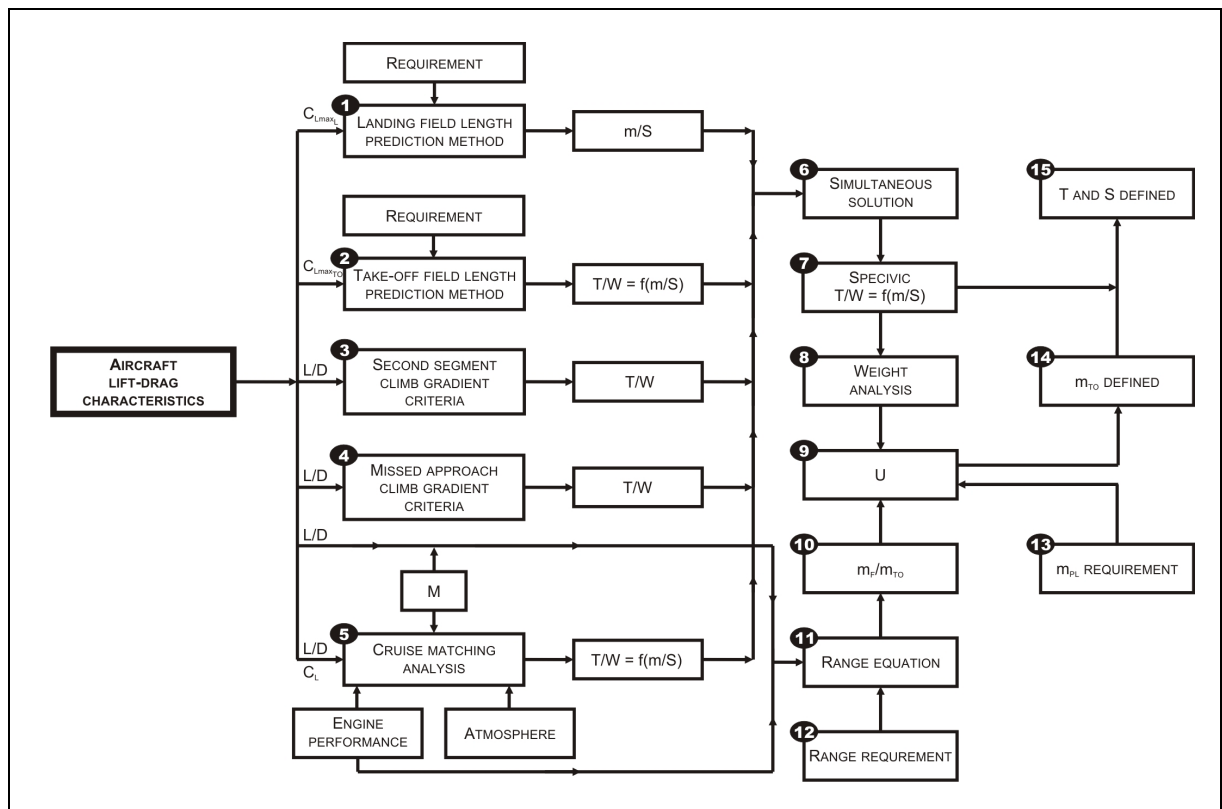


Fig. 5.1 Flow chart of the aircraft preliminary sizing process for jets based on **Loftin 1980**

Fig. 5.1 needs some explanation: The blocks in the first column represent calculations for various flight phases.

Block 1 "LANDING DISTANCE" provides a maximum value for the *wing loading* m/S (reference value: m_{MTO}/S_w). The input values of the calculation are the maximum lift coefficient with flaps in the landing position $C_{L,max,L}$ as well as the landing field length s_{LFL} according to CS/FAR. The maximum lift coefficient $C_{L,max,L}$ depends on the type of high lift system and is selected from data in the literature.

Block 2, "TAKE-OFF DISTANCE" provides a minimum value for the *thrust-to-weight ratio as a function of the wing loading*: $T/(m \cdot g) = f(m/S)$ with reference value: $T_{TO}/(m_{MTO} \cdot g)$. The functional connection $T/(m \cdot g) = f(m/S)$ is dependent on the maximum lift coefficient with flaps in the take-off position $C_{L,max,TO}$ and the take-off field length s_{TOFL} . The maximum lift coefficient $C_{L,max,TO}$ is selected with the aid of data in the literature.

Blocks 3 and 4 examine the "CLIMB RATE IN THE SECOND SEGMENT" and the "CLIMB RATE DURING THE MISSED APPROACH". The blocks provide minimum values for the *thrust-to-weight ratio* $T/(m \cdot g)$. The input value for the calculations: the lift-to-drag ratio, 'L over D') L/D is estimated on the basis of a simple approximation calculation.

Block 5 "CRUISE" represents the cruise analysis that provides a minimum value for the *thrust-to-weight ratio as a function of the wing loading*: $T/(m \cdot g) = f(m/S)$. The thrust-to-weight ratio thus determined is sufficient to facilitate a stationary straight flight with the assumed Mach number for the respective wing loading. The calculation is carried out for the design lift coefficient $C_{L,DESIGN}$. The *cruise altitude* is also obtained from the cruise analysis. Input values are the lift-to-drag ratio $E = L/D$ during cruise, the assumed cruise Mach number $M = M_{CR}$, engine parameters and the characteristics of the atmosphere.

The output values of the blocks in the first column of Fig. 5.1 provide a set of relationships between the thrust-to-weight ratio and the wing loading. Taken together, these relationships give, in a "MATCHING CHART" (**Blocks 6 and 7**), a *single pair of values: thrust-to-weight ratio and wing loading* that meets all requirements and constraints in an economical manner.

The thrust-to-weight ratio (also referred to as the maximum take-off mass or range by other authors) are the input values for a mass estimate according to statistics. In **Blocks 8 and 9**, first the OPERATING EMPTY MASS m_{OE}/m_{MTO} or the *RELATIVE USEFUL LOAD* u is estimated, defined as

$$u = \frac{m_F + m_{PL}}{m_{MTO}} = 1 - \frac{m_{OE}}{m_{MTO}} \quad . \quad (5.1)$$

The useful load is $m_F + m_{PL}$, maximum take-off mass m_{MTO} and operating empty mass m_{OE} .

In **Blocks 10 and 11** the RELATIVE FUEL MASS m_F / m_{MTO} is calculated, using the "Breguet range equation", from the range requirement (**Block 12**). Other input values are the assumed cruise Mach number $M = M_{CR}$, the lift-to-drag ratio during cruising $E = L / D$ and the specific fuel consumption during cruising $c = SFC_{CR}$.

"MAXIMUM TAKE-OFF MASS m_{MTO} ", "TAKE-OFF THRUST AND WING AREA": in **Block 14** the *maximum take-off mass* m_{MTO} is calculated from relative useful load u , relative fuel mass m_F / m_{MTO} and the *payload requirement* m_{MPL} (**Block 13**). With the maximum take-off mass m_{MTO} the necessary *take-off thrust* $T = T_{TO}$ and the *wing area* $S = S_W$ can then be calculated in **Block 15** from thrust-to-weight ratio $T / m \cdot g$ and wing loading $S = S_W$.

5.1 Landing Distance

The basis for analyzing the landing distance are the aviation regulations. The key passages are reproduced here from CS. Further details can be found in the regulations.

CS 25.125 Landing

- (a) The horizontal distance necessary **to land** and to come to a complete stop **from a point 50 ft above the landing surface** must be determined
- (1) The aeroplane must be in the landing configuration.
 - (2) A stabilised **approach**, with a calibrated **airspeed** of not less than **1.3 VS**, must be maintained down to the 50 ft height.

CS - OPS 1.515 Landing - Dry Runways

- (a) An operator shall ensure that the landing mass of the aeroplane ... allows a full stop landing from 50 ft above the threshold:
- (1) Within **60% of the landing distance available** at the destination aerodrome and at any alternate aerodrome for **turbojet** powered aeroplanes; or
 - (2) Within **70% of the landing distance available** at the destination aerodrome and at any alternate aerodrome for **turbopropeller** powered aeroplane ...

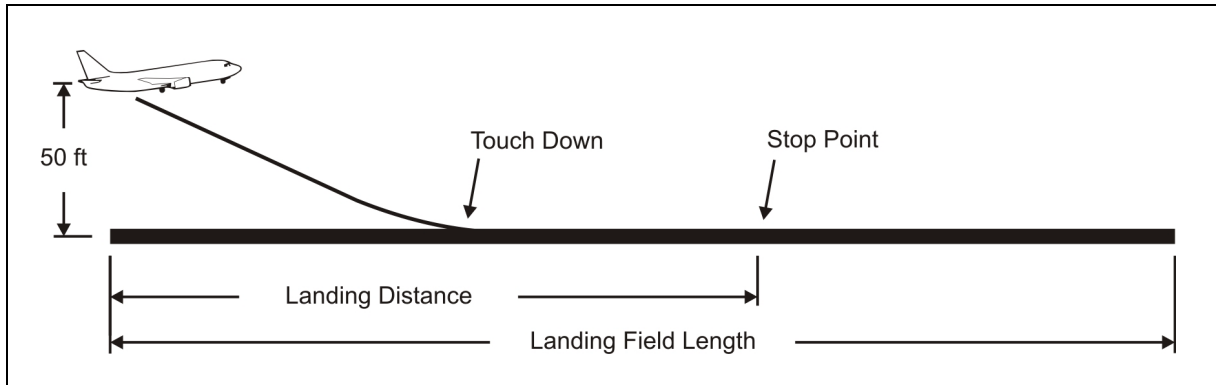


Fig. 5.2 Definition of the landing field length according to CS and FAR

An aircraft may land at an airfield if the *landing field length* s_{LFL} is shorter than the *landing distance available*, LDA s_{LDA} . The landing field length is calculated according to CS/FAR from the landing distance s_L and a **safety factor**. This safety factor is $1/0.6 = 1.667$ for **jets** and $1/0.7 = 1.429$ for **turboprops**. **Fig. 5.2** shows the landing procedure.

Loftin 1980 contains a statistic that gives the relationship between the landing field length and the approach speed for aircraft with jet engines. This is summarized as follows (**Loftin 1980**, Fig. 3.4)

$$V_{APP} = k_{APP} \cdot \sqrt{s_{LFL}} \quad (5.2)$$

$$\text{with } k_{APP} = 1.70 \sqrt{\text{m/s}^2}.$$

The wing loading at maximum landing mass is

$$m_{ML} / S_W = \frac{\rho \cdot V_{S,L}^2}{2 \cdot g} \cdot C_{L,max,L} \quad . \quad (5.3)$$

ρ is the atmospheric density. To simplify subsequent calculations, we want to relate the atmospheric density ρ to the atmospheric density at sea level $\rho_0 = 1.225 \text{ kg/m}^3$ under standard atmospheric conditions first of all.

$$\rho = \sigma \cdot \rho_0 \quad . \quad (5.4)$$

If we now insert equation (5.2) and equation (5.4) into equation (5.3), we get

$$m_{ML} / S_W = k_L \cdot \sigma \cdot C_{L,max,L} \cdot S_{LFL} \quad (5.5)$$

$$\text{with } k_L = 0.107 \text{ kg/m}^3 \quad .$$

Empirical values for maximum lift coefficients $C_{L,max}$ are contained in **Table 5.1**, **Fig. 5.3** and **Fig. 5.4**. **Table 5.3** and **Table 5.2** contain the ratio of maximum landing mass m_{ML} to maximum take-off mass m_{MTO} , which gives

$$m_{MTO} / S_W = \frac{m_{ML} / S_W}{m_{ML} / m_{MTO}} \quad . \quad (5.6)$$

This **wing loading must not be exceeded** if the aircraft is to meet requirements.

Table 5.1 Maximum lift coefficients for take-off (TO), landing (L) and cruise configuration (based on **Roskam I**)

type of aircraft	$C_{L,max}$	$C_{L,max,TO}$	$C_{L,max,L}$
business jet	1.4 – 1.8	1.6 – 2.2	1.6 – 2.6
jet transport	1.2 – 1.8	1.6 – 2.2	1.8 – 2.8
single engine propeller driven	1.3 – 1.9	1.3 – 1.9	1.6 – 2.3
twin engine propeller driven	1.2 – 1.8	1.4 – 2.0	1.6 – 2.5
fighter	1.2 – 1.8	1.4 – 2.0	1.6 – 2.6
supersonic cruise	1.2 – 2.8	1.6 – 2.0	1.8 – 2.2


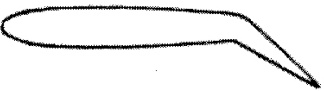


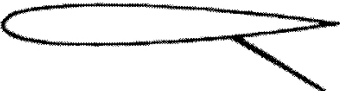




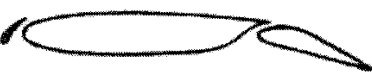


		$C_{L,max}$	$\Delta C_{L,max}$
Clean Airfoil		1,45	-
Plain Flap		2,25	0,80
Single-Slotted Flap		2,60	1,15
Double-Slotted Flap		2,80	1,35
Split Flap		2,40	0,95
Double-Wing (Junkers)		2,25	0,80
Fowler Flap		2,80	1,35
Slat		2,00	0,55
Combinations:			
Plain Flap and Slat		2,45	1,00
Single-Slotted Flap and Slat		2,70	1,25
Double-Slotted Flap and Slat		2,90	1,45
Fowler Flap and Slat		3,00	1,55

Fig. 5.3 Maximum lift coefficient of profiles with different high-lift devices (based on data from Dubs 1987)

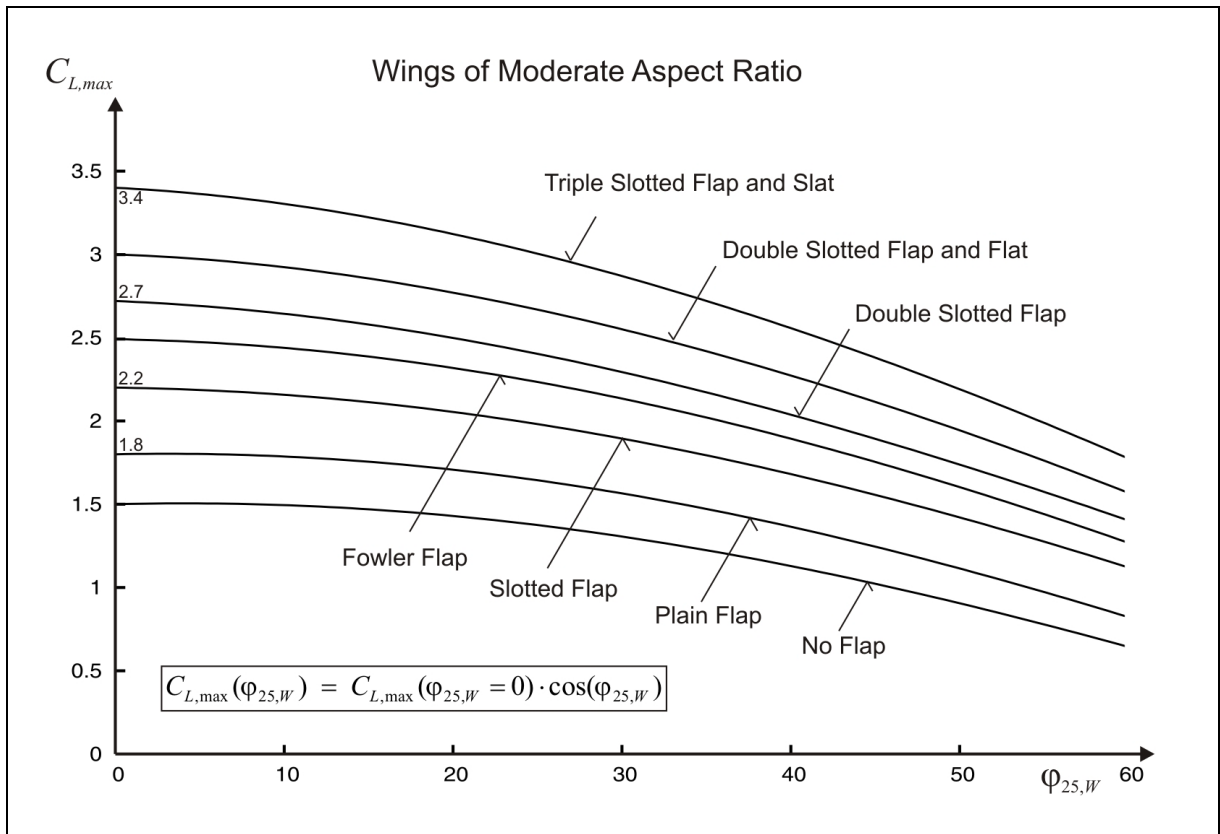


Fig. 5.4 Maximum lift coefficient of aircraft with different high-lift devices as a function of wing sweep. For take-off configuration the given values have to be reduced by 20 percent (based on data from **Raymer 1989**)

Table 5.2 Statistical values of maximum landing mass over maximum take-off mass m_{ML} / m_{MTO} for different types of aircraft (based on **Roskam I**)

type of aircraft	$\frac{m_{ML}}{m_{MTO,min}}$	$\frac{m_{ML}}{m_{MTO,av}}$	$\frac{m_{ML}}{m_{MTO,max}}$
business jet	0.69	0.88	0.96
short range jet transport	0.9	0.93	0.97
medium range jet transport	0.76	0.88	0.95
long range jet transport	0.65	0.78	0.95
ultra long range jet transport	0.65	0.71	0.73
fighter	0.57	-	1
supersonic cruise	0.63	0.75	0.88

Table 5.3 Statistical values of maximum landing mass over maximum take-off mass m_{ML} / m_{MTO} for jets of different design range (based on **Loftin 1980**)

design range classification	design range (NM)	design range (km)	m_{ML} / m_{MTO}
short range	up to 1000	up to 2000	0.93
medium range	1000 – 3000	2000 – 5500	0.89
long range	3000 – 8000	5500 – 15000	0.78
ultra long range	more than 8000	more than 15000	0.71

5.2 Take-off Distance

The basis for analyzing the take-off distance are the aviation regulations. The key passages are reproduced here according to CS-25. Further details can be found in the regulations.

CS 25.113 Take-off distance and take-off run

- (a) Take-off distance is **the greater of** -
 - (1) The horizontal **distance** along the take-off path from the start of the take-off **to** the point at which the aeroplane is **35 ft above the take-off surface**, determined under CS 25.111 (d.h. mit *Triebwerksausfall* und Geschwindigkeit V₂); or
 - (2) **115% of the horizontal distance** along the take-off path, **with all engines operating**, from the start of the take-off **to** the point at which the aeroplane is **35 ft above the take-off surface**, as determined by a procedure consistent with CS 25.111.

CS 25.111 Take-off path

- (a) ...
- (2) **The aeroplane must be accelerated** on the ground to VEF, at which point **the critical engine must be made inoperative** and remain inoperative for the rest of the take-off; and
- (3) After reaching VEF, the aeroplane must be accelerated to V₂.
- (b) During the acceleration to speed V₂, the nose gear may be raised off the ground ... However, landing gear retraction may not be begun until the aeroplane is airborne.
- (c) During the take-off path determination in accordance with sub-paragraphs (a) and (b) of this paragraph -
 - (2) **The aeroplane must reach V₂ before it is 35 ft above the take-off surface** *

CS 25.109 Accelerate-stop distance

- (a) The accelerate-stop distance is ...
- (2) The **sum of the distances necessary to** -
 - (i) **Accelerate the aeroplane** from a standing start to V₁ and continue the acceleration for 2.0 seconds after V₁ is reached with all engines operating; **and**
 - (ii) **Come to a full stop** from the point reached at the end of the acceleration period prescribed in sub-paragraph (a)(2)(i) of this paragraph, assuming that the pilot does not apply any means of retarding the aeroplane until that point is reached ...

* nach CS 25.107 (take-off speeds) muss V₂ auf jeden Fall größer sein als 1.2 V_S.

Should an engine fail during take-off **before** the take-off decision speed V_1 has been reached, the pilot must reject take-off and brake. The distance from the take-off point to the point at which the aircraft comes to a standstill again is the *accelerate-stop distance* and must be shorter than the *accelerate-stop distance available*, ASDA.

If the pilot notices an engine failure **after** the take-off decision speed V_1 has already been exceeded, she must continue the take-off with the remaining engine(s). This results in the *take-off distance OEI*, which must be shorter than the *take-off distance available*, TODA. OEI stands for *one engine inoperative*.

If engine failure is noticed precisely when the take-off decision speed V_1 has been reached, the pilot has both possibilities, namely either to continue the take-off or to reject the take-off.

The take-off decision speed V_1 can be set arbitrarily, but there is only one take-off decision speed V_1 where the following applies:

Accelerate-stop distance = take-off distance OEI.

The take-off distance produced from meeting this condition is called *balanced field length*.

Fig. 5.5 shows the take-off procedure without *clearway* and without *stopway*.

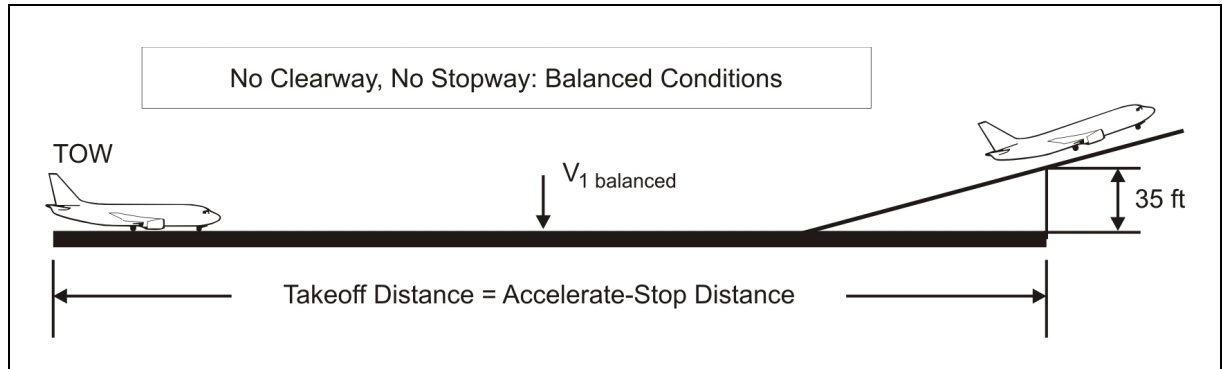


Fig. 5.5 Definition of the balanced field length according to CS and FAR (engine failure after V_1)

According to CS 25.113 (a)(2), the take-off distance AEO is 115% of the distance required to fly over an obstacle of 35ft. AEO stands for *all engines operating*. It must be shorter than the *take-off distance available*, TODA. The *take-off field length* s_{TOFL} is the larger distance in a comparison of *balanced field length* and *take-off distance AEO*.

Assuming that the thrust T , air resistance D and lift L are constant during take-off, the following applies to the *take-off ground roll*¹:

$$s_{TOG} = \frac{1}{2} \cdot \frac{m_{TO} \cdot (V_{LOF} - V_w)^2}{T_{TO} - D_{TO} - \mu \cdot (m \cdot g - L_{TO}) - m_{TO} \cdot g \cdot \sin \gamma} \quad (5.7)$$

V_{LOF} Lift-off speed, $V_{LOF} \approx V_2 \approx 1.2 \cdot V_{S,TO}$

$V_{S,TO}$ Stall speed in take-off configuration

V_w Wind speed

μ Rolling friction

γ Runway slope

Equation (5.7) is simplified to make it usable for the aircraft design. First we calculate the *lift-off speed* from the formula $m_{TO} \cdot g = L = \frac{\rho}{2} V_{LOF}^2 \cdot C_{L,LOF} \cdot S_w$

¹ See "Flight Mechanics" lecture

$$V_{LOF} = \sqrt{\frac{2g}{\rho} \cdot \frac{m_{TO}}{S_W} \cdot \frac{1}{C_{L,LOF}}} . \quad (5.8)$$

The following assumptions are made:

- V_{LOF} is only slightly less than V_2 . Therefore, we calculate $V_{LOF} = 1.2 \cdot V_{s,TO}$.
- The take-off takes place on a level runway with no wind.
- The thrust T is much greater than resistance D and rolling friction.

We are taking into consideration the assumptions and insert equation (5.8) in equation (5.7) and obtain a *simplified equation for the take-off ground roll*:

$$s_{TOG} = \frac{g \cdot m_{MTO}^2}{\rho \cdot C_{L,LOF} \cdot S_W \cdot T} = \frac{g}{\rho \cdot C_{L,LOF}} \cdot \frac{m_{MTO} / S_W}{T_{TO} / (m_{MTO} \cdot g)} . \quad (5.9)$$

This equation provides values which are too small for the take-off ground roll, as the drag has been ignored. However, the equation is suitable as a basis for statistical evaluations: it is assumed that the take-off field length s_{TOFL} is proportional to the take-off ground roll s_{TOG} . Furthermore, the lift coefficient $C_{L,LOF}$ is replaced by the maximum lift coefficient with flaps in take-off position $C_{L,max,TO}$. In a statistical evaluation (**Loftin 1980**, Fig. 3.7) for aircraft with jet engines the following is produced in conjunction with equation (5.4)

$\frac{T_{TO} / (m_{MTO} \cdot g)}{m_{MTO} / S_W} = \frac{k_{TO}}{s_{TOFL} \cdot \sigma \cdot C_{L,max,TO}} \quad (5.10)$ <p style="text-align: center; margin-top: 10px;">with $k_{TO} = 2.34 \text{ m}^3/\text{kg}$</p>
--

Table 5.1 contains values for the maximum lift coefficient with flaps in take-off position $C_{L,max,TO}$. The **ratio from thrust-to-weight ratio and wing loading** pursuant to equation 5.10 **must not be undershot** if the aircraft is to meet requirements.

5.3 Climb Rate during 2nd Segment

The take-off path is defined in several paragraphs of the certification regulations. The climb path is shown clearly in **Fig. 5.6**. The key passages regarding requirements in the second segment are quoted here according to CS-25. Further details can be found in the regulations.

CS 25.121 Climb: one-engine-inoperative

(b) *Take-off; landing gear retracted.*

In the take-off configuration existing at the point of the flight path at which the landing gear is fully retracted, ... the **steady gradient of climb may not be less than**

2·4% for two-engined aeroplanes,

2·7% for three-engined aeroplanes and

3·0% for four-engined aeroplanes,

at V_2 and with -

- (1) The critical engine inoperative and the remaining engines at the available maximum continuous power or thrust; and
- (2) The weight equal to the weight existing at the end of the take-off path ...

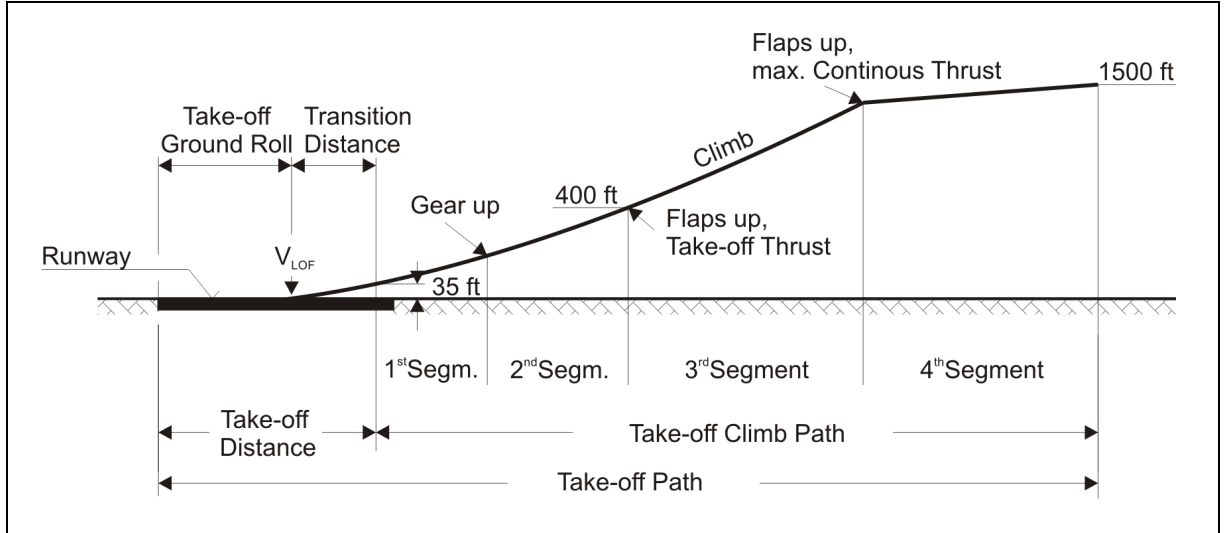


Fig. 5.6 Take-off path, definitions and nomenclature (based on **Brüning 1993**)

In the climb with climb angle γ thrust T is required to overcome drag D and weight $m \cdot g$. The following equation gives the sum of the forces in the flight direction

$$T = D + m \cdot g \cdot \sin \gamma \quad . \quad (5.11)$$

In addition, the following equation gives the force balance vertical to the flight direction (with simplification for small climb angle)

$$L = m \cdot g \cdot \cos \gamma \approx m \cdot g \quad . \quad (5.12)$$

Equation (5.11) divided by $m \cdot g$ and equation (5.12) gives

$$\frac{T}{m \cdot g} = \frac{1}{E} + \sin \gamma \quad . \quad (5.13)$$

If the climb is also to be possible with a failed engine, the thrust-to-weight ratio – *relative to the thrust of all the engines* – must be correspondingly greater. For a number of n_E engines, **at least a thrust-to-weight ratio of**

$$\frac{T_{TO}}{m_{MTO} \cdot g} = \left(\frac{n_E}{n_E - 1} \right) \cdot \left(\frac{1}{E} + \sin \gamma \right) \quad (5.14)$$

must be stipulated.

The climb angle is used in equation (5.14). However, in the regulations, the climb gradient is stated as a percentage. A conversion is simple. As

$$\tan \gamma = \frac{\text{climb gradient}}{100} \quad (5.15)$$

follows

$$\gamma = \arctan \frac{\text{climb gradient}}{100} \quad (5.16)$$

where *climb gradient* means the *value from the regulations as a percentage*. In the present calculations, the angle is small and so one can dispense with the task of conversion and directly insert the value from the regulation (e.g. for 3 % climb rate, insert 0.03) in equation (5.14), as

$$\sin \gamma \approx \frac{\text{climb gradient}}{100} \quad (5.17)$$

5.4 Lift-to-Drag Ratio with Extended Landing Gear and Extended Flaps

In equation (5.14) the **lift-to-drag ratio** $E = L/D$, which is to be **calculated** here **with an approximation procedure**, is still unknown. It is

$$E = L/D = \frac{C_L}{C_D} \quad (5.18)$$

The drag is comprised of profile drag and induced drag. The induced drag depends on the lift coefficient, the wing aspect ratio and Oswald's efficiency factor

$$C_D = C_{D,P} + \frac{C_L^2}{\pi \cdot A \cdot e} \quad (5.19)$$

$$E = \frac{C_L}{C_{D,P} + \frac{C_L^2}{\pi \cdot A \cdot e}} \quad (5.20)$$

The profile drag is comprised of the zero-lift drag and the additional drags due to the high lift system and, if applicable, the landing gear.

$$C_{D,P} = C_{D,0} + \Delta C_{D,flap} + \Delta C_{D,slat} + \Delta C_{D,gear} \quad (5.21)$$

The approximation procedure according to **Loftin 1980** applied to normal passenger aircraft makes the following assumptions to estimate lift-to-drag ratio:

e	0.7	due to extended flaps and slats
$C_{D,0}$	0.02	
$\Delta C_{D,flap}$	for $C_L = 1.3$: flaps $15^\circ \Rightarrow \Delta C_{D,flap} = 0.01$ for $C_L = 1.5$: flaps $25^\circ \Rightarrow \Delta C_{D,flap} = 0.02$ for $C_L = 1.7$: flaps $35^\circ \Rightarrow \Delta C_{D,flap} = 0.03$	
$\Delta C_{D,slat}$	negligible	
$\Delta C_{D,gear}$	0.015	in case landing gear is extended.

The *maximum* lift coefficients in the case of the three stated flap positions are naturally higher. In the climb after take-off at $V_2 = 1.2 \cdot V_{S,TO}$, the $C_{L,max,TO} = 1.44 \cdot C_L$ and during the missed approach after the landing approach at $V_{MA} = 1.3 \cdot V_{S,L}$, the $C_{L,max,L} = 1.69 \cdot C_L$. In this case the procedure is such that the following conversion is used to estimate the maximum lift coefficient from the predefined maximum lift coefficients:

$$C_L = C_{L,max} \left(\frac{V_s}{V} \right)^2 \quad (5.21a)$$

The values according to **Loftin 1980** for $\Delta C_{D,flap}$ can also be summarized in a formula

$\Delta C_{D,flap} = 0.05 C_L - 0.055 \quad (5.21b)$ <p style="text-align: center;">for $C_L \geq 1.1$.</p>

5.5 Climb Rate during Missed Approach

During a missed (discontinued) approach the aircraft is in the process of making the final approach. For some reason a decision is taken not to land. Take-off thrust is applied, the aircraft climbs and makes a new approach according to a predefined procedure. The aircraft climbs, although it is still in the landing configuration – with considerable drag: the landing gear has already been extended and the flaps are in landing position. The regulations require sufficient installed thrust to carry out this maneuver safely. The key passages relating to requirements for the missed approach are quoted here according to CS-25. Further details can be found in the regulations.

CS 25.121	Climb: one-engine-inoperative
(d)	Discontinued Approach. ... the steady gradient may not be less than
	2·1% for two-engined aeroplanes,
	2·4% for three-engined aeroplanes and
	2·7% for four-engined aeroplanes, with -
(1)	The critical engine inoperative , the remaining engines at the available take-off power or thrust;
(2)	The maximum landing weight; and
(3)	A climb speed established in connection with normal landing procedures (these are 1·3 VS), but not exceeding 1·5 VS.
(4)	Landing gear retracted. *
*	(4) is only contained in CS-25 <u>not</u> in den FAR Part 25 !!!

The calculation method for the missed approach is very similar to the method used for the second segment. When estimating the lift-to-drag ratio $E = L/D$ it must be borne in mind that (according to FAR Part 25, but not according to CS-25!!!) the landing gear is still extended. The necessary thrust-to-weight ratio is

$$\frac{T_{TO}}{m_{ML} \cdot g} = \left(\frac{n_E}{n_E - 1} \right) \cdot \left(\frac{1}{E} + \sin \gamma \right) \quad (5.22)$$

and in this case relates initially to the maximum landing mass. However, as all the calculations in the matching chart (Blocks 6 and 7) use parameters which relate to take-off, the thrust-to-weight ratio has to be converted to the maximum take-off mass.

$$\frac{T_{TO}}{m_{MTO} \cdot g} = \frac{T_{TO}}{m_{ML} \cdot g} \cdot \frac{m_{ML}}{m_{MTO}} \quad (5.23)$$

For the missed approach the equation to determine the **minimum value of the thrust-to-weight ratio** is as follows:

$$\frac{T_{TO}}{m_{MTO} \cdot g} = \left(\frac{n_E}{n_E - 1} \right) \cdot \left(\frac{1}{E} + \sin \gamma \right) \cdot \frac{m_{ML}}{m_{MTO}} \quad (5.24)$$

5.6 Cruise

For calculations in the cruise phase, a **stationary straight flight** at cruise altitude is assumed. Therefore two equations can be used:

- a) lift is equal to weight;
- b) drag is equal to thrust.

With these two equations a statement can then be made on:

- a) the wing loading;
- b) the thrust-to-weight ratio.

The connection between the **wing loading** and the **thrust-to-weight ratio** is determined in such a way that both parameters are **initially calculated separately** as a function of altitude. The connection between the two parameters is then obtained automatically from the individual results via the connection with the altitude.

5.6.1 Thrust-to-Weight Ratio

In cruise flight – i.e. in a stationary straight flight – the following applies to the thrust T_{CR} and the drag D_{CR}

$$T_{CR} = D_{CR} = \frac{m_{MTO} \cdot g}{E} \quad . \quad (5.25)$$

Strictly speaking, the performance requirement in cruise flight is that of a climb. The reason for this is the definition of the service ceiling. The definition states that when flying at service ceiling, a jet still has to reach a climb speed of 500 ft/min. Accordingly, for flights at any other, lower altitude, at least the same climb speed of 500 ft/min would be expected. The formula $T_{CR} = D_{CR}$ is therefore not a conservative estimate, but has the advantage of producing a simple equation. However, this is balanced out in (5.25) by the fact that the maximum take-off mass is assumed as the aircraft mass. The actual mass in cruise flight is less than m_{MTO} due to the consumption of fuel since take-off. At this point this leads to a small safety margin. It is assumed that this safety margin balances out the non-conservative assumption $T_{CR} = D_{CR}$ for the cruise flight.

The equation (5.25) is divided by the take-off thrust T_{TO} . This gives

$$\frac{T_{CR}}{T_{TO}} = \frac{m_{MTO} \cdot g}{T_{TO} \cdot E} \quad (5.26)$$

or

$$\frac{T_{TO}}{m_{MTO} \cdot g} = \frac{1}{(T_{CR}/T_{TO}) \cdot E} \quad (5.27)$$

Lift-to-drag ration E is estimated from the wing aspect ratio, as is explained below in Section 5.7.

T_{CR} / T_{TO} can be read off engine diagrams for a given altitude and Mach number. For normal cruise Mach numbers of jet transports ($M_{CR} \approx 0,8$) a simplified equation is given: Depending on the cruise altitude h_{CR} and by-pass ratio, BPR μ the thrust ratio is

$$\frac{T_{CR}}{T_{TO}} = (0,0013 \mu - 0,0397) \frac{1}{\text{km}} h_{CR} - 0,0248 \mu + 0,7125 \quad (5.28)$$

or with a cruise altitude in ft:

$$\frac{T_{CR}}{T_{TO}} = (3,962 \cdot 10^{-7} \mu - 1,210 \cdot 10^{-5}) \frac{1}{\text{ft}} h_{CR} - 0,0248 \mu + 0,7125 \quad (5.29)$$

5.6.2 Wing Loading

In cruise flight the lift is equal to the weight and the following applies:

$$\frac{m_{MTO}}{S_W} = \frac{C_L \cdot q}{g} = \frac{C_L \cdot M^2}{g} \cdot \frac{q}{M^2} \quad (5.30)$$

q is the dynamic pressure calculated from $q = 1/2 \cdot \rho \cdot V^2$, M is the Mach number. The actual mass in cruise flight is less than m_{MTO} due to the fuel consumption since take-off. If we calculate with m_{MTO} here too, this again leads to a small safety margin with regard to the dimensioning.

Here the question arises as to what lift coefficient C_L is demanded in (5.30). The cruise phase must take place at an altitude where it is possible to reach the design lift coefficient specified for the profile. Often the design lift coefficient $C_{L,DESIGN} = C_{L,md}$ is chosen *for jets*. $C_{L,md}$ is the lift coefficient for minimum drag or for maximum lift-to-drag ratio. This lift coefficient is reached if the aircraft is flown at the speed of the lowest drag V_{md} . However, the speed V is practically already fixed due to the requirement for a cruise Mach number. We therefore choose a ratio V/V_{md} and therefore ultimately fix V_{md} and C_L . For a flight with maximum lift-to-drag ratio $V/V_{md} = 1.0$. A flight that produces the biggest range for a jet – and thus meets the range requirement most easily – requires $V/V_{md} = 1.316$ (see Flight Mechanics). If an aircraft has been optimized for slow flight, then its wing might be too big for cruise flight. The lift coefficient in cruise flight C_L is then less than $C_{L,md}$ and $V/V_{md} > 1.316$. However, the following should apply to many aircraft: $V/V_{md} = 1.0 \dots 1.316$. Thus, by choosing V/V_{md} , the lift coefficient C_L in cruise flight is established, see equations (5.39) and (5.40). The practical significance of choosing V/V_{md} is that ultimately one has the option of moving the cruise flight curve in the matching chart (**Fig. 5.9**) and thus optimizing the design!

For q/M^2 in (5.25) the following is obtained:

$$\frac{q}{M^2} = \frac{\frac{1}{2} \cdot \rho \cdot V^2}{V^2 / a^2} = \frac{1}{2} \cdot \rho \cdot a^2 \quad . \quad (5.31)$$

We take the correlation for the sound velocity a from the thermodynamics

$$a^2 = \gamma \cdot \frac{p}{\rho} \quad (5.32)$$

γ is the ratio of specific heats (known as κ in the relevant German literature). For air, $\gamma = 1.4$ applies. When equation (5.32) is inserted in equation (5.31) this gives:

$$\frac{q}{M^2} = \frac{\gamma}{2} \cdot p(h) \quad . \quad (5.33)$$

The pressure $p(h)$ is determined from the standard atmosphere (see Flight Mechanics). Here it is important to bear in mind that the equation for the troposphere has to be used for an altitude h up to 11 km, and at an altitude h of between 11 km and 20 km the equation for the stratosphere applies.

Equation (5.33) inserted in equation (5.30) finally gives the wing loading as a function of the chosen parameters: lift coefficient C_L , Mach number M and altitude (h).

$$\frac{m_{MTO}}{S_w} = \frac{C_L \cdot M^2}{g} \cdot \frac{\gamma}{2} \cdot p(h) \quad . \quad (5.34)$$

The results of a separate calculation of **wing loading** and the **thrust-to-weight ratio** are entered at the end of the cruise analysis in a table like **Table 5.4**.

Table 5.4 Example table for the collection of cruise performance data

altitude h	wing loading m / S	thrust-to-weight ratio $T / (m \cdot g)$
...
...
5000 m
...
...

The values can then be transferred from this table to the matching chart, thus producing the function $T / (m \cdot g) = f(m / S)$.

5.7 Lift-to-Drag Ratio during Cruise

Lift-to-drag ratio not only increases with increasing wing aspect ratio, but also with a small wetted area of the aircraft relative to the wing area S_{wet} / S_W . **Fig. 5.7** shows that the lift-to-drag ratio is a function of the

$$\text{"Wetted Aspect Ratio"} = A / (S_{wet} / S_W). \quad (5.35)$$

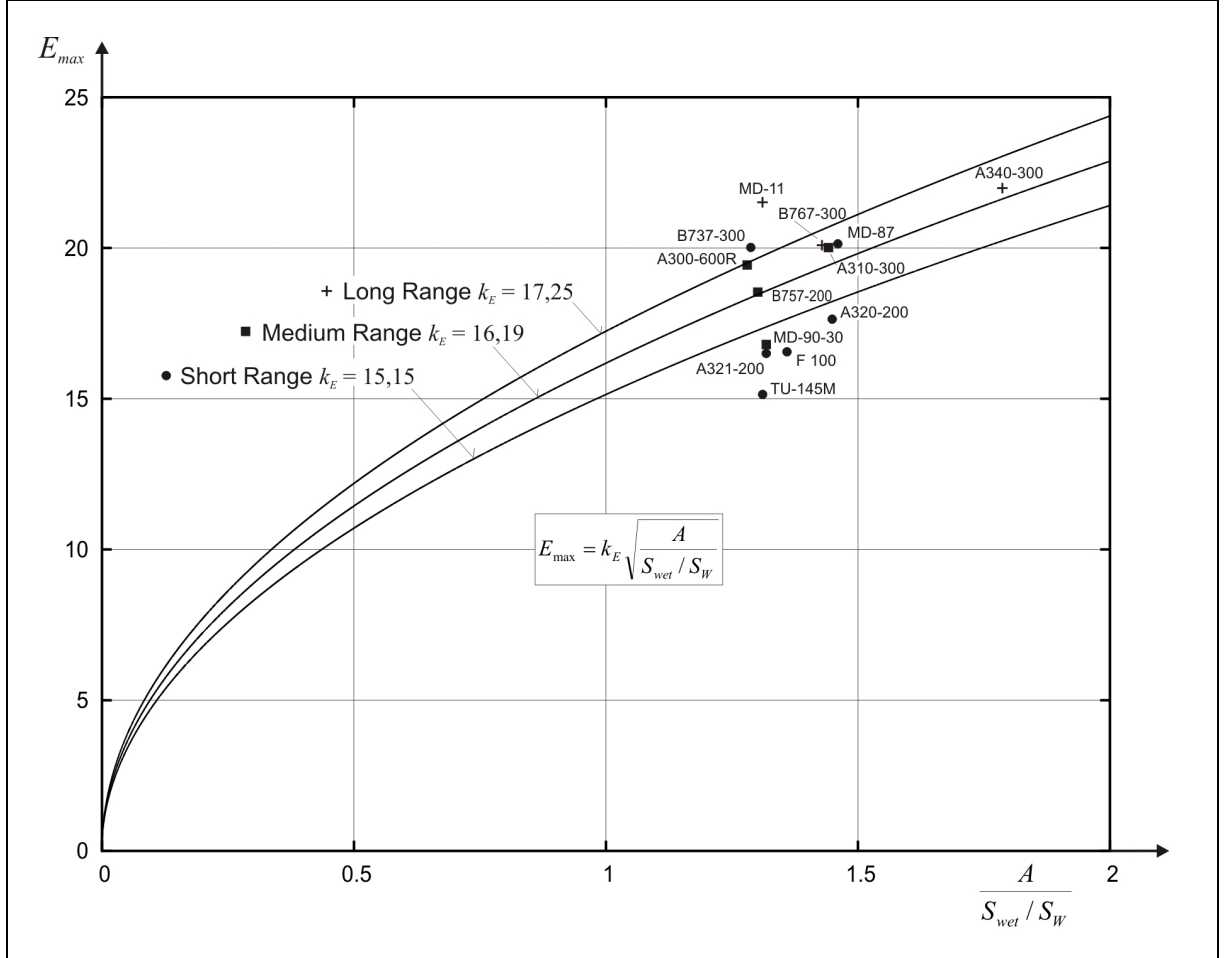


Fig. 5.7 Estimation of glide ratio, wetted area and wing area (based on **Raymer 1989**)

The relationship of **Fig. 5.7** can also be expressed by equations. Taking a closer look at underlying principles, it becomes apparent that one is dealing with functions $y = \sqrt{x}$ in **Fig. 5.7**. This can be derived, but it will be dispensed with at this point. It is then

$$E_{max} = k_E \sqrt{\frac{A}{S_{wet} / S_W}} \quad (5.36)$$

A derivation would yield

$$k_E = \frac{1}{2} \sqrt{\frac{\pi e}{c_f}} \quad (5.37)$$

Loftin 1980 chooses $e = 0.85$ for all jet aircraft in the cruise configuration. $\overline{c_f} = 0.003$ is a common value in literature for jet transports. Thus, giving

$$k_E = \frac{1}{2} \sqrt{\frac{\pi e}{c_f}} = 14.9 \quad .$$

k_E , according to the data used by **Raymer 1989** (Fig. 5.7 evaluated) gives

$$k_E = 15.8 \quad .$$

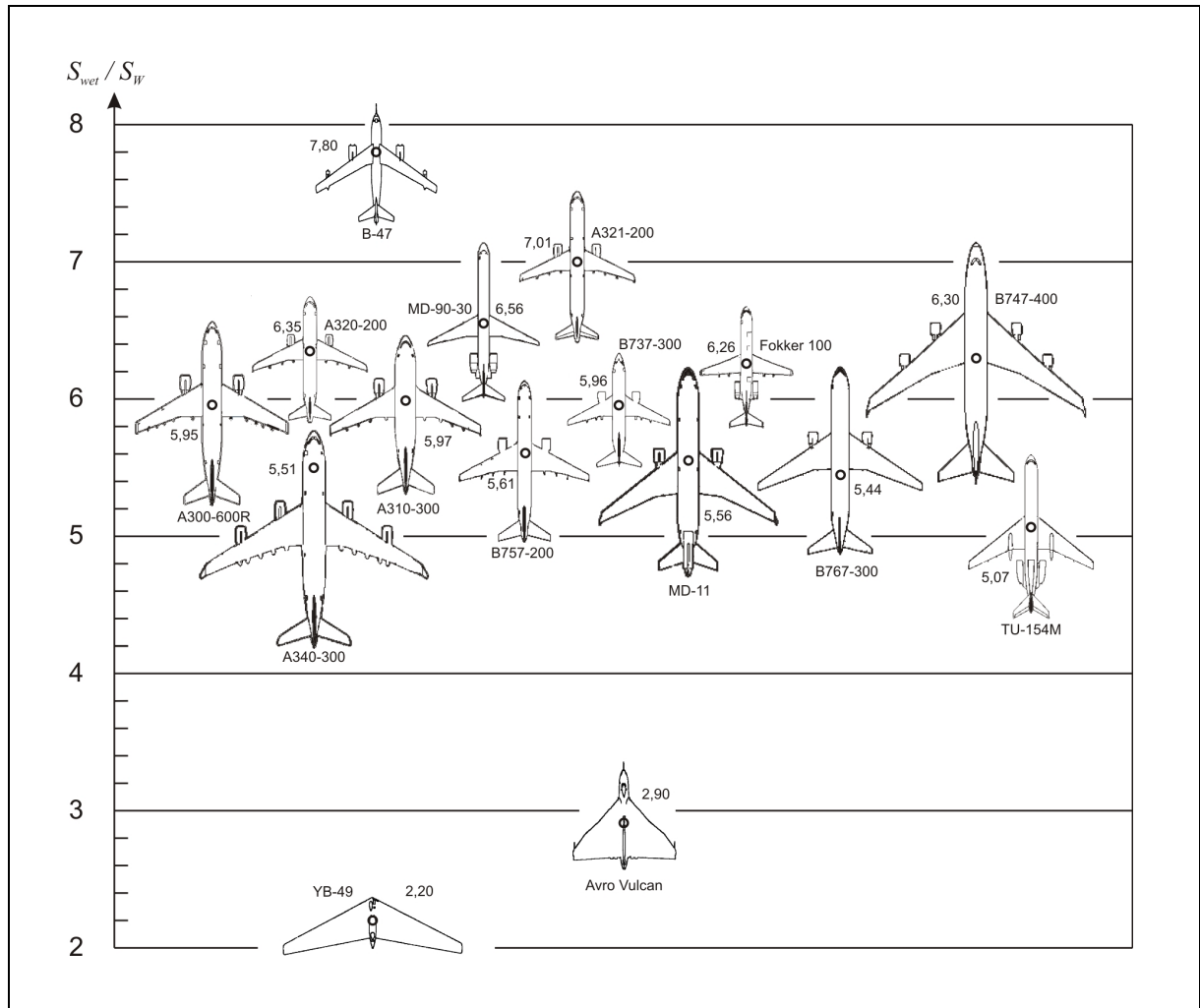


Fig. 5.8 Aircraft plan forms and their relative wetted area S_{wet} / S_W (based on **Raymer 1989**)

Fig. 5.8 illustrates which aircraft categories have which ratio S_{wet} / S_W and shows for conventional aircraft configurations:

$$S_{wet} / S_W = 6.0 \dots 6.2 \quad (5.38)$$

Lift coefficient in cruise flight for flight with minimum drag, i.e. with E_{max} :

$$C_{L,md} = \frac{\pi A e}{2 E_{max}} \quad (5.39)$$

Actual lift coefficient divided by lift coefficient for flight with minimum drag

$$C_L / C_{L,md} = 1 / (V / V_{md})^2 \quad \text{and therefore}$$

$$C_L = \frac{C_{L,md}}{(V / V_{md})^2} \quad (5.40)$$

The actual lift-to-drag ratio in cruise flight is

$$E = \frac{2 E_{max}}{\frac{1}{\left(\frac{C_L}{C_{L,md}}\right)} + \left(\frac{C_L}{C_{L,md}}\right)} \quad (5.41)$$

5.8 Matching Chart

In the matching chart a two-dimensional optimization problem is solved graphically. The two **optimization variables** are:

- thrust-to-weight ratio, $T_{TO} / (m_{TO} \cdot g)$ and
- wing loading, m_{MTO} / S_W .

In previous sections it was demonstrated how, from the various performance requirements, either the wing loading or the thrust-to-weight ratio can be calculated. For all calculations it was ensured that wing loading and thrust-to-weight ratio always refer to take-off with MTOW, which made it possible to compare the values of different flight phases. The results are plotted on the matching chart. **Fig. 5.9** shows such a hypothetical matching chart.

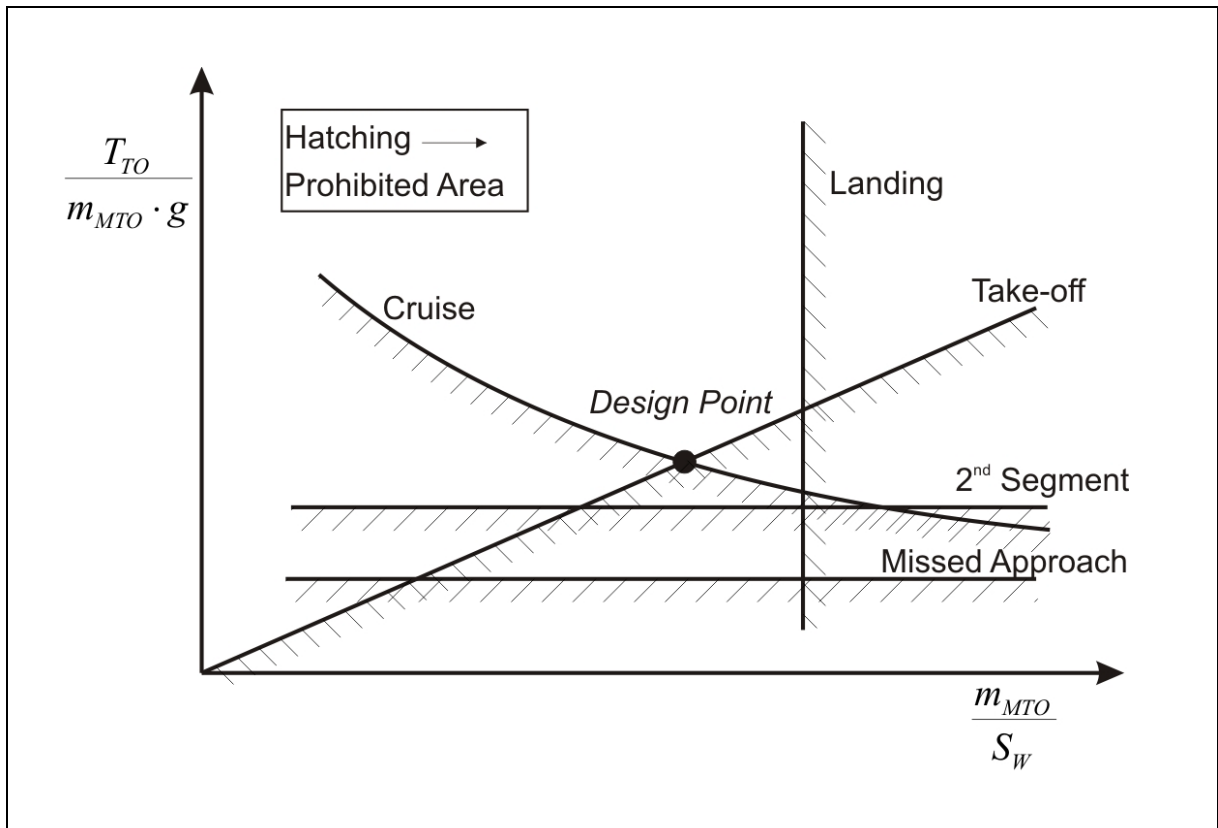


Fig. 5.9 Hypothetical matching chart

The aim of optimization is to achieve the following:

- *Priority 1:* to achieve the smallest possible thrust-to-weight ratio;
- *Priority 2:* to achieve the highest possible wing loading.

The resultant pair of values with the elements "wing loading" and "thrust-to-weight ratio" constitutes a solution to the design problem which meets the examined constraints and also involves a comparatively low weight.

The results thus gained should still be examined for plausibility. To do this, statistical values of designed aircraft can be referred to, as contained in **Fig. 5.10** and **Fig. 5.11**, as well as in **Table 5.5** and **Table 5.6**.

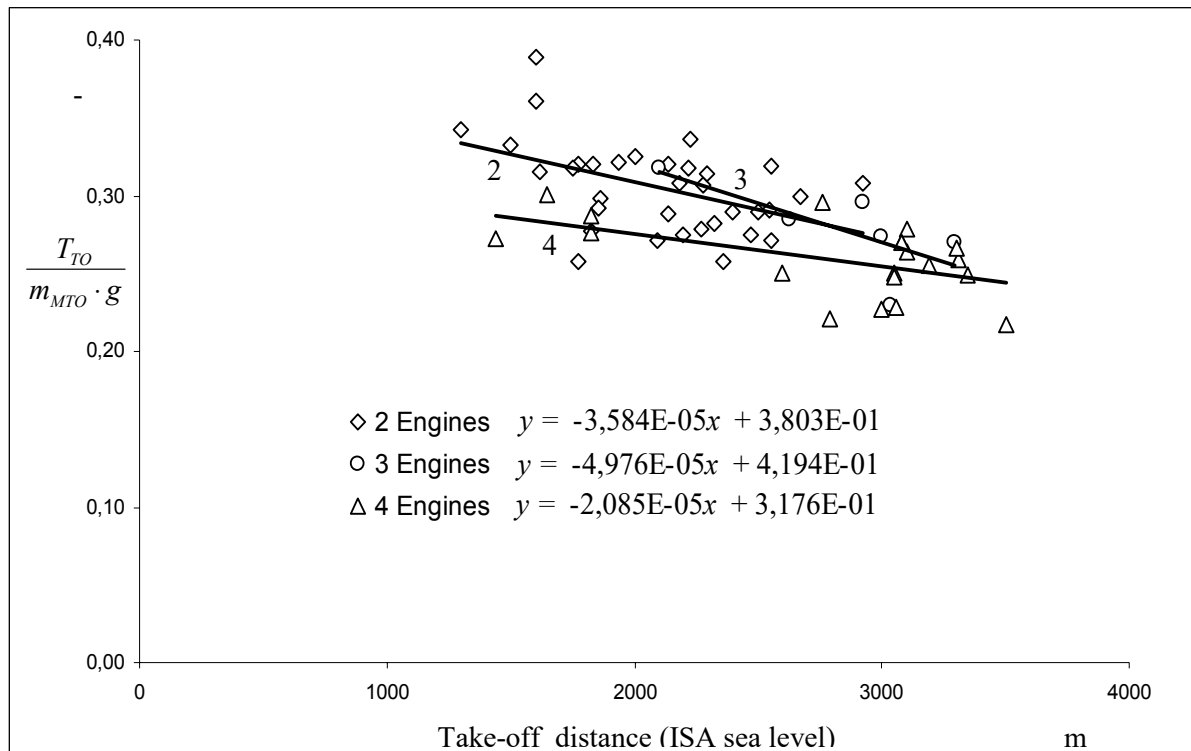


Fig. 5.10 Thrust-to-weight ratio as a function of balanced field length (data from **Jenkinson 1999**)

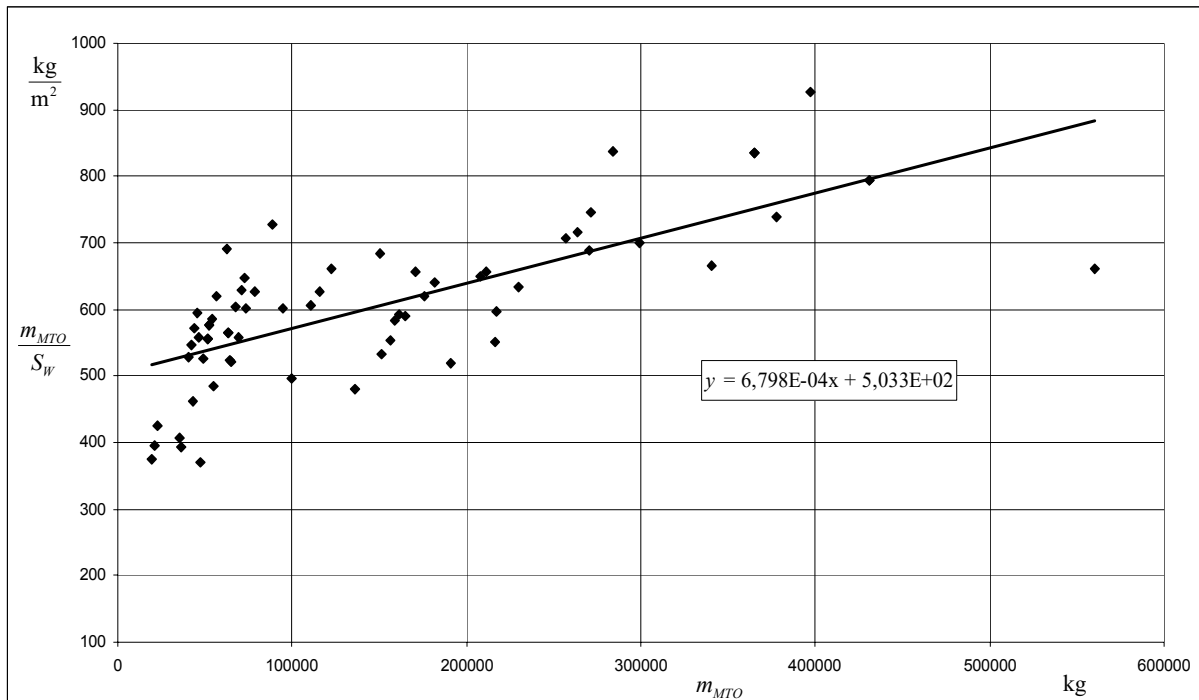


Fig. 5.11 Wing loading as a function of maximum take-off mass (data from **Jenkinson 1999**)

Table 5.5 Thrust- respectively power-to-weight ratio of different types of aircraft (based on **Raymer 1989**)

type of aircraft	typical value	unit	
jet transport	0.25	-	$T_{TO} / m_{MTO} \cdot g$
single engine piston propeller	12	W/N	$P_{TO} / m_{MTO} \cdot g$
twin engine piston propeller	28	W/N	$P_{TO} / m_{MTO} \cdot g$
twin turboprop	34	W/N	$P_{TO} / m_{MTO} \cdot g$

Table 5.6 Wing loading of different types of aircraft (based on **Raymer 1989**)

type of aircraft	m_{MTO} / S_W (kg/m²)
glider	29
homebuilt	54
single engine piston propeller	83
twin engine piston propeller	127
twin turboprop	195
jet transport	586

5.9 Maximum Take-Off Mass

The maximum take-off mass m_{MTO} is comprised of payload, fuel mass (for a specific range R at a specific payload m_{PL}) and the operating empty mass:

$$m_{MTO} = m_{PL} + m_F + m_{OE} \quad . \quad (5.42)$$

If we recast this, we get

$$m_{MTO} - m_F - m_{OE} = m_{PL} \quad (5.43)$$

$$m_{MTO} \cdot \left(1 - \frac{m_F}{m_{MTO}} - \frac{m_{OE}}{m_{MTO}} \right) = m_{PL} \quad (5.44)$$

$$m_{MTO} = \frac{m_{PL}}{1 - \frac{m_F}{m_{MTO}} - \frac{m_{OE}}{m_{MTO}}} \quad . \quad (5.45)$$

The relative fuel mass m_F / m_{MTO} and relative operating empty mass m_{OE} / m_{MTO} are discussed in two sub-sub sections that follow.

5.9.1 Relative Operating Empty Mass

The relative operating empty mass m_{OE} / m_{MTO} or relative useful load u are estimated from aircraft statistics. Definitions are

$$u = \frac{m_F + m_{PL}}{m_{MTO}} = 1 - \frac{m_{OE}}{m_{MTO}} \quad . \quad (5.46)$$

Two approaches are given here to calculate m_{OE} / m_{MTO} .

Approach 1:

Marckwardt 1998a uses a regression calculation for *jet transports*:

$$\frac{m_{OE}}{m_{MTO}} = 0.591 \cdot \left(\frac{R [\text{km}]}{1000} \right)^{-0.113} \cdot \left(\frac{m_{MTO} [\text{kg}]}{1000} \right)^{0.0572} \cdot n_E^{-0.206} \quad . \quad (5.47)$$

Equation (5.47) provided m_{OE} / m_{MTO} for all aircraft examined by **Marckwardt 1998a** with an error rate of less than 10%. Note: equation (5.47) has to be used iteratively:

1. select a starting value $m_{OE} / m_{MTO} = 0.5$
2. insert m_{OE} / m_{MTO} into equation (5.45) and obtain (with m_F / m_{MTO} from 5.9.2) m_{MTO}
3. calculate a new value for m_{OE} / m_{MTO} from equation (5.47)
4. go back to step 2 and repeat until convergence.

Approach 2:

Loftin 1980 (unlike other authors) uses the thrust-to-weight ratio obtained in the preliminary sizing procedure to determine the relative operating empty mass or the relative useful load u from a statistical analysis. Various civil jets from a business jet to a Boeing 747 were included in the analysis, and a thrust-to-weight ratios of between 0.23 and 0.46 was taken into account. The result can be summarized (**Loftin 1980**, Fig. 3.21)

$$u = 0.77 - 1.04 \cdot \frac{T_{TO}}{m_{MTO} \cdot g} \quad (5.48)$$

or

$\frac{m_{OE}}{m_{MTO}} = 0.23 + 1.04 \cdot \frac{T_{TO}}{m_{MTO} \cdot g} \quad (5.49)$
--

Equation (5.49) provided the relative operating empty mass m_{OE} / m_{MTO} for virtually all aircraft examined by **Loftin 1980** with an error rate of less than 10%. The relative operating empty mass m_{OE} / m_{MTO} increases with increasing thrust-to-weight ratio. As a high thrust-to-weight ratio requires high-performance and therefore heavy engines, equation (5.49) reflects the expected tendency. Furthermore (5.49) is in very good agreement with independent statistical data from **Fig. 5.12**.

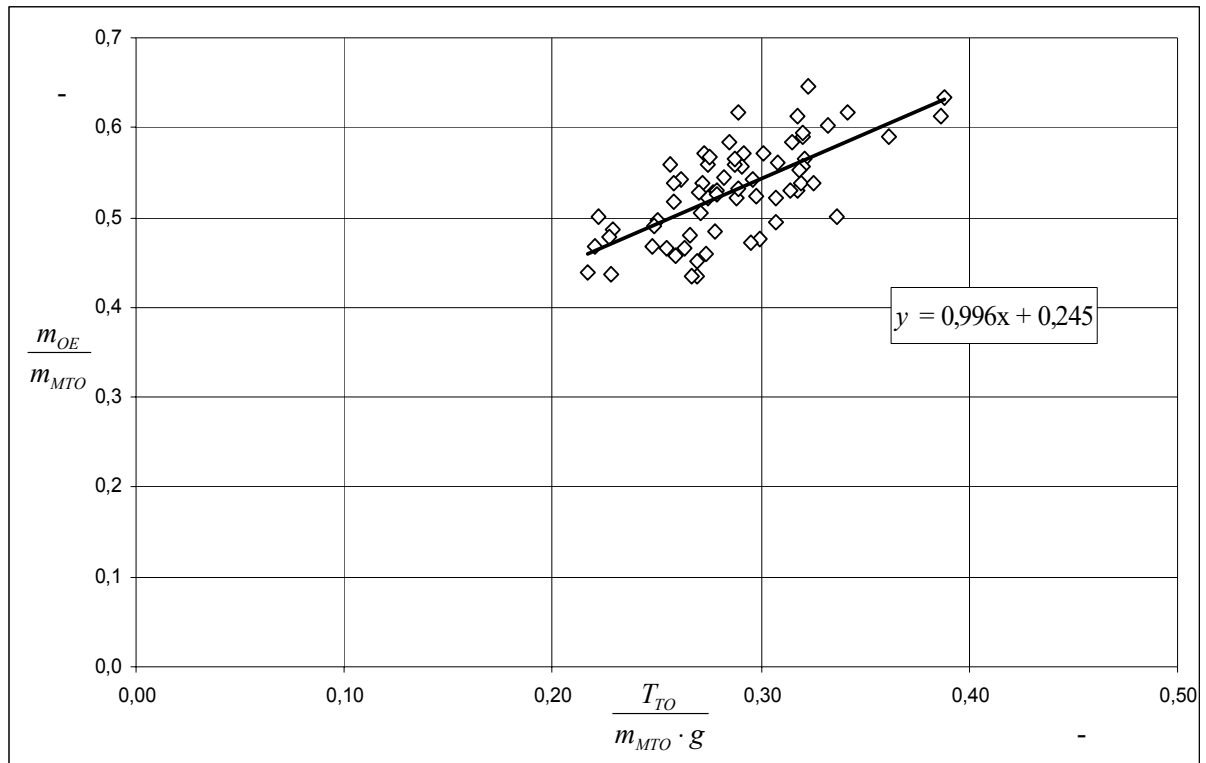


Fig. 5.12 Relative operating empty mass m_{OE} / m_{MTO} as a function of thrust-to-weight ratio (data from **Kallmeyer 1999**, **Jenkinson 1999**)

Fig. 5.13 and **Fig. 5.14** give further inside into dependencies of m_{OE} / m_{MTO} .

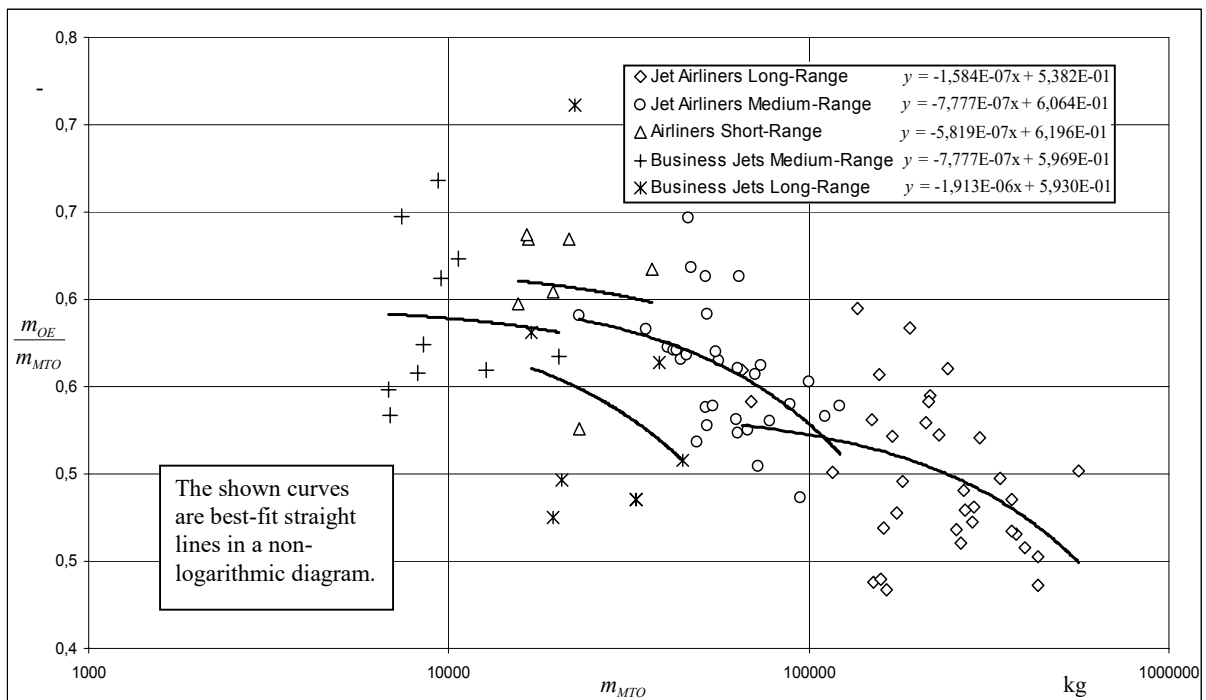


Fig. 5.13 Relative operating empty mass m_{OE} / m_{MTO} as a function of maximum take-off mass m_{MTO} (data from **Jenkinson 1999**, www.wikipedia.de)

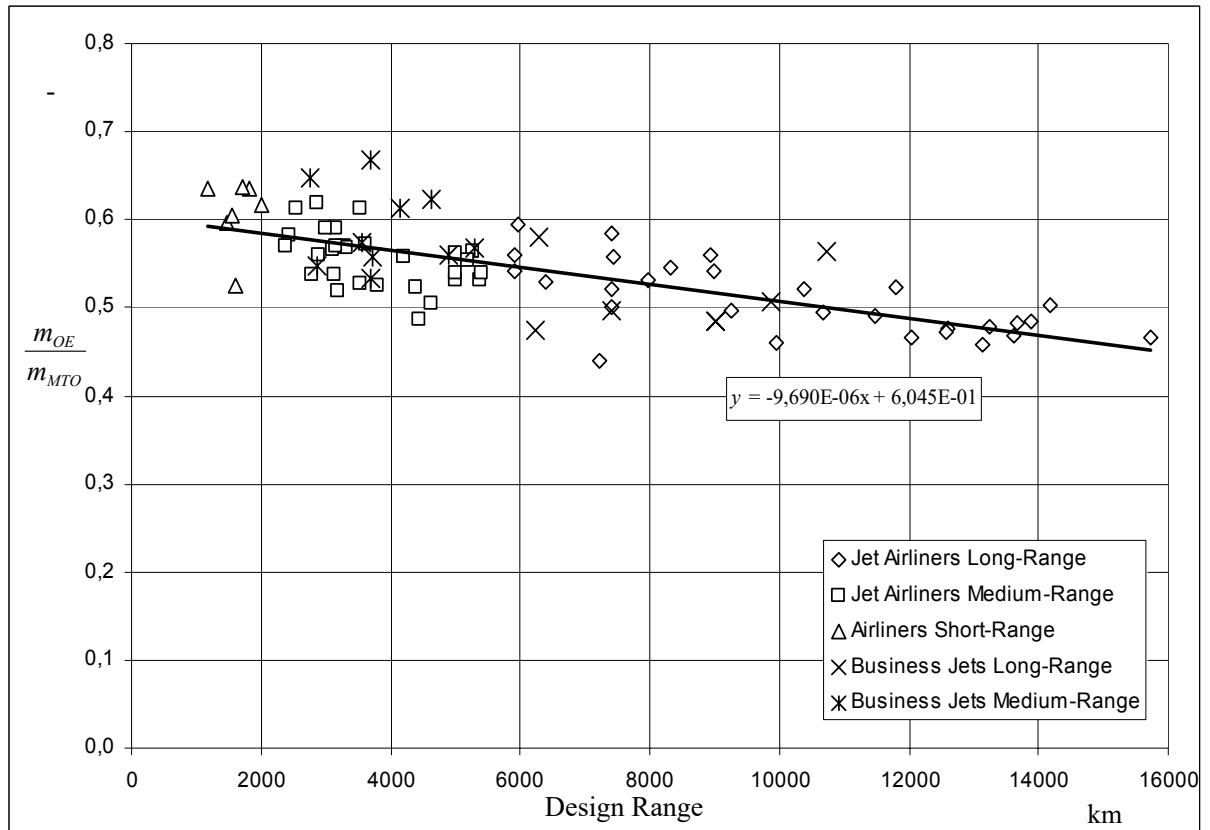


Fig. 5.14 Relative operating empty mass m_{OE} / m_{MTO} as a function of design range (no fuel reserves) (data from **Jenkinson 1999** and www.wikipedia.de)

5.9.2 Relative Fuel Mass

The relative fuel mass m_F / m_{MTO} is inserted in equation (5.45) to estimate the maximum take-off mass m_{MTO} . Fuel is required during all flight phases from starting the engines to taxiing off after landing. The flight phases can be named as shown in **Fig. 5.15**. To simplify the calculation the descent (DES) is often omitted. Instead it can be assumed that the distance covered during descent is already covered during cruise flight.

m_i is the mass at the beginning of a flight phase ($i = TO, CLB, CR, \dots$). m_{i+1} is the mass at the start of the next flight phase. m_L is the mass at the beginning of the landing phase, m_T mass at the beginning of "taxi to apron". Lets call m_{SO} the mass at the end the flight "after switch off". The parameter m_{i+1} / m_i refers to flight phase i and is called *mission segment mass fraction*. The parameter $1 - m_{i+1} / m_i$ is then the relative fuel consumption in the respective flight phase i . The flight phases engine start (ES) and taxi (T) can be omitted if only the take-off mass has to be calculated. This is the case here. All *mission segment mass fractions*

taken together then provide a parameter for calculating the fuel consumption for the entire flight: This parameter is called *mission fuel fraction* M_{ff} .

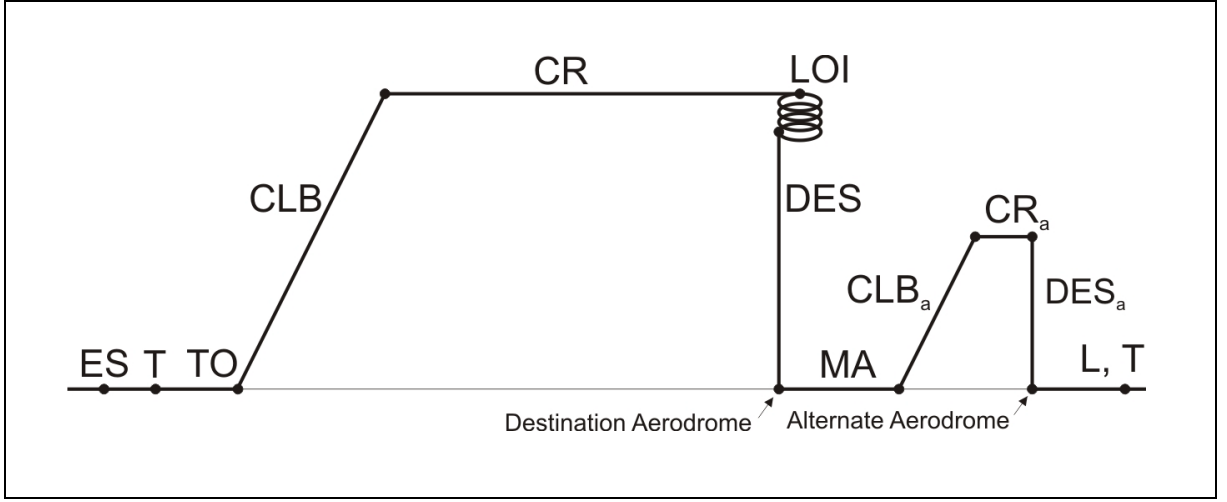


Fig. 5.15 Typical flight phases of a civil transport flight mission

$$M_{ff} = \frac{m_{SO}}{m_T} \cdot \frac{m_T}{m_L} \cdot \frac{m_L}{m_{DES}} \cdot \frac{m_{DES}}{m_{CR,alt}} \cdot \frac{m_{CR,alt}}{m_{CLB}} \cdot \frac{m_{CLB}}{m_{MA}} \cdot \frac{m_{MA}}{m_{DES}} \cdot \frac{m_{DES}}{m_{LOI}} \cdot \frac{m_{LOI}}{m_{CR}} \cdot \frac{m_{CR}}{m_{CLB}} \cdot \frac{m_{CLB}}{m_{TO}} = \frac{m_{SO}}{m_{TO}} \quad (5.50)$$

The entire mass of the fuel consumed on the flight is then calculated from the *mission fuel fraction* M_{ff}

$$m_F = m_{TO} - m_{SO} = m_{TO} \cdot \frac{m_{TO} - m_{SO}}{m_{TO}} = m_{TO} \cdot (1 - M_{ff}) \quad (5.51)$$

The relative fuel mass for equation (5.45) follows from the mission fuel fraction

$$\frac{m_F}{m_{TO}} = 1 - M_{ff} \quad (5.52)$$

The *mission segment mass fractions* m_{i+1} / m_i first have to be determined in order to be able to work with equation (5.50) and (5.52):

- The mass ratios for cruise and loiter *must* be determined according to *Breguet* (see below).
- For the remaining flight phases it is scarcely possible or worthwhile to calculate the mass ratio with the resources available here, so that the data in **Table 5.9** has to be resorted to.

For the cruise flight of a jet, the Breguet range factor is

$$B_s = \frac{L / D \cdot V}{SFC_T \cdot g} \quad (5.53)$$

For the cruise flight of a propeller aircraft the corresponding Breguet range factor is

$$B_s = \frac{L / D \cdot \eta}{SFC_P \cdot g} \quad (5.54)$$

In equation (5.54) $c = SFC_T$ is the *thrust*-specific fuel consumption. In equation (5.55) SFC_P is the *performance*-specific fuel consumption and η is the propeller efficiency. The mission segment mass fraction for the cruise phase then comes to the following with the Breguet range factor B_s

$$\frac{m_{LOI}}{m_{CR}} = e^{-\frac{s_{CR}}{B_s}} \quad (5.55)$$

s_{CR} is the distance covered in the cruise phase. **Table 5.7** and **Table 5.8** provide information on the specific fuel consumption.

More details to the calculation of fuel mass (taking into account the regulations on fuel reserves) are given in a spreadsheet based method for aircraft preliminary sizing that accompanies these lecture notes.

Table 5.7 Specific fuel consumption $c = SFC_T$ for jets (based on **Raymer 1989**)

SFC_T	cruise		loiter	
	lb/lb/h	mg/N/s	lb/lb/h	mg/N/s
turbojet	0.9	25.5	0.8	22.7
turbofan, low bypass ratio	0.8	22.7	0.7	19.8
turbofan, high bypass ratio	0.5	14.2	0.4	11.3

Table 5.8 Specific fuel consumption SFC_P and propeller efficiency η for propeller aircraft (based on **Raymer 1989**)

	cruise			loiter		
	SFC_P	η		SFC_P	η	
	lb/hp/h	mg/W/s	-	lb/hp/h	mg/W/s	-
piston, fixed pitch propeller	0.4	0.068	0.8	0.5	0.085	0.7
piston, variable pitch propeller	0.4	0.068	0.8	0.5	0.085	0.8
turboprop	0.5	0.085	0.8	0.6	0.101	0.8

Table 5.9 Generic mission segment mass fractions (based on **Roskam I**)

type of aircraft	engine start	taxi	take-off	climb	descent	landing
business jet	0.99	0.995	0.995	0.98	0.99	0.992
jet transport	0.99	0.99	0.995	0.98	0.99	0.992
fighter	0.99	0.99	0.99	0.96 – 0.9	0.99	0.995
supersonic cruise	0.99	0.995	0.995	0.92 – 0.87	0.985	0.992

5.10 Take-off Thrust and Wing Area

Take-off thrust and wing area can easily be calculated with the now known maximum take-off mass m_{MTO} from the thrust-to-weight ratio $T_{TO} / (m_{MTO} \cdot g)$ and the wing loading m_{MTO} / S_W

$$T_{TO} = m_{MTO} \cdot g \cdot \left(\frac{T_{TO}}{m_{MTO} \cdot g} \right) \quad (5.56)$$

$$S_W = m_{MTO} / \left(\frac{m_{MTO}}{S_W} \right) . \quad (5.57)$$

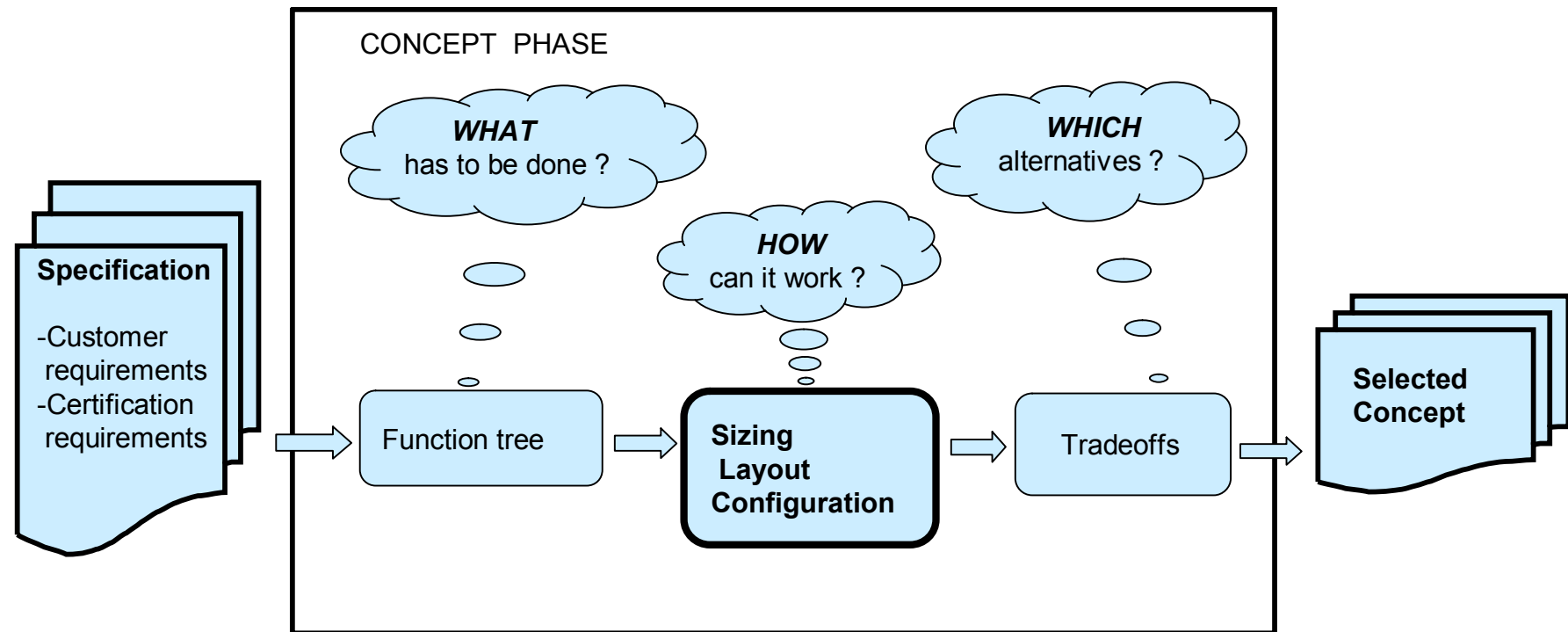
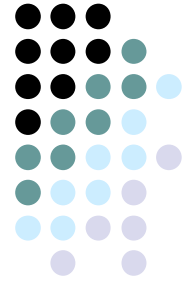
Landing mass m_L , operating empty mass m_{OE} , fuel mass m_F and some other parameters can now easily be calculated.

Erhard Rumpler

Chapter 6

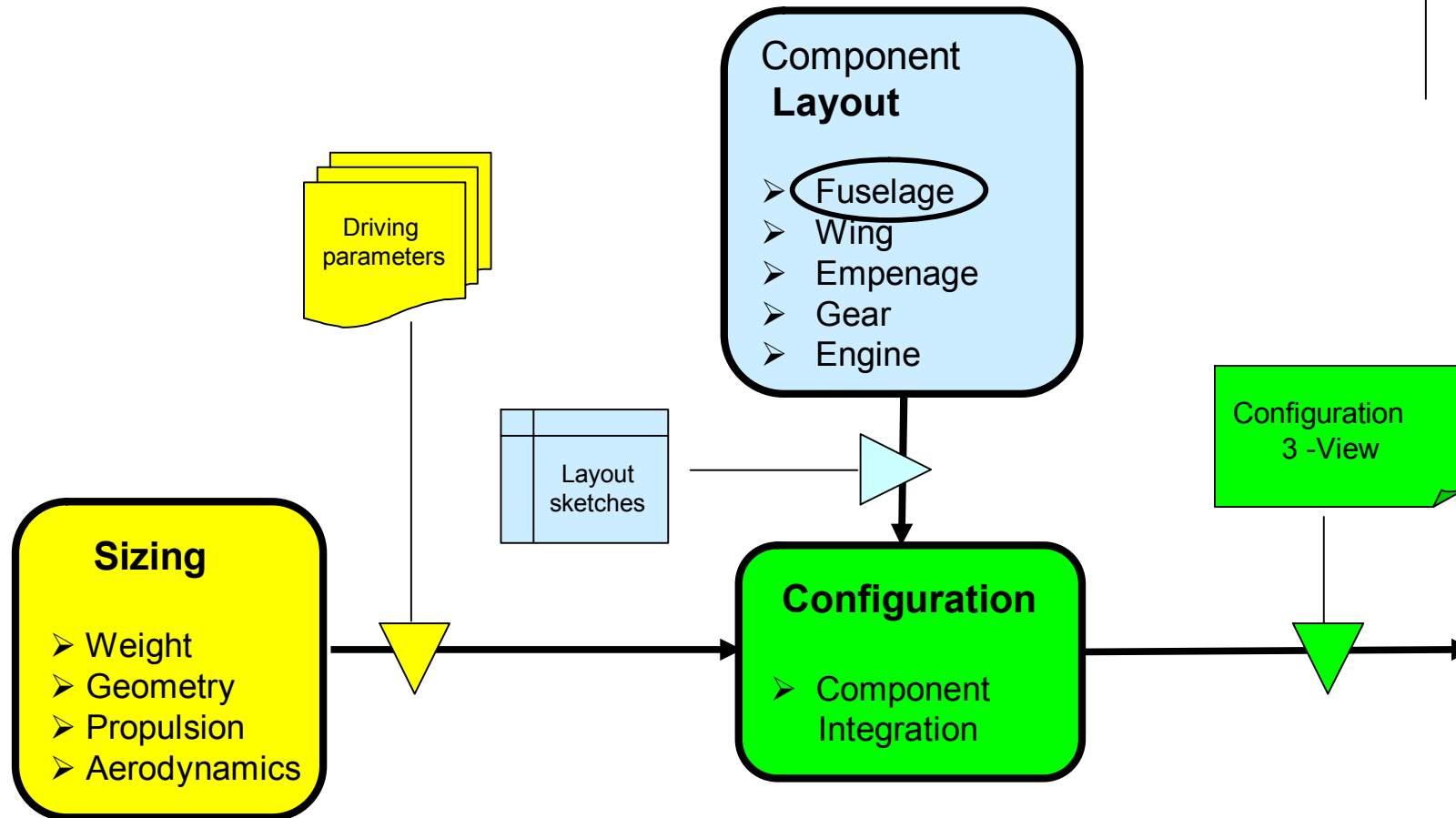
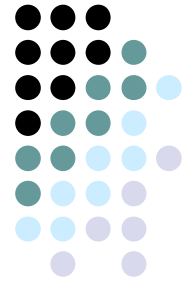
Fuselage Design

Design methodology



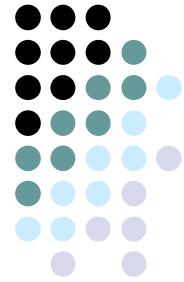
Short course covers Specification, Sizing, Layout and Configuration

Sizing — component layout — configuration

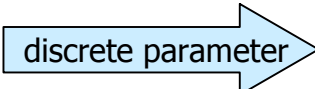


Sizing and component layout prepare prerequisites for configuration design

Fuselage layout considerations : cabin crossection



PAX / Cargo Container Accomodation

- Seats abreast  discrete parameter Fuselage Dia

$$D_f = 0,45 / n_{PAX}$$

- Main Configurations

3 abreast
6 abreast
8 abreast

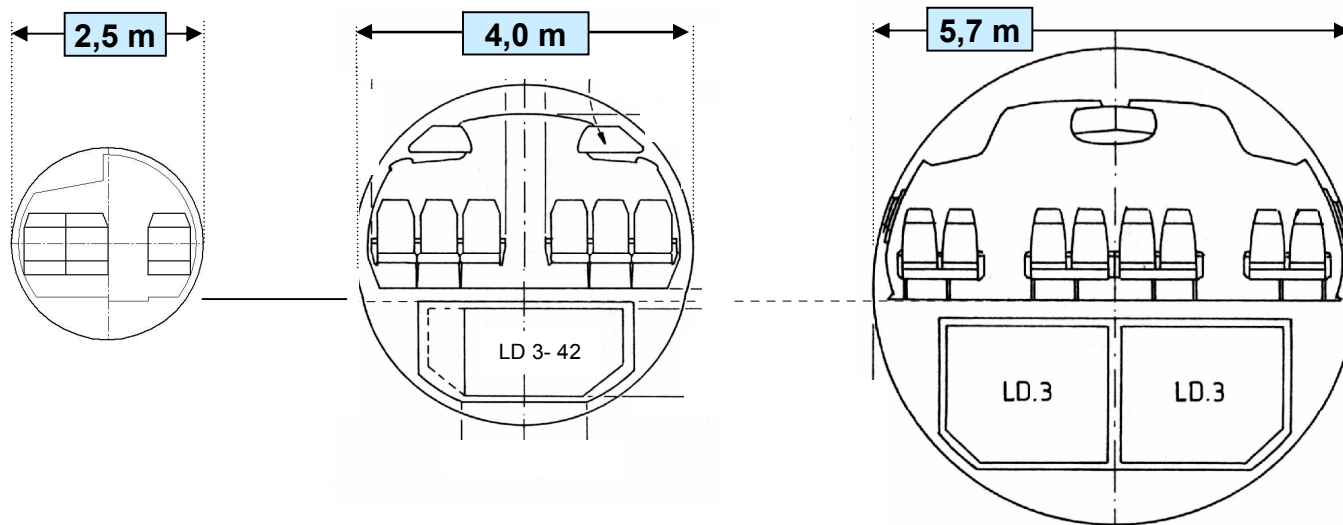
single aisle
single aisle
twin aisle

regional a/c
medium range a/c
long range a/c

$$D_f = 2,5 \text{ m}$$

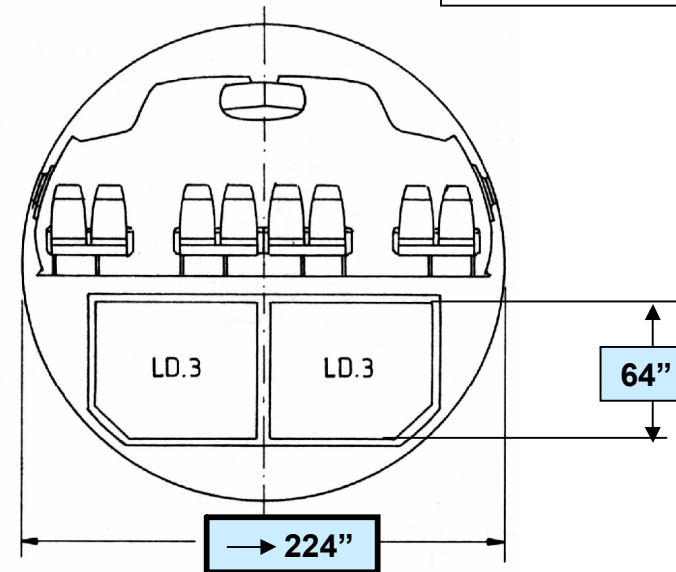
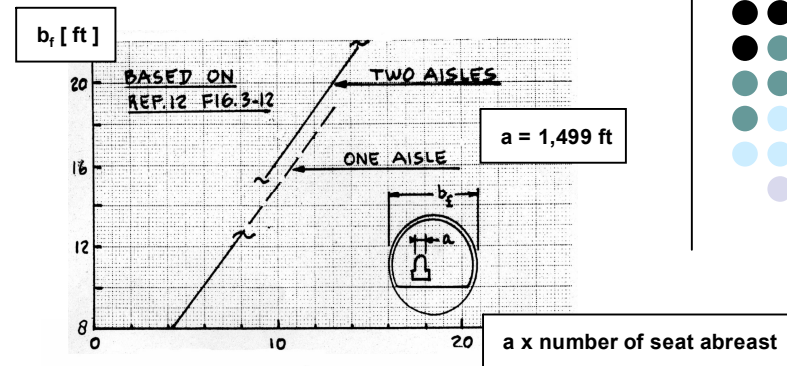
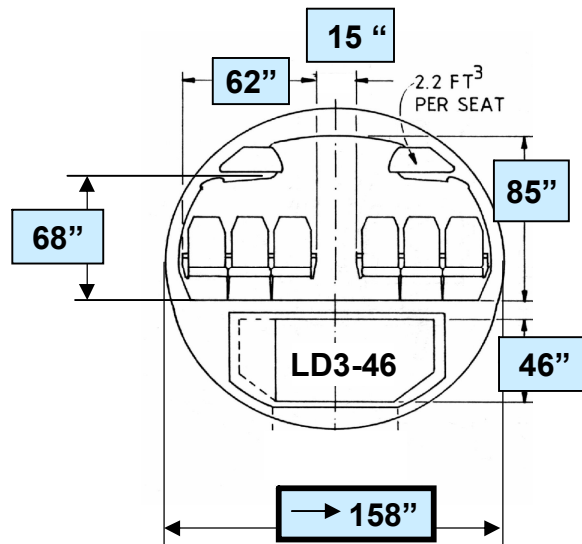
$$D_f = 4,0 \text{ m}$$

$$D_f = 5,7 \text{ m}$$



Cabin crossection

- FAR requirements for seats, ceiling, aisle
- Standard cargo containers LD3, LD3-46
- Decision : Seats abreast
- Design goal : Fuselage diameter



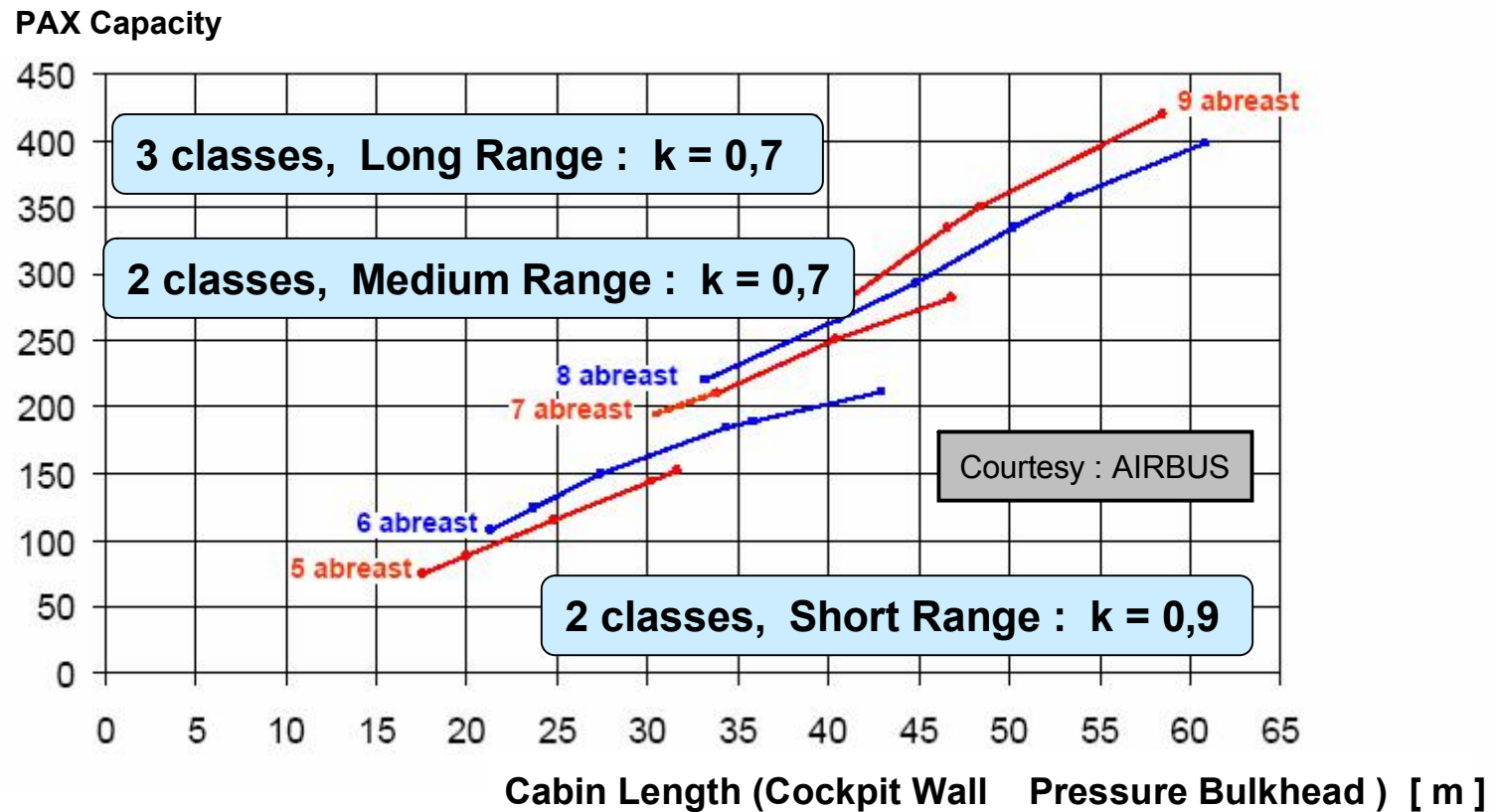
Historical note : Seat abreast configurations :

2-a LearJet	3-a Gulfstream, Do328	4-a Dash8, F28
5-a DC-9	6-a A320, B727	7-a B767
8-a A300	9-a L1011	10-a A380

Courtesy : ROSKAM

Cabin length

$$\text{Cabin length} = n_{\text{PAX}} / n_{\text{abreast}} \cdot K$$



Airworthiness considerations

- Aircraft components have to meet the requirements given by authorities
- FAA (authority) → FAR (requirements)
- Small FAR selection useful for layout design
- 2 Categories of design loads :

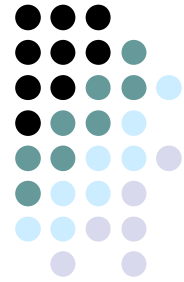
Flight Loads

Burst pressure FAR 25.365

Flare- and gust loads FAR 25.331 - 341

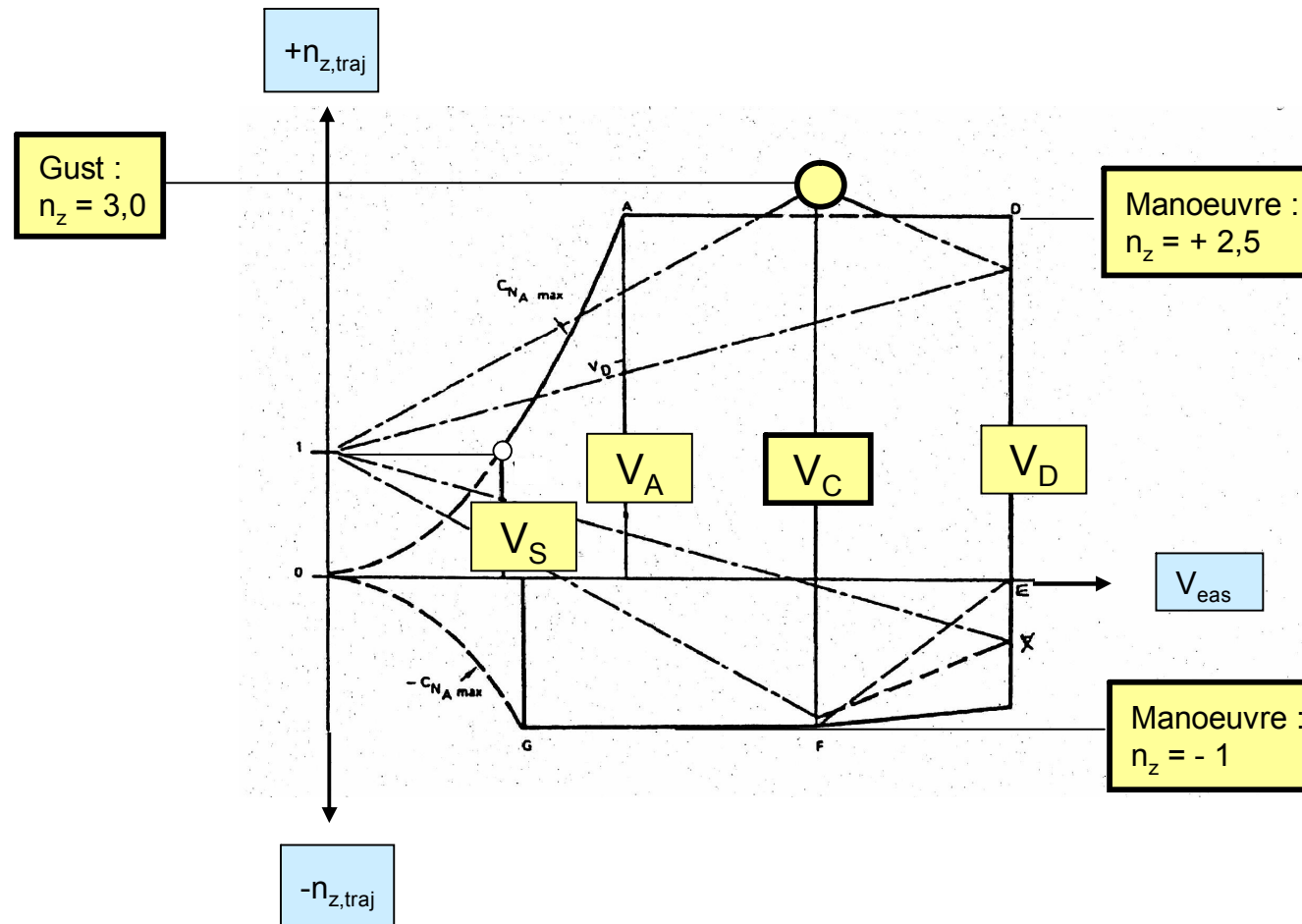
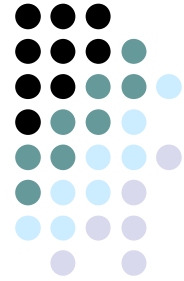
Ground Loads

Landing FAR 25.449 - 481



Flight loads

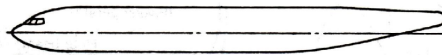
- Important source : **V-n Diagram**
- Load factor estimates for transport aircraft



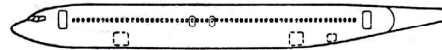
Fuselage shape refinement



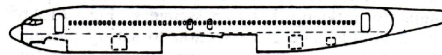
Ideal pressure shell.



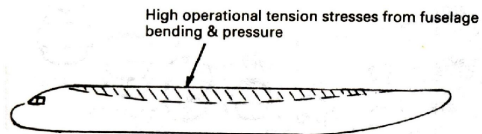
Aerodynamic smoothness.



Passenger requirements (cutouts).



Final configuration of a commercial transport.



High operational tension stresses from fuselage bending & pressure

Requirements of a Pressure vessel

- cylinder
- pressure domes

Requirements of aerodynamic drag

- fore body
- aft body

Requirements of a transportation system

- window cutouts
- door cutouts

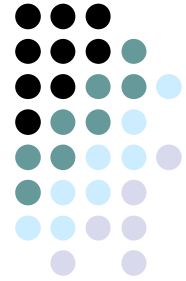
Requirements of an aircraft fuselage

- wing cutout
- gear wells cutouts

Requirements of a highly loaded lightweight structure

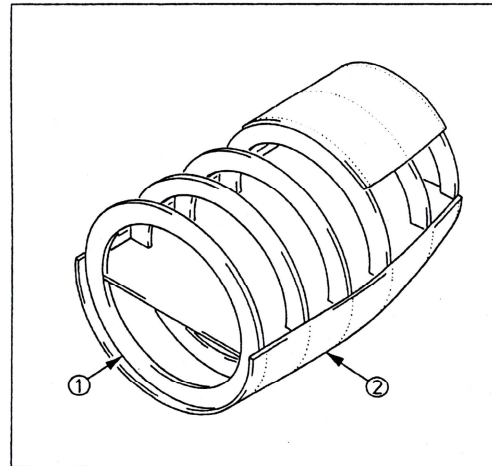
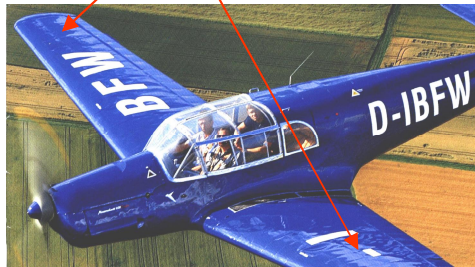
- handling of stresses on upper fuselage

Courtesy : NIU

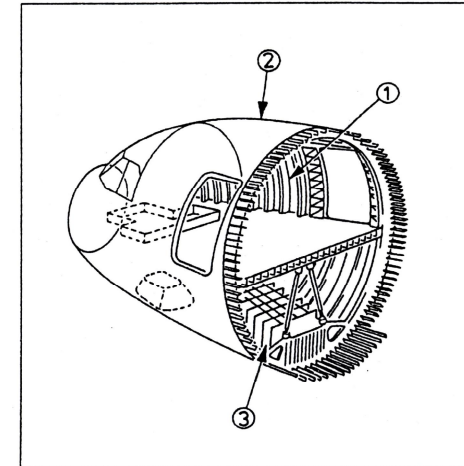


Structural technology applied to a refined shape

➤ skin - buckling of 1930-aircraft :



MONOCOQUE



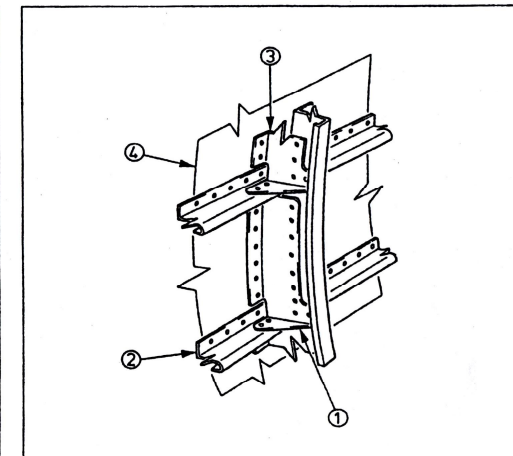
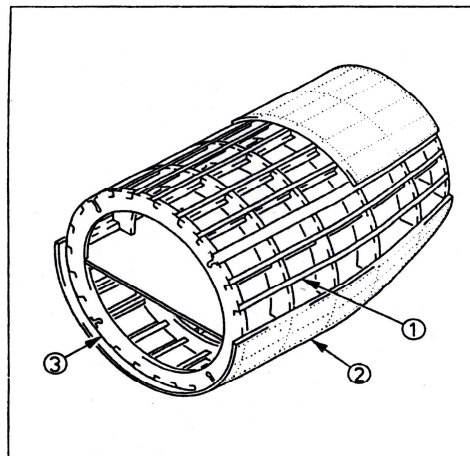
Courtesy :ENGMANN

➤ technology of 1980+ -aircraft :

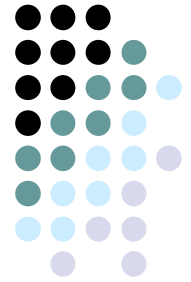
buckling not accepted

➔ **monocoque** – technology

➔ **semi- monocoque** - technology



Structures-related definitions



- **SKIN** : loft defining structural member
- **STRINGER** : longitudinal skin stiffening member
- **PANEL** : skin + stringer assembly
- **FRAME** : circumference panel stiffening member
- **BULKHEAD** : massive frame, able to transfer concentrated loads
- **CLIP** : connecting member between frame and stringer or skin
- **SHELL** : panel + frame assembly

Structural technology

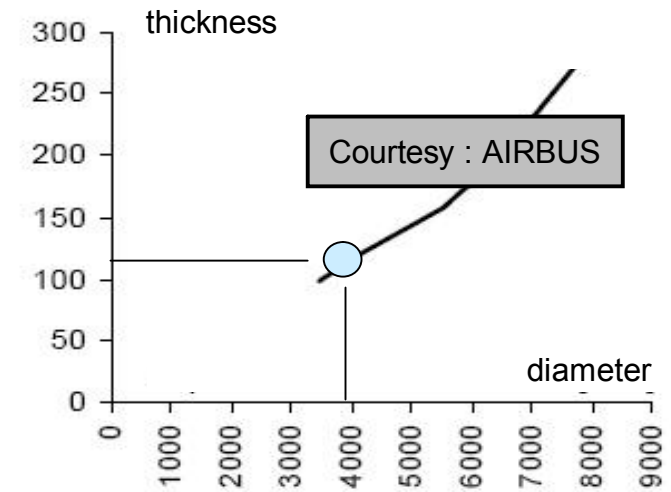
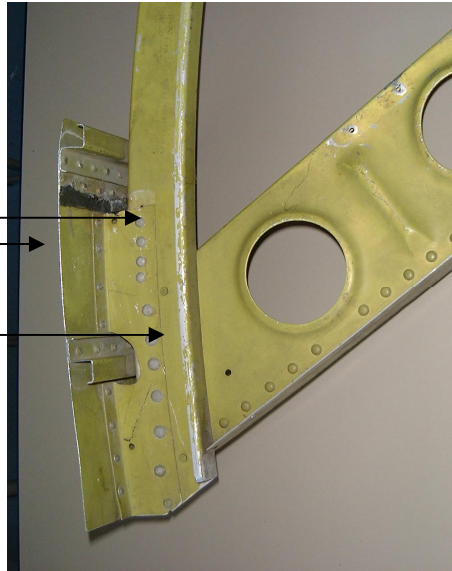
➤ SEMI - MONOCOQUE

Version AIRBUS

-CLIP

between

SKIN and FRAME

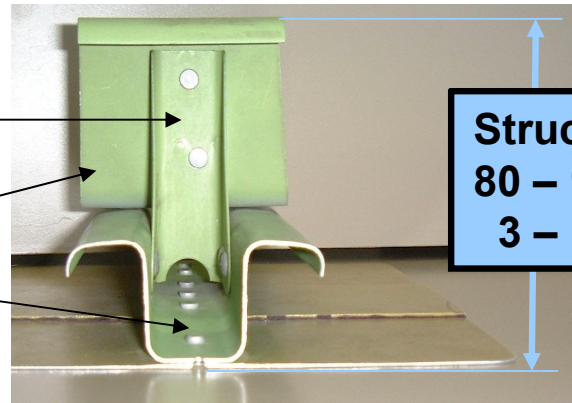


Version BOEING

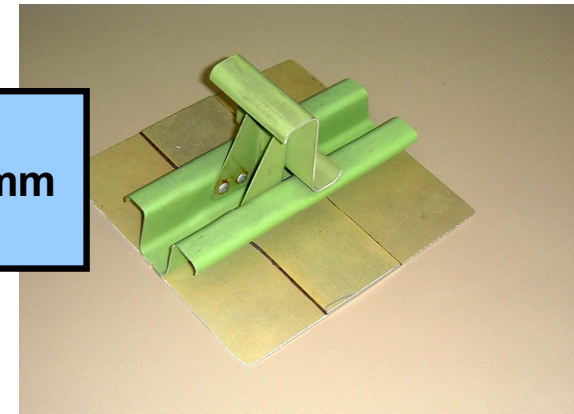
-CLIP

between

FRAME and STRINGER



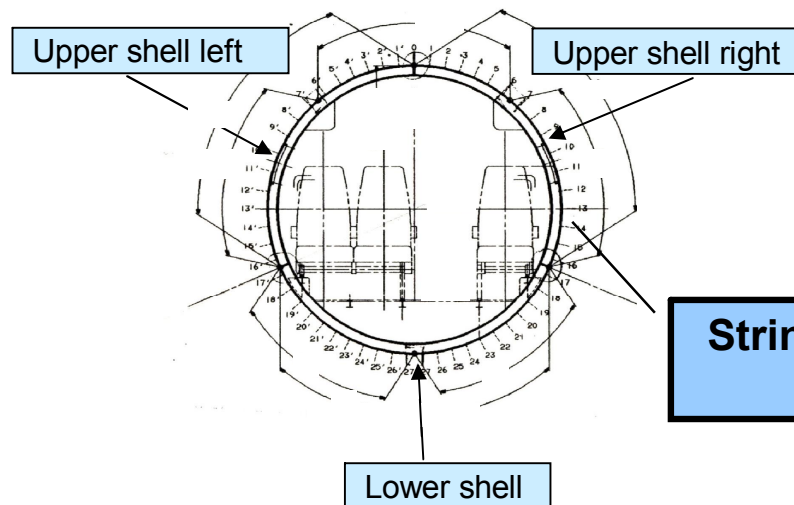
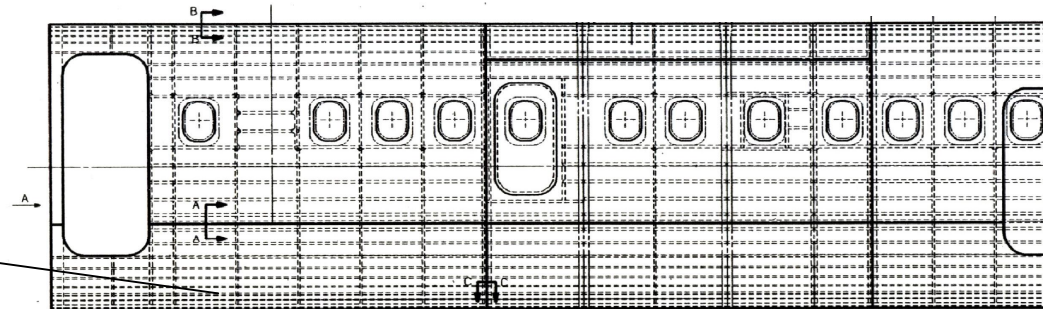
Structure
80 – 140 mm
3 – 5,5 “



Shell layout 3-abreast

- Frame / stringer spacing defined by buckling resistance requirements

**Frame spacing
18 – 28"**

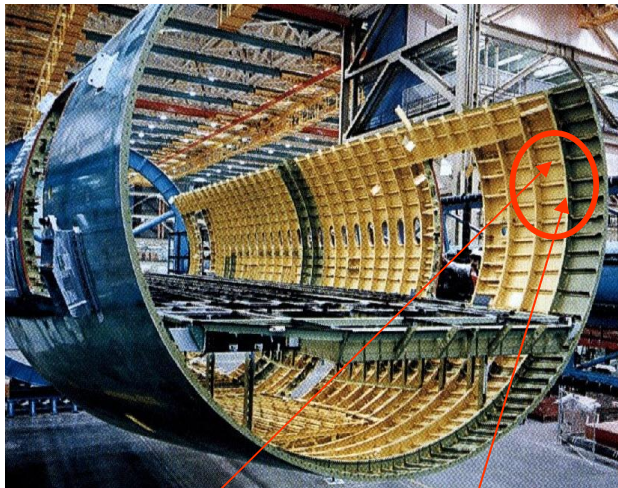


Courtesy : DORNIER

**Stringer spacing
8 – 12"**

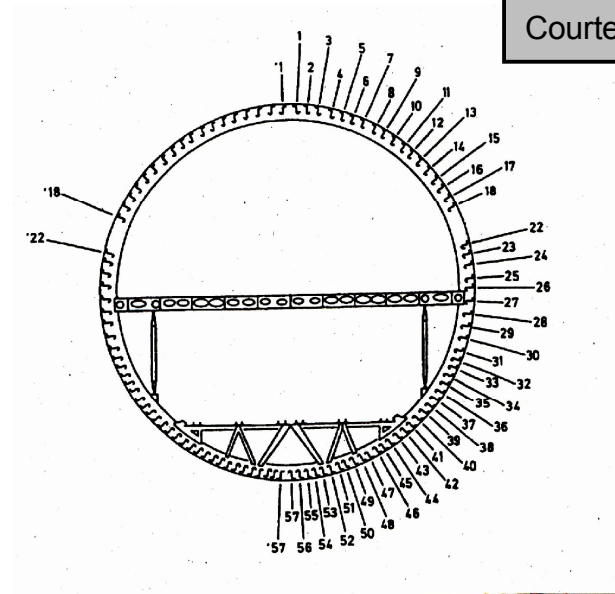
Shell layout 8-abreast +

- Frame/stringer offset defined by buckling requirements

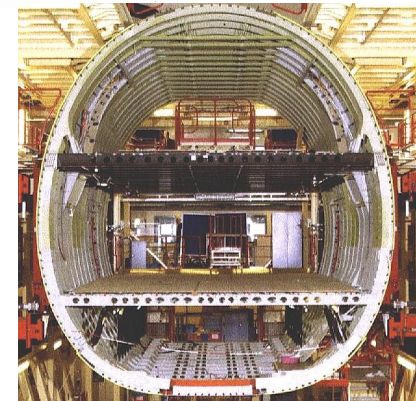


**Stringer spacing
6 – 10"**

**Frame spacing
18 - 22"**



Courtesy : AIRBUS



Fuselage Structural Sections

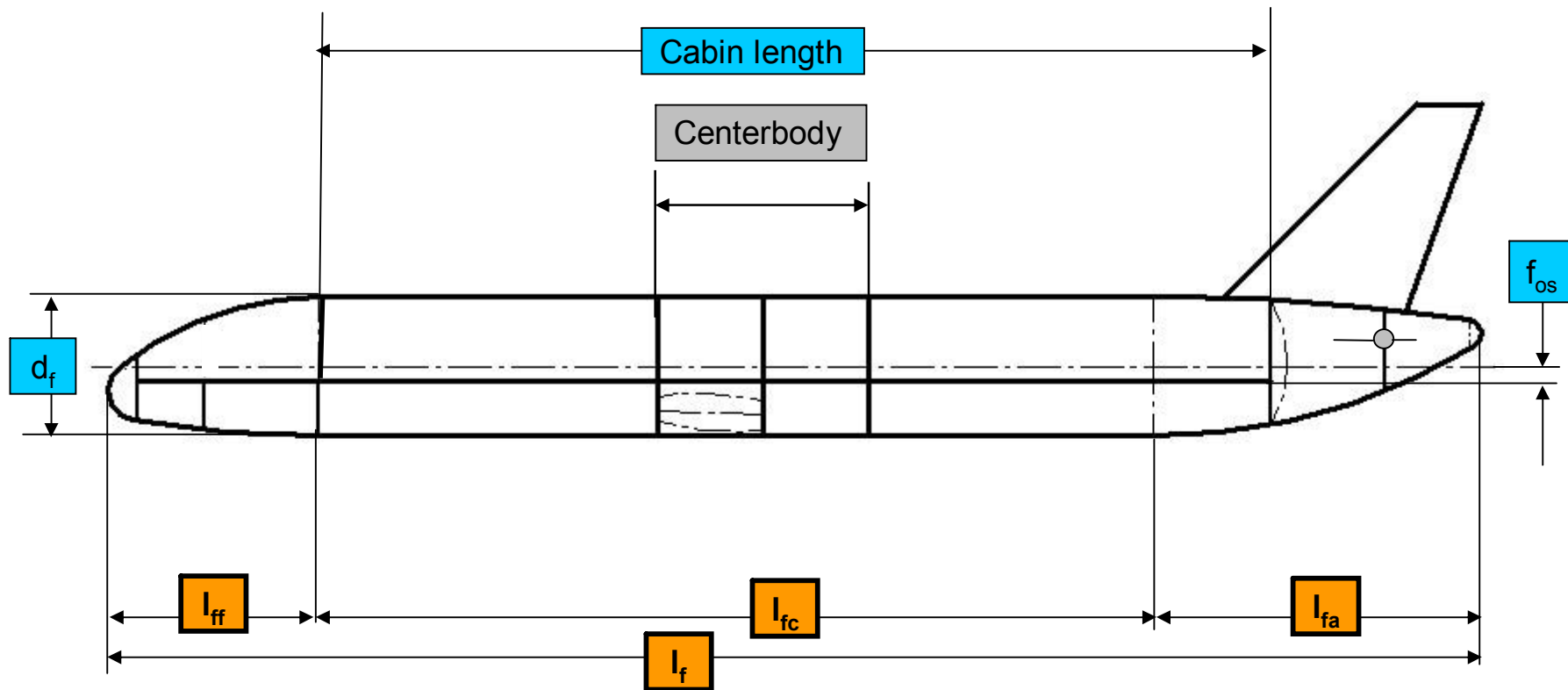
- Cylindrical section l_{fc}
- Non cylindrical sections l_{ff} , l_{fa} defined by aerodynamics

➤ Estimates :

$$l_{ff} \sim 1,4 \cdot d_f$$

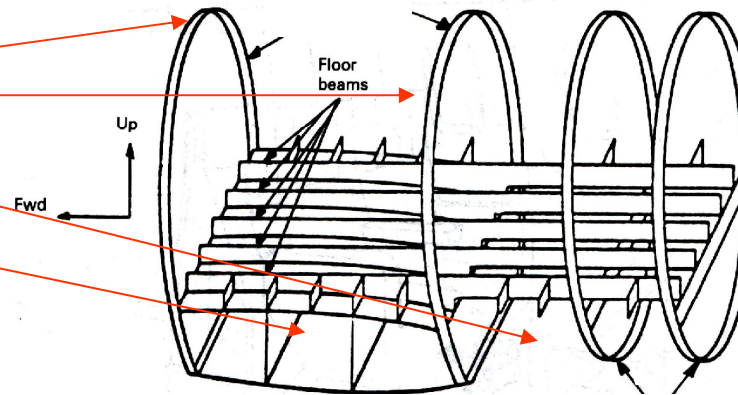
$$l_{fc} \sim 5,8 \cdot d_f$$

$$l_{fa} \sim 2,6 \cdot d_f$$

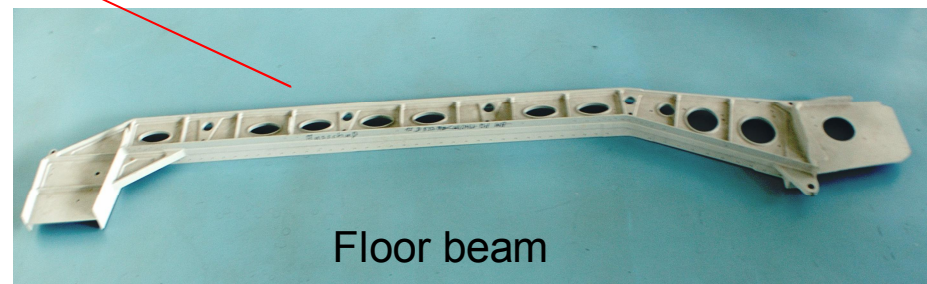
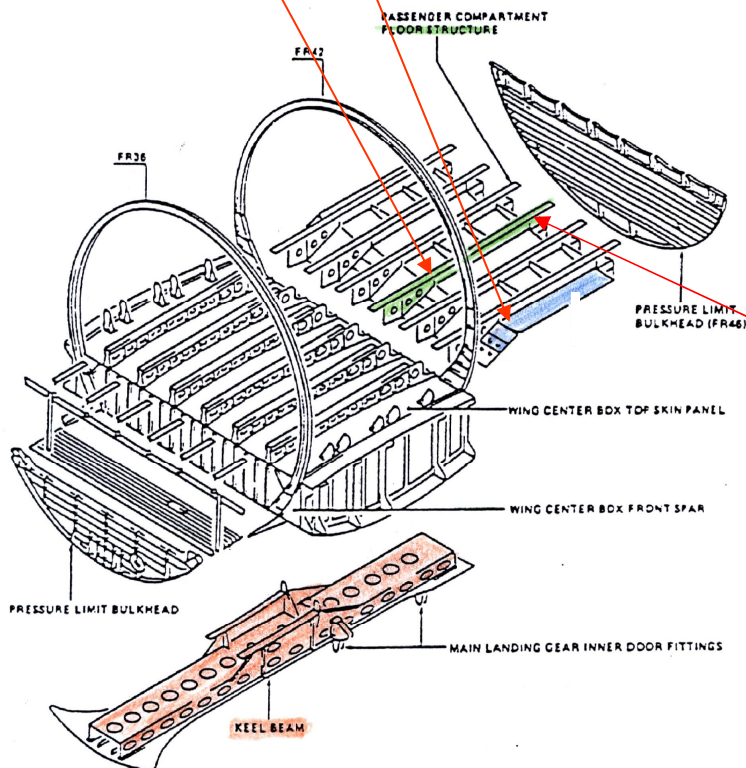


Center body (“ Static Heart “)

- Main bulkheads
- Main gear wheel well
- Center wing box
- Pressure diaphragms
- Floor beam

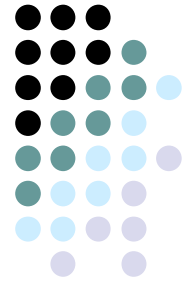


Courtesy : AIRBUS

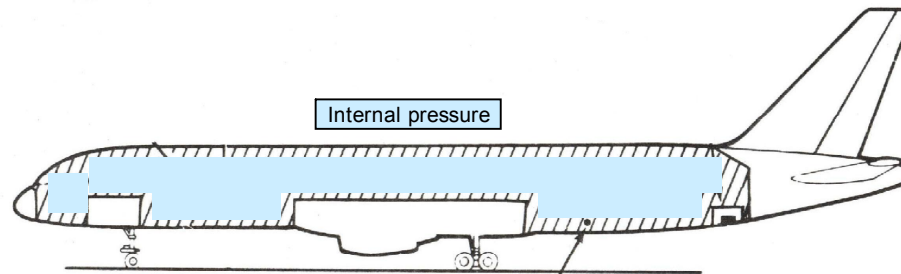


Floor beam

Stress conditions on structural sections

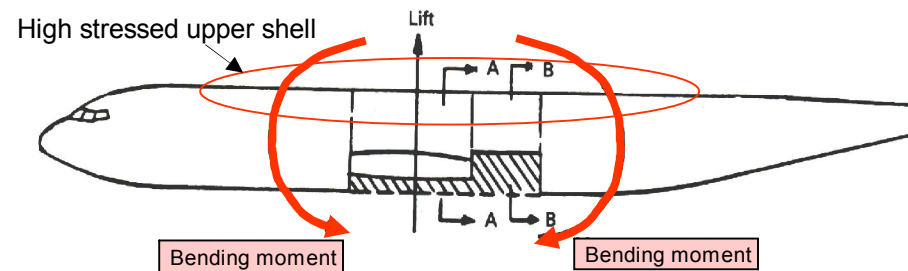


➤ Internal pressure

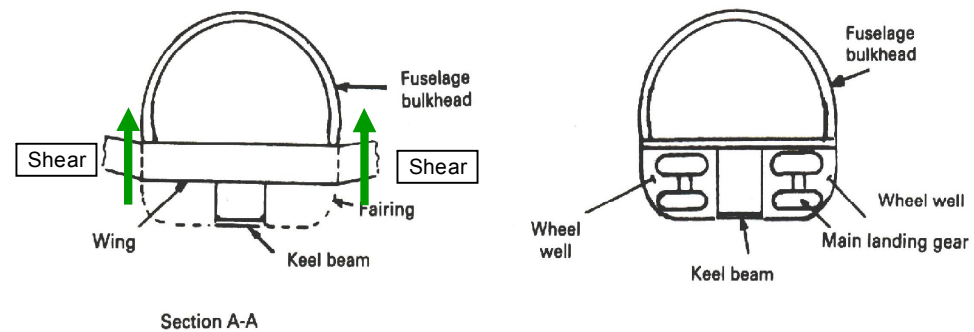


Courtesy : NIU

➤ Bending

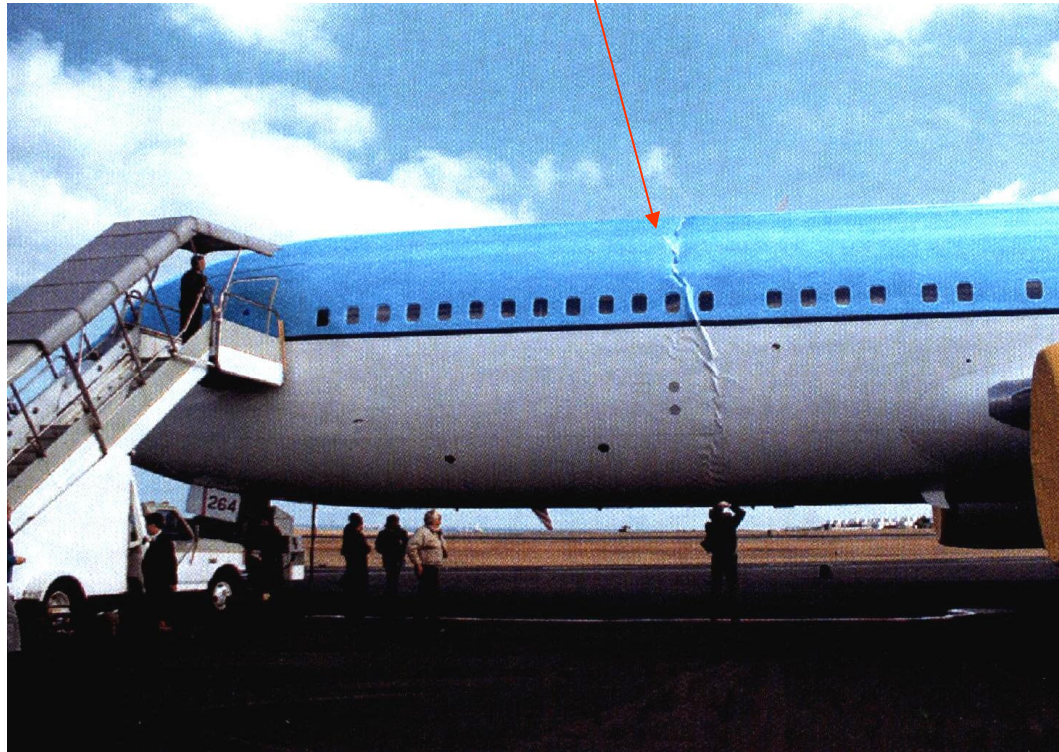


➤ Shear



High stressed shell sections

- High bending stress as a result of a hard level landing (Ref. Gear design)
- Buckling of compressed upper shells



High stressed shell sections

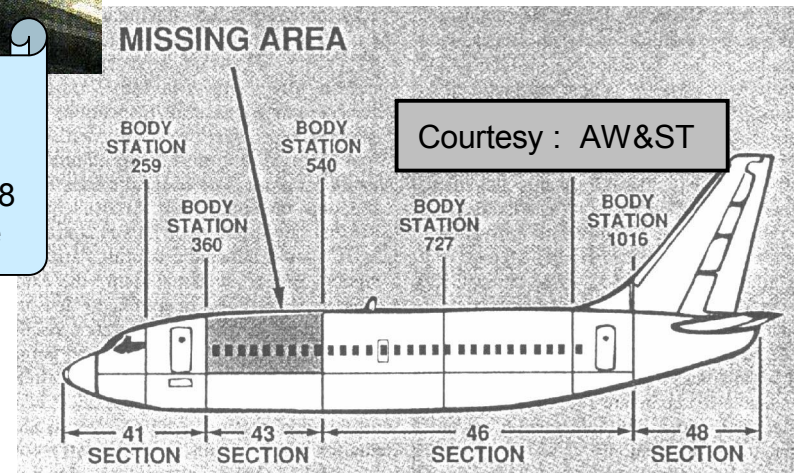
- GLARE technology for high stressed upper shells



Historical note :

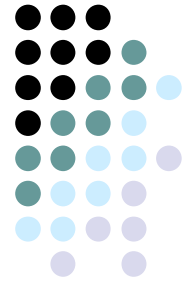
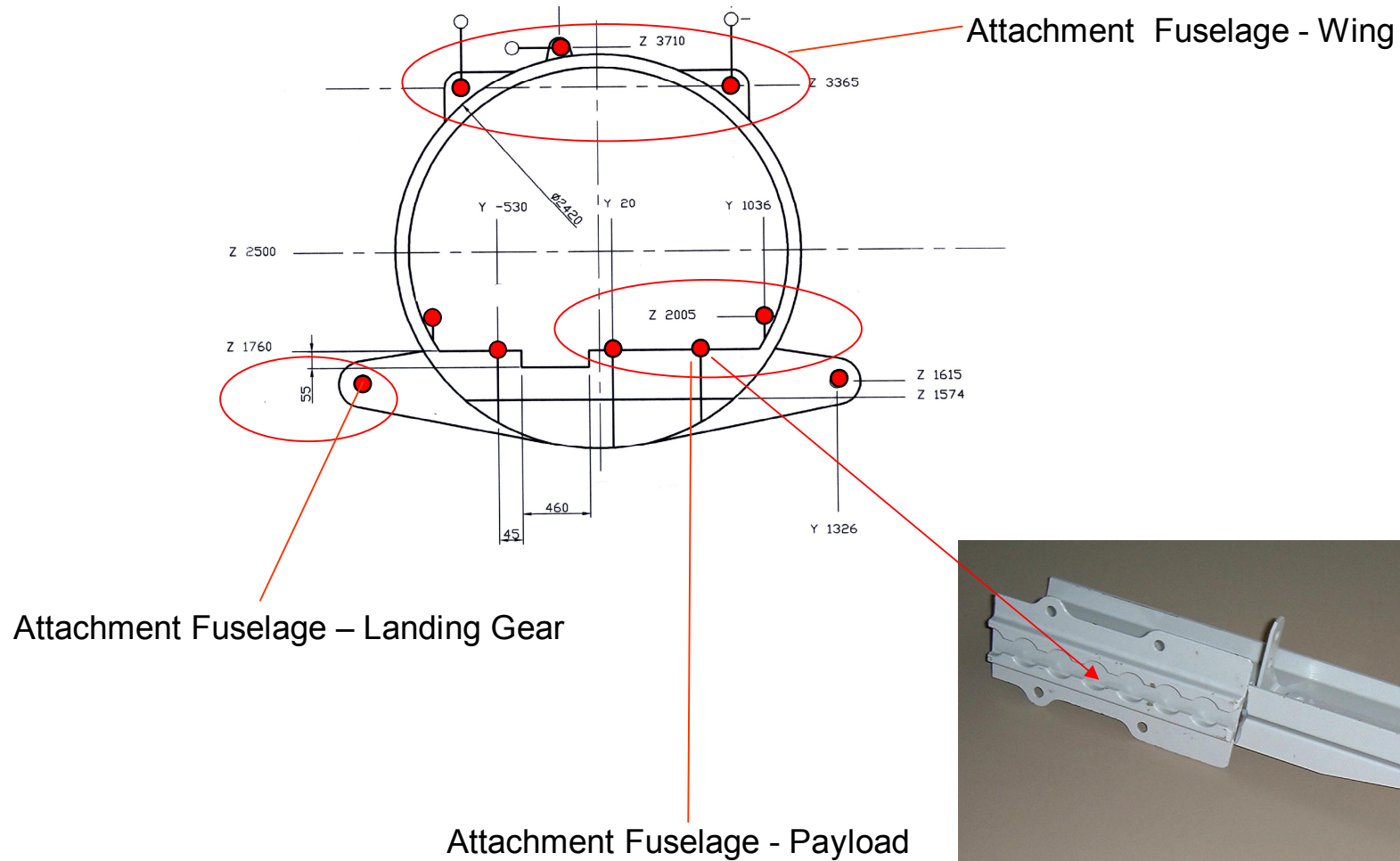
B737

Accident 04/28/1988
- Upper shell failure



Attachment Points

➤ Transfer of concentrated loads : main bulkheads

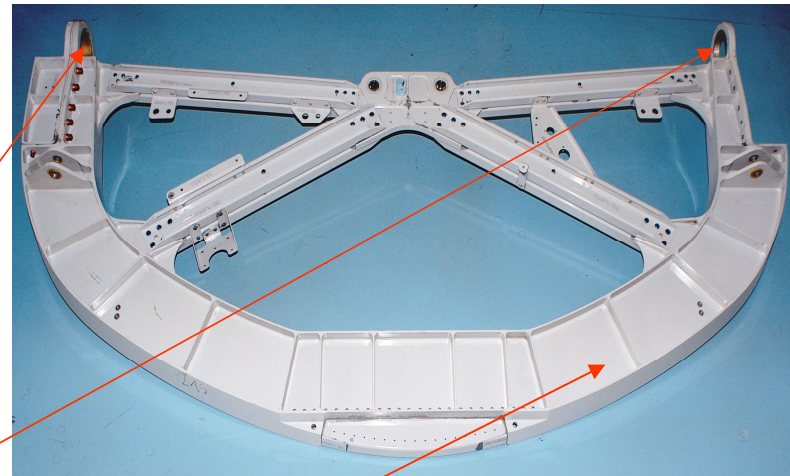


Attachment Points



Attachment Fuselage – Horizontal Stabilizer :

- Methods of pitch trim
 - elevator
 - stabilizer
- Shown decision
 - stabilizer trim
 - require pivots on bulkhead



Pivots

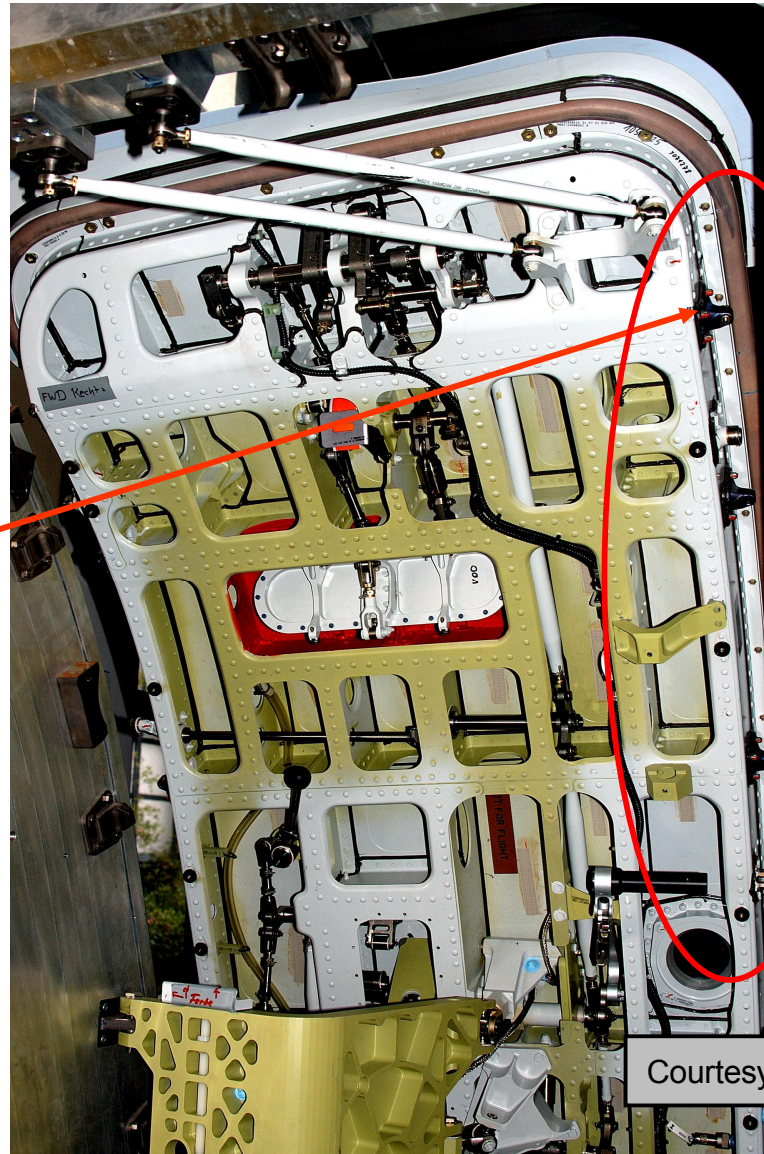
Horizontal stabilizer
bulkhead

Attachment Points

Attachment Fuselage – Passenger Door

“ PLUG – TYPE ” Doors

- Door loaded by differential pressure
- Load transfer via a discrete number of hardpoints
.... **stops** or **plugs**
- Special structural members on door and fuselage



Courtesy : EC

Cutouts

Door cutout requires special provisions for concentrated load transfer to the fuselage shell

- bulkheads in front and rear of door cutout
- inforced upper and lower sill
- Special structural member between door stop, bulkhead and following frame ... **"intercostal"**

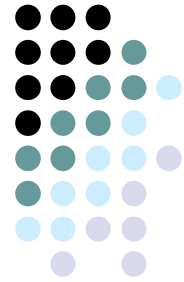
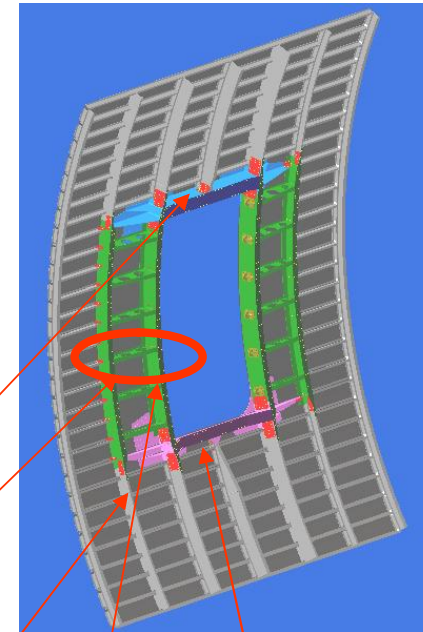
Transfer of a highly concentrated Load into a thin-walled shell ... "intercostal"

upper sill

regular frame

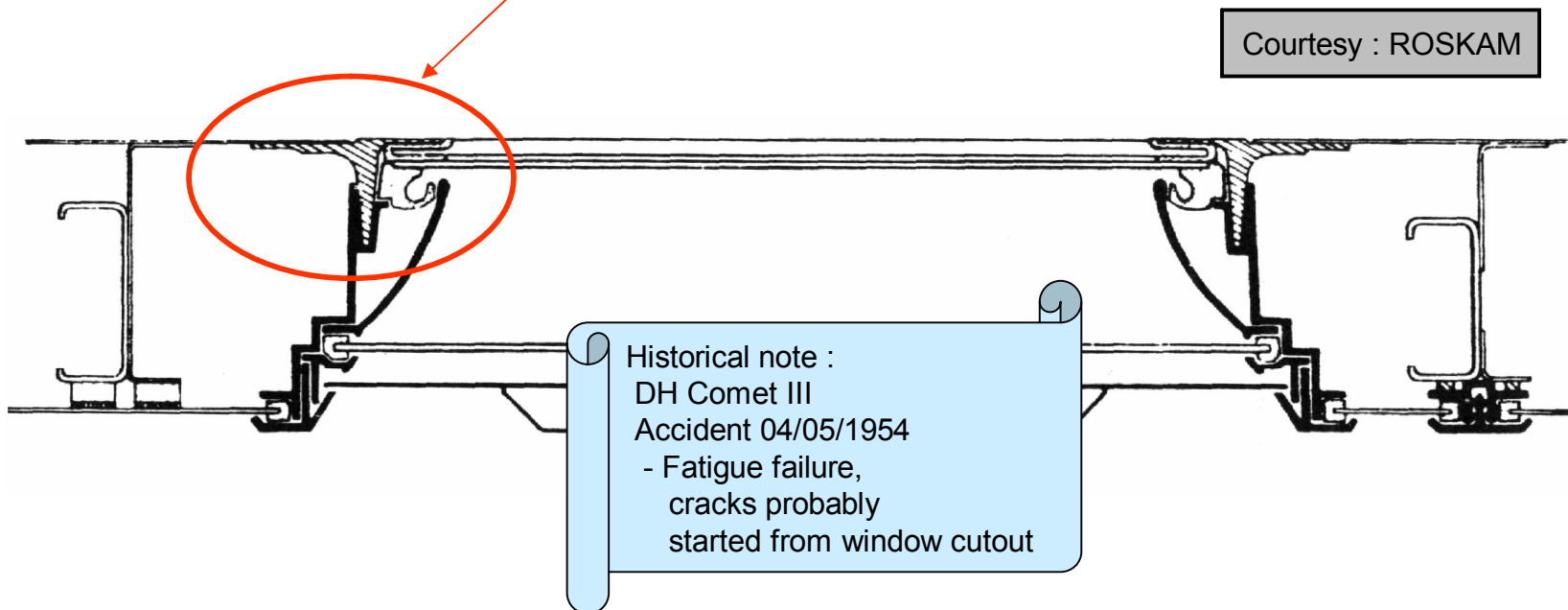
bulkhead

lower sill



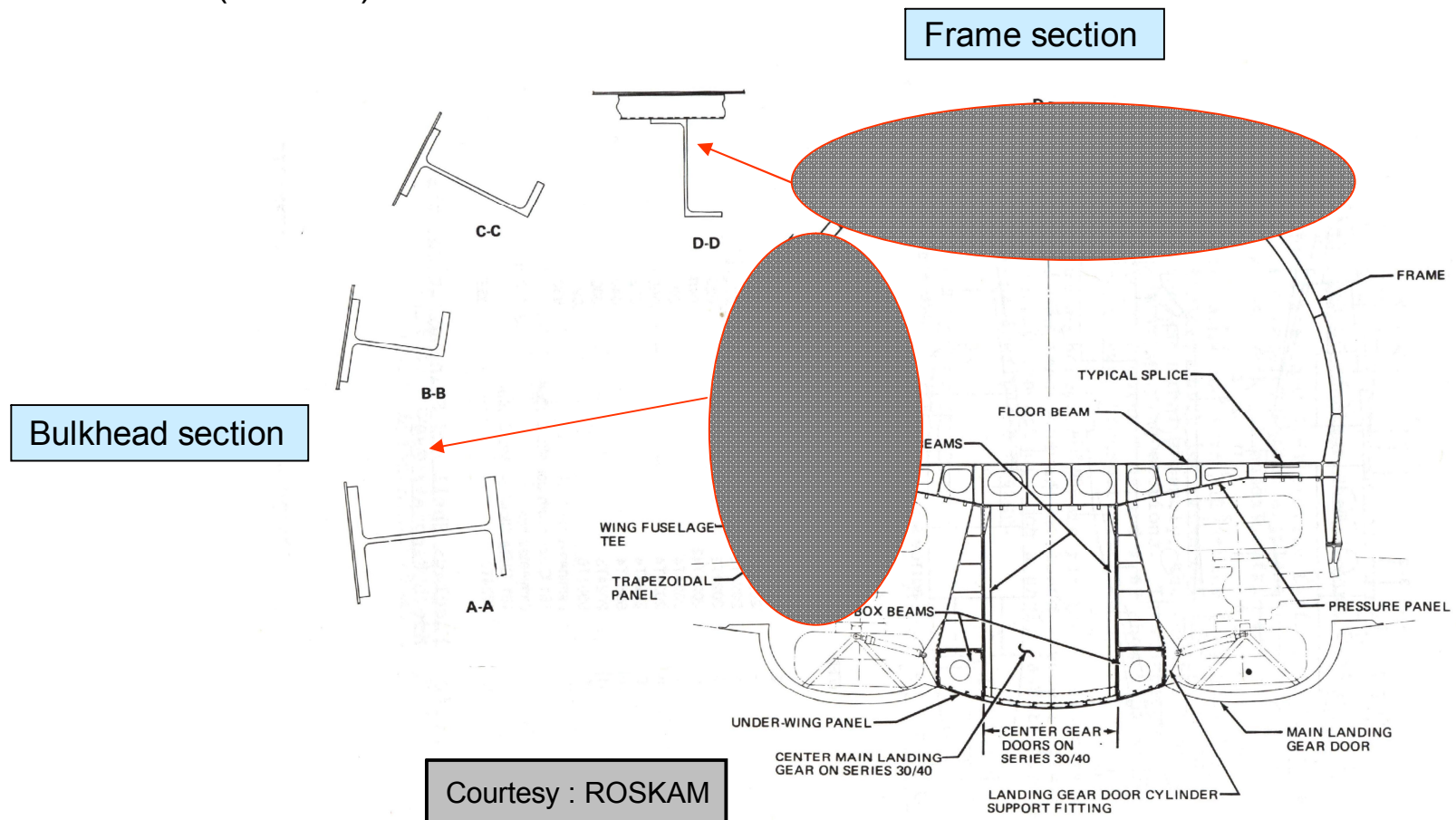
Cutouts

- Window cutout requires special provisions for fatigue loads on account of frequent pressurizing / depressurizing of the fuselage
- Standard solution : Precision forged Al 2024 frame



Cutouts

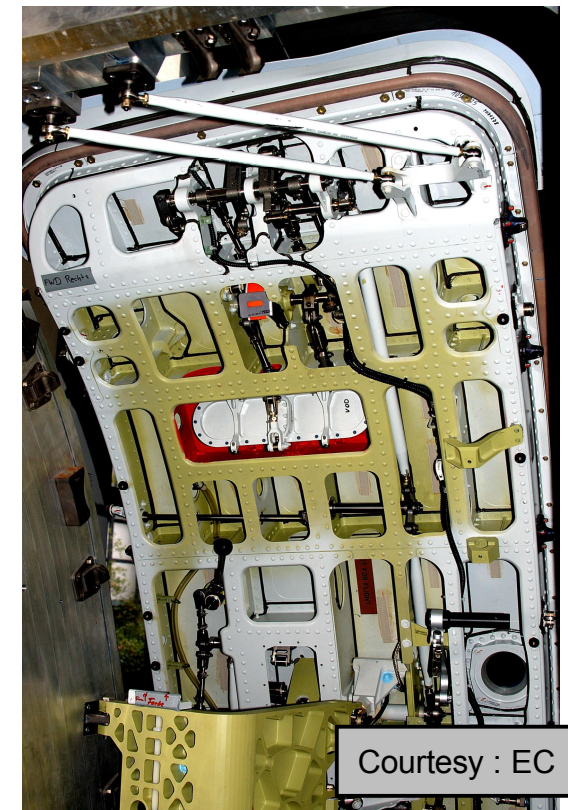
- Main gear wheel well largest cutout in fuselage
- Special “bridging” elements
- Keel beam (keelson)



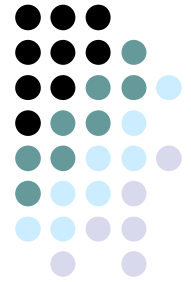
Passenger Doors

- 8 door types available
- differences in dimensions
- FAR requests door dimensions in relation to PAX number
- FAR requests further pressure load, safety items

	Abmaße der verschiedenen Türen und Notausstiege nach JAA und FAA							
Ausstieg	A	B	C	I	II	III	TwinIII	IV
max. zugelassene Passagieranzahl	110	75	55	45	40	35	65	9
Türhöhe in Zoll (mm)	72" (1828,3)	72" (1828,3)	48" (1219,2)	48" (1219,2)	44" (1117,6)	36" (914,4)	36" (914,4)	26" (660,4)
Türbreite in Zoll (mm)	42" (1066,8)	32" (812,8)	30" (762)	24" (609,6)	20" (508)	20" (508)	20" (508)	19" (482,6)
max. Eckenradius in Zoll (mm)	7" (177,8)	6" (152,4)	10" (254)	8" (203,2)	7" (177,8)	7" (177,8)	7" (177,8)	6,3" (160,02)
step up	0	0	0	0	10" (254)	20" (508)	20" (508)	29" (736,6)
step down	0	0	0	0	17" (431,8)	27" (685,8)	27" (685,8)	36" (914,4)
Anzahl der Zugänge / Notrutschenbahnen	2	2	1	1	1	1	1	1
Gangbreite	36" (914,4)	36" (914,4)	20" (508)	20" (508)	20" (508)	20" oder 2x6" und kein Sitz vorn Fenster	20" oder 2x6" und kein Sitz vorn Fenster	6" (152,4)
Flugbegleitersitz erforderlich	Ja	Ja	Nein	Nein	Nein	Nein	Nein	Nein



Courtesy : EC



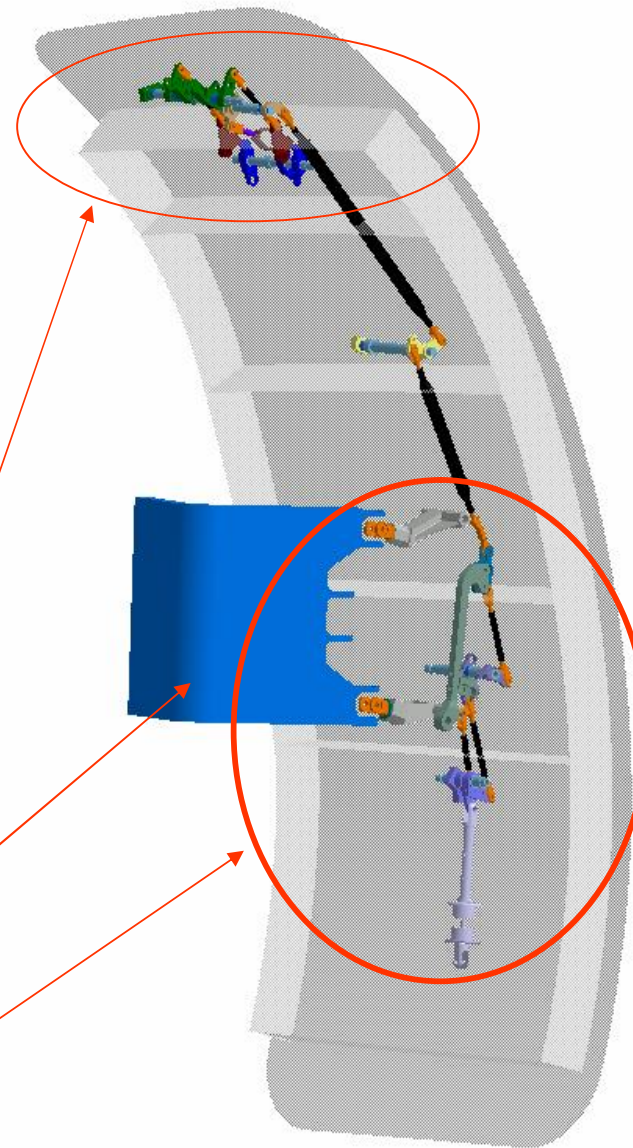
Passenger Doors

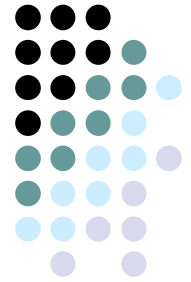
- Safety-relevant latch and lock mechanisms sophisticate the door design
- Ergonomic operation request limited forces on door handle despite increasing door weight
- High stressed component due to pressure difference

LOCK - mechanism

Main support arm

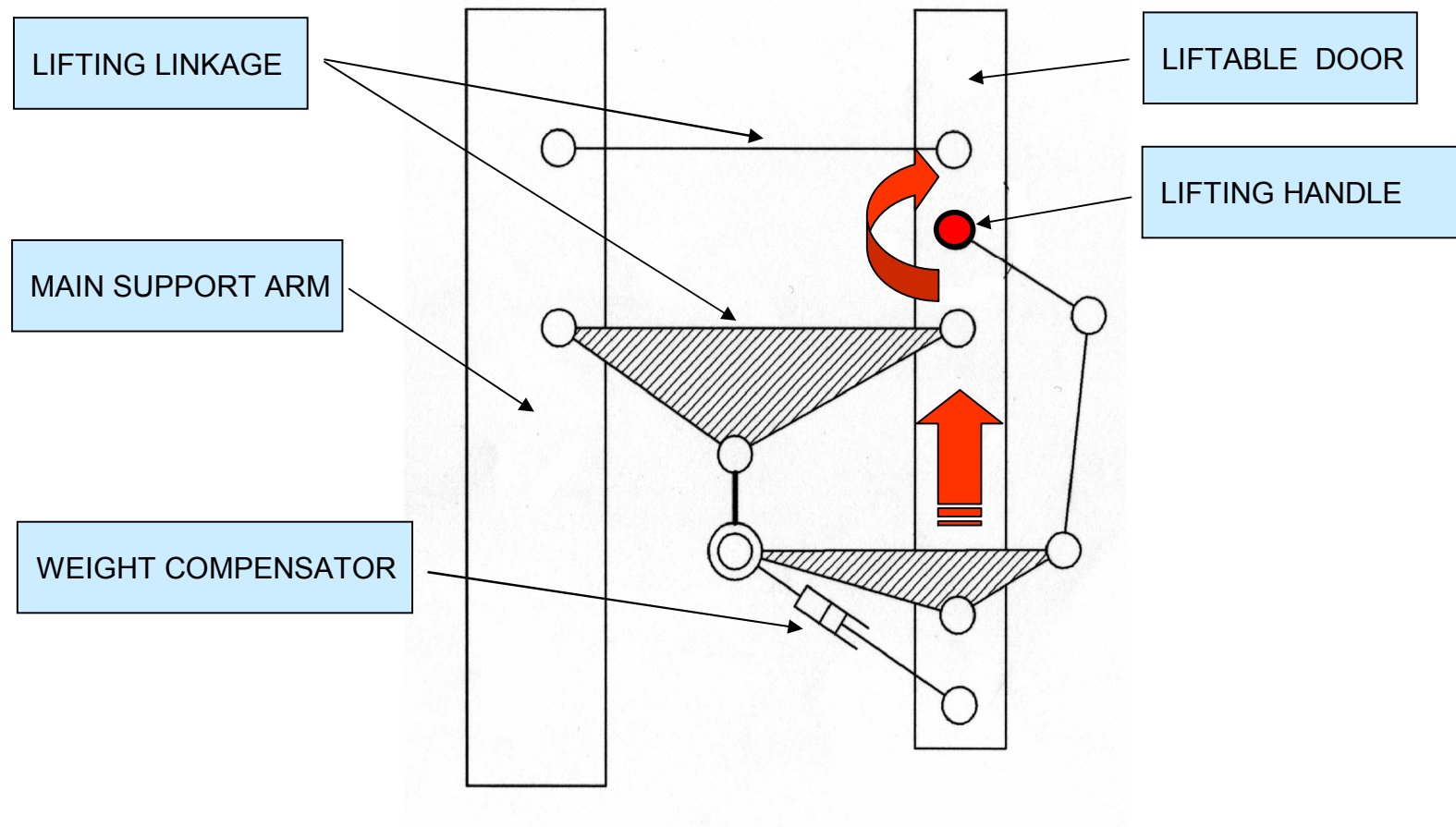
LATCH – BY – LIFT mechanism





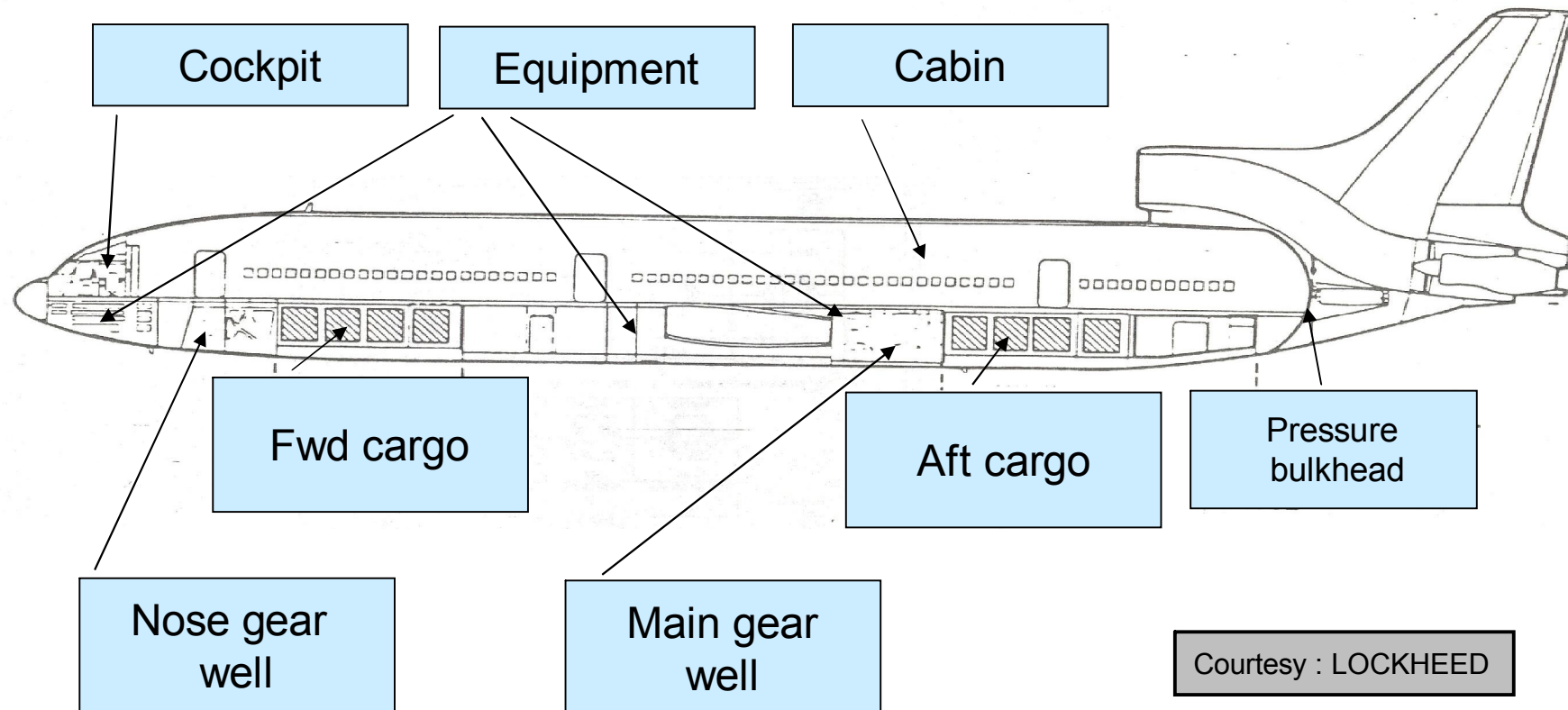
LATCH – BY - LIFT mechanism

- Swivel of the handle lifts the door free from the stops

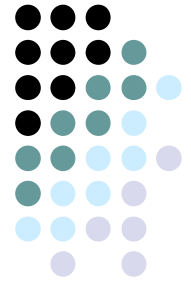


Fuselage General Arrangement

➤ **INBOARD PROFILE** visualizes arrangement of fuselage inventory



Conclusion



Fuselage design meets the requirements for

Payload containment (PAX and / or cargo)

- Ergonomics
- Environment
- Stowage

Leverage for tail control surfaces

- Weight minimum

Aerodynamics

- Drag minimum

References .

- J. ROSKAM : Airplane design
- M. NIU : Airframe structural design
- K. Engmann : Technologie des Flugzeuges
- N. N. : Dornier publications
- N. N. : Airbus publications
- N. N. : Lockheed publications

Dieter Scholz

Chapter 7

Wing Design

7 Wing design

During the preliminary sizing, the wing was merely described in terms of the *wing area* S_w and the *wing aspect ratio* A_w . When designing the wing, other wing parameters are determined. This involves the definition of the *wing section* and the *planform*.

7.1 Wing Parameters

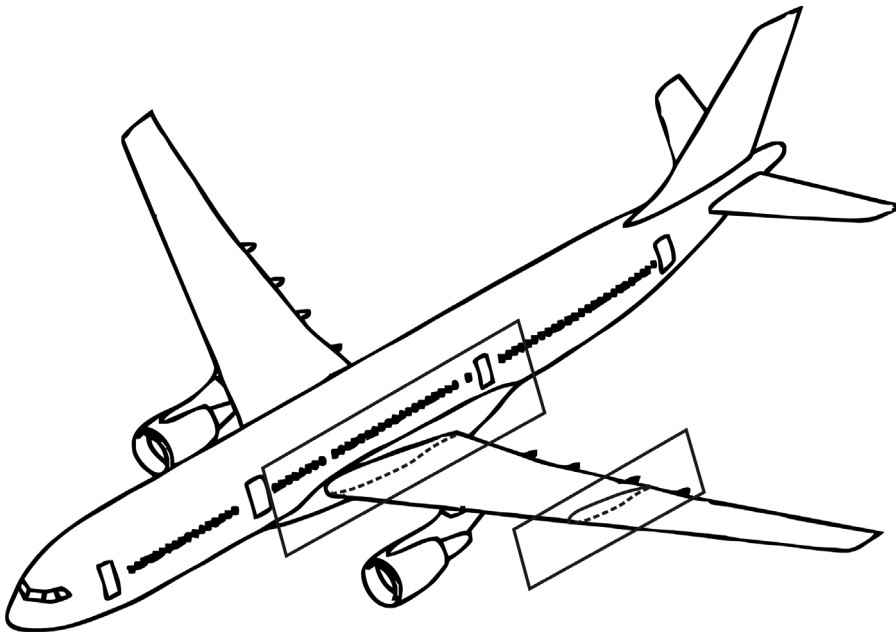


Fig. 7.1
Definition of the wing sections

Wing sections are positioned parallel to the plane of symmetry of the aircraft (**Fig. 7.1**). A wing section is produced by scaling up an airfoil section. The *airfoil section* is described by the section coordinates of the top of the section $y_u = f(x)$ and the bottom of the section $y_l = f(x)$ with $0 \leq x \leq 1$. Sections can also be described by the *thickness distribution* $t = f(x)$ combined with the *camber* $y_c = f(x)$. **Fig. 7.2** contains additional parameters for describing the section geometry:

Chord	c
Thickness	t
Camber	$(y_c)_{max} / c$
Position of maximum thickness	x_t
Position of maximum camber	$x_{(y_c)_{max}}$
Leading edge radius	r
Trailing edge angle	Φ_{TE}

Fig. 7.2 also defines the following:

Chord line

(Mean) camber line

Leading edge LE

Trailing edge TE

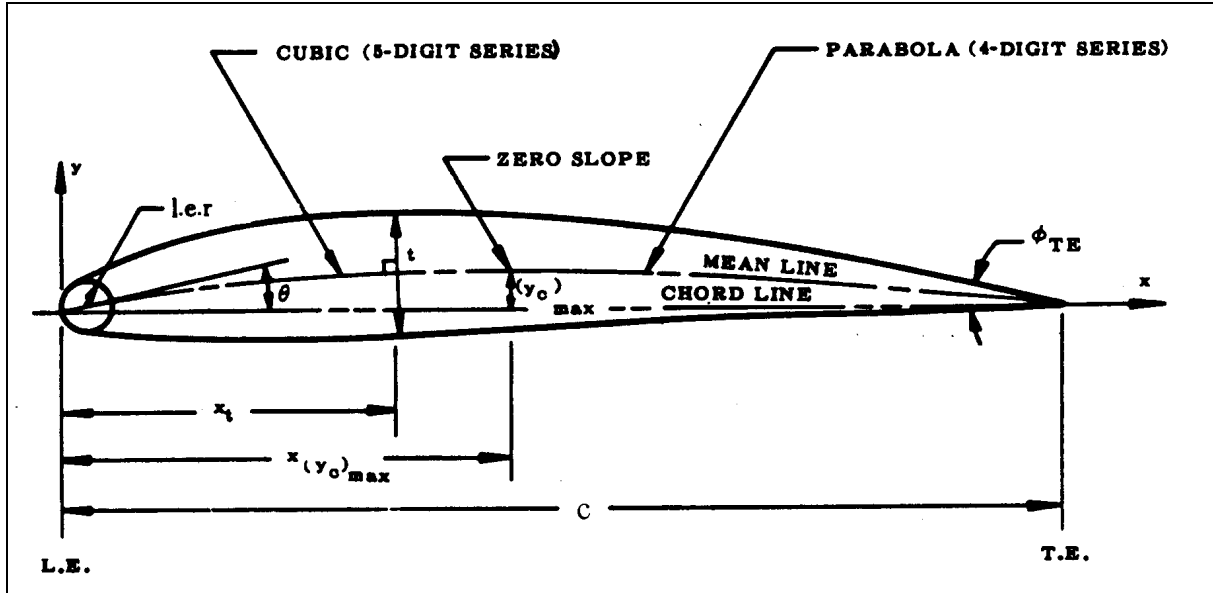


Fig. 7.2: Airfoil geometry (DATCOM 1978)

For simplicity of production, planforms with a curved leading and trailing edge are rare. Wings can therefore very often be described as double tapered wings (Fig. 7.3). The simple tapered wing and the rectangular wing can be seen as special versions of the double tapered wing. The sweep angle ϕ depends on the % line¹ on which it is measured. Normally the sweep angle of the leading edge ϕ_{LE} , trailing edge ϕ_{TE} , 25% line ϕ_{25} (quarter chord sweep) and 50% line ϕ_{50} are stated.

The point where the inner and outer taper meet is called the kink. At this *kink*, the local chord is called c_k . In contrast to the chord at the *wing tip* c_t , a chord does not actually exist on the *wing root* c_r , but is only created by graphically extending the leading and trailing edge as far as the plane of symmetry – and therefore into the fuselage. The *mean aerodynamic chord* c_{MAC} is the chord of an equivalent untwisted, unswept rectangular wing that achieves the same lift and the same pitching moment as this wing. The *aerodynamic center*, *AC* lies on the mean aerodynamic chord. The aerodynamic center is characterized by the following feature: if we

¹ n% point: point on a local chord that is located n% of the local chord behind the leading edge.

n% line: line formed by the geometric locations of the n% points of the chords.

Note: In this case “n%” is replaced by a percentage (e.g. 25%) or another figure symbolizing the percentage (e.g. $c/4$).

take an axis that is perpendicular to the plane of symmetry of the aircraft and passes through the aerodynamic center, the pitching moment of the wing about this axis is constant and independent of the lift. The position of the aerodynamic center X_{AC} on a rectangular wing with a thin symmetrical section is $0.25 \cdot c_{MAC}$. **Torenbeek 1988** (Fig. E10) contains details of the position of the aerodynamic center on simple tapered wings.

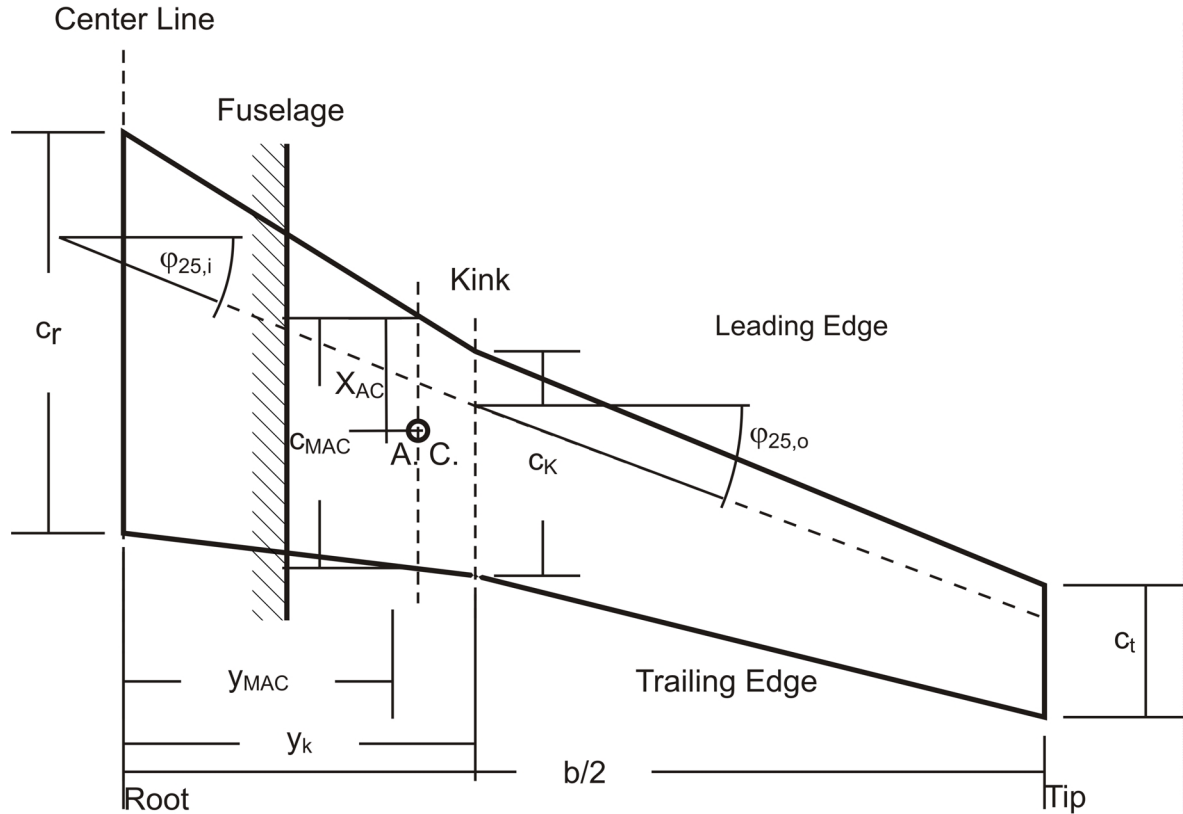
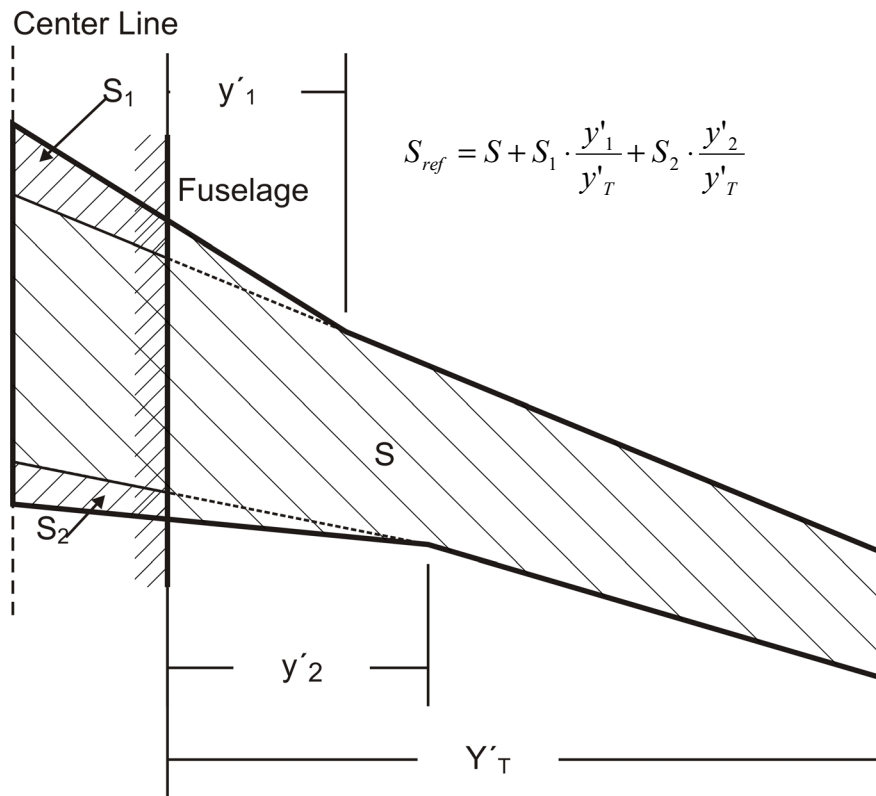


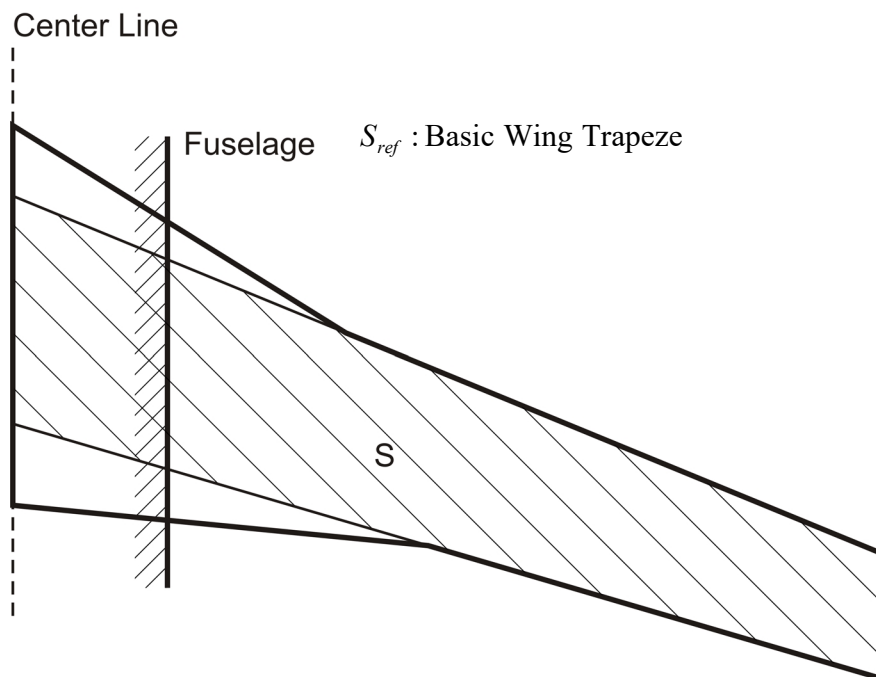
Fig. 7.3 Geometry of the double tapered wing

Wing area S_w does not just include the visible part of the wing. The wing area also includes the area of the inner taper in the fuselage. The exact size of the wing area is not really important. All that is needed for the calculations is a standard reference wing area S_{ref} . Why is this? Let's take a look at the calculation for lift in cruise flight, for example: $m \cdot g = L = 1/2 \rho v^2 \cdot C_L \cdot S_{ref}$. If S_{ref} is changed, only the lift coefficient C_L changes (by definition). For this reason, aircraft manufacturers often use their own in-house definition of the (reference) wing area. **Fig. 7.4** and **Fig. 7.5** show such differing definitions of the wing area.

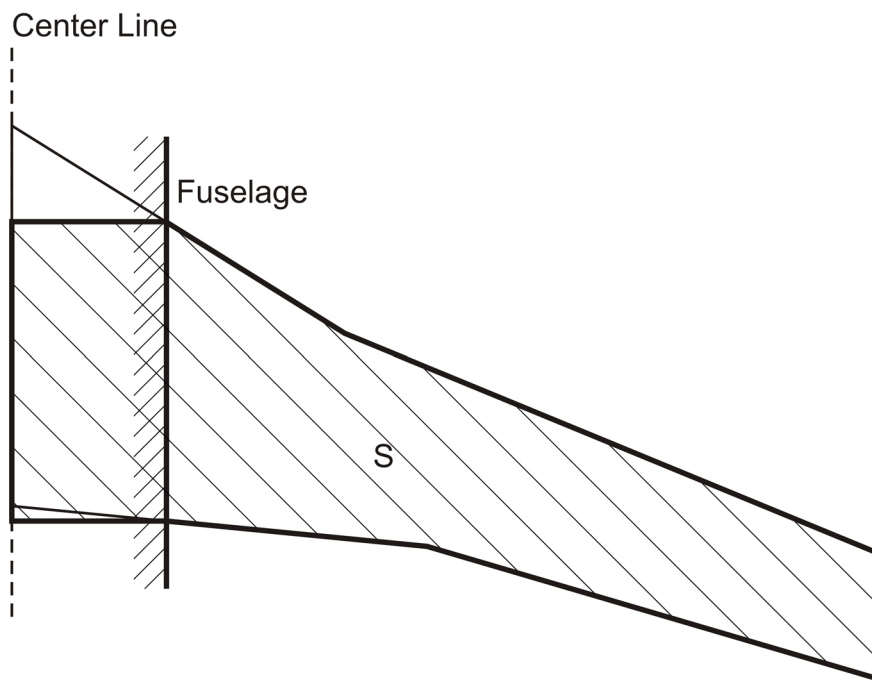
**Fig. 7.4**

a)
Definition of the reference wing area according to Boeing.

Note: The Boeing B-747 has a different definition of the reference wing area: $S_{ref} = S$



b)
Definition of the reference wing area according to Fokker and McDonnell Douglas

**Fig. 7.5**

Definition of the reference wing area according to Airbus

Wing parameters in aircraft design

The following have **already been determined** (to a large extent) (see Section 5):

- Wing area S_w
- Wing aspect ratio A_w .

When searching for a suitable aircraft configuration (see Section 4) consideration was already given to transmitting the forces from the wing to the fuselage by means of the following configuration:

- cantilever wing
- braced wing

and to the position of the wing in relation to the fuselage

- low wing position
- mid wing position
- high wing position

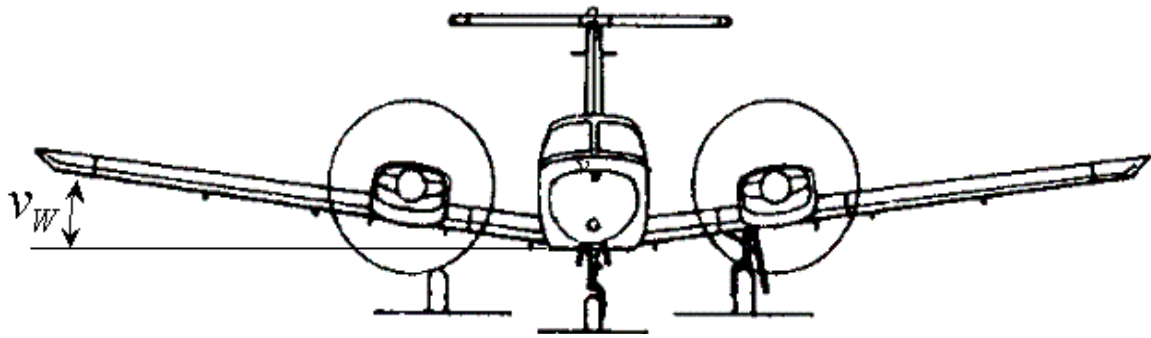


Fig. 7.6 (Positive) dihedral angle of the wing v_W

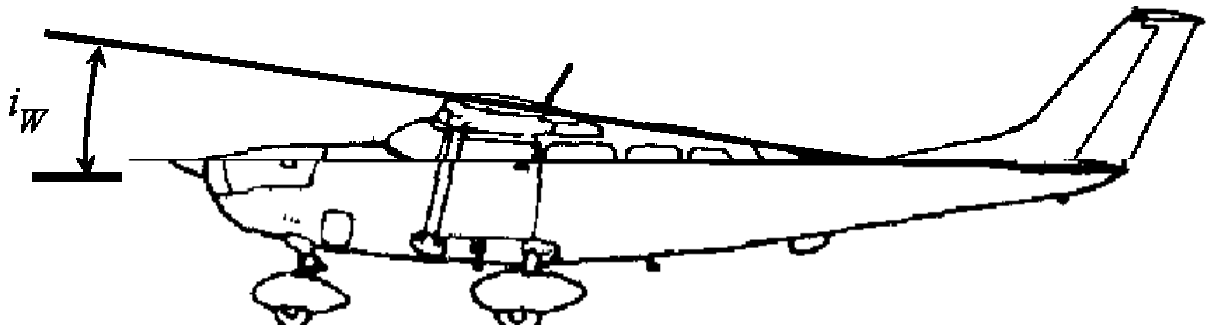


Fig. 7.7 (Positive) incidence angle i_W : angle between the chord line of the wing root and a reference line of the fuselage (e.g. cabin floor)

The following still have **to be determined** (here in Section 7):

Taper ratio, λ_W

Sweep angle, $\phi_{25,W}$

Thickness ratio, $(t/c)_W$

Airfoils

Dihedral angle, v_W (**Fig. 7.6**)

Incidence angle, i_W (**Fig. 7.7**)

Wing twist, ε_t (**Fig. 7.8**)

Subsections 7.2 and 7.3 below contain equations and estimates for these parameters. It is important to compare and check the calculation results with the values from the aircraft statistics. Tables with wing parameters are, for example, included in **Roskam II** (Section 6) and **Torenbeek 1988** (Section 7). Further comprehensive information can be found in “Jane's All The World's Aircraft” (**Lambert 1993**).

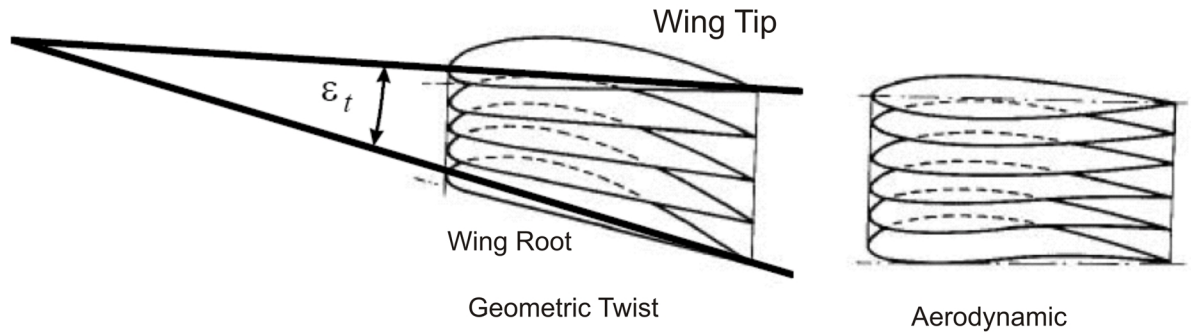


Fig. 7.8 Wing twist ε_t . The twist shown in the diagram is negative. There are two types of wing twist:

- 1.) Geometric twist:
change in the angle between the chord lines.
- 2.) Aerodynamic twist:
change in the zero-lift line along the span of an airfoil.
The diagram shows the typical case of reduced lift at the wing tip, i.e. “wash out”.
The opposite effect is called “wash in”.

The following must be **taken into account** when choosing parameters:

- Take-off/landing: maximum lift coefficient, required high lift systems, lift-to-drag ratio, attitude, lift curve slope $dC_L / d\alpha$
- Cruise: lift-to-drag ratio L/D , drag divergence Mach number M_{DD} , buffet onset boundary
- Fuel tank volume
- Flight characteristics, stalling behavior, flight in turbulence
- Landing gear actuation and stowage
- Wing mass
- Production costs

These characteristics, which depend on the choice of the above-mentioned wing parameters, are discussed in Subsection 7.3.

Definitions

Aspect ratio

$$A = \frac{b^2}{S} \quad , \quad (7.1)$$

with Span b .

Mean aerodynamic chord

$$c_{MAC} = \frac{2}{S} \int_0^{b/2} c^2 dy \quad , \quad (7.2)$$

Area

$$S = 2 \int_0^{b/2} c \, dy \quad , \quad (7.3)$$

Spanwise location of mean aerodynamic chord

$$y_{MAC} = \frac{2}{S} \int_0^{b/2} c \cdot y \, dy \quad . \quad (7.4)$$

with y spanwise location.

Relative span position

$$\eta = \frac{y}{b/2} \quad , \quad (7.5)$$

Taper ratio

$$\lambda = \frac{c_t}{c_r} \quad , \quad (7.6)$$

The following additionally applies to double tapered wings:

on the inner wing (index: i) $\lambda_i = \frac{c_k}{c_r} \quad , \quad (7.7)$

on the outer wing (index: o) $\lambda_o = \frac{c_t}{c_k} \quad . \quad (7.8)$

Equations for the geometry of the simple tapered wing

$$A = \frac{b^2}{S} = \frac{2b}{c_r(1+\lambda)} \quad , \quad (7.9)$$

$$c_{MAC} = \frac{2}{3} c_r \frac{1+\lambda+\lambda^2}{1+\lambda} \quad , \quad (7.10)$$

$$S = \frac{b}{2} c_r (1+\lambda) \quad , \quad (7.11)$$

$$\frac{y_{MAC}}{b/2} = \frac{1 - \frac{c_{MAC}}{c_r}}{1 - \lambda} = \frac{1}{3} \left(\frac{1+2\lambda}{1+\lambda} \right) \quad , \quad (7.12)$$

Conversion of the sweep of an $m\%$ line to the sweep of an $n\%$ line (m and n are the % values):

$$\tan \varphi_n = \tan \varphi_m - \frac{4}{A} \left[\frac{n-m}{100} \cdot \frac{1-\lambda}{1+\lambda} \right] . \quad (7.13)$$

Equations for the geometry of the double tapered wing

$$A = \frac{b^2}{S} = \frac{2b}{c_r [(1-\lambda) \cdot \eta_k + \lambda_i + \lambda]} , \quad (7.14)$$

with

$$\eta_k = \frac{y_k}{b/2} .$$

$$c_{MAC} = \frac{c_{MAC,i} \cdot S_i + c_{MAC,o} \cdot S_o}{S} , \quad (7.15)$$

$$S = S_i + S_o = \frac{b^2}{A} = \frac{b}{2} c_r [(1-\lambda) \cdot \eta_k + \lambda_i + \lambda] , \quad (7.16)$$

$$y_{MAC} = \frac{y_{MCA,i} \cdot S_i + (y_k + y_{MAC,o}) \cdot S_o}{S_i + S_o} . \quad (7.17)$$

Please note: The index $()_w$ for wing was omitted in equations 7.1 to 7.16 because the equations are thus also applicable to a horizontal tailplane. When calculating the geometry of a vertical tailplane, it is important to take into account that the tailplane only consists of half the area. Thus, for example, equation (7.3) can be used to produce the definition for the area of the vertical tailplane S_V :

$$S_V = \int_0^{b/2} c \, dy . \quad (7.17)$$

7.2 Basic Principle and Design Equations

Pressure coefficient

The flow configurations around an airfoil are shown with the aid of the pressure coefficient (see Fig. 7.12). The **pressure coefficient** is defined as

$$c_p = \frac{p - p_\infty}{q_\infty} . \quad (7.18)$$

The index “ ∞ ” refers to a parameter of the free flow (undisturbed by the airfoil section). By definition: $q_\infty = \frac{1}{2} \rho V_\infty^2$ and for incompressible flow (Bernoulli) $p_\infty + \frac{1}{2} \rho V_\infty^2 = p + \frac{1}{2} \rho V^2$ hence $p - p_\infty = \frac{1}{2} \rho (V_\infty^2 - V^2)$. With the local *super velocity* $v = V - V_\infty$

$$c_p = \frac{\frac{1}{2} \rho \cdot (V_\infty^2 - V^2)}{\frac{1}{2} \rho V_\infty^2} = 1 - \left(\frac{V}{V_\infty} \right)^2 \approx -\frac{2 \cdot v}{V_\infty} . \quad (7.19)$$

The approximation (\approx) applies for v much smaller than V_∞ . The local velocity at the airfoil is

$$V = V_\infty \cdot \sqrt{1 - c_p} . \quad (7.20)$$

For compressible flow, the equation is as follows, with the ratio of specific heats γ :

$$c_p = \frac{2}{\gamma \cdot M} \left[\left(\frac{2 + [\gamma - 1] \cdot M_\infty^2}{2 + [\gamma - 1] \cdot M^2} \right)^{\frac{\gamma}{\gamma - 1}} - 1 \right] \approx -\frac{2 \cdot v}{V_\infty} . \quad (7.21)$$

The derivation and background to equation (7.21) can be found e.g. in **Anderson 1991**.

Mach number correction

From a flow speed of approximately $M = 0.3$, it is necessary to correct coefficients such as c_p , c_L , c_D . This can be done with the aid of the Prandtl-Glauert compressibility correction, as is shown here using the example of the pressure coefficient:

$$c_p = \frac{c_{p,M=0}}{\sqrt{1 - M_\infty^2}} . \quad (7.22)$$

The **Mach number correction factor according to Prandtl-Glauert** is therefore $\frac{1}{\sqrt{1 - M_\infty^2}}$,

but it only applies to

- 2-dimensional flow (i.e. for airfoils),
- thin airfoil sections,
- small angles of attack,
- pure subsonic flow, i.e. for $M < M_{crit}$. (See below for a definition of M_{crit}).

Despite these restrictions, the Mach number correction according to Prandtl-Glauert is often used as the first approximation.

Lift curve slope

The lift curve slope gives the increase in the lift coefficient with the angle of attack

$$C_{L,\alpha} = \frac{dC_L}{d\alpha} . \quad (7.23)$$

The **lift curve slope of a wing** is calculated here according to **DATCOM 1978** (Section 4.1.3.2). Corrections will be necessary for the combination of wing-fuselage and wing-fuselage-empennage. $C_{L,\alpha}$ is calculated from the equation in 1/radian [1/rad].

$$C_{L,\alpha} = \frac{2 \cdot \pi \cdot A}{2 + \sqrt{\frac{A^2 \cdot \beta^2}{\kappa^2} \cdot \left(1 + \frac{\tan^2 \varphi_{50}}{\beta^2}\right) + 4}} \quad (7.24)$$

β is the reciprocal of the Mach number correction factor

$$\beta = \sqrt{1 - M^2} \quad (7.25)$$

and

$$\kappa = \frac{C_{L,\alpha}}{2\pi / \beta} . \quad (7.26)$$

Some authors use $\kappa = 1$ for simplicity's sake and obtain the following from equation (7.24)

$$C_{L,\alpha} = \frac{2 \cdot \pi \cdot A}{2 + \sqrt{A^2 \cdot (1 + \tan^2 \varphi_{50} - M^2) + 4}} . \quad (7.27)$$

In equation (7.26) for equation (7.24), $c_{L,\alpha}$ is the **lift curve slope of the airfoil section**. $c_{L,\alpha}$ can be estimated from

$$c_{L,\alpha} = \frac{1.05}{\beta} \cdot \left[\frac{c_{L,\alpha}}{(c_{L,\alpha})_{theory}} \right] \cdot (c_{L,\alpha})_{theory} \quad (7.28)$$

with data from **Fig. 7.9** and with the theoretical lift curve slope of the airfoil

$$(c_{L,\alpha})_{theory} = 2 \cdot \pi + 4.7 \cdot (t/c) \cdot [1 + 0.00375 \cdot \Phi_{TE}] \quad (7.29)$$

In equation (7.29), Φ_{TE} is the trailing edge angle according to Fig. 7.2 in degrees. Equation (7.29) gives the result $(c_{L,\alpha})_{theory}$ in 1/radian [1/rad].

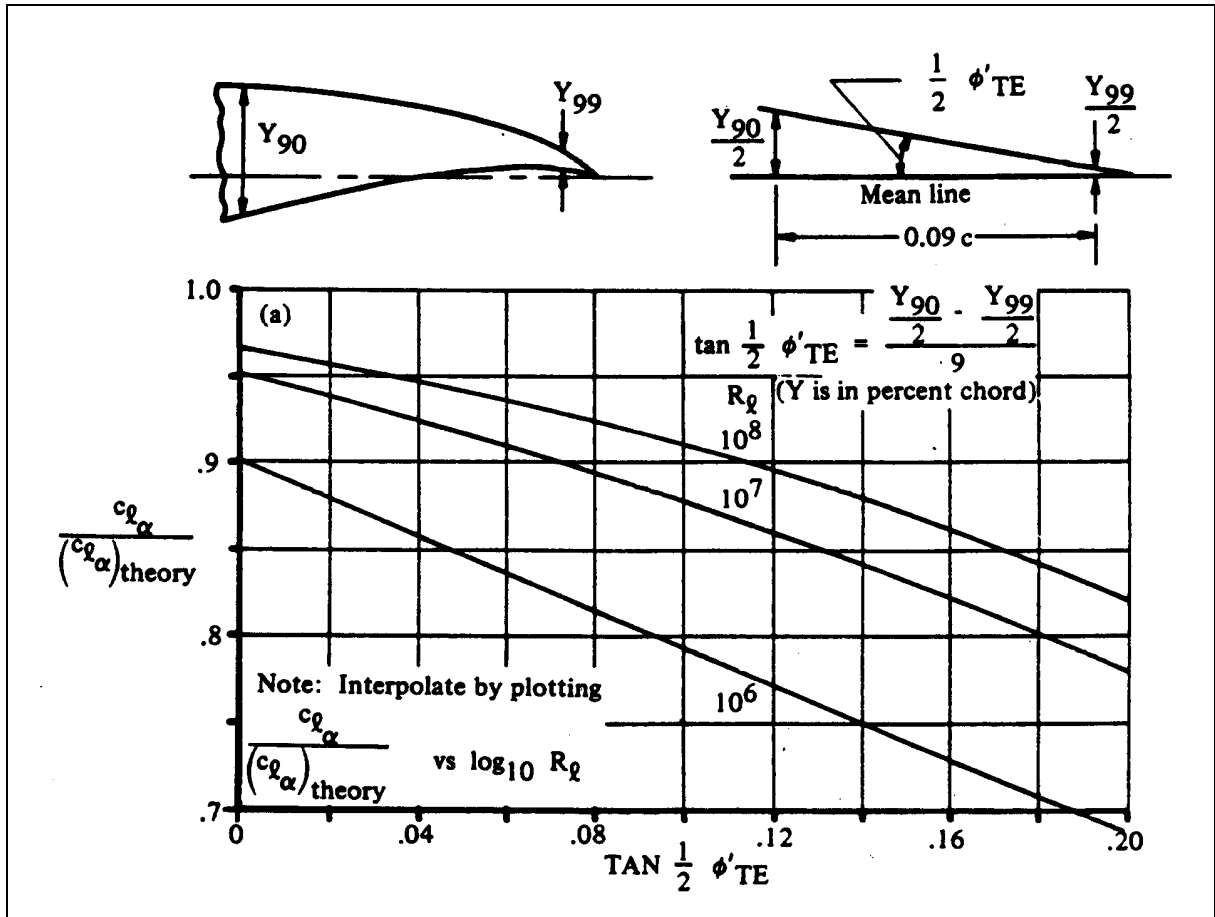


Fig. 7.9 Calculating the lift curve slope of an airfoil section according to **DATCOM 1978**

Critical Mach number and shock wave

If the flight Mach number M is increased to close to $M = 1$, the **flow speed** in the vicinity of the airfoil will at some point **exceed the speed of sound** (i.e. exceed $M = 1$). The flight Mach number achieved at this point is called the *critical Mach number* M_{crit} . The critical Mach number is smaller than 1 because, due to the super velocities v , the local flow speeds may be higher than the airspeed. According to equation (7.21), one would expect the super velocities to occur where there are negative pressure coefficients – i.e. on the suction or upper surface of the airfoil. After the critical Mach number has been exceeded a localized area with $M > 1$ appears first on the upper surface of the airfoil and only later on the lower surface as well (see **Fig. 7.10**). As this local flow $M > 1$ finally recombines with the free stream behind the airfoil, it has to be reduced to $M < 1$ again at some point. This reduction involves an increase in pressure. A *shock wave* occurs. In the shock wave, the local Mach number drops from an initial value of $M > 1$ to a value of $M < 1$. The shock wave leads to an **increase in the drag and to the separation of the boundary layer**. As the Mach number increases, the shock waves above and below the airfoil section move more and more to the rear. If the flow speeds increase even further, the shock waves are finally located at the end of the airfoil section and form the so-called “wake”.

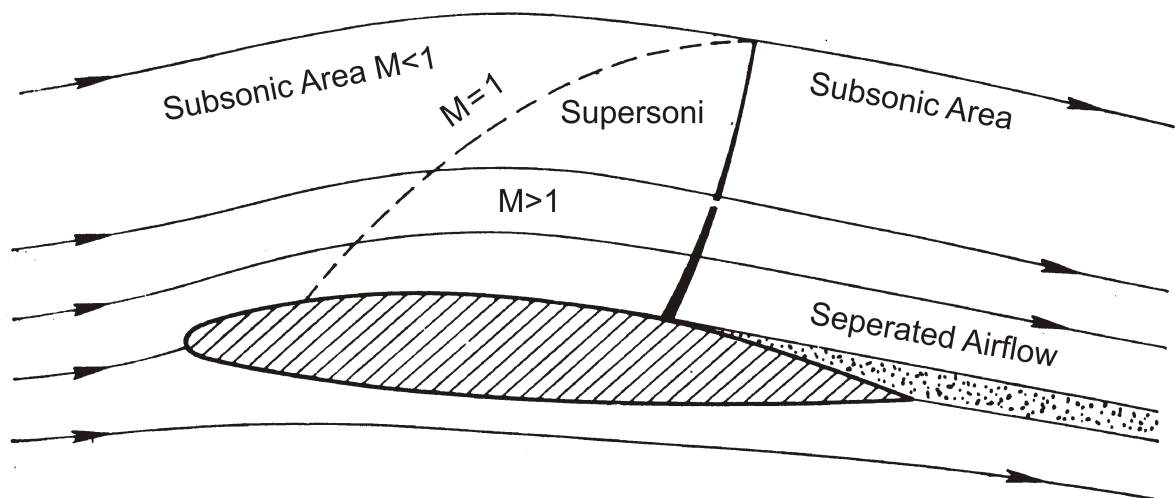


Fig. 7.10 Airfoil section subjected to subsonic flow speed $M_{crit} < M < 1$. After the flow has passed through the supersonic area, the flow is then decelerated in the shock wave from a local speed $M > 1$ to a speed $M < 1$

Drag divergence Mach number

The parameters of a wing must be chosen so as to ensure that the drag increase of the aircraft is not too high at the required cruise Mach number M_{CR} . As the Mach number increases, the critical Mach number M_{crit} will first be reached. This is the flight Mach number where the speed of sound occurs locally at the wing for the first time (see above). The drag divergence

Mach number M_{DD} is – according to a definition applied by Airbus and Boeing – the Mach number where the wave drag (that is the additional drag due to Mach effects) amounts to 0.0020. M_{DD} is larger than M_{crit} . How much bigger depends on the type of airfoil section. Typically, M_{DD} is 0.08 Mach higher than the critical Mach number M_{crit} (**Raymer 1989**).

The increase in drag, caused by the wave drag, is shown in **Fig. 7.11**. At $M = 1.0$, the drag is only approximately half as big as at $M = 1.2$ or at $M = 1.05$. The wave drag at $M = 1.05$ is approximately as big as the wave drag at $M = 1.2$.

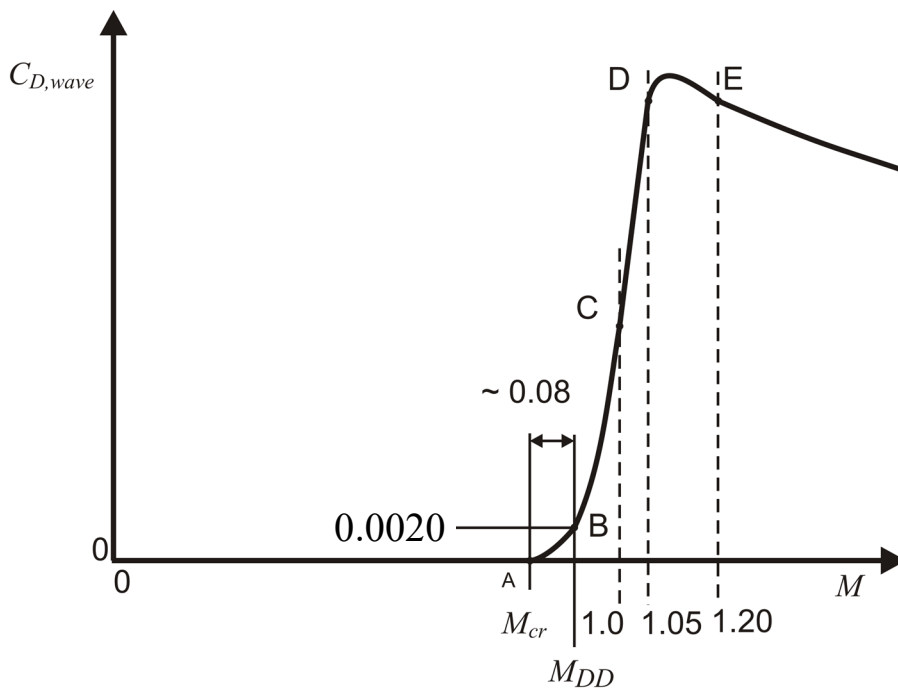


Fig. 7.11
A typical progression of the wave drag $C_{D,wave}$ as a function of the flight Mach number M

The drag divergence Mach number M_{DD} rises with

- decreasing lift coefficient C_L ,
- decreasing relative thickness (t/c) ,
- increasing leading edge radius,
- increasing sweep ϕ .

Transonic airfoils

Special transonic airfoils (called “supercritical airfoil” by NASA) increase the cruise Mach number or allow the use of a larger relative thickness. Through a larger relative thickness, the wing weight can be reduced and therefore, at the end of the day, the operating costs are also cut.

During the Second World War, airfoils were already being developed with a view to increasing the critical Mach number. In particular, **NACA 6-series sections (Abbott 1959)** showed improvements in the drag increase at high Mach numbers without having too detrimental an effect on the slow flight characteristics. These airfoils were used in the first generation of subsonic jet aircraft, such as for the Caravelle.

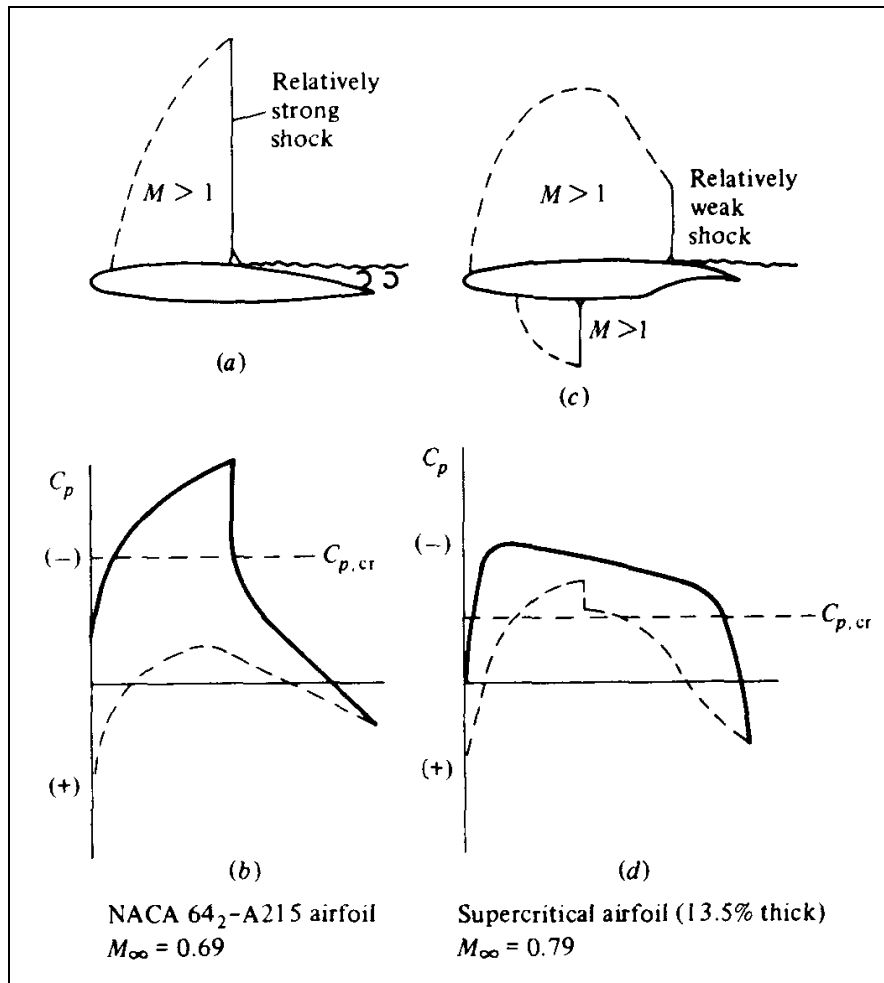
The first airfoils for the supercritical area were the **sections with peaky pressure distribution** from PEARCY in England. It was already known that by means of thinner sections, M_{crit} could be increased. The idea was to increase the distance between M_{crit} and M_{DD} . This was achieved by a virtually isentropic pressure increase prior to a weak shock wave. The drag increase could thereby be delayed by $M = 0.02$ to 0.03 compared to the airfoils of the NACA 6 series. This type of airfoil was used, for example, in the BAC 1-11, VC-10 and DC-9.

At the start of the sixties, WHITCOMB at NASA was working on **supercritical sections**. His work still forms the basis for the airfoils used in civil transports and business jets.

Fig. 7.12 compares a conventional airfoil with a supercritical airfoil. With the conventional airfoil, the flow on the upper surface of the airfoil section is accelerated even more after the speed of sound has been exceeded locally, so that a strong shock wave is created approximately in the middle of the airfoil. Due to the strong increase in pressure in the shock wave, separation of the flow occurs with a large increase in drag and stochastic force fluctuations on the wing. This phenomenon is called buffeting. On the other hand, in the case of the supercritical airfoil, a uniform supercritical distribution of pressure occurs at a lower level, which is concluded by a weaker shock wave in the rear section of the airfoil.

Supercritical airfoils differ from conventional airfoils in the following ways:

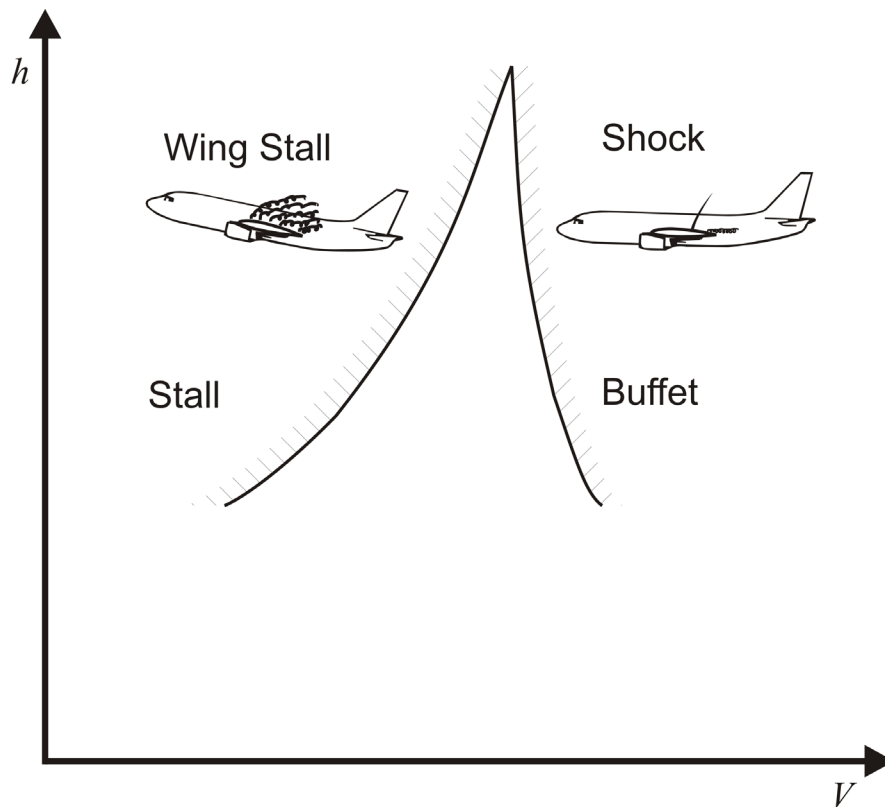
1. The **upper surface of the airfoil is only slightly curved in the middle section**. Therefore the low pressure, and thus also the flow speed, is reduced, so that the shock wave is shifted to the trailing edge and the intensity of the impact shock can be reduced.
2. The **lower surface of the airfoil has a concave curvature in the rear section** with a so-called S shock. This produces a greater increase in pressure, which increases the lift with the same angle of attack and therefore allows a reduced angle of attack for the required lift, thus taking the strain off the upper surface of the airfoil (rear loading). The rear loading, however, leads to a not insignificant pitching moment, which must be compensated for by correspondingly larger empennages.
3. The **leading edge radius of the section is increased** to avoid excessive super velocities.
4. The **airfoil leading edge** may also be curved downward somewhat. This means that acceptable lift coefficients can be achieved in slow flight – despite the disadvantage of having only a slight curvature in the middle section of the airfoil.

**Fig. 7.12**

Standard airfoil of the NACA 6 series compared to a supercritical airfoil at cruise Mach number (Andersen 1991)

High-altitude flight and buffet onset boundary

At high altitudes the speed of sound is low, and therefore the Mach number is high for a given airspeed. Due to the low air density, a high lift coefficient and a high angle of attack are necessary. A flight in gusty air or with maneuvers such as a turn requires still higher lift coefficients and angle of attack. In doing so, the aircraft may **stall** (the aircraft is too *slow*). On the other hand, the Mach number may be too high for the required lift coefficient, so that **buffeting** occurs (the aircraft is too *fast*). As shown in **Fig. 7.13**, the usable speed range becomes more and more limited as the altitude increases. When designing the wing, this phenomenon must be taken into account. It is important to ensure that a usable airspeed range is retained at cruise altitude.

**Fig. 7.13:**

Stall boundary and buffet boundary. The usable speed range becomes smaller as the altitude increases

The certification regulations contain the following requirements:

CS 25.251**Vibration and buffeting**

- (b) Each part of the aeroplane must be shown in flight to be **free from excessive vibration**, under an appropriate speed and power conditions **up to** at least the minimum value of **VD** allowed in CS 25.335.
- ...
- (d) There may be **no perceptible buffeting** condition in the cruise configuration in straight flight at any speed **up to VMO/MMO** ...

ACJ 25.1585(c)**Cruise Maneuvering Capability**

... it is possible to achieve a positive normal **acceleration increment of 0.3 g** without exceeding the **buffet onset** boundary ...

In cruise flight up to V_{MO} (maximum operating limit speed) or M_{MO} (maximum operating limit Mach number) with a load factor of 1.3g, no buffeting may occur. Up to V_D (design diving speed) or M_D (design diving Mach number) (M_D is approximately 0.05 to 0.09 above M_{MO}) acceptable flying characteristics must be retained. Buffeting is, however, allowed. Unfortunately, there is no simple way to calculate the buffet onset boundary.

Calculation of wing parameters from the design Mach number

Airbus and **Boeing** use the following design Mach number (= cruise Mach number)

$$M_{design} = M_{CR} :$$

$M_{DD} = M_{CR} \quad (7.30)$

and thereby obtains (by definition, see above) a wave drag of 0.002.

There are certainly other possibilities to place M_{DD} with respect to M_{CR} . **Obert 1997** (reporting from experience at **Fokker**) recommends setting the cruise Mach number so as to achieve a wave drag of 0.0015. If we bear in mind that $M_{DD} = M_{crit} + 0.08$ (see Fig. 7.11), roughly the following applies:

$$M_{DD} \approx M_{CR} + 0.02.$$

As we can see, to some extent it is up to the design engineer to set the drag divergence Mach number M_{DD} in relation to the required cruise Mach number M_{CR} .

The **effective Mach number** and **effective speed** for a swept wing are according to the geometric considerations and the **cosine rule** from Fig. 7.14:

$$V_{eff} = V \cdot \cos \phi_{25} \quad \text{and} \quad M_{eff} = M \cdot \cos \phi_{25}$$

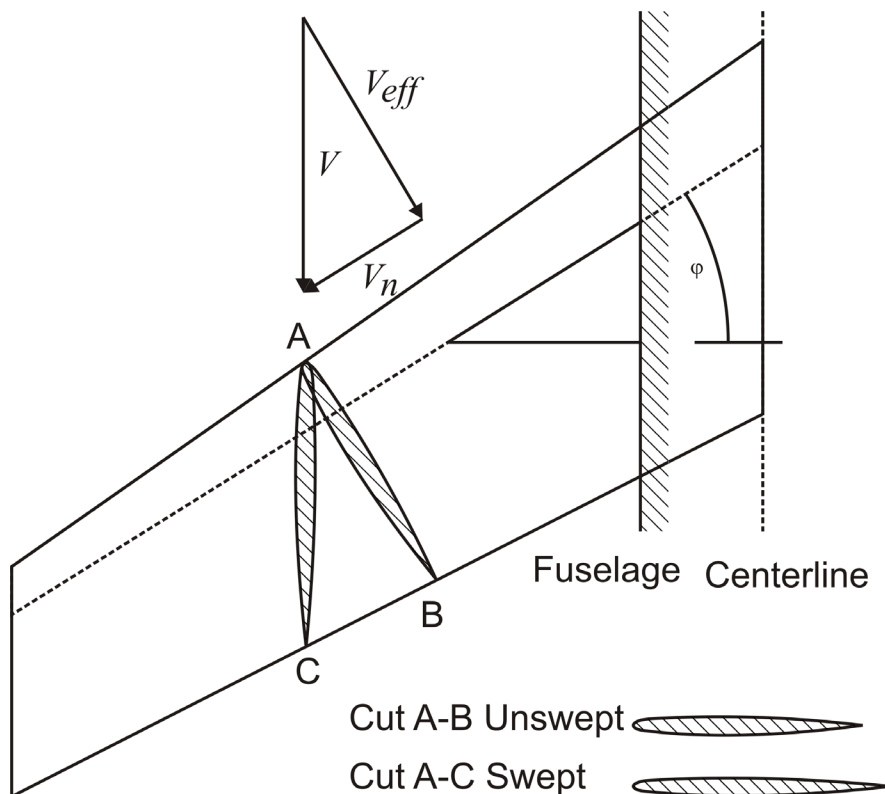


Fig. 7.14:

Decomposition of the vector V of the flow speed into an effective component perpendicular to the wing (index: eff) and a component along the wing quarter chord line (index: n)

Furthermore it is

$$\begin{aligned}c_{eff} &= c \cdot \cos \varphi_{25} \quad , \\t_{eff} &= t \quad , \\(t/c)_{eff} &= (t/c) / \cos \varphi_{25} \quad .\end{aligned}$$

However, experience has shown that sweep does not enable the effective Mach number to be reduced as much as the geometric considerations would lead one to assume. Therefore the following general equation is used:

$$M_{eff} = M \cdot (\cos \varphi_{25})^x \quad . \quad (7.31)$$

The cosine rule corresponds to $x = 1.0$

STAUFENBIEL suggests: $x = 0.75$.

Torenbeek 1988 and many other authors suggest: $x = 0.5$.

If we stick with **Torenbeek 1988** and $x = 0.5$, then the following also applies:

$$M_{DD,eff} = M_{DD} \cdot \sqrt{\cos \varphi_{25}} \quad . \quad (7.32)$$

Bearing in mind that $(t/c) = (t/c)_{eff} \cdot \cos \varphi_{25}$ applies, according to **Torenbeek 1988** the maximum permissible relative thickness of an airfoil parallel to the aircraft's plane of symmetry is as follows:

$$(t/c) = 0.3 \cdot \cos \varphi_{25} \cdot \left(\left[1 - \left(\frac{5 + M_{DD,eff}^2}{5 + (k_M - 0.25 \cdot C_L)^2} \right)^{3.5} \right] \cdot \frac{\sqrt{1 - M_{DD,eff}^2}}{M_{DD,eff}^2} \right)^{\frac{2}{3}} \quad (7.33)$$

$k_M = 1.00$	conventional airfoils; maximum t/c at about $0.30c$,
$k_M = 1.05$	high-speed (peaky) airfoils, 1960-1970 technology,
$k_M = 1.12$ to 1.15	supercritical airfoils.
C_L :	the design lift coefficient (for cruise) chosen in Section 5

The calculated t/c applies for an average spanwise position on the wing. **Jenkinson 1999** calculates an average relative thickness from the relative thickness at the tip (t) and root (r) of the wing:

$$t/c = \frac{3(t/c)_t + (t/c)_r}{4} \quad .$$

The accuracy of the calculation (estimation) of relative thickness turns out to be limited with simple equations like (7.33). Further information on calculating the maximum permissible relative thickness of a wing can be found in **Scholz 2005**.

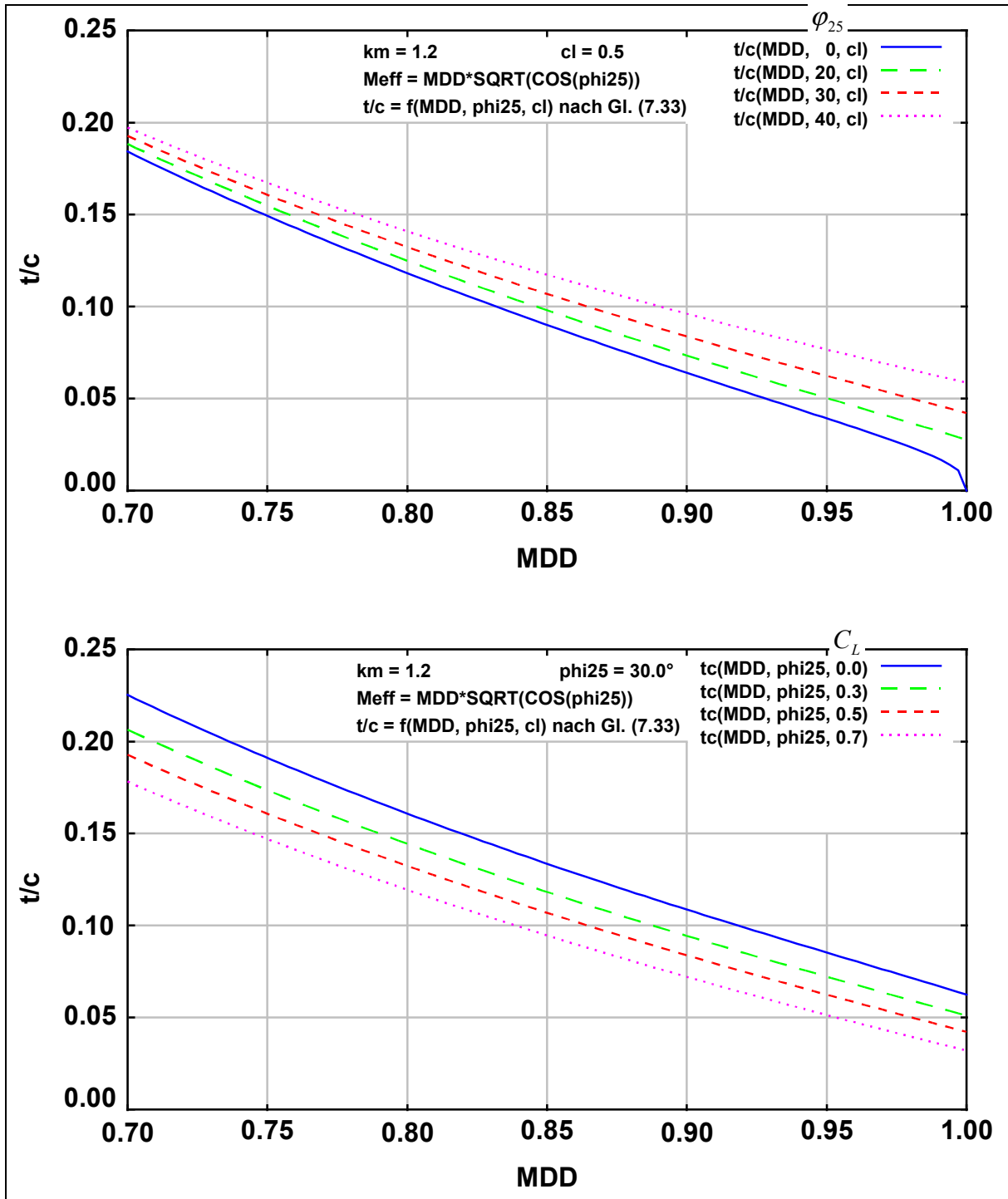


Fig. 7.15 (top) and Fig. 7.16 (bottom)

Influence of drag divergence Mach number M_{DD} on the relative thickness t/c using sweep angle ϕ_{25} (top) and of the design lift coefficient C_L (bottom) as further parameter. Calculated with equation (7.32) and (7.33)

Fig. 7.15 shows the influence of M_{DD} , ϕ_{25} and C_L on t/c . Fig. 7.15 was calculated with equations (7.32) and (7.33).

Winglets and End Plates

The effective aspect ratio can be increased by means of winglets without increasing the span. This can make sense if the span is limited due to the structural specifications of the airfield, hangar or gate. The effective span for a wing with winglets or end plates can be estimated according to **Dubs 1987** with

$$A_{eff} = A / (1 + \delta_E) \quad (7.34)$$

with $(1 + \delta_E)$ from **Fig. 7.18** according to the geometry from **Fig. 7.17**.

Practical note: In Section 5 an aspect ratio was used to determine the glide ratio L/D in cruise configuration. This aspect ratio may now be considered as the effective aspect ratio. (7.34) may now be used to calculate the geometric aspect ratio from

$$A = A_{eff} (1 + \delta_E) \quad .$$

It follows the span from

$$b = \sqrt{A S_W} \quad .$$

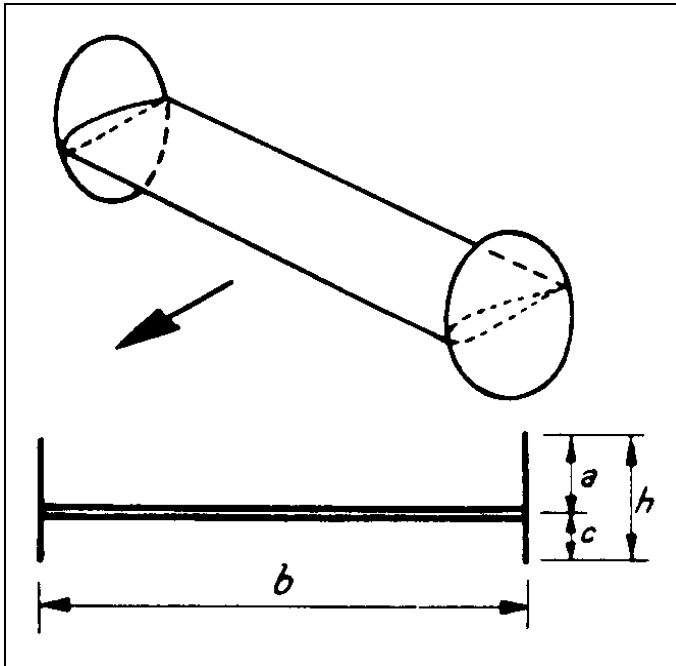
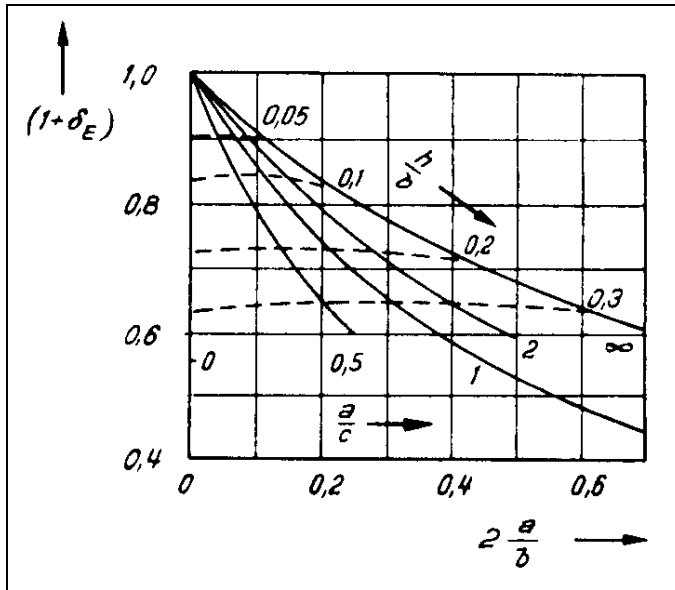


Fig. 7.17

Geometry of a wing with winglets or end plates (**Dubs 1987**)

**Fig. 7.18**

Factor for calculating the effective aspect ratio of a wing with winglets or end plates (Dubs 1987)

Volume of the fuel tank

Torenbeek 1988 specifies a semi-empirical equation for estimating the volume of the fuel tank. This equation is reported to have a degree of precision of $\pm 10\%$.

$$V_{\text{tank}} = 0.54 \cdot S_w^{1.5} \cdot (t/c)_r \cdot \frac{1}{\sqrt{A}} \cdot \frac{1 + \lambda \cdot \sqrt{\tau} + \lambda^2 \cdot \tau}{(1 + \lambda)^2} \quad (7.35)$$

with

$$\tau = \frac{(t/c)_t}{(t/c)_r}.$$

When deriving the equation, it was assumed that a simple tapered wing was involved with a linear thickness distribution. Statistical data was used to calculate the correction factor of 0.54. The sweep has virtually no impact on the tank volume. Equation (7.35) can also be used to calculate the tank volume of a tank that only covers part of the span of the wing. The parameters of the wing root r and the wing tip t then have to be set to the values on the inner and outer end of the tank.

7.3 Flight and Operational Characteristics

Cantilever or braced wing

Braced wings can be constructed so that they are approximately 30% lighter than cantilever wings. However, the struts cause considerable form and interference drag. They are therefore

only used for comparatively slow aircraft (less than approximately 200 kt). An aircraft configuration with joint wings (see Section 4) tries to achieve both advantages simultaneously.

Position of the wing in relation to the fuselage

The optimum position of the wing in relation to the fuselage depends on the type of aircraft use. In the case of a **cargo aircraft**, the emphasis is on ease of loading and unloading. If the aircraft is to be loaded directly from a lorry or by using an on-board ramp, a high-wing aircraft is required. In the case of a **passenger aircraft**, the high-wing offers passengers good visibility. However, landing gear mounted on the wing will be heavy in the case of the high wing aircraft due to its length. Landing gear mounted on the fuselage will require additional drag-inducing fuselage cladding. In most cases, a mid-wing configuration is not possible on passenger and cargo aircraft because it would prevent a continuous free cross section for the cabin or the hold. **Seaplanes** achieve the necessary distance between the wing and the water surface by means of a high wing configuration. For **small aircraft**, no wing position has established itself as the best compromise up to now. In general the following applies:

- A mid-wing configuration creates the least interference drag. (Interference drag is produced by the mutual influence of the airflow over the fuselage and wing).
- The high positioning of the wing has a stabilizing effect around the rolling axis (**Fig. 7.19**), but has a destabilizing influence on Dutch roll. Aft swept wings also have a positive stabilizing effect around the longitudinal axis and a positive dihedral angle. The connections are assessed in the subsection “Dihedral”.

Table 7.1 Summary evaluation of wing position in relation to the fuselage

	High wing	Mid wing	Low wing
Interference drag	average	low	high
Stability around the longitudinal axis	stable	neutral	unstable (requires dihedral for stability)
Visibility from cabin and cockpit ^a	good	average	poor
Landing gear:			
on the wing	long and heavy	-	short and light
on the fuselage	high drag	-	-
Loading	easy	average	requires steps and loading aids

^a Visibility depends on where the wing cuts through the fuselage.

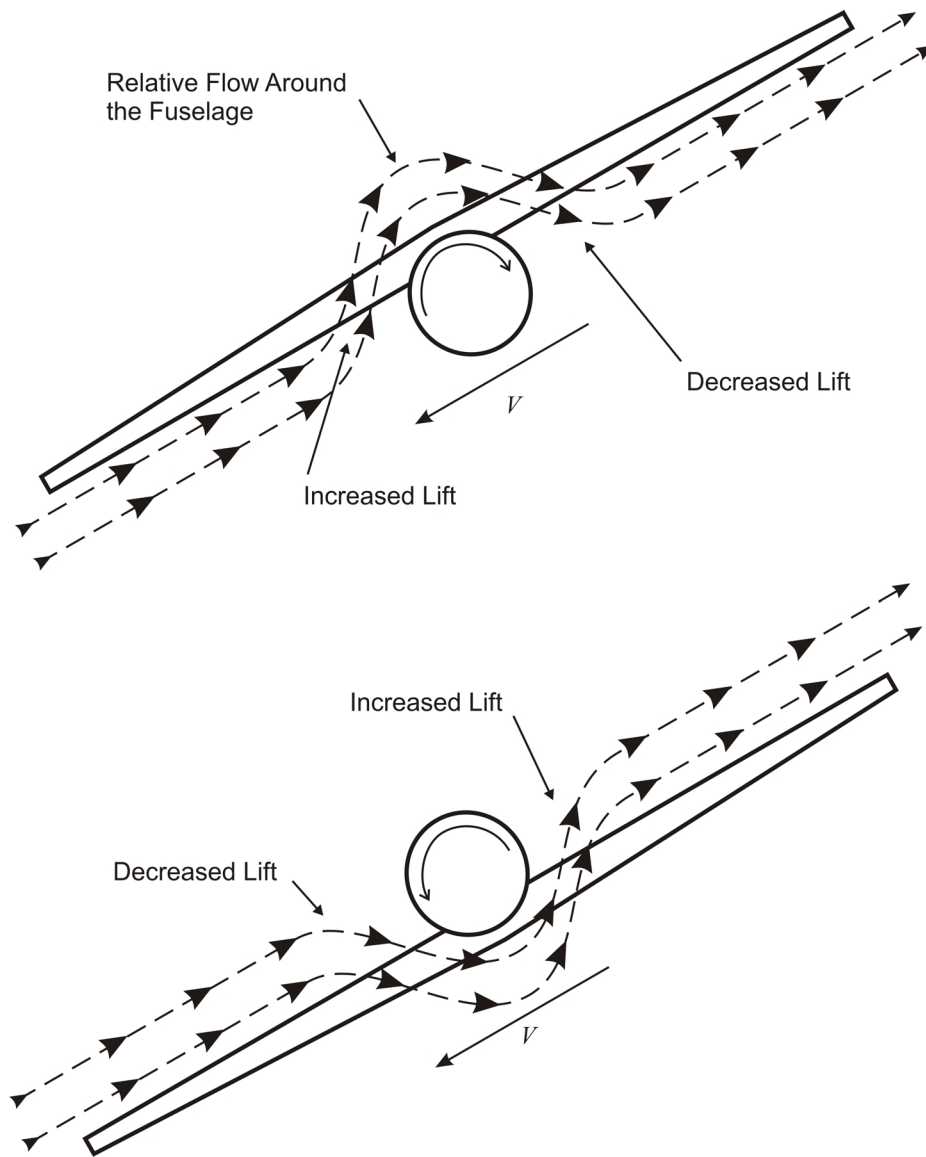


Fig. 7.19 Effect of wing position on roll stability

Wing area and wing loading

The wing area was determined from the requirements to be met by the aircraft in the **preliminary sizing**. Then the smallest possible thrust-to-weight ratio and the smallest possible wing were chosen, and consequently the highest possible wing loading. In doing so, it was assumed that **the larger the area of a wing, the heavier and more expensive it becomes**.

If a specific **approach speed** or a specific **landing distance** is not to be exceeded, the wing area should not be too small.

In the case of a **flight in turbulent air** the aircraft is especially influenced by vertical gusts. These vertical gusts momentarily change the wing's angle of attack. For example, the angle of attack is increased by a vertical gust from below (in addition to the flow acting on the wing due to the airspeed). The aircraft's response to the vertical gust is expressed by the change in the load factor with the angle of attack

$$n_{\alpha} = \frac{dn}{d\alpha} = \frac{1}{m \cdot g} \cdot \frac{dL}{d\alpha} = \frac{\frac{1}{2} \rho v^2 \cdot C_{L\alpha}}{g \cdot \left(\frac{m}{S_w} \right)} . \quad (7.36)$$

Consequently the smaller the wing loading, the more intensely the aircraft reacts to the vertical gust.

The **tank volume** is proportional to $S_w^{1.5}$. This is demonstrated by equation (7.35).

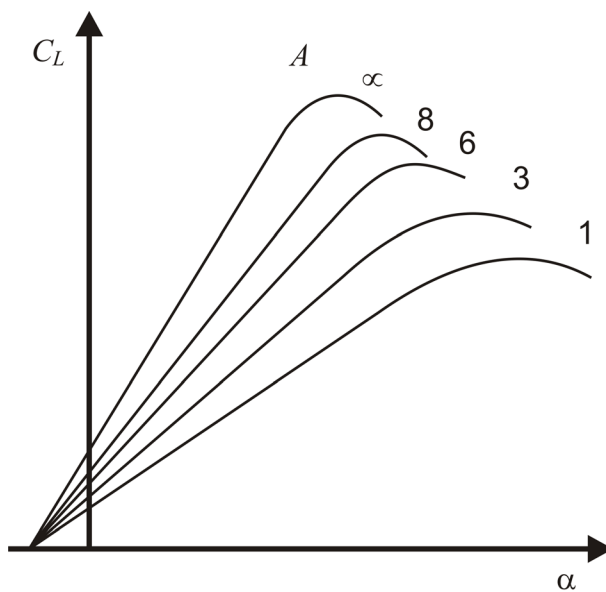
Wing aspect ratio

The wing aspect ratio $A = b^2 / S$ has an impact on various parameters:

- A high aspect ratio reduces the **induced drag** $C_L^2 / (\pi \cdot A \cdot e)$.
- The **wing mass** of wings with a high aspect ratio is greater than that of wings with a small aspect ratio.
- With an equal wing area, a wing with a higher aspect ratio also has a bigger **span** pursuant to $b = \sqrt{A \cdot S}$.
- The smaller the aspect ratio, the smaller the **lift curve slope** (Fig. 7.20). However, this means that visibility from the cockpit during approach is reduced due to an increased pitch attitude angle. According to equation (7.36), the greater the lift curve slope, and therefore the greater the aspect ratio, the more the aircraft reacts to a vertical gust. In addition, a larger angle for rotating the aircraft at take-off is required.
- The tank volume is proportional to $\frac{1}{\sqrt{A}}$. As the aspect ratio increases, the tank volume therefore decreases. This is demonstrated by equation (7.35).

Table 7.2 Summary evaluation of wing aspect ratio A

	Large aspect ratio	Small aspect ratio
Induced drag	small	large
Lift-to-drag ratio L/D	large	small
Lift curve slope	large	small
Pitch attitude angle during approach	small (i.e. good visibility from the cockpit)	large (i.e. poor visibility from the cockpit)
Flight in turbulent air	bumpy	smooth
Required angle for rotation	small	large
Wing mass	large	small
Tank volume	small	large
Span (for $S_W = \text{const}$)	large	small

**Fig. 7.20**

Effect of aspect ratio on the lift curve slope

Sweep

As explained above, the **critical Mach number** is increased by the sweep. It is irrelevant whether this occurs with the aid of forward sweep or aft sweep.

As a rule, the **maximum lift coefficient** of the wing is reduced due to sweep. The following applies:²

$$C_{L,max,swept} = C_{L,max,unswept} \cdot \cos \phi_{25} \quad . \quad (7.37)$$

² Section 8 contains a more precise method for calculating the maximum lift coefficient of swept wings, taking into account the shape of the airfoil leading edge.

This relationship applies approximately to the normally used airfoils with a less sharply defined leading edge. If the wing area is sized by $C_{L,max}$, then a larger wing area must be chosen in the case of a larger sweep angle. The **mass of the wing** increases due to the sweep.

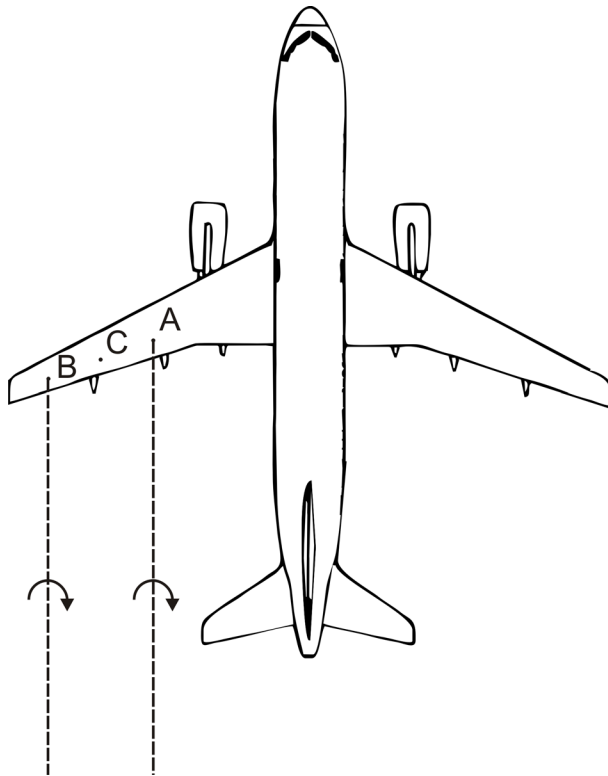
As a rule, the angle of attack of the forward swept wing increases due to the deflection with increasing load. The load increases further due to the increased angle of attack. This positive feed back affecting the forward swept wing leads to divergent behavior. The divergence can be counteracted by an especially stiff wing. However, the necessary additional stiffening increases the wing mass. Consequently **forward swept wings are heavier than aft swept wings**.

The **stall behavior** of forward swept wings is considerably better than that of aft swept wings. The aim is to stall the inner wing first and then the outer wing. In this way, the outer aileron remains effective in the stalled state, so that one-sided “tipping” of the aircraft over one wing can be prevented. **Fig. 7.21** and **Fig. 7.22** explain why a forward swept wing has better lift distribution for the stall behavior. In the case of the aft swept wing, the flow separates first at the wing tip (**tip stall**). This undesirable behavior is also exacerbated by the fact that the boundary layer moves outward with the flow. In older aircraft an attempt was made to keep the inner wing's boundary layer in place on the inner wing with the aid of stall fences (**Fig. 7.23**).

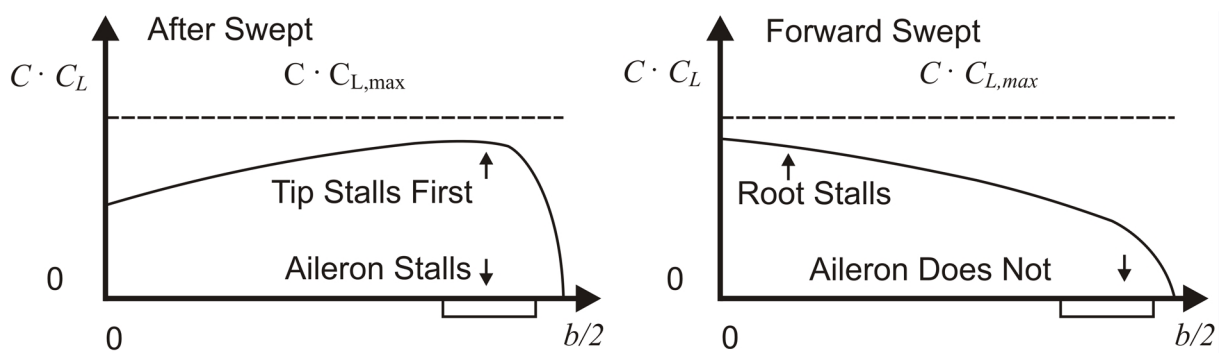
An additional problem associated with tip stall is the change in the pitching moment. As the wing tips are behind the center of gravity in the case of the aft swept wing, the tip stall results in a nose up moment and **pitch up** of the aircraft. If the pilot does not counteract this immediately, the aircraft will stall even more.

The main landing gear and the wing are approximately located at the center of gravity of the aircraft. In the case of swept wings the mean aerodynamic chord is approximately at the center of gravity, but not the wing root. Swept wings therefore cause problems with the **installation of landing gear**. An additional area on the double tapered wing S_3 according to Fig. 7.4 and Fig. 7.5 may solve the problem.

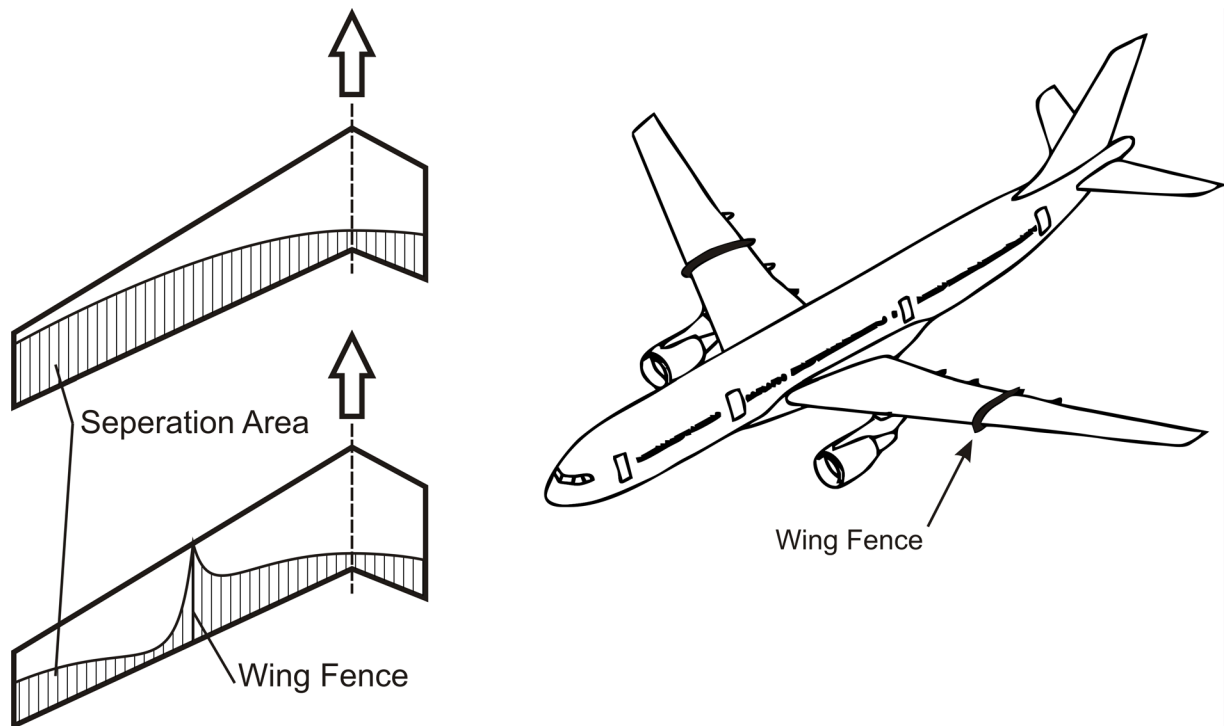
Equation (7.24) shows that the **lift curve slope** decreases as the sweep increases. Thus, the flying characteristics improve in gusty weather, but visibility from the cockpit is worse during the approach due to an increased pitch attitude angle. A larger angle is required at take-off for rotating the aircraft.

**Fig. 7.21**

A filament of flow emanating from Point A has a greater influence on Point C than the influence traveling back from Point B to C. Therefore Point C experiences a greater downwash overall than would be the case for a wing without sweep. The effect thus described results in a lift distribution on the aft swept wing, as shown in Fig. 7.22 (left). In the forward swept wing, the argumentation applies accordingly and leads to the lift distribution in Fig. 7.22 (right)

**Fig. 7.22**

Influence of the sweep on the lift distribution and the stall behavior. The reason for the differing lift distribution is explained by Fig. 7.21

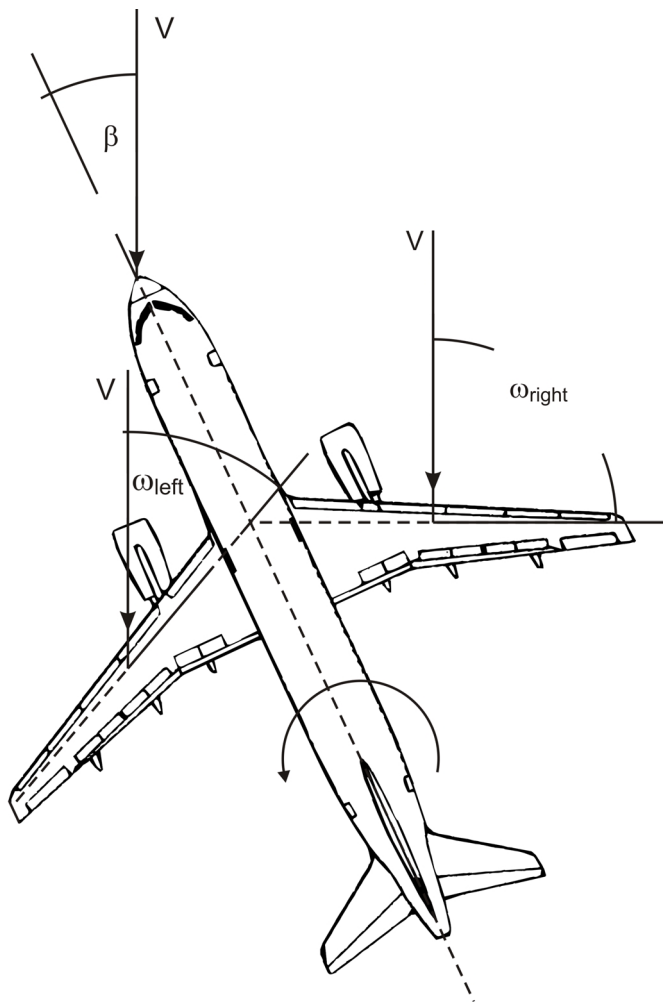
**Fig. 7.23**

High angles of attack lead to separation of the flow, usually beginning at the trailing edge. An aft swept wing has a larger area of separated flow at the outer wing than at the inner wing. A stall fence is used in an attempt to positively influence the boundary layer and the separation zone at the outer wing

Aft swept wings exhibit positive **stability around the longitudinal axis**. This is explained with help of (Fig. 7.24) the effect is based on $C_{L,max,swept} = C_{L,max,unswept} \cdot \cos \phi_{25}$ as given in (7.37). If we assume a positive side slip angle (as drawn in Fig. 7.24) $\omega_{right} > \omega_{left}$ and hence $C_{L,right} > C_{L,left}$. This causes a rolling moment to the left.

Aft swept wings however exhibit a destabilizing effect on the **Dutch roll**. The aircraft may need an electronic yaw damper to cope with this problem.

Forward swept wings are basically unstable around the longitudinal axis and therefore require a positive dihedral angle to compensate. The dihedral effect is examined in more detail in the subsection on the dihedral.

**Fig. 7.24**

Positive stability around the longitudinal axis by means of aft swept wings

The **appearance of an aircraft** should not be underestimated. According to general opinion, a swept wing looks better, and what looks good also sells better. This all the more true in the case of private aircraft and business jets. However, experience has shown that tastes tend to be conservative. Designs which are too futuristic might experience problems on the market.

Table 7.3 Summary evaluation of wing sweep ϕ_{25}

	Large sweep	Small sweep
Critical Mach number	large	small
Maximum lift coefficient	small	large
Lift curve slope	small	large
Pitch attitude angle during approach	large (i.e. poor visibility from the cockpit)	small (i.e. good visibility from the cockpit)
Flight in turbulent air	smooth	bumpy
Required angle for rotation	large	small
Integration of landing gear	difficult	minor problems
Wing mass	large	small

Table 7.4 Summary evaluation of type of wing sweep

	Forward sweep	No sweep	Aft sweep
Risk: tip stall	none	none	large
Risk: pitch up	minor	none	large
Maximum lift coefficient	small	large	very small
Risk: one-sided stall	minor	very minor	large
Risk: divergent wing deflection	yes	no	no
Wing mass	very large	small	large
Stability around the longitudinal axis	unstable (requires dihedral for stability)	neutral	stable

Variable sweep is chosen for the following reasons:

- good take-off and landing characteristics,
- minimal drag and good flying characteristics in cruise flight,
- optimum lift-to-drag ratio in all flying ranges.

Variable sweep has the following drawbacks:

- the structure of the pivoting mechanism is heavy and expensive,
- the drive system of the variable swept wing is heavy and expensive
- changing the sweep angle causes considerable shifts in the aerodynamic center; large empennages are required to compensate for the resulting moments.

Relative thickness

- **Drag.** Large airfoil thickness causes a high profile drag³ in the subsonic range. It also causes high wave drag at transonic and supersonic speed. In the case of supersonic speed, the wave drag is proportional to $(t/c)^2$. This explains why supersonic aircraft require extremely thin wings.
- Large relative thickness reduces the **wing mass** because both the bending stiffness and the torsional stiffness are increased.
- The **maximum lift coefficient** rises as the relative thickness increases. This applies up to a relative thickness of approximately 12% to 14%.
- The **volume of the fuel tank** in the wing increases in proportion to the relative thickness. This is shown in equation (7.35).

Conclusion: The relative thickness should always be as large as possible while still being compatible with drag requirements.

³ Profile drag = frictional drag + form drag

Table 7.5 Summary evaluation on relative thickness

	Small relative thickness	Large relative thickness
Maximum lift coefficient	small	large
Lift curve slope Equation (7.24)	small	large
Drag	small	large
Tank volume	small	large
Wing mass	large	small

Taper ratio

The taper ratio $\lambda = c_t / c_r$ has an influence on the **lift distribution** in the direction of the span. Lift distribution means the graphical representation (**Fig. 7.25**) of the function $c \cdot c_L$ over the dimensionless distance from the plane of symmetry in the direction of the span $y / (b / 2)$. The smallest induced drag is obtained for an elliptical lift distribution. This elliptical lift distribution is achieved if all the airfoils are geometrically similar and all chords lines are parallel, and the wing also has an elliptical chord distribution over the span. The lift coefficient (which is calculated by dividing the value $c \cdot c_L$ by c) is *constant* over the span in this case.

Important: 1.) The *lift distribution* (Fig. 7.25) $c \cdot c_L$ in the direction of the span $y / (b / 2)$ must be carefully distinguished from 2.) the *distribution of the lift coefficient* (Fig. 7.26) c_L in the direction of the span $y / (b / 2)$. 1) refers to the aerodynamic quality, and 2) refers to the stall behavior of the wing.

The lift distribution on a **rectangular wing** is too “thick” due to the larger chord at the wing tip. The result is roughly 7% higher induced drag. For an unswept wing, the elliptical lift distribution can be approximately achieved by a **tapered wing** with $\lambda = 0.45$. The induced drag is then less than 1% higher than the induced drag of the wing with the elliptical lift distribution.

The position of the center of pressure of a wing section moves to the wing root as the taper ratio decreases. The root bending moment (caused by the lift) decreases accordingly. As the thickness of the wing root becomes larger at the same time, a wing with small λ can achieve a smaller **wing mass** than a rectangular wing.

The necessary thickness at the wing tip constitutes a lower limit for the taper ratio λ , as sufficient **installation space** must be available to accommodate ailerons and the relevant mechanisms in the wing.

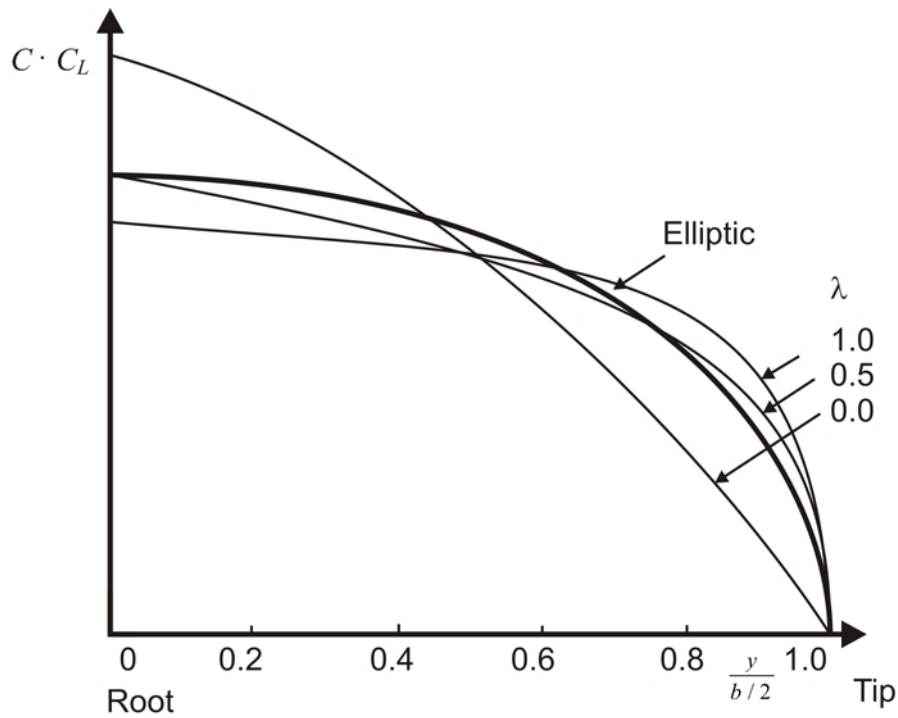


Fig. 7.25 Lift distribution for various taper ratios at $\varphi = 0$

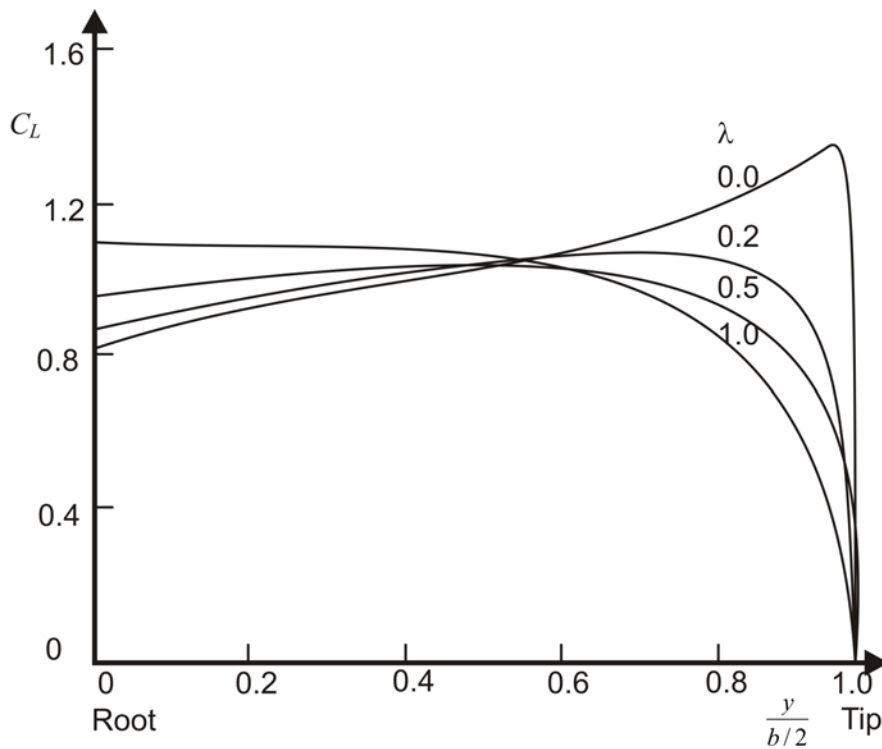


Fig. 7.26 Distribution of the lift coefficient for various taper ratios at $\varphi = 0$ and aspect ratio $A = 10$ on a wing with $C_L = 1$

The taper ratio is an important parameter for controlling **stall behavior**. The lift coefficient distribution in the direction of the span (**Fig. 7.26**) is helpful for the assessment. The flow will separate from the wing first at the point where the lift coefficient distribution reaches its maximum level. To a first approximation the following applies:

$$\text{(only) for } \underline{\varphi = 0} : \quad c_{L,max} \text{ is at: } \eta = y / (b / 2) = 1 - \lambda . \quad (7.38)$$

With a taper ratio of 0.45, for example, one would consequently expect the flow separation to start at $\eta = 0.55$. This is close to the inner end of the aileron and leaves the aileron largely in attached flow. At the same time with a tapered wing with $\lambda = 0.45$ one also obtains the best approximation for the elliptical lift distribution.

Wings with a positive **sweep** tend to have a “thicker” lift distribution in the vicinity of the wing tip (see above). In order to get close to the elliptical lift distribution again, λ must have smaller values. The optimum taper ratio for the smallest induced drag according to **Torenbeek 1988** can be estimated from the following to a first approximation:

$$\lambda_{opt} = 0.45 \cdot e^{-0.036 \cdot \varphi_{25}} . \quad (7.39)$$

In equation (7.39) the sweep angle is entered in degrees. e is the Euler number.

λ smaller than 0.2 should be avoided because the short chord at the wing tip can only have small Reynold number. This results in small maximum lift coefficients and **tip stall**. Also the distribution of the lift coefficient (Fig. 7.26) shows a danger of tip stall in the case of small λ values.

It can be ascertained from equation (7.35) that for wings with a constant relative thickness over the span, a taper ratio of $\lambda = 0$ (triangular wing) offers the largest **tank volume**.

Rectangular wings ($\lambda = 1$) can be manufactured with minimal **production costs**.

Commercial jet transports use double tapered wings, as shown in Fig. 7.5. The additional area S2 is called a “glove”, and area S3 is called “yehudi”. The benefits are:

- an increase in the thickness at the wing root,
- a reduction in the relative thickness at the wing root in order to achieve higher drag divergence Mach numbers M_{DD} ,
- increase in the sweep (by means of the glove) in order to achieve higher drag divergence Mach numbers,
- increase in the installation space for the landing gear (by means of “yehudi”),

- reduction in the sweep of the inner flaps (by means of “yehudi”) in order to achieve a larger maximum lift coefficient.

Table 7.6: Summary evaluation with regard to taper ratio

	Taper ratio λ small	Taper ratio λ large
Tip stall	bad	good
Tank volume at t/c = const	large (optimum for $\lambda = 0$)	small
Production costs	-	advantage only for $\lambda = 1$
Installation space for aileron	small	large
Wing mass	small	large
Induced drag in the case of small large sweep	small	large

Twist

The twist is defined as

$$\varepsilon_t = i_{w,tip} - i_{w,root} \quad (7.40)$$

Many wings are built with negative wing twist ε_t , so that the incidence angle i_w decreases in the direction of the wing tip (Fig. 7.8). This measure is used to **prevent tip stall**. Especially aft swept wings must be given negative twist in order to prevent tip stall.

Twist helps to achieve an elliptical **lift distribution**. However, it is only possible to achieve this with *one* lift coefficient. With other lift coefficients, reduced lift-to-drag ratios are produced, compared to the elliptical lift distribution. If the twist is limited to 5° , these losses can be kept to a minimum. Wash out reduces the root bending moment. Thus the **wing mass** can be reduced. In preliminary design the following can be applied if no other data is given:

$\varepsilon_t = -3^\circ$ (wash out). However the A310 (see Subsection 7.5) shows $\varepsilon_t = -8^\circ$.

Dihedral

Dihedral may occur as a positive dihedral angle, as shown in Fig. 7.6, or as a negative dihedral angle (anhedral). In sideslip, a positive dihedral angle causes a **moment around the longitudinal axis**, which causes the wings to level. A positive dihedral angle therefore leads to positive stability around the longitudinal axis. **Fig. 7.27** shows how the flow acts on a wing with a dihedral: The aircraft flies with its left wing down. This causes the aircraft to slip to the left. The side slip velocity V approaches the wing from the left. Due to dihedral this causes a difference in the angle of attack on wing section 1 respectively 2. On section 1 lift is increased whereas on section 2 lift is decreased. The resultant moment causes the wing to level again. The wing leveling moment increases with dihedral angle:

$$\Delta\alpha_1 = \frac{V_n}{U}$$

$$\beta = \frac{V}{U} \quad \text{and} \quad V_n = V v_w$$

$$\text{hence} \quad \Delta\alpha_1 = \beta v_w .$$

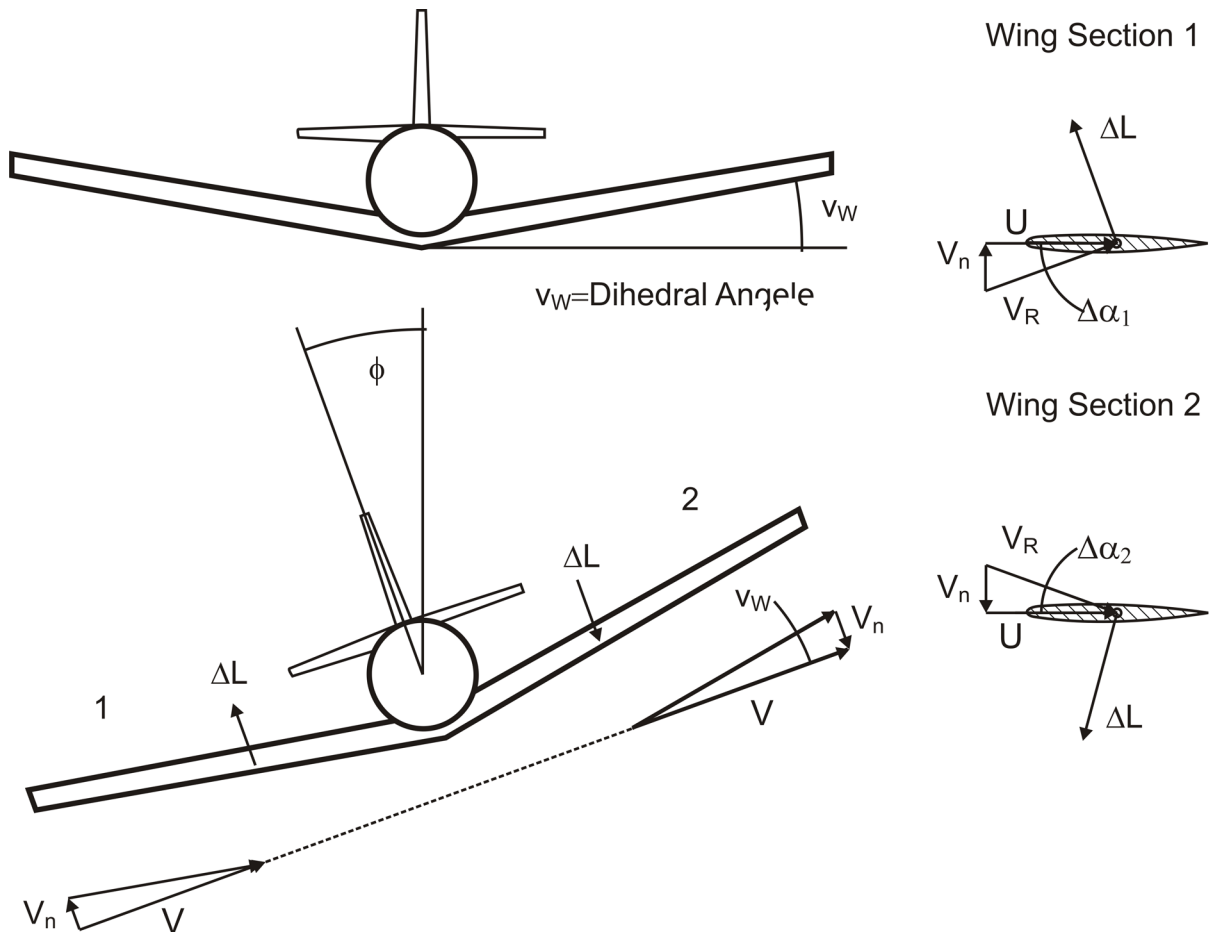


Fig. 7.27 The flow on the wing with a positive dihedral leads to a moment around the longitudinal axis that causes the wings to level.

V velocity due to sideslip
 V_n normal component of side velocity
 U forward velocity
 V_R resultant velocity

The moment around the longitudinal axis in sideslip leads to

- a stable **spiral mode**,
- an unstable **Dutch roll**.

A stabilizing moment around the longitudinal axis in sideslip is achieved by

- a positive dihedral angle,
- a wing configuration in relation to the fuselage in the form of a high-wing aircraft,
- an aft swept wing.

A destabilizing moment around the longitudinal axis in sideslip is achieved by

- a negative dihedral angle (anhedral),
- a wing configuration in relation to the fuselage in the form of a low-wing aircraft,
- forward swept wing.

10° sweep achieves roughly as much as 1° dihedral.

Moving the wing position in relation to the fuselage by “one step”
(e.g. from high to middle, or from middle to low)
achieves roughly as much as 3.5° dihedral

The combination of aft sweep and high-wing configuration together achieve so much stability that it has to be counteracted with an anhedral. For example, Avro RJ85 (see Section 4).

Table 7.7 Instructions for choice of dihedral

Dihedral angle in °	Low wing	Mid wing	High wing
Unswept wing	5 to 7	2 to 4	0 to 2
Swept wing	3 to 7	-2 to 2	-5 to -2

Dihedral is also used to ensure the necessary **clearance of engines and wing tips from the ground**.

Incidence angle

The incidence angle i_w is defined in Fig. 7.7.

The incidence angle should be chosen so as to ensure that the **drag in cruise flight** is as low as possible. For this, the fuselage longitudinal axis should be parallel to the direction of the flow. In case of doubt, the fuselage can have a small positive incidence angle in cruise flight. However, if the incidence angle is negative, the fuselage produces negative lift and therefore additional drag.

The incidence angle should be chosen so that the **cabin floor is horizontal in cruise flight**. If the cabin floor diverges too much from the horizontal, it can become difficult for the cabin crew to push the trolleys through the aisles. Furthermore, servicing in a passenger aircraft

should start already towards the end of the climb. Labor unions define which floor angle is acceptable for the crews during servicing. On the basis of the requirement of a horizontal fuselage in cruise, the incidence angle can be estimated (**Roskam III**):

$$i_w = \frac{C_{L,CR}}{C_{L_\alpha}} + \alpha_0 - 0.4 \cdot \varepsilon_t . \quad (7.41)$$

In this equation:

- C_{L_α} the lift curve slope according to equation (7.24),
- $C_{L,CR}$ the necessary lift coefficient in cruise flight,
- α_0 the angle of attack at zero wing lift or a characteristic profile of the wing,
- ε_t the twist (see above).

The factor 0.4 tries to account for the fact that we have a tapered wing with the inboard wing having more area and hence more contribution towards overall lift than the outboard wing.

It must be borne in mind

- that α_0 and ε_t are negative, as a rule.
- that C_{L_α} from equation (7.24) is obtained in radian (rad) and has to be converted into degrees (°) for equation (7.40) if α_0 and ε_t are also in degrees.

If the incidence angle is too small, **visibility from the cockpit** onto the runway may no longer fulfill the requirement in the **landing approach**.

If the incidence angle is too great, the **nose wheel** may touch down first during **landing**. This must always be avoided, as the nose landing gear is not designed to absorb landing impact. It is only possible to determine whether such a risk exists after defining the high lift system. In this respect, it is critical if only flaps, but no slats, are envisaged for an aircraft. In this case, the aircraft will reduce its pitch attitude angle during landing approach after extending the flaps.

Summary of key characteristics

Table 7.8 contains a summary of key characteristics of wing design parameters.

Table. 7.8 Summary of key characteristics of wing design parameters based on **Schmitt 1998**

effect of an increase off → on ↓	S_w	A	ϕ	λ	t/c
low speed flight	+++ lifting capacity	+++ 2. segment	- $C_{L \max}$	++ depending on plan view	++ $C_{L \max}$
high speed flight	++ aerodyn. quality buffeting M_{Dive}	++ aerodyn. quality	++ M_{Dive}	-	-- M_D
wing mass m_w low => +	- big wing => heavy	--- $h_{Wingbox}$ bending moment	-- bending moment	- $h_{Wingbox}$	+++ $h_{Wingbox}$
fuel tank V_F high => +	++ $\sim S^{1.5}$	- $\sim \frac{1}{\sqrt{A}}$	≈ 0	- $\frac{1 + \lambda + \lambda^2}{(1 + \lambda)^2}$	+++ $\sim t/c$
wing stiffness	++ $h_{Wingbox}$	-- $h_{Wingbox}/b$	-- $b_{50\%}$	- $h_{Wingbox}$	+++ $h_{Wingbox}$

7.4 Ailerons and Spoilers

Most aircraft use ailerons and/or spoilers for rolling. In doing so, the large lever arm of the wings can be utilized. Some fighter aircraft create an (additional) roll moment through the asymmetrical deflection of the elevator.

The yawing movement initiated by the vertical rudder also leads to rolling (due to a positive yaw/roll moment). However, this coupling is so weak that no satisfactory maneuverability can be achieved around the longitudinal axis in normal operation with the rudder alone.

Ailerons

Ailerons are simple plain flaps that are normally mounted close to the left and right wing tips. The position of the ailerons enables a large lever arm to be utilized. The ailerons on both wing tips deflect in opposite directions.

Ailerons cause an **adverse yaw**. This adverse yaw causes the aircraft to first yaw in a direction that is contrary to the initiated turn. The adverse yaw has to be compensated for with the rudder, and can be reduced if the ailerons are designed so as to deflect further upward than

downward. A special aileron geometry, which also serves to reduce the adverse yaw, is shown in **Fig 7.28**.

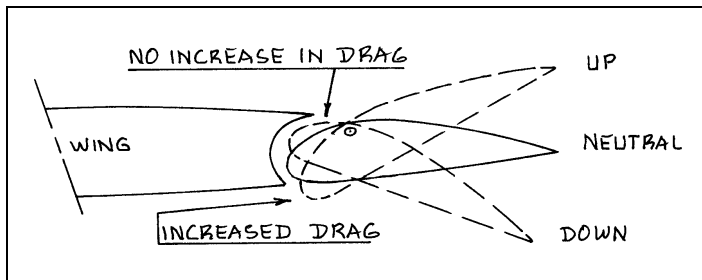


Fig. 7.28

Aileron with special geometry to reduce the adverse yaw (**Roskam III**)

The deflection of an aileron on a wing tip (outer aileron) can twist the wing so such an extent that the aircraft performs a roll movement that is contrary to what was initially intended by the aileron deflection. The phenomenon is called **aileron reversal** and can occur in the case of high dynamic pressures and wings with low torsional rigidity. In such cases, the aileron must be fixed when high dynamic pressures occur. Roll movements are then initiated with spoilers – or with ailerons that are mounted further inboard on the wing (inner aileron).

It is important to bear in mind that ailerons “compete” with flaps for the space on the trailing edge. The high lift system can be especially effective if the entire span is available for flaps. The problem can be solved in some cases by deflecting the ailerons downward symmetrically together with the flaps, e.g. 20% of their full deflection (**aileron droop**), so that they support the high lift system. However possibilities for aileron droop are limited because flaps are used in low speed flight and this is exactly the situation when high aileron deflections are needed. Thus aileron droop may not cause aileron efficiency to be reduced too much.

When choosing the geometry of the ailerons, the geometry of completed aircraft can be used as a guide in the preliminary design. The chord of the ailerons is normally **20% to 40% of the wing chord**. Typical values are roughly 30% of the wing chord. Ailerons are normally in the region of 40% to 100% of the semi-span. Typical ailerons cover **65% to 95% of the semi-span**.

Spoilers

Spoilers do what their name says, i.e. they “spoil” the flow over the part of the wing that is located directly behind the spoilers. **Fig. 7.29** shows the effect. Spoilers are very effective with extended flaps. In contrast to ailerons, spoilers do not cause adverse yaw, but rather a yawing movement in the direction of the turn being flown. Due to the principle on which spoilers function, drag is also produced by spoiler deflection. Therefore, the flight control system is often designed so that the ailerons are used first and the spoilers are only employed when higher roll rates are required.

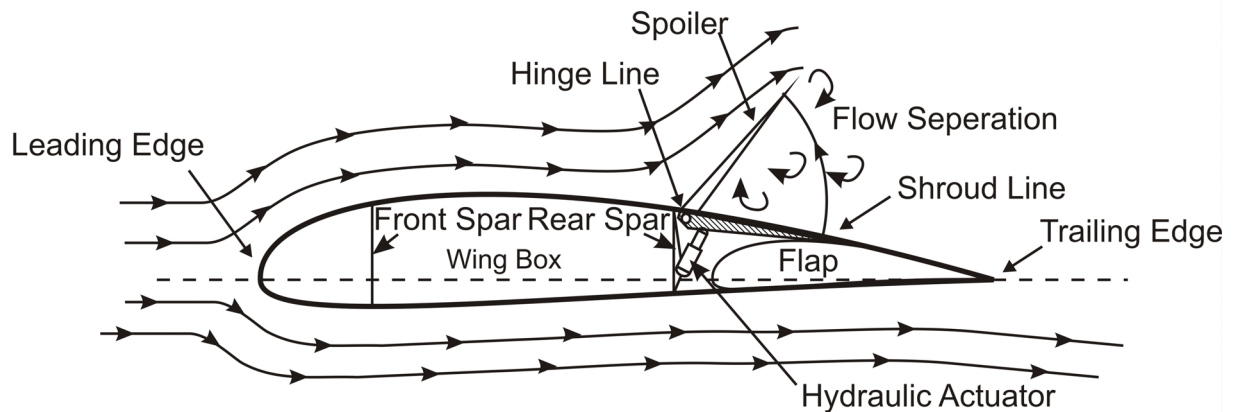


Fig. 7.29 Arrangement of a spoiler on a wing section

Spoiler geometries can be found in “Jane's all the World's Aircraft” (**Lambert 1993**). The three-views from Section 4 can also be used to gain an initial impression of spoiler geometries.

Most aircraft use a **wing box** to absorb forces and moments. The front and rear limits of the wing box are defined by the front and rear spars. The **location of the spars** must be chosen so as to be **compatible with the high lift system** and the **control surfaces**. As can be seen in Fig. 7.29, the hinge line of the spoilers is located directly behind the rear spar. Space has to be left between the rear spar and the hinge line to accommodate the drive mechanism of the ailerons. **Typical locations for the spars** are as follows:

- Front spar: 15% to 30% of the chord,
- Rear spar: 65% to 75% of the chord.

After deciding where to locate the spars, it is possible to calculate the **volume of the fuel tank** more precisely than was possible with the semi-empirical equation (7.35).

7.5 Example: The Wing of the Airbus A310

Table 7.9 A310 wing characteristics

Reference surface area (Sref) (aerodynamic)	219 m ²
Aspect ratio (aerodynamic)	8,8
Total wing span (b)	43,90 m
Sweep at 25% MAC (aerodynamic)	27,97 °
Root chord	8,381 m
Kink chord (basic trapezium)	4,946 m
Tip chord	2,175 m
Mean aerodynamic chord (MAC)	5,829 m
Root thickness/chord ratio	15,2 %
Kink thickness/chord ratio	11,8 %
Tip thickness/chord ratio	10,8 %
Inner trailing edge dihedral	11,8°
Outer trailing edge dihedral (Jig shape)	4,3°
Root wing setting	5,3°

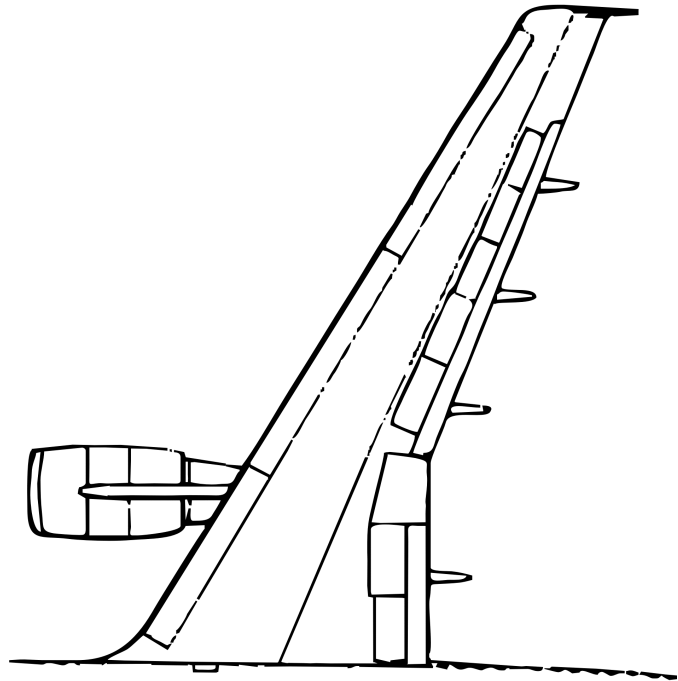


Fig. 7.30 A310 wing planform

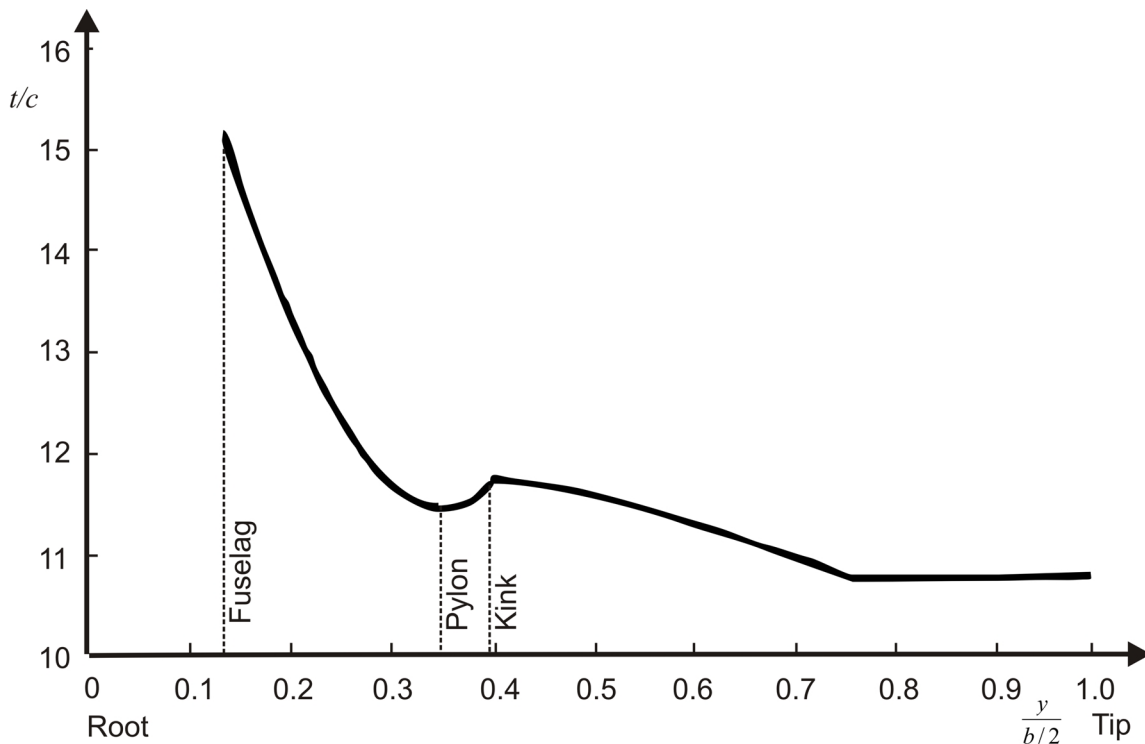


Fig. 7.31 A310 distribution of relative wing thickness

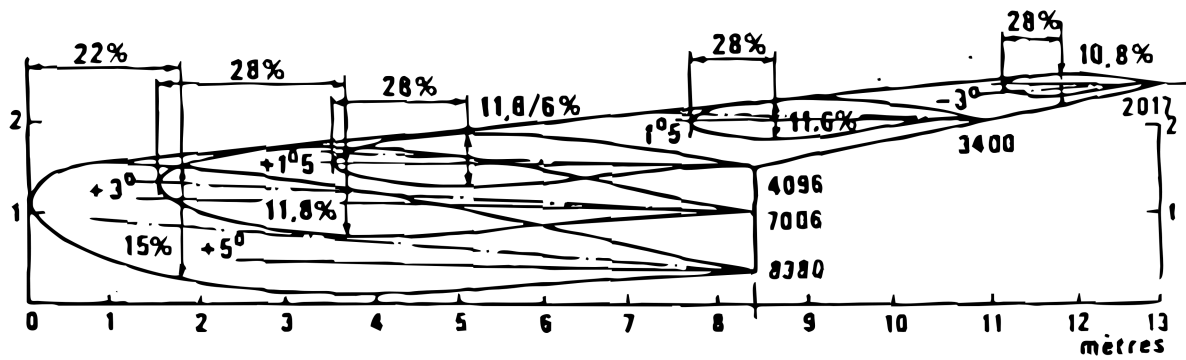


Fig. 7.32 Airbus A310 wing: sections, chord, relative thickness, wing twist, and incidence angle (quoted from Obert 1997)

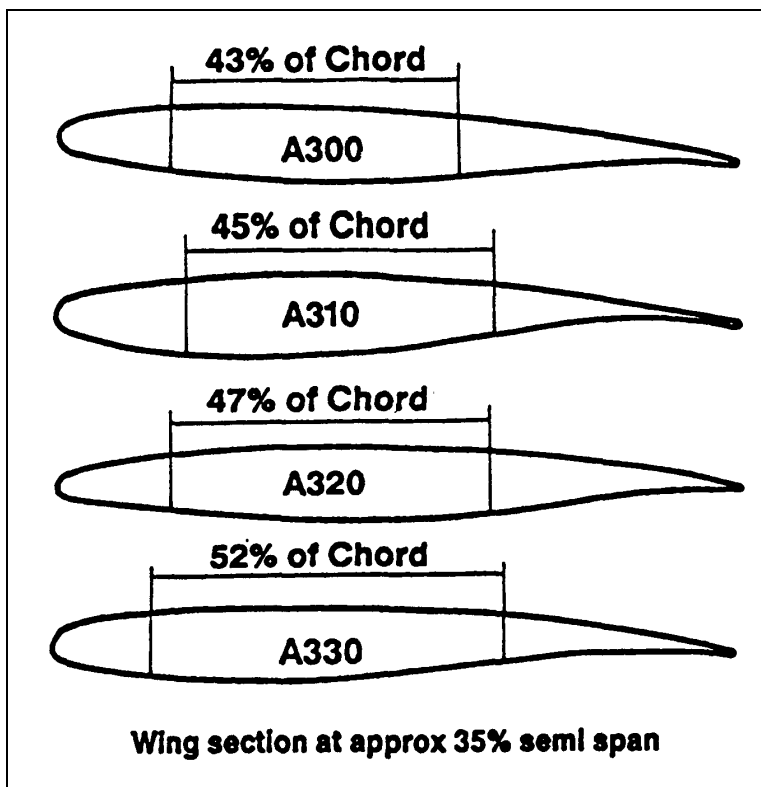


Fig. 7.33 Wing section and wing box at 35% semi-span of Airbus A310 in comparison with other Airbus aircraft

Acknowledgement: Table 7.9, Fig. 30, Fig. 31, and Fig. 33 are courtesy of Airbus.

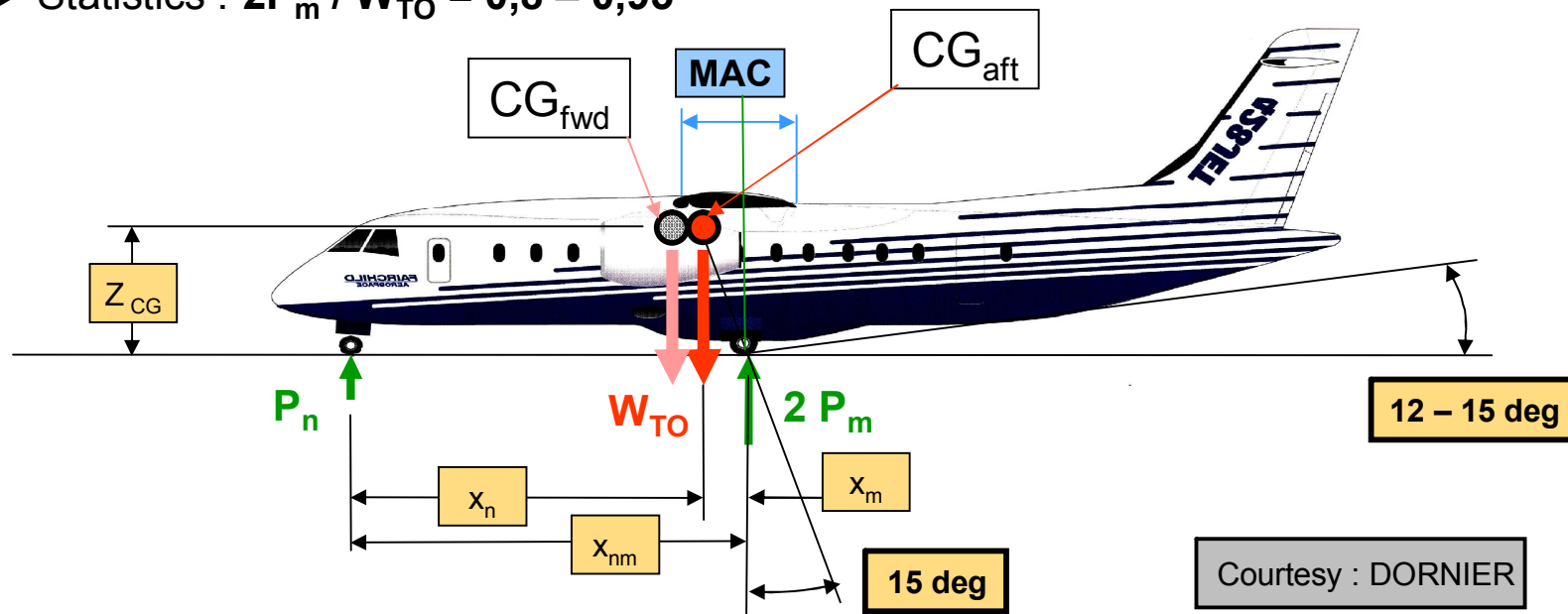
Erhard Rumpler

Chapter 8

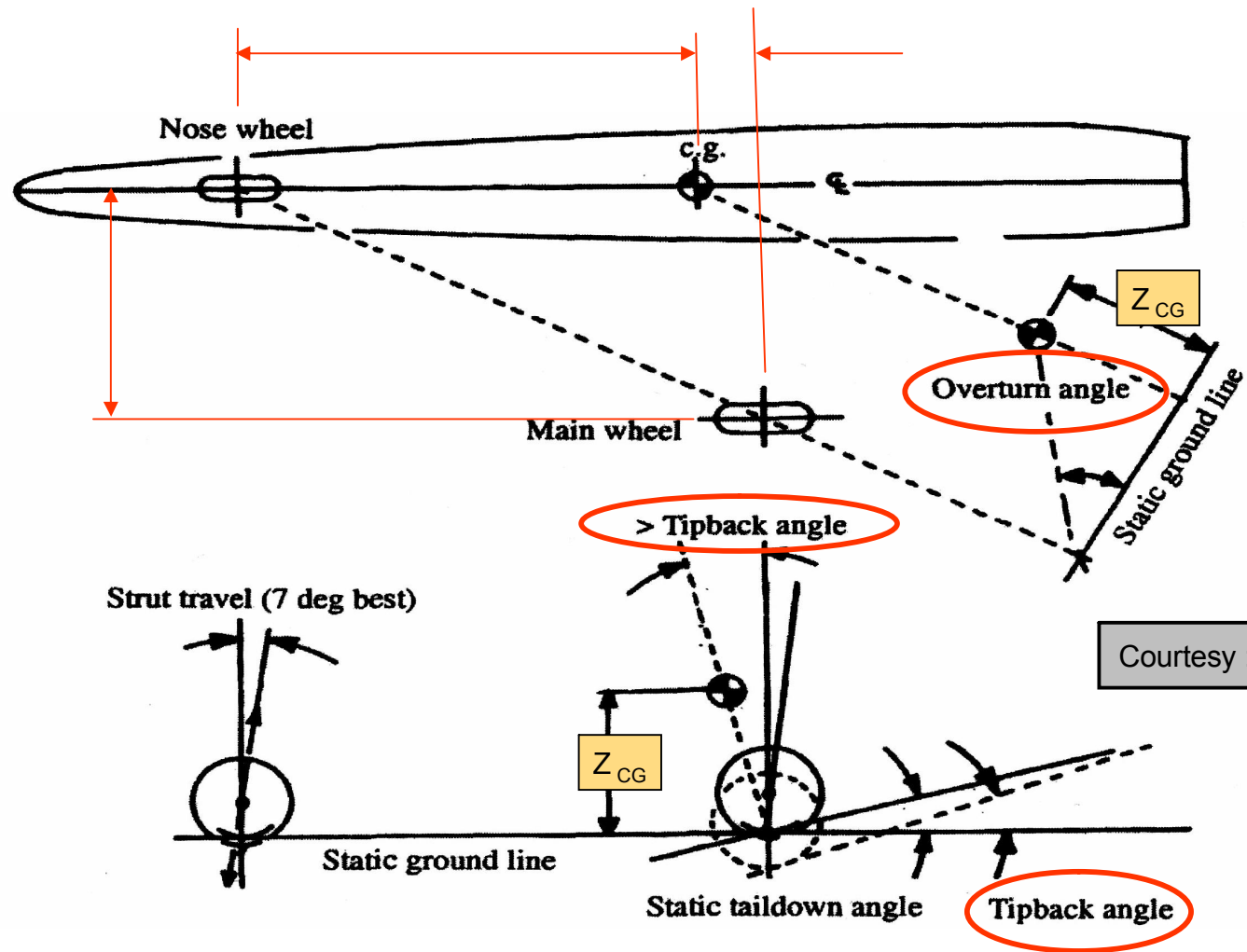
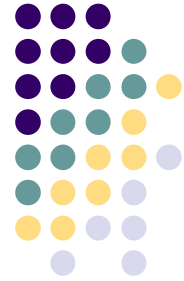
Landing Gear Design

Gear arrangement

- Standard nose gear
- Static load distribution leads to basic design data
- Cases : CG_{fwd} relevant for nose gear
 CG_{aft} relevant for main gear
- main gear position between about **50 – 55 % MAC**
- $W_{TO} = P_n + 2P_m$
- Statistics : $2P_m / W_{TO} = 0,8 – 0,95$



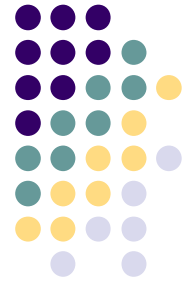
Gear arrangement

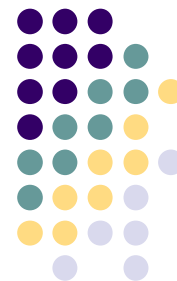


Landing gear airworthiness

- FAR specifies required landing conditions
- Landing conditions imply loads on gear components
- FAR selection useful for layout design
- For more details check relevant FAR §§

FEDERAL AIRWORTHINESS REQUIREMENTS	
LANDING CONDITIONS	FAR §§
All wheel level landing without drag	25.479
All wheel level landing with drag	25.479
All wheel level landing with lateral drift	25.485
Main gear level landing without drag	25.479
Main gear level landing with drag	25.479
Tail-down landing without drag	25.481
One-wheel landing	25.483



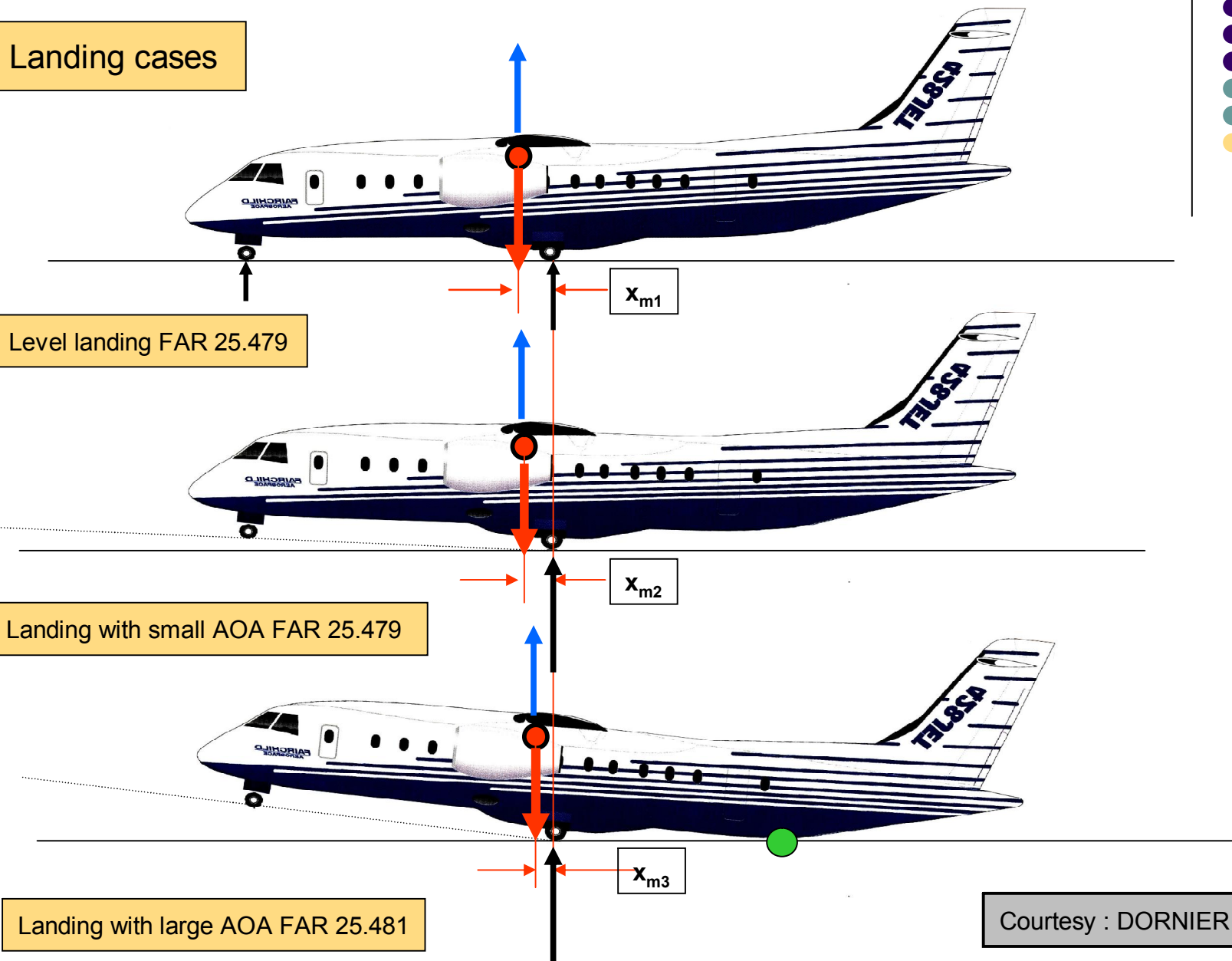


Landing cases

Level landing FAR 25.479

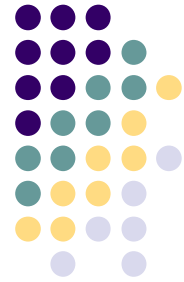
Landing with small AOA FAR 25.479

Landing with large AOA FAR 25.481



Courtesy : DORNIER

Landing impact energy dissipation



$$T_{\text{kin}} = W_L \cdot v_s^2 / 2g$$

$$T_{\text{pot}} = (W_L - L) \cdot f$$

$$A_{\text{gear}} = W_L \cdot f \cdot n \cdot k \cdot V$$

$$T_{\text{kin}} + T_{\text{pot}} = A_{\text{gear}}$$

f [m] ... vertical travel

v_s [m/s] ... vertical velocity

k [-] ... number of working gear struts

n [-] ... load factor

V [-] ... oleo – pneumatic shock absorber efficiency

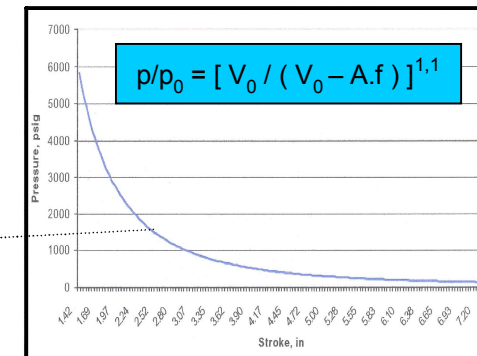
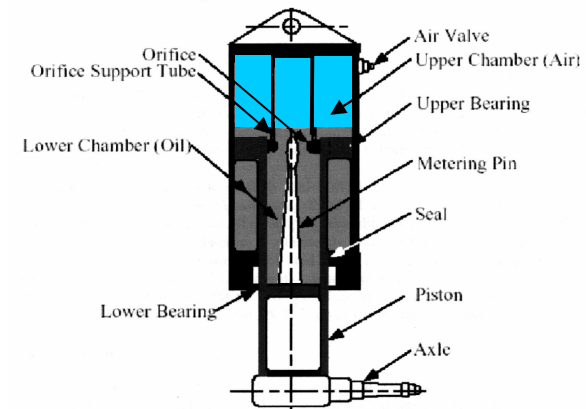
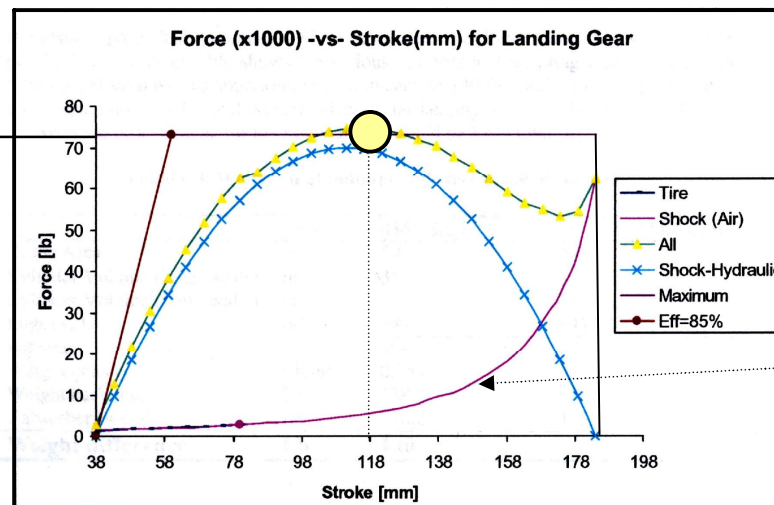
FAR 25.473

- Limit energy condition : $v_s = 8 \text{ fps} = 2,54 \text{ [m/s]}$
- Reserve energy condition : $v_s = 10 \text{ fps} = 3,11 \text{ [m/s]}$
- Wing residual lift :
 $L = 2 \cdot W_L / 3 \dots \text{FAR 23}$
 $L = W_L \dots \text{FAR 25}$

Landing impact energy dissipation

➤ Working details of oleo-pneumatic shock absorbers

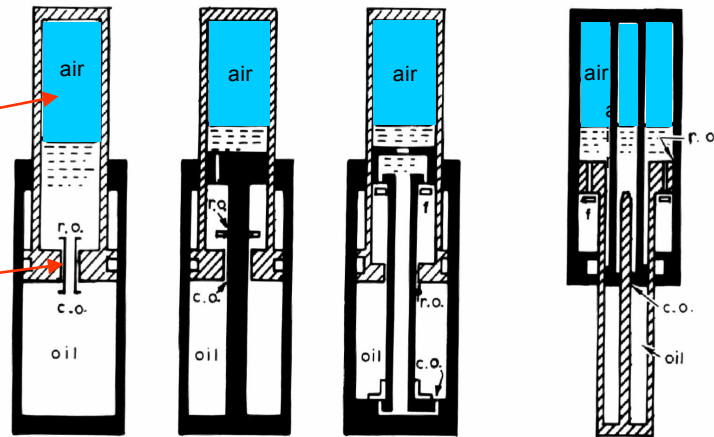
Oleo Adjustment :
 $n = 2,7 - 3$
 $V = 0,75 - 0,8$



Oleo-pneumatic shock absorbers

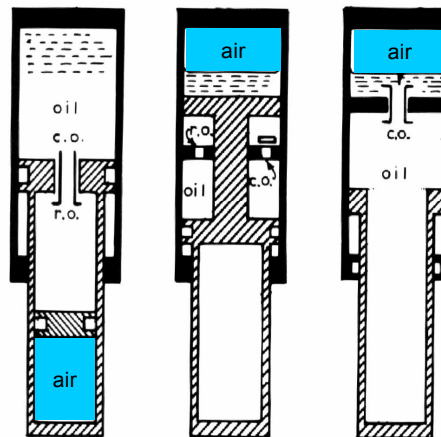
➤ Design basics :

- Pneumatic spring
- Friction damping by oil flow through recoil orifice

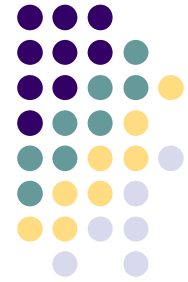


➤ Different Layouts :

- sketches 1 - 7



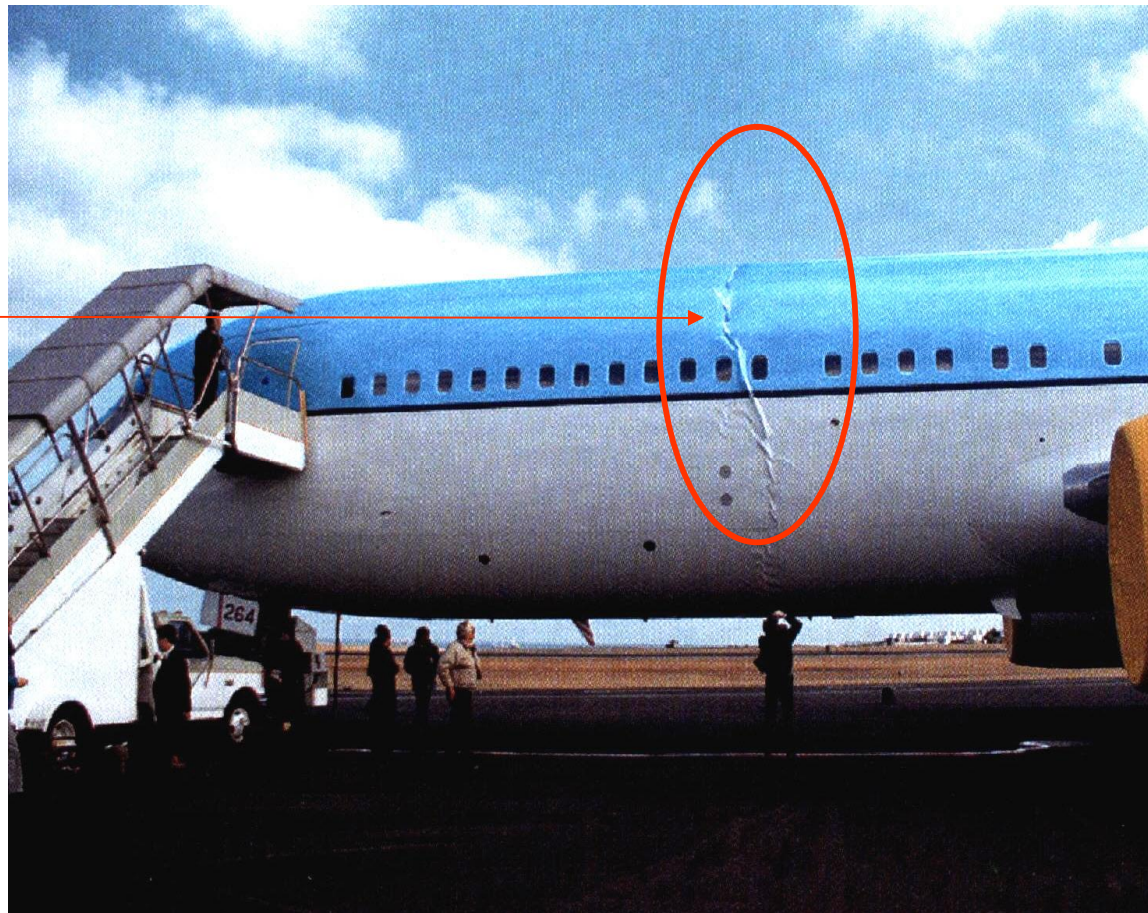
Courtesy : CURREY



Hard landing impact hazards

- All wheel level landing
- V_S exceeding FAR reserve energy condition of 10 fps

Upper fuselage shells
damaged due to
bending compression
loads



Braking energy dissipation

➤ Performance details of aircraft brakes :

Rejected takeoff condition :

- $v_h = 80$ [m/s]
- $s_{STOP} = 1200$ [m]
- $m = 132\ 000$ [kg]
- $T_{br} = 422$ [mJ]
- $P_{br} = 14\ 067$ [kW]
- 8 brakes → **53 [mJ/br]**



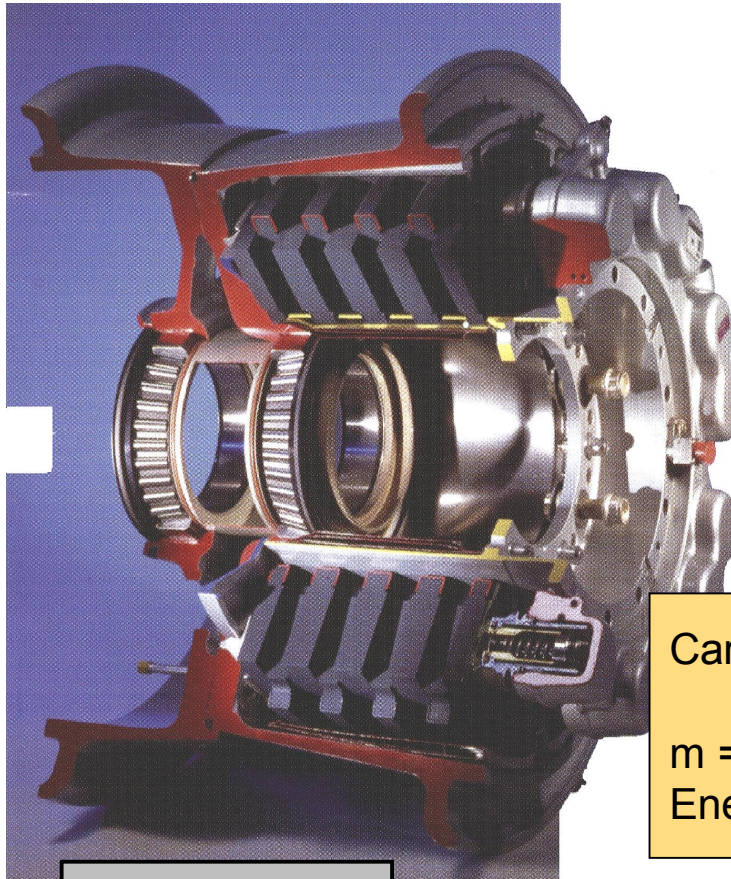
Courtesy : AW&ST

Rejected Take Off

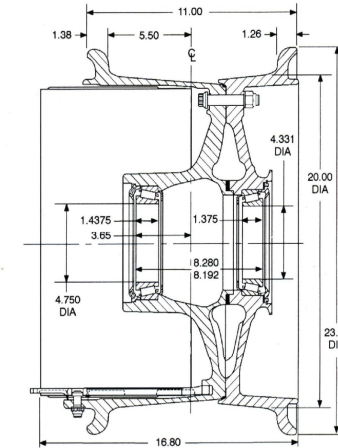
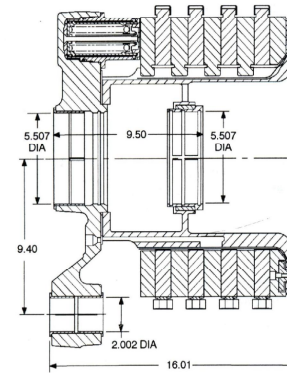
- Gloomng brakes showdown
- One of the hardest moments in an aircraft's life

Aircraft brakes and wheels

➤ Components to handle a RTO :



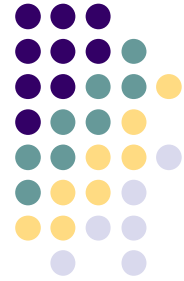
Courtesy : MESSIER



Carbon / Carbon aircraft brake

$m = 74 \text{ kg}$

Energy capacity $T_{br} = 70 \text{ [mJ]}$



Retract kinematics (sketch)

- 6-bar linkage
- side brace/downlock links “**perpendicular**”
- downlock links in overcenter position
- downlock springs hold overcenter position

UPPER SIDE BRACE LINK

LOWER SIDE BRACE LINK

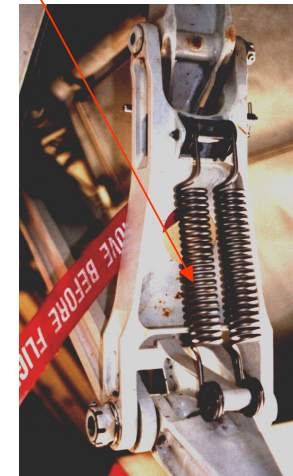
MAIN STRUT

OLEO-PNEUMATIC SHOCK ABSORBER

BOGIE

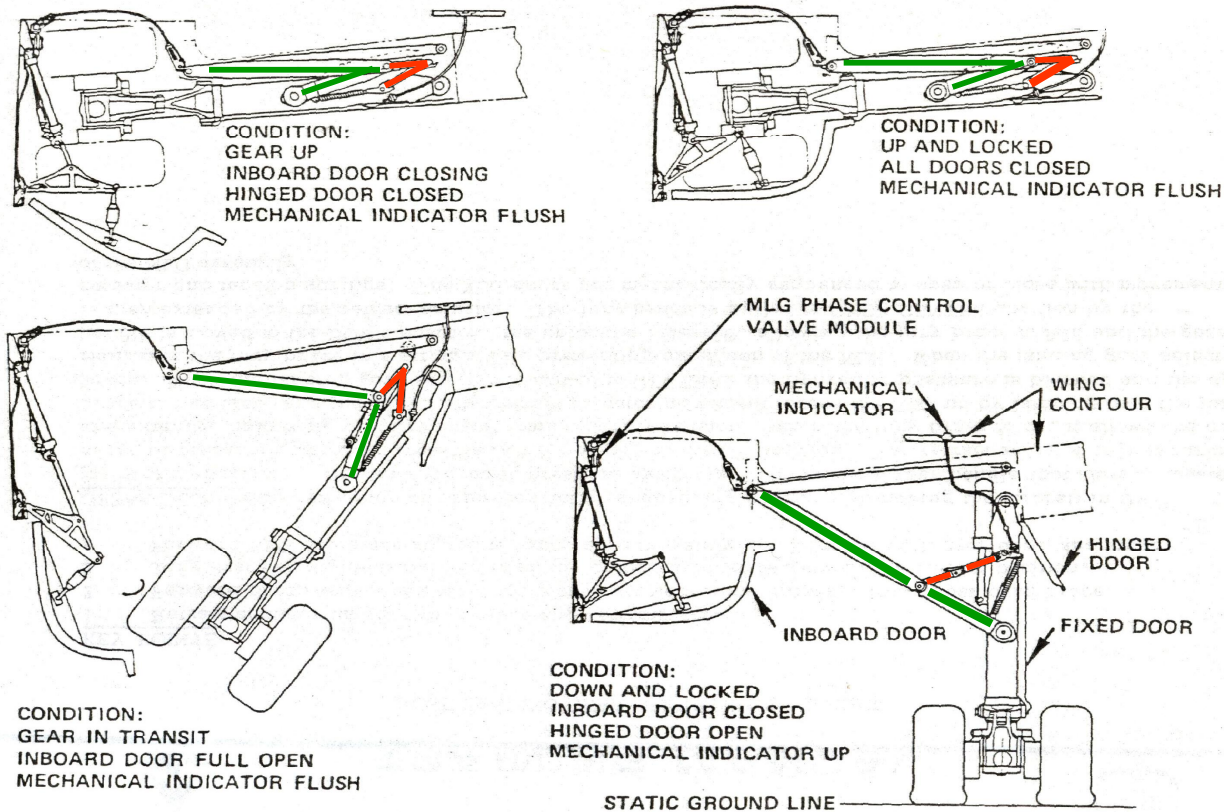
DOWNLOCK LINKS

DOWNLOCK SPRING



Retract operation sequence

- most modern gears retract inwards into a fuselage bay (“wheel well”)

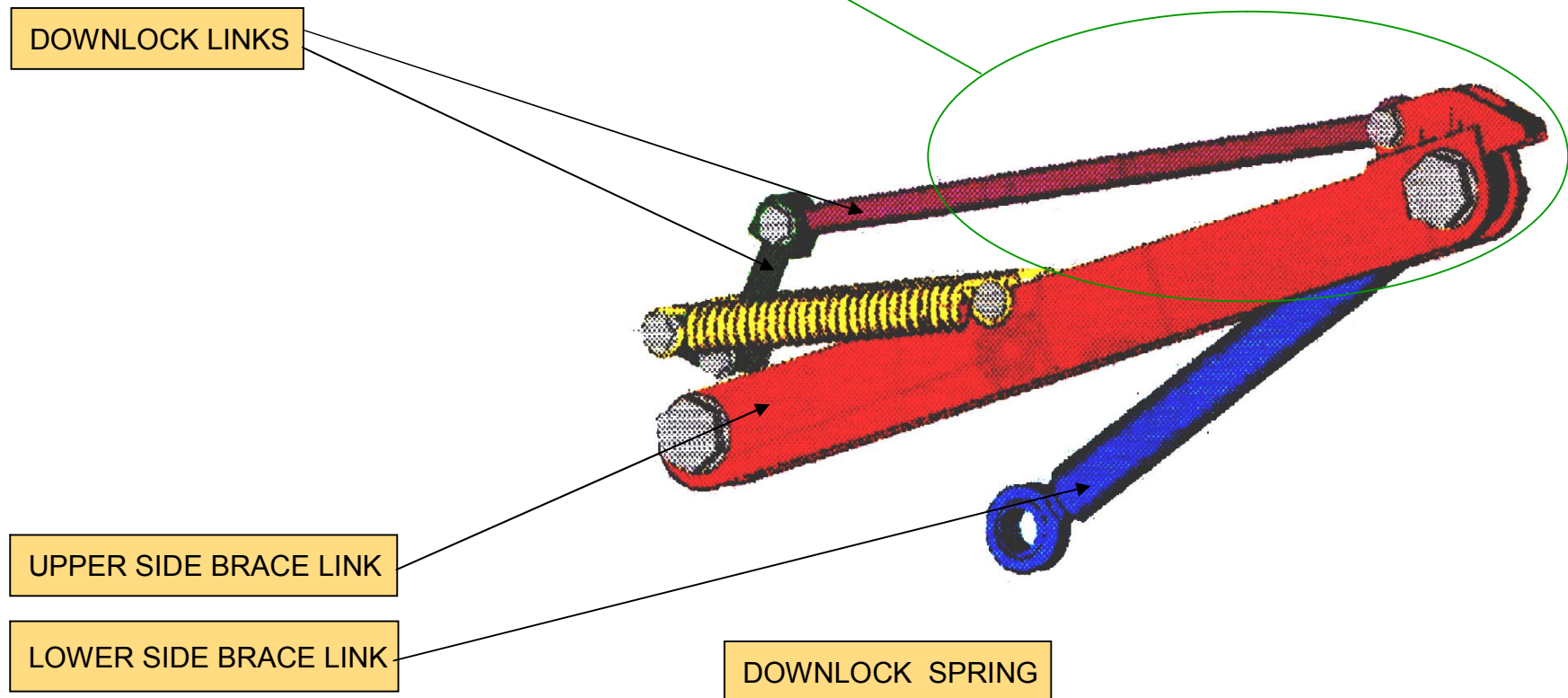


Courtesy : LOCKHEED

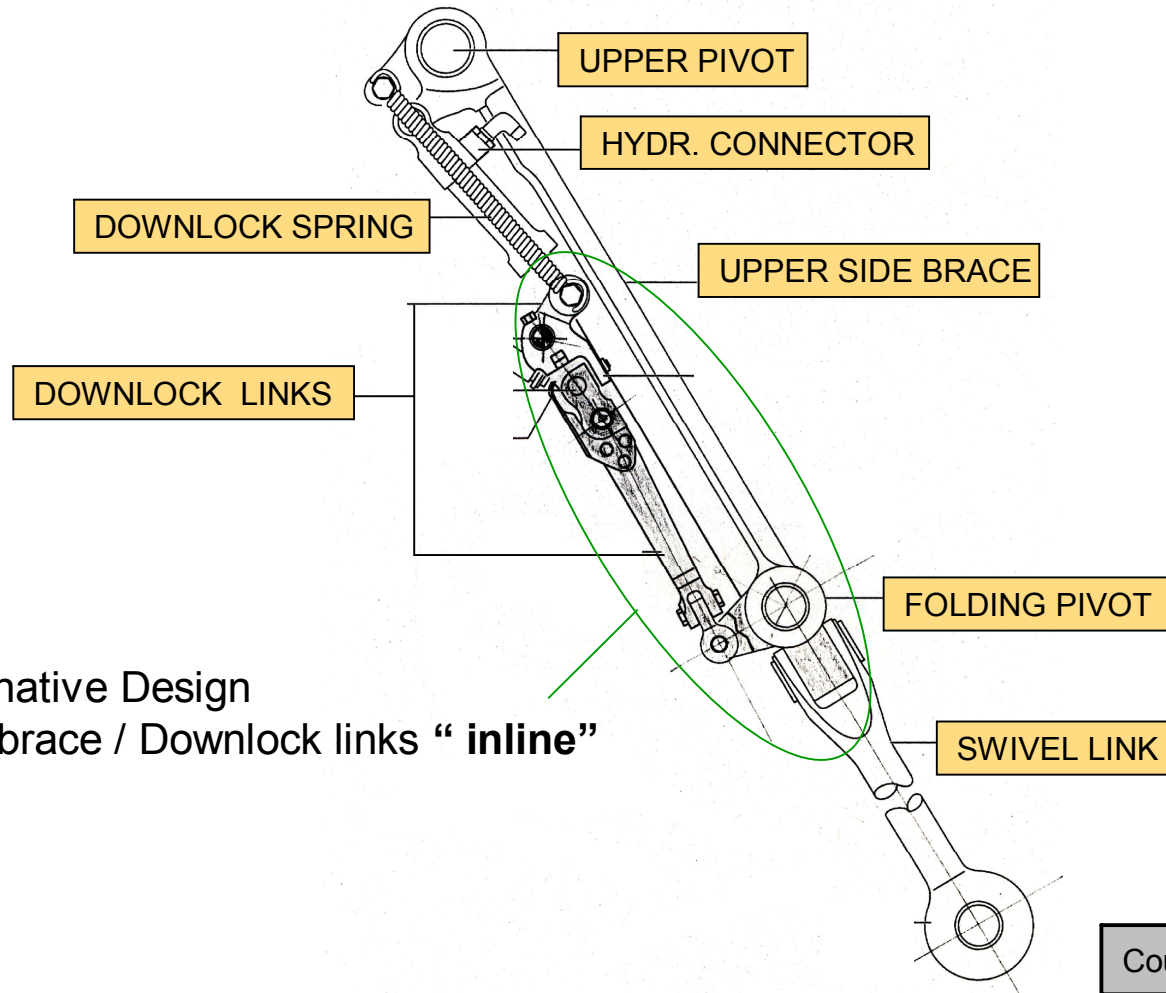


Retract mechanism example

- Alternative design
Side brace / downlock links “**inline**”



Retract mechanism example

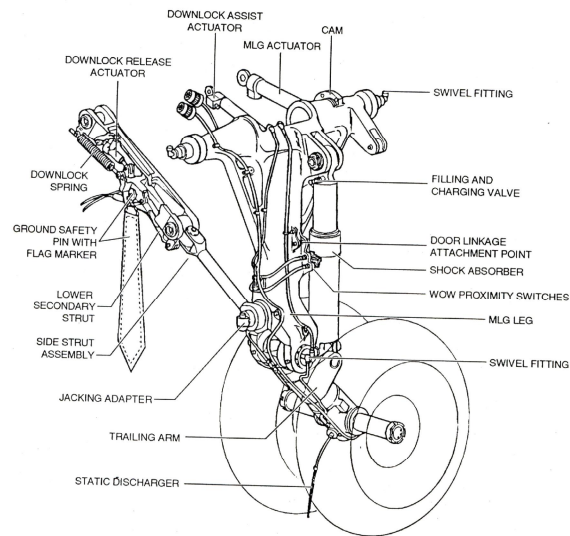


- Alternative Design
Side brace / Downlock links “**inline**”

Courtesy : DORNIER

Landing gear configurations

➤ Different size, similar layout



Courtesy : DORNIER

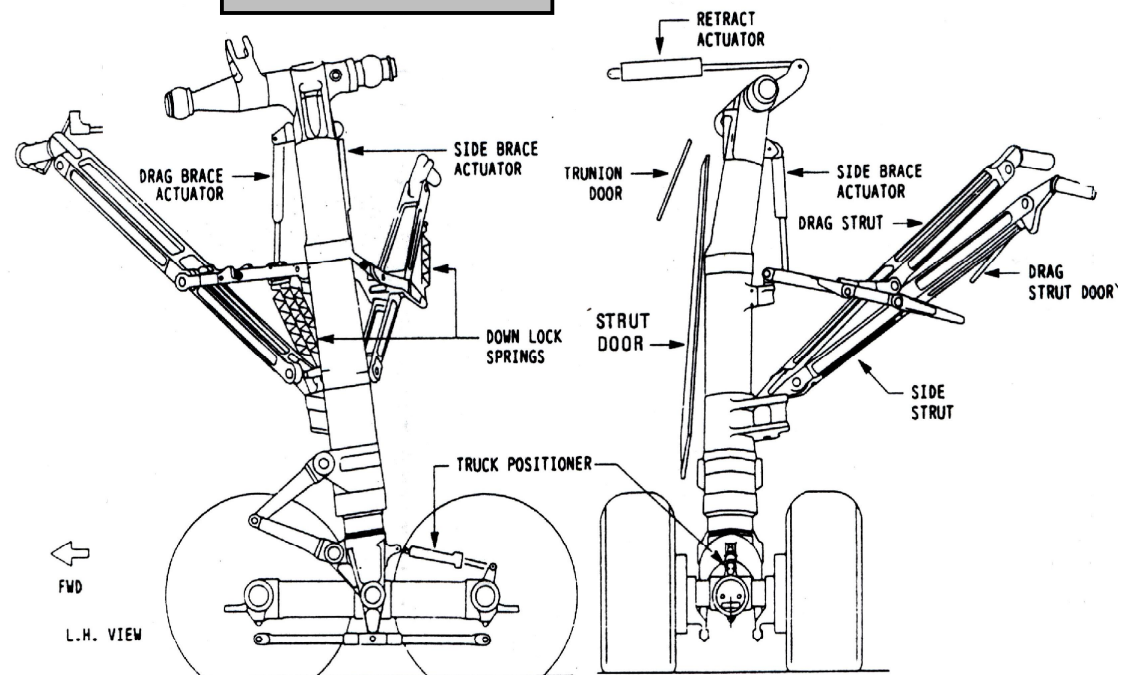
Design 1 :

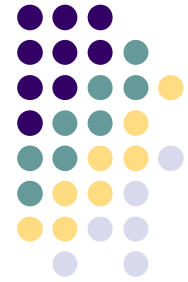
- Regional transport
- Fuselage mount
- Downlock inline

Design 2 :

- Medium / LR transport
- Wing mount
- Downlock perpendicular

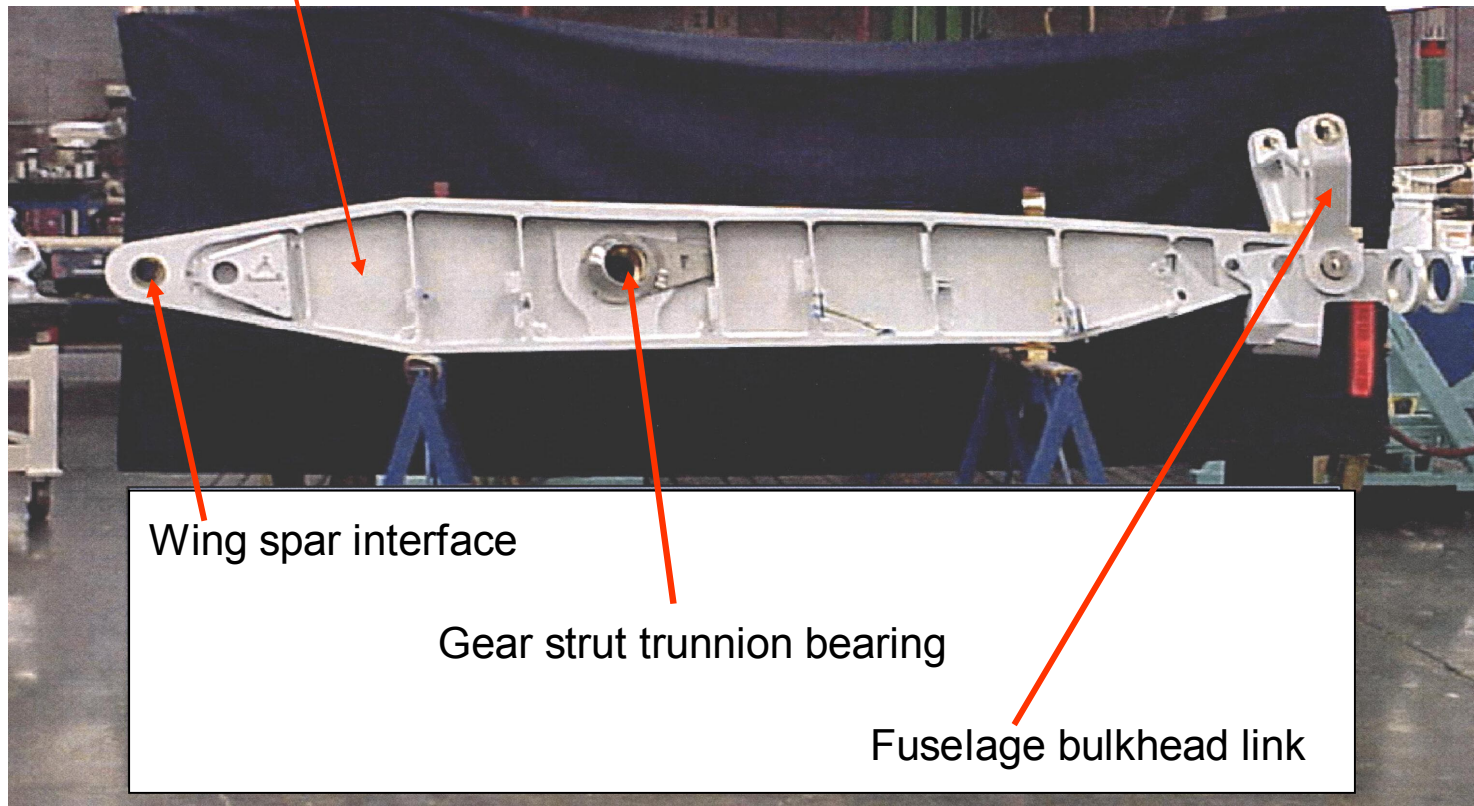
Courtesy : BOEING



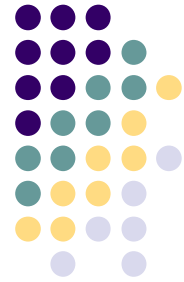


Landing gear attachment : gear strut —————> wing / fuselage structure

➤ Landing gear beam



Load distribution : gear strut → wing / fuselage structure

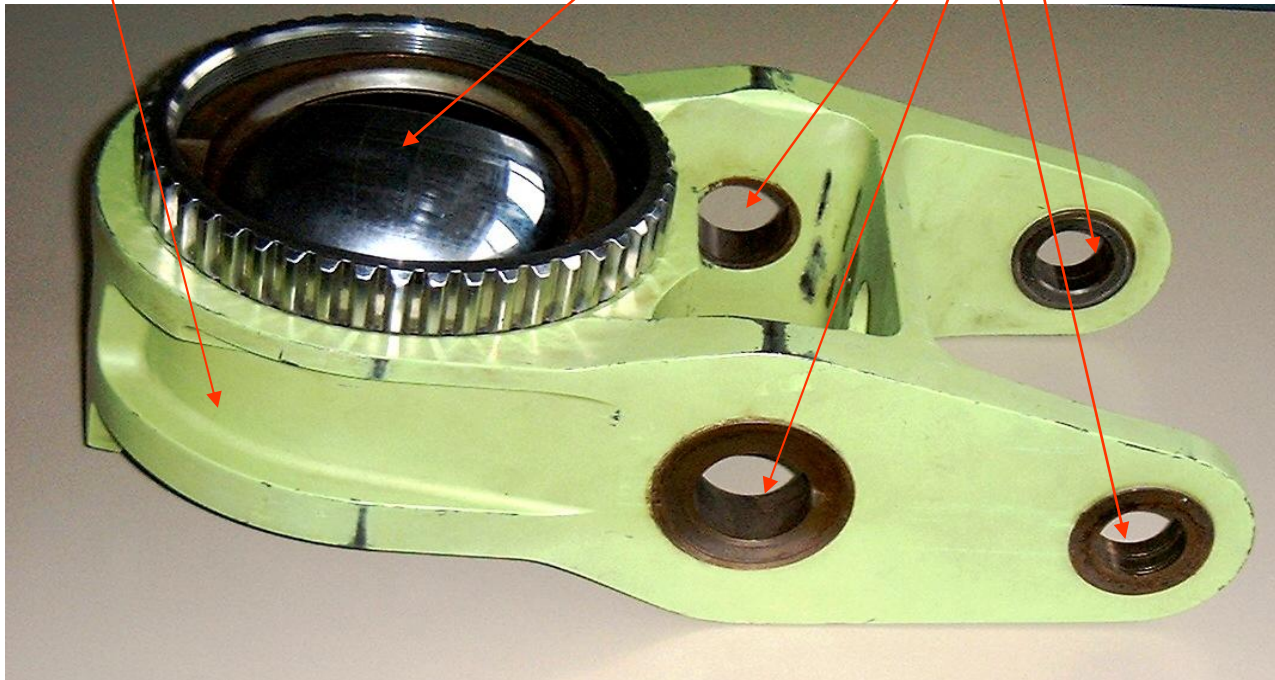


➤ Wing fitting

- Concentrated load distribution
- Trunnion bearing

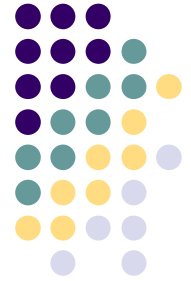
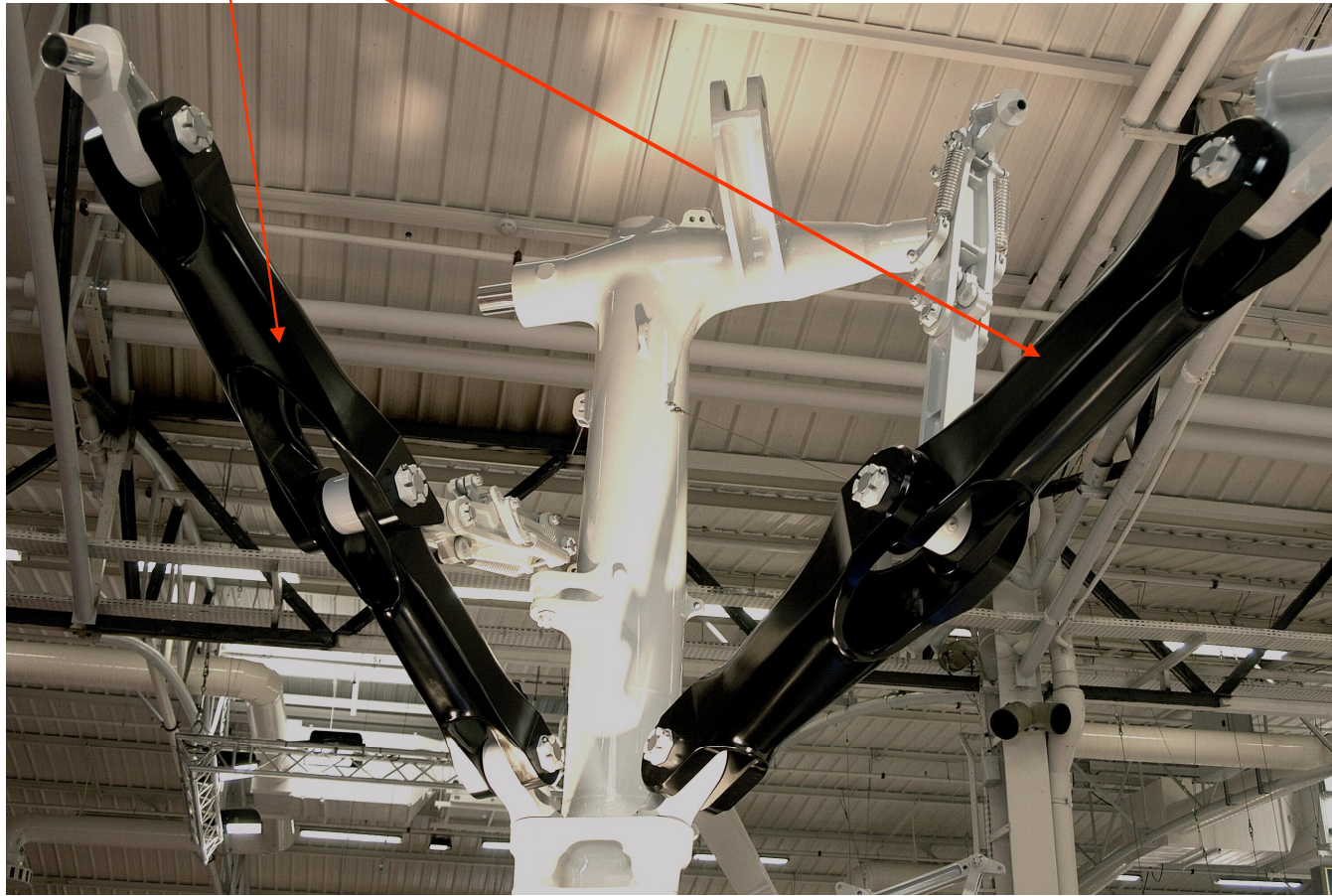
Concentrated load ...strut trunnion bearing

Distributed load ...wing rear spar



Component technology innovations

- Side brace in composite technology



Conclusion



Gear layout meets the requirements for

- Ground mobility of an airplane
 - Take off and landing run
 - Taxi
- Energy dissipation
 - Landing impact
 - Braking
- Aerodynamics
 - Retractability

References :

- J. ROSKAM : Airplane design
- M. NIU : Airframe structural design
- N. CURREY : Landing gear design
- N. N. : Dornier publications
- N. N. : Messier publications
- N. N. : Boeing publications

Dieter Scholz

Chapter 9

Empennage General Design

9 Empennage General Design

Empennage design is subdivided into Section 9 (Empennage General Design) and Section 11 (Empennage Sizing). In this first section basic information on empennage design is provided. The size of the empennage is estimated with the aid of the so-called tail volume. This initial estimate of empennage size is important for calculating the aircraft mass and center of gravity. Afterwards detailed calculation methods for determining empennage size will be dealt with in Section 11.

The basic configuration of the empennage has already been established in Section 4 with the configuration of the aircraft. In this section the various types of empennage will be looked at more closely, in order to define the exact configuration.

Empennages are "small wings". Therefore, many of the aspects described in Section 7 (Wing Design) also apply to empennages. The main difference is that empennages – unlike wings – normally only use a small part of the potential lift. If an empennage should come close to its maximum lift coefficient in flight, the empennage design is likely to be faulty.

9.1 Functions of Empennages

Empennages create a force that acts upon a lever arm. Consequently a moment is created through empennages:

- the horizontal tailplane creates a moment around the lateral axis (pitch),
- the vertical tailplane (fin) principally creates a moment around the vertical axis (yaw).

Ailerons and spoilers on the wing (see Section 7) principally create a moment around the longitudinal axis (roll).

Control surfaces on empennages and on the wing are the customary way to create moments. However, there are other possibilities for creating moments:

- moving the center of gravity (tail aft aircraft),
- engine thrust (control jets on the VTOL aircraft).

Empennages ensure trim, stability and control. These three aspects are detailed in the next paragraphs.

Trim

The moment created by an empennage balances out moments occurring on the aircraft for another reason. The horizontal tailplane, for example, balances out the wing moment (Fig. 9.1). In the case of propeller aircraft, the rotating slipstream causes a moment at the rear of the fuselage and at the vertical tailplane. The vertical tailplane has to compensate for this moment. If an engine fails on a multi-engine aircraft, the vertical tailplane compensates for an asymmetrical moment distribution around the vertical axis.

CS 25.161 defines the term "trim":

- (a) Each aeroplane must meet the **trim requirements** of this paragraph **after being trimmed**, and **without further pressure upon**, or movement of, either the **primary controls** or their corresponding trim controls by the pilot or the automatic pilot.

In simple terms: an aircraft is trimmed when the primary flight controls (pitch, roll, yaw) are free of forces in controlled flight.

The trim has to be guaranteed for all prescribed center-of-gravity positions, airspeeds, flap and landing gear positions and in the event of engine failure (for details see: CS 25.161).

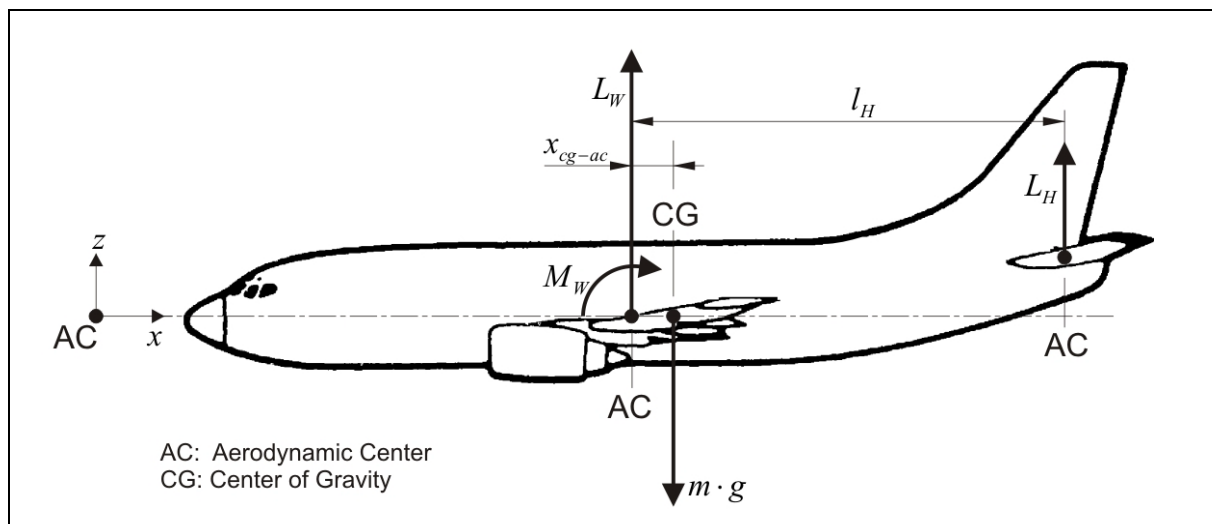


Fig. 9.1 Forces and moments acting on an aircraft during trimmed horizontal flight.

Stability

Stability refers to the capacity of the aircraft to return to the original flying position after a disturbance from outside or after a brief control input. Details are contained in the certification regulations in CS 25.171 to CS 25.181. A distinction is made between static stability and dynamic stability.

- *Static stability.* Longitudinal static stability ensures that the airspeed remains stable. The following is required according to CS 25.173:

- | | |
|-----|---|
| (a) | A pull must be required to obtain and maintain speeds below the specified trim speed, and a push must be required to obtain and maintain speeds above the specified trim speed. |
| (c) | The average gradient of the stable slope of the stick force versus speed curve may not be less than 1 pound for each 6 knots. |

The lateral static stability returns the aircraft to a slip-free flight. CS 25.177 requires the following:

- | | |
|-----|---|
| (b) | The static lateral stability (as shown by the tendency to raise the low wing in a sideslip with the aileron controls free) for any landing gear and wing-flap position and symmetric power condition, may not be negative at any airspeed |
|-----|---|

- *Dynamic stability* is contingent upon static stability. But an aircraft is not necessarily dynamically stable when it is statically stable, because if the aircraft returns to its original position after a disturbance, it can, of course, easily overshoot the original position. If this oscillation ceases after a while (or an overshoot does not occur), this oscillation of the aircraft is dynamically stable. But if the amplitude of oscillation becomes greater and greater, this oscillation of the aircraft is dynamically unstable. Conventional aircraft exhibit the following "oscillation forms" or, to be more precise, modes (it does not always have to be an oscillation; it might also be a heavily damped movement):

- in a *longitudinal movement* (i.e. around the lateral axis): short period mode, phugoid.
- in a *lateral movement* (i.e. around the longitudinal and vertical axis): spiral mode, Dutch roll mode.

The modes can best be explained with a small model aircraft in the hand or in flight. Therefore, a further description is dispensed with at this point.

CS 25.181 requires that certification flights must demonstrate the following features:

- | | |
|-----|--|
| (a) | Any short period oscillation ... must be heavily damped with the primary controls - |
| (1) | Free; and |
| (2) | In a fixed position. |
| (b) | Any combined lateral-directional oscillations ('Dutch roll') ... must be positively damped with controls free, and must be controllable with normal use of the primary controls without requiring exceptional pilot skill. |

Control

An aircraft must be sufficiently controllable in all critical flight states (CS 25.143 to CS 25.149). The control forces should not become too extreme (see CS 25.143(c)). In addition, the increase in control forces is dealt with using the limit load factor (CS 25.143):

- | | |
|-----|--|
| (f) | ... the stick forces and the gradient of the curve of stick force versus manoeuvring load factor must lie within satisfactory limits. The stick forces must not be so great as to make excessive demands on the pilot's strength ... and must not be so low that the aeroplane can easily be overstressed inadvertently. |
|-----|--|

Critical flight states for the empennage dimensioning from the point of view of control are:

- *Horizontal tailplane*: critical combination of center-of-gravity position, flap position and airspeed; rotation during take-off; flare when landing: control with trimmed horizontal stabilizer (CS 25.255).
- *Vertical tailplane (fin)*: Engine failure in cruise and during take-off and landing. Engine failure during take-off run, landing with crosswind (sideslip to compensate for crosswind component), spinning (CS 23.221).

An aircraft must possess sufficient **maneuverability** in accordance with its flight mission. It is scarcely possible to derive maneuverability criteria from the civil certification regulations. Instead the findings contained in military regulations – also for transport aircraft – are used in the design (see **MIL-F-8785C** and **MIL-STD-1797**). In the development phase a simulator model is created and the future aircraft is "flown" and assessed by test pilots. The lever arm and aileron must be large enough for sufficient maneuverability. In addition, it must be possible to deflect the control surfaces quickly enough.

9.2 Shapes of the Empennage

Different empennage shapes are shown on selected aircraft in Fig. 9.2.

The **conventional tail** provides appropriate stability and control and also leads to the most lightweight construction in most cases. Approximately 70 % of aircraft are fitted with a conventional tail. Spin characteristics can be bad in the case of a conventional tail due to the blanketing of the vertical tailplane (Fig. 9.3). The downwash of the wing is relatively large in the area of the horizontal tailplane. Rear engines cannot be teamed with conventional tails. Stabilizer trim is possible with comparatively low complexity. A larger vertical tailplane height is more appropriate for a conventional tail than a T-tail.

The **T-tail** is heavier than the conventional tail because the vertical tailplane has to support the horizontal tailplane. However, the T-tail has advantages that partly compensate for the described main disadvantage (weight). Owing to the end plate effect, the vertical tailplane can be smaller. The horizontal tailplane is more effective because it is positioned out of the airflow behind the wing and is subjected to less downwash. It can therefore be smaller. For the same reason the horizontal tailplane is also subject to less tail buffeting. The T-tail creates space for engines that are to be placed at the rear. The T-tail looks good, according to general opinion.

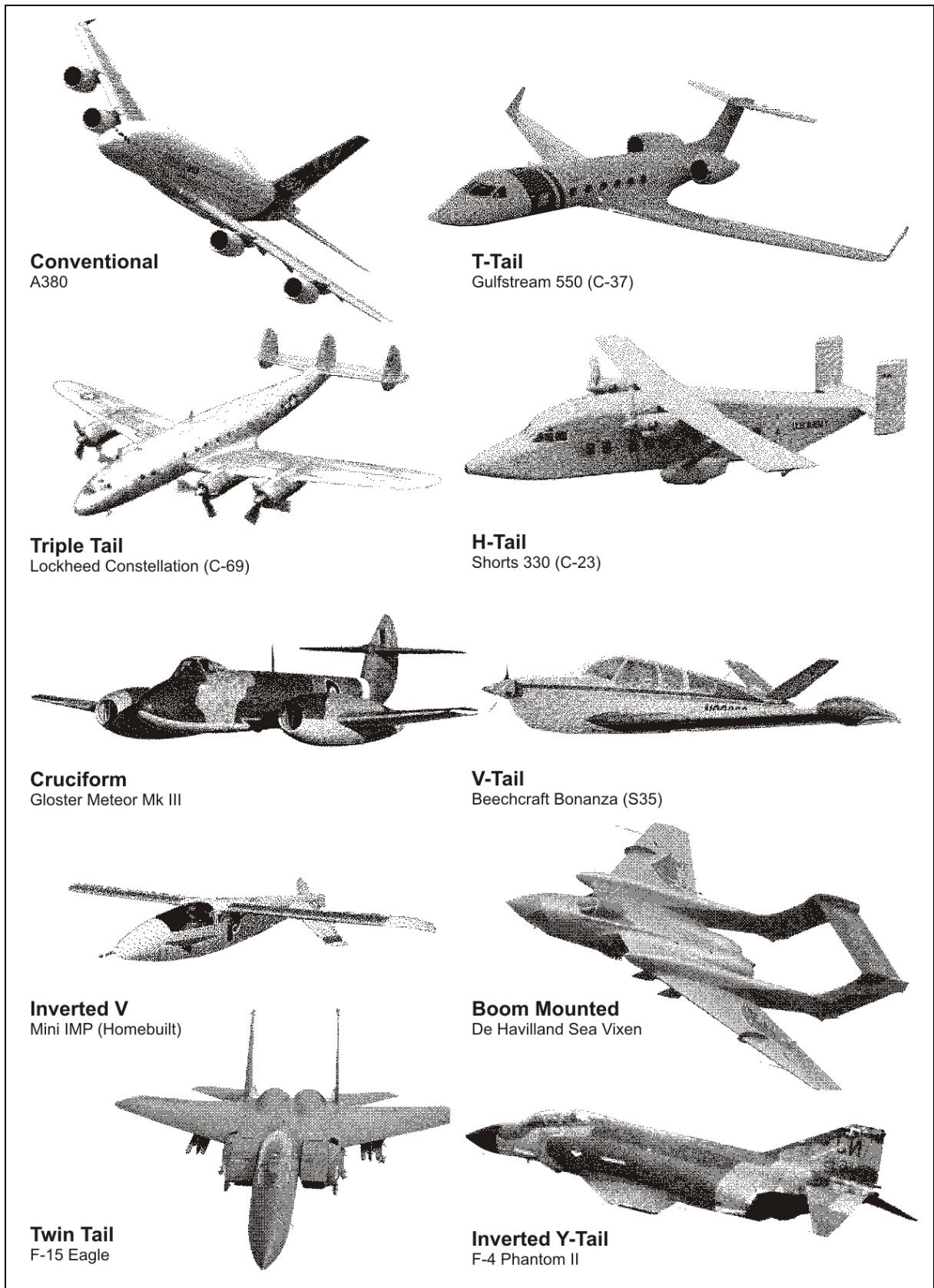


Fig. 9.2 Empennages of conventional aircraft configurations

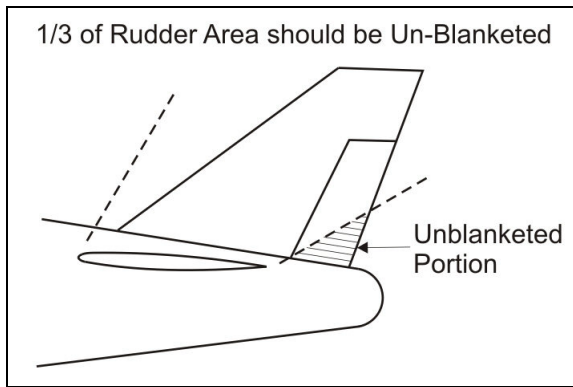


Fig. 9.3 Influence of the empennage design on the spin recovery characteristics

With T-tails the problem of *deep stall* must be taken into account (Fig. 9.4). In the case of high angles of attack the horizontal tailplane can be caught up in the airflow behind the wing and be blanketed. If, in addition, the wing tends to make the aircraft pitch up at high angles of attack (see Section 7), a situation may arise in which the aircraft can no longer be recovered from the stall. Fig. 9.5 shows admissible positions of the horizontal tailplane.

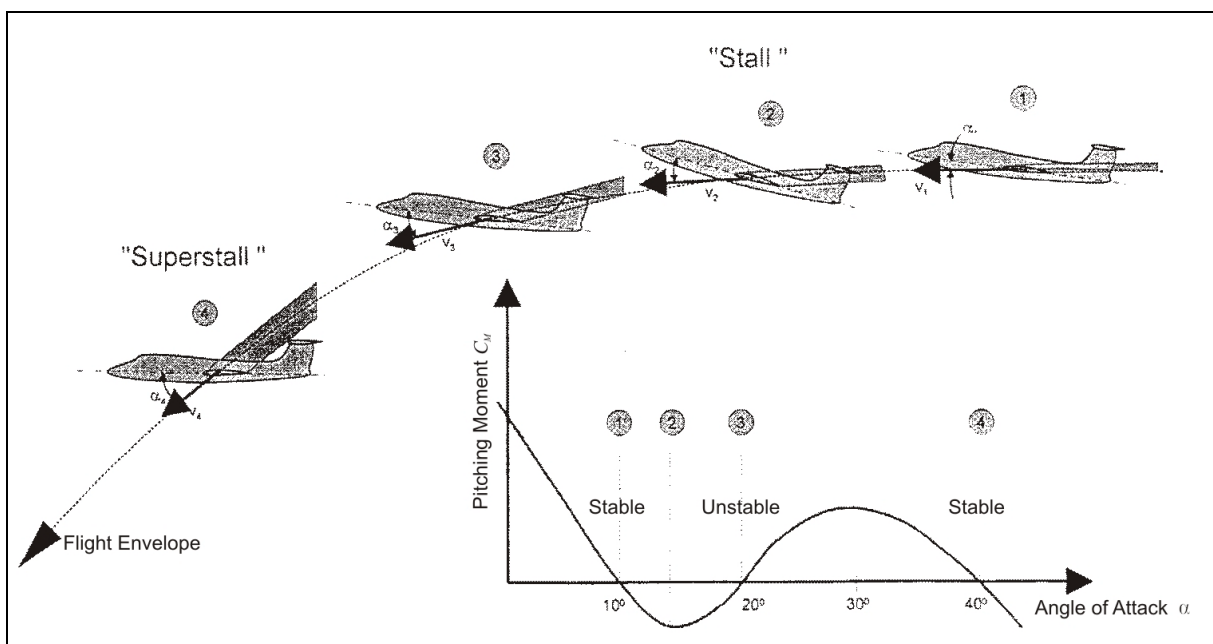


Fig. 9.4 Flight envelope, angle of attack and pitching moment during deep stall and super stall (Schmitt 1998)

The **cruciform tail** is a compromise between a conventional tail and a T-tail. The cruciform tail weighs less than the T-tail and allows the engines to be placed at the rear (e.g. Caravelle). However, the cruciform tail does not have a surface area advantage due to the end plate effect like the T-tail.

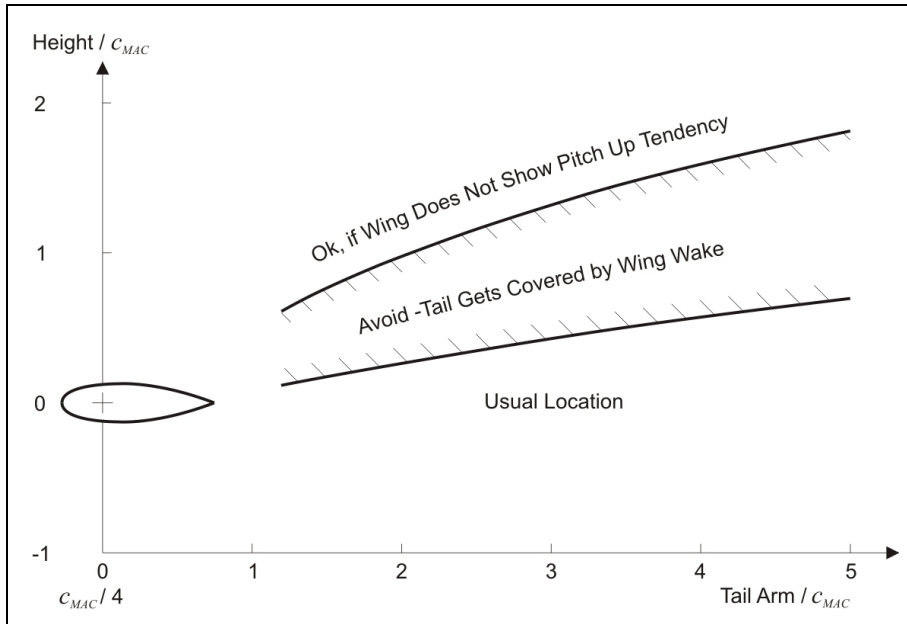


Fig. 9.5 Positioning of horizontal tailplanes

The aim of the **V-tail** is to achieve a smaller tail area than with horizontal and vertical tailplanes, for example in the form of the conventional tail. The V-tail is designed as follows: In the first step the required areas of a conventional horizontal tailplane S_H and vertical tailplane S_V are determined (see below). Theoretically the V-tail provides efficiency as a horizontal and vertical tailplane, corresponding to the projection of the V-tail in the horizontal and vertical. This theoretical approach gives the necessary V angle for the V-tail

$$v = \arctan \frac{S_V}{S_H} \quad (9.1)$$

and the necessary area

$$S_{V-Tail,theory} = \sqrt{S_H^2 + S_V^2} \quad (9.2)$$

On the basis of this theoretical analysis the V-tail only requires a tail area of $S_{V-tail} / (S_V + S_H) = 70.7\%$ compared to the conventional tail with $S_V / S_H = 1$. With other S_V / S_H ratios the area saving is less. According to the **NACA 823** report, the V-tail must, however, be larger in practice than the theory suggests for the same efficiency, so that the advantage of the smaller area is lost and a tail area

$$S_{V-Tail} = S_H + S_V \quad (9.3)$$

is necessary.

With a V-tail the control surfaces deflect in the same direction in the function of the elevator and in opposite directions in the function of the rudder. If the right rudder pedal is pressed, the right control surface of the V-tail moves down and the left control surface up. One of the dis-

advantages of the V-tail is the complicated mechanics required to combine the elevator and rudder inputs. Inconveniently a "rudder deflection" of the V-tail causes a roll moment against the desired turn. A roll moment in the direction of the desired turn is, on the other hand, achieved with the inverted V-tail. However, many aircraft configurations will not be able to accommodate an inverted V-tail due to the necessary ground clearance.

A **twin tail** can be used if a single vertical tailplane would be too big. Twin tails are covered less by the front fuselage in the case of high angles of attack than a vertical tail in the plane of symmetry. For the latter reason twin tails are seen on fighter aircraft that operate in the high angle of attack range. Fig. 9.2 shows additional tail configurations that might be advantageous under certain circumstances.

Other tail features:

- Through the **dorsal fin** (Fig. 9.6) the efficiency of the vertical tailplane where high angles of yaw exist is improved through vortex formation. The stall is thereby moved to higher angles of yaw.
- The **ventral fin** (Fig. 9.6) is not blanketed even with high angles of attack. The ventral fin also serves to prevent lateral instabilities in high-speed flight.

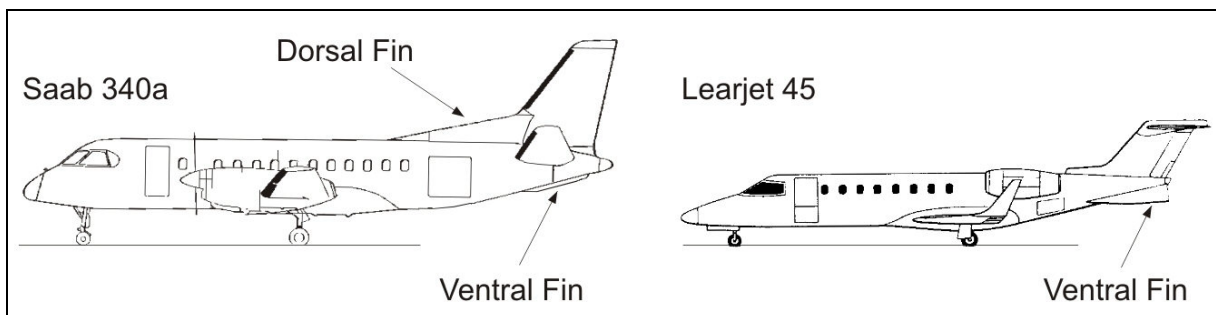


Fig. 9.6 Examples of aircrafts with dorsal fin and ventral fin

The **canard tails** (Fig. 9.7) are subdivided into *control canard* and *lifting canard*.

- In the case of a *control canard* the wing bears the aircraft's weight. Wings and fuselage alone show neutral stability; the canard is only used for control, but makes the system comprising fuselage, wing and tail instable. An electronic flight control system, EFCS, carries out the regulation and stabilization of the instable aircraft. An aircraft with canard must be designed in such a way that the wing can never be stalled. Instead the canard is first stalled. This necessitates that the wing's lift potential cannot be fully utilized.
- The *lifting canard* has less drag theoretically because the canard – in contrast to the horizontal tailplane of the tail aft configuration – creates lift (instead of negative lift) (compare with Fig. 9.1). By using the *lifting canard* the wing must be placed further to the rear. Through this placement the lifting canard is able to facilitate a center-of-gravity range that

is normally required. However, the lifting canard displays various disadvantages that restrict its overall utility considerably: the placement of the wing further back on the fuselage increases the nose-heavy moment when using the landing flaps due to the larger lever arm. The wing of the canard must therefore have a greater area with less effective flaps than is customary with the tail aft configuration. Another way of solving this problem is to fit the canard with effective flaps or provide a variable sweep of the canard.

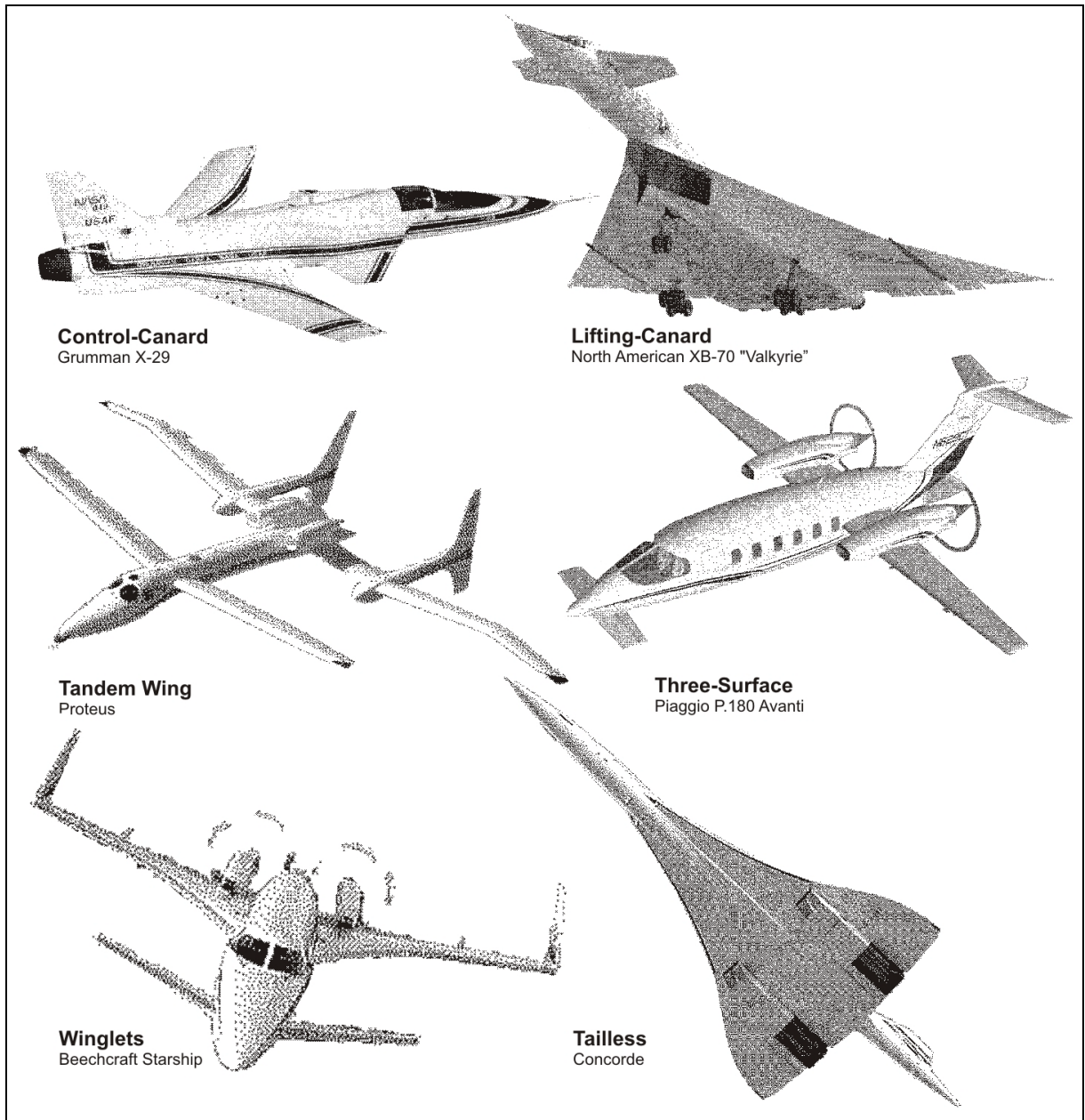


Fig. 9.7 Empennages of unconventional aircraft configurations

The **tandem wing** is a *lifting canard* where the lift forces are approximately evenly distributed between the wing and the canard.

The **three-surface configuration** makes it possible to create a pitching moment without influencing the lift on the wing. Therefore it is possible to better optimize the distribution of lift on the wing and thereby reduce the drag. One of the disadvantages is the additional complexity due to an additional area.

All configurations with canards have the disadvantage that the wing lies in a flow disturbed by the empennage placed at the front.

9.3 Design Rules

- The horizontal tailplane should be installed in a **position** so that it does not lie in the slipstream. If this rule is not observed, it may have the following effects:
 - structure fatigue due to tail buffeting;
 - increased noise in the cabin due to tail buffeting;
 - considerable trim changes with differing choice of engine performance.

In some small single-engine aircraft the empennage is deliberately placed in the slipstream. Then one benefits from an increased efficiency of the tail assembly during take-off and landing, but may have to accept the disadvantages described above.

- The detailed **placement of the horizontal tailplane** can be determined from Fig. 9.5: low-lying horizontal tailplanes are most suitable for getting an aircraft out of a stall. With subsonic aircraft the empennage can also be installed at the same height as the wing. A T-tail may only be used if the wing is uncritical and is not susceptible to excessive pitch-up (compare Section 9.2: "T-tail").
- The **lever arm** of the empennage should be as large as possible, thereby making it possible to keep the tail areas small, which reduces weight and drag.
- The **aspect ratio** of the horizontal tailplane should be about half the aspect ratio of the wing. T-tails have a smaller aspect ratio of the vertical tailplane than conventional tails (Table 9.1). This allows weight disadvantages to be kept to a minimum.
- Tails with a taper ratio of $\lambda = 1$ are built in some cases as **rectangular tail** especially for general aviation aircraft. Rectangular tails reduce production costs.
- The **critical Mach number** of the empennage $M_{crit,H}$ und $M_{crit,V}$ should be $\Delta M = 0.05$ higher than the critical Mach number of the wing $M_{crit,W}$. Through this measure the efficiency of the tail assembly should also be guaranteed at high speed. Relative thickness,

drag divergence Mach number, sweep, and the lift coefficient of the empennage must be chosen so as to ensure that a $\Delta M = 0.05$ can be achieved. With an equation from Section 7 in the form

$$t/c = f(M_{DD}, \phi_{25}, C_L, \text{airfoil})$$

these parameters can be chosen to approximately suit each other if the drag divergence Mach number M_{DD} of the tail is $\Delta M = 0.05$ higher than for the wing.

- The **sweep of the horizontal tailplane** should be approximately 5° larger than the sweep of the wing. Thus a higher critical Mach number of the horizontal tailplane can be achieved and a loss of efficiency due to shock waves is avoided. In addition, the lift gradient of the horizontal tailplane can be less than the lift gradient of the wing due to the increased sweep, so that the horizontal tailplane only reaches the stall state at larger angles of attack than the wing.
- The **sweep angle of the vertical tailplane** is 35° to 55° for aircraft with "high airspeeds" (flight with compressibility effects). The sweep angle of the vertical tailplane for aircraft with "low airspeeds" (flight without compressibility effects) should be less than 20° . A large sweep angle increases the lever arm and the angle where the vertical tailplane goes into stall, but reduces the maximum lift coefficient.
- The **horizontal tailplane** should have a **relative thickness** that is approximately 10 % less than the relative thickness in the outer wing. Thus, a higher critical Mach number of the horizontal tailplane can be achieved and a loss of efficiency due to shock waves is prevented.
- Symmetrical **airfoils** are chosen exclusively for vertical tailplanes. Symmetrical or virtually symmetrical airfoils with 9% to 12% relative thickness are chosen for horizontal tailplanes. For example, NACA 0009 or NACA 0012 (**Abbott 1959**) can be chosen. Asymmetrical horizontal tailplane airfoils are installed "upside-down" because the horizontal tailplane has to create negative lift.
- If the **left and right elevators** are to be **connected**, the sweep and the taper ratio must be selected so as to ensure that a hinge line is produced perpendicular to the aircraft's plane of symmetry. Reasons for connecting the elevators may be:
 - to reduce the elevators' tendency to flutter;
 - to facilitate joint actuation of the elevators.

- The **dihedral angle** can be chosen so that the empennage is positioned outside the engine slipstream. Dihedral of the horizontal tail is not used to modify roll stability as this is much more influenced by the wing.
- If the horizontal tailplane is fixed, an **incidence angle** of around 2° to 3° downwards should be chosen to create negative lift. A more flexible alternative is a movable, i.e. **trimmable horizontal stabilizer**, THS, which facilitates a larger center-of-gravity range.
- The horizontal tailplane can be designed as an **all moving tail**. An all moving tail only consists of one surface with an adjustable incidence angle. The all moving tail is more effective – especially at high Mach numbers – but also heavier than a fixed empennage with control surface. In the case of large aircraft high output may be required to move the all moving tail in flight with the necessary actuating speed. A compromise is the **trimmable horizontal stabilizer** mentioned above: the horizontal stabilizer is used to trim and is only adjusted gradually (with a low actuating power); the elevator is deflected correspondingly quicker for maneuvering. The trimmable horizontal stabilizer is the standard solution for transport aircraft.
- **Lifting canard** or **tandem wing** are designed like wings (see Section 7).

Tables 9.1, 9.2 and 9.3 contain parameters that can be referred to as guides for empennage design.

Table 9.1 Conventional aspect ratios A and taper ratios λ from empennages on transport category airplanes (**Raymer 1989**)

Type	Horizontal Tailplane		Vertical Tailplane	
	A	λ	A	λ
Conventional Tail	3.00 ... 5.00	0.3 ... 0.6	1.3 ... 2.0	0.3 ... 0.6
T-Tail	as Conventional Tail	as Conventional Tail	0.7 ... 1.2	0.6 ... 1.0

Table 9.2: Conventional design parameters for horizontal tails (**Roskam II**)

Type	Dihedral Angle $\nu [^\circ]$	Incidence Angle $i_h [^\circ]$	Aspect Ratio $A_h [-]$	Sweep Angle $\phi [^\circ]$	Taper Ratio $\lambda_h [-]$
Business Jets	- 4 ... 9	-3.5 fixed	3.2 ... 6.3	0 ... 35	0.32 ... 0.57
Transport Jets	0 ... 11	variable	3.4 ... 6.1	18 ... 37	0.27 ... 0.62
Fighters	-23 ... 5	0 fixed or variable	2.3 ... 5.8	0 ... 55	0.16 ... 1.00
Supersonic Civil Transport	-15 ... 0	0 fixed or variable	1.8 ... 2.6	32 ... 60	0.14 ... 0.39

Table 9.3: Conventional design parameters for vertical tails (**Roskam II**)

Type	Dihedral Angle $\nu [^\circ]$	Incidence Angle $i_h [^\circ]$	Aspect Ratio $A_h [-]$	Sweep Angle $\phi [^\circ]$	Taper Ratio $\lambda_h [-]$
Business Jets	90	0	0.8 ... 1.6	28 ... 55	0.30 ... 0.74
Transport Jets	90	0	0.7 ... 2.0	33 ... 53	0.26 ... 0.73
Fighters	75 ... 90	0	0.4 ... 2.0	9 ... 60	0.19 ... 0.57
Supersonic Cruise Airplanes	75 ... 90	0	0.5 ... 1.8	37 ... 65	0.20 ... 0.43

9.4 Design According to Tail Volume

The area of the horizontal tailplane S_H or the vertical tailplane S_V multiplied by the lever arm l_H or l_V is called tail volume. The tail volume coefficient is defined for the horizontal tailplane as

$$C_H = \frac{S_H \cdot l_H}{S_W \cdot c_{MAC}} \quad (9.4)$$

and for the vertical tailplane as

$$C_V = \frac{S_V \cdot l_V}{S_W \cdot b} \quad (9.5)$$

l_H the lever arm of the horizontal tailplane is the distance between the aerodynamic centers of wing and horizontal tailplane,

l_V the lever arm of the vertical tailplane is the distance between the aerodynamic centers of wing and vertical tailplane.

As a good approximation the 25 % - point on the mean aerodynamic chord can also be referred to instead of the distances between the aerodynamic centers.

Table 9.4 Conventional tail volume coefficients of horizontal and vertical tails (**Raymer 1989**)

type	horizontal C_H	vertical C_V
General Aviation - Twin Engine	0.80	0.07
Transport Jets	1.00	0.08
Jet - Trainer	0.70	0.06
Jet - Fighter	0.40	0.07

The tail size can be estimated from the tail volume coefficient if the tail lever arms l_H and l_V are known. The lever arms are not, however, fixed until the position of the wing has been established. However, this only takes place in Step 11 "Mass and Center of Gravity". For this reason the tail lever arms can only be estimated from the length of the fuselage in this case (Table 9.5).

Table 9.5: Conventional tail lever arms of horizontal and vertical tails (**Raymer 1998**)

aircraft configuration	average of l_H and l_V
propeller in front of fuselage	60% of fuselage length
engines on the wing	50 ... 55% of fuselage length
engines on the tail	45 ... 50% of fuselage length
control canard	30 ... 50% of fuselage length
sailplane	65% of fuselage length

- The tail volume coefficients can be reduced by 10% to 15% in the case of **trimmable horizontal stabilizers**.
- In the case of a **T-tail**, the tail volume coefficients can be reduced by 5% for horizontal and vertical tailplane due to the end plate effect and the improved flow.
- In the case of a control **canard** a tail volume coefficient of 0.1 can be set. In the case of a *lifting canard* the tail volume coefficient method cannot be applied. Instead a ratio of the areas of canard and wing is established.
- If the criteria for stability and control determine the dimensioning of an aircraft's tail design, the tail volume coefficients can be reduced by approximately 10% if the aircraft has an electronic flight control system, **EFCS**. However, for transport aircraft other criteria (such as engine failure for the rudder) often determine the dimensioning, so that tail area cannot necessarily be saved through an EFCS.

9.5 Elevator and Rudder

Elevator and rudder start on the fuselage and extend to approximately 90% of the (semi-) span of the tail, or up to the tip of the tail (Fig. 9.8). They have a chord which accounts for approximately **25 % to 40 % of the chord of the tail**. Elevators are deflected downwards by a maximum of 15° to 25° and upwards by a maximum of 25° to 35°. Rudders are **deflected** by a **maximum of 25° to 35°**. **Torenbeek 1988** and **Roskam II** contain detailed tables with tail and control surface data.

The maximum lift (negative lift or transverse force) that an elevator or rudder on a tail can achieve can be calculated using the method from Section 8 because an elevator or rudder is a plain flap.

Particularly in the case of aircraft with a reversible flight control system (Fig. 9.7) it is important to know the hinge moment required to deflect the rudder in the various flight states. The

reason is that the hinge moment determines the hand and foot forces on the flight controls, which may not exceed specific maximum values according to CS 25.143(c). The hinge moment is calculated with

$$M_c = \frac{1}{2} \rho V^2 \cdot C_h \cdot S_F \cdot c_F \quad . \quad (9.6)$$

V is the airspeed, S_F is the control surface area, c_F is the rudder depth (measured from the hinge line to the trailing edge). The hinge moment coefficient C_h of a control surface is calculated from the hinge moment derivatives C_{h_α} and C_{h_δ} (see **DATCOM 1978** or **Roskam VI**). It is important to bear in mind that asymmetrical airfoils already have a hinge moment coefficient C_{h_0} at $\alpha = \delta = 0$.

$$C_h = C_{h_0} + C_{h_\alpha} \cdot \alpha + C_{h_\delta} \cdot \delta \quad . \quad (9.7)$$

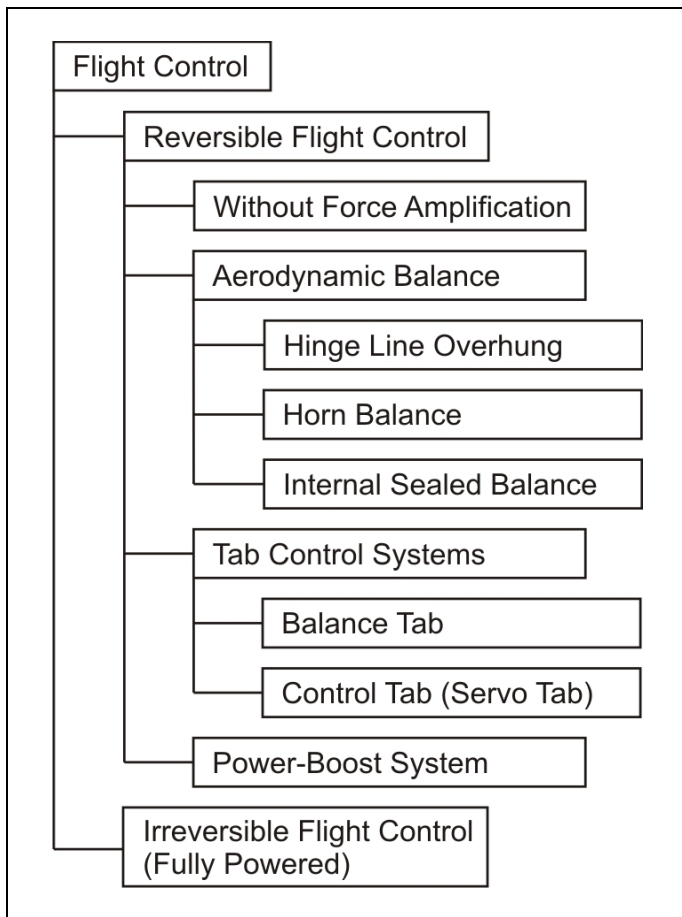


Fig. 9.8 Classification of flight controls and hinge moment reduction possibilities

According to equation (9.6) the aerodynamic hinge moment increases with the size and speed of an aircraft. As the control forces may become too large even in small aircraft, measures must be taken to reduce them. The hinge moment is fully or partially carried by the pilot's muscular force on reversible flight controls. On irreversible flight controls the hinge moment

is countered by the aircraft's onboard energy systems. Fig. 9.8 shows the main options for reducing control forces. The options are arranged according to increasing effectiveness but also complexity. Fig. 9.9 shows two of these methods for hinge moment reduction. Horn and overhang balance are often applied on small aircraft owing to their simple design.

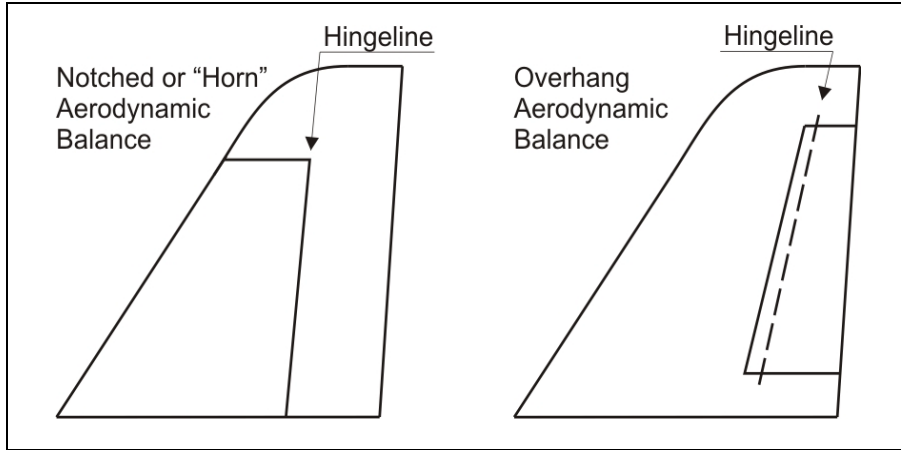


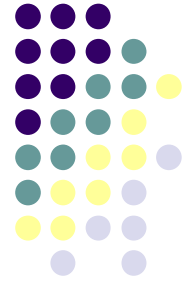
Fig. 9.9 Typical methods of hinge moment reduction

Erhard Rumpler

Chapter 10

Engine Integration

Engine integration (mechanical)



➤ Power plant components :

- Engine (turbofan or turboprop)
- Nacelle (aerodynamics, thrust reverser)
- Pylon (mechanical link, optimal engine position)
- Accessory systems (starter, fuel supply, generators, lubrication, ...)

➤ Engine integration (mechanical) :

- connection engine / airframe
- relevant component : pylon

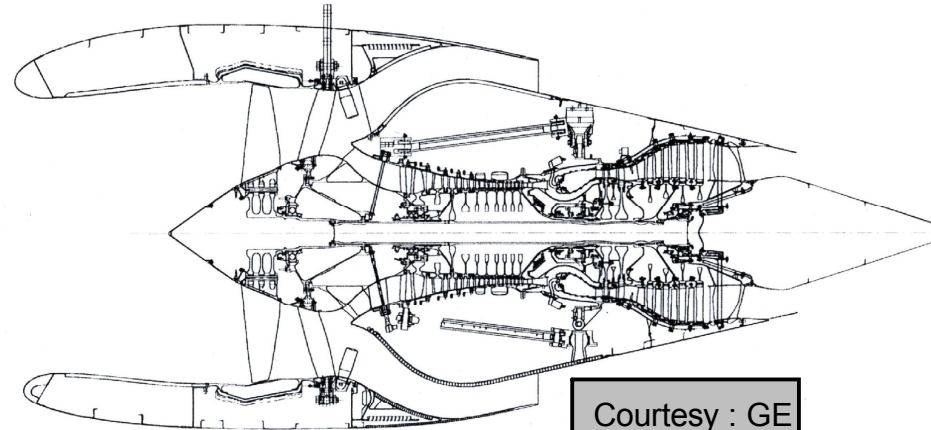


Standard turbofans 2000

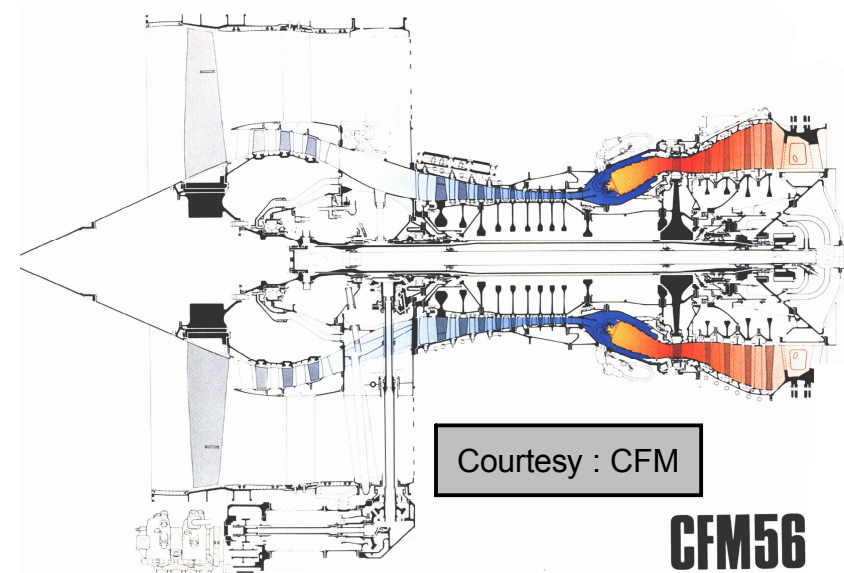
Thrust	41 kN
Fan dia	1,24 m
Length	2,62 m

Thrust :	89 -139 kN
Fan dia	1,84 m
Length	2,62 m

CF34-3A1



Courtesy : GE



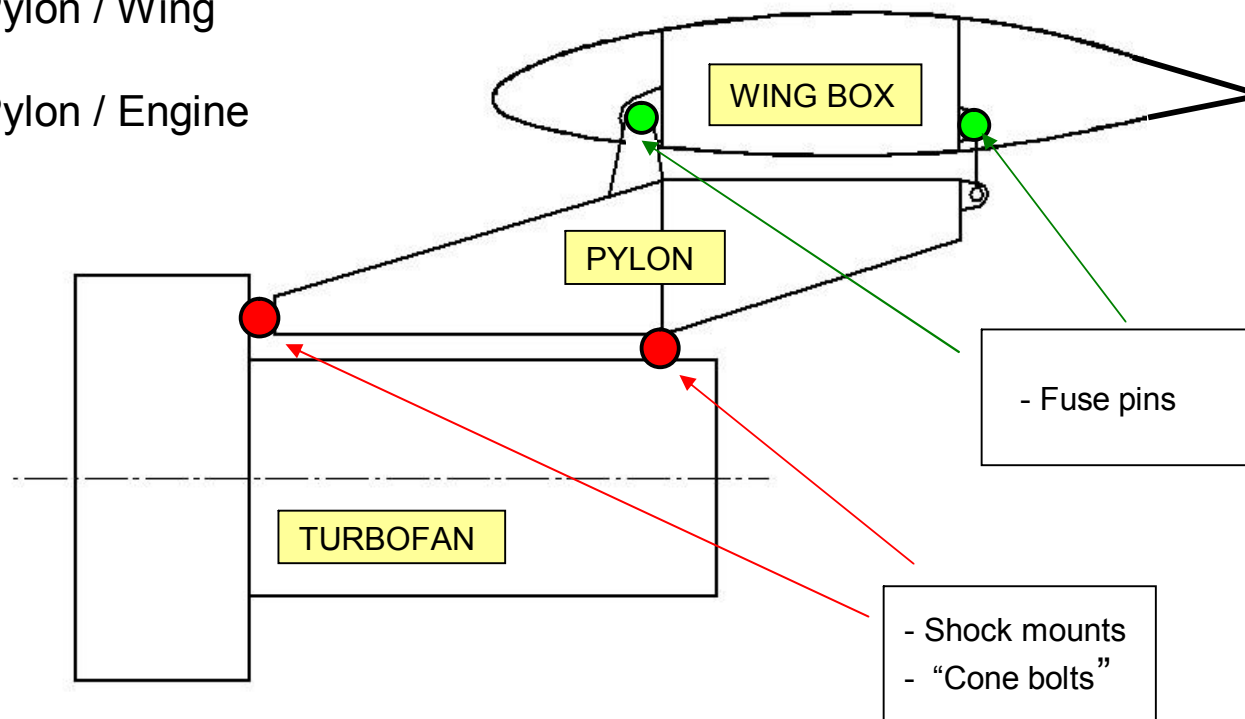
Courtesy : CFM

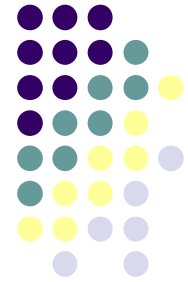
CFM56

Turbofan engine installation

➤ Attachment Points :

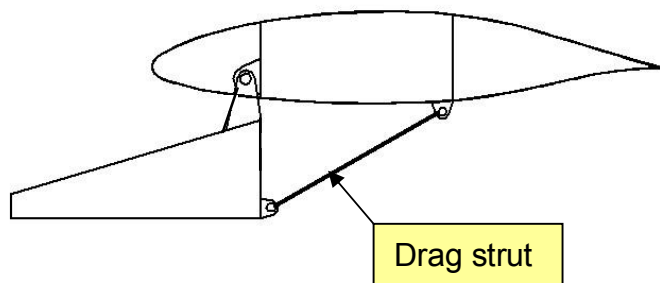
- - Pylon / Wing
- - Pylon / Engine





Wing / pylon interface

➤ Interface designs

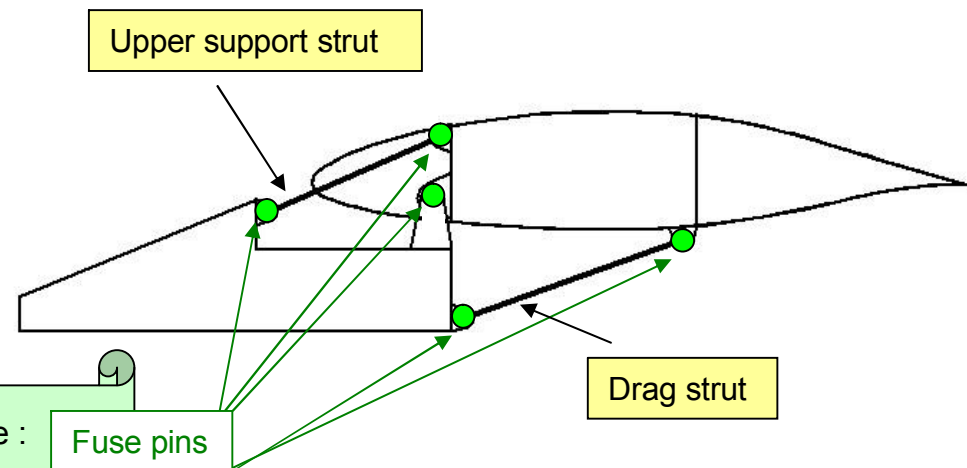


Design 1 for smaller engines

- Static determinated
- No redundancy

Design 2 for larger engines

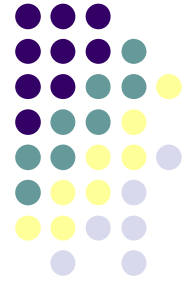
- Static indeterminated
- Redundancy
- Load splitting



Historical note :
B747
Accident 10/04/1992
- Fuse pin failure

Interface morphologic matrix

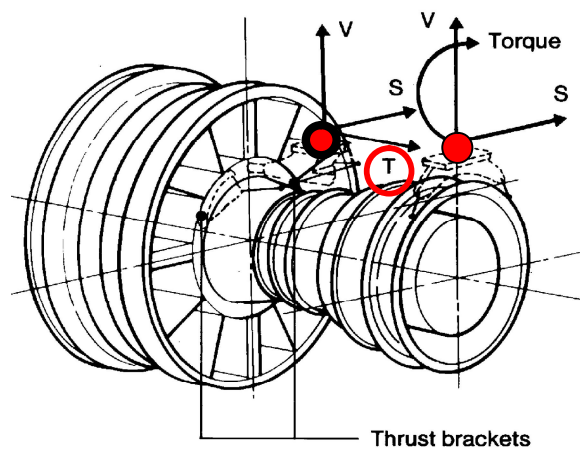
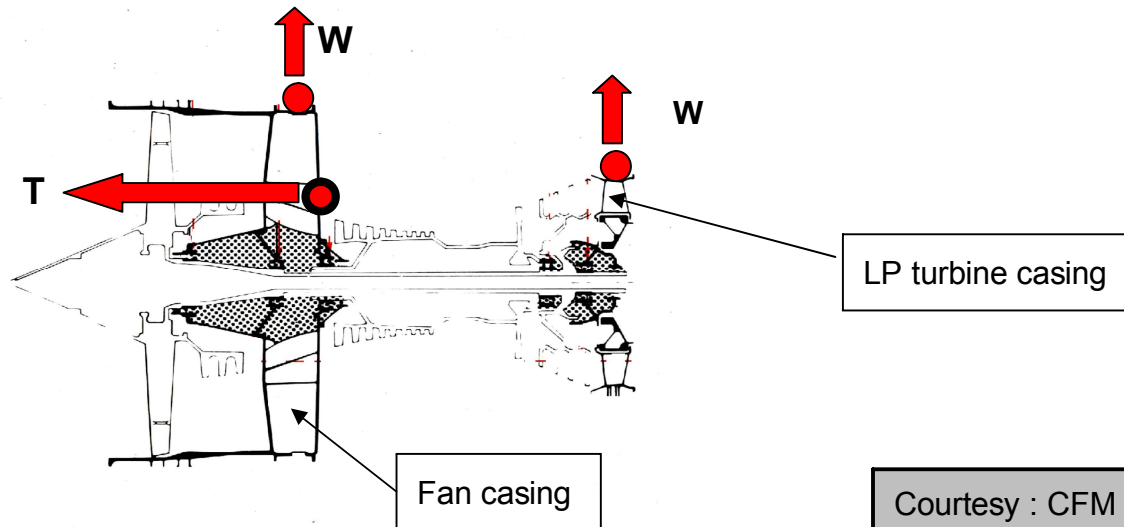
- complete range of interface designs



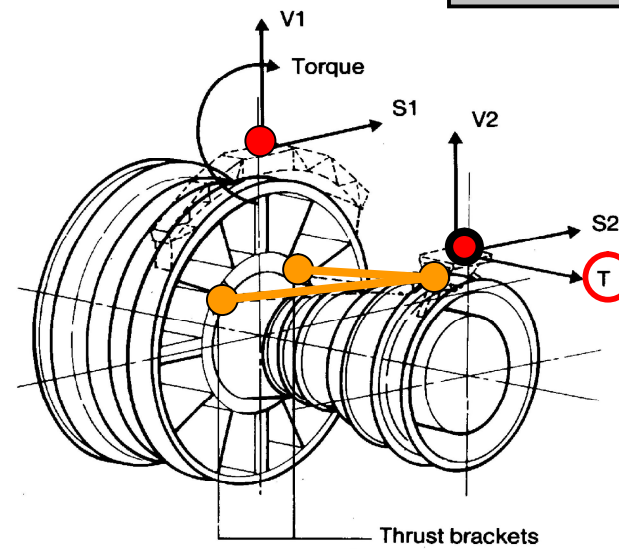
Triebwerk – Pylon	vorne: Fachwerk mit 2 Thrust-Links 	hinten: 2 Pendelstützen & Bolzen 	hinten: Bolzen 				
Pylon Struktur	langer Kasten o. Druckstrebe 	kurzer Kasten m. Druckstrebe 	langer Kasten o. Druckstrebe 	Fachwerk mit Interface 	Fachwerk 	Fachwerk m. Druckstrebe 	
Pylon – Wing vorne	Brücke 	Brücke m. Mittelrippe 	Brücke m. Thrust-Link 	reines Fachwerk 	Fachwerk m. Schubwänden 		2 Pendelstützen
Pylon – Wing hinten	1 Pendelstütze 	2 Pendelstützen 	Bolzen 	2 Pendelstützen & Bolzen 	2 Pendelstützen & Bolzen (Dormier-Lösung) 	Brücke 	

Turbofan engine attachment points

- “Hardpoints” on fan and turbine casings



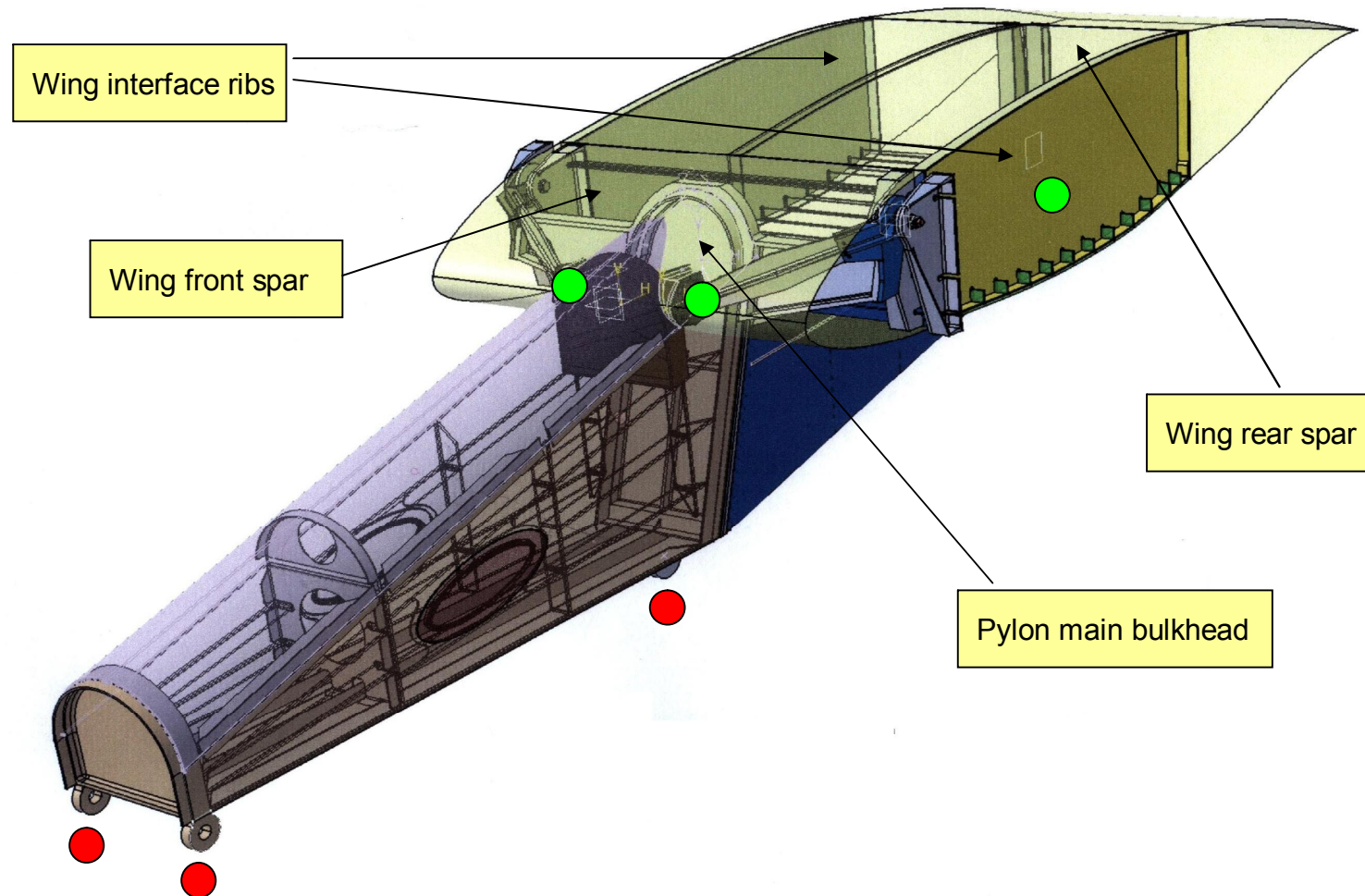
1B - Underwing mounting



3B - Underwing mounting

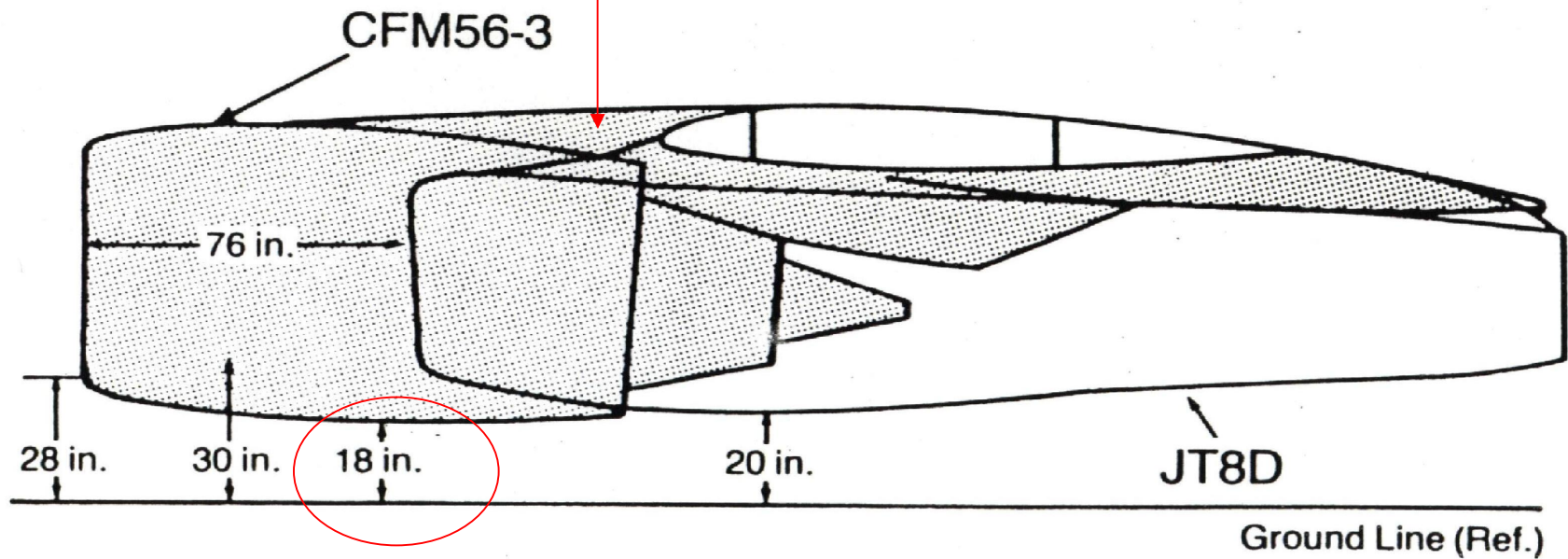
Engine pylon design

- Design 1 exercise for a smaller pylon

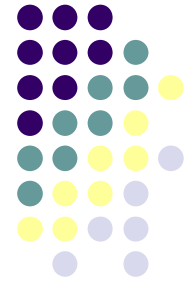


Ground clearance

- Special flat pylon design to ensure ground clearance in case of an existing landing gear

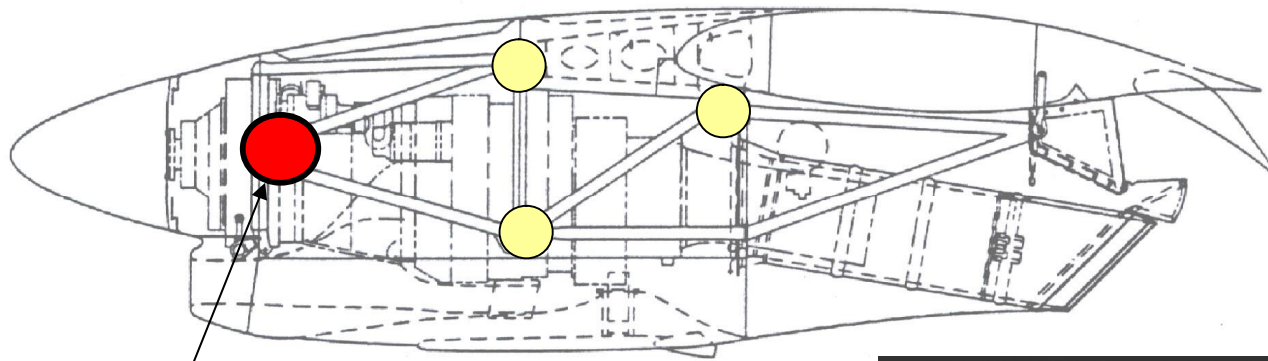


Courtesy : CFM



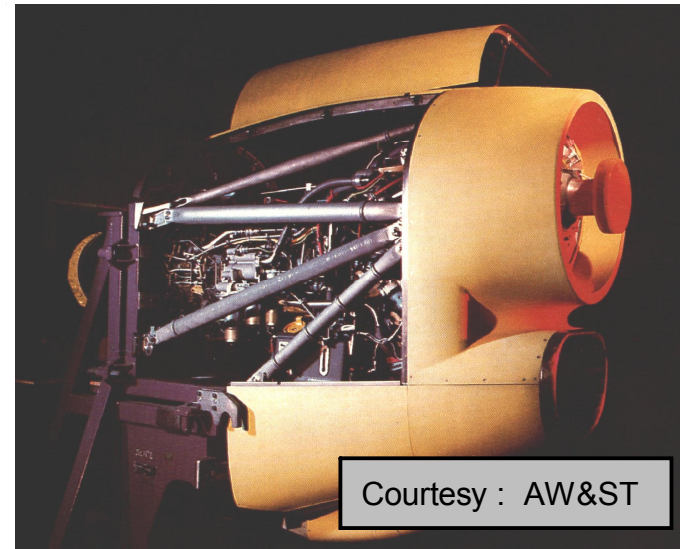
Turboprop engine integration

- Truss between gearbox and wing



Propeller thrust
Propeller torque
Gearbox weight
Propeller weight

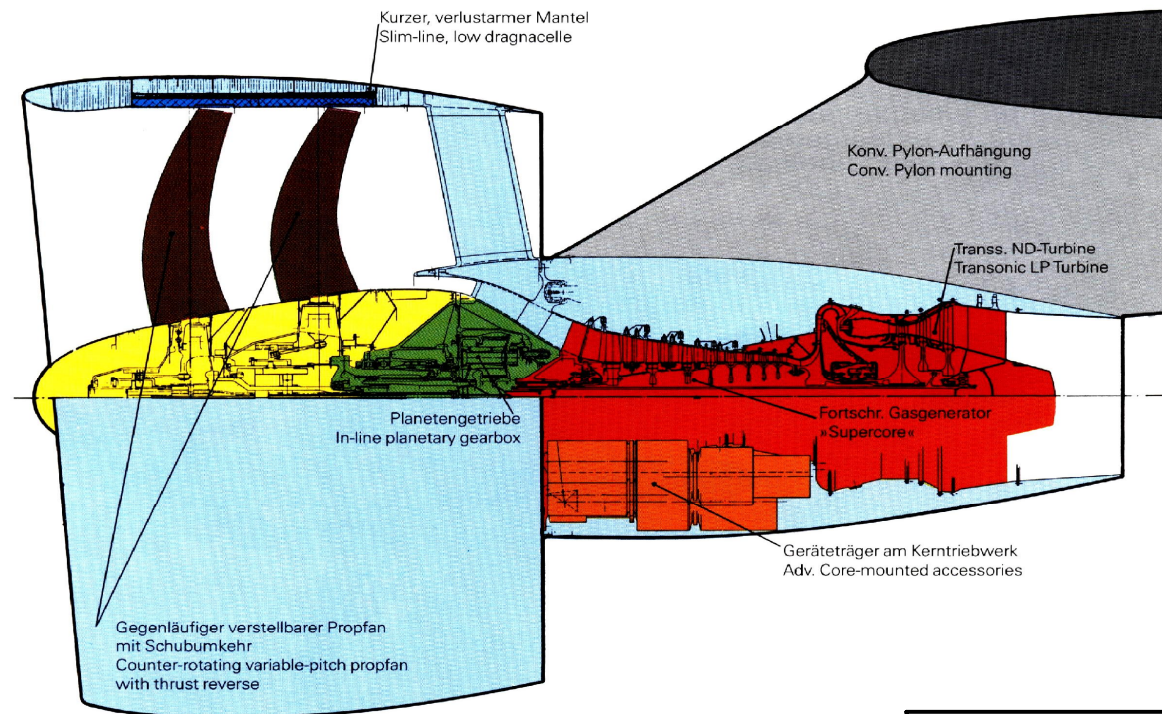
Courtesy : DORNIER



Courtesy : AW&ST

Innovative concepts

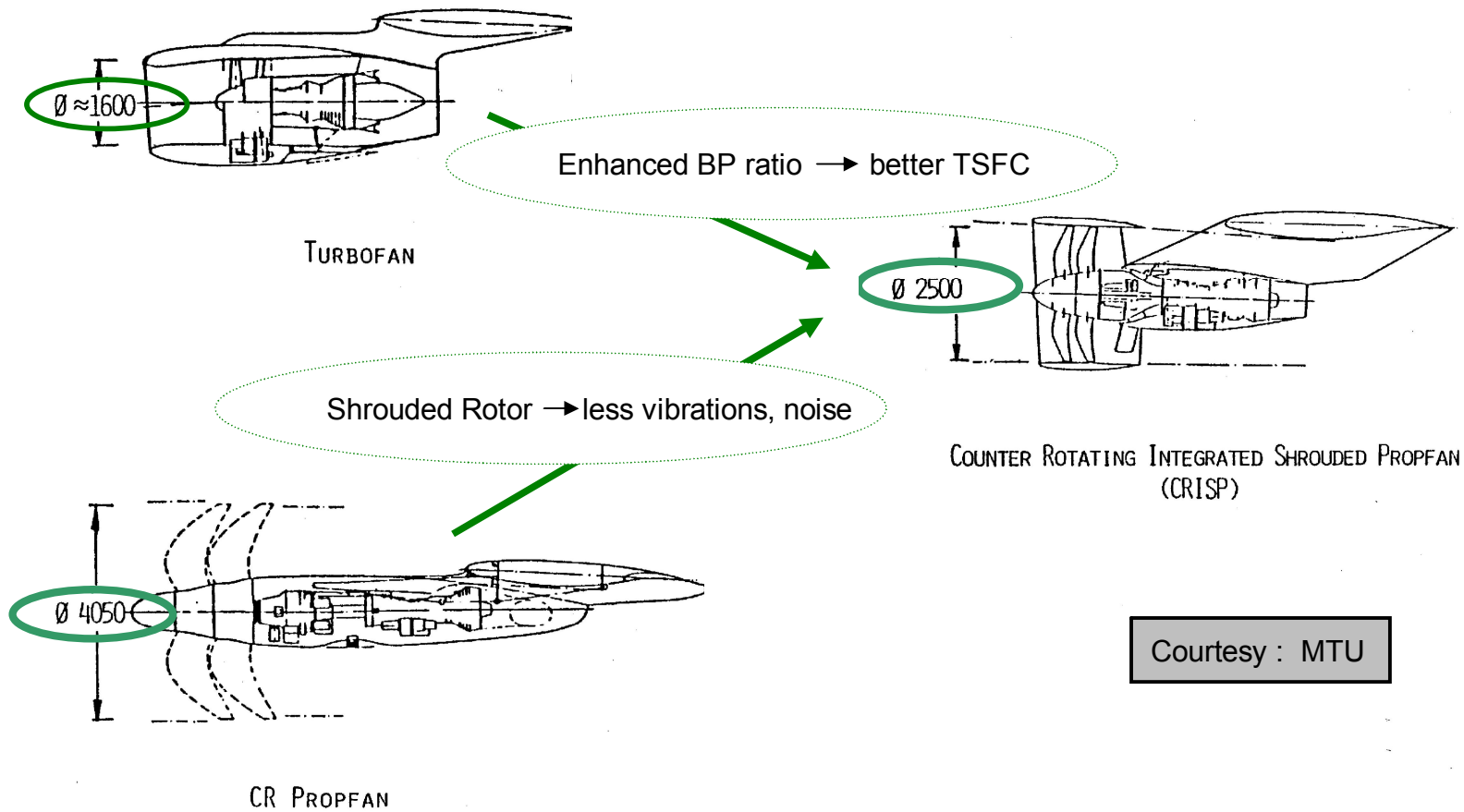
- Further enhanced bypass ratio
- Shrouded propfan
- 2 Rotors, counterrotating



Courtesy : MTU

Innovative concepts

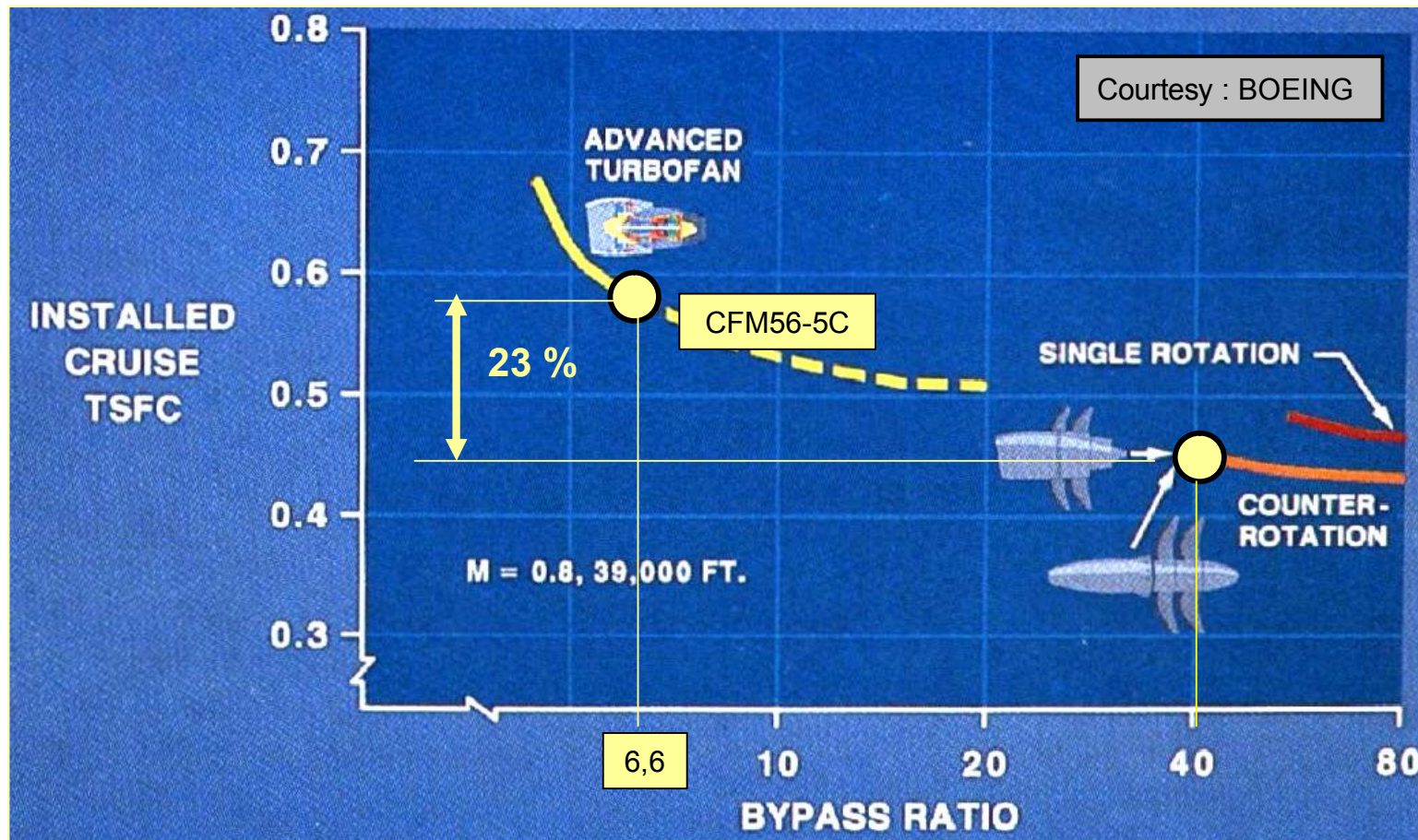
- Combination of enhanced bypass ratio, shrouded rotor



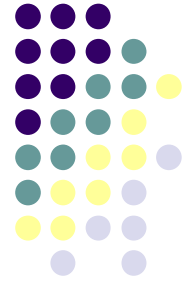
Courtesy : MTU

Innovative concepts

- TSCF decrease as a result of further bypass ratio increase



Conclusion



Engine integration layout meets the requirements for

- Thrust transfer from engine to airframe
 - Short load pathes
 - Safety (fail-safe, defined separation pattern)
- Engine Position
 - Interference engine / wing or engine / fuselage
 - CG control
- Aerodynamics
 - Nacelle (also interface for thrust reverser)

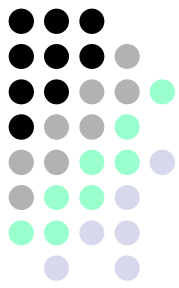
References .

- J. ROSKAM : Airplane design
- M. NIU : Airframe structural design
- N. N. : MTU publications
- N. N. : Airbus publications
- N.N. : GE publications

Erhard Rumpler

Chapter 11

Aircraft Configuration Design



Chapter 11.1

Configuration Design Process

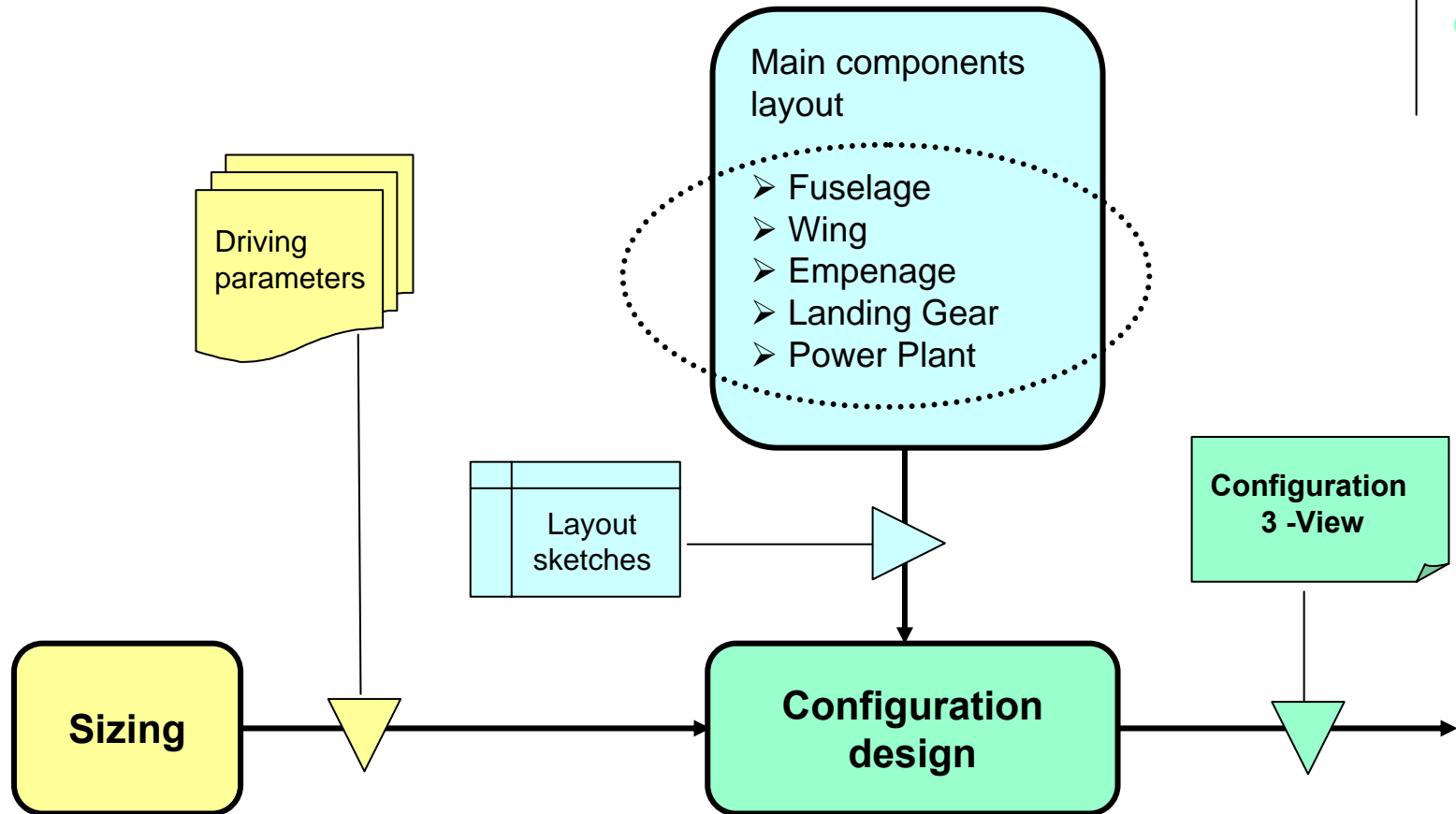
- Methodology
- Component Integration
- Center of Gravity
- Zero - lift Drag
- Design Loads
- Airworthiness Requirements
- Structural Concept

Configuration design methodology

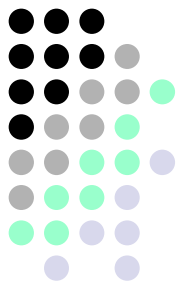


- *SIZING* procedure defines parameter values meeting the specification
- Main documentation form : Diagrams, Sketches
- *CONFIGURATION DESIGN* procedure integrates sized main components to an aircraft concept assisted by :
 - Statistical database
 - Standard solutions
 - New technologies
 - Innovative ideas
- Prerequisite for the configuration design process :
 - Preliminary layouts of main aircraft components
- Main documentation form : Configuration 3-view

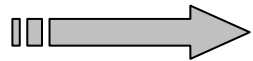
Configuration design methodology



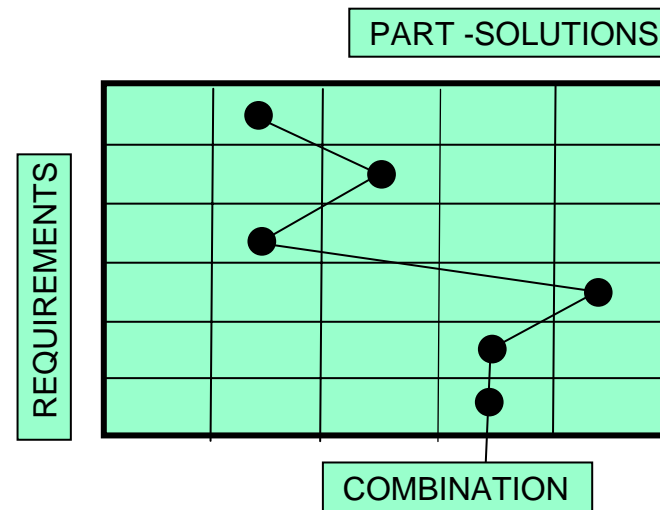
Configuration design methodology



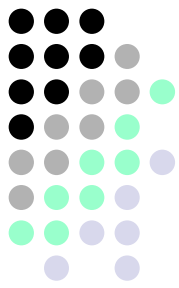
- Sized candidates for main structural components are identified
- Configuration design is now in a position to integrate these components to a number of specification – meeting aircraft concepts
- frequently used tool for that step (to avoid “forgotten” solutions) :



MORPHOLOGIC MATRIX



Configuration design methodology



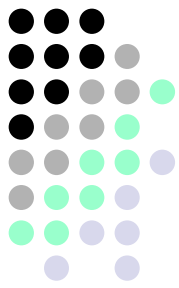
➤ Morphologic Matrix of main structural component arrangement

		MAIN STRUCT. COMPONENT	PART -SOLUTIONS			
REQUIREMENT	LIFT	WING	LOW	HIGH		MID
				OFFSET	CENT-BOX	
	PAYLOAD CONTAINMENT	FUSELAGE	1-AISLE	2 -AISLE		2-LEVEL
	PROPULSION	ENGINE	UNDER WING	REAR FUSELAGE		BURIED
	GROUND MOBILITY	GEAR	TRICYCLE NOSE	TRICYCLE TAIL		MULTI
	STABILIZING & CONTROL	EMPENAGE	CONVENT-IONAL TAIL	T-TAIL		CANARD

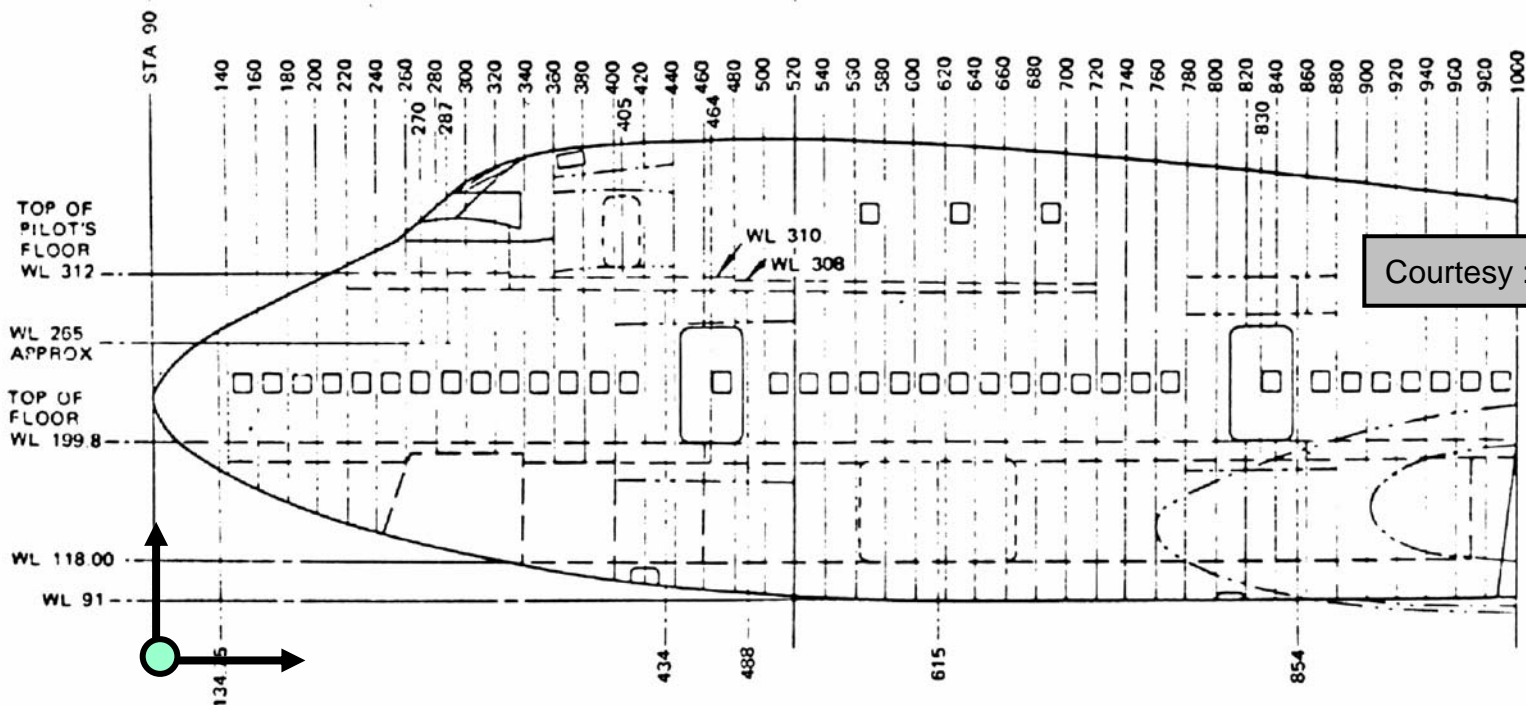
CONFIGURATION 1

CONFIGURATION 2

Design coordinate system (Station – Waterline Plan)



- Start with a design coordinate system
- Origin in front / below fuselage with respect to to later added components
- x ... STA,
- z ... WL



Component Centers of Gravity (CG)

- Design statistics gives a first estimate of main components CG's

- Wing:

$$0,37 - 0,42 \bar{c}$$

- Hor./ Vert. Stabilizer :

$$0,30 \bar{c}$$

- Fuselage :

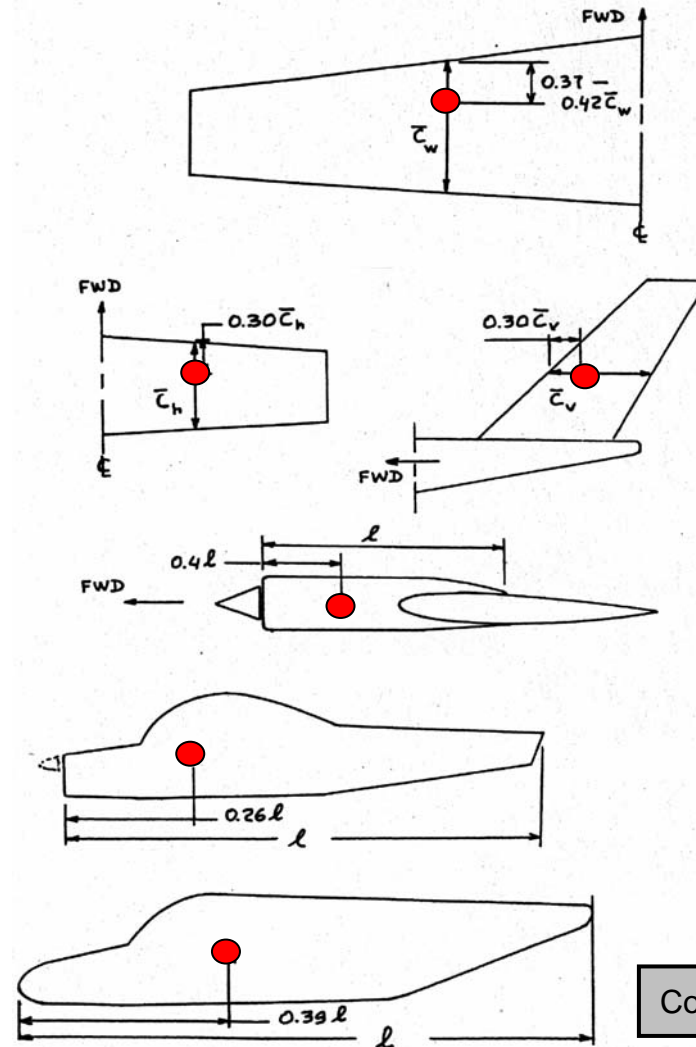
$$0,26 l_{fus} \quad \dots \text{Canopy type}$$

$$0,39 l_{fus} \quad \dots \text{Cabin type}$$

$$0,45 - 0,5 l_{fus} \quad \dots \text{Airliner}$$

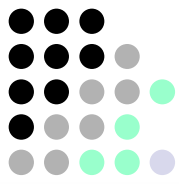
- Engine /Nacelle :

$$0,4 l_{nacelle}$$

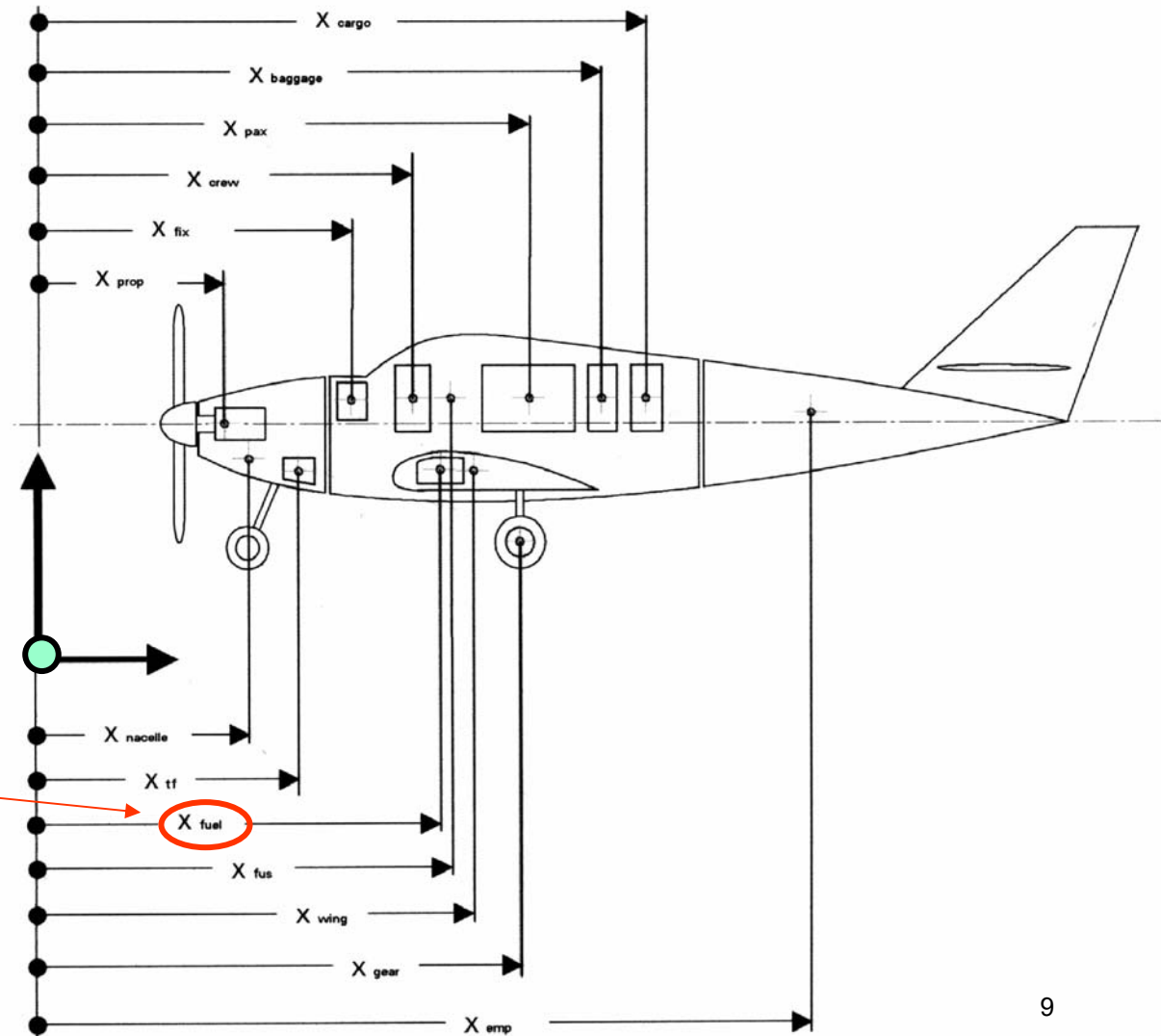


Courtesy : ROSKAM

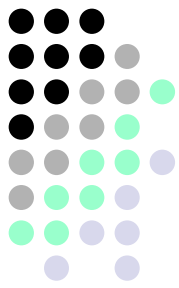
Component Centers of Gravity (CG`s)



- Origin from STA / WL - Plan
- Components weights from breakdown statistics
- Components CG`s from design statistics
- CG travels during loading / deloading
- Fuel to be placed close to the CG



Integration main structural components

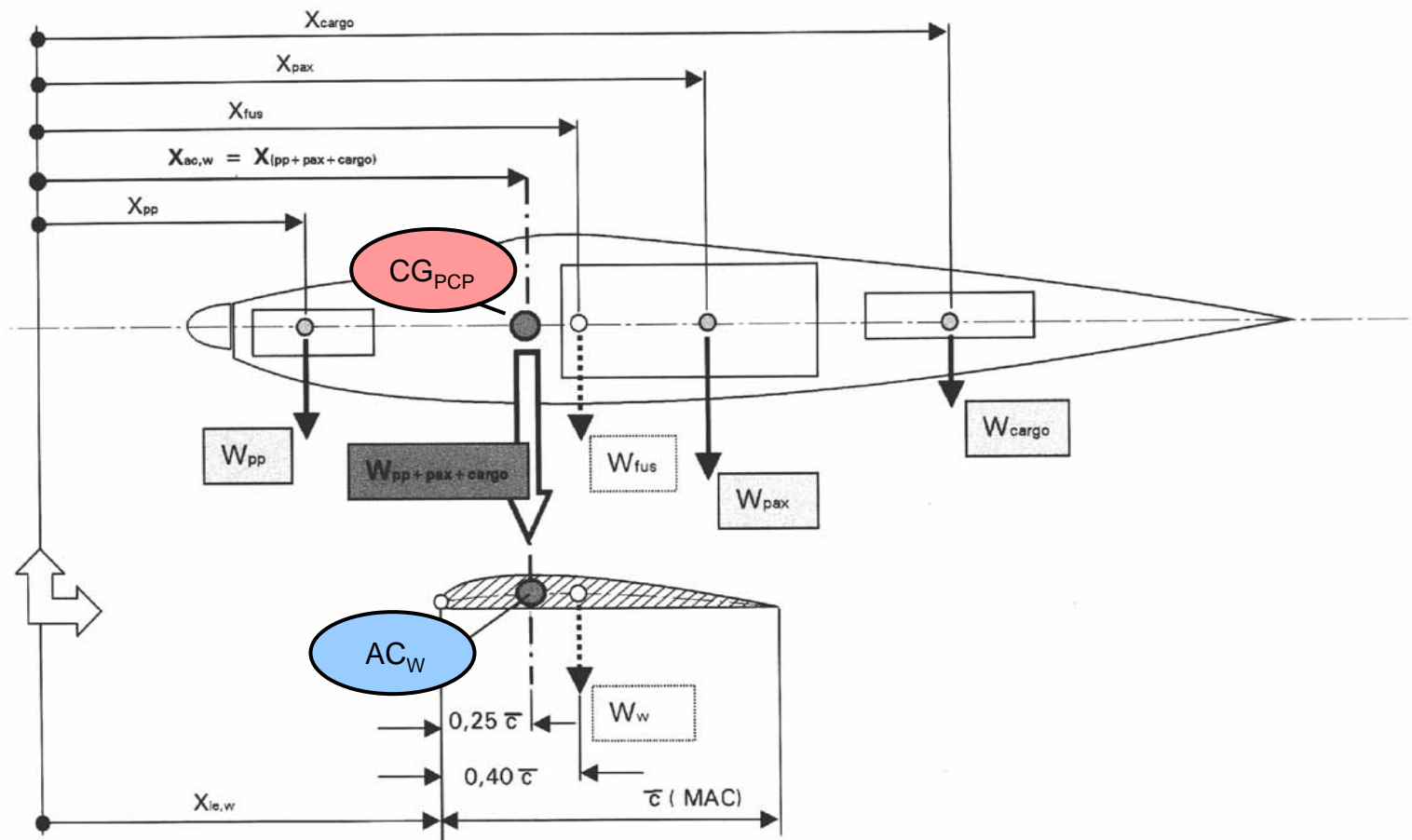
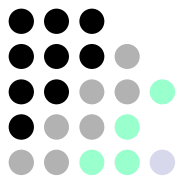


Integration Procedure Fuselage / Wing :

- Preliminary positioning of
 - Payload 1 (PAX)
 - Payload 2 (Cargo)
 - Power Plant
- Identification of their **CG`s** \longrightarrow **CG**_{PAX+CARGO+PP}
- Identification of the Aerodynamic Center of the sized wing \longrightarrow **AC**_w

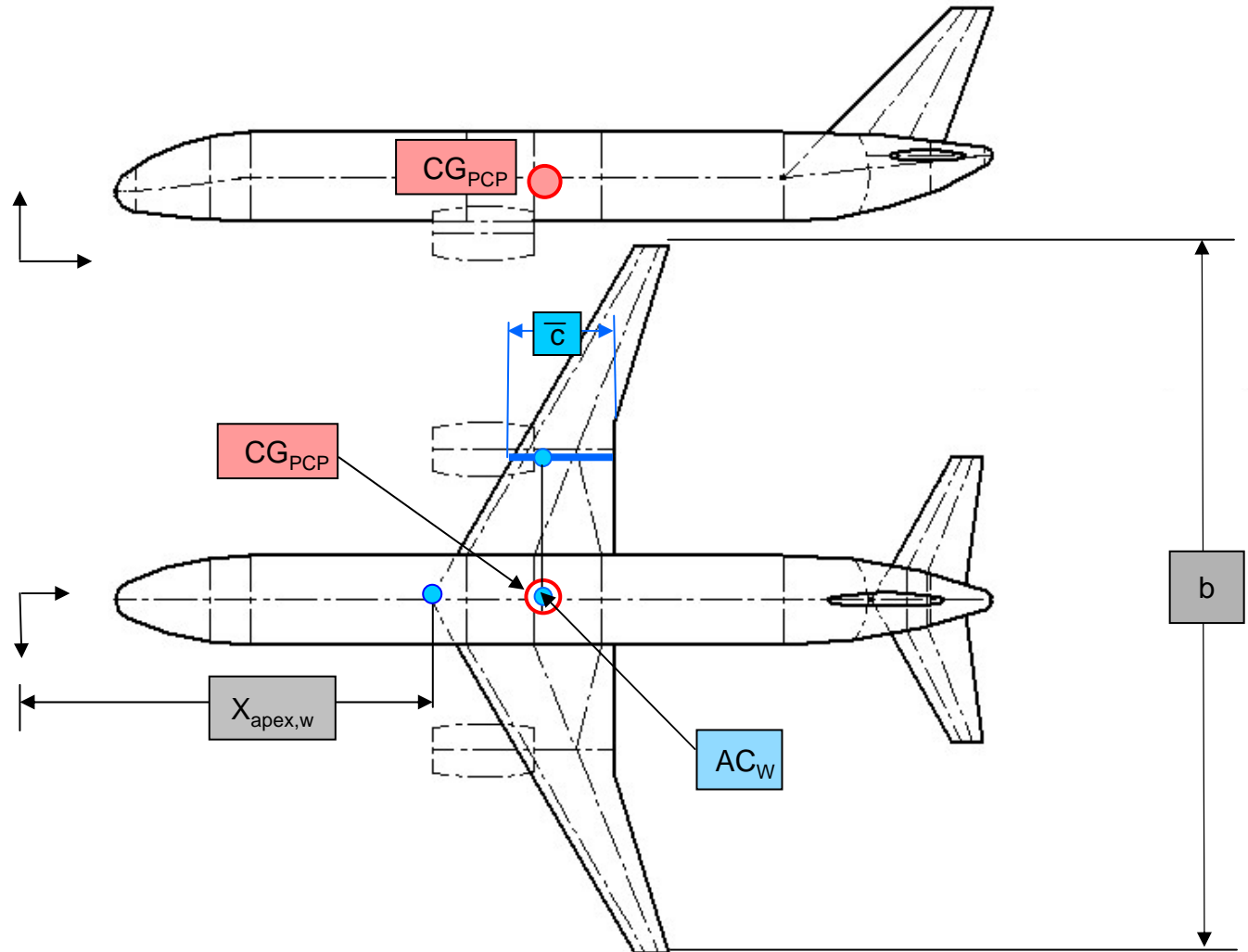
Superposition of **CG**_{PAX+CARGO+PP} and **AC**_w \longrightarrow preliminary position of the wing

Integration main structural components



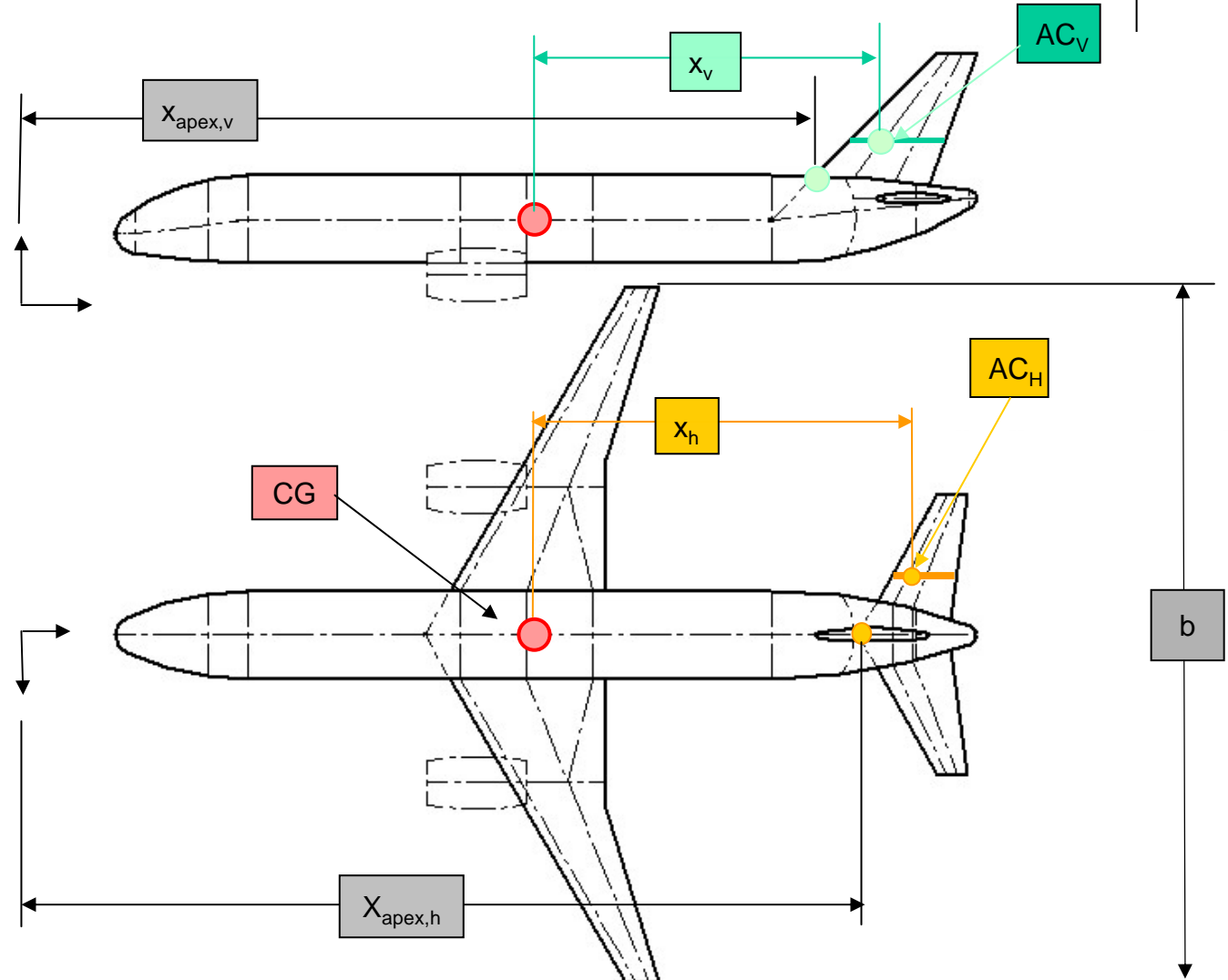
Integration main structural components

Integration procedure Fuselage / Wing :



Integration main structural components

Integration procedure Horizontal Stabilizer / Vertical Stabilizer :

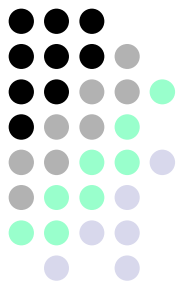


Volume Method :

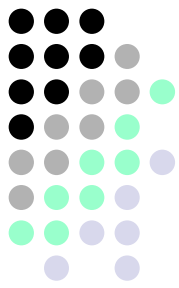
$$V_h = x_h \cdot S_h / S_w \cdot \bar{c}$$

$$V_v = x_v \cdot S_v / S_w \cdot b$$

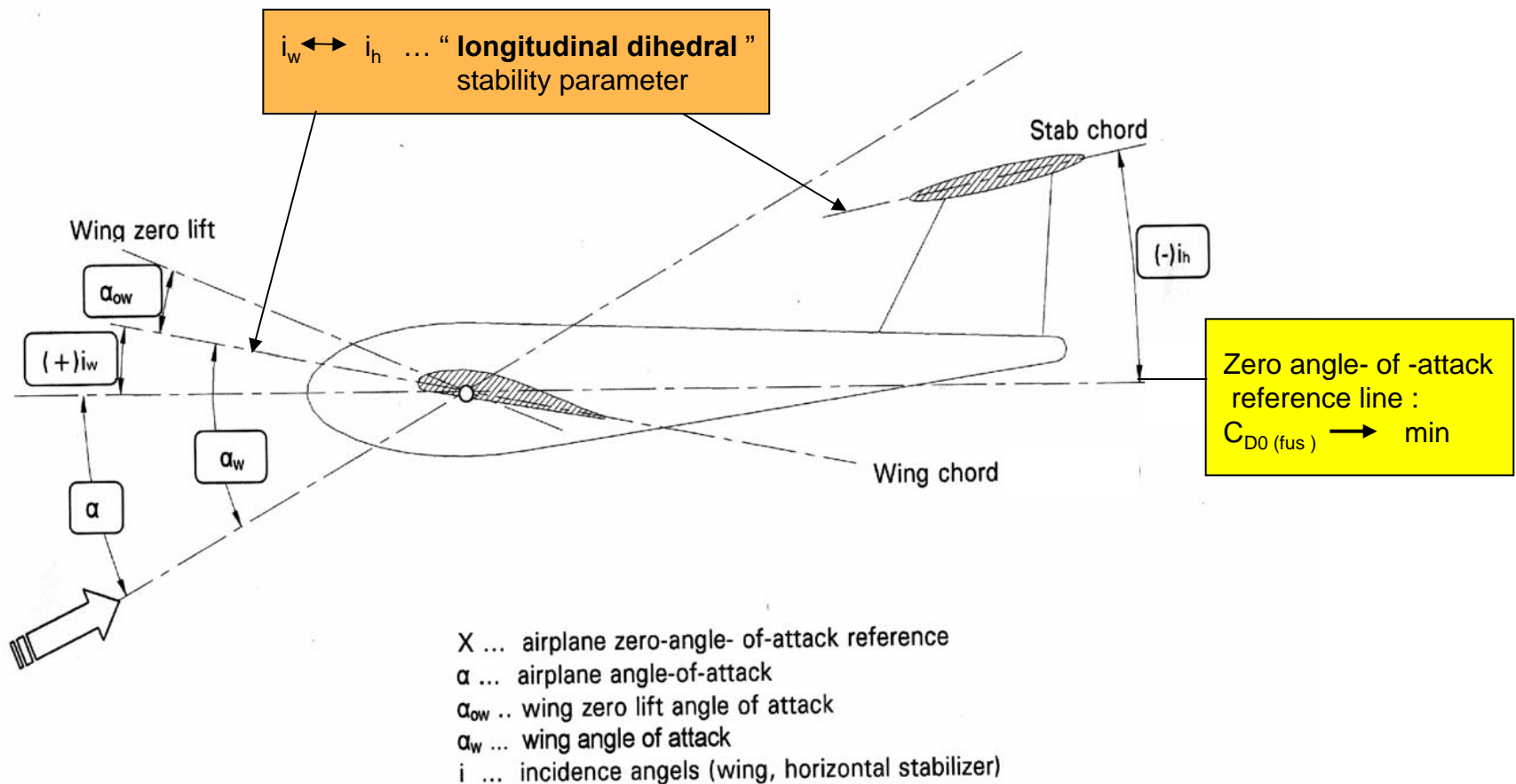
$V_h, V_v \dots$ **Statistics**



Integration of main structural components

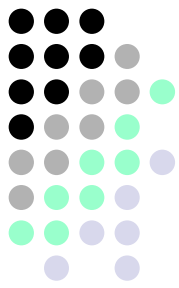


Integration procedure HS / VS : incidence angles

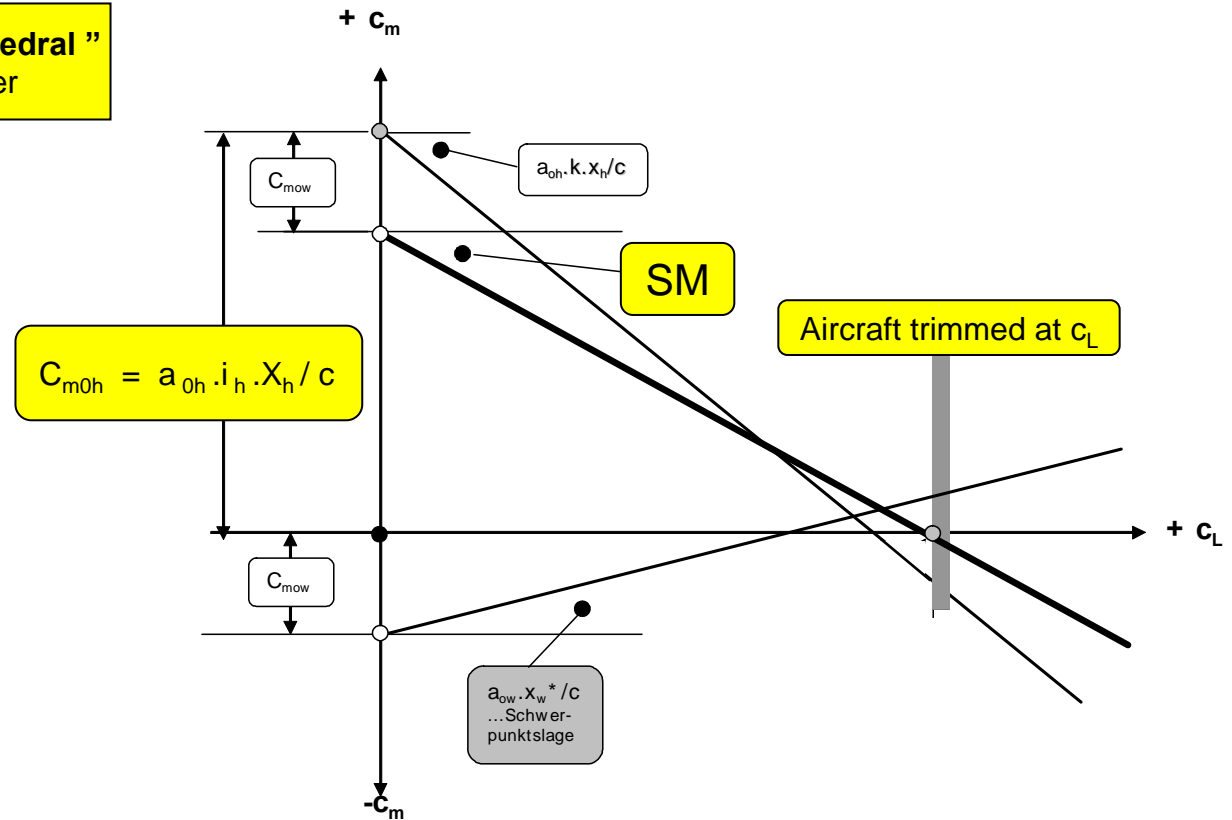


Integration of main structural components

Integration procedure HS : Stability Margin (SM)

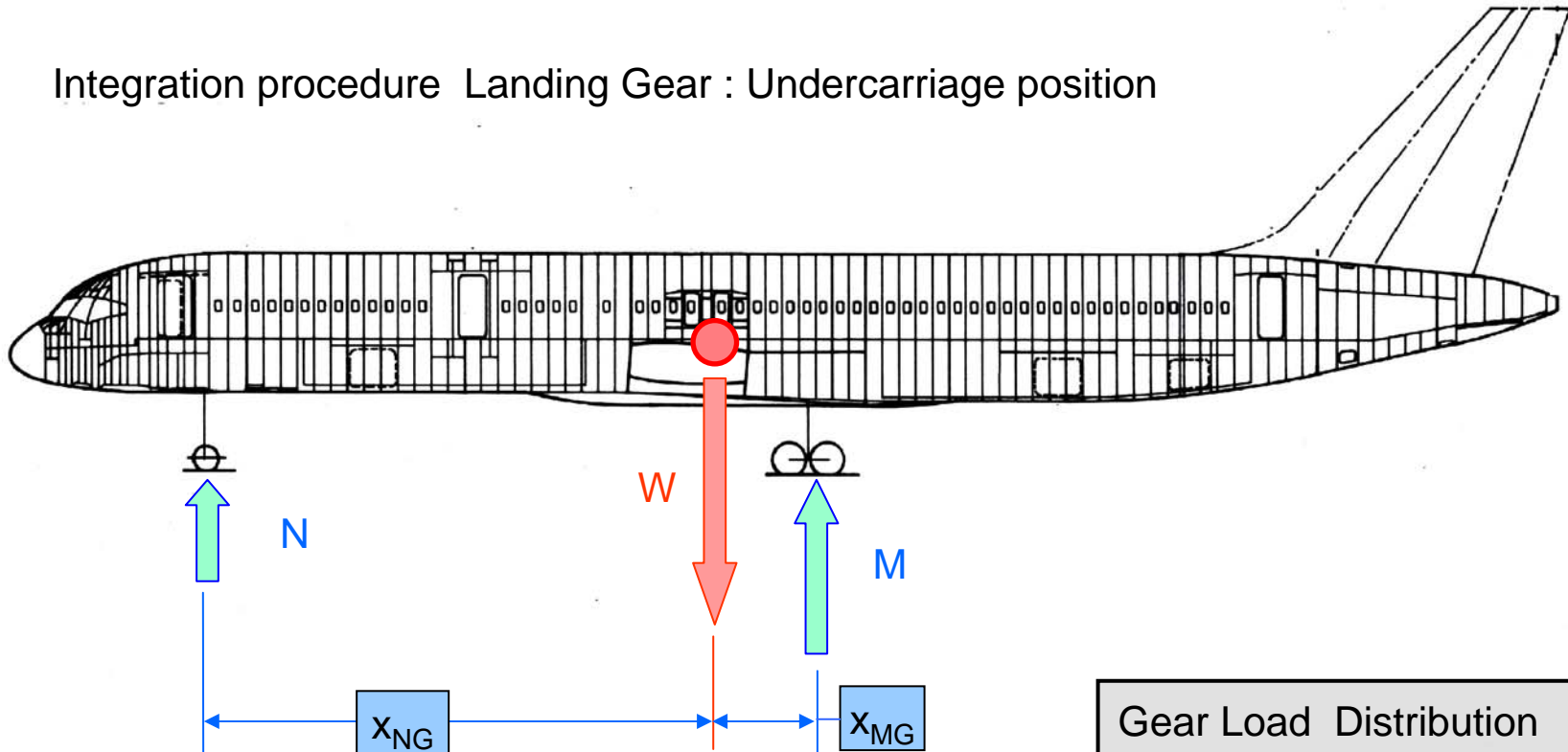


$i_w \leftrightarrow i_h$... “longitudinal dihedral” stability parameter



Integration of main structural components

Integration procedure Landing Gear : Undercarriage position



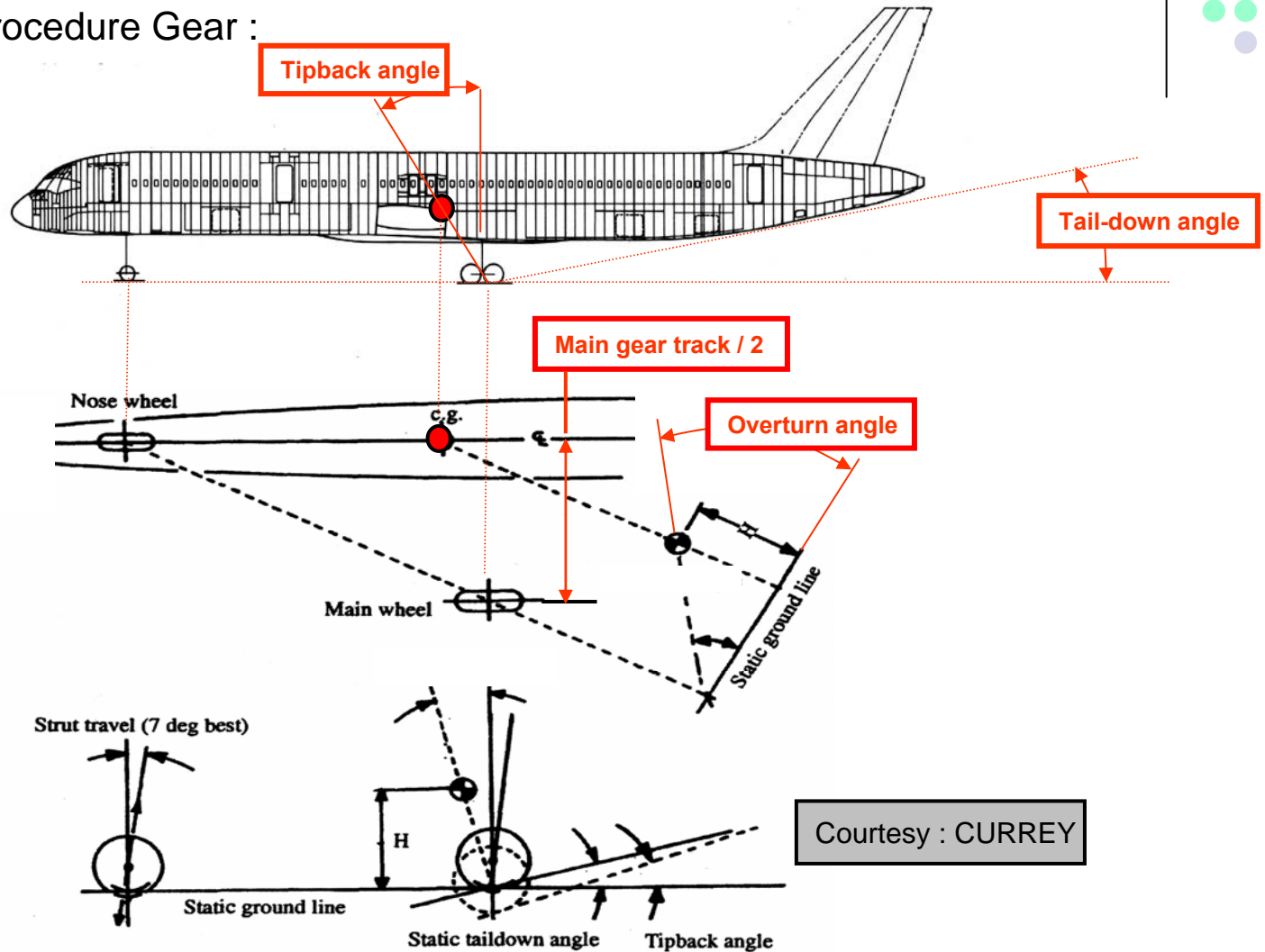
Gear Load Distribution

5 – 20 % Nose Gear
80 – 95 % Main Gear

→ x_{NG} , x_{MG}

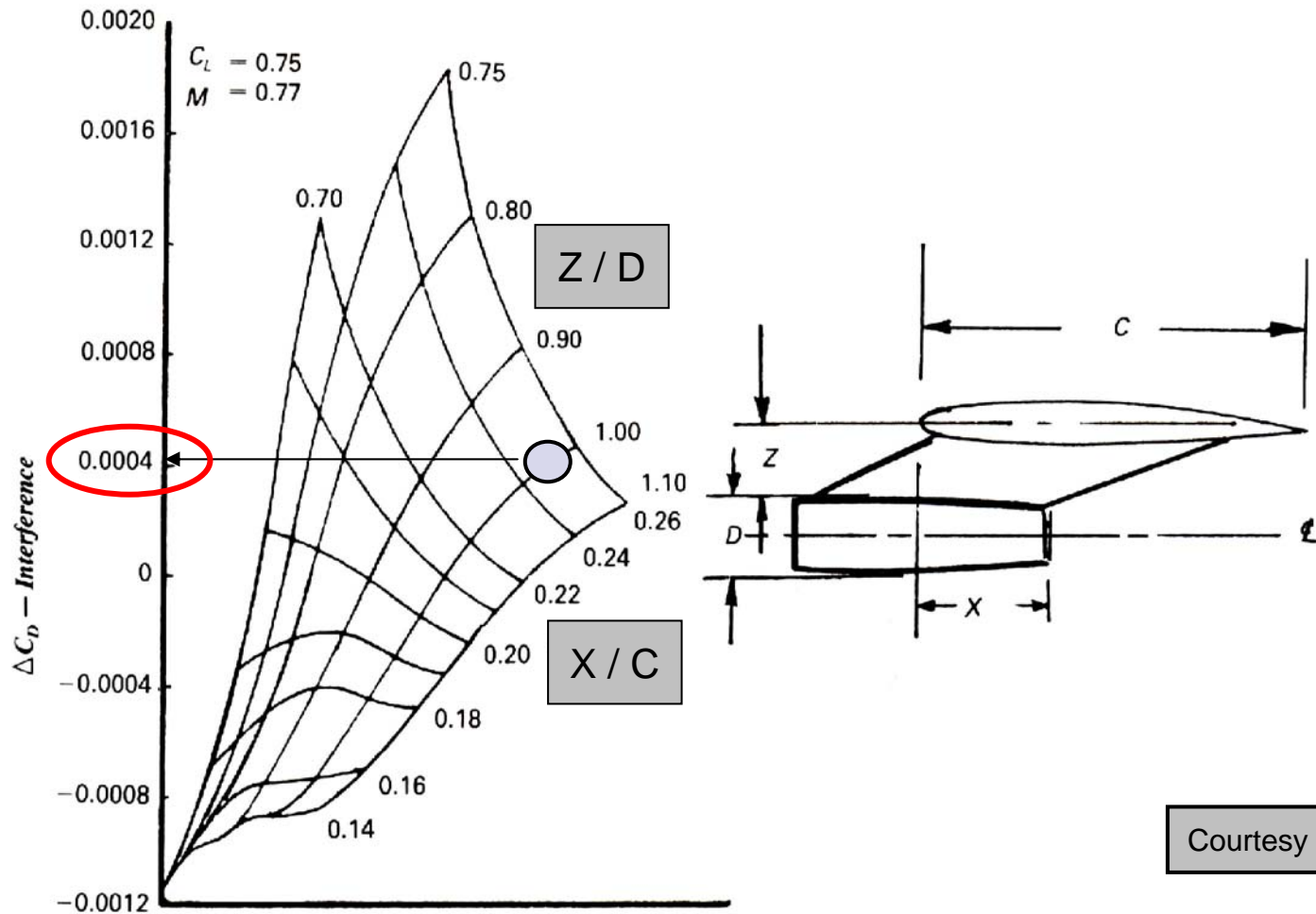
Integration of main structural components

Integration procedure Gear :



Integration of main structural components

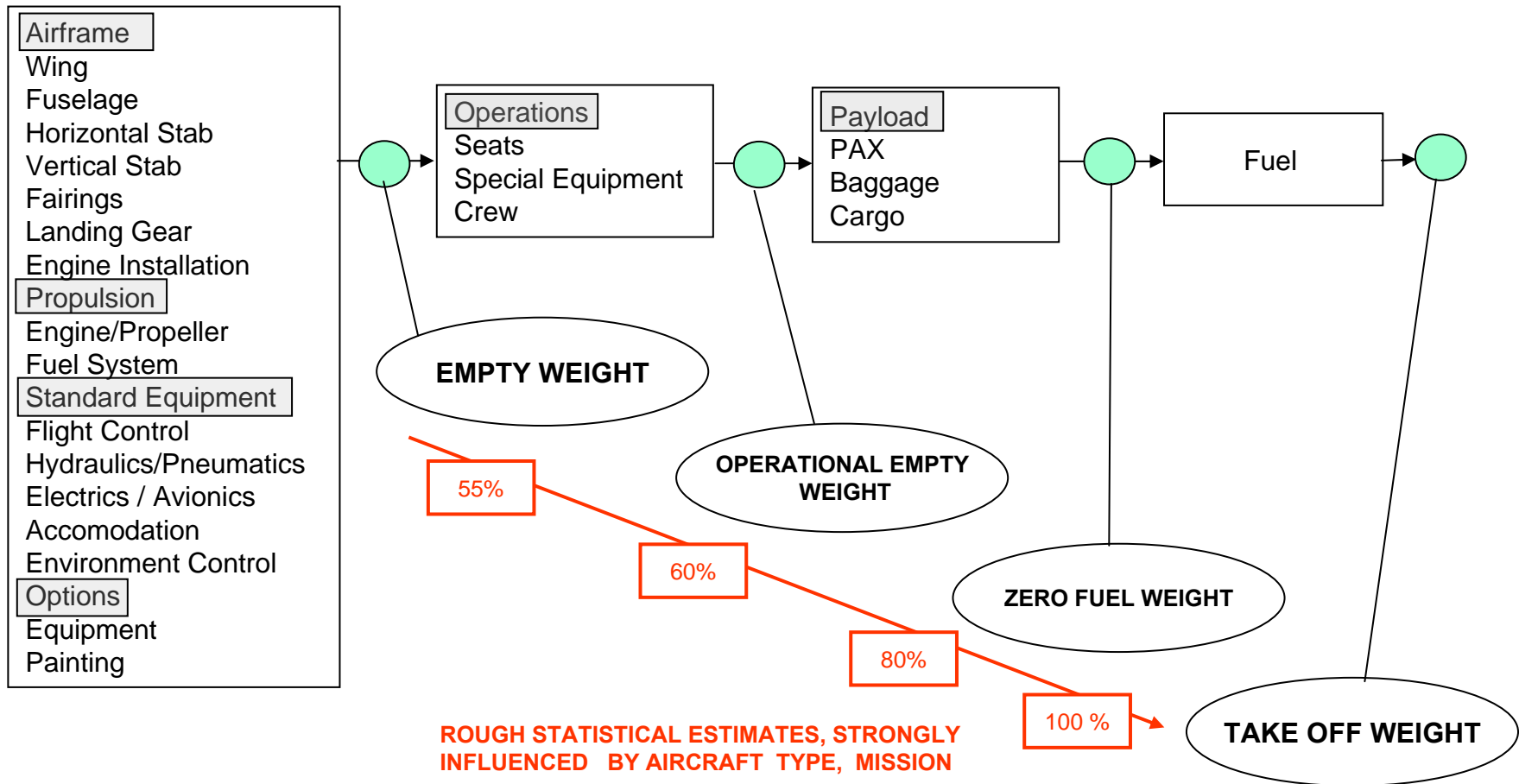
Integration procedure Power Plant : Interference drag



CG refinement



Weight Breakdown → Weight Trends → Center of Gravity

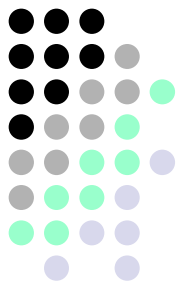


A 10x10 grid of colored dots representing a 2D histogram. The dots are colored black, gray, green, and purple. The distribution is roughly bell-shaped, centered around the middle of the grid.

- CG Travel of a General Aviation light airplane :



Zero –lift drag estimate



- Main component integration completes first configuration loop
- Next step : drag estimate for propulsion / performance calculations
- Component build-up method applied to the established configuration

$$C_{D0} = (1 / S_w) \cdot \sum C_{Di} \cdot A_i$$

COMPONENT CROSSSECTION AREA

- Wetted area method applied to the established configuration

$$C_{D0} = (1 / S_w) \cdot C_{fe} \cdot S_{wet}$$

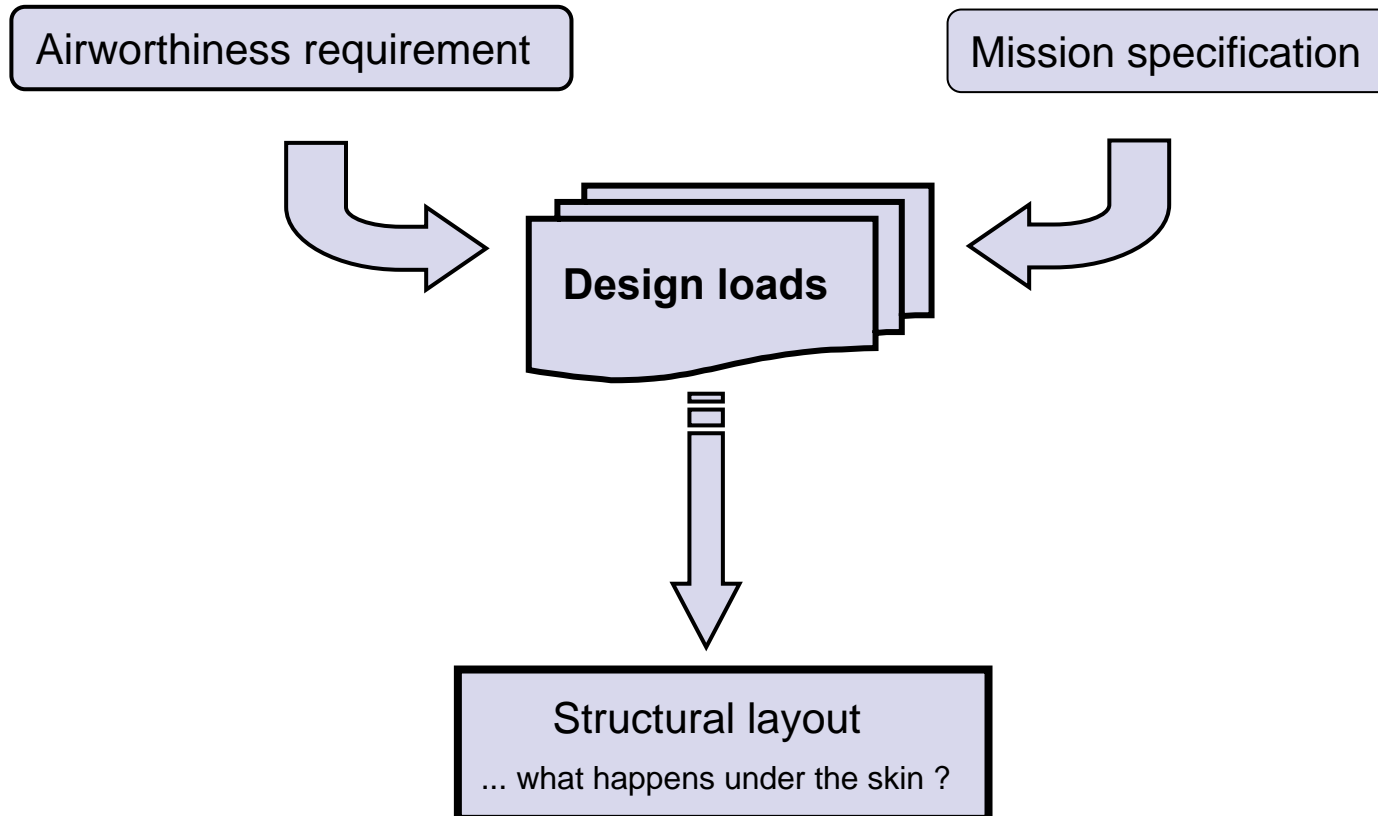
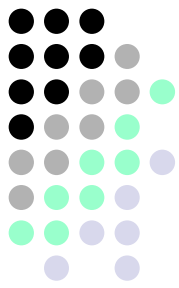
AIRCRAFT WETTED AREA

EQUIVALENT SKIN FRICTION COEFFICIENT , ~ 0,003

- Asset for interference drag : 10 – 15 %

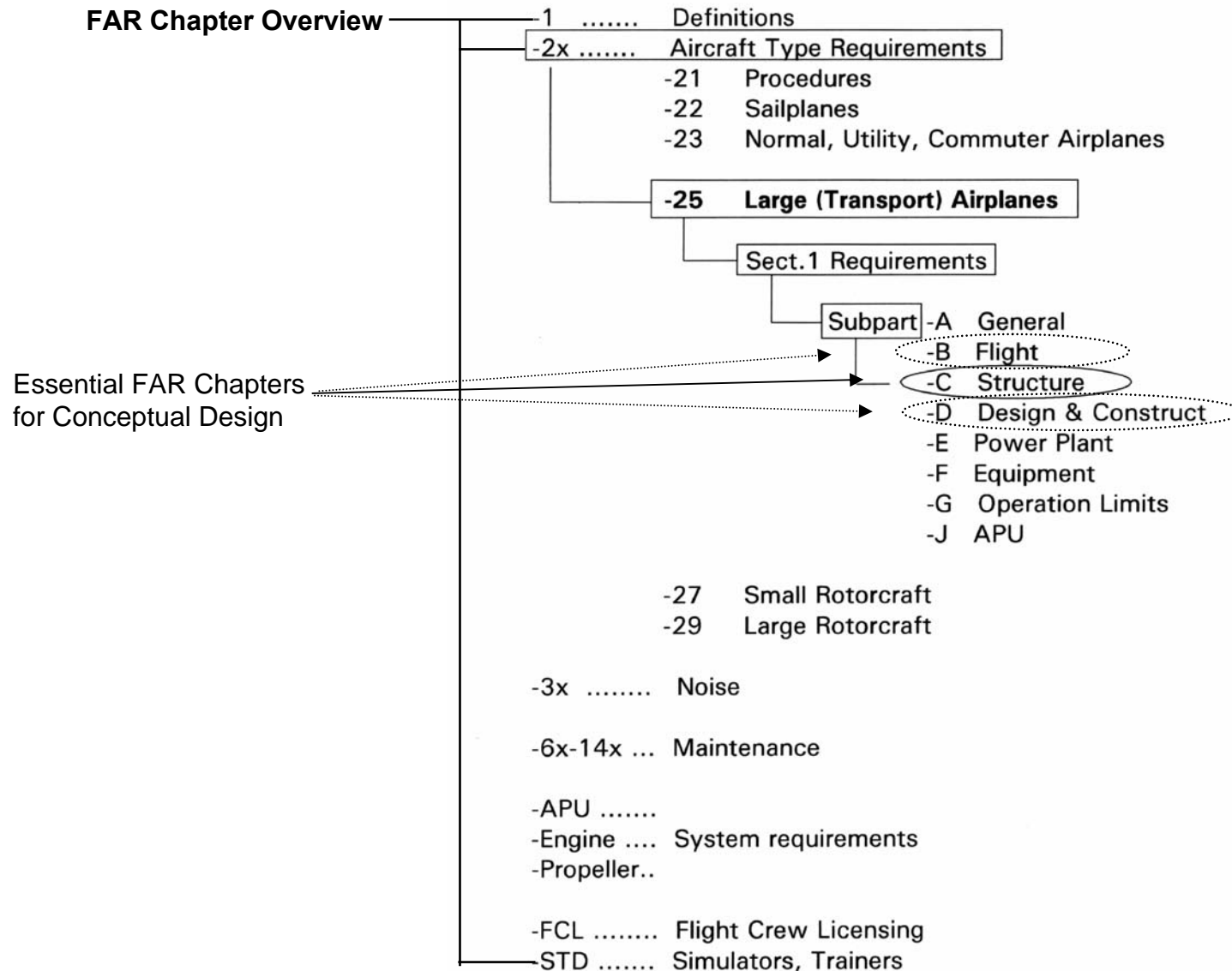
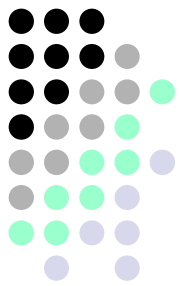
Design loads

- Start of the **STRESS / WEIGHT ITERATION** loop

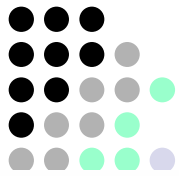


Airworthiness requirements

FAR / JAR



Airworthiness requirements → design loads



FAR / JAR 25

Sect. 1 - Requirements

Subpart B - Flight

■ General

■ Performance

Stall
Speeds
Stability
Trim

■

FAR / JAR 25

Sect. 1 - Requirements

Subpart C - Structure

■ General

■ Flight Loads

■ Control Surfaces Loads

■ Ground Loads

■ Fatigue

FAR / JAR 25

Sect. 1 - Requirements

Subpart D - Design & Construction

■ General

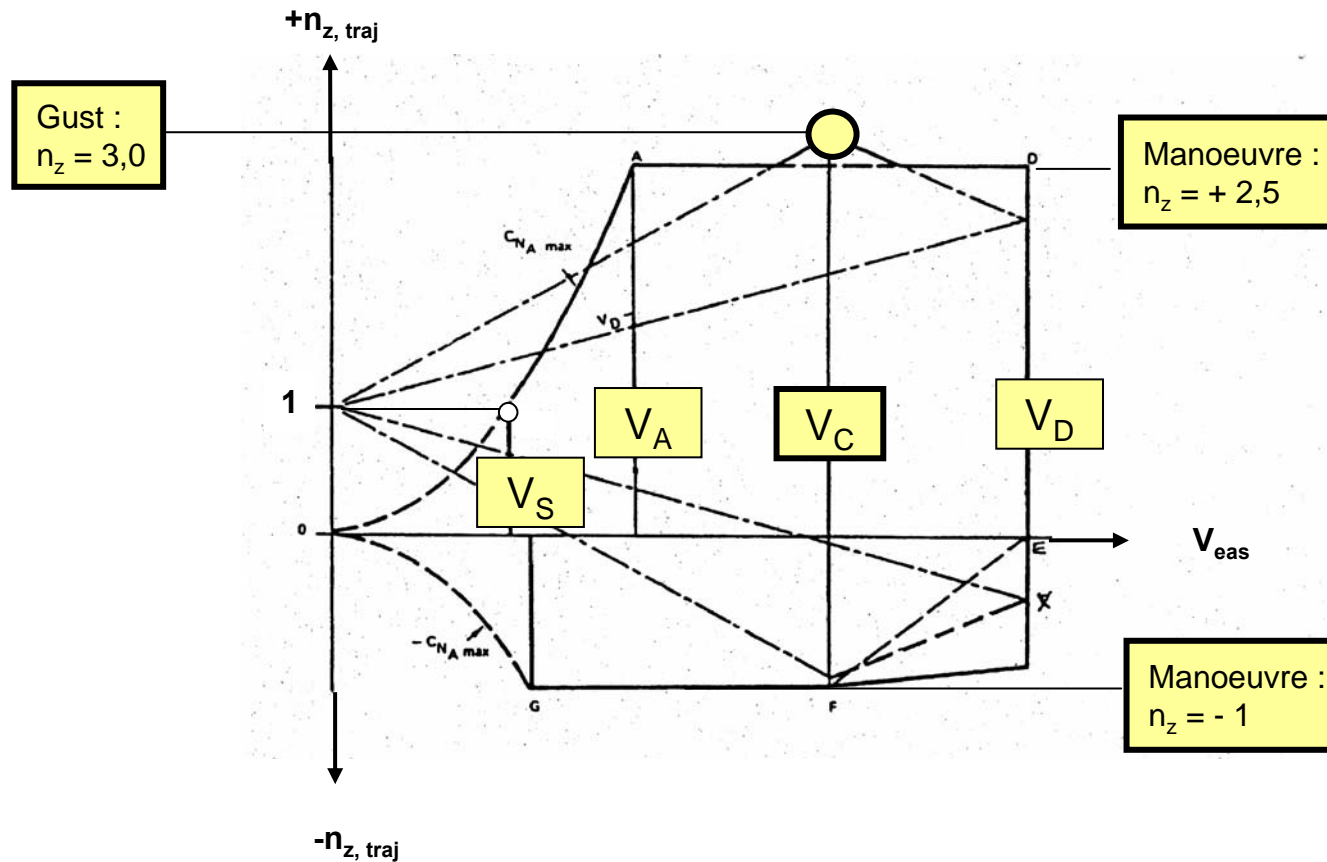
■ Control Surfaces

■ Control Systems

■ Landing Gear

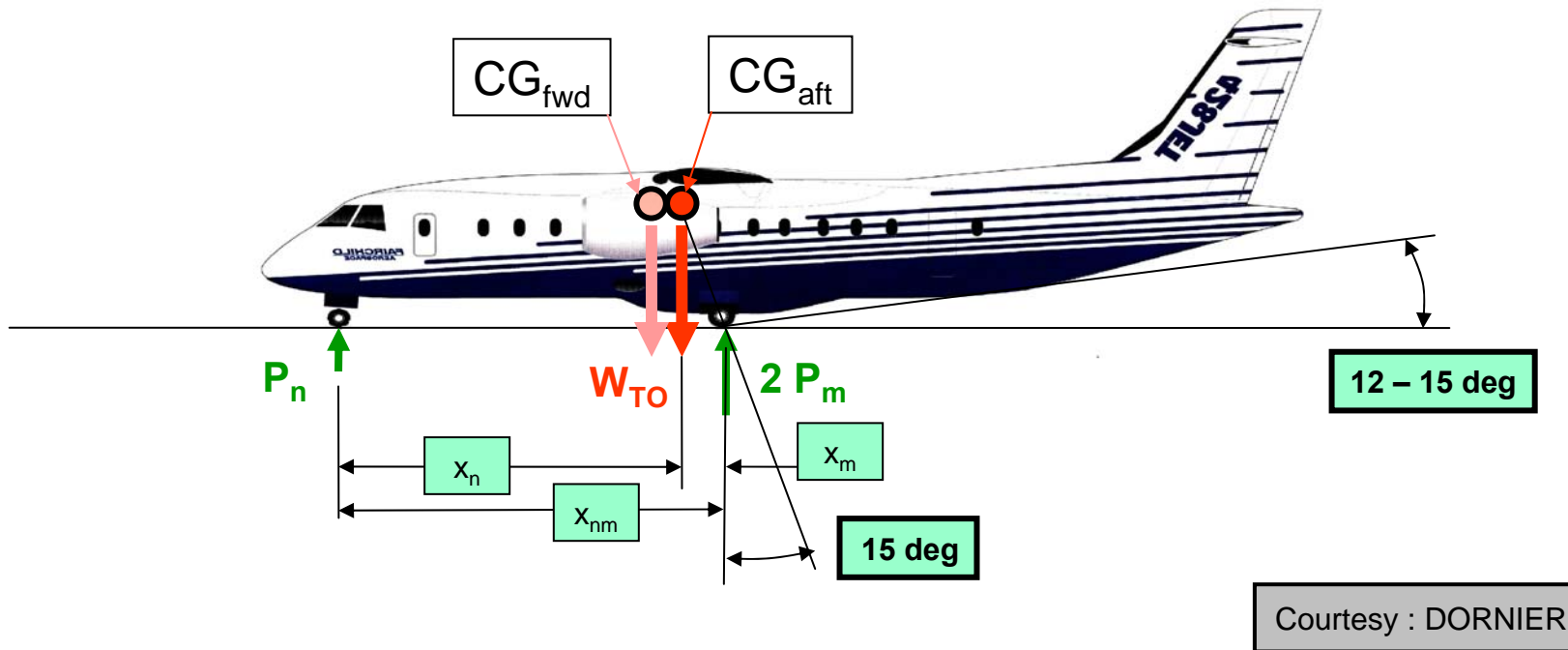
Flight loads

➤ Important source for design loads : **V – n Diagram**



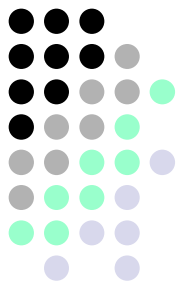
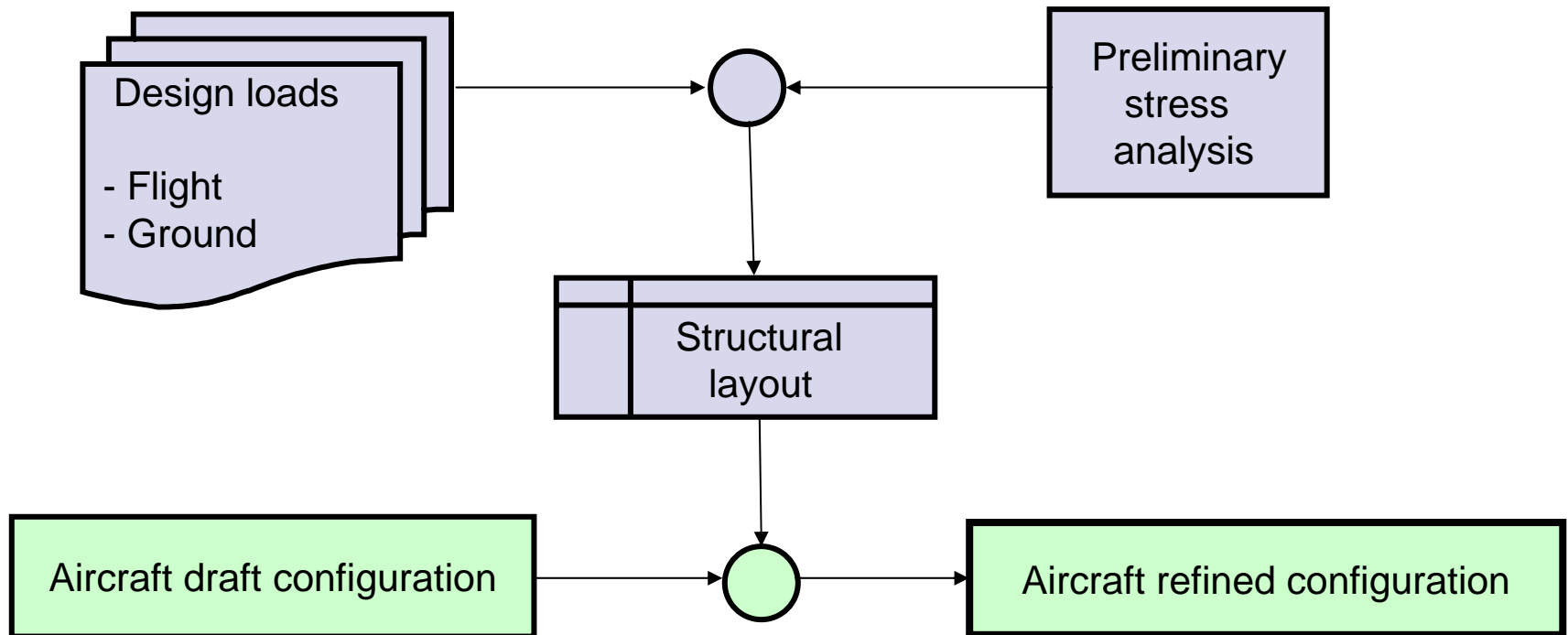
Ground loads

- Basic static ground loads : Ref Landing gear
- Landing impact load factor : Ref Landing gear

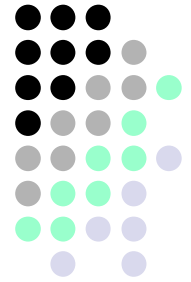


Configuration design

- A structural layout is a prerequisite for a refined configuration



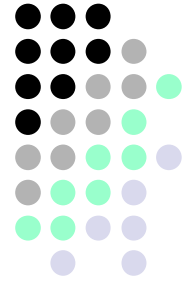
Chapter 11.2



Configuration Design Problems

11.2.1 160 – 200 Seat Medium Transport

Configuration layout 1 : Medium Range Transport



Configuration Decisions :

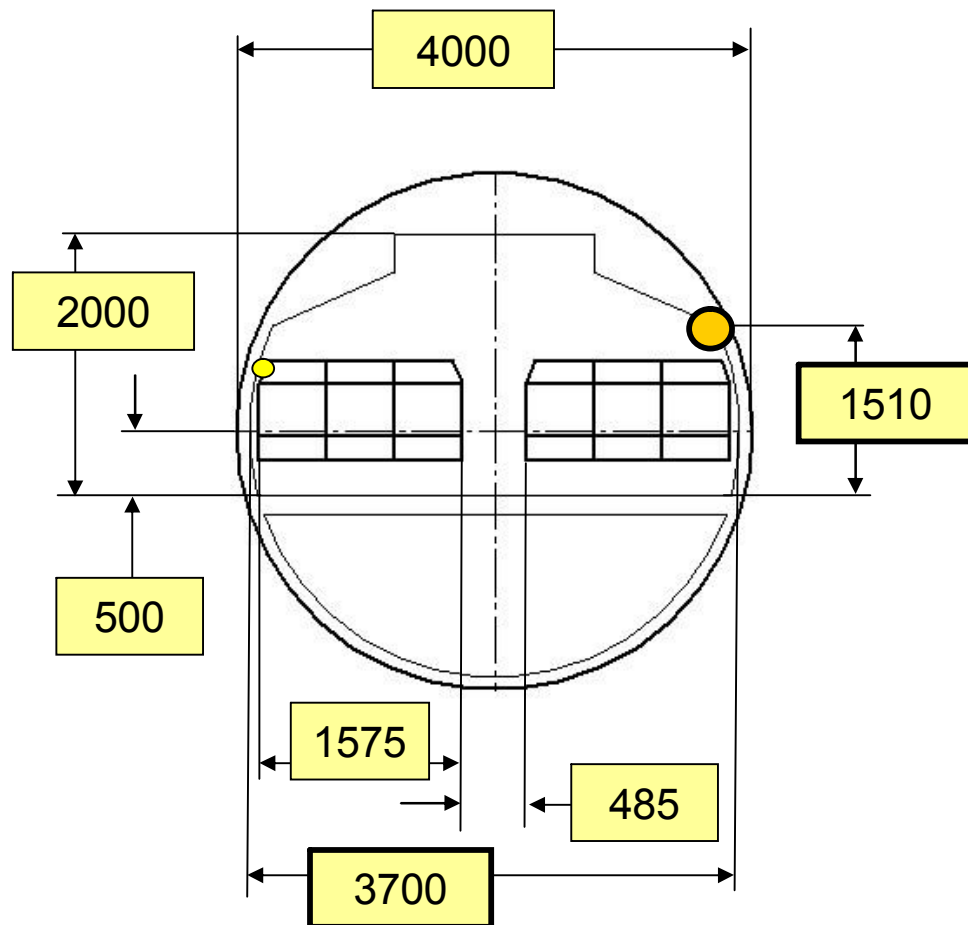
- 150 – 200 PAX, 6 - abreast, Single aisle
- Low Wing
- Conventional Tail
- 2 Underwing Engines
- Tricycle Nose Gear

Basic Geometry Data (requested) :

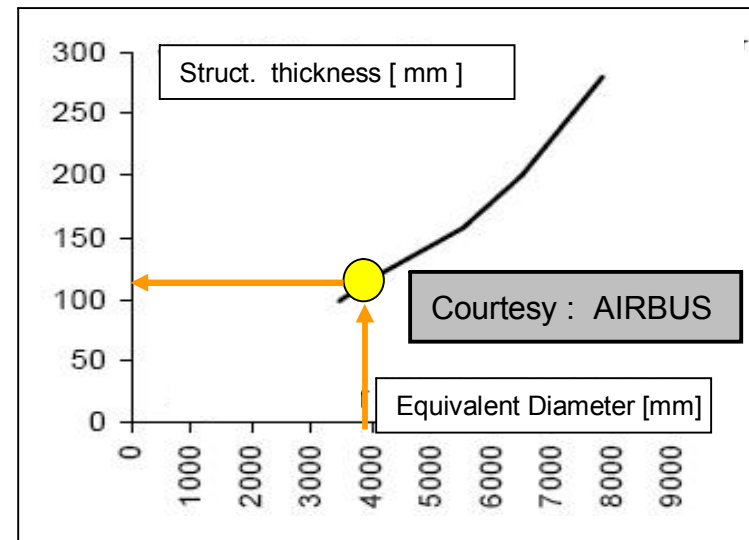
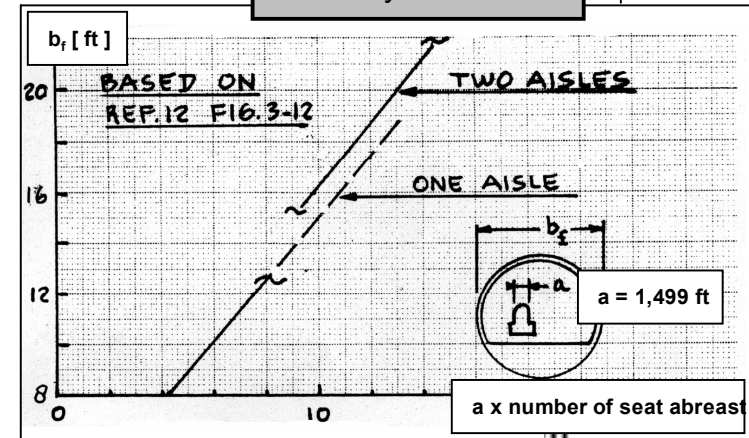
- Fuselage Inner Dia / Outer Dia
- Cabin Length
- Floor Level
- Length Cylindrical Section
- Length Forebody
- Length Aftbody
- Length Fuselage

Configuration layout 1 : Medium Range Transport

➤ Fuselage Dia

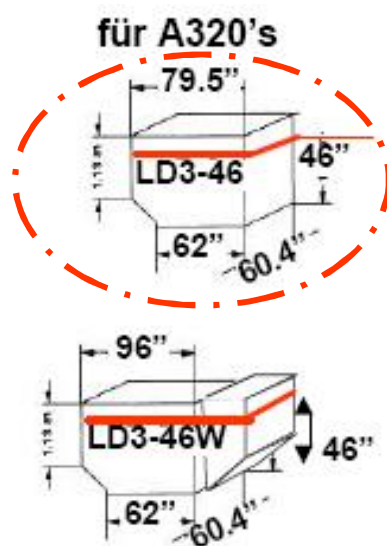


Courtesy : ROSKAM

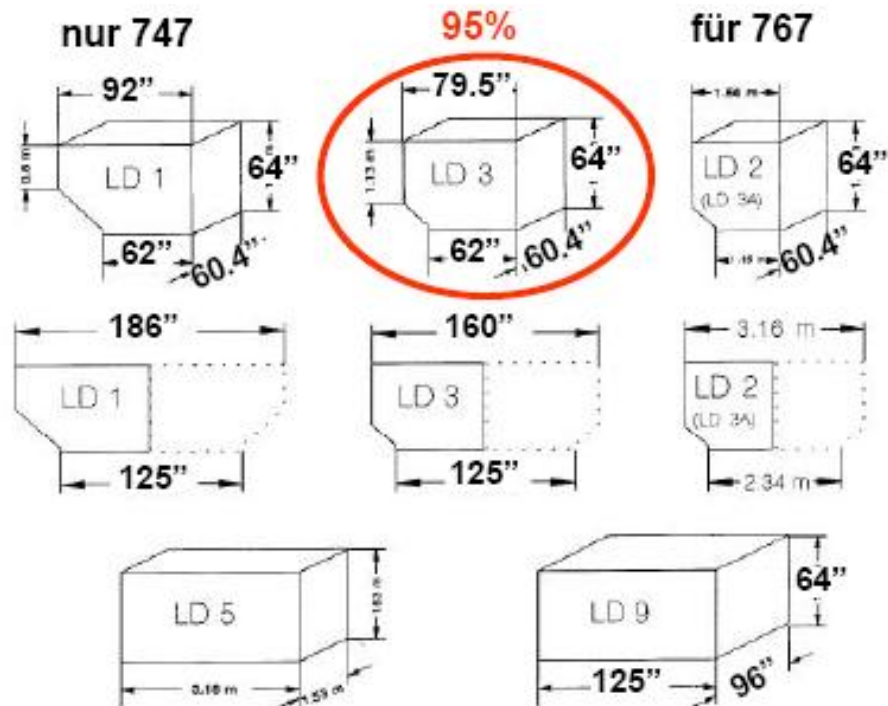


Configuration layout 1 : Medium Range Transport

➤ Container Dimensions

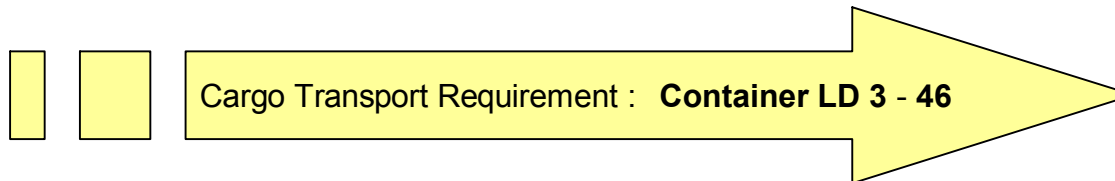
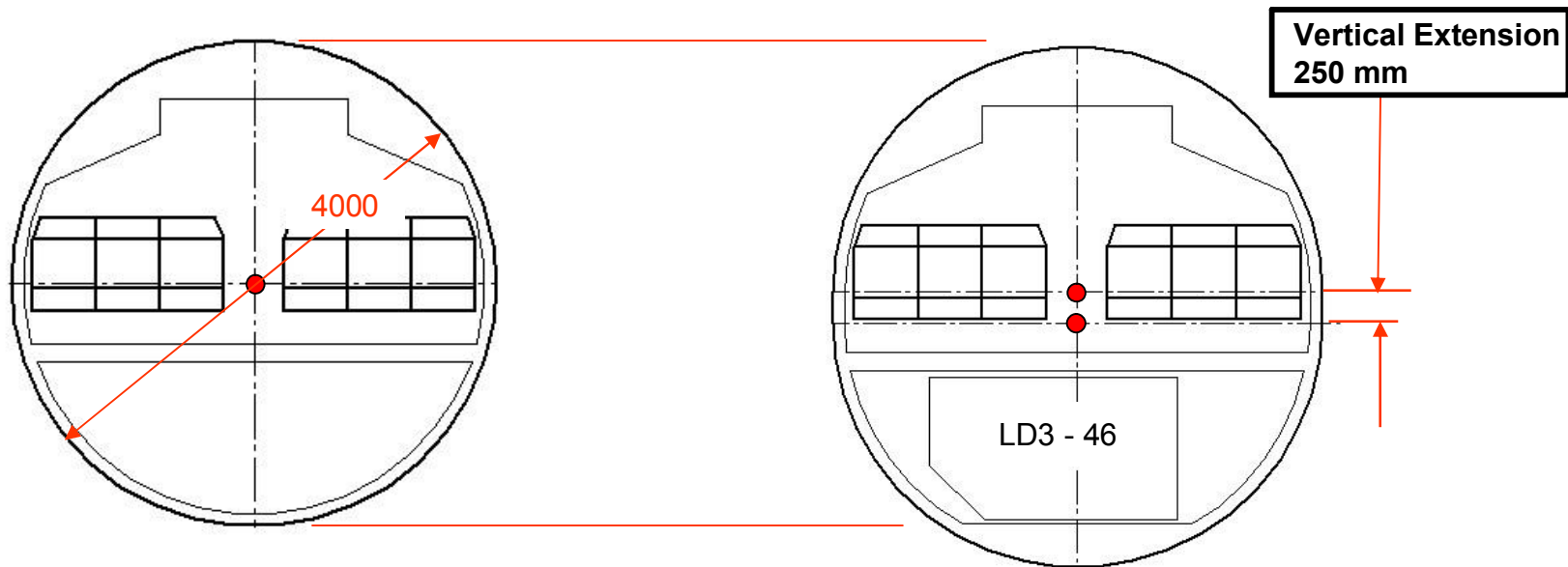


Courtesy : AIRBUS



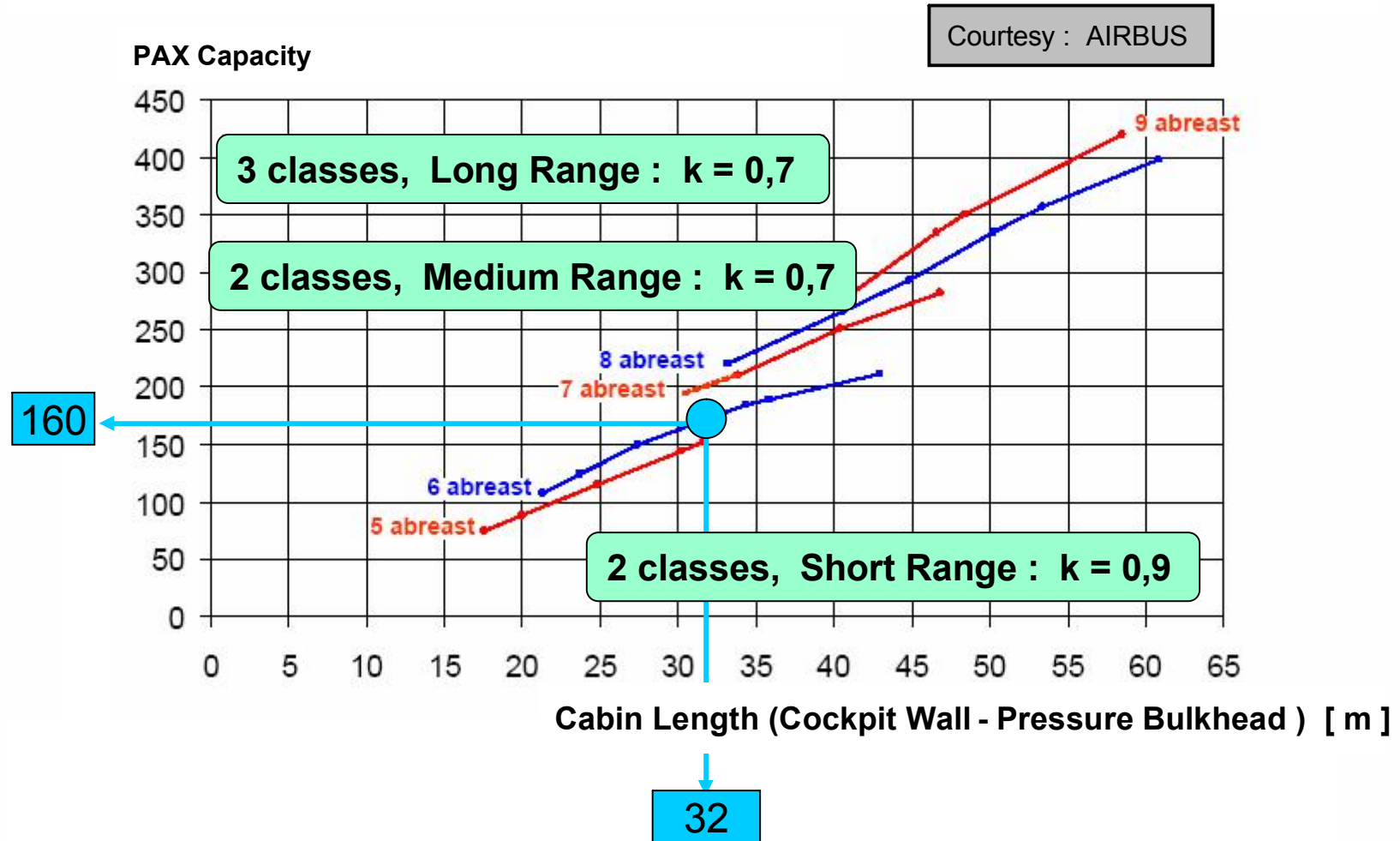
Configuration layout 1 : Medium Range Transport

➤ Fuselage Dia / Container

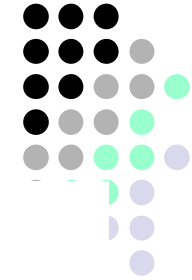


Configuration layout 1 : Medium Range Transport

➤ Cabin length = $n_{\text{PAX}} / n_{\text{abreast}} \cdot K$

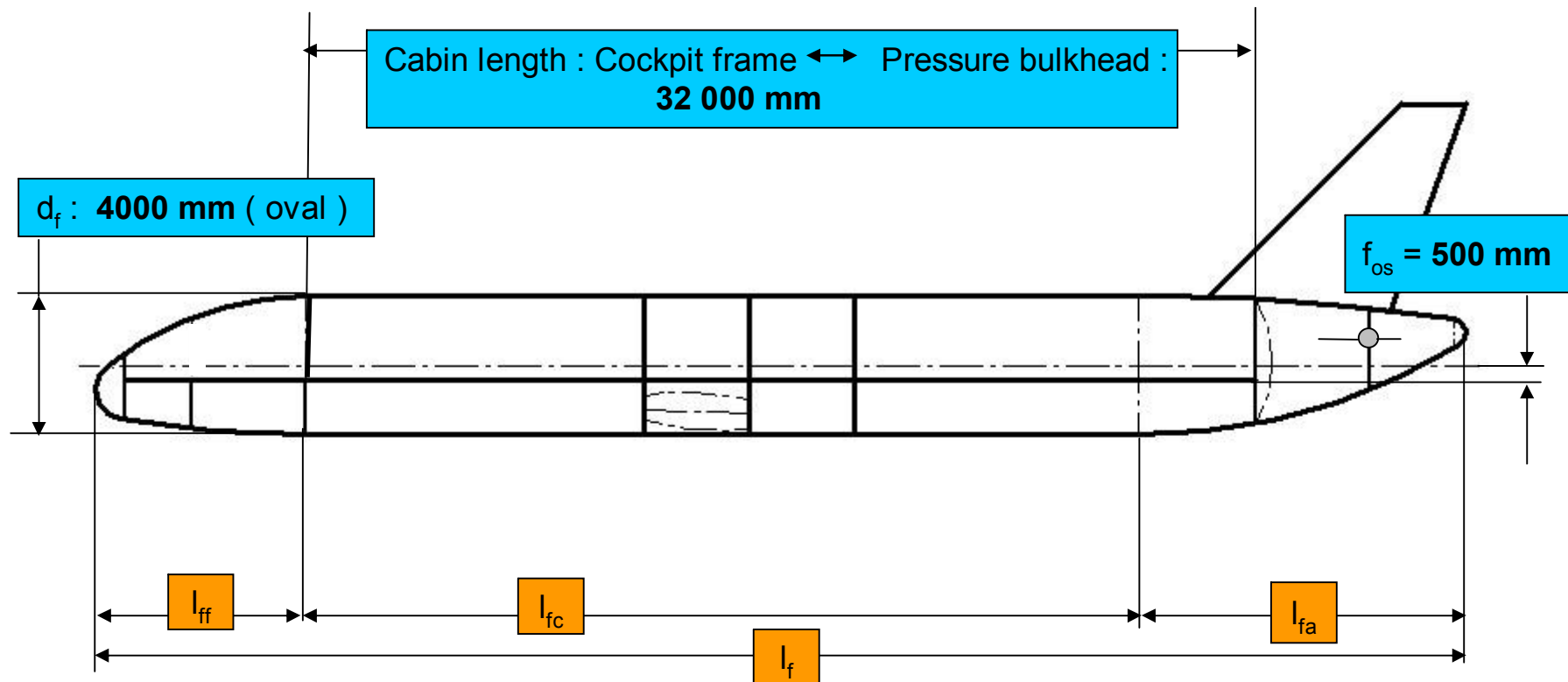


Configuration layout 1 : Medium Range Transport

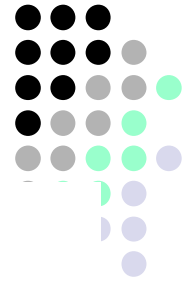


➤ Fuselage basic layout

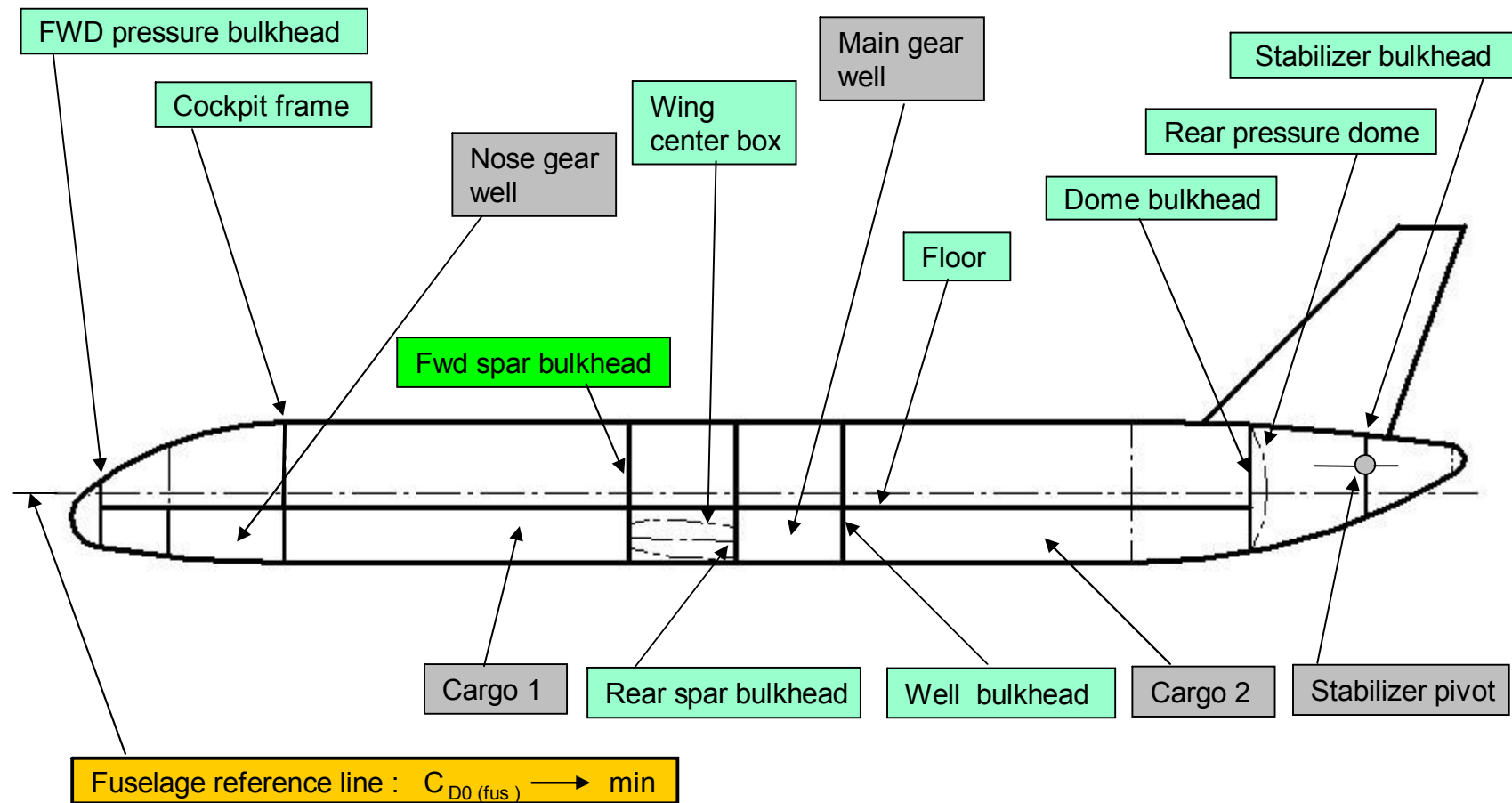
$$l_f / d_f = 5 - 8 - 14$$



Configuration layout 1 : Medium Range Transport

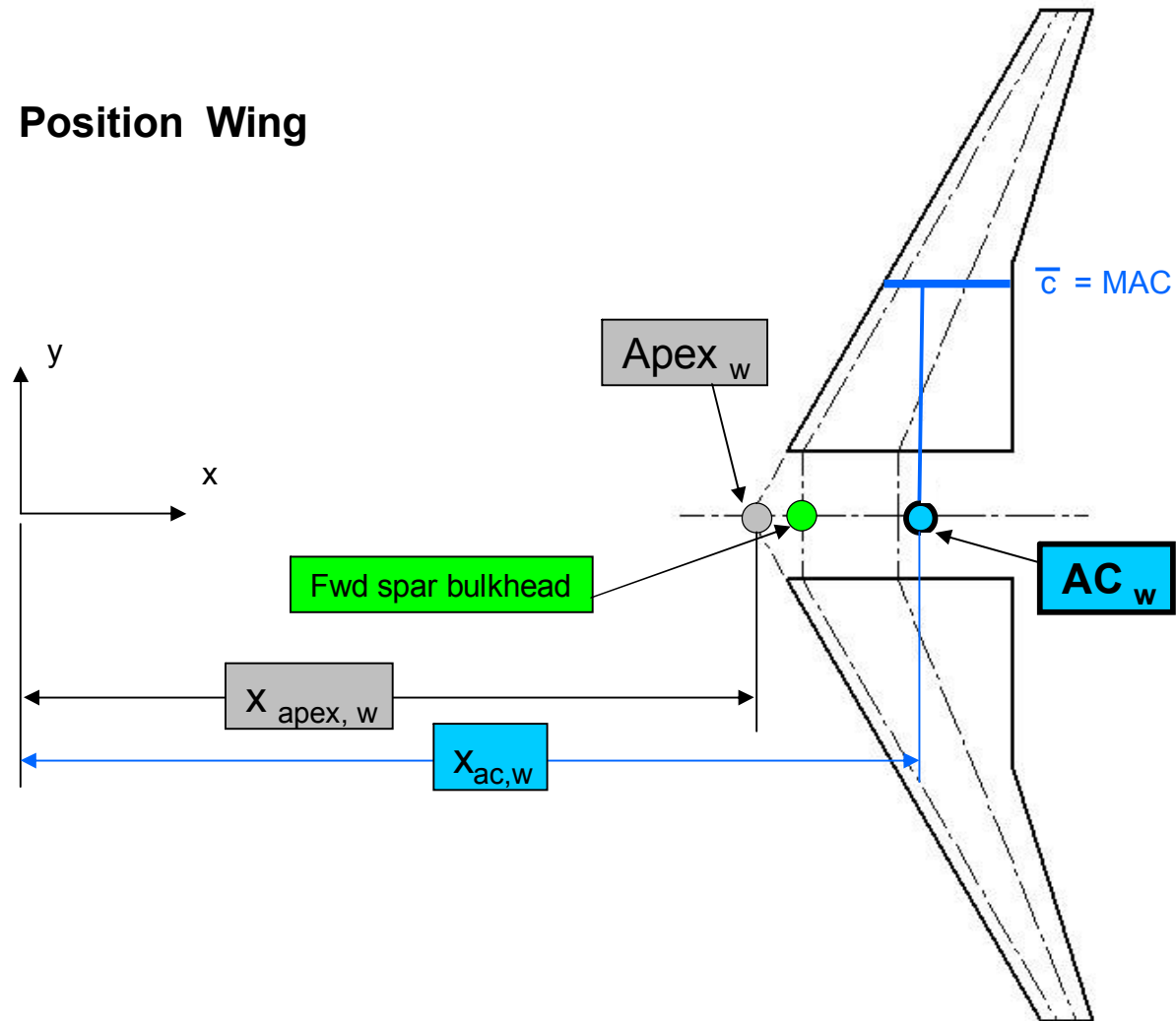


➤ Fuselage structural arrangement

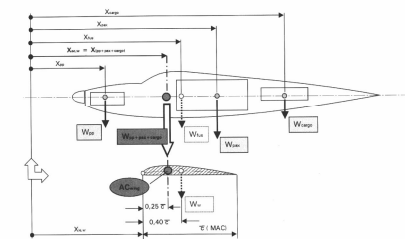


Configuration layout 1 : Medium Range Transport

➤ Position Wing

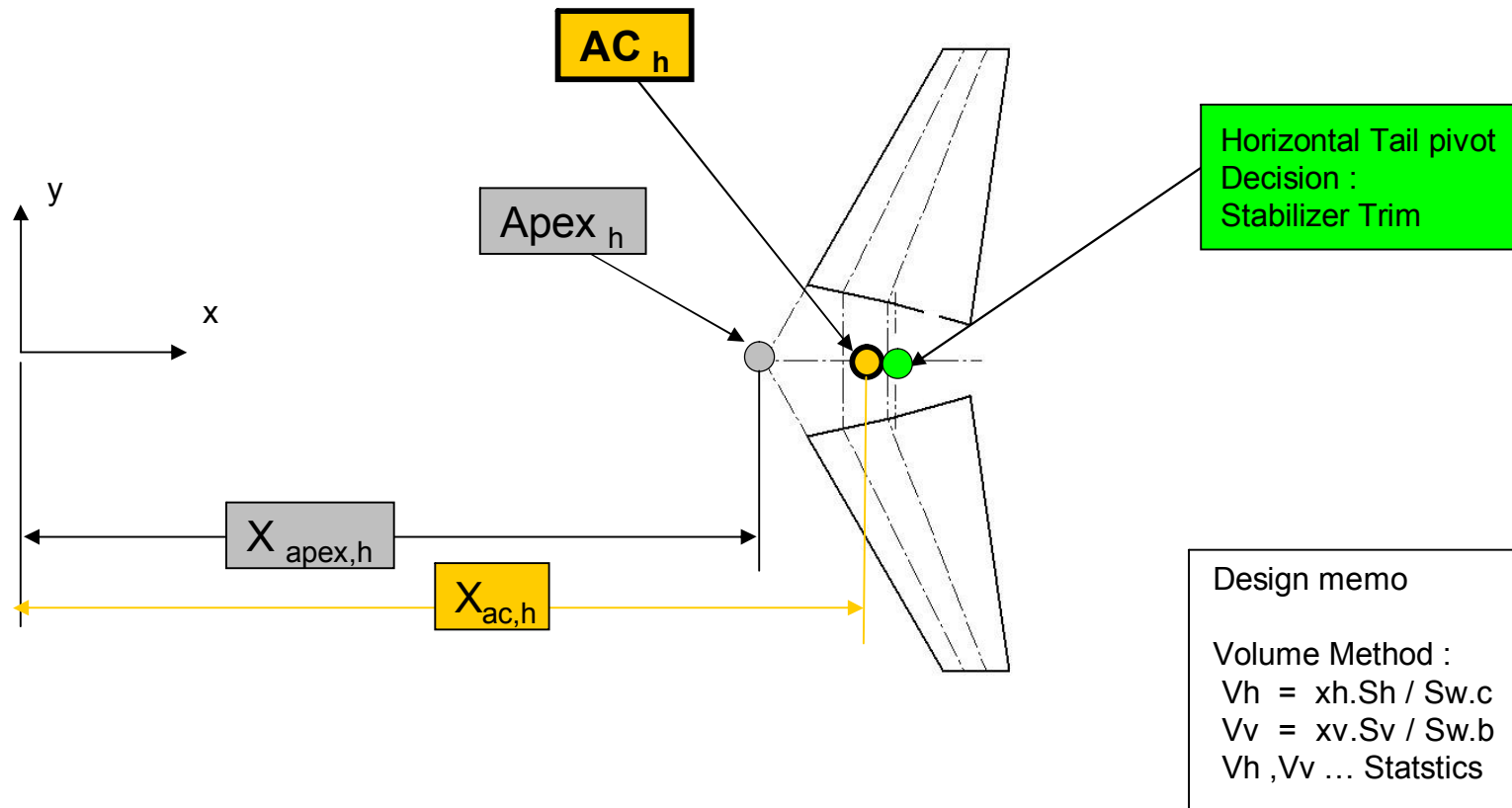


Design memo



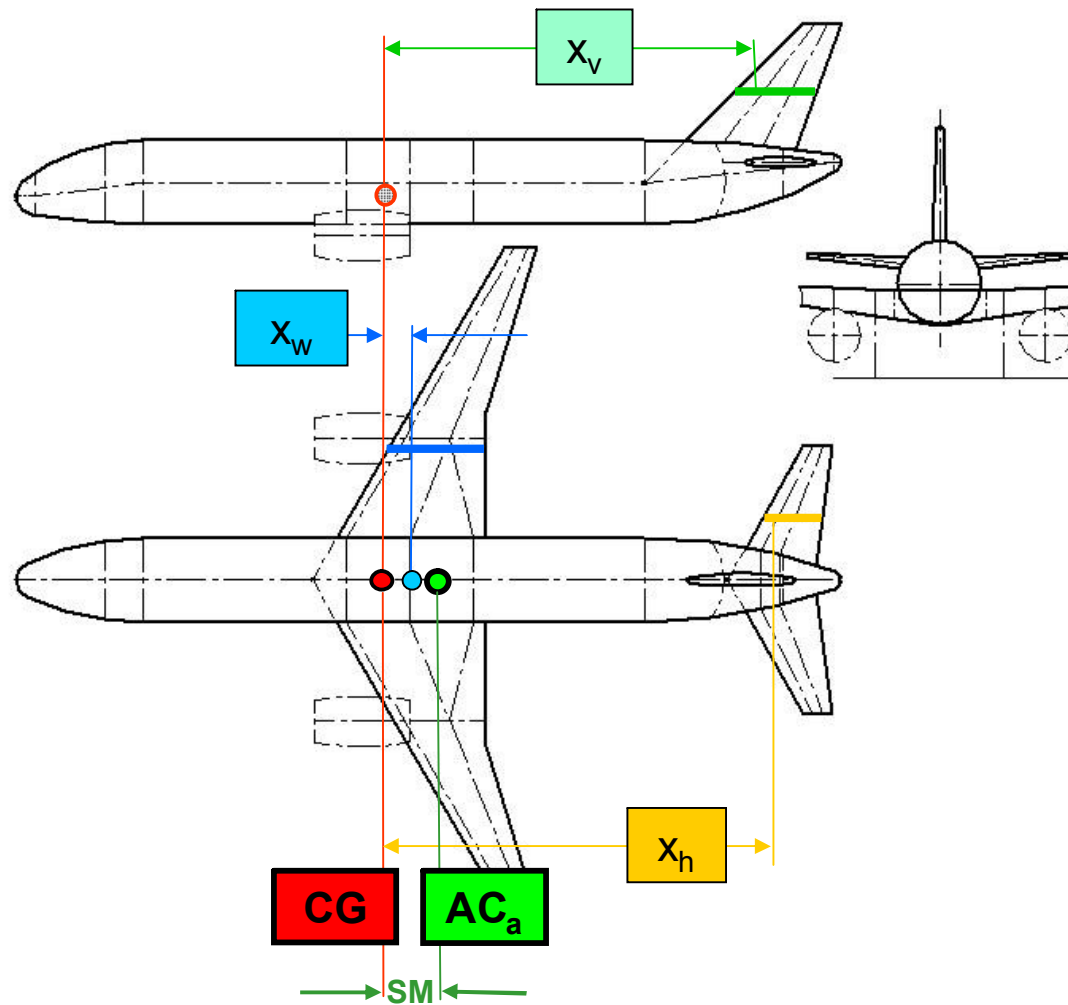
Configuration layout 1 : Medium Range Transport

➤ Position Horizontal Tail



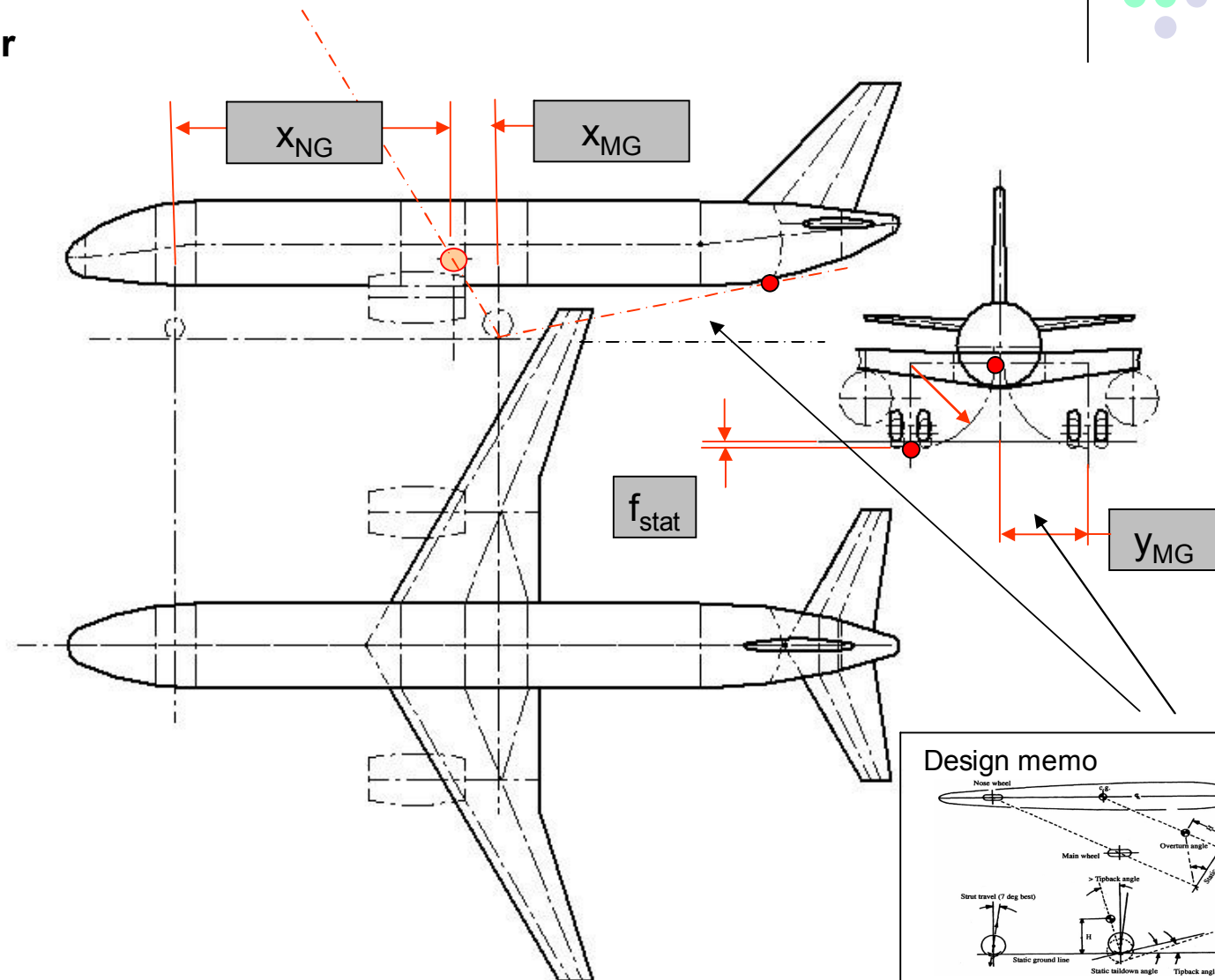
Configuration layout 1 : Medium Range Transport

➤ Integration Airframe



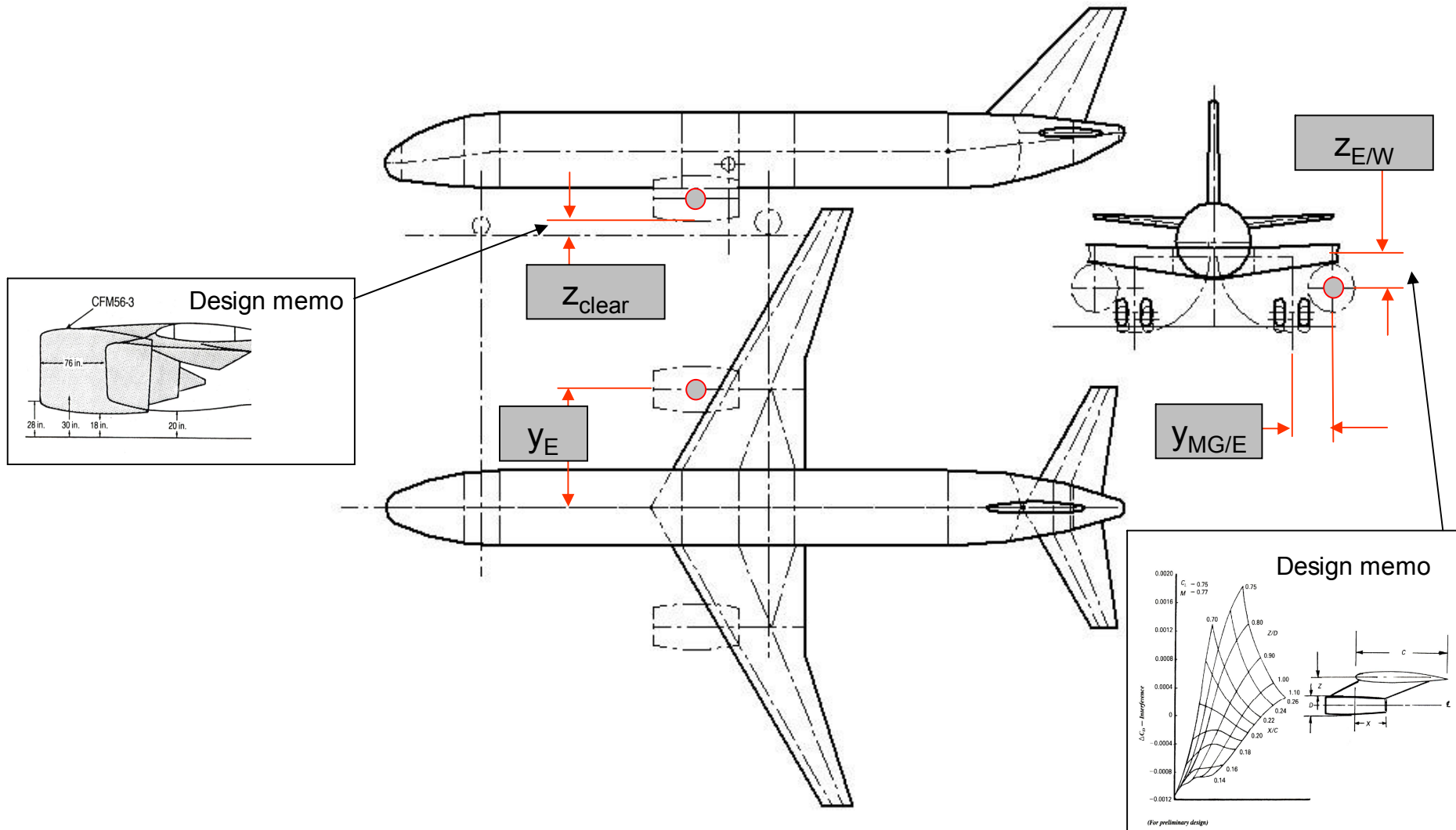
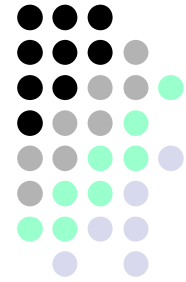
Configuration layout 1 : Medium Range Transport

➤ Position Gear



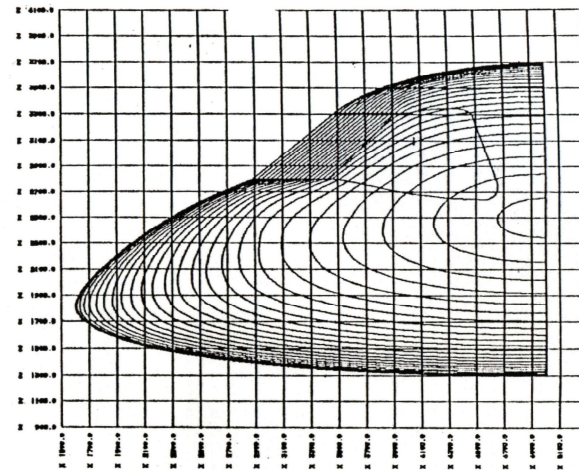
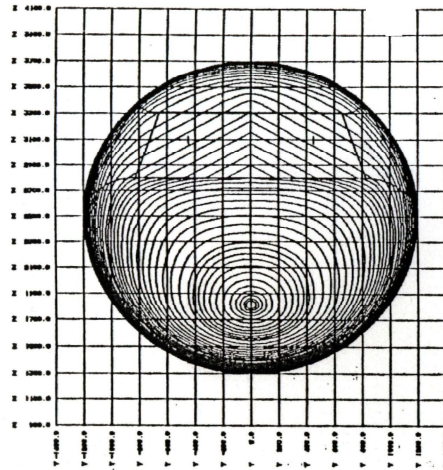
Configuration layout 1 : Medium Range Transport

➤ Position Engine



Configuration layout 1 : Medium Range Transport

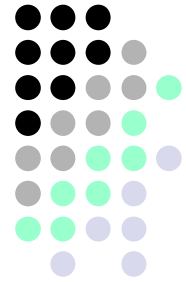
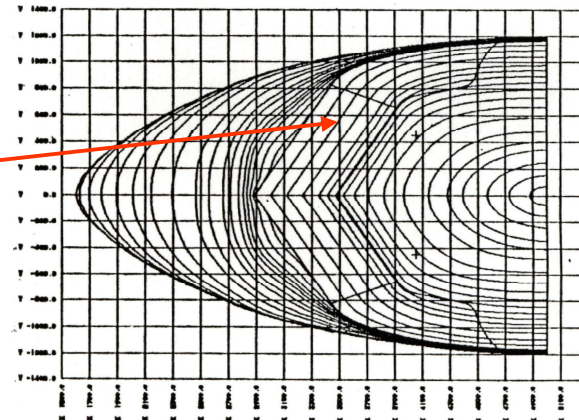
➤ Loft



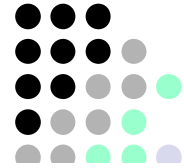
Fore Body Loft :

Influence of Windshields

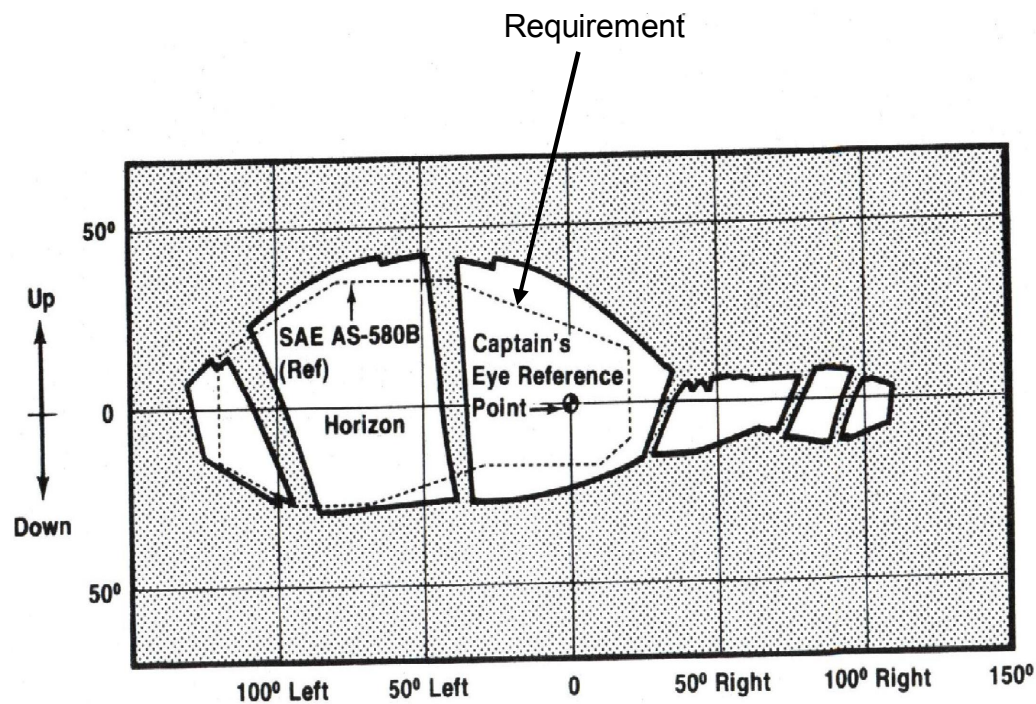
- flat
- spherical (curved)



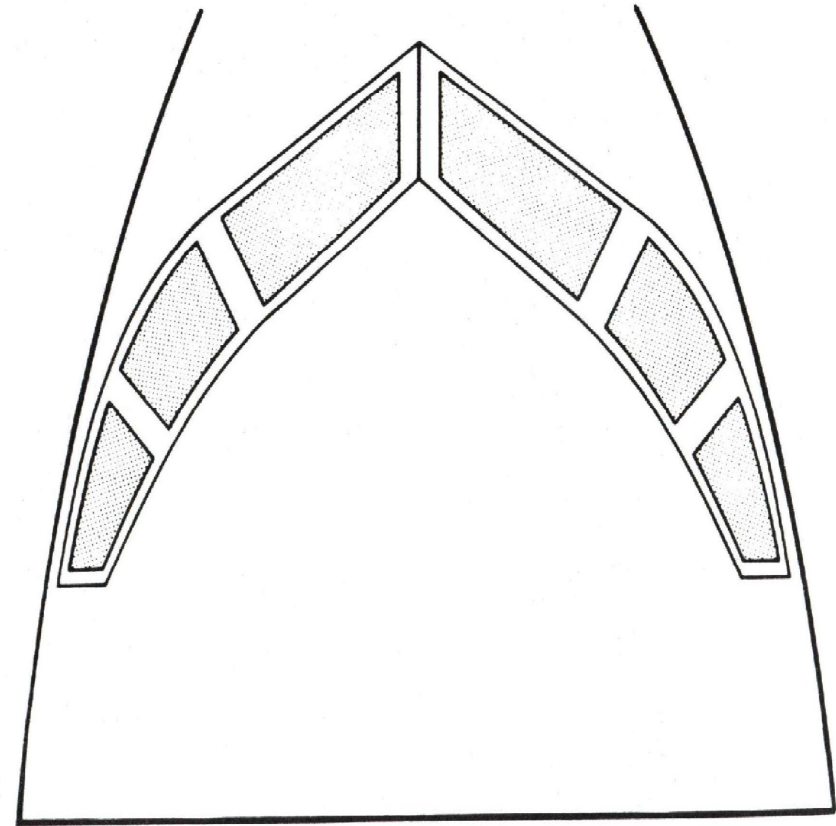
Configuration layout 1 : Medium Range Transport



➤ Vision Polar Diagram



Captain's Clear View Vision

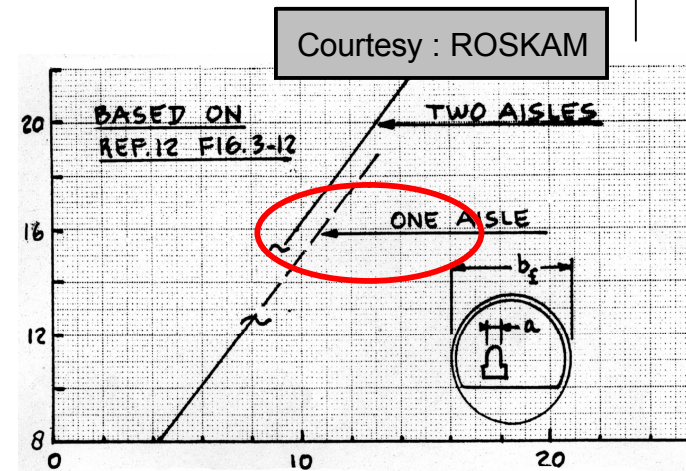


Courtesy : ROSKAM

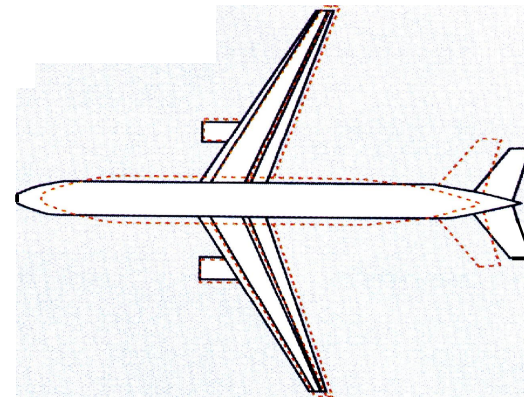
Configuration layout 1 : Medium Range Transport

- Interference sector 1-aisle / 2 – aisle in 200 PAX category

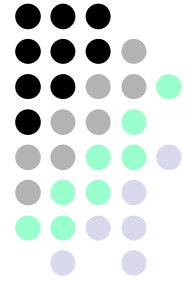
-Seats abreast	6	8
-Fuselage dia	4m	5,7m
-Fuselage length	49m	43m
-Lift/Drag	20	19
-MTOW	123 t	138 t



- Technical advantages to favor narrow-body, BUT higher comfort level, container capability for wide-body



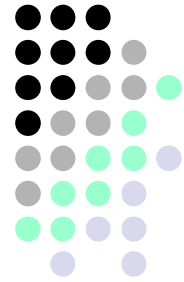
Chapter 11.2



Configuration Design Problems

11.2.2 30 Seat Regional Transport

Configuration layout 2 : Regional Transport



Configuration Decisions :

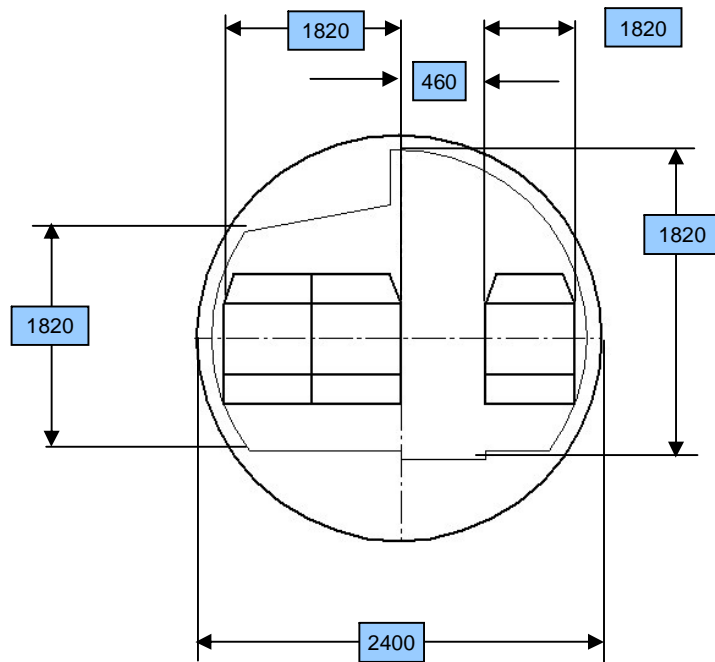
- 30 PAX, 3 - abreast, Single aisle
- High Wing
- T - Tai
- 2 Underwing Engines
- Tricycle Nose Gear

Basic Geometry Data (requested) :

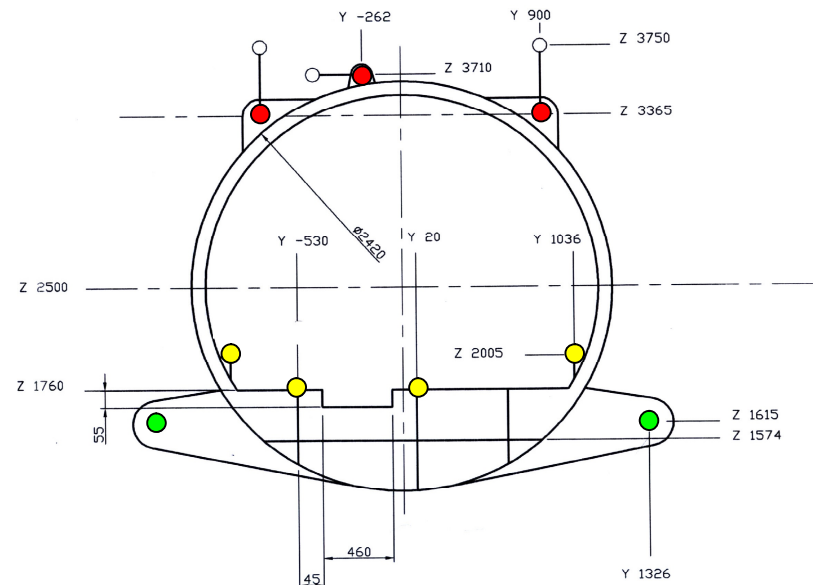
- Fuselage Inner Dia
- Outer Dia
- Cabin Length
- Cabin Ceiling
- Length Cylindrical Section
- Length Forebody
- Length Aftbody
- Length Fuselage
- Wing position
- Gear Position

Configuration layout 2 : Regional Transport

➤ Fuselage Dia



Cabin Cross Section

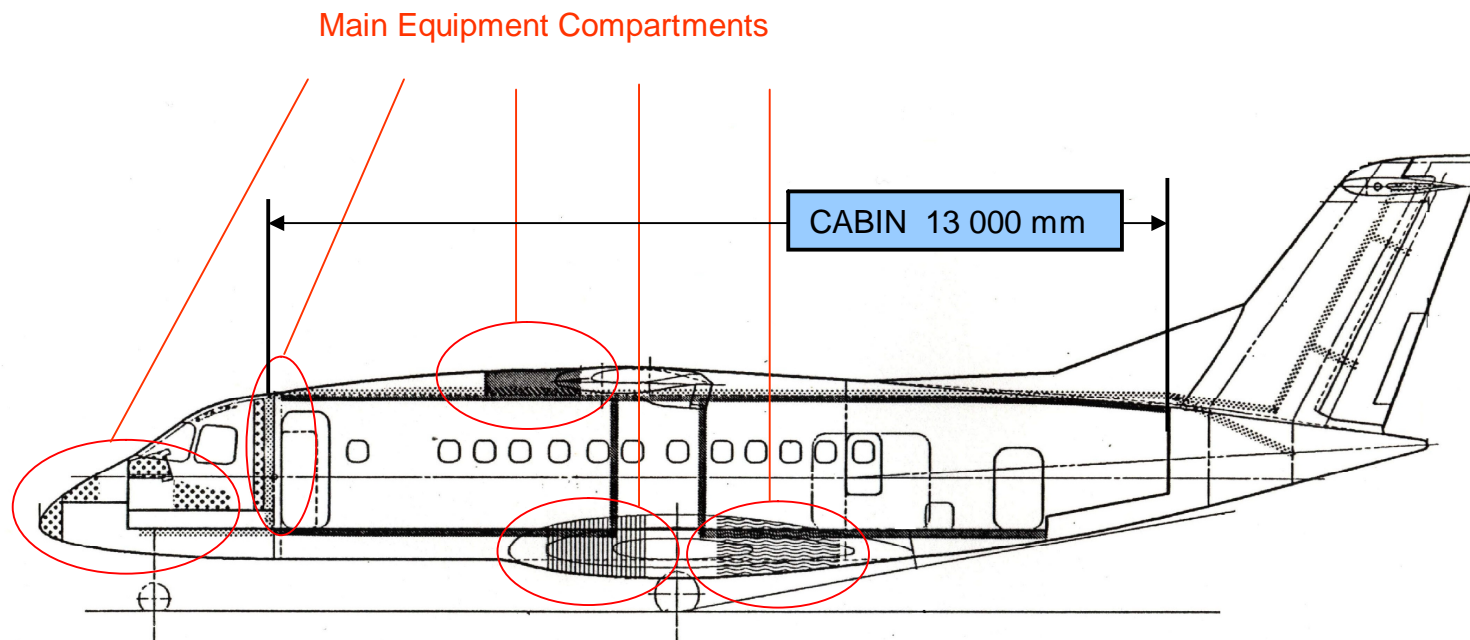
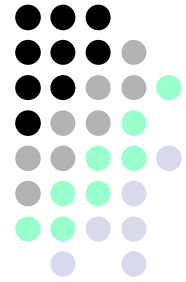


- Wing Loads
- Seat Loads
- Gear Loads

Main Bulkhead

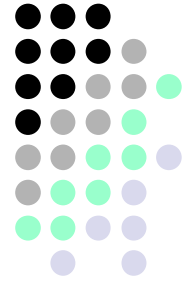
Configuration layout 2 : Regional Transport

- **Fuselage Inboard Profile** : Small fuselage, space for systems, equipment



Courtesy : DORNIER

Configuration layout 2 : Regional Transport



Configuration details will be found as shown in Configuration1

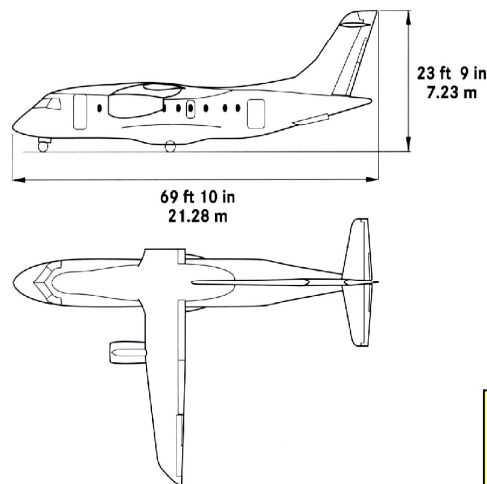
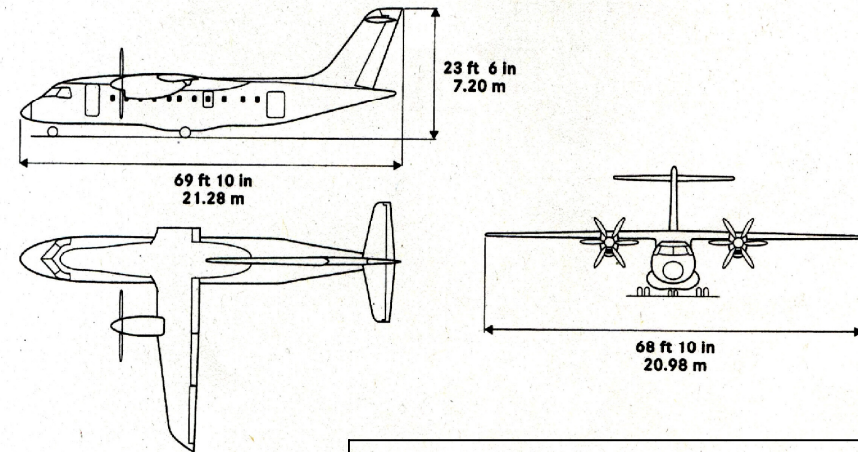
- Component Positions
- CG Travel
- Airworthiness
- Design Loads
- Loft
- Vision Polar

Configuration layout 2 : Regional Transport



Design Special :

- 2 Versions of an Aircraft
- Identical Airframe
- Different Propulsion



Performance Parameters

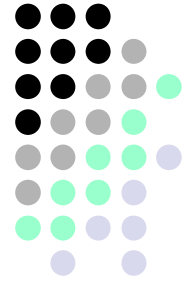
Max .Cruise Speed (FL 200)	335 KTAS
Design Range (32 PAX)	730 nm
Max. Operating Altitude	25 000 ft
MTOW	13 640 kg

Performance Parameters

Max .Cruise Speed (FL 230)	375 KTAS
Design Range (32 PAX)	870 nm
Max. Operating Altitude	31 000 ft
MTOW	14 990 kg

Courtesy : DORNIER

Chapter 11.3



Special Configurations

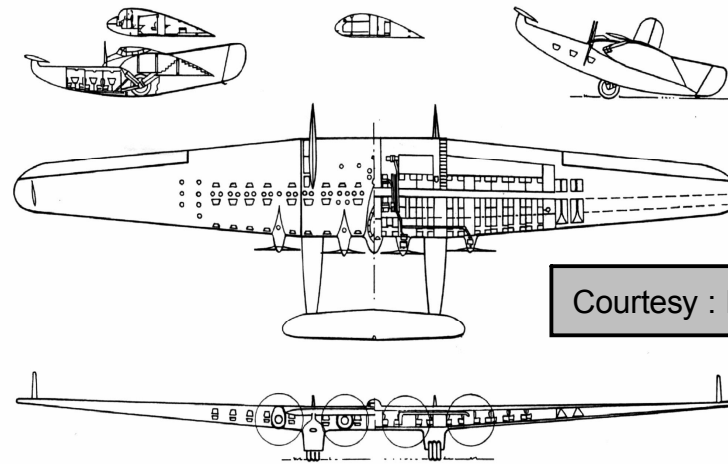
- Spanloading
- Joined Wing
- Military Transport

Special Configurations

- **Spanloading :** *Payload distribution spanwise*

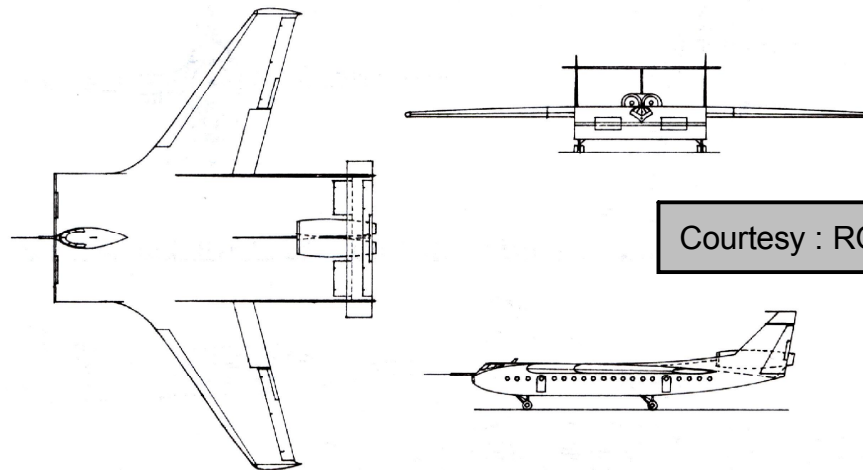
Early concepts
- low altitude
- not pressurized

JUNKERS



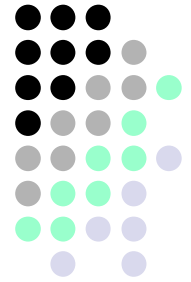
Courtesy : DT. MUSEUM

BURNELLI



Courtesy : ROSKAM

SpanloadingFlying Wing ...BWB



➤ **Spanloading** : *Payload distribution spanwise*

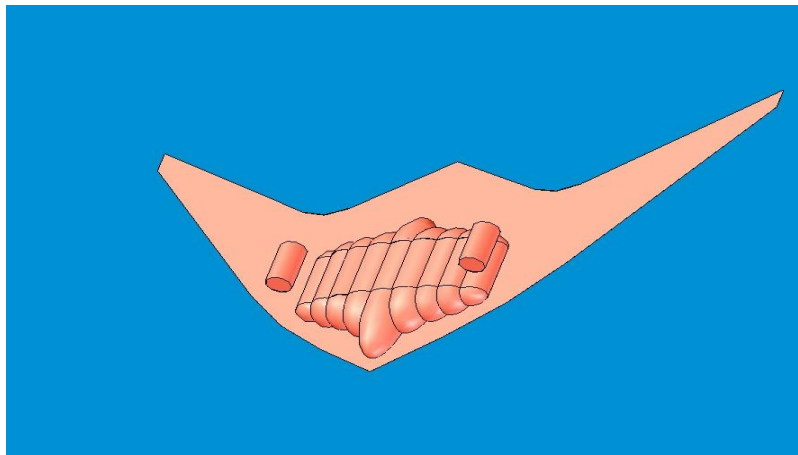
Modern concepts
- high altitude
- pressurized

NORTHROP



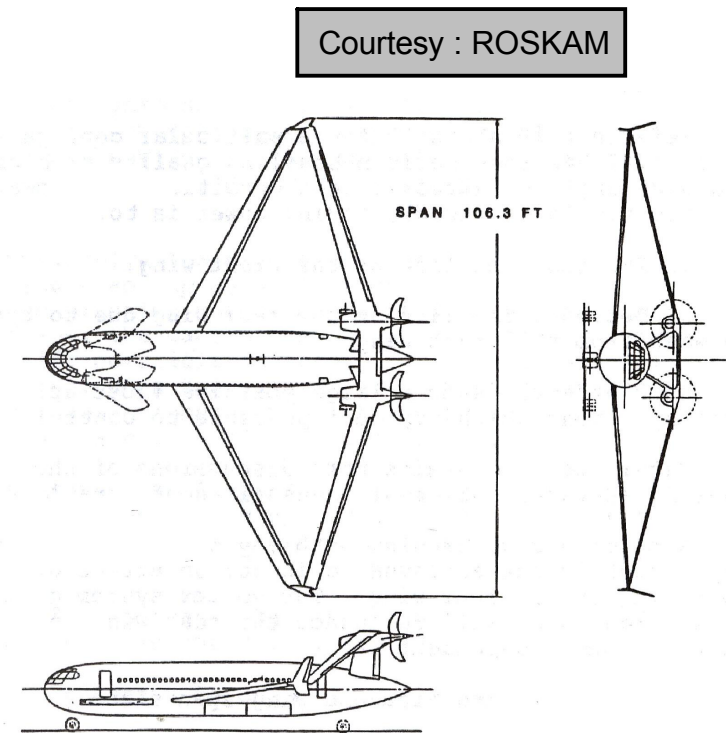
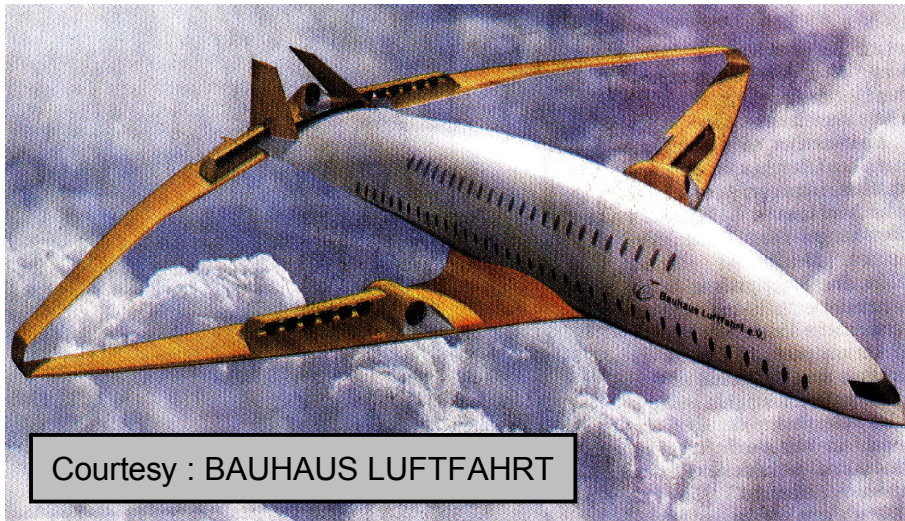
BWB

- multi bubble



➤ Special Configurations

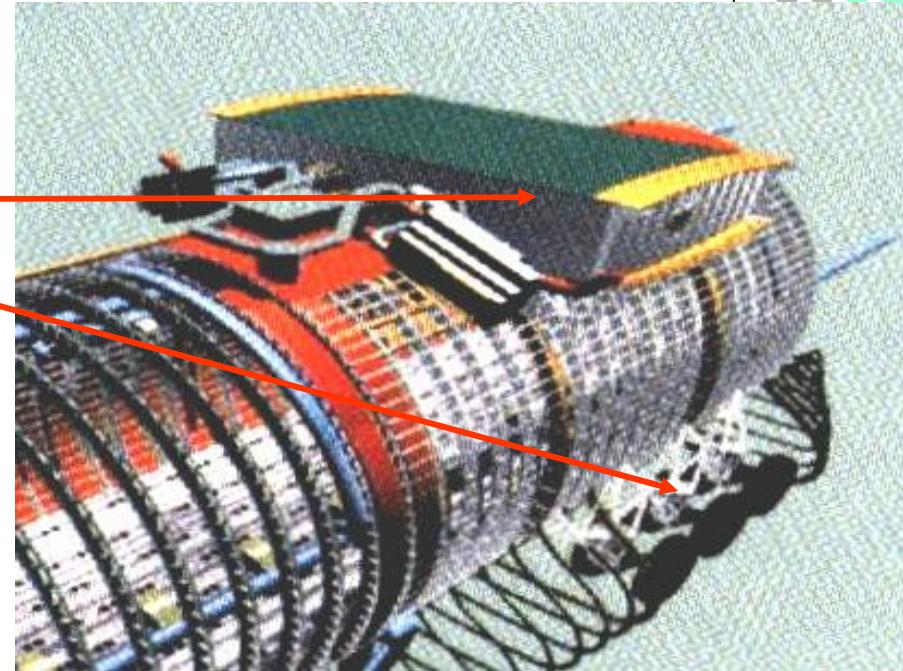
➤ **Joined Wing** : enhanced wing stiffness



Special Configurations

➤ Military Transport :

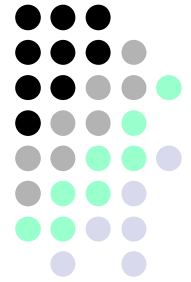
- High wing, Centerbox
- Gear with “kneeling” capability
- Low floor
- Turboprop propulsion



Courtesy : AIRBUS

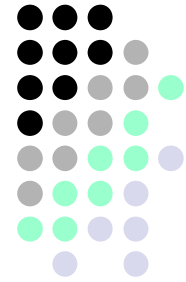
Chapter 11.4

Conclusions

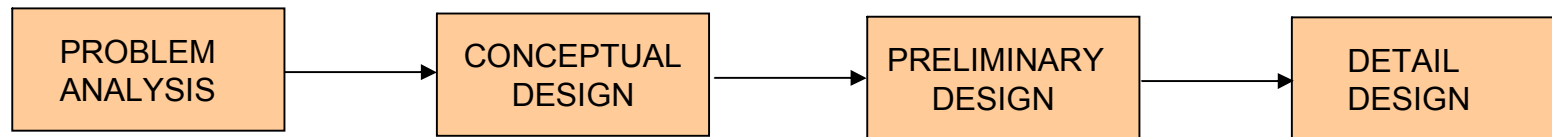


Conclusions

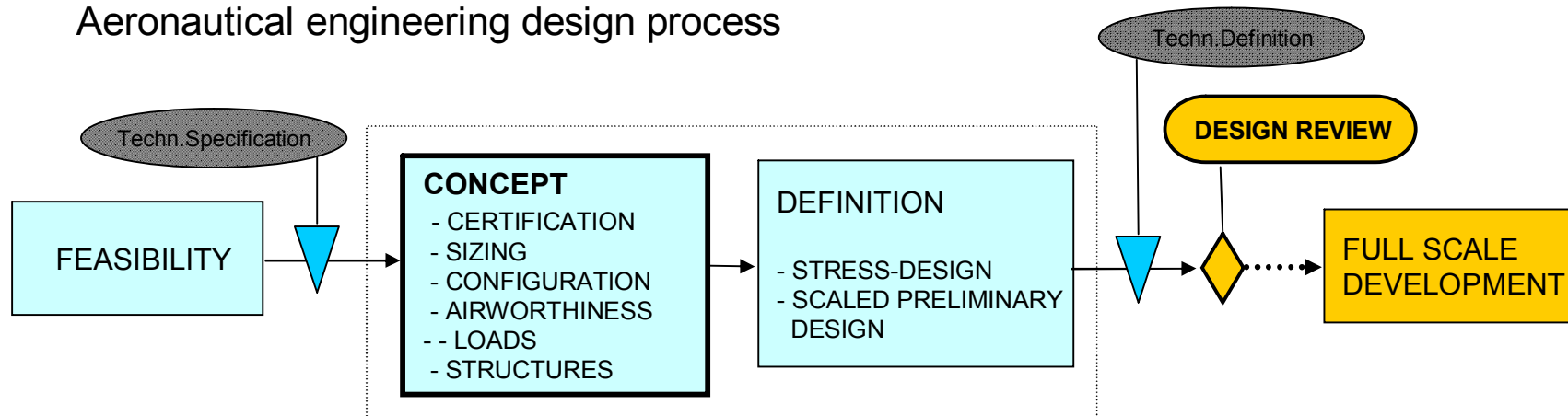
- Aircraft conceptual design utilizes a defined methodology
- This methodology goes confirm with general engineering design methods
- Special is an extended concept/definition phase which incorporates large parts of general preliminary design tasks



General engineering design process



Aeronautical engineering design process



Jürgen Thorbeck

Chapter 12

**From
Aircraft Performance
to
Aircraft Assessment**

From Aircraft Performance to Aircraft Assessment

1. Objectives of the Lecture
2. Preface for a Simple Approach to DOC
3. Operational Cost Structure
4. A Simplified DOC Model
 1. DOC Notations
 2. Fuel Demand
 3. Average Aircraft Weight
 4. Payload Range Diagram
 5. Unit Cost
 6. JAVA DOC Applet
5. Aircraft Family Economics
6. Presentation of DOC Calculation Results
7. Total Quality Assessment

- ▶ Understand
 - the structure of direct operation cost (DOC) of commercial aircraft
 - the different notations for DOC
 - how flight physical properties (flight performance) of the aircraft are affecting the DOC
 - how to interpret the payload range diagram as the ultimate performance statement and as basis for DOC calculations
 - how to distinguish between physical and operational flight conditions
 - how the major design requirements are affecting the DOC
 - how to simply assess DOC
 - the DOC differences of aircraft family members
 - how to interpret different DOC representations
 - the basics for a total value analysis

- ▶ Enable
 - to assess aircraft design weights by statistical means
 - to create a payload range diagram from known design weights (top-down)
 - to create a payload range diagram from technological performance data (bottom-up)
 - to convert a payload range diagram into a DOC range diagram
 - to perform simple DOC calculations for comparison purposes
 - to construct meaningful aircraft assessment diagrams

- ▶ The major objective in commercial aircraft design is to find a viable solution for an aircraft configuration and size which fulfills all the given requirements (operational and certification) and represents an optimum with respect to a given function of merit
- ▶ Objective functions can be parameters such as weight (e.g. MTOW, OEW), performance (e.g. speed, climb distance), flight comfort (non quantifiable) or in most cases direct operating cost (DOC)
- ▶ An objective function is necessary for the aircraft design process
- ▶ Airlines usually perform both a total quality assessment which includes a DOC evaluation and a thorough route analysis with cost simulation
- ▶ DOC assessment in the scope of aircraft design is not intended to simulate the operational cost of an arbitrary airline operation under its specific conditions, but to provide for a merit function which reflects cost trends as accurate as possible even when the aircraft is still poorly defined, i.e. in the concept phase



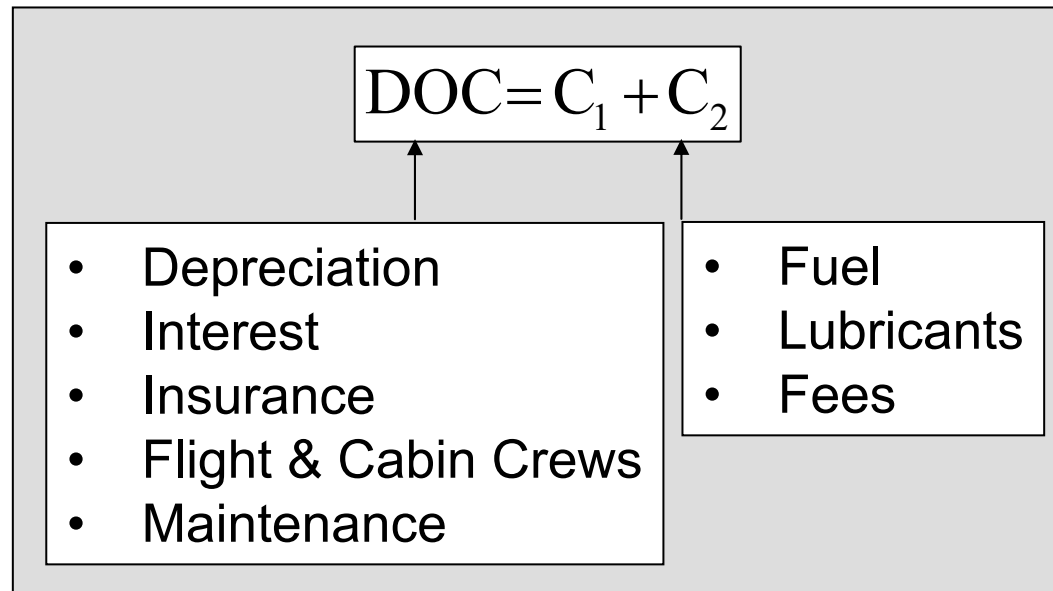
Preface for a Simple Approach to DOC

*Aircraft Design &
Aero Structures*

- ▶ A suitable function of merit has to be simple in structure in order to allow for design optimizations
- ▶ A function of merit is to be used for comparison purposes only
- ▶ It has to reflect the flight physical properties of the aircraft as well as operational cost parameters
- ▶ As engineers or technically thinking people we use to be a little bit afraid when it comes to financial considerations, because that seems to touch another strange world
- ▶ However, dealing with DOC we have to be bold enough to create a simplified artificial world by our own, which reflects, as accurate as possible, the complex real world
- ▶ We consequently have to set-up a cost scenario by means of averaging the non-uniform real life cost scenario parameters such as prices for hardware, fuel or operational services
- ▶ We are going to notice on the way that flight physics plays also an important role in economics of flight
- ▶ Let us enter in that adventure

- ▶ Indirect Operation Cost (IOC)
 - Corporate Management
 - Marketing
 - Facilities
 - ...
- ▶ Direct Operation Cost (DOC)
 - Flight dependent
 - Fuel and Lubricants
 - Fees (Ground handling & landing & air traffic control)
 - Flight independent
 - Capital Cost (Depreciation & Interest & Insurance)
 - Flight & Cabin Crew
 - Maintenance facilities
 - Maintenance (flight cycle, flight time, calendar time dependent)
- ▶ The sum of IOC and DOC is called total operating cost (TOC)
- ▶ DOC excluding capital cost used to be called cash operating cost (COC)

- ▶ Two elements are required for the most simple DOC model :
 - C1: Route dependent (variable) Cost
 - C2: Route independent (fixed) Cost



- ▶ How does a typical cost scenario look like?
- ▶ Which parameters do we need to know in order to use that formula?

- ▶ Simplifications to be made:
- ▶ All **route independent cost** are primarily based on the aircraft size and its respective operational empty weight (OEW)
- ▶ The major element is the capital cost which can be assumed to be a linear function of the OEW (if the aircraft market influence is considered negligible) and thus

$$C_1 = P_{\text{OEW}} \cdot \text{OEW} \cdot a \quad \text{whereas} \quad a = \text{IR} \cdot \frac{1 - f_{\text{RV}} \cdot \left(\frac{1}{1 + \text{IR}} \right)^{\text{DP}}}{1 - \left(\frac{1}{1 + \text{IR}} \right)^{\text{DP}}}$$

with a: Annuity factor

P_{OEW} : Price per kg OEW

IR: Interest rate

DP: Depreciation period (years)

f_{RV} : Residual value factor (Residual value / aircraft price)

- ▶ That does assume that an operator is buying an aircraft for a constant price per kg and spends the corresponding capital cost constantly per year all over the depreciation period



A Simplified DOC Model

- ▶ That annuity formula, which is based on a modified mortgage equation, addresses both depreciation and interest
- ▶ The reason for the a.m. modification is to include the residual aircraft value at the end of the depreciation period into the capital cost, which is occasionally meaningful
- ▶ All non capital cost elements are accounted for by adjustment of the price factor P_{OEW}
- ▶ Insurance cost are also proportional to the aircraft price
- ▶ Personnel cost are assumed to be route independent because an airline has to provide a sufficient number of crews to ensure flight operations over the entire service time and therefore are proportional to the payload (e.g. number of passengers) and in so far approximately also to the aircraft OEW
- ▶ Note: The flight crew cost are independent of the aircraft size. In so far the error made by that assumption decreases with capacity

- ▶ Within the **route dependent cost** lubrication cost can be assumed to be of minor order of magnitude compared to the fuel cost and can be addressed by a minor correction of the fuel price
- ▶ The fees are comprising payload dependent handling fees and maximum take-off weight (MTOW) dependent ATC and landing fees
- ▶ The second term can thus be calculated by

$$C_2 = FC \cdot \left(P_F \cdot m_F + P_{PL} \cdot PL + P_L \cdot MTOW + R \cdot \sqrt{\frac{MTOW}{50000}} \right)$$

with

- P_F : Fuel price [€/kg]
- m_F : Mission fuel [kg]
- PL : Payload
- P_{PL} : Handling fees [€/kg]
- P_L : Landing fees [€/kg]
- FC : Yearly flight cycles

Note: The fourth term represents the EUROCONTROL formula for ATC-fees



A Simplified DOC Model

- ▶ Landing fees are charged on basis of aircraft MTOW whereas ATC fees are based on both the secured flight distance (Range) and the discounted (square root!) MTOW
- ▶ Due to the dependency of the aircraft utilization on the range it doesn't make sense to estimate DOC on a flight-by-flight basis
- ▶ In that case capital cost, which are spent over the lifetime (or at least the depreciation period) of the aircraft have to be distributed over all cumulated flight
- ▶ It is therefore common to look at the yearly DOC because various statistical utilization data on that basis are available (IATA, ATA, AIA, airline balance sheets)

- ▶ A basic structure of a generic utilization formula is

$$FC = \frac{FT_{p.a.}}{(FT + BT)} = \frac{FT_{p.a.}}{\left(\frac{R}{v} + BT\right)}$$

with $FT_{p.a.}$: Yearly flight time (365 days · 24 h – downtime)

FT: Flight time

BT: Block time supplement per flight

R: Average stage length

v: Cruise speed

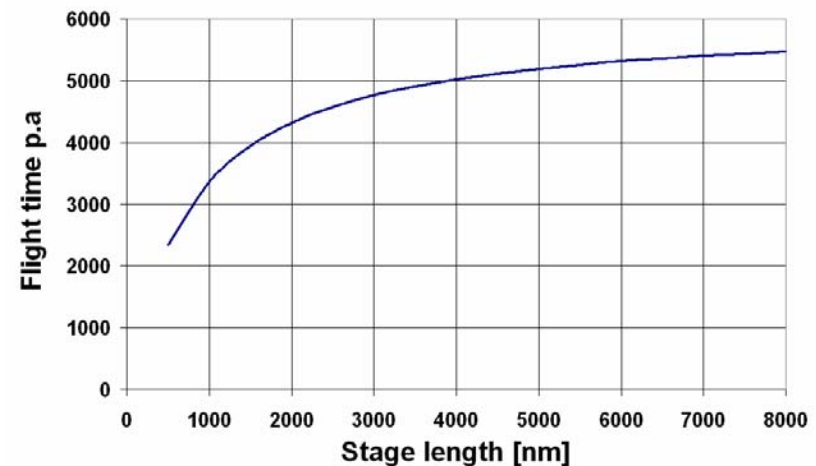
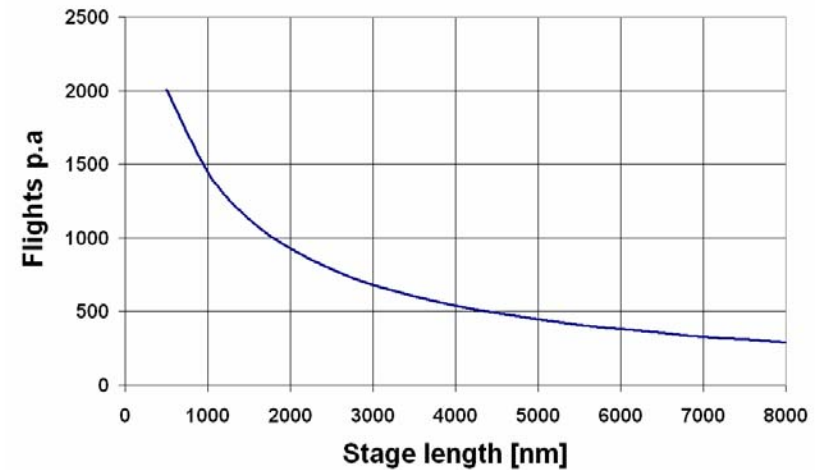
- ▶ Note: It is hereby assumed, that the flight is performed with constant speed, which is not the actual case (ref. climb/descent/approach segments)

- ▶ Statistical values for large airlines operating in the European scenario are
 - Average downtime: 2750 h (Maintenance, night curfews)
 - Average block time: 1,83 h
- ▶ With that the Utilization formula can be written

$$FC = \frac{6011}{\left(\frac{R}{v} + 1,83 \right)}$$

- ▶ The yearly flight time yields

$$\begin{aligned} FH_{p.a.} &= FC \cdot t_{flug} \\ &= \frac{6011}{1 + v \cdot \frac{1,83}{R}} \end{aligned}$$



- ▶ We have seen that only a limited number of parameters are necessary to calculate DOC
 - Financial parameters (Interest rates, depreciation period, residual value)
 - Operational parameters (Yearly flight cycles & downtime, block time supplement)
 - Aircraft design weights (MTOW, OEW, PL)
- ▶ Whereas financial and operational parameters can be obtained from statistical investigations, the aircraft weights have a flight physical origin

- ▶ The absolute DOC as monetary value is usually not well suited for the assessment of different aircraft because the aircraft size and technology is heavily driving that figure.
- ▶ For aircraft evaluation purposes it is better to reference the DOC to a term which addresses the benefit of the aircraft, e.g. the
 - range potential
 - Trip cost (TC)
 - DOC/km
 - passenger mile potential
 - Unit cost
 - Seat mile cost (SMC, DOC per seat-km offered, DOC/SKO)
 - DOC/Passenger km (DOC per passenger-km offered, DOC/PKO)
 - payload mile potential
 - Unit cost
 - Ton kilometer cost (DOC per ton-km offered, DOC/TKO)

- ▶ It is unusual to base cost expressions on revenue, e.g. sold seat-km (Revenue passenger kilometers, RPK), because revenue is strongly influenced by the market situation and is therefore varying
- ▶ Trip cost are giving an assessment towards the risk of operating the aircraft, e.g. if there is no revenue
- ▶ Unit cost rather are a means to assess the changes of operating the aircraft
- ▶ The mentioned cost expressions are calculated by

$$\text{DOC} / \text{TKO} = \frac{\text{DOC}}{\text{PL} \cdot \text{R}} \left[\frac{\text{€}}{\text{to} \cdot \text{km}} \right]$$

$$\text{DOC} / \text{km} = \frac{\text{DOC}}{\text{R}} \left[\frac{\text{€}}{\text{km}} \right] = \text{TK} \quad \text{or} \quad \text{TC} = \frac{\text{DOC}}{\text{TKO}} \cdot \text{PL} \left[\frac{\text{€}}{\text{km}} \right]$$

$$\text{DOC} / \text{SKO} = \frac{\text{DOC}}{\text{PAX} \cdot \text{R}} \left[\frac{\text{€}}{\text{km}} \right] = \text{SMC} \quad \text{or} \quad \text{SMK} = \frac{\text{TC}}{\text{PAX}} \left[\frac{\text{€}}{\text{km}} \right]$$

- ▶ Thrust specific fuel consumption SFC reflects the engine technology level

$$\text{SFC} = \frac{\dot{m}_F}{T} = \frac{dm_F}{dt} \cdot \frac{1}{T} = \frac{dm_F}{dt} \cdot \frac{dR}{dR} \cdot \frac{1}{T} = \frac{dm_F}{dR} \cdot \frac{dR}{dt} \cdot \frac{1}{T} = \frac{dm_F}{dR} \cdot \frac{v}{T}$$

with m_F : Fuel mass (dot indicates time derivative)
 T : Thrust [N]
 R : Range [km]
 v : Air speed [km/h]

- ▶ Thus the range specific fuel consumption is

$$\frac{dm_F}{dR} = \frac{\text{SFC} \cdot T}{v}$$

- ▶ The required thrust for steady **cruise flight** conditions equals the drag D of the aircraft and can be expressed by the aerodynamic efficiency D/L and the gross weight W :

$$T = D = D / L \cdot W$$

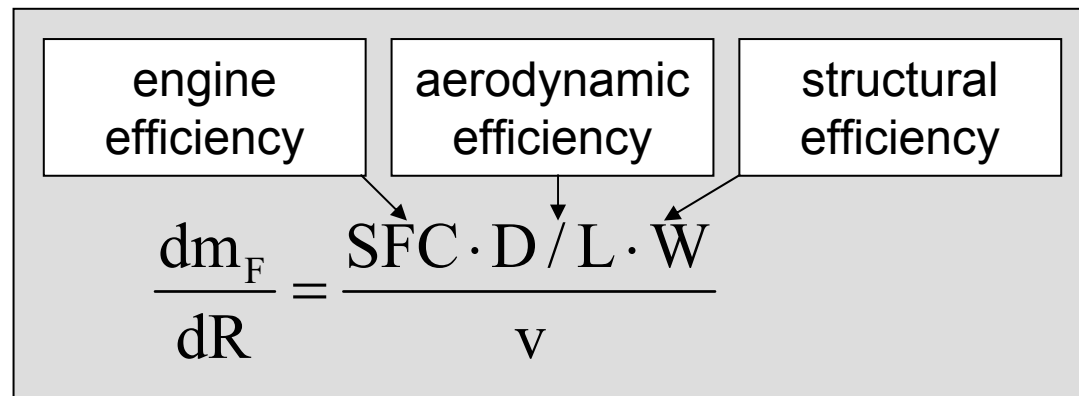
- ▶ Now the **range specific fuel demand** can be rewritten

$$\frac{dm_F}{dR} = \frac{SFC \cdot D / L}{v} \cdot W$$

- ▶ The factor of W is known as Breguet-factor and the reciprocal as so called **fuel mileage**

$$\frac{dR}{dm_F} = \frac{v}{SFC \cdot D / L \cdot W}$$

- ▶ It becomes obvious that all important flight physical properties of the aircraft are driving the fuel burn:



- ▶ The above formula represents the momentary fuel burn which is varying by the decreasing gross weight during a flight due to burned fuel
- ▶ It can be assumed that for a rough estimate of the fuel demand it is sufficient to calculate with an average flight weight (W_{ave} , average between TOW and LW) of the magnitude

$$W_{ave} = \frac{TOW + LW}{2} = TOW - \frac{W_{MF}}{2}$$

with TOW: Take-off mass
 LW: Landing mass
 W_{MF} : Mission fuel weight

- ▶ With that, now range independent, average gross weight the momentary fuel burn for a given range can be converted into a total fuel consumption

$$m_F = \frac{SFC \cdot D / L \cdot W_{ave} \cdot R}{V}$$

- Assuming that the overall efficiency η_{tot} of an aero-engine is consisting of two elements, the thermal and the propulsion efficiency

$$\eta_{\text{tot}} = \eta_{\text{therm}} \cdot \eta_{\text{prop}} = \frac{\text{Benefit}}{\text{Expense}}$$

it can be written

$$\eta_{\text{tot}} = \frac{N_{\text{internal}}}{N_{\text{Fuel}}} \cdot \frac{N_{\text{Prop}}}{N_{\text{internal}}} = \frac{N_{\text{Prop}}}{N_{\text{Fuel}}} = \frac{T \cdot v}{\dot{m}_F \cdot H_L} = \frac{v}{\text{SFC} \cdot H_L}$$

with

- N_{internal} : Power of the turbo mechanical engine
- N_{Fuel} : Chemical power of the fuel
- N_{Prop} : Propulsion power
- H_L : Lower heat value of fuel

- From that the thrust specific fuel consumption results in

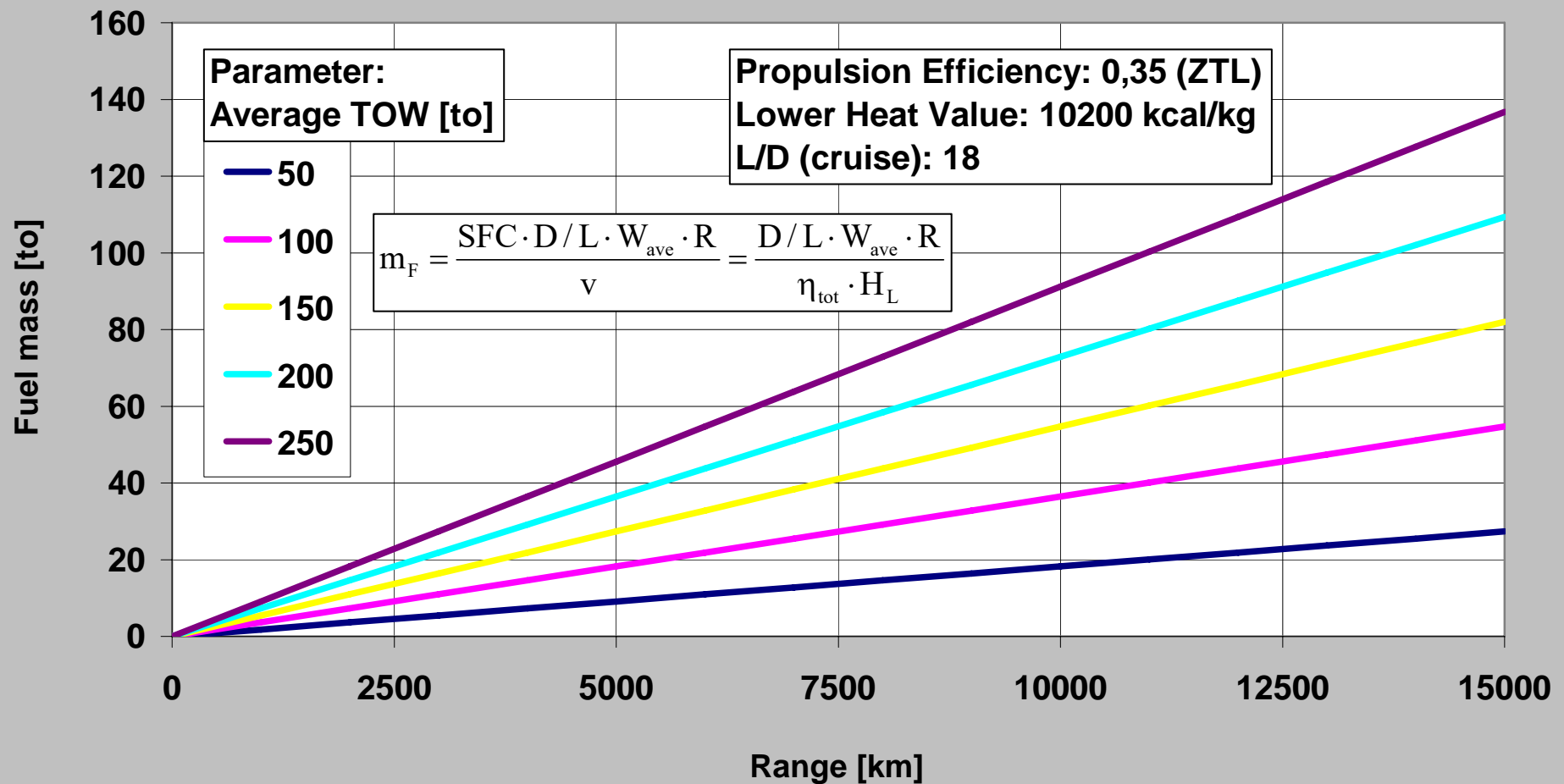
$$\text{SFC} = \frac{v}{\eta_{\text{tot}} \cdot H_L}$$

- ▶ Thus the fuel demand for a given range can also be written as a function of the fuel specific heat and the engine total efficiency

$$m_F = \frac{D / L \cdot W_{ave} \cdot R}{\eta_{tot} \cdot H_L}$$

- ▶ Note: For typical aviation fuels (Kerosene: $H_L = 10200$ kcal/kg) and a high bypass ratio engine (SFC of 0,6 1/sec) the cruise efficiency of an aero-engine can be assessed by approx. 0,35
- ▶ Note: Because the flight segment dependent SFC values are not considered, that calculation method does reflect the cruise flight only

Fuel Demand (no reserves, cruise conditions only)



- ▶ Note: The calculated fuel demand so far does neither consider reserve fuel nor the non cruise parts of a flight mission
- ▶ An entire flight mission (so called off-blocks to on-blocks) is much more complex and consists of the segments
 - Engine start
 - Taxi to start point with ground idle
 - Accelerated round run with maximum power
 - Accelerated initial climb with maximum power
 - Steady climb with maximum climb power
 - Cruise flight (with or without step climb segments) with cruise power
 - High speed descent with flight idle
 - Reduced speed descent with flight idle
 - Approach with power according to flap setting
 - Landing and ground run with ground idle (or thrust reverse power)
 - Taxi to park position with ground idle
 - Engine cut

- ▶ The cumulative fuel demand has to be calculated for each given payload and range mission
- ▶ A full mission calculation does require a precise definition of the fuel policy of the operator in regard to the
 - climb strategy (best climb angle, best rate of climb, economic climb)
 - cruise strategy (const. altitude, const. angle of attack, const. speed)
 - descent strategy (minimum rate of descent, best descent range)
- ▶ Thus the calculation requires a lot of sub-optimizations and is very exhausting
- ▶ For an operational range calculation the reserve fuel has to be considered according to the European or American rules defined by definition of
 - Alternate distance, flight level & speed to alternate
 - Holding time, holding altitude, holding speed
 - contingency fuel (European scenario only)

- ▶ For practical aircraft conceptual design analysis it is helpful to use normalized statistical data for aircraft design weights
- ▶ Weight fraction factors are typically used for normalization
- ▶ The maximum gross weight (MTOW) is the sum of the weight elements

$$\text{MTOW} = \text{OEW} + \text{PL} + W_{\text{fuel}}$$

with OEW: Operation empty weight

PL: Payload

W_{fuel} : Total fuel weight (including reserves)

- ▶ Dividing by MTOW leads to weight factors (fractions)

$$1 = \frac{\text{OEW}}{\text{MTOW}} + \frac{\text{PL}}{\text{MTOW}} + \frac{W_{\text{fuel}}}{\text{MTOW}} = \beta + \gamma + \kappa$$

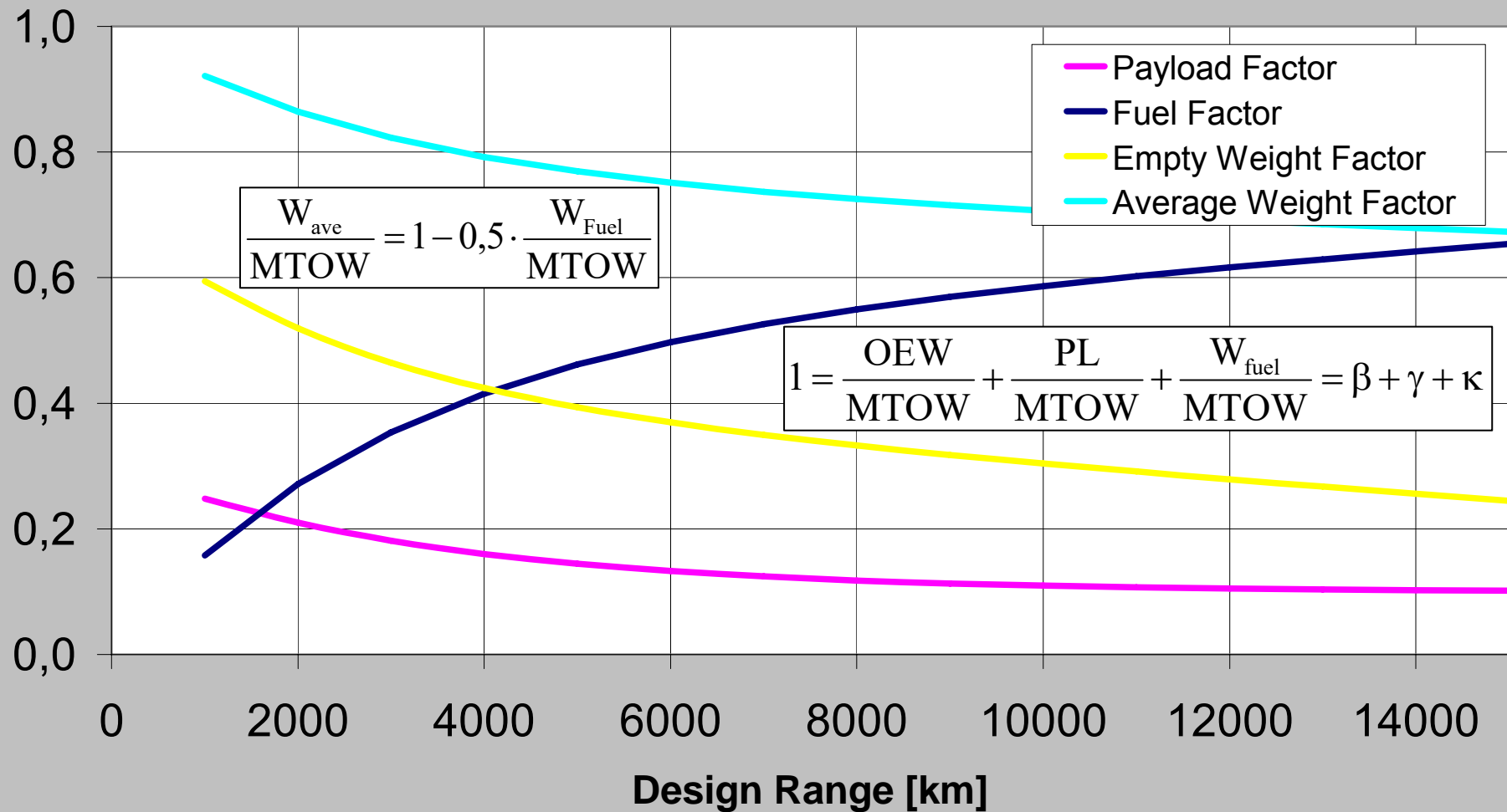
with β : Empty weight factor

γ : Payload factor

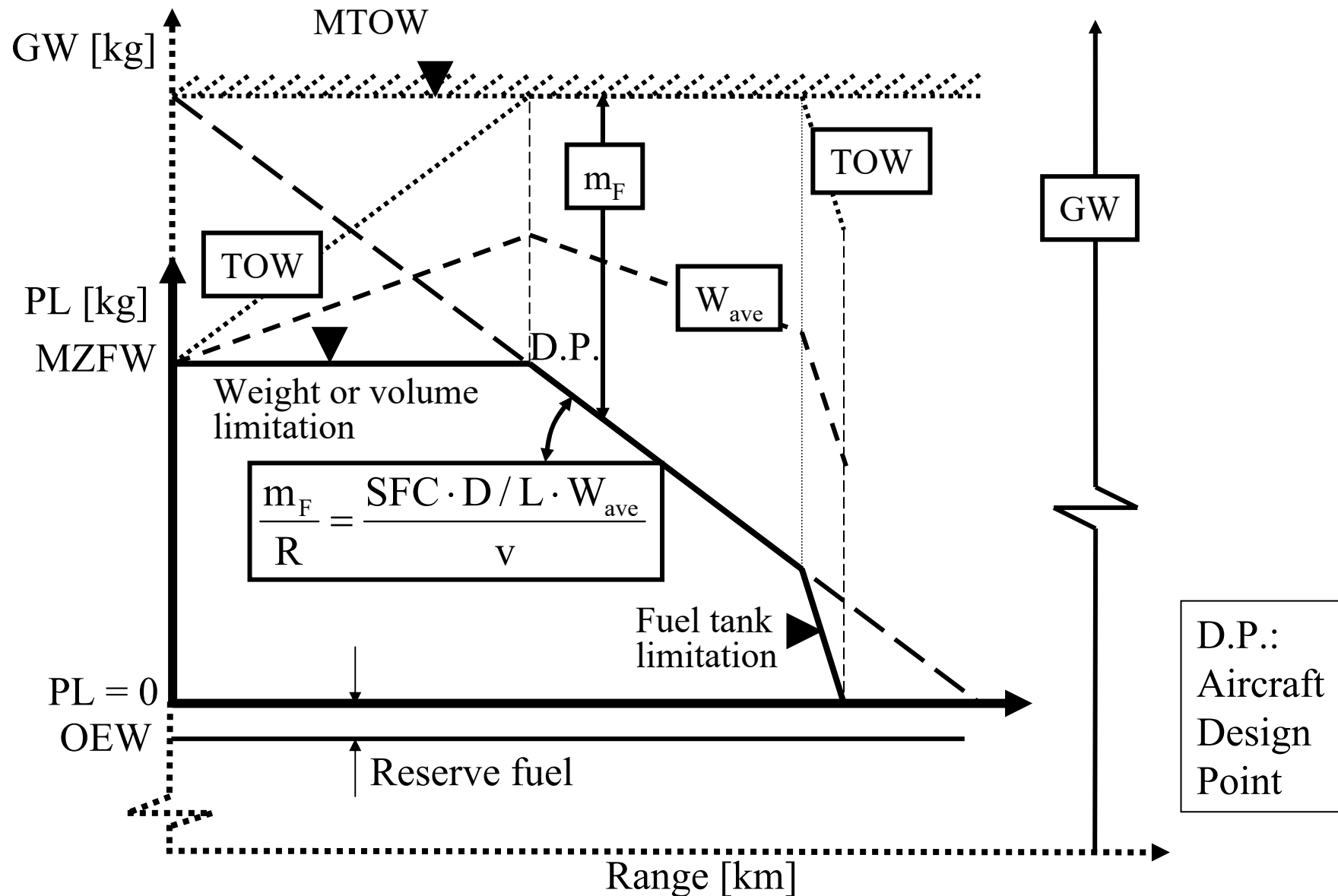
κ : Fuel factor

- ▶ Knowing the payload factor and therewith the MTOW and consequently the fuel factor for a given payload it is easy to assess the OEW

Aircraft Design Weight Statistics



- ▶ The payload range diagram constitutes a series of mission calculations for the entire aircraft range regime ranging from zero to maximum range → **bottom-up** calculation
- ▶ In order to facilitate the calculation some assumptions are justified
 - cruise calculation with const. SFC, speed and aerodynamic efficiency
 - statistic correction factor for all non-cruise segments
- ▶ Those simplifications are the basis for a **top-down** approach
- ▶ The payload range diagram is part of a gross weight range diagram
- ▶ Gross weight consists of two main elements
 - non range dependent weights (fixed weights)
 - OEW
 - reserve fuel (approximately)
 - range dependent weights (variable weights)
 - Payload
 - Mission fuel
- ▶ For range variation only the variable weight elements are interchangeable



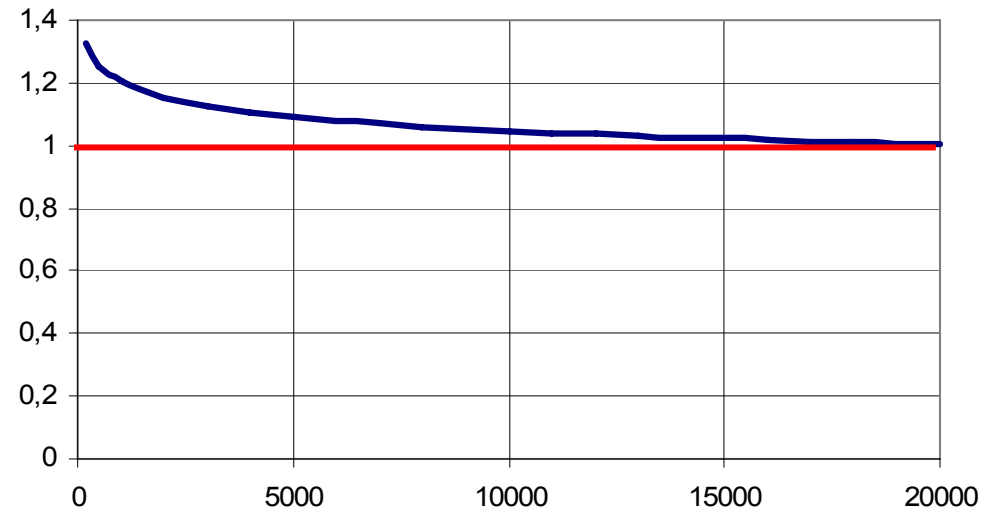
- ▶ Explanation of the payload range diagram
 - For zero range there is no need for mission fuel
 - The fuel required for an increasing range is increasing slightly progressively, because the average gross weight (coarse dotted line) is increasing
 - At design point (required payload and range) there is no need to increase the take-off weight any further because that would unnecessarily compromise the approach speed and take-off and landing distance
 - Further increase of the range is possible by exchanging payload with additional fuel thereby keeping the take-off weight at maximum. According to the now decreasing average gross weight the payload range characteristic is declining in that domain
 - When the fuel reaches the tank limitation only a steep decrease of the average gross weight by further reducing the payload can increase the range up to the point where the payload is zero (maximum range)
 - The payload range diagram (bold lines) ultimately appears as a part of the gross weight diagram
- ▶ Note: The substitution line is straight only under the assumption of a constant average gross weight (sometimes taken as the D.P. average gross weight) over range

- ▶ In the given format the payload range diagram reflects the operational performance of an aircraft
- ▶ If no reserve fuel is considered, which results in lower MTOW, lower average gross weight and consequently in a smaller slope of the substitution line, the payload range diagram reflects the physical performance of an aircraft
- ▶ A slope correction which accounts for the ignorance of the non cruise segments of the mission can be done by means of a statistical investigation of exact mission calculation results
- ▶ The difference to the results of a cruise condition based Breguet factor and a “true” average Breguet factor resulting from that study can be expressed by a simple regression factor:

$$\frac{dm_F}{dR \cdot G_{ave}} = f \cdot \frac{SFC \cdot D / L}{V} \quad \text{with} \quad f = 1,82 \cdot DMR^{-0,06}$$

- ▶ For a bottom-up generation of a payload range diagram that factor can be successfully used in order to construct the substitution line

Average Breguet factor /
Cruise Breguet factor



Design Mission Range [km]

- ▶ Assuming that the D/L ratio is approximately constant during the entire flight the declining character of that factor with increasing range primarily is explained by a decrease of the average SFC because the flight with higher SFC at lower than cruise altitude (climb segment) takes an increasingly smaller share of the entire flight ($\rightarrow 1$)
- ▶ The same applies for the speed which is on average higher with increasing range

- ▶ Note: In contrast to the American scenario in the European scenario the reserve fuel is defined by two elements
 - Fuel for a flight to an alternate airport with landing weight
 - Additional contingency fuel defined by a fixed fraction of the cruise fuel as safety margin for unknown wind influences
- ▶ In so far the horizontal line of the reserve fuel is increasing with range up to the maximum tank capacity, thereafter being constant
- ▶ That can lead to exceeding the maximum landing weight and thus to a third, normally flat shaped restriction of the payload close to the design point edge

- ▶ Constructing a simplified payload range diagram (see above) for a newly designed aircraft **bottom-up** requires accomplishment of an entire design synthesis which at least results in data such as design weights (MTOW, OEW, $W_{\text{max fuel}}$, PL_{max}), D/L_{cruise} (drag polar) and SFC_{cruise} (engine characteristic map)
- ▶ The starting point is defined by the maximum payload at zero range
- ▶ From that point draw a horizontal line to the design range
- ▶ The Breguet factor can be calculated by the a.m. fuel consumption formula using the calculated cruise SFC, D/L and speed
- ▶ Knowing the range corrected average Breguet factor, representing its slope, the substitution line can be drawn
- ▶ That line ends at the payload which is remaining if the aircraft started with MTOW, maximum fuel and with a given OEW:

$$PL_{\text{max fuel}} = MTOW - OEW - W_{\text{fuel max}}$$
- ▶ Finally the maximum range can be depicted by dissolving the fuel formula to the range, setting the fuel mass to the maximum and the average gross weight to $OEW + W_{\text{fuelmax}}/2$

- ▶ By doing so the maximum range can be depicted by the formula

$$R_{\max} = \frac{V \cdot W_{\text{fuelmax}}}{\text{SFC} \cdot D / L \cdot \left(\text{OE}W + \frac{W_{\text{fuelmax}}}{2} \right)}$$

- ▶ For comparison purposes it is often helpful to construct a payload range diagram of an existing aircraft by application of the same principle as used for a synthetic aircraft
- ▶ A determination of the **physical payload range diagram** using known aircraft weight data is easily possible in a top-down approach
- ▶ With knowledge of the typically available aircraft data the way is as follows:
 - Determination of the design point (design payload & range)
 - Drawing the horizontal volume limitation line (for passenger planes) or the weight limitation line (for cargo aircraft) through the design point
 - Determining the maximum payload at maximum fuel

$$PL_{\max \text{ fuel}} = \text{MTOW} - \text{OE}W - W_{F, \max}$$

with $W_{F, \max}$: Fuel tank capacity

- Determination of the approximate slope of the substitution line by

$$\frac{\Delta m_F}{\Delta R} = \frac{MTOW - OEW - DPL}{DMR}$$

with DMR: Design range

DPL: Design payload

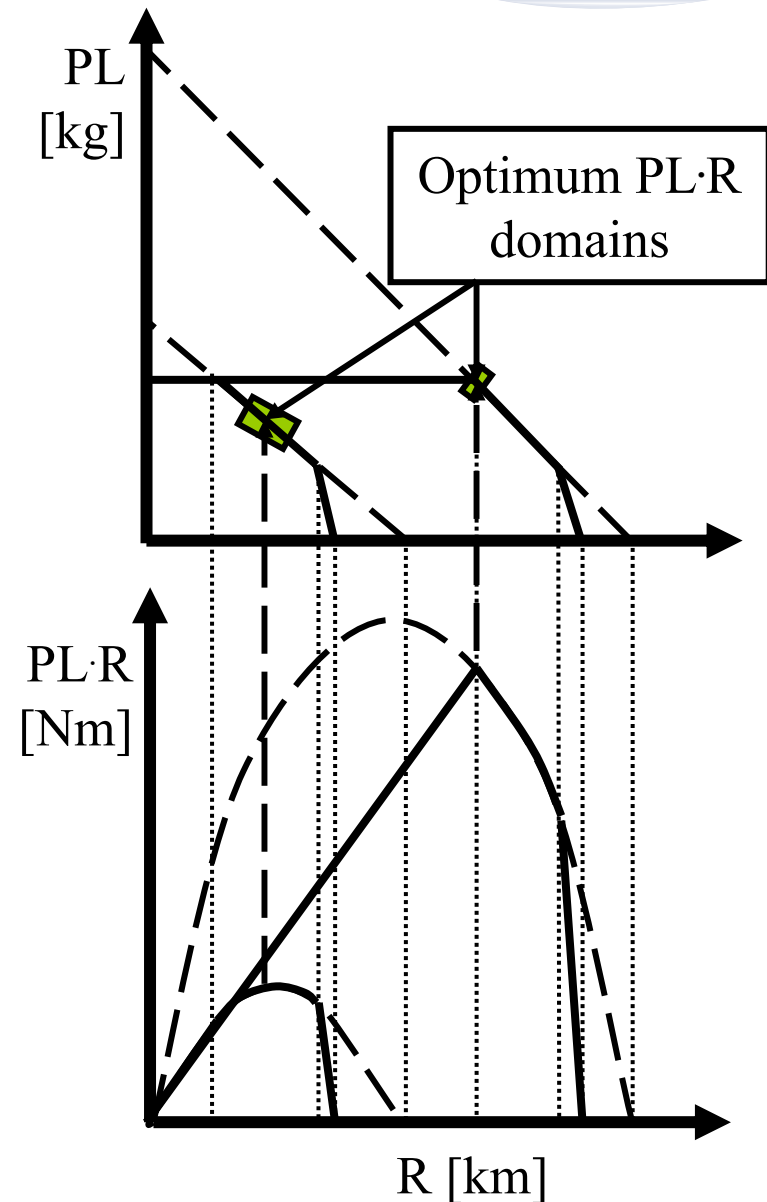
- Because the slope is also valid for the maximum fuel point it can be written for the range at that point

$$\frac{\Delta m_F}{\Delta R} = \frac{W_{F,max}}{R_{max fuel}} \Rightarrow R_{max fuel} = \frac{W_{F,max}}{\frac{\Delta m_F}{\Delta R}}$$

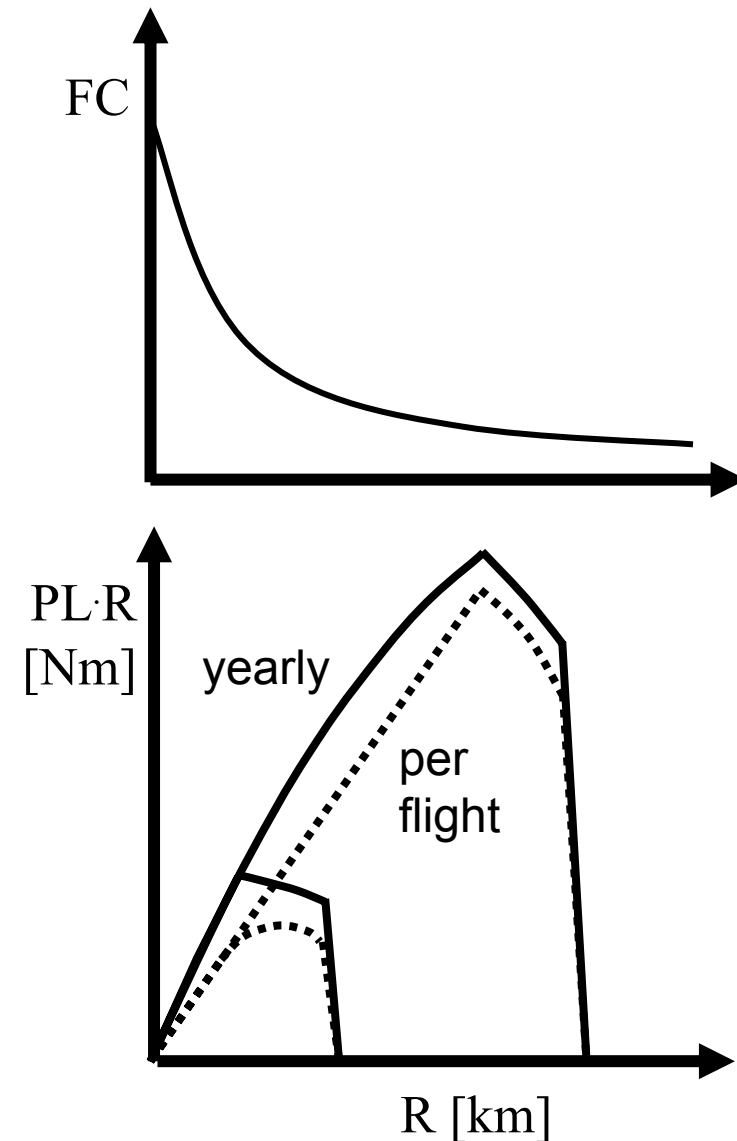
- Draw a straight line between design and fuel point as approximation for the substitution line
 - The maximum range point is most often published by the aircraft manufacturer
- Of course, for a comparison the synthesized aircraft physical payload range diagram has also to be used

- ▶ In order to calculate the unit cost defined as DOC/TKO it is necessary to know the denominator of that equation, which is the productivity of the aircraft and which is defined by the product of payload times range
- ▶ The productivity can be directly derived from the payload range diagram simply by multiplying both scale values
- ▶ An example which compares a long and a small range aircraft with equal capacity is given next

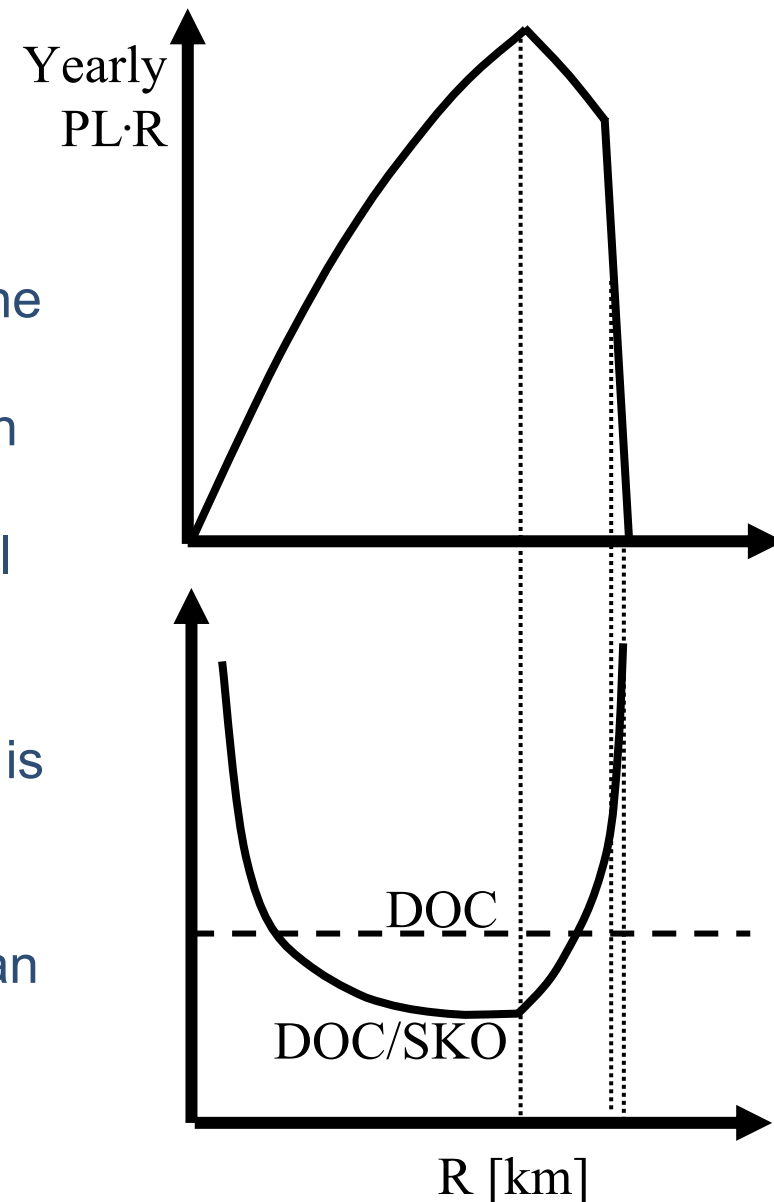
- ▶ Multiplying PL and R results, along the unrestricted payload range substitution line, in a quadratic parabola
- ▶ The payload restriction leads to a straight line through the origin
- ▶ In the domain of the fuel tank restriction we get again a steep quadratic parabola
- ▶ As the comparison of a short and a long range aircraft with equal capacity shows, the long range aircraft delivers a much bigger productivity, however, the point of its maximum is always the design point, whereas with the short range aircraft the maximum can be on the substitution line
- ▶ That consideration is of course valid for a single flight only



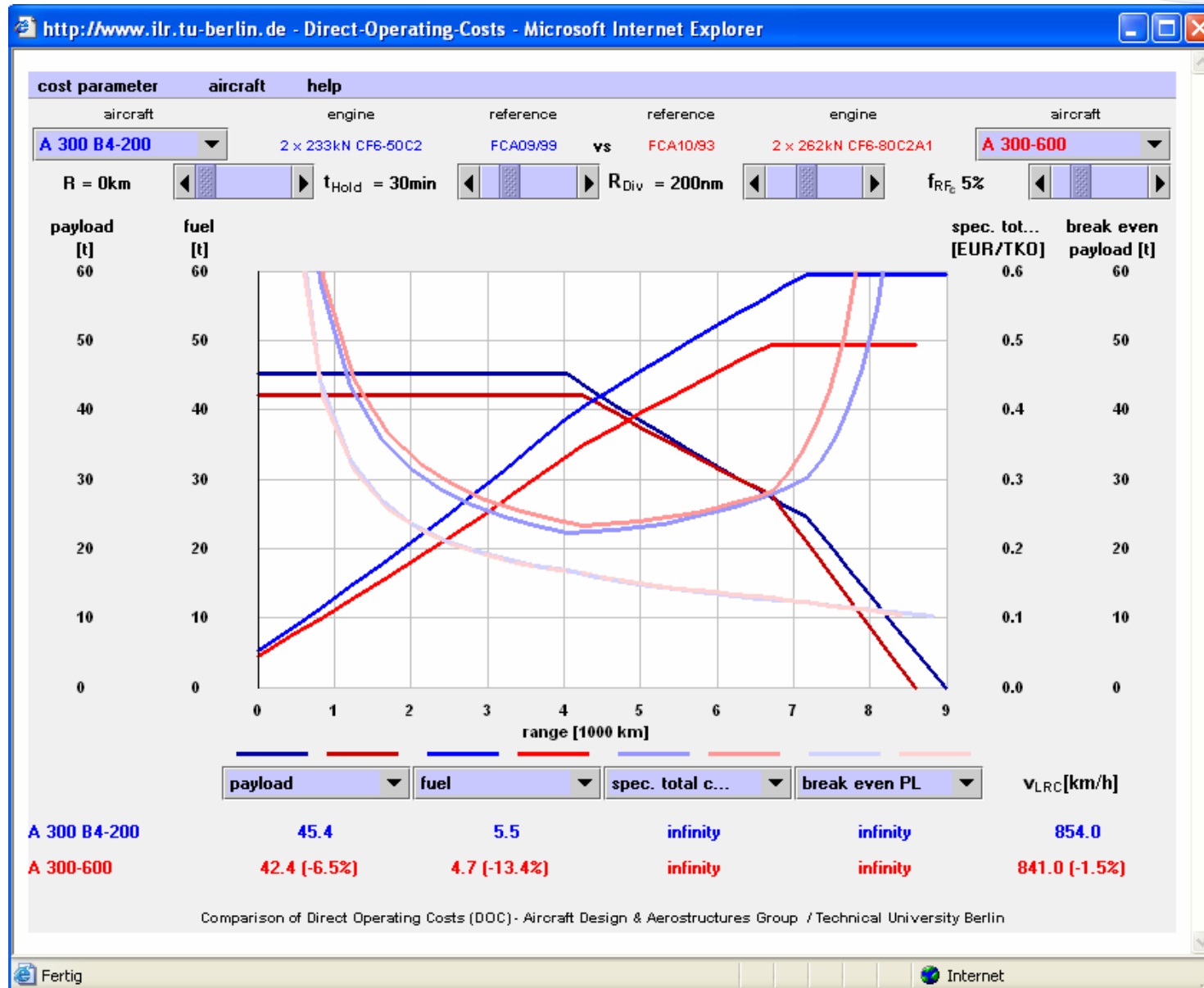
- ▶ A further calculation is necessary in order to calculate the yearly productivity which is defined as $FC \cdot PL \cdot R$
- ▶ The yearly flight cycles (see the rationale above) are decreasing with range due to the increase of flight time
- ▶ The shape of the resulting productivity curve is being deformed by becoming slightly elevated on the left hand side
- ▶ The straight lines through origin become slightly curved, depending on the design range
- ▶ In the domain of volume restriction there is no productivity difference between the long and short range aircraft



- ▶ The unit cost can now be determined by dividing the absolute yearly DOC by the yearly productivity
- ▶ Assuming constant yearly DOC over range, which can be approximately the case for a specific cost scenario (increasing fuel cost compensate with decreasing fees), the shape of unit cost directly result from the reciprocal productivity
- ▶ The minimum unit cost for the given characteristic of a long range aircraft is positioned at the design point
- ▶ For short range aircraft it could possibly be positioned at a bigger than design range (see page 28)

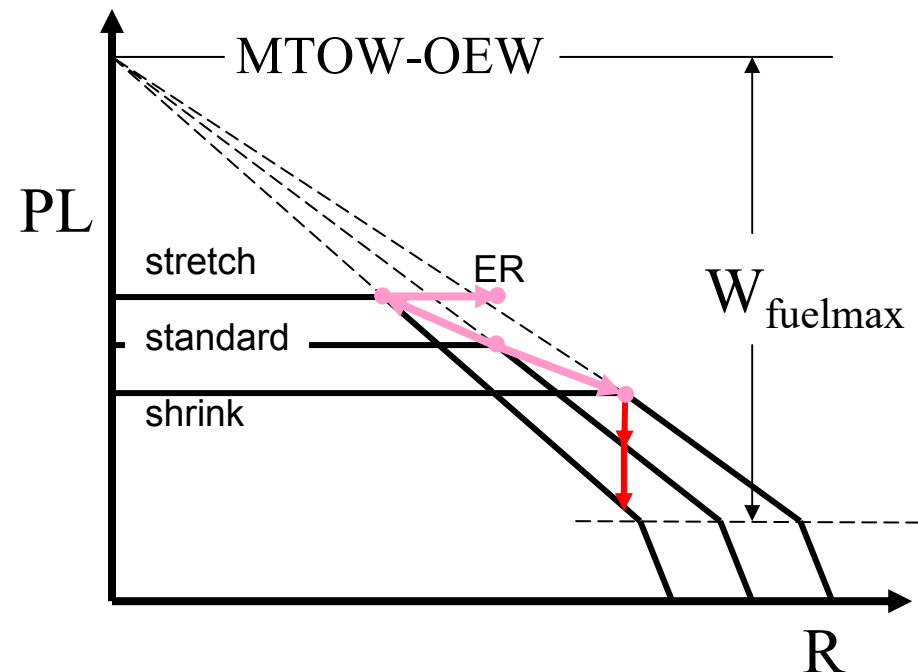


- ▶ For exercising the presented method an internet based java applet is available under <http://www.ilr.tu-berlin.de/LB/> (Luftfahrzeugbau / Applets / Betriebskosten)
- ▶ It provides the option to compare two different commercial aircraft, which can be selected out of a thorough data base or created individually by the user
- ▶ The results are presented in a diagram which can show simultaneously up to four parameters which can be selected out of several choices
- ▶ The calculation results for both aircraft are presented simultaneously
- ▶ Please note the progressive slope of the required fuel curve left of the design point and the declining slope thereafter

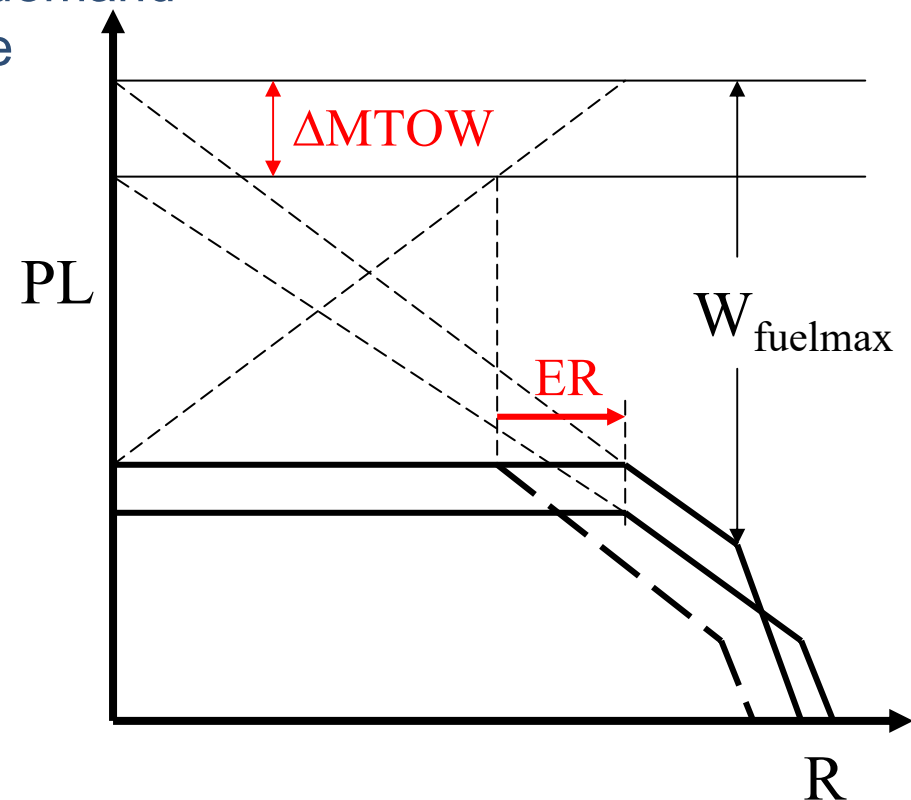


- ▶ Aircraft families are basically created by introducing constant section fuselage plugs of more or less length in front of and behind the wing, all other components remain unchanged
- ▶ Aircraft families have their commercial justification in
 - Reduction of development cost (non recurring cost, NRC)
 - Parts commonality
 - Common crew qualification (training reduction)
- ▶ However, only the high capacity family member (ultimate stretch) has the best economics, all others represent, from the flight physical standpoint, compromised designs (e.g. too large wing, too heavy, too much thrust) compared with an optimum design
- ▶ A typical family development encompasses three basic and one advanced steps
 - Standard capacity (e.g. A320)
 - Stretch version (e.g. A321)
 - Shrink version (e.g. A319)
 - Extended range stretch (e.g. A321ER)

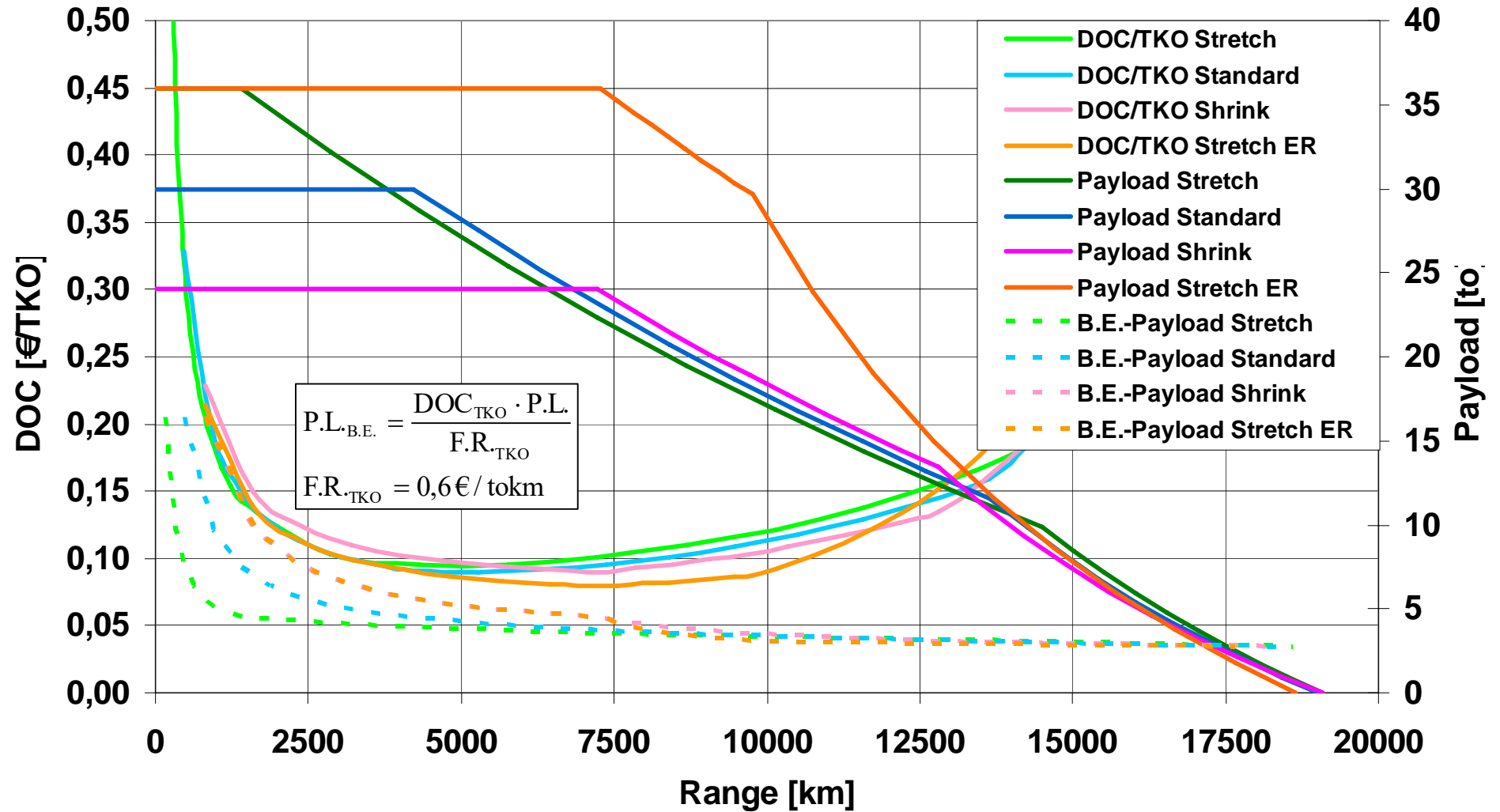
- ▶ The natural family development is characterized by varying Breguet factors due to fact that increasing capacity is leading to both larger fuselage Reynolds numbers and fineness ratios and subsequently to lower friction and pressure drag, however, also to an increase in empty weight (additional fuselage barrel and equipment)
- ▶ Therefore the family development shows up in the payload range diagram as follows:
- ▶ From standard to shrink the design range increases, the standard and even more the stretch payload cannot match the payload of the shrink at its design point
- ▶ If the market is defined by a range requirement which is matched by the shrink, all longer versions are producing at inferior economics
- ▶ The range has to be recovered by increase of the MTOW (ER)



- ▶ In order to solve the range problem of the bigger capacity aircraft it is common to increase the MTOW to an extent that the extended range (ER) design point matches the range requirement of the standard
- ▶ Note: The structural allowances for that increase have to be provided even in the smallest variant for the sake of commonality
- ▶ The higher MTOW allows for an operation of a origin-destination pair with capacities according to the demand
- ▶ Note: However, by increasing the MTOW the corresponding wing loading increases which leads to both longer take-off runs and lower initial cruise altitudes (lower available weight related thrust)
- ▶ Therefore an extension of the range by a MTOW increase can lead to unloading of the aircraft, depending on the available field length



Payload and DOC- Comparison



- ▶ In the previous diagram also the so called break-even payload (BEPL) is shown
- ▶ For a given revenue rate (RR) in terms of €/TKO the comparison of cost (DOC) and revenue leads directly to the break even payload (BEPL) because for BE the condition must be

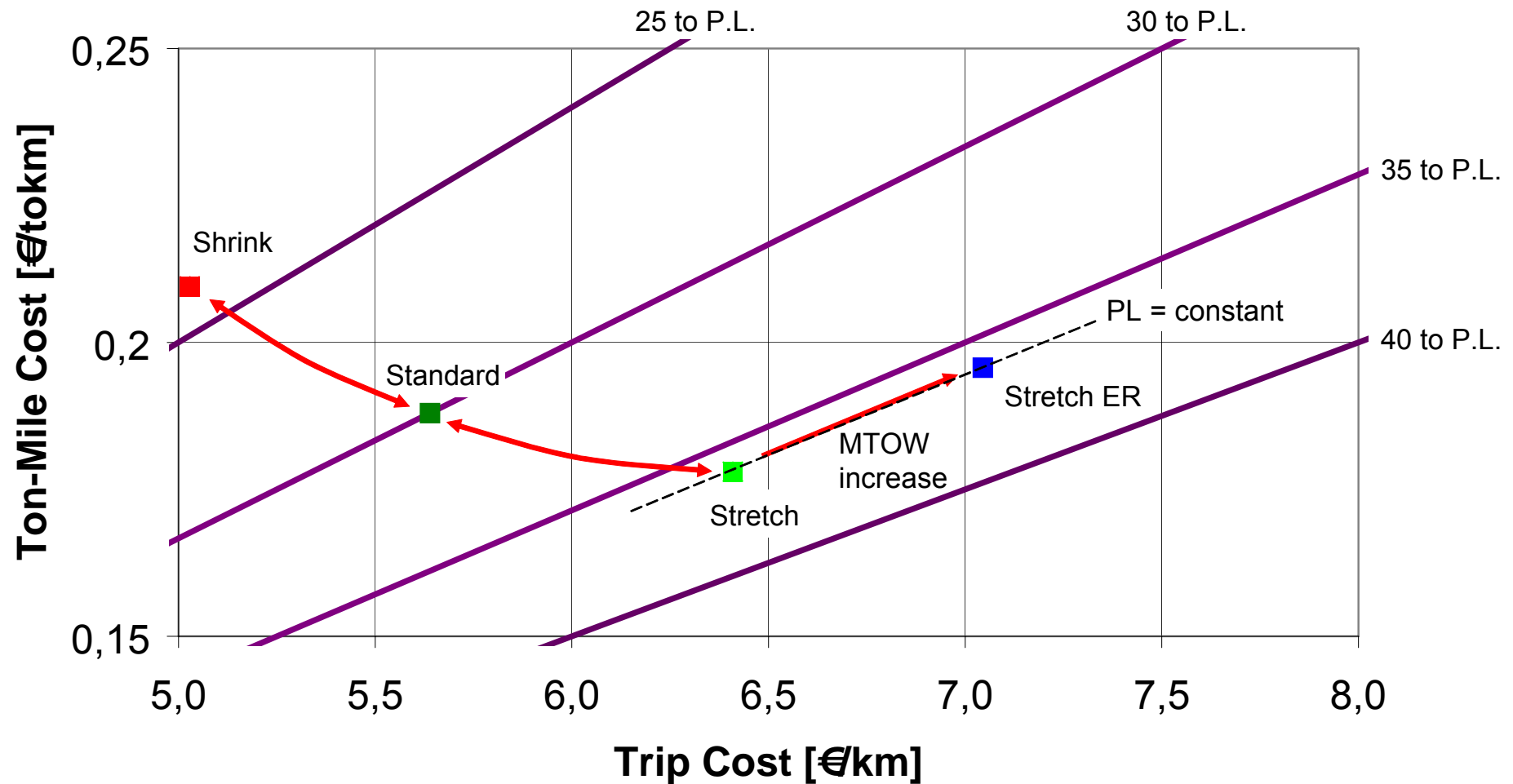
$$\text{Revenue} = \text{DOC} \quad \Rightarrow \quad \text{RR} \cdot \text{BEPL} = \text{SMC} \cdot \text{PL}$$

$$\text{BEPL} = \frac{\text{SMC} \cdot \text{PL}}{\text{RR}}$$

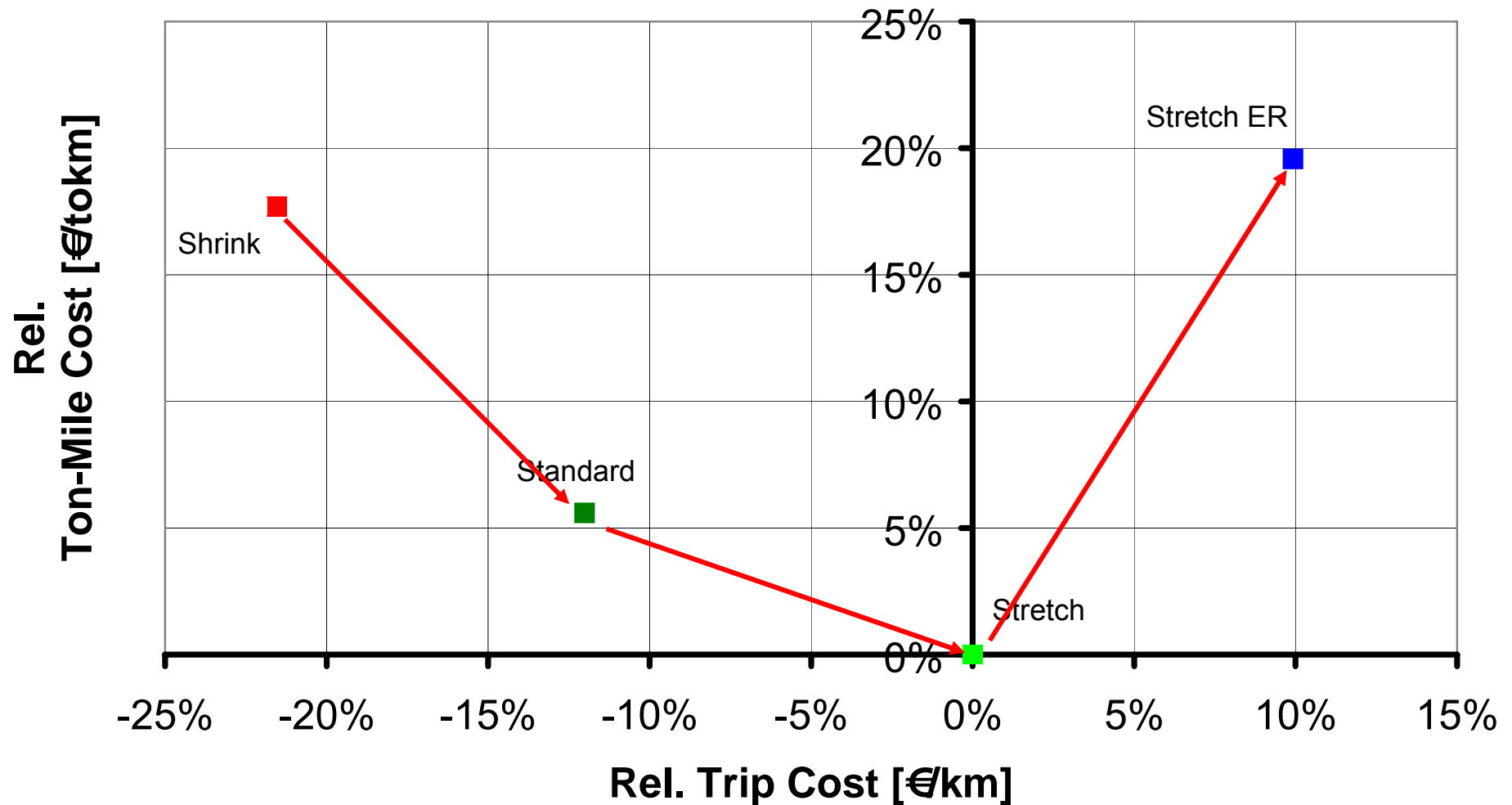
- ▶ The area between the BEPL and PL line indicates the profitable domain of operations
- ▶ Below BEPL the operation is prone to financial losses
- ▶ The best result is achieved if the aircraft is operated with maximum payload in the domain close to design range

- ▶ One of the most meaningful diagrams for the economical assessment of commercial aircraft compares the unit cost, which represent the opportunities, over the trip cost, which represent the risk of operation
- ▶ The parameter capacity (seats) is showing up as straight lines through the origin
- ▶ The three family members are located on a curved line ranging from the ultimate shrink at high unit cost and a low trip cost to the ultimate stretch at low unit cost and high trip cost
- ▶ An extended range is not for free because the ER-version is located at both higher unit and trip cost compared to the stretch on the same capacity line
- ▶ For a short range aircraft family cost diagrams are shown on the next two pages
- ▶ The first shows the two representations of the DOC values, the second shows the values relative to the stretch version

Ton-Mile Cost vs. Trip Cost (1000 km Mission)



Rel. Ton-Mile Cost vs. Rel. Trip Cost (1000 km Mission)



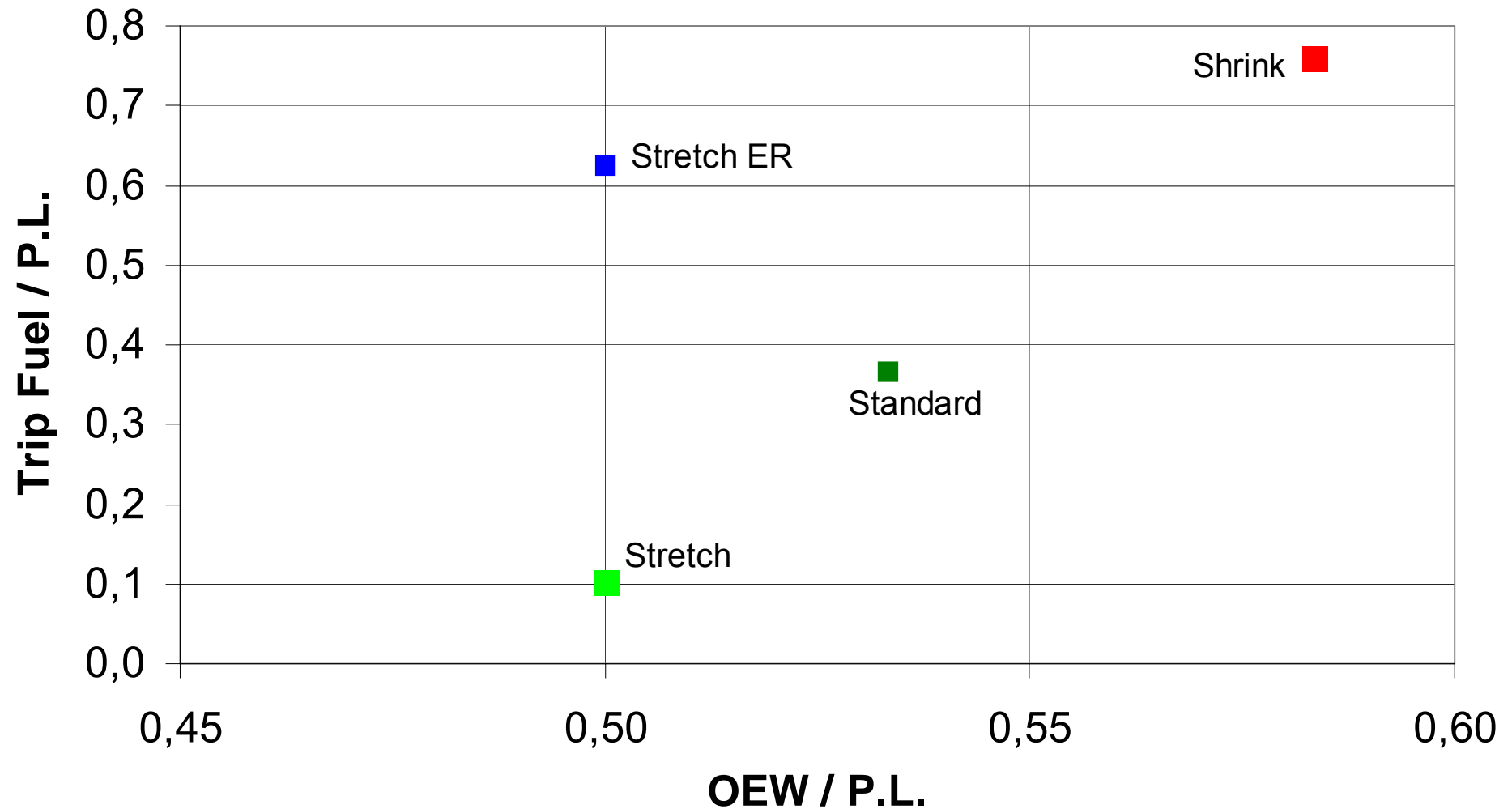


Presentation of DOC Calculation Results

*Aircraft Design &
Aero Structures*

- ▶ The presented economical results can be also explained to some extent when looking at the flight physical comparison data such as OEW per design PL and kg fuel per design PL
- ▶ It becomes clear again, that the stretch version burns less fuel and its structure is lighter compared to the shorter versions
- ▶ However, the extended range stretch version burns a lot more fuel as the low MTOW version

Technology Comparison



- ▶ Not only DOC are driving the decision of an airline to buy a fleet of a specific airplane
- ▶ Additional considerations include
 - Aircraft related aspects
 - Operation cost
 - Performance
 - Comfort
 - Marketing
 - Environment
 - Industry related aspects
 - After sales support
 - Competition (market share)
 - Product quality
 - Financial standing
- ▶ Only a few of these aspects can be quantified
- ▶ The overall assessment has to deal simultaneously with quantifiable and non-quantifiable aspects

Assessment criteria for a total value analysis

- **Economics**

- Price per Seat
- Fuel per Seat
- Weight per Seat
- Revenue Potential
- Trip Cost
- Seat Mile Cost

- **Marketing**

- Family Concept
- Product Development
- Container Capability
- Airport Compatibility

- **Performance**

- Range
- Speed
- T/O Capability
- Cruise Altitude
- Climb Performance
- ETOPS
- Cargo Capability

- **Comfort**

- Cabin Standard
- Hat-rack Volume
- Internal Noise
- Cabin Flexibility

- **Commonality**

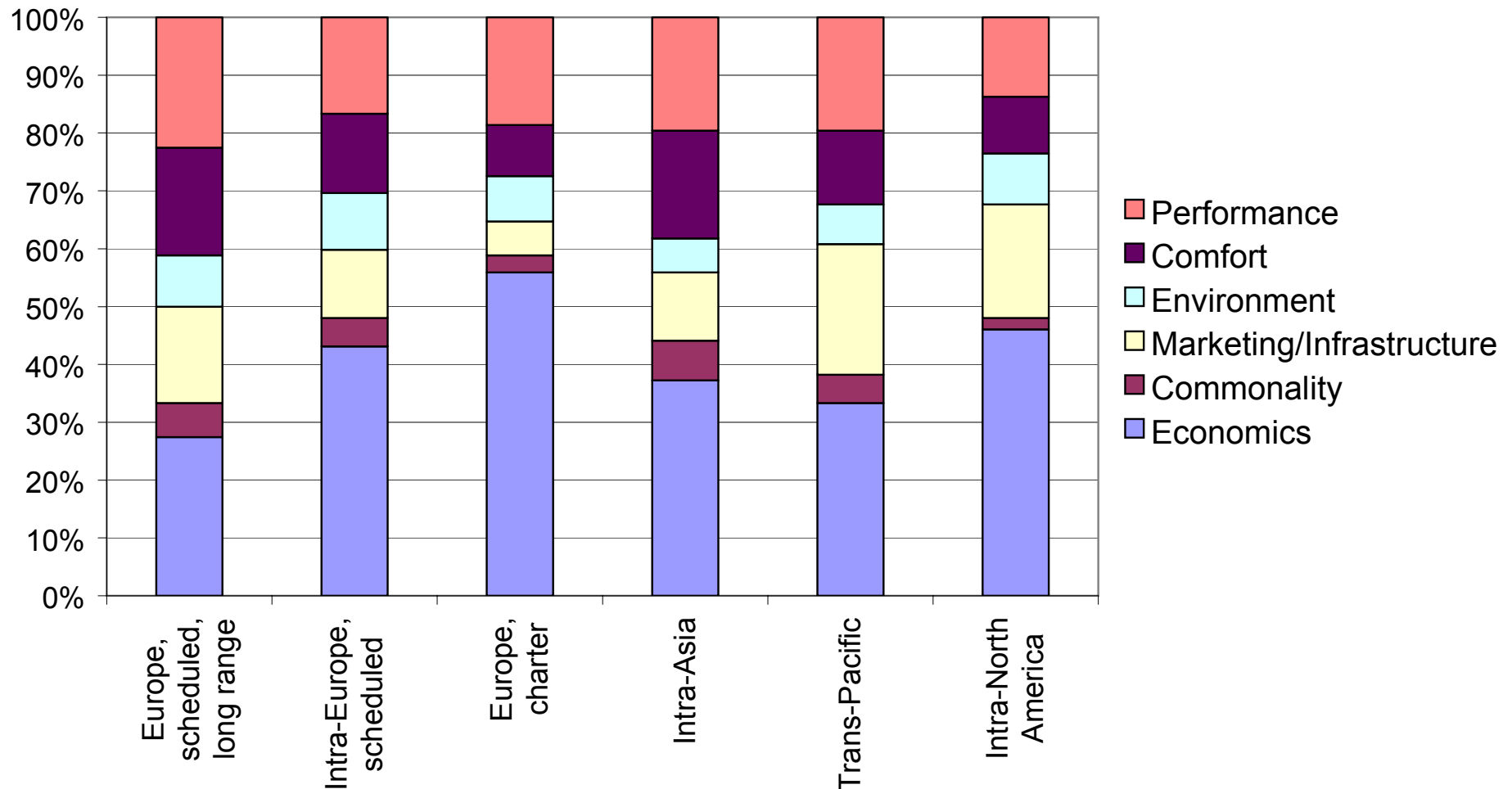
- Cockpit
- Cabin
- Spare parts

- **Environment**

- Noise
- Emission

- ▶ Different operators have different views on the same criteria

Relative value of Criteria



- ▶ Basic method: After establishing a list of criteria, the criteria are weighted by an assessment of knowable globalist's
- ▶ Thereafter the available options are assessed by each criteria on a comparison basis
- ▶ The assessment for each category of criteria is calculated by summing up the products of assessments and weights

Aircraft Total Value Analysis

Category	Criteria	Weight	Assessment			Weighed Assessment		
			A/C #1	A/C #2	A/C #3	A/C #1	A/C #2	A/C #3
1	Performance	83				13	14	13
1	Passenger Payload	10	1	2	3	10	20	30
1	Cargo Payload	3	3	2	1	9	6	3
1	Range	10	2	2	2	20	20	20
1	Runway limitations	5	3	3	3	15	15	15
1	CAT III capability	7	2	2	2	14	14	14
1	Cruise altitude	7	2	1	3	14	7	21
1	One-engine-out ceiling	5	1	1	3	5	5	15
1	Speed	7	3	3	1	21	21	7
1	OEI	5	2	3	1	10	15	5
1	MTOW	7	2	3	1	14	21	7
1	Fuel consumption	10	1	1	1	10	10	10
1	Turn-around capability	7	2	2	2	14	14	14
2	Cabin capability	25				8	8	11
2	Cabin flexibility	7	1	1	3	7	7	21
2	Cargo door location	5	2	2	2	10	10	10
2	Baggage storage	5	1	2	3	5	10	15
2	Galley flexibility	5	3	2	1	15	10	5
2	In-flight entertainment	3	1	1	1	3	3	3
3	Environment	19				13	11	12
3	Noise	7	1	1	1	7	7	7
3	Emission	7	3	3	2	21	21	14
3	Cabin noise	5	2	1	3	10	5	15
4	Industrial aspects	40				9	10	8
4	Engine choices	5	1	1	1	5	5	5
4	Product support	5	3	3	3	15	15	15
4	Family concept	7	2	3	1	14	21	7
4	Manufacturers image	3	3	1	2	9	3	6
4	Technology level & risk	5	2	3	3	10	15	15
4	Market share	3	2	2	2	6	6	6
4	Resale value guaranty	5	1	1	1	5	5	5
4	Jet/Turbo-Prop	7	1	1	1	7	7	7
5	Cost	15				7	13	14
5	Maintenance program	3	3	3	2	9	9	6
5	Seat mile cost	7	1	3	3	7	21	21
5	Trip cost	5	1	2	3	5	10	15
6	Commonality	6				6	6	6
6	Spares commonality	3	1	2	3	3	6	9
6	Cross crew qualification	3	3	2	1	9	6	3
7	Financial aspects	16				11	9	6
7	Financing	3	3	3	3	9	9	9
7	Price escalation	3	2	2	1	6	6	3
7	A/C price	7	3	2	1	21	14	7
7	Introductory cost	3	2	2	2	6	6	6
	Total Weight	204						

Note: Weight figures range from 0 (not important at all) <---> 10 (utmost important)

- ▶ If the categories have been determined properly (e.g. on a equal weight basis) their assessments can be summed up to an overall assessment
- ▶ The total value analysis is not at all precise, however, it is supporting a purchase decision because it is helpful in
 - improving the understanding of the problem
 - structuring that complex problem
 - considering all the different particular interests of parties involved
 - providing transparency and thus a common understanding for the decision

Aircraft Total Value Analysis Result

			Assessment		
Category	Criteria	Weight	A/C #1	A/C #2	A/C #3
1	Performance	14,3%	13	14	13
2	Cabin capability	14,3%	8	8	11
3	Environment	14,3%	13	11	12
4	Industrial aspects	14,3%	9	10	8
5	Cost	14,3%	7	13	14
6	Commonality	14,3%	6	6	6
7	Financial aspects	14,3%	11	9	6
Ranking	Total	100,0%	66	71	71

Hannes Ross

Chapter 13

Military Aircraft Development

Foreword

The objective of this lecture is to give the reader, who is primarily involved in and familiar with commercial aircraft design and development, a brief overview of the different aspects, which have to be considered in the design of military aircraft vehicles (other than transport aircraft), particularly in Europe. The content is limited to the areas which are different from the commercial world. Weapons and avionic systems are not addressed in detail.

Contents

	Page
List of Figures	M 0-4
List of Abbreviations	M 0-8
1 Development Scenario and Environment	M 1-1
2 Requirements	M 2-1
3 Design Process and Tools	M 3-1
4 Technologies	M 4-1
4.1 Composites	M 4-1
4.2 Ejection Systems and Pilot "g" Protection	M 4-5
4.3 Unstable Configurations and Digital Flight Controls	M 4-9
4.4 Thrust Vectoring	M 4-12
4.4.1 X-31 Enhanced Fighter Manoeuvrability (EFM) Program	M 4-12
4.4.2 The VECTOR Program	M 4-26
4.5 Aircraft Signature	M 4-30
5 Unmanned Systems	M 5-1
6 Future Aspects	M 6-1

List of Figures

- Fig.1-1 Weapon System Life Cycle
- Fig.1-2 Development Phases
- Fig.1-3 Life Cycle Cost Breakdown and Phase Duration
- Fig.1-4 Objectives during development phases
- Fig.1-5 Improved design freedom by earlier knowledge

- Fig.2-1 Differences between commercial and military requirements
- Fig.2-2 Thrust/Weight and Wingloading
- Fig.2-3 Wing Loading and Aspect Ratio
- Fig.2-4 Ideal Design Process
- Fig.2-5 Typical missions for military aircraft
- Fig.2-6 Mission Profile
- Fig.2-7 Mission Segments
- Fig.2-8 Manoeuvre Requirements
- Fig.2-9 Manoeuvre Performance Plott
- Fig.2-10 Design Requirements (1)
- Fig.2-11 Design Requirements (2)

- Fig.3-1 Design Parameter
- Fig.3-2 Baseline Configuration
- Fig.3-3 Specialists dream of their aircraft design
- Fig.3-4 Aircraft design, a multidisciplinary activity = systems integration
- Fig.3-5 Computer Aided Design Program (CADE)
- Fig.3-6 Growth Factor Definition
- Fig.3-7 Design Window
- Fig.3-8 Sensitivity Matrix
- Fig.3-9 Growth Factors
- Fig.3-10 One Solution for one Requirement?
- Fig.3-11 A10 vs. A-11 Competition
- Fig.3-12 YF-16 vs. YF 17: Light Weight Fighter Competition
- Fig.3-13 F-18 Leading Edge Vortex Generation
- Fig.3-14 The latest US Competition: X-32(Boeing) vs. X-35 Lockheed Martin
- Fig.3-15 European Competition
- Fig.3-16 Full scale mock-up of MBB design, 1978 ILA Hannover
- Fig.3-17 Design Status Eurofighter, Mid 80ies
- Fig.3-18 Design windows for different missions
- Fig.3-19 Development Plan, Eurofighter 1986
- Fig.3-20 Concurrent Development and Production of the F-22
- Fig.3-21 Digital Line Definition for the Airbus A300

- Fig.3-22 Digital line definition by modern computer programs
- Fig.3-23 Surface definition utilization
- Fig.3-24 Utilization of surface data for aerodynamic and flight control
- Fig.3-25 Cross-section determination for drag calculation
- Fig.3-25 Inboard Profil
- Fig.3-26 Equipment installation in secondary power bay

- Fig.4.1-1 F-15 Fuselage Design
- Fig.4.1-2 Eurofighter Centre Fuselage Design
- Fig.4.1-3 Eurofighter Centre Fuselage Carbon Fibre Skin
- Fig.4.1-4 CFC structure lay-up
- Fig.4.1-5 CFC Utilization at Tornado and Eurofighter
- Fig.4.1-6 Evolution of CFC utilization in fighter aircraft
- Fig.4.1-7 Material Breakdown, commercial and military aircraft
- Fig.4.1-8 Lear Fan 2100, the first commercial all composite aircraft, 1981

- Fig.4.2-1 Ejection clearance
- Fig.4.2-2 Pilot Seating in an F-16 and an Ultra Light sailplane
- Fig.4.2-3 Ejection through the canopy
- Fig.4.2-4 Ejection Tests
- Fig.4.2-5 Pilot Ejection, Su-27
- Fig.4.2-6 Ejection Reality, MiG-29
- Fig.4.2-7 Pilot “g” tolerance

- Fig.4.3-1 Stable Configuration Arrangement
- Fig.4.3-2 Stable and unstable configuration
- Fig.4.3-3 Improved drag polar by reduced stability
- Fig.4.3-4 Modified F-104

- Fig.4.4-1 Otto Lilienthal in his Hang Glider, ~1894
- Fig.4.4-2 Out of Control Military Accidents, US Airforce and Navy
- Fig.4.4-3 Crash of Birgen Air, 6th Febr. 1996
- Fig.4.4-4 Two dimensional calculation of flow separation
- Fig.4.4-5 Evolution of Thrust/Weight Ratio
- Fig.4.4-6 Post-Stall Landing Gear, Grashopper, 1973
- Fig.4.4-7 Post Stall Regime
- Fig.4.4-8 Flow visualisation in a water tunnel
- Fig.4.4-9 Results of Close in Combat Simulations, IABG, Ottobrunn 1979
- Fig.4.4-10 Government / Industry Organization & X-31 Program Objectives
- Fig.4.4-11 Configuration Selection Process
- Fig.4.4-12 Size Comparison of X-31 and Eurofighter

- Fig.4.4-13 Primary MBB Workshare
- Fig.4.4-14 Thrust Vectoring Tests behind a F-18
- Fig.4.4-15 Side force generation with the vane system
- Fig.4.4-16 Vane with delaminations after first curing cycle
- Fig.4.4-17 General arrangement of TV vanes at X-31 and F-18 HARV
- Fig.4.4-18 Trailing edge pitch power vs. angle of attack
- Fig.4.4-19 Canard pitch power vs. angle of attack
- Fig.4.4-20 Rudder power vs. angle of attack
- Fig.4.4-21 Total Control Power, Aero and Thrust Vectoring
- Fig.4.4-22 X-31 conventional and PST flight envelope
- Fig.4.4-23 Post-Stall Test Milestones
- Fig.4.4-24 Trim surface bolted on to aft fuselage
- Fig.4.4-25 Addition of nose strakes
- Fig.4.4-26 Close in Combat effectiveness: Simulation vs. Flight Test
- Fig.4.4-27 Post-Stall Manoeuvre
- Fig.4.4-28 Vector Program Elements
- Fig.4.4-29 Extremely Short Take-off and Landing (ESTOL)
- Fig.4.4-30 ESTOL automated landing procedure
- Fig.4.4-31 Landing attitude at 24° approach, just before derotation
- Fig.4.4-32 Thrust Vectoring is a reality and used on operational aircraft of the
- Fig.4.4-33 Thrust vectoring is difficult to implement on commercial aircraft US and Russia

- Fig.4.5-1 Intentionally High Signature Aircraft: the “Red Baron”
- Fig.4.5-2 Optical Signature Reduction by Camouflage Paint
- Fig.4.5-3 Sun Reflection on Canopy and Structure
- Fig.4.5-4 Radar Cross-Section Definition
- Fig.4.5-5 Relative magnitude of Radar reflection for different body shapes
- Fig.4.5-6 Comparison radar reflection of sphere and cube
- Fig.4.5-7 Major contributors to radar cross section
- Fig.4.5-7 Desired radar beam reflection
- Fig.4.5-9 Measures to reduce radar reflections
- Fig.4.5-10 First “Stealth” aircraft, code name “Have Blue”, Lockheed Skunk Works
- Fig.4.5-11 First operational low signature aircraft: F-117, Lockheed
- Fig.4.5-12 F-22 air superiority fighter to replace F-117!?
- Fig.4.5-13 B-2 Bomber, Northrop-Grumman
- Fig.4.5-14 The MBB developed Lampyridae (Glühwürmchen)
- Fig.4.5-15 Metal mockup for RCS testing
- Fig.4.5-16 “Flight Test” of Lampyridae in the DNW Wind Tunnel
- Fig.4.5-17 Horten Ho IX/Gotha Go 229, First Flight January 1945
- Fig.4.5-18 British Aerospace RCS Model, code name “Replica”, 1994-1999
- Fig.4.5-19 Stealth aircraft development

- Fig.4.5-20 US developed and flight tested stealth aircraft
- Fig.4.5-21 EADS RCS test facilities
- Fig.4.5-22 Tornado RCS Tests, Manching
- Fig.4.5-23 Infrared Signature is very difficult to reduce
- Fig.4.5-24 Flare dispensing
- Fig.4.5-25 Stealth Technology Gap between the US and Europe

- Fig.5-1 Unmanned Aerial Vehicles (UAV) are more than 50 years old
- Fig.5-2 Why do we want UAV's?
- Fig.5-3 Involvement of Crew members in accidents
- Fig.5-4 UAV System Elements
- Fig.5-5 UAV utilization in "d,d,d" missions
- Fig.5-6 UAV missions and vehicle types
- Fig.5-7 Technical Challenges for Reconnaissance UAV's
- Fig.5-8 Cost considerations
- Fig.5-9 UAV Categories, Characteristics
- Fig.5-10 UAV Categories, Altitude and Range
- Fig.5-11 Quantity of UAV types developed and procured per country (only >5 considered)
- Fig.5-12 Number of vehicles per category (source Euro UAV)
- Fig.5-13 Conflicting Autonomy Requirements
- Fig.5-14 Range of UAV's in use or planned for the German forces.
- Fig.5-15 GMOD Plan for Euro-Hawk
- Fig.5-17 Global Hawk acquisition cost changes
- Fig.5-18 Global Hawk cost escalation
- Fig.5-19 Simulated Unmanned Vehicle ATTAS in controlled German air space
- Fig.5-20 Current Certification classes for UAV's in Germany
- Fig.5-21 Open Questions from NASA "ACCESS" Study
- Fig.5-22 Expected UAV development sequence
- Fig.5-23 Example of European cooperation

- Fig.6-1 How do we maintain the knowledge base of the development and production team?
- Fig.6-2 Aerospace industries turnover and employment
- Fig.6-3 National company consolidation
- Fig.6-4 Scenario change since 1940: From all out war to singular strikes
- Fig.6-5 World fighter inventory
- Fig.6-6 Distribution of fighter inventory
- Fig.6-7 German Fighter Inventory Planning, status 2003
- Fig.6-8 European fighter inventory
- Fig.6-9 European options for a new Future Airborne Weapon System (FAWS)
- Fig.6-10 Fighter aircraft production quantities

- Fig.6-11 The Lockheed Martin Joint Strike Fighter, the “Blue Threat”
- Fig.6-12 Home Market Relations, Annual Volume
- Fig.6-13 R&D Expenditure, 1995 – 1999
- Fig.6-14 High Priority Technologies for Europe
- Fig.6-15 Potential new systems in Europe
- Fig.6-16 Europe must grow together!

List of Abbreviations

A/A	Air-to-Air
A/C	Aircraft
A/D	Analogue/Digital
A/G	Air-to-Ground
AADS	Advanced Air Data System
AAIH	Aircent Air Interoperability Handbook
AB	After Burner
ABCCC	Airborne battlefield command and control centre (USA)
ACA	Associate Contractors Agreement
ACCS	Air Command and Control System
ACO	Airspace control order
ACS	Armament Control System
ACTE	Active control technology equipment
AD	Air Defence
ADA	Airborne Data Acquisition
ADT	Avionic Demonstrator
ADV	Air Defence Variant
AECMA	Aircraft European Contractors Manufacturers Association
AFB	Air Force Base
AGE	Aerospace Ground Equipment
AGS	Aircraft Ground Surveillance
AIT	Air Italia (Italian Eurofighter Partner Company)
AMAD	Aircraft Mounted Accessories Drive
AMP	Amplitude (nav)
AMRAAM	Advanced Medium Range Air to Air Missile
AOA	Angle Of Attack
AOC	Automatic Overload Control
APACHE	US –Hubschrauber
APU	Auxiliary Power Unit
ARMIGER	Zukünftige Bordwaffe des Eurofighter
ARS	Advanced radar sensing
AS	Air Superiority
ASRAAM	Advanced Short Range Air to Air Missile
ASSTA	Avionik System Software Tornado in ADA
ATC	Air Traffic Control
ATO	Assisted Take-Off
ATR	Automatic Target Recognition

ATTAS	Advanced technologies testing aircraft system
AV-Week	Aviation Week
AVE	Air Vehicle Engineering
AWACS	Airborne Warning and Control System
BAe	British Aerospace
BDA	Bomb Damage Assessment
BME	Basic Mass Empty
BMVg	Bundesministerium der Verteidigung
Bö	Bölkow
BSD	Bulk Storage Device
BUS	Digital electrical connection
BWB	Bundesamt für Wehrtechnik und Beschaffung
C ³	Command, Control, Communications
C2	Command and Control
CA	Counter Air
CAIS	Computer-aided instruction system
CAP	Combat Air Patrol
CAS	Close Air Support
CBR	California Bearing Ratio
CCV	Control Configured Vehicle
CFK	Kohlenstofffaserverstärkter Kunststoff
CG	Center of Gravity
CIC	Close In Combat
CMS	Configuration Management System
COMINT	Communications Intelligence
CONOPS	Concept of Operations
CR	Close Range
CRC	Control and Reporting Centre
CRE	Create
CS	Control System
CSAS	Command Stability Augmentation System
CTOL	Conventional Take Off and Landing
DARO	Reconnaissance Organisation of DARPA
DARPA	Defense Advanced Research Projects Agency
Dasa	Today EADS
DASS	Defensive Aids Sub System
DCM	Pitching moment coefficient
DFM	Direct Force Modes
DFS	Deutsche Flugsicherung
DLR	Deutsches Forschungszentrum für Luft- und Raumfahrt

DoD	Department of Defense
DTD	Design Techniques Department
DUL	Design Ultimate Load
EADS	European Aeronautic Defence and Space Company
EADS-M	European Aeronautic Defence and Space Company - Military
EASAMS	US Electronic Company
EBM	Electronic bearing marker
ECM	Electronic Counter Measures
ECR	Electronic Combat/Reconnaissance
ECS	Environmental Control System
EF	Eurofighter
EFA	European Fighter Aircraft
EFM	Enhanced Fighter Maneuverability
EG	Emergency Generator
ELINT	Electronic Intelligence
EMC	Electromagnetic Compatibility
EMV	Elektromagnetische Verträglichkeit (=EMC)
EnMC	Enhanced Main Computer
EO	Electro-Optical
EOB	Electronic Order of Battle
EPC	Eurofighter Partner Companies
EPU	Emergency Power Unit
ERWE	Enhanced Radar Warning Equipment
ESG	German Electronic Company, Munich
ESM	Electronic Support Measures
ESTOL	Extremely Short Take-Off and Landing
ETAP	European Technology Acquisition Program
EW	Electronic Warfare
F/F	Front Fuselage
FA	Fix Attack
FADS	Flush Air Data System
FAR	Federal Aviation
FAWS	Future Airborne Weapon System
FCC	Flight Control Computer
FCS	Flight Control System
FEBA	Forward Edge of Battle Area
FF	Freefall; Full Fire
FH	Flight Hours
FLIR	Forward Looking Infrared
FMOD	Federal Ministry of Defense

FOAS	Future Offensive Air System
FOC	Final Operational Clearance
FRG	Federal Republic of Germany
FTH	Flight Test Hours
FUS	Flugzeug Union Süd
FY	Financial/Fiscal Year
G/A	Ground to Air
GAF RECCE	German Air Force Reconnaissance
GASP	Gemeinsame Sicherheits und Aussenpolitik
GD	Ground defence
GE	General Electric
GFK	Glasfaserverstärkter Kunststoff
GH	Global Hawk
GPS	Global Positioning System
HAA	High Angle of Attack
HALE	High Altitude, Long Endurance
HARM	High Speed Anti Radiation Missile
HARV	High-AOA Research Vehicle
He	Heinkel
HF	High Frequency
HFB	Hamburger Flugzeugbau
HH	
HMD	Helmet Mounted Display
HP	Hewlett Packard
IABG	Industrieanlagen Betriebsgesellschaft
IBS	Integrated bridge system (ship)
IDG	Integrated Drive Generator
IDS	Interdiction Strike
IFF	Identification Friend or Foe
ILS	Integrated Logistic Support; Instrument Landing System
IMINT	Image Intelligence
IMLFP	Improvement Life Program
IO	Input/Output
IOC	Initial Operational Clearance
IR	Infra Red
IRIS-T/HMS	German IR Missile with Thrust vectoring
IRLS	Infrared Line Scanner
IRST	Infrared Search and Track
ITO	Internationale Test-Organisation
IVN	Initial voice network

JAST	Joint Advanced Strike Technology
JFS	Jet Fuel Starter, or Joint Strike Fighter
JSF	Joint Strike Fighter
JSTARS	Joint surveillance and target attack radar system
JTIDS	Joint Tactical Information Distribution System
KEPD	Kinetic Energy Penetration Destroyer
KWE	Kampfwertterhaltung
KWS	Kampfwertsteigerung
KZO	Kleinfluggerät zur Zielortung
L/D	Lift over drag
LAA	Low Angle of Attack
LADP	Low Altitude Deep Penetration
LALE	Low Altitude Long Endurance
Ldg	Landing
LDP/GBU 33	Laser Designator Pod, GBU is a weapon
Lfz	Luftfahrzeug
LINS/GPS	Laser Inertial Navigation System/Global Positioning System
LL/HS	Low Level/High Speed
LO	Landing order
LOC1	Location 1
LOI	Letter of intent
LTV	Ling Temco Vought , US company
LVT	Low Volume Terminal
MAFT	Major Airframe Fatigue Test
MALE	Medium Altitude, Long Endurance
MAST	Major Airframe Static Test
MBB	Messerschmitt Bölkow-Blohm
MC	Main Committee; Main Contractor
Me	Messerschmitt
MEADS	Medium Extended Air Defense System
MFD	Multi Function Display
MIDS	Multifunction Information Distribution System
MIL STD	US Military Standard
MLG	Main Landing Gear
MLI	Mid Life Improvement
MMI	Man Machine Interface
mmW	Millimeterwellen-Radar
MOA	Memorandum of Agreement
MPA	Man-Powered Aircraft; Maritime Patrol Aircraft
MR	Medium Range

MRA	Multi Role Aircraft
MRCA	Multi Role Combat Aircraft
MRE	Medium Range Endurance
MTI	Moving Target Indicator
MTOW	Maximum Take-Off Weight
NAMMA	Tornado Industrial Management Organization
NAMMO	Tornado Government Management Organization
NARMCO	Werkstoffbezeichnung, CFC
NATO	North Atlantic Treaty Organization
NC	Numerical Controlled Machine
NDV	Nutzungsdauerverlängerung
NETMA	NATO Eurofighter and Tornado Management Agency
NKF	Neues Kampfflugzeug
NLG	Nose Landing Gear
NTR	Normalised Time/Range
OA	Order Administration
OCAMS	On-Board Checkout and Monitoring System
OCCAR	Organisation Conjointe de Coopération en matière d'Armement
OFP	Operational Flight Program
OSZE	Organisation für Sicherheit und Zusammenarbeit in Europa
PDS	Portable Data Store
PFP	Partnership for Peace
PG	Policy Group
PI	Point Intercept
PNU	Precision Navigation Upgrade
POC	Point of Contact
PSD	Post Stall Display
PST	Post Stall Technology
R&D	Research and Development
RABE	Radar automatic track extractor
RAM	Radar Absorbing Material
RAT	Ram Air Turbine
RCFAM	Role Coupled Fuselage Aiming
RCS	Radar Cross Section
RECCE	Reconnaissance
RF	Radio Frequency
RFQ	Request For Quotation
RIU	Receiver Interface Unit
RJ	Right Main Beam Jamming
RQS	Rescue Squadron

RSTA	Reconnaissance, Surveillance and Target Acquisition
RVDT	Rotary variable displacement transducer
RWE	Radar Warning Equipment
S/G	= T/W= Thrust Weight Ratio
S/M/LR	Short/Middle/Long Range
SA	Situation Awareness
SAM	Surface-to-Air Missile
SAR	Semi Aperture Radar
SAS	Stability Augmentation System
SATCOM	Satellite Communication
SC	Sub Committee; Sub Contractor
SDD	System Development and Demonstration
SDR	System Design Responsibility
SEAD	Suppression of Enemy Air Defence
SEP	Specific Access Power
SFH	Simulated Flight Hours
SIA	Societa Italiana Avionica
SIGINT	Signal Intelligence
SOC	Struck off Charge
SOM	Stand-Off Missile
SPS	Secondary Power System
SR	Short Range
SRM	Short Range Missile
SS	Sight Setting; Single Shot
STANAG	Standardization Agreement (NATO)
STOL	Short Take Off and Landing
STOVL	Short Take-off Vertical Landing
SVS	Schubvektorsteuerung
SW	Software
T/O	Take Off
T/W	Thrust /Weight
TACAN	Tactical Air Navigation
TBD	To Be Determined/Defined
TBM	Tactical Ballistic Missile
TDP	Technology Demonstration Program
TDV	Technology Demonstration Vehicle
TE	Training equipment
TF	Terrain Following
TG	Task group
TOGW	Take Off Gross Weight

TOR	Tornado
TOS	Time on Station
TS	Twin Seat; Test Squadron
TV/TAB	Television Tabular Display
UAV	Unmanned Air Vehicle
UCAV	Unmanned Combat Air Vehicle
UCS	Utilities Control System
UE	Unplanned ERWE
UFA	Unmanned Fighter Aircraft
UH	Unplanned HARM
UHF	Ultra High Frequencies
URAV	Unmanned Reconnaissance Air Vehicle
USAF	United States Air Force
USMC	United States Marine Corps
USN	United States Navy
V/STOL	Vertical Short Take Off and Landing
VFW	Vereinigte Flugtechnische Werke
VG	Variable Geometry
VHF	Very High Frequencies
VIS-CCD	Vehicle intercommunication system
VJ	Vertikal startender Jäger
VTOL	Vertical Take Off and Landing
W/S	Wing Loading: Weight/Wing Area s
WEU	Western European Union
WFG	Wave Form Generator
WS	Weapon System
WSO	Weapon System Officer
WTD	Wehrtechnische Dienststelle

1 Development Scenario and Environment

The German situation is particular peculiar: The development of VSTOL aircraft (VJ 101, VAK 191, Do 31) during the fifties and sixties were the last national development programs. All military programs conducted after 1970 were international (Transall, Tornado, Alfa-Jet, Eurofighter). An exception are smaller vehicles like unmanned reconnaissance UAV's. The development process is further determined by the following characteristics:

- No national development programs → Cooperation
- Only one (national) customer
- Development cost is (primarily) Government financed
- Difficult/time consuming agreements between partner nations
- National participants: Military Customer, Government, Industry
- Cooperative industrial development means: no prime contractor
- Cost share = Work share, determined by number of a/c ordered
- No money across the border
- National interests (political, military, economical) result in slow decision/agreement processes and/or delays.

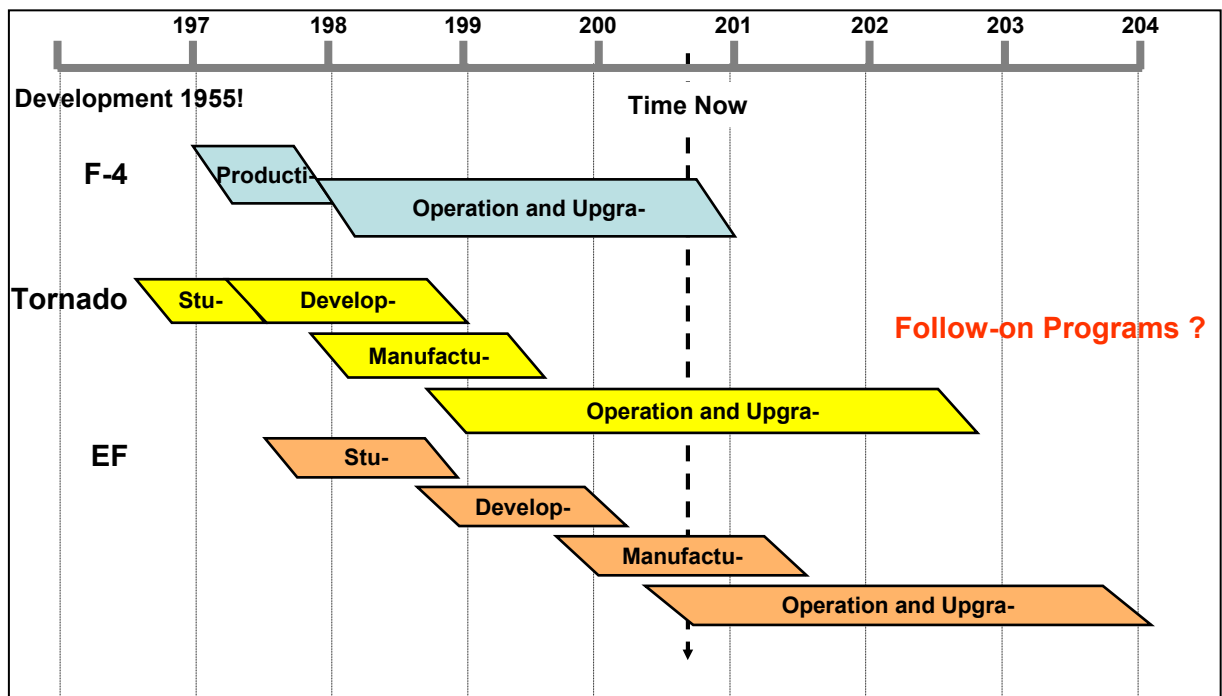


Fig. 1-1 Weapon System Life Cycle

The development cycle (and the associated cost and manpower required) during World War II were extremely short. This has completely changed during the last 50 years. Predevelopment, development and production of a new weapon system take now a time period of 20 to 30 years as shown for F-4, Tornado und Eurofighter as shown in **Fig. 1-1** and **Fig. 1-2**. A life cycle

(from initial studies to phase out) for a modern weapon system now covers a time period of 50 to 60 years.

In spite of all modern technologies in design, manufacturing, testing the development cycles have not decreased but increased. However, one has to admit, that the capabilities and complexity of modern military aircraft systems is considerably higher than those developed 50 years ago, so are flight safety and lifetime.

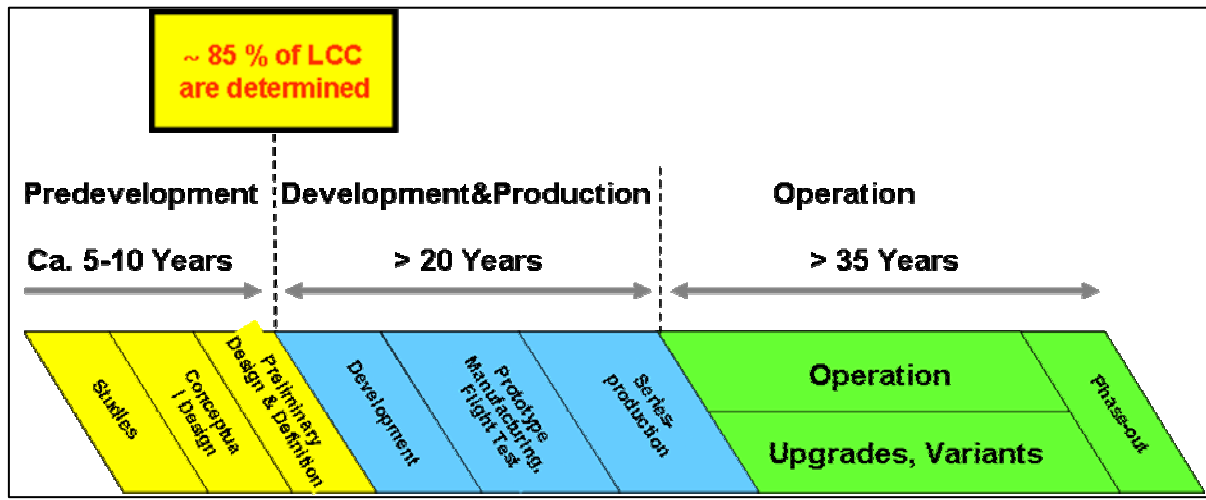


Fig. 1-2 Development Phases

Fig. 1-3 shows the relative cost and duration of weapon system development phases for an aircraft developed in the late sixties in the USA and one started about 15 years later in Europe. In particular the elapsed time for the initial phases has grown considerably, a result of the difficult harmonization effort required between the various nations (Government, air force, industry) to define the development objectives, the work- and cost share. It is important to realize, that the concept and definition phases determine the primary characteristic of the weapon system which is to operate throughout 30 to 40 years. That means not only the acquisition cost but, even more important, the operational cost.

Phase	1970		2000
	Cost [%]	Duration Years	Duration Years
Concept	0,04	0,5 + 0,5 = 1	5
Definition	0,2	0,5 + 0,5 = 1	5
Development	6,8	3 (F-15)	10 (EF)
Production (500 A/C)	31,0	5	12 (EF 620)
Operation	62,0	15	40
Life Cycle	100		

Fig. 1-3 Life Cycle Cost Breakdown and Phase Duration

Phase	Objective
Concept	Find optimum configuration (Sub- / Supersonic A/C, variable geometry, basic requirements, ...)
Contract Definition	Optimize and specify total system (System specific offer for contract signature)
Development	Control technical development, meet cost and schedule constraints
Production	Prepare series production, meet cost and schedule constraints

Fig. 1-4 Objectives during development phases

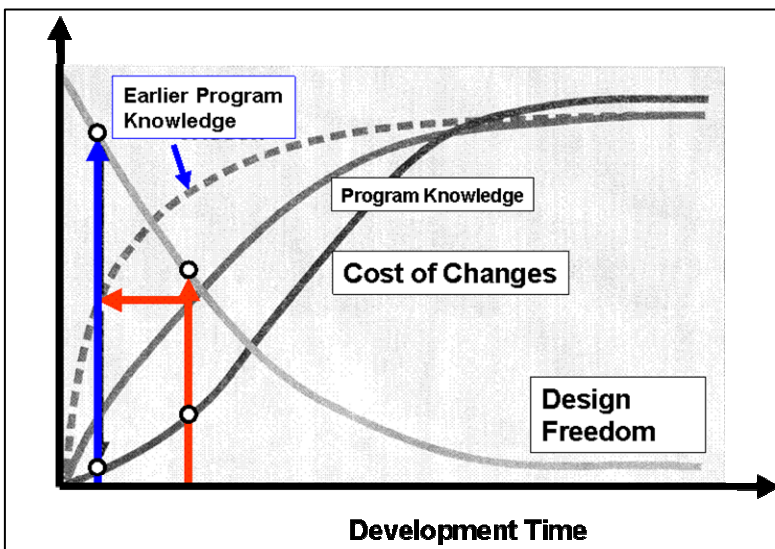


Fig. 1-5 Improved design freedom by earlier knowledge

The objective for the industry is changing during these phases, **Fig. 1-4**. The amount of money involved in the early phases is significantly lower than in the latter ones. However it should be noted that the definition of the vehicle/system take place in the concept and definition phase. During this time period the characteristics which will determine the "performance" and acceptability of the system are defined. Introducing changes becomes significantly more expensive, if incorporated at a later point in time. Therefore all modern tool developments and processes aim to increase the knowledge base and its quality about a system in the early stages of the development, **Fig. 1-5**.

2 Requirements

Fig. 2-1 summarizes significant differences between commercial and military aircraft design. They are very obvious; most of them will be addressed within this paper. Note that the wing loading is not so much different, however the thrust/weight ratio is about three times as high for fighter aircraft, **Fig. 2-2**. The aerodynamic is characterized by the small aspect ratio for fighter aircraft, essential for high maneuverability, in particular roll rate **Fig. 2-3**.

Requirement	Fighter	Commercial
Load factor	9g/-3 g	3,5/-1,5
Fatigue life	4 – 8000 hrs	50000 hrs
Payload	external/internal	internal
Maximum Speed	Mach >1	Mach < 1
Max.sink rate for Ldg.gear	3,6 m/s	3,6 m/s
Mission Equipment	Customer	Customer
Fuel	wing & fuselage	wing
Vulnerability considered	Yes	(NA)
Crew Escape	Ejection	None
Technologies	High performance	economical
Engine arrangement	fuselage integrated	in gondolas
Thrust/weight	>0.7	<0,4
Mission duration*	~1-2 hrs	1 – 12 hrs
Export	Government contr.	Free market
Production size	<1000	>1000

* For combat vehicles w/o external tanks and /or in flight refueling

Fig. 2-1 Differences between commercial and military requirements

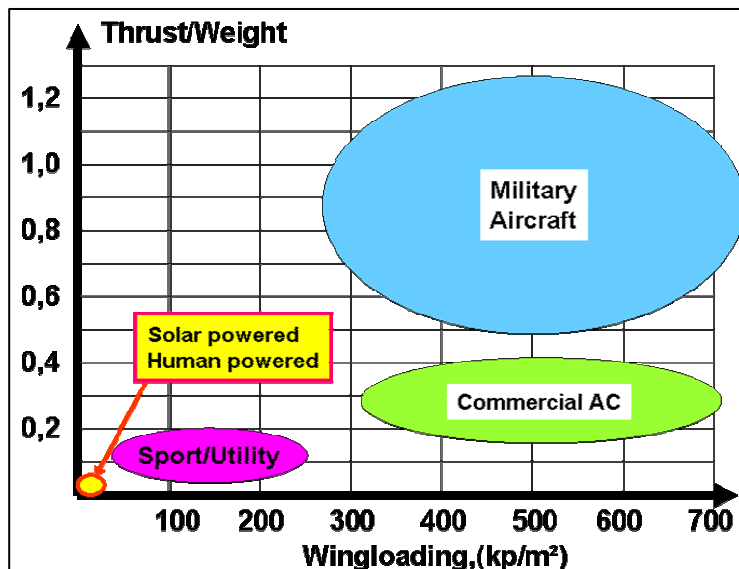


Fig. 2-2 Thrust/Weight and Wing Loading

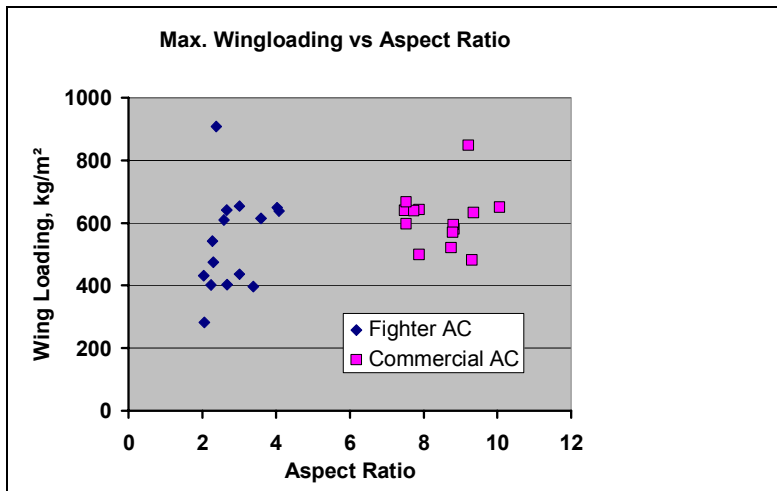


Fig. 2-3 Wing Loading and Aspect Ratio

Usually an aircraft was designed to certain technical "requirements" (range, payload, flight performance, etc.) defined by the customer and/or the company. Nowadays the expression "requirements", is replaced by "capabilities". This provides more flexibility for the customer because he does not have to specify a weapon system but the task he needs to perform. A new weapon system does not have to be the same type as the one to be replaced. E.g. the need to transport a certain mass from A to B could be satisfied by an air-vehicle or a surface vehicle. The specification of time, distance and geographic location will then allow evaluating the options.

The four basic tasks for which a military aircraft can be designed are

- Training
- Transport
- Reconnaissance
- Defense/Attack

The scope of this lecture is primarily oriented towards the latter two.

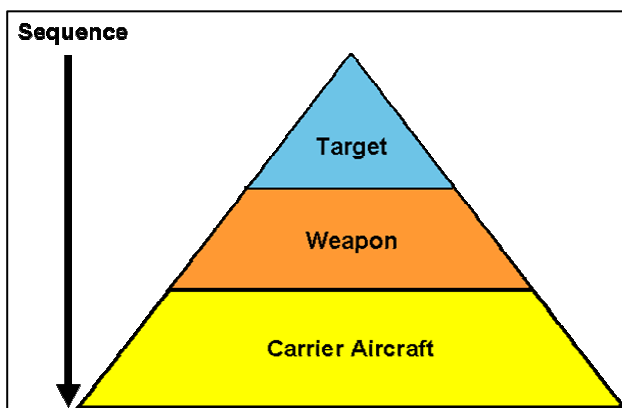


Fig. 2-4 Ideal Design Process

The ideal design process would start with the objective/target, determine the means to achieve it (sensors/weapons) and would then proceed to the definition of the vehicle (**Fig. 2-4**). The real world is quite different if one looks at some typical examples like the

- F-104 G: Designed for Point Intercept, used in GER for A/G missions
- Tornado (MRCA = Multi Role Combat Aircraft)
Initial A/G Weapons 1970 (iron bombs; Today: smart bombs)
Modified for AD, and guided weapons (A/G)
- F-4 Phantom (a true multirole ac designed 1955)
Carrier Airplane used in Germany for AD, adapted to Sparrow and AG 65 in the 80ies
- Eurofighter
Designed for A/A : AMRAAM, Sparrow (Skyflash, Aspide), Aim 9L. Now upgraded for IRIS-T,
Now modified for Dual Role, i.e. also A/G: Precision Weapons, Stand-off Weapon

Changes due to new sensors, avionic software, weapons, require flexible (multi-role) configurations and modular avionic systems.

Another recent example is the acquisition of the carrier aircraft F-18 by Switzerland which does neither have a Navy nor an aircraft carrier. Political and economic aspects are important contributors to weapons system development or acquisition programs.

The consequence of the significant scenario changes to be expected and the extremely long life span of a combat aircraft is, that the basic air-vehicle should be rather flexible and in particular capable to satisfy air/air and air to ground missions. It should allow easy changes in the sensor and weapon suite. This is in particular true, since the number of aircraft types in the inventory of most air forces has steadily decreased.

Typical air/air, air/ground and reconnaissance missions are identified in **Fig. 2-5**. Each (alternate) mission is defined by a mission profile (**Fig. 2-6**), the load and the external fuel required. Typical segments of a mission are defined in **Fig. 2-7**.

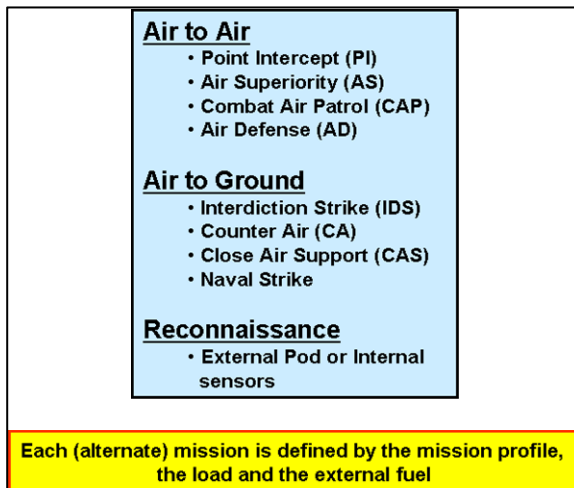


Fig.2-5 Typical missions for military aircraft

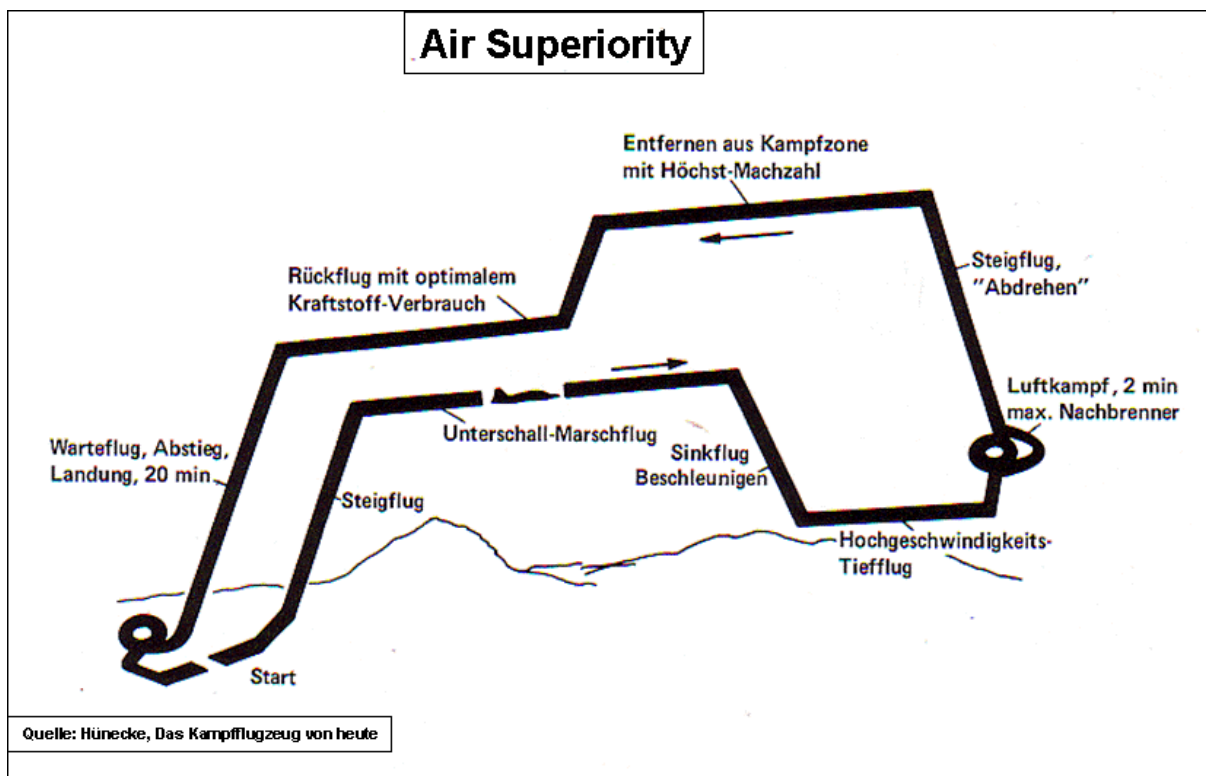


Fig. 2-6 Mission Profile

For each aircraft system there is one "design mission". The design mission determines the internal fuel carried by the aircraft; alternate mission performance is then a fall out. Of equal importance are the maneuver requirements (**Fig. 2-8**), which determine the thrust/weight and wing loading of the vehicle. A graphical presentation of maneuver performance is given in **Fig. 2-9**. For a fixed altitude the specific excess power, the turn rate, the turn radius and the load factor are being presented.

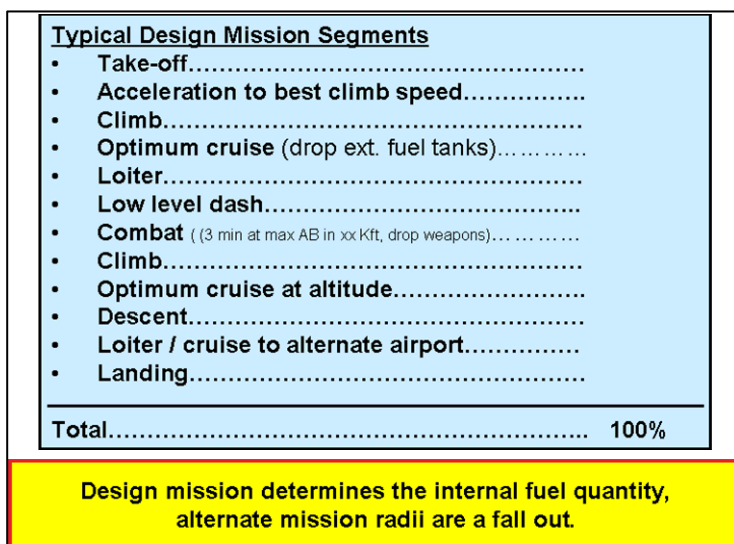


Fig. 2-7 Mission Segments

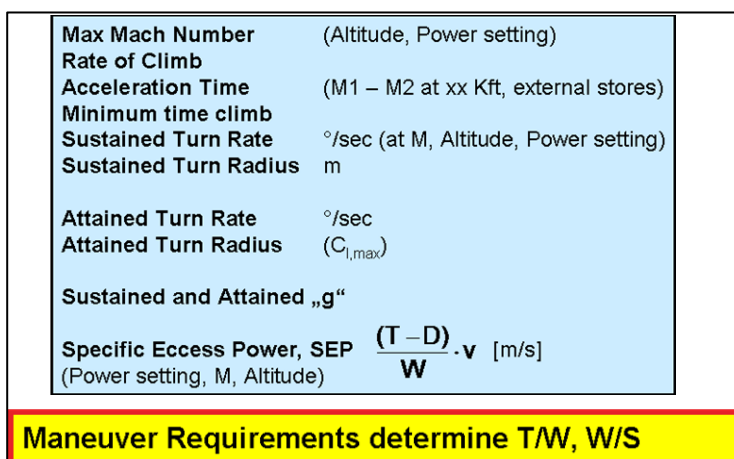


Fig. 2-8 Maneuver Requirements

More detailed requirements/criteria for the design of the vehicle are described in **Fig. 2-10** and **Fig. 2-11**. They include performance, equipment, engines, number of crew, structural design, maintenance, survivability safety etc.

The question, whether the design requirements for a new system will still be correct after 20 to 40 years is very difficult to answer, because of potential scenario changes which are very hard to predict. While the "east/west" scenario was pretty stable from 1950 to 1990, it has dramatically changed in the last 15 years.

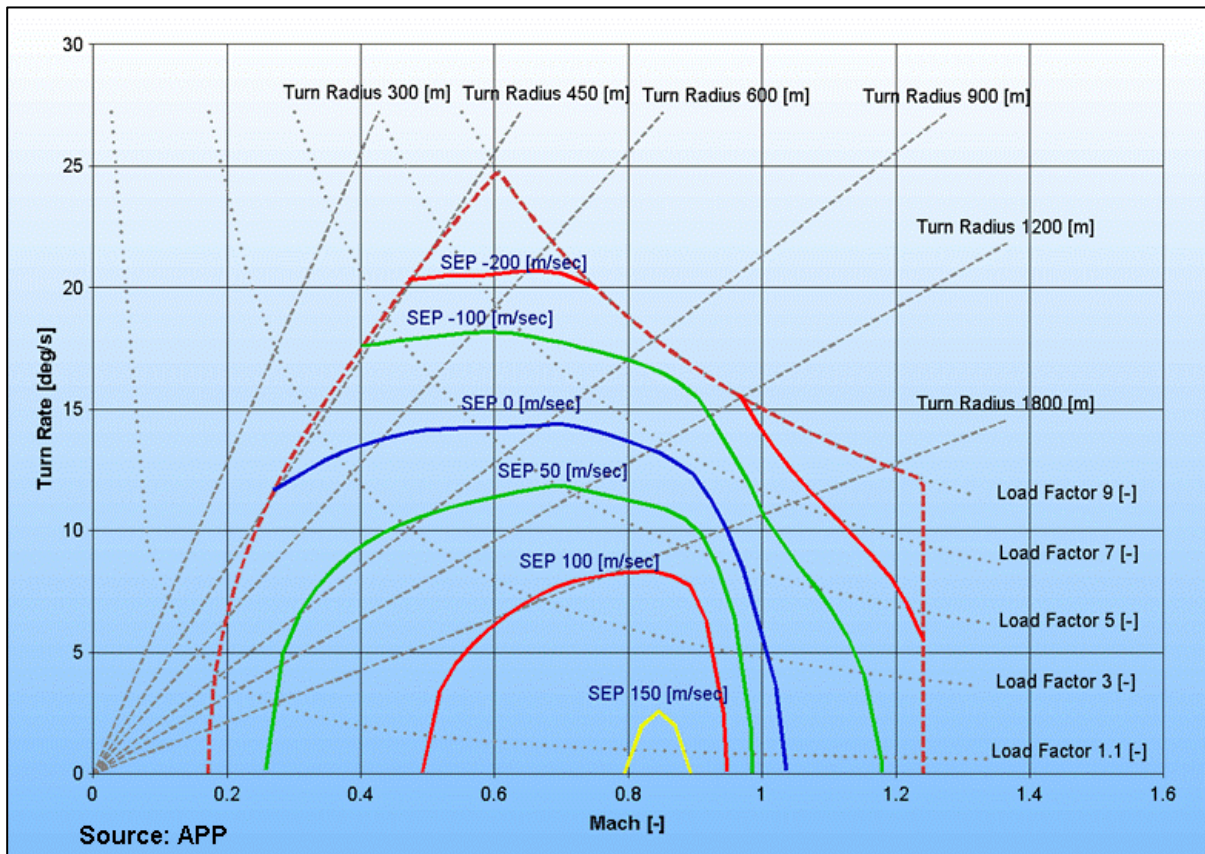


Fig. 2-9 Maneuver Performance Plot

Flight Performance	<ul style="list-style-type: none"> • Field length • Mission: payload radius • Maneuver
Equipment & Mission Requirements	<ul style="list-style-type: none"> • Navigation • Communication/Identification • Detection, recognition, location • Weapon delivery • Flight control modes (e.g. TF) • ECM capabilities • Signature
Armament, GFE (Government Furnished Equipment)	<ul style="list-style-type: none"> • Gun • Missiles • (Smart) bombs • beam weapons
Crew	<ul style="list-style-type: none"> • members: 0/1/2.... • Ejection/Rescue (seat, capsule)
Engine (GFE)	<ul style="list-style-type: none"> • Type • Number

Fig. 2-10 Design Requirements (1)

Structural Criteria	<ul style="list-style-type: none"> • design load factor and mass • dynamic loads – gusts, maneuver
Mass	<ul style="list-style-type: none"> • Design mass (@ xx %, load factor, payload)
Design Life	<ul style="list-style-type: none"> • xxxx Flight hours (Tornado e.g. 4000)
Maintenance	<ul style="list-style-type: none"> • man hours/flight hours
Reliability	<ul style="list-style-type: none"> • Mission probability of success • MTBF (Mean Time between Failures)
Survivability	<ul style="list-style-type: none"> • survival against certain caliber guns (G/A)
Safety	<ul style="list-style-type: none"> • Criticality of systems (FCS !!!), MTBF • Redundancy • Probability of a/c loss
Cost	<ul style="list-style-type: none"> • Development • Production • Operation

Fig.2-11 Design Requirements (2)

3 Design Process and Tools

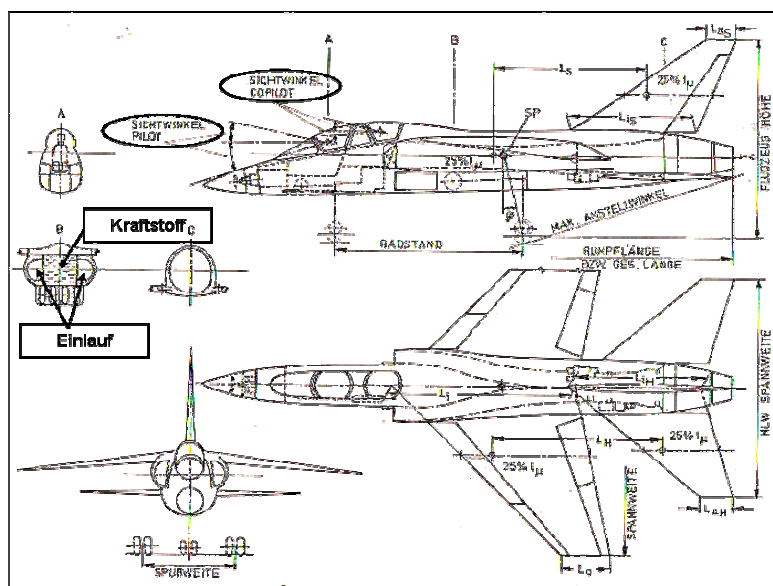
During the conceptual phase various design alternatives have to be investigated to find the optimum configuration. Wing and tail plan form, number and type of engines, the technology level to be incorporated etc. need to be investigated and the impact on system characteristics and cost identified.

Quite a few parameters are fixed from the beginning (such as crew size, engine type, weapons etc. see **Fig. 3-1**) which leaves primarily the integration as a very challenging and difficult job to the designer. The external shape of the aircraft, fuselage and wing/tail design show the signature of a capable design team. Like in many other disciplines, there is not just one solution for a given set of requirements.

	Fixed Parameter (GFE)	„Freely“ selectable Parameters
1. Radar dish diameter	X	
2. Equipment	X	
3. Armament (Gun)	X	
4. Cockpit		
Field of View (Mil-Std.)	X	
Ejection Seat	X	
5. Inlet ($M > 1$, $M < 1$), Type and Location	(X)	X
6. Landing gear (CBR)	X	
7. Wing geometry		X
8. Horizontal tail geometry		X
9. Vertical tail geometry		X
10. Engine type, size und dimension	X	X
11. Fuel tank location		X

GFE=Government Furnished Equipment

Fig. 3-1 Design Parameter



In the old days often a sketch on a small piece of paper was the start of a configuration layout. Today, modern computer programs allow to quickly design and investigate a configuration in 3 dimensions. But now and then it is usually one man, with broad knowledge and experience, who conceives the vehicle (**Fig. 3-2**), which will then be used as a baseline design. This is a very demanding job and unfortunately the number of engineers having participated in many development programs to accumulate this knowledge base is very low and shrinking. Every specialist is trying to optimize his own little equation (**Fig. 3-3**), but project managers/leaders have to be generalists and need to integrate all system aspects (**Fig. 3-4**). Aircraft design is a multidisciplinary iteration process.

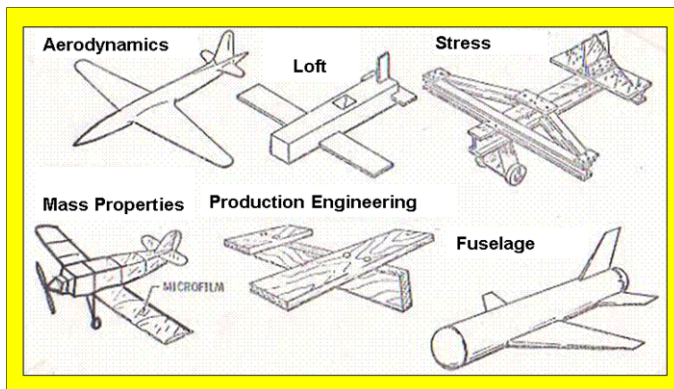


Fig. 3-3 Specialists dream of their aircraft design

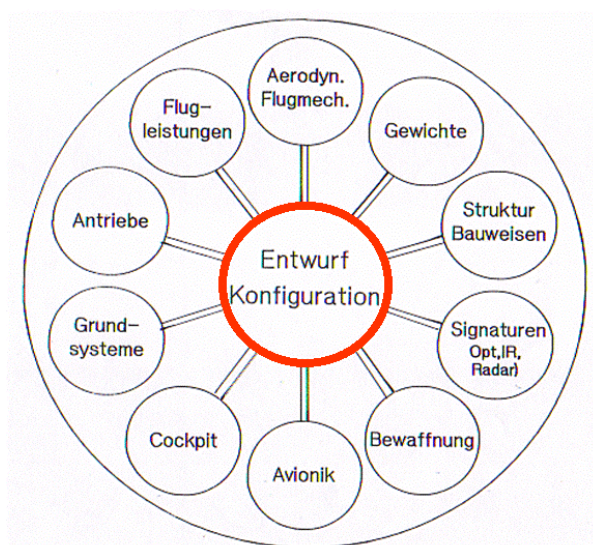


Fig. 3-4 Aircraft design, a multidisciplinary activity = systems integration

Once a Baseline concept is established, this will be used as an input for a computer aided design and evaluation program (CADE), which allows to scale the aircraft to make it meet (or exceed) the performance criteria, i.e. design mission and maneuver requirements **Fig. 3-5**. Such a computer program also allows defining the design window (**Fig. 3-6**), where viable solutions for configurations exist, perform numerous trade-off studies, and establishing a sensitivity matrix/growth factors for quick assessments of trade off's, **Fig. 3-7 / Fig. 3-8**.

In combination with an optimization routine such a CADE program provides the opportunity to optimize the configuration using pay-off functions and constraints. Typical weight growth factors generated with such a CADE program are given in **Fig. 3-9**.

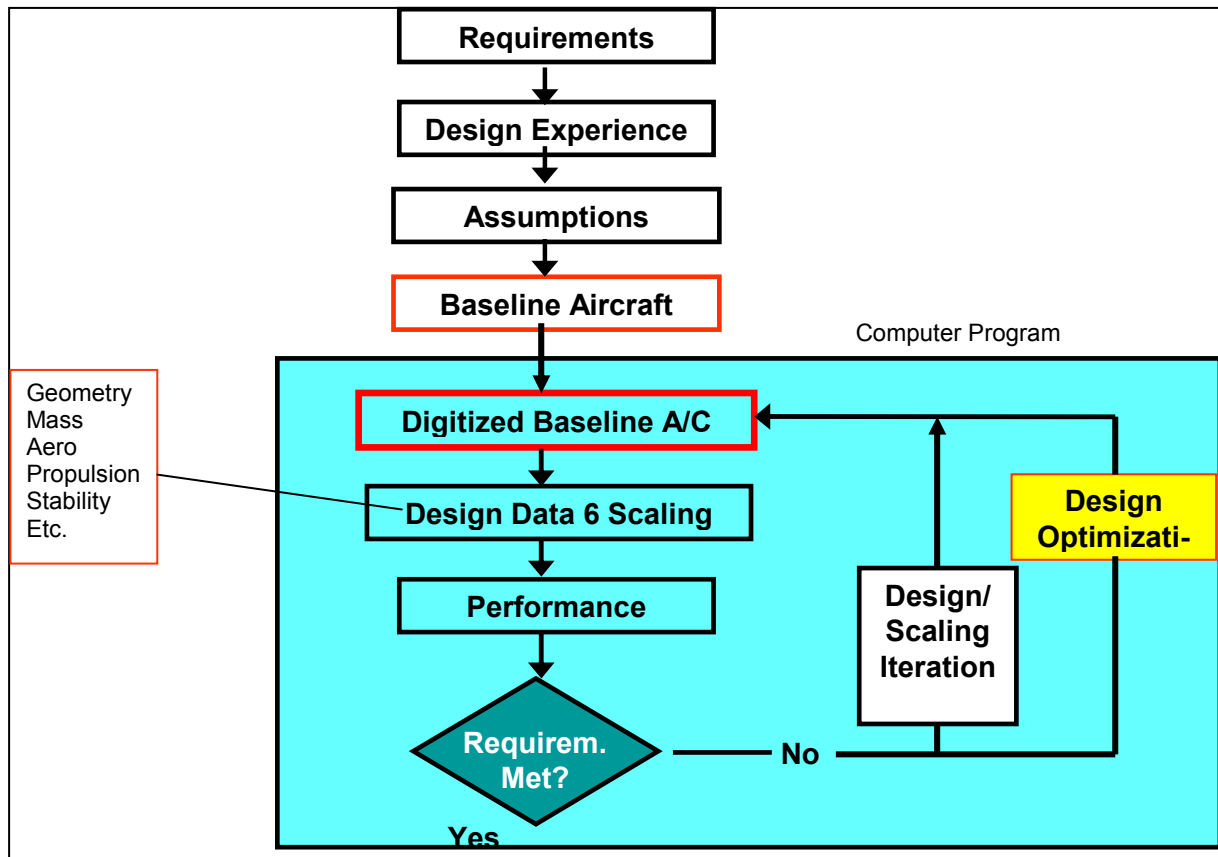


Fig. 3-5 Computer Aided Design Program (CADE)

Change of an aircraft characteristic by changing another aircraft parameter maintaining a defined/constant performance level

$$K_1 = \frac{\partial \text{Take-off Weight}}{\partial \text{Weight increment}}$$

$$K_2 = \frac{\partial \text{Take-off Weight}}{\partial \text{Drag increment}}$$

$$\text{Take-off Weight} = \text{Take-off weight}_0 + \sum_{i=1}^n \frac{\partial A}{\partial Z} \cdot \Delta Z$$

The sensitivity of mass, drag, thrust ect. to initial changes will result in a sensitivity matrix

Fig. 3-6 Growth Factor Definition

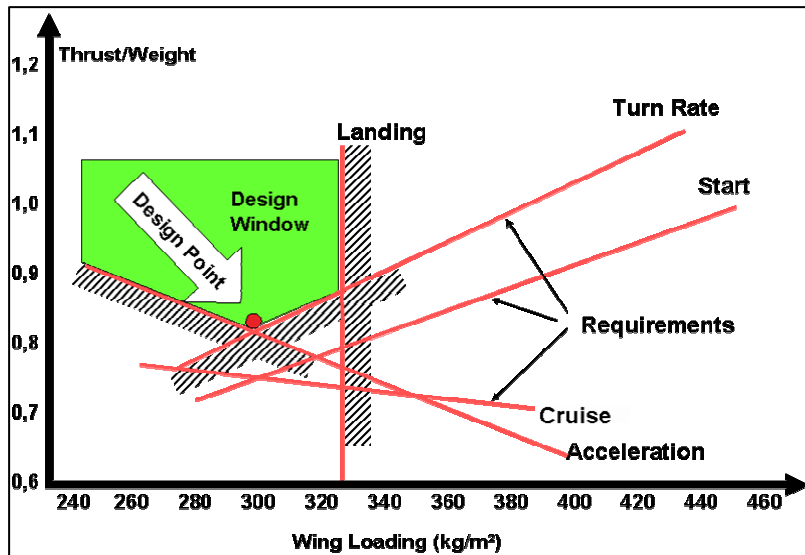


Fig. 3-7 Design Window

Delta	Mass	Drag	Thrust	SFC
TOGW	$\frac{\Delta TOGW}{\Delta Mass}$	$\frac{\Delta TOGW}{\Delta Drag}$	$\frac{\Delta TOGW}{\Delta Thrust}$	$\frac{\Delta TOGW}{\Delta SFC}$
Cruise Drag				
Thrust				

Fig. 3-8 Sensitivity Matrix

Rubber engine = constant mission & maneuver performance)	
Structure...	3,5
Avionic...	3,9
Laser with external window	6,9
Pylon	8,9
Fin	17,6
Camouflage paint	70
Weight Growth factor for fighter ac depending on requirements: 1.5 – 3.5	

Fig. 3-9 Growth Factors

In the USA a number of development programs have been performed with the aim to satisfy the requirements of Air Force and Navy. This was – so far – never really achieved. The F-111 was one example; the Navy pulled back and developed their own aircraft, the F-14. The Joint

Strike Fighter (JSF) is the latest try. A land- (USAF), a carrier- (Navy) and a STOVL (Marines) version are being developed with the aim to maintain a high degree of commonality thereby reducing development and operational cost. Another try to have a joint Air Force/Navy development program for an unmanned combat aircraft in the USA was cancelled in 2005.

One strategy, which keeps the competition going and allows the customer to better judge the products offered, is the prototype approach, usually conducted in the USA: At least two companies are contracted to develop a prototype aircraft and perform flight test, after which the final evaluation and selection of the winner takes place.

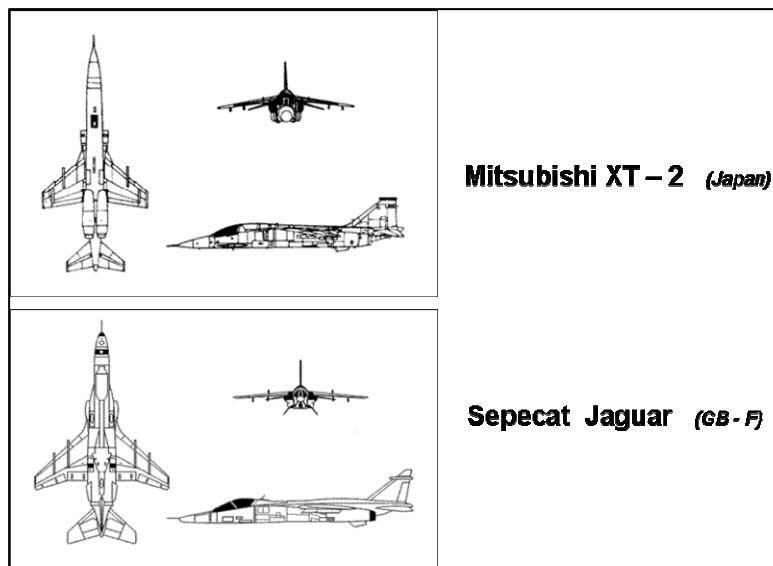


Fig. 3-10 One Solution for one Requirement?

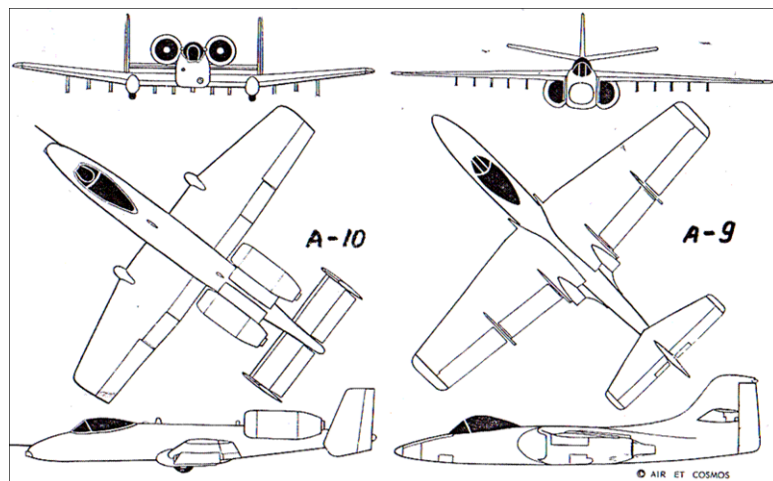


Fig. 3-11 A10 vs. A-11 Competition

Looking at the Mitsubishi XT2 and the Jaguar (**Fig. 3-10**), both of which are using the same engine, one may conclude that there is only one solution/configuration for one requirement. However, considering the A-9/A-10 competition for a ground attack aircraft, primarily sized

by the requirement to attack tanks with a gun (**Fig. 3-11**), it becomes obvious, that the designer does have different options for the layout of the configuration. Wing-, engine-, landing gear location and tail arrangement are considerably different. What is identical is the wing geometry. As can be seen in many other competitions: the wing geometry (aspect ratio, sweep, wing loading, wing thickness etc.) is determined by the mission definition and the maneuver requirements.

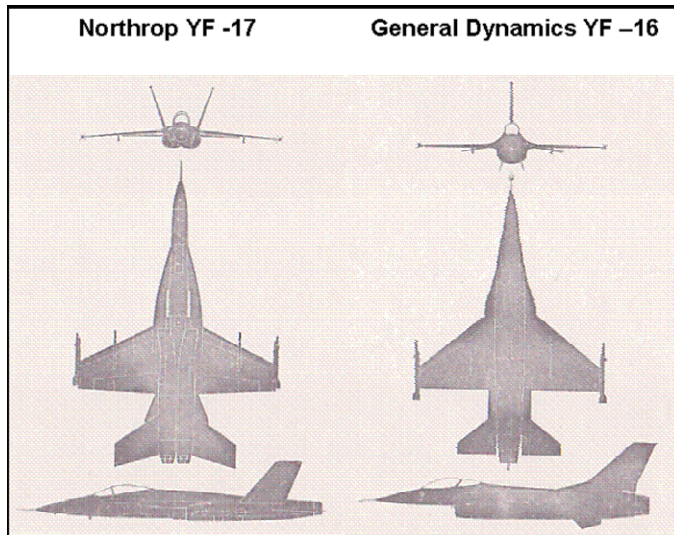


Fig. 3-12 YF-16 vs. YF 17: Light Weigh Fighter Competition

Another typical prototype competition conducted in the USA was the YF-16 vs. the YF-17, **Fig. 3-12**. It was the competition for a light weight fighter, a complementary aircraft to the existing F-15 covering the high end. Both aircraft are characterized by a strake wing geometry, which provides very good aerodynamic characteristics at high angles of attack through the generation of a large vortex by the leading edge extension at the wing root (**Fig. 3-13**). The YF-16 was using one existing engine of the larger F-15. This guaranteed high reliability, low development cost, because the basic engine was there and paid for by the F-15 program. It required only some adaptation for a single engine ac.



Fig. 3-13 F-18 Leading Edge Vortex Generation

The YF-17 philosophy included the twin engine safety aspect, and a strong argument for a low bypass ratio engine, perfectly suited for a fighter aircraft with its low sensitivity to quick changes of power settings. The YF-16 was selected by the USAF, yet McDonnell-Douglas was smart, quick and successful selling the YF-17 to the US Navy, which became the F-18.

The latest and very important competition in the US was for the Joint Strike Fighter. The winner was to get a sole contract for the development with an expected number of around 3000 ac production run for all US services. The two competing aircraft, X-32 designed by Boeing and X-35 by Lockheed Martin are shown in **Fig. 3-14**. If somebody has a feeling for aircraft design it is evident who came out to be the winner. There is still truth in the saying "what looks good flies good". Even the slogan "form follows function" did not help Boeing.

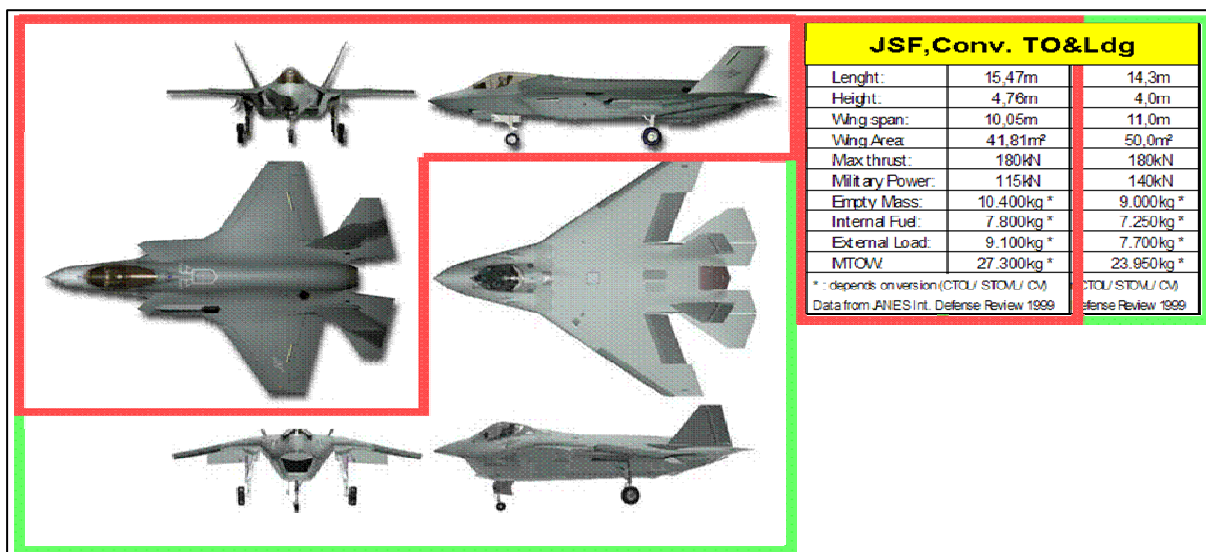


Fig. 3-14 The latest US Competition: X-32(Boeing) vs. X-35 Lockheed Martin (Winner)

Fig. 3-15 shows the European approach. There was no real competition in the development, because the requirements for Gripen, Rafale and Eurofighter were not identical. It was rather a national approach by Sweden and France, and a "joint" multinational program with Germany, Italy, UK, as partners, later joined by Spain. Gripen and Rafale have a relative small number of aircraft on order by their own nation. Hence the development cost share per aircraft is large and a problem, when trying to sell the aircraft. All three aircraft have a delta- canard wing arrangement with Gripen and Rafale having a short coupled, the Eurofighter a long coupled canard. Now, that the aircraft are in production, we have a real competition when the aircraft are offered for sale on the world market.

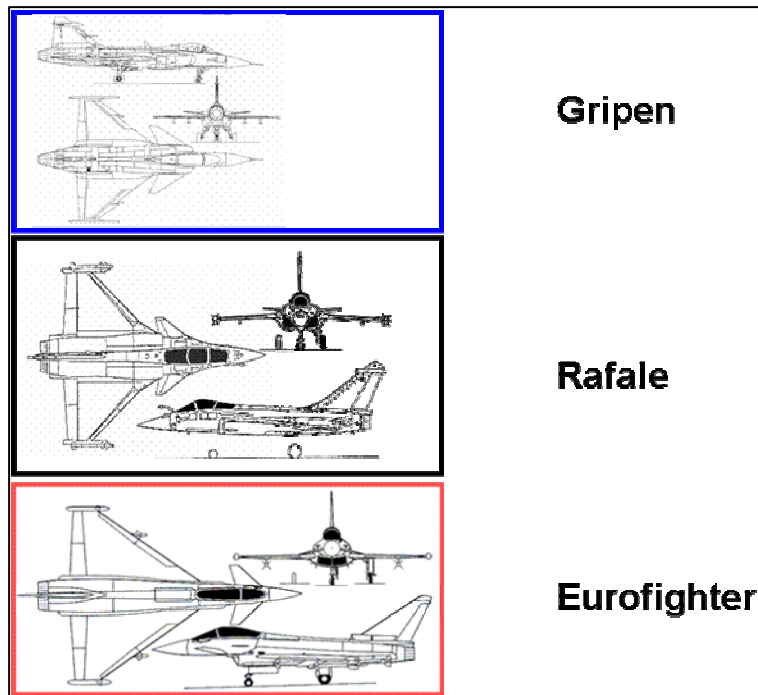


Fig. 3-15 European Competition

Configuration/Design data which must be generated during a conceptual phase include

- **Three View:** Geometry, wetted area, cross section
- **Inboard profile:** Critical cross sections, equipment bays, fuel tanks
- **Structural design:** primary load path (bulkheads, spars, wing/tail attachment, landing gear, major doors)
- **Manufacturing breakdown:** Fuselage sections, including inlet and engine sections, wing, tail, flaps, airbrake, fairings, pylons
- **External/Internal stores:** Type, numbers, location of fuel and armament
- **Mass Properties:** Mass breakdown, material distribution, c.g. travel, moments of inertia.



Fig. 3-16 Full scale mock-up of MBB design, 1978 ILA Hannover

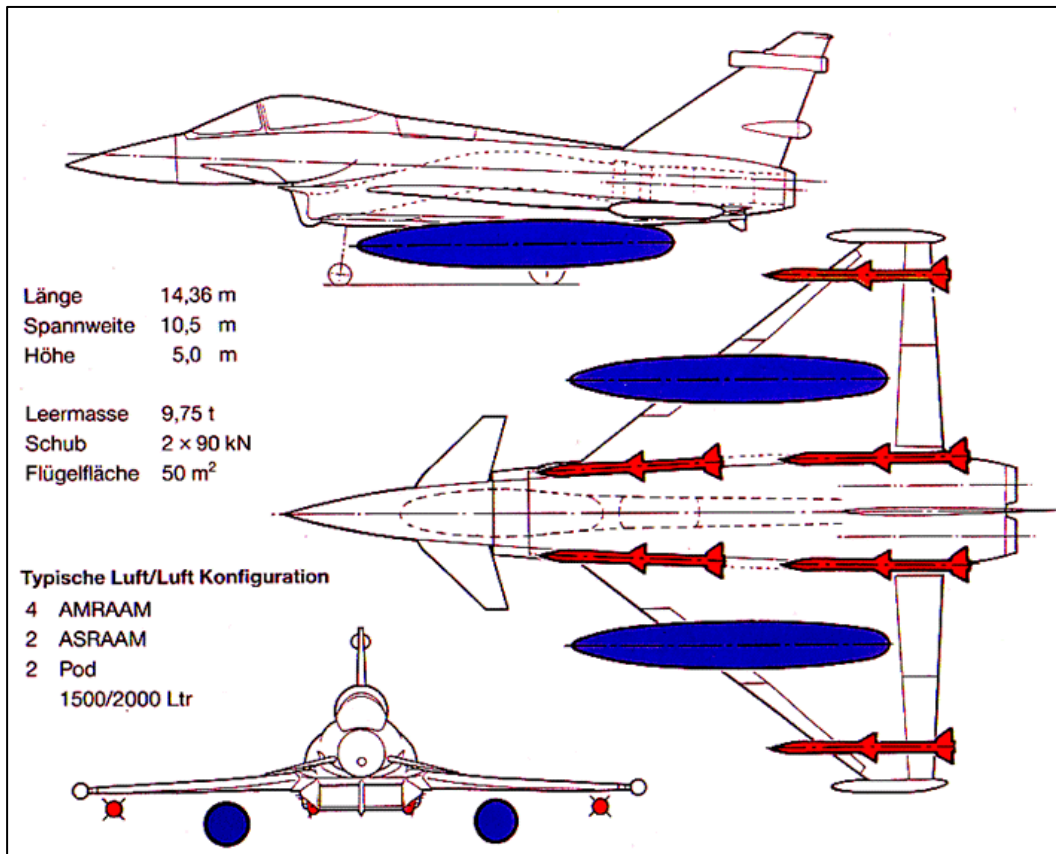


Fig. 3-17 Design Status Eurofighter, Mid 80ies

Fig. 3-16 shows a full scale wooden mock-up of the original MBB design which was already on display on the ILA 1978 in Hannover. It shows some features which are not present in the actual Eurofighter configuration: The twin vertical tails were replaced by a single vertical, the rectangular inlet was bent around the lower fuselage and the wing got a straight leading edge. These were the visible impact of BAe to the outside configuration, a very important aspect of

the acceptance of the MBB configuration by BAe. **Fig. 3-17** shows a project status in the mid eighties.

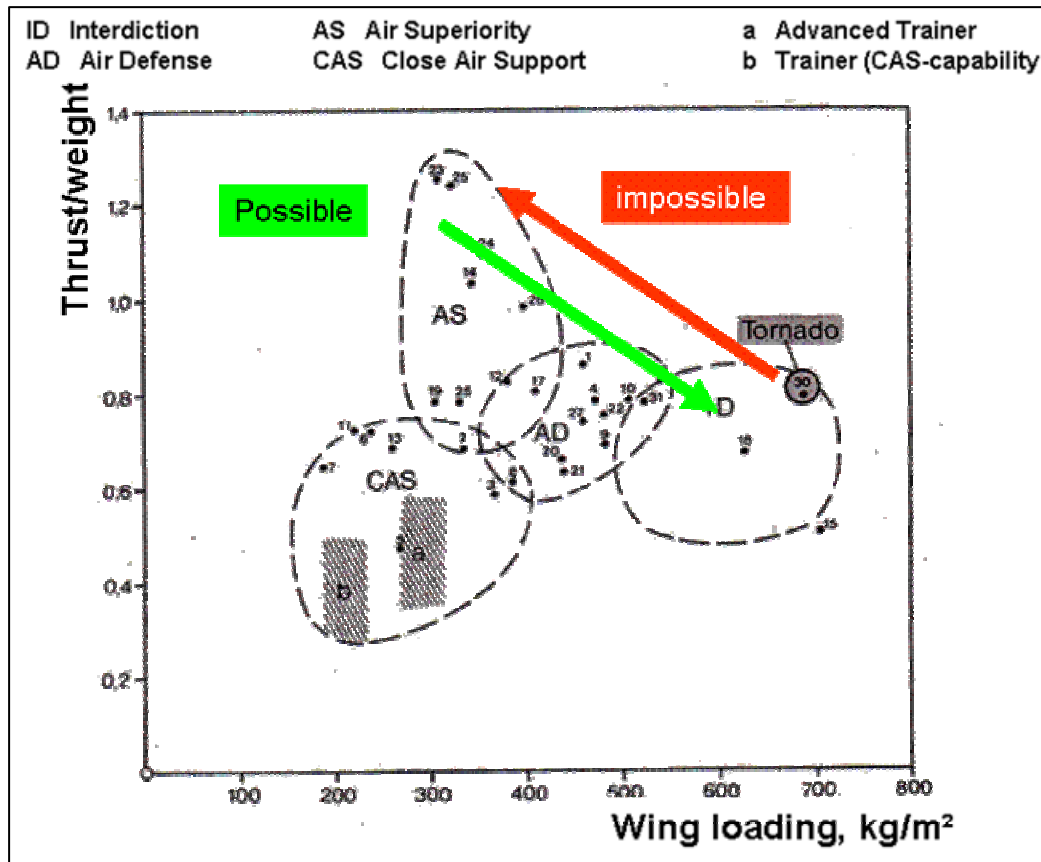


Fig. 3-18 Design windows for different missions

If one compares the famous design characteristics thrust/weight vs. wing loading for various missions (**Fig. 3-18**), it becomes immediately clear that a true multirole aircraft has to be designed for the air superiority role, because additional weapons as required for air/ground missions will automatically reduce thrust/weight and increase wing loading. I.e., a Eurofighter can be used for air to air and air to ground, provided that the avionics is adapted for the different weapon types. However, a Tornado can never be converted to perform air/air missions against the high performance fighter, simply because it is lacking thrust to weight and has too high a wing loading for that mission.

The Eurofighter development schedule drafted in 1986 called for the delivery of the first production vehicle in early 1996 (**Fig. 3-19**). The actual date was 2003, which means a delay of 7 years. Reasons for this include political aspects (a redefinition of major requirements by the Defence ministers), delays in contract releases due to financial considerations a new cost share resulting in further work share negotiations and – last but not least – technical challenges, initially in the flight control system area, later in the avionics system.

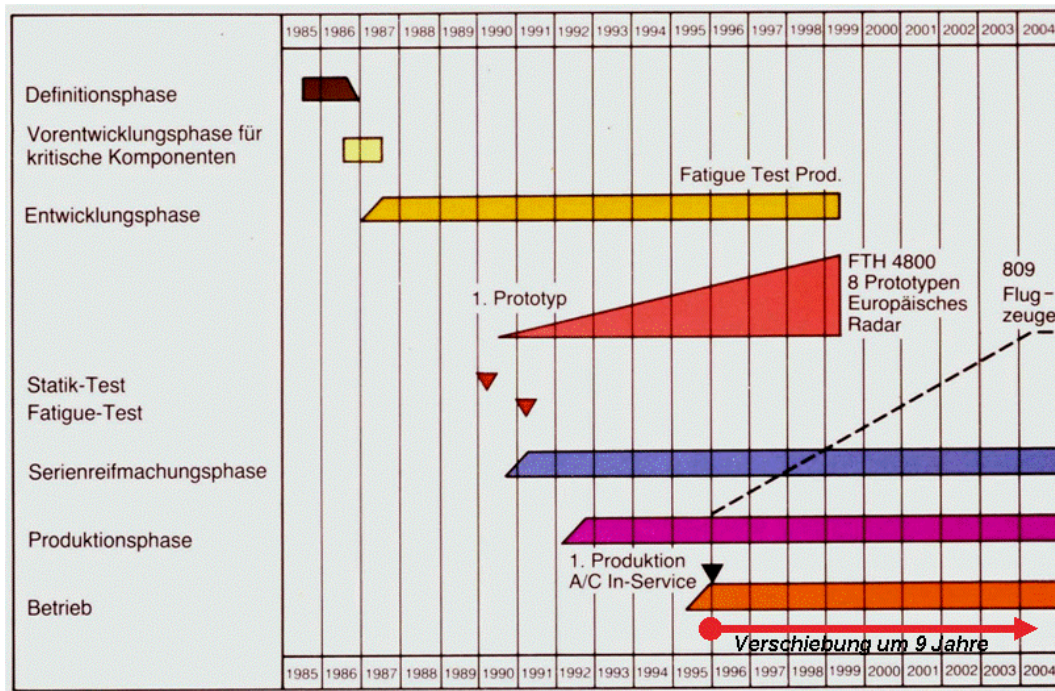


Fig. 3-19 Development Plan, Eurofighter 1986

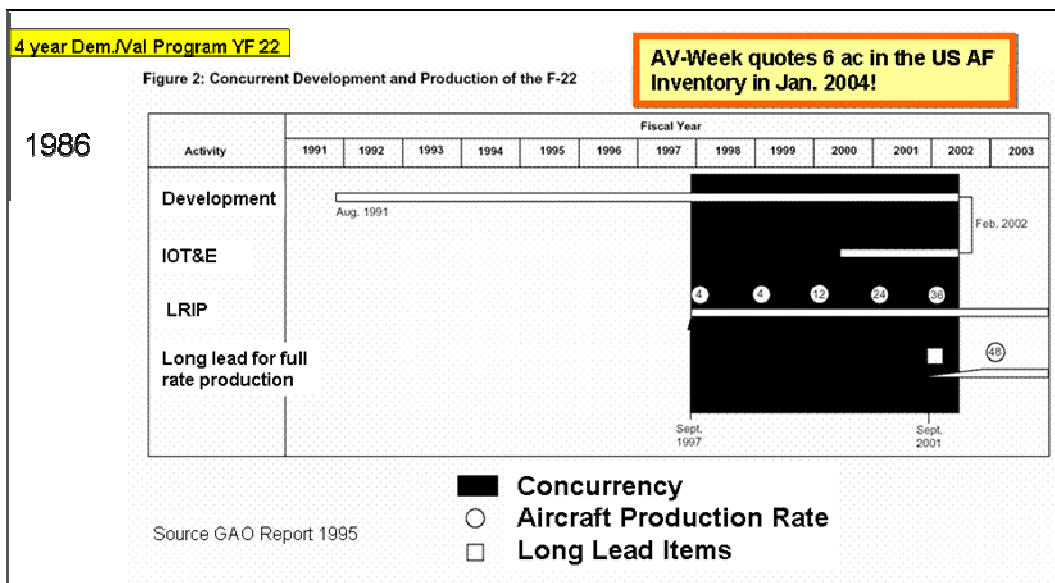


Fig. 3-20 Concurrent Development and Production of the F-22

The Eurofighter was not the only development program experiencing program delays. The American F-22 started with a prototype program in 1986 (YF 22 vs. YF 23 McDonnell-Douglas) followed by a full scale development program in 1991. It is a single nation program and yet in 2004 there were only 6 AC delivered to the US Air Force. In spite of all the modern tools and processes the development time of new aircraft has not been reduced. Part of the problem is certainly the increased complexity of modern systems with all the electronic features in the sensor area, on board processing and communication networks. But the fact, that fewer and fewer aircraft are being developed in a certain time span leads to a situation, where

less experienced personal has to perform a more complex integration work with bigger technology steps. Hence the technical risk and the likelihood of failures is increasing.

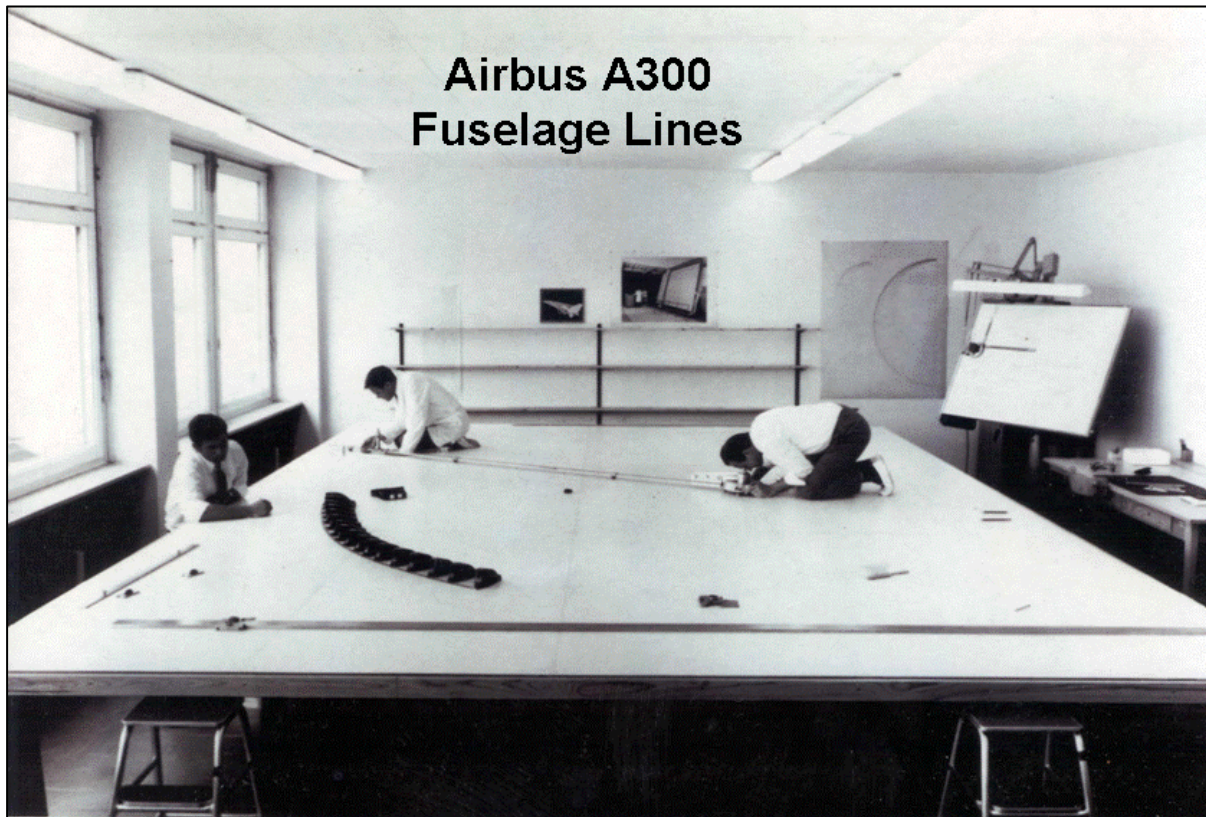


Fig. 3-21 Digital Line Definition for the Airbus A300, 1970

Fig. 3-21 shows the conversion of a fuselage drawing into digital coordinates for an Airbus using magnifiers. At that time lines were manually generated using the graphical procedures developed by shipbuilders. With the rapid development of computer hard- and software in the eighties generating and changing lines is very easy and allows a quick and precise mathematical definition of surfaces, cross sections and volumes at any station of the aircraft (**Fig. 3-22**). It is interesting that the CATIA program developed by Dassault is the most widely used one in the aeronautical industry, even in the US. The utilisation of such three dimensional models for other disciplines is presented in **Fig. 3-23** through **Fig. 3-25**. These features are a very important part of "concurrent engineering".

A much improved analysis of the available and used internal volumes in an aircraft is possible at an early point of the design process and allows the generation of "digital mock-ups". These have almost eliminated the need to build wooden or metallic mock-ups for the investigation of internal bays, routing of cables, pipes and equipment installation. To allow the engineer generating drawings to concentrate on the new and important items of the configuration, files for standard parts and -elements must be available (nuts, bolts, clamps, brackets, connectors, joints, fittings, etc). An inboard profile of a trainer aircraft (**Fig. 3-26**) and a detail design of a fuselage compartment (**Fig. 3-27**) illustrate the use of these new tools.

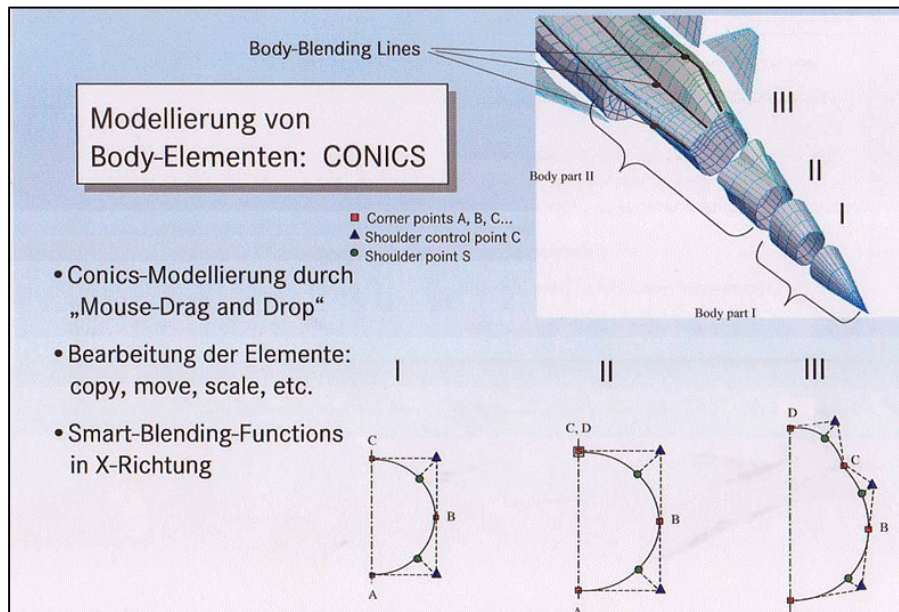


Fig. 3-22 Digital line definition by modern computer programs

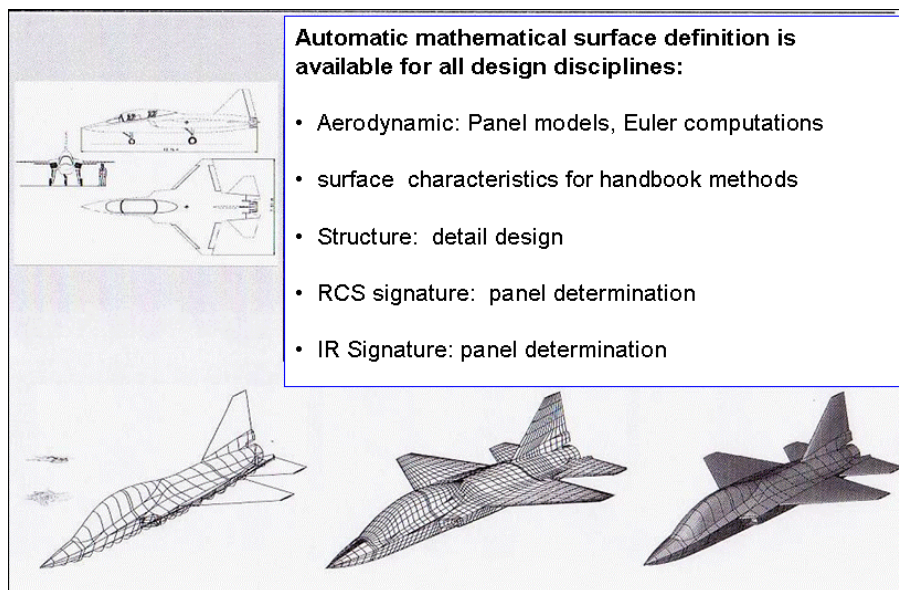


Fig. 3-23 Surface definition utilization

It should be noted that geometry information, drawings, part lists, equipment lists, material data etc. are all part of a huge data base which need to be properly defined with all the necessary interfaces and need to be under configuration control throughout development, production and operation. There is no unique system available (like Microsoft, SAP etc) and most companies are inventing/developing their own system.

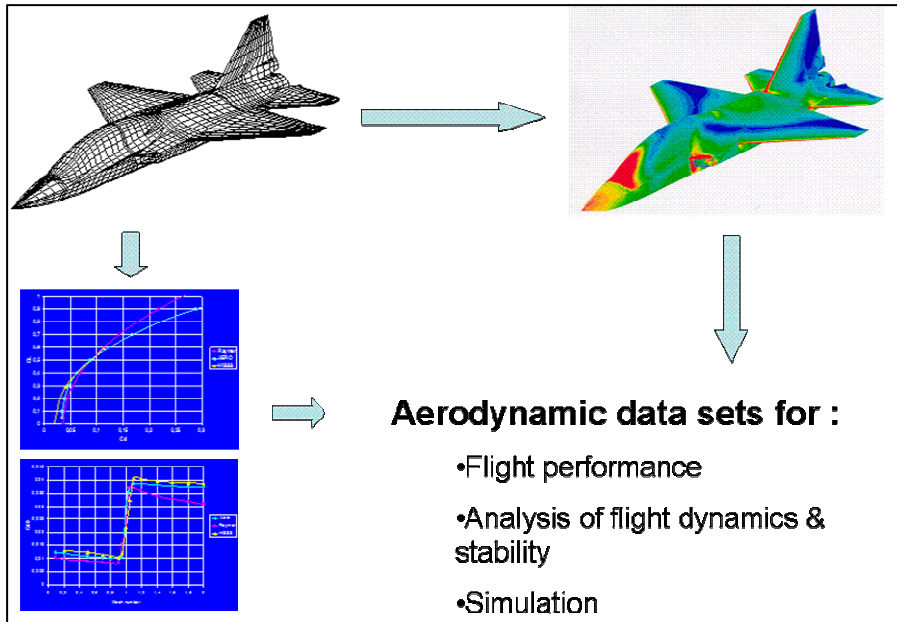


Fig. 3-24 Utilization of surface data for aerodynamic and flight control

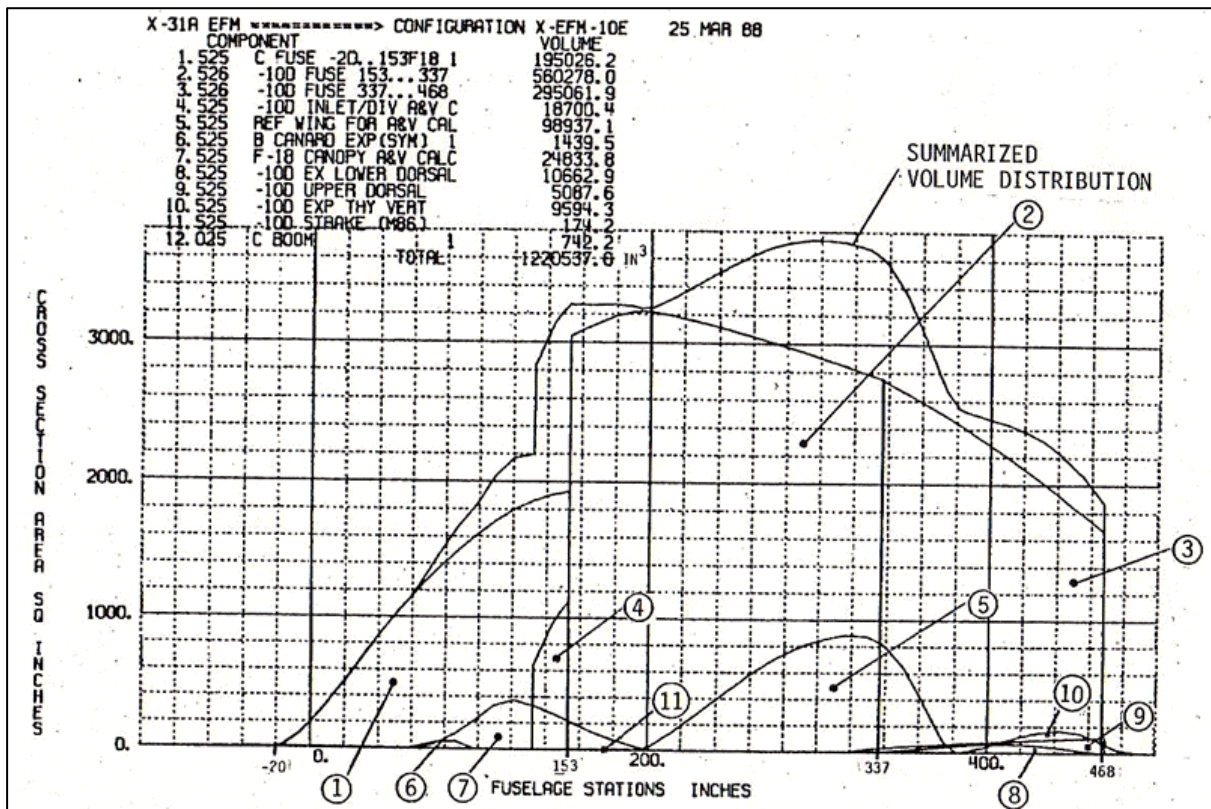


Fig. 3-25 Cross-section determination for drag calculation

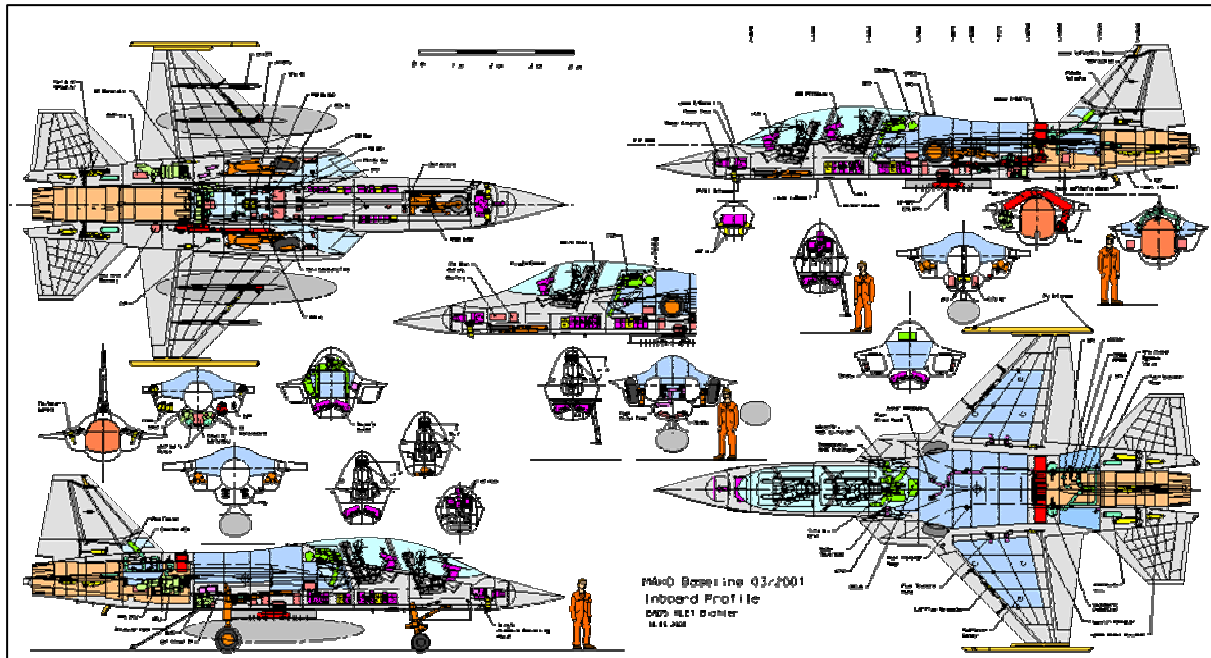


Fig. 3-26 Inboard Profile

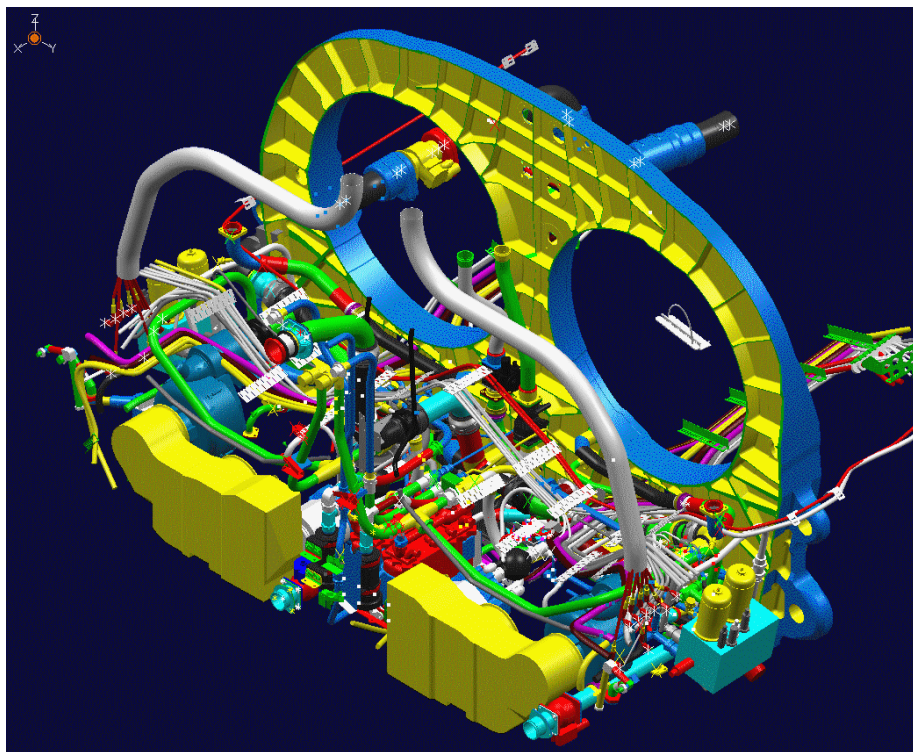


Fig. 3-27 Equipment installations in secondary power bay

4 Technologies

4.1 Composites

Composites have been used for fighter aircraft since the mid 60ies. Boron fibres were initially used, primarily because at that time they were cheaper than carbon fibres. The design to load-path option, the superior stiffness and material data, fatigue behaviour and corrosion resistance have led to a continuous increase of the fibre content in the structure of military aircraft.

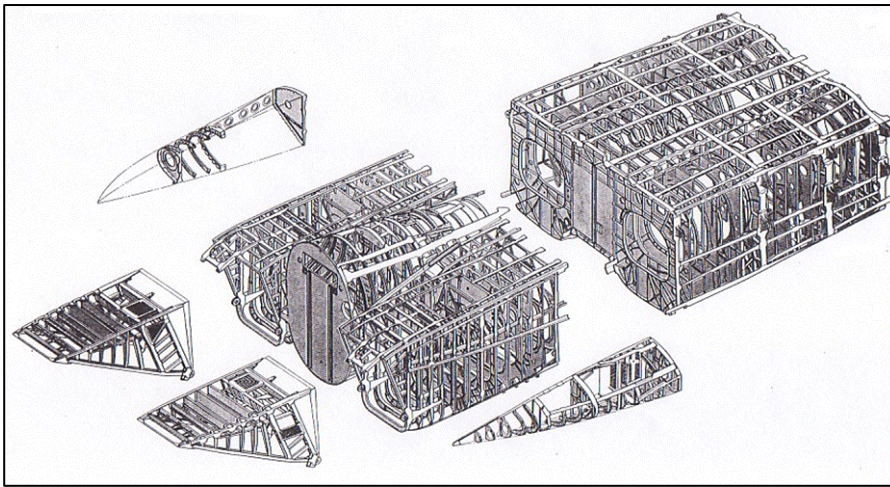


Fig. 4.1-1 F-15 Fuselage Design

A comparison of the F-15 metal fuselage with many small bulkheads to support the skin (**Fig. 4.1-1**) and the Eurofighter fuselage (**Fig. 4.1-2** and **Fig. 4.1-3**) using few metal frames and a carbon fibre skin with integrated cocured stiffeners show the development of structural concepts in the time span of twenty years from 1967 to 1987. Access to and volume for integral tanks within the fuselage have much improved.

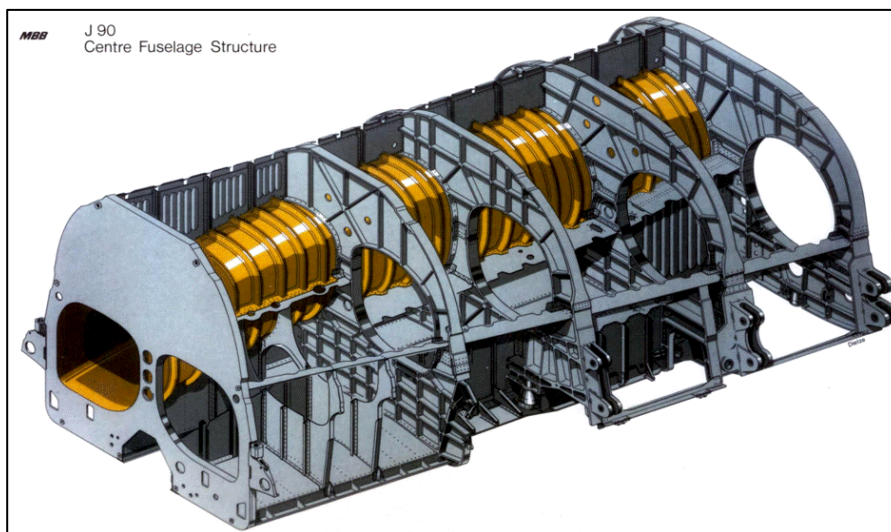


Fig. 4.1-2 Eurofighter Centre Fuselage Design

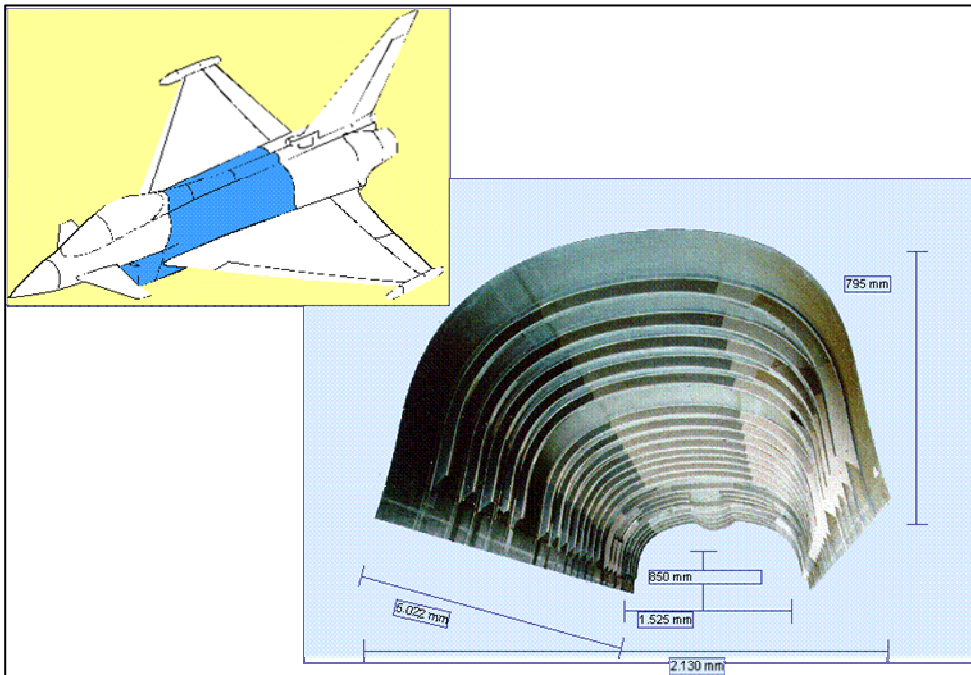


Fig. 4.1-3 Eurofighter Centre Fuselage Carbon Fiber Skin

The primary reason for CFC utilisation of course was –and still is- weight reduction. Unfortunately the second objective "cost reduction" has not yet been equally successful. While the military side was primarily arguing via the weight reduction and hence performance improvement, the commercial side put much more emphasis on the economic pay-off. Improved material properties and cost, manufacturing processes, design- operational experience have greatly contributed to the wide spread utilization of composites.

One of the problems, which still need further improvement, is the automation of the manufacturing processes from cutting to curing. **Fig. 4.1-4** shows that 5500 plies have to individually cut to size and then laid down at the right position for the Eurofighter centre fuselage skin. It is clear that this process can not be done economically without automation.

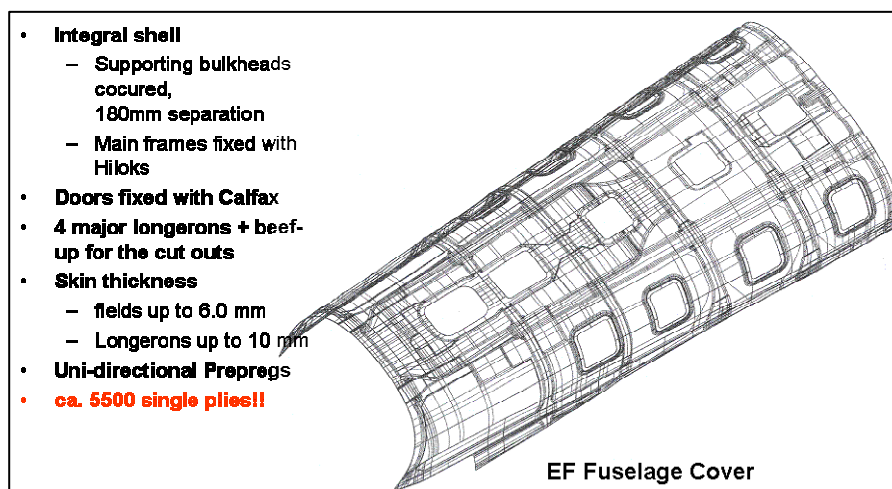


Fig. 4.1-4 CFC Structure Lay-Up

While on the Tornado aircraft only test articles have been manufactured from CFC (Fig. 4.1-5) the Eurofighter surface area is 70% CFC, which is equal to ~29% of the structural weight. All the modern European fighter aircraft have caught up with the Americans in the CFC utilization, however, with a time delay of about 5 years. All modern fighter aircraft in the US and Europe show a CFC share of 25 to 30% of structural weight (Fig. 4.1-6).

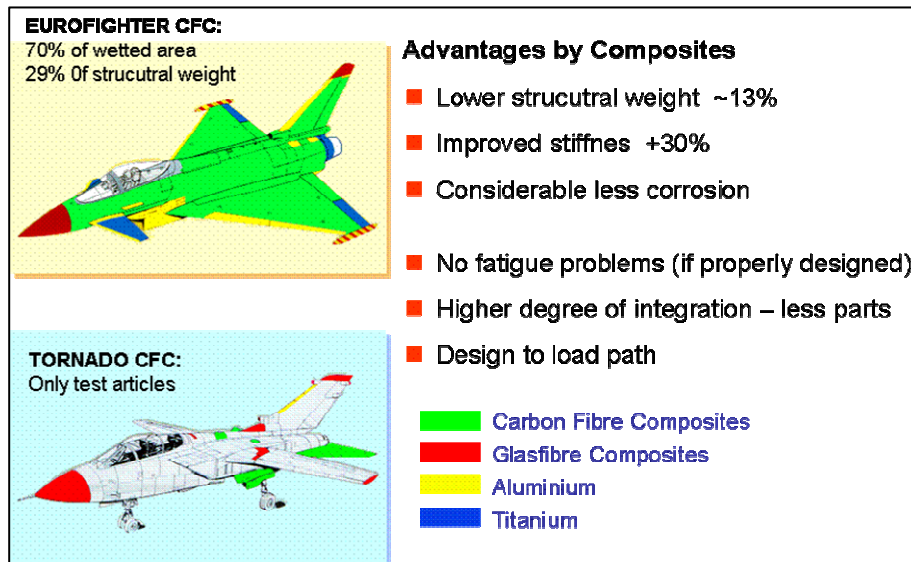


Fig. 4.1-5 CFC Utilization at Tornado and Eurofighter

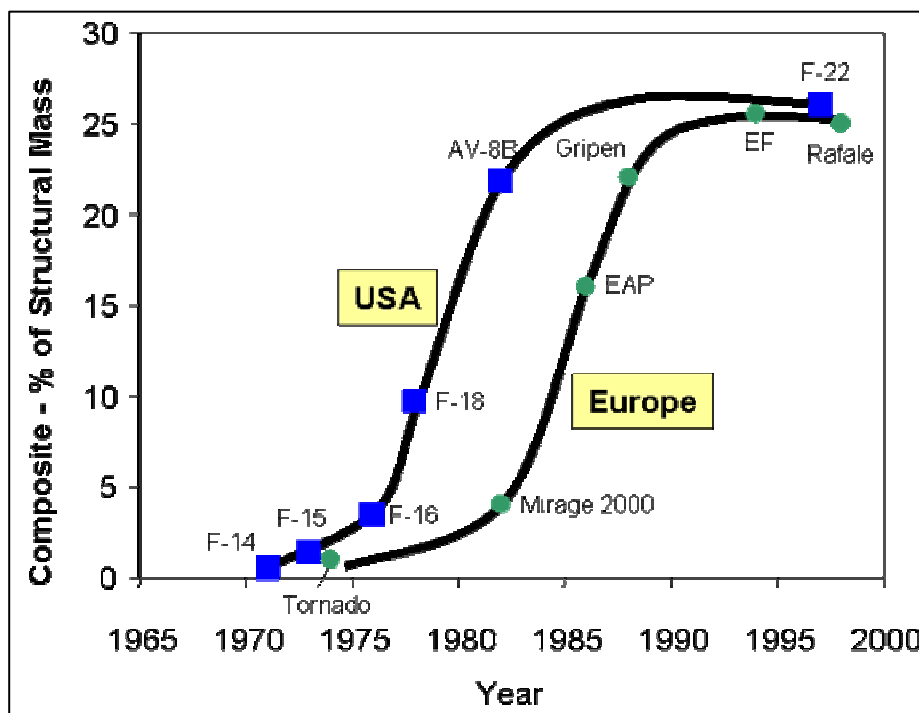


Fig. 4.1-6 Evolution of CFC utilization in fighter aircraft

While commercial aircraft have so far used less than 15% CFC in their structural mass, this figure is about to be changed dramatically with the introduction of the Boeing Dreamliner

B-787 and the Airbus A350 XWB. Boeing claims about 50% of structural weight to be in CFC! Wing and fuselage in CFC are the major steps toward that goal, **Fig. 4.1-7**.

	Military Aircraft			Comercial Aircraft		
Material	TOR	EF2000	F-22	Airbus		Boeing B 7E7 A350XWB
				A320	A330/ A340	
Alu	65 %	44 %	16 %	71 %	75 %	Wings Tails Fuselage!
TI	16 %	13 %	39 %	3 %	3 %	
Composites	1 %	29 %	24 %	16 %	12 %	
Steel	13 %	3 %	6 %	3 %	3 %	
Miscellaneous	5 %	11 %	15 %	7 %	7 %	
		↓		↓		
Composite Parts	Flaps	Fuselage skin Spine Airbrake Wing skin, spars,ribs Tails	Wings Tails Fuselage	Vertical Tail Horizontal Tail		
				Wing Flaps Fuselage pressure bulkhead		

Fig. 4.1-7 Material Breakdown, commercial and military aircraft

It is noteworthy that earlier civil aircraft had already achieved almost 100% CFC, like the Lear-Fan 2100 in 1985 (**Fig. 4.1-8**), now also the German Grob SP Very Light Jet. The Lear Fan 2100 was unfortunately killed by the enormous time delays and the costly effort to simultaneously develop the aircraft and the certification procedures with the US authorities.

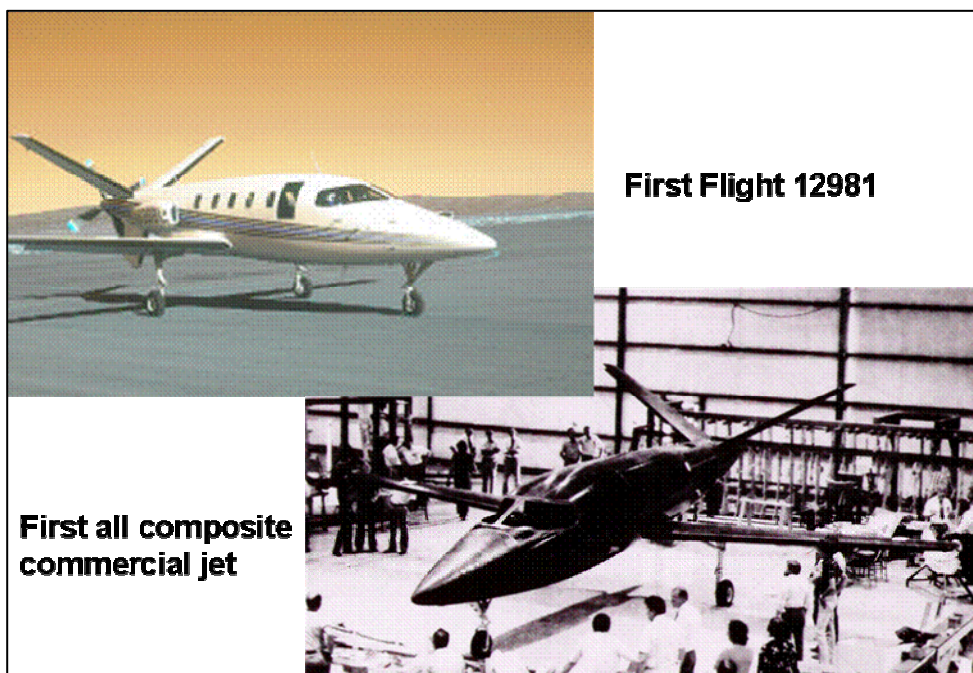


Fig. 4.1-8 Lear Fan 2100, the first commercial all composite aircraft, 1981

4.2 Ejection Systems and Pilot "g" Protection

Military fighter aircraft have an ejection system to save the crew in an emergency within the whole flight envelope, i.e. from zero airspeed/altitude to maximum altitude/speed. The ejection system requires special provisions to assure, that the pilot is within the clearance envelope for the ejection (Fig. 4.2-1 and Fig. 4.2-2).

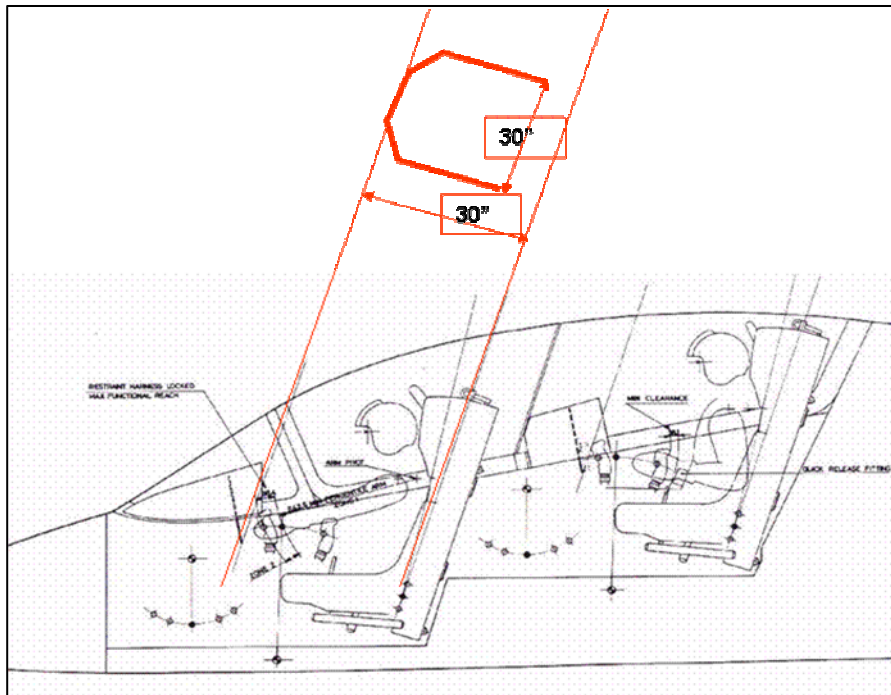


Fig. 4.2-1 Ejection clearance



Fig. 4.2-2 Pilot Seating in an F-16 and an Ultra Light sailplane

The modern cockpit is roomy, with good view; however, arms and legs have to be in the right position during the ejection. Arms are at the ejection handle, legs will be automatically pulled

towards the seat. To leave the airplane, the seat either penetrates the canopy or the canopy is separated before the ejection, **Fig. 4.2-3**. Seats are ground tested on rocket propelled sleds using dummy pilots, **Fig. 4.2-4**.

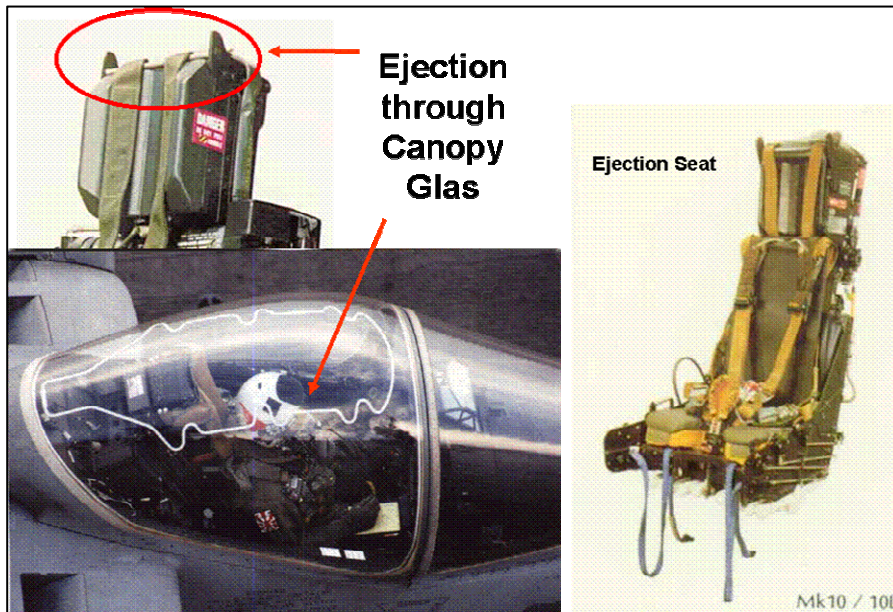


Fig. 4.2-3 Ejection through the canopy

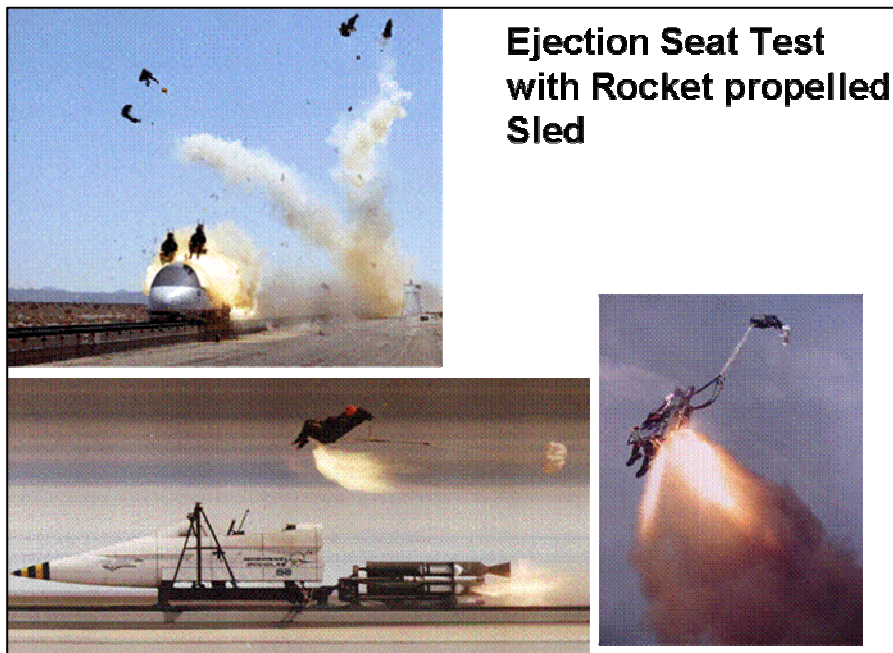


Fig. 4.2-4 Ejection Tests

Russia did have the most advanced seat since about 1985: the company Svesda developed a seat with a controllable ejection nozzle. At any point in time a seat mounted computer has the aircraft's state vector information (velocity, attitude, rates etc). This information is used to control the nozzle during the ejection in such a way, that an optimum recovery trajectory is

achieved (**Fig. 4.2-5** and **Fig. 4.2-6**). Quite a few Russian aircraft have successfully demonstrated the superiority of their ejection system.



Fig. 4.2-5 Pilot Ejection, Su-27

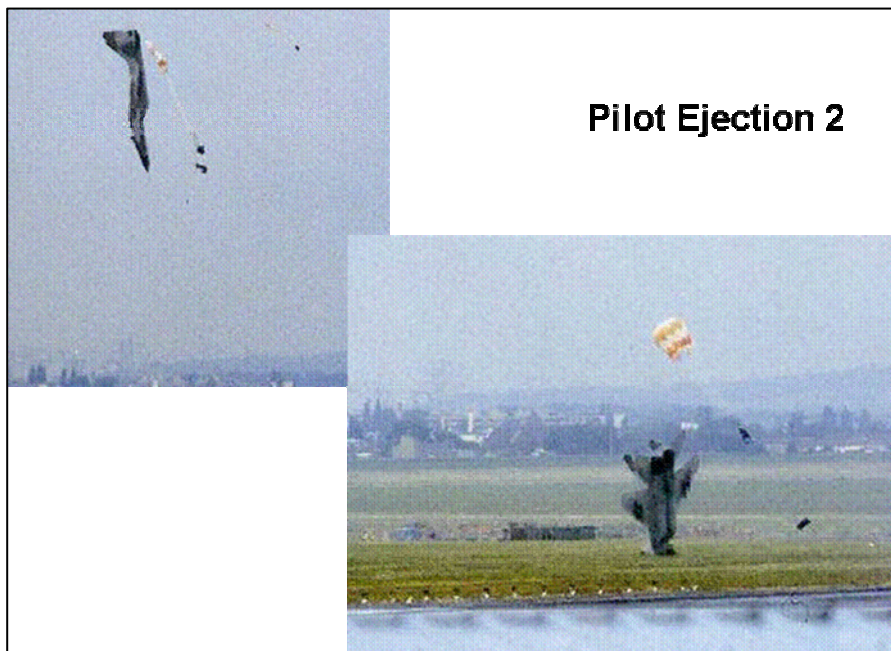


Fig. 4.2-6 Ejection Reality, Mig-29

Modern fighter aircraft are designed for high structural "g" loads (positive +9g, negative -3g). The most sensitive parameters affecting the "g" capability of an unprotected pilot are: "g" on-set rate, g- level and time exposure (**Fig. 4.2-7**)

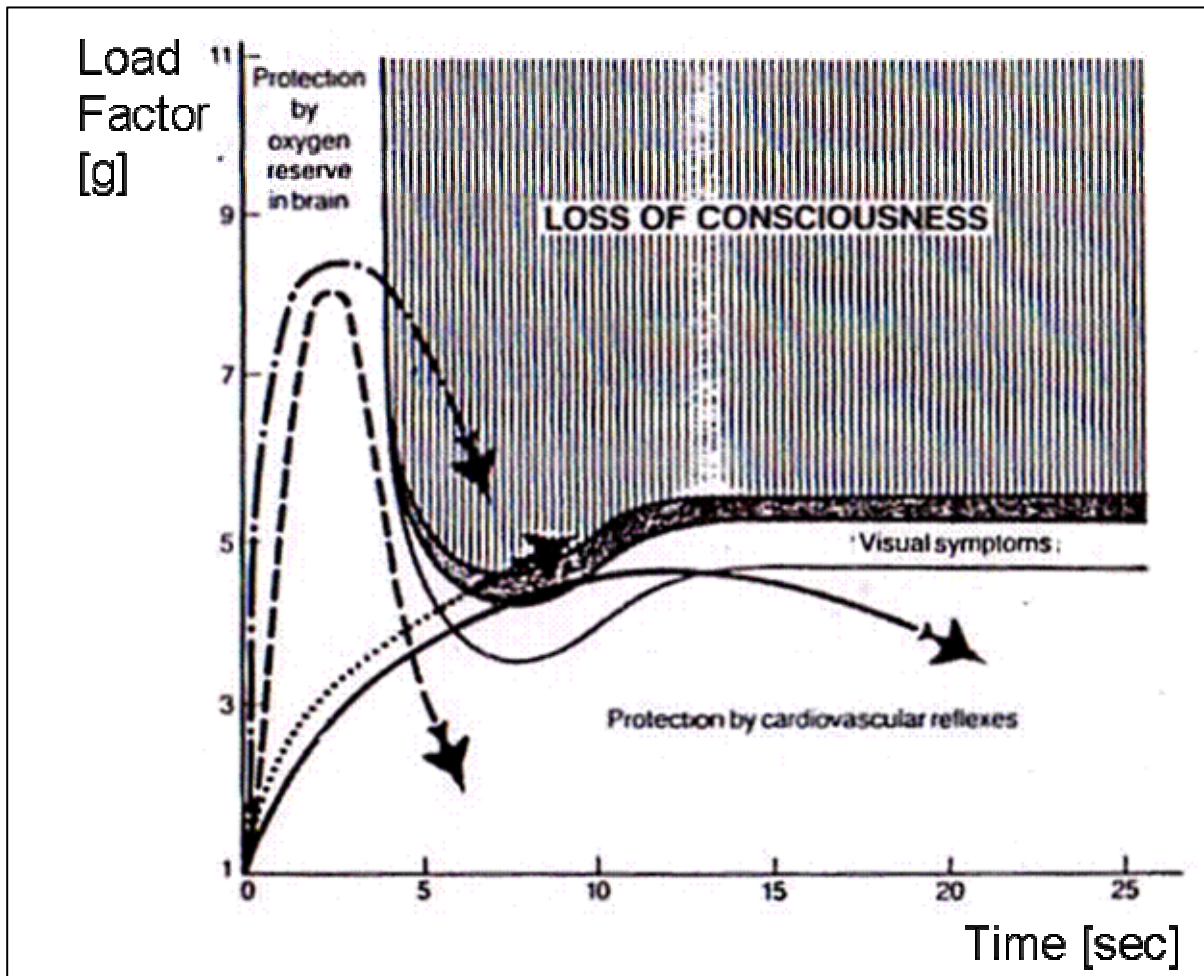


Fig. 4.2-7 Pilot "g" tolerance

Exceedance of those limits leads to reduced field of view, grey out, black out (pilot can't see but can still fly the aircraft), and eventually unconsciousness. If the g onset is more than 5 g per second, as experienced during operational flights for the first time at the end of the 70s in fighters like the F-16, blackouts can happen instantaneously and without physical warning. Between 1982 and 1997 the US Air Force lost twelve F-16 through G-LOC (loss of consciousness). As a result nine pilots lost their lives. With proper protection (anti g-suit) the pilot can sustain much higher values and the structural design limits can fully be used for aircraft manoeuvres.

A novel suit system made by the Zurich Firm Life Support System (LSS) solves this problem. The Swiss physicist Andreas Reinhard has been working on his version of the "anti-g-suit", the "Libelle", which has a liquid filling. In principle the body of a Pilot wearing "Libelle" is surrounded by liquid of the same density, which compensates any difference in pressure caused by centrifugal forces almost entirely and without delay. The "Libelle Suit" makes sure that organs do not become displaced, as is the case with the classical pneumatic suits when the pilot is exposed to g forces. The Eurofighter will be equipped with this system.

4.3 Unstable Configurations and Digital Flight Control

Air vehicle performance used to be the prime driver in configuration development. Initially the maximum speed was the key parameter and led to the development of ever faster vehicles, eventually supersonic aircraft. However, thermal effects and material limitations limited the number of aircraft designed to go significantly faster than $M = 2.2$. Manoeuvrability and agility became more dominant in the 70ies and 80ies. One way to improve these characteristics is to reduce the static stability of the aircraft.

A stable configuration will return to its initial condition, i.e. angle of attack, after a disturbance occurs, e.g. by a gust **Fig. 4.3-1**. This is achieved by the fact that the neutral point is aft of the c.g. and the additional lift at increasing AoA can generate a pitch down moment which forces the aircraft back to the initial trimmed AoA. Since stable configurations have a considerable trim drag, in particular at higher angles of attack (because the tail has to generate a down-draft rather than lift (**Fig. 4.3-2**), an unstable configuration can generate more lift at less drag (**Fig. 4.3-3**).

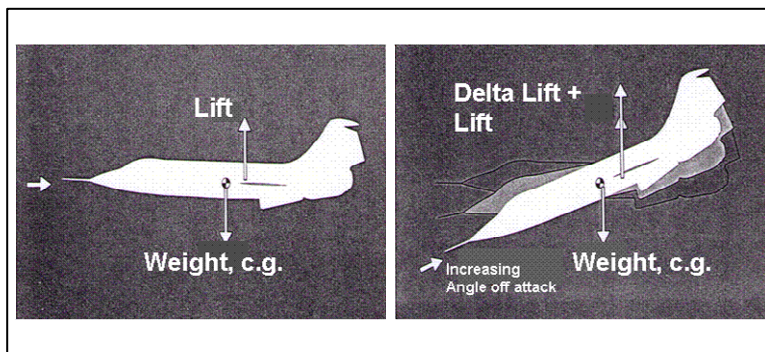


Fig. 4.3-1 Stable Configuration Arrangement

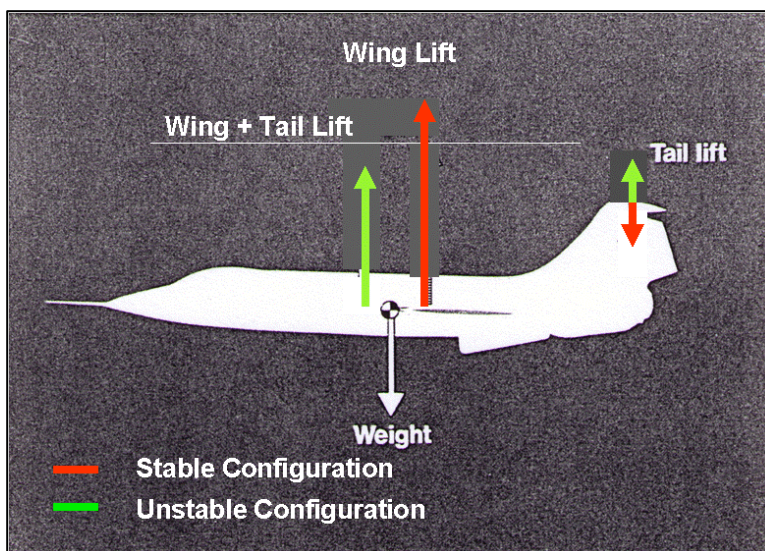


Fig. 4.3-2 Stable and unstable configuration

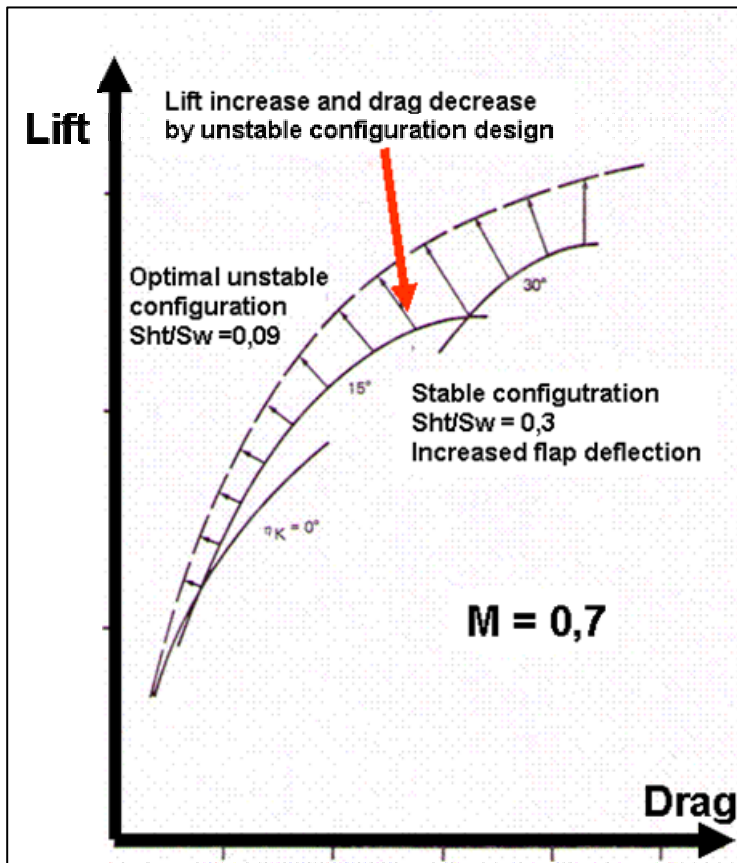


Fig. 4.3-3 Improved drag polar by reduced stability

However, to actually utilize this benefit such a configuration needs a stabilization system since the pilot is not capable to perform this function for the desired instability level. Though analog systems did provide a stabilisation (e.g. for the VSTOL aircraft), the real break through was only possible with the improvement of digital high speed computing capabilities.

MBB did develop the first quadruplex digital fly by wire system in the late 70ies. An F-104 was modified for the development and test. Mods included the addition of:

- the flight control system itself,
- air data sensors
- actuators
- droppable ballast weight at the aft tail (to move the c.g. aft)
- fixed canard behind the cockpit (to move the neutral point forward)

The system did still have a reversionary mode: if required, one could go back to the conventional mechanical flight control system, **Fig. 4.3-4**. Program start was 1974, the program ended in 1979.



Fig. 4.3-4 Modified F-104

The quadruplex system is based on a "voting" process using the results of all available lines: At the first failure or deviation from the average value of the 4 systems, three systems remain and do allow a voting in case of a second failure. No voting can be performed in case of a third failure.

The quadruplex system has per definition identical channels. If there is an inherent failure, it is contained in every channel and can not easily be detected. One option is the dissimilar redundancy, whereby one channel is for example analog or has been programmed by a different person. Also neural network/self adapting systems are being investigated. The problem with these systems is still the certification, because the results are not based on a deterministic approach.

The results and experience with the CCV-104 program provided the basis for the X-31 and Eurofighter FCS development at EADS.

The availability of digital flight control systems offers yet another feature: Known constraints and limitations can be incorporated in the FCS and the pilot does no longer have to worry about them. If his commands would lead to an unacceptable/forbidden manoeuvre, the FCS automatically limits his input. In particular structural overloads can be prevented, e.g. excessive roll rates or g loads with external stores or AoA or sideslip angles. This feature is called "**carefree handling**" and is incorporated in the Eurofighter.

4.4 Thrust Vectoring

4.4.1 X-31 Enhanced Fighter Manoeuvrability (EFM) Program

Loosing control at high angles of attack is still a very common source of airplane accidents. Otto Lilienthal crashed and died in such a situation (**Fig. 4.4-1**).



Fig. 4.4.1-1 Otto Lilienthal in his Hang Glider, ~1894

The US air force lost about 550 aircraft in 20 years in "out of control" situations, **Fig. 4.4-2**. And even today's commercial aircraft are not fool proof as the Birgen Air accident in 1996 indicates, **Fig. 4.4-3**.

<i>STALL / SPIN OUT - OF - CONTROL OPERATIONAL ACCIDENTS 1965 - 1986</i>			
Total losses (fighter / attack, bomber, trainer, etc): 566			
Fatalities per accident: 0.85			
Fighter / Attack			
<u>USAF</u>		<u>USN</u>	
F-4	68	F-4	73
F-100	30	A-4/TA-4	54
F-111	17	F-8	35
A-7	14	A-7	33
F-5	10	EA-6	21
F-15	10	F-14	18
A-10	8	T-2	17
F-16	5	A-6	14
Total value of fighter / attack losses: \$3.95 Billion			

Fig. 4.4-2 Out of Control Military Accidents, US Airforce and Navy

Nine months after the **crash of the Birgenair 757** off the coast of the Dominican Republic, the official accident report was published on November 8. The document states that the main reason for the disaster, which cost the lives of 178 passengers and 11 crew, was the failure of the crew to **interpret the signs of impending stall correctly and act accordingly**. The pilots were confused by false speed displays due to a blocked pitot.

Fig. 4.4-3 Crash of Birgen Air, 6th Febr. 1996

The loss of control starts with flow separation at the trailing edge of an airfoil and is progressing towards the leading edge at increasing angle of attack. As soon as the flow starts to separate from a control surface the control power is being reduced, as shown in **Fig. 4.4-4**, a pictorial presentation of flow separation, generated with a two dimensional flow calculation.

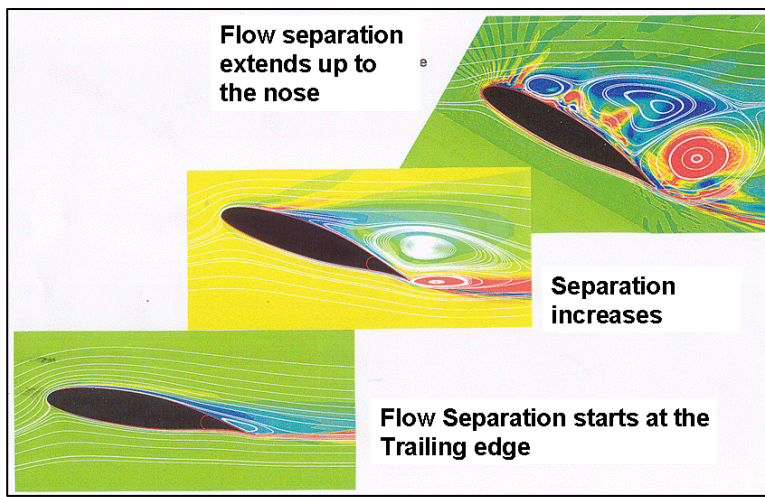


Fig. 4.4-4 Two dimensional calculation of flow separation

If there is the need or the desire to control an aircraft even in these situations, i.e. at high angles of attack when aerodynamic control surfaces quit working and/or at very low dynamic pressure, a different approach has to be taken.

Impulse control systems and thrust deflection systems are well known from the development of vertical take off and landing aircraft. With the increase of the thrust/weight system in fighter aircraft to values above one (**Fig. 4.4-5**) the question arises: can one use this capability to reduce take-off and landing distance without the complexity of full vertical take-off/landing capability. Birds do it all the time, in particular if they have a long "landing gear".

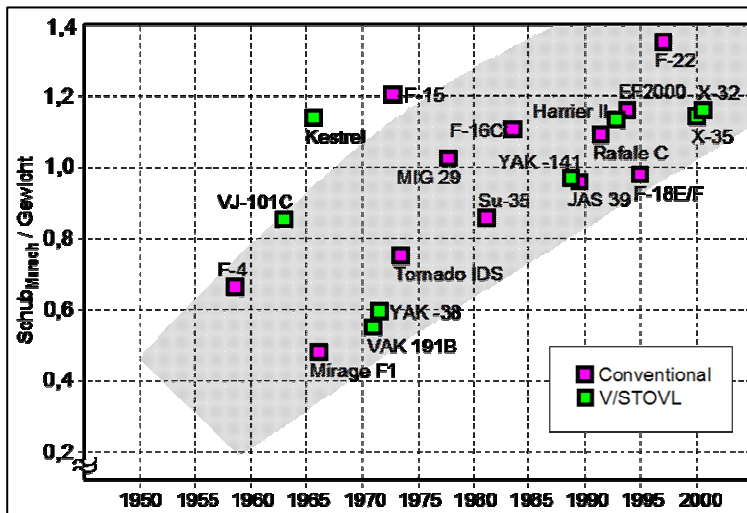


Fig. 4.4-5 Evolution of Thrust/Weight Ratio

Fig. 4.4-6 shows a landing gear design which provides sufficient tail clearance to allow landings at high angles of attack. During the derotation the aircraft c.g. is to be maintained right above the landing gear. This concept was discarded at MBB in the early 70ies since the computer technology available did not allow to develop a sophisticated control system including the use of a vectoring nozzle for pitch and yaw control at low dynamic pressure/high AoA.

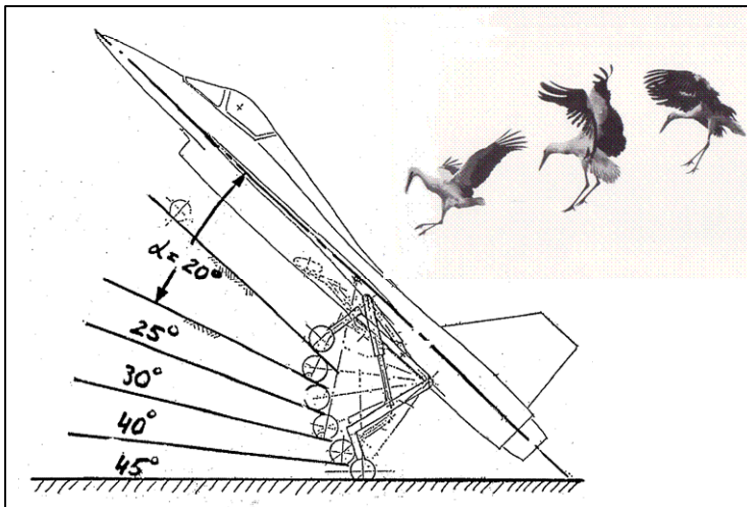


Fig. 4.4-6 Poststall Landing Gear, Grashopper, 1973

The activities were redirected by Dr. W. Herbst to investigate controllability and maneuverability at high angles of attack with the aid of a thrust vectoring system. Fig. 4.4-7 illustrates the principle characteristic of lift vs. angle of attack. With increasing AoA the linear relationship is lost and the lift reaches a maximum, thereafter lift decreases and at 90° AoA the lift becomes zero (Post-Stall regime). The flow field for a delta canard configuration reflects this behaviour: The steady flow at lower AoA is becoming more and more disturbed with increasing α . It is evident, that the disturbances are starting at the trailing edge of the wing moving forward with increasing α .

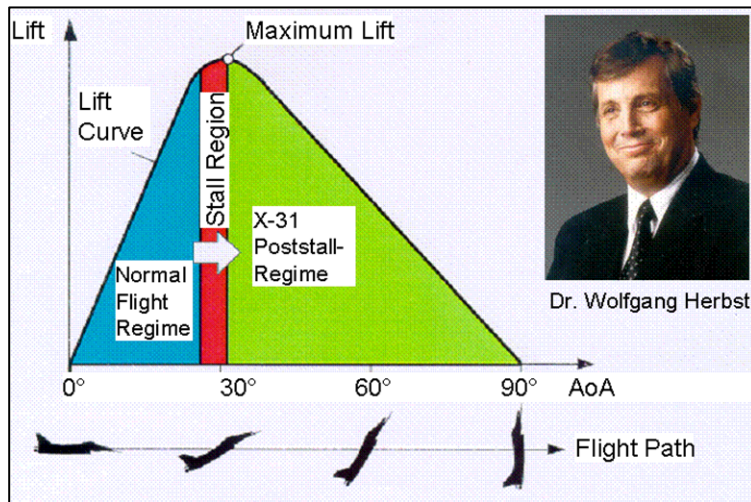


Fig. 4.4-7 Post Stall Regime

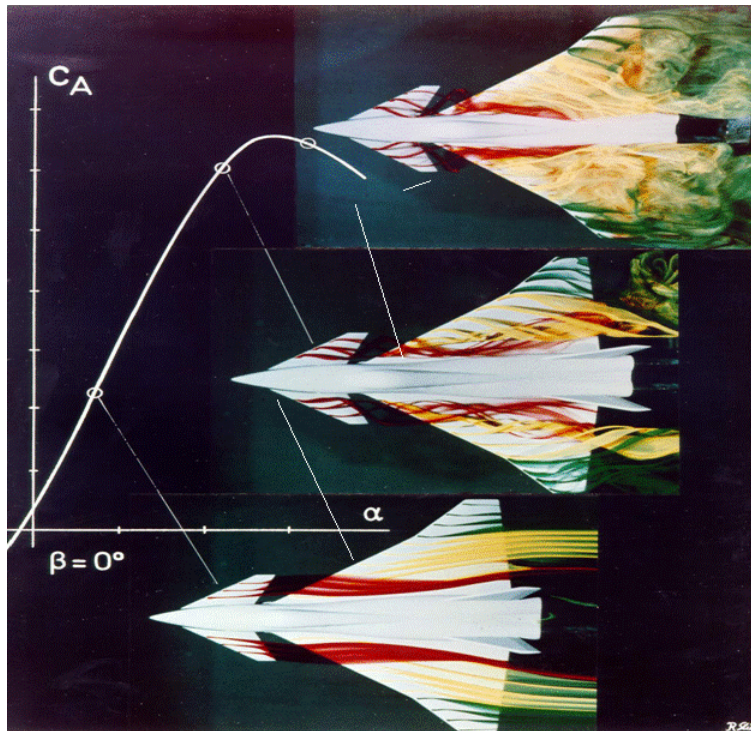


Fig. 4.4-8 Flow visualisation in a water tunnel

By adding a thrust vectoring capability to deflect the engine exhaust, pitch- and yaw control moments can be generated. Roll control around the body axis is zero for single engine ac and small for twin engine configuration, depending on engine separation.

Initial digital and manned simulation in the late 70ies confirmed, that flying high angle of attack manoeuvres during close in air to air combat leads to a significant improvement in the exchange ratio, in particular for the gun (**Fig. 4.4-9**).

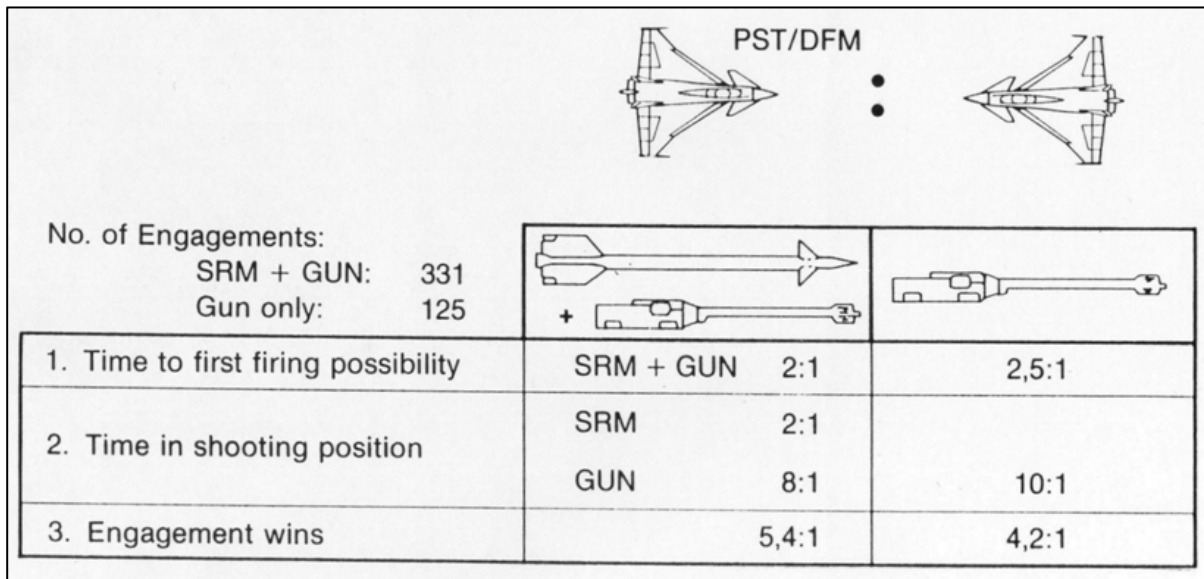


Fig. 4.4-9 Results of Close in Combat Simulations, IABG, Ottobrunn 1979

Based on these results MBB tried to convince European companies to join in a demonstrator program. Neither Dassault nor BAe or Alenia were willing to engage in such a program, though their independent studies confirmed MBB's simulation results. However, contacts to the US finally brought the desired result. North American Rockwell, eager to get back into the fighter business, proposed such a program to DARPA (Defence Advanced Research Agency). After an evaluation of the MBB proposed vehicle in the manned Simulator at the IABG in Ottobrunn by DARPA pilots the program got real.

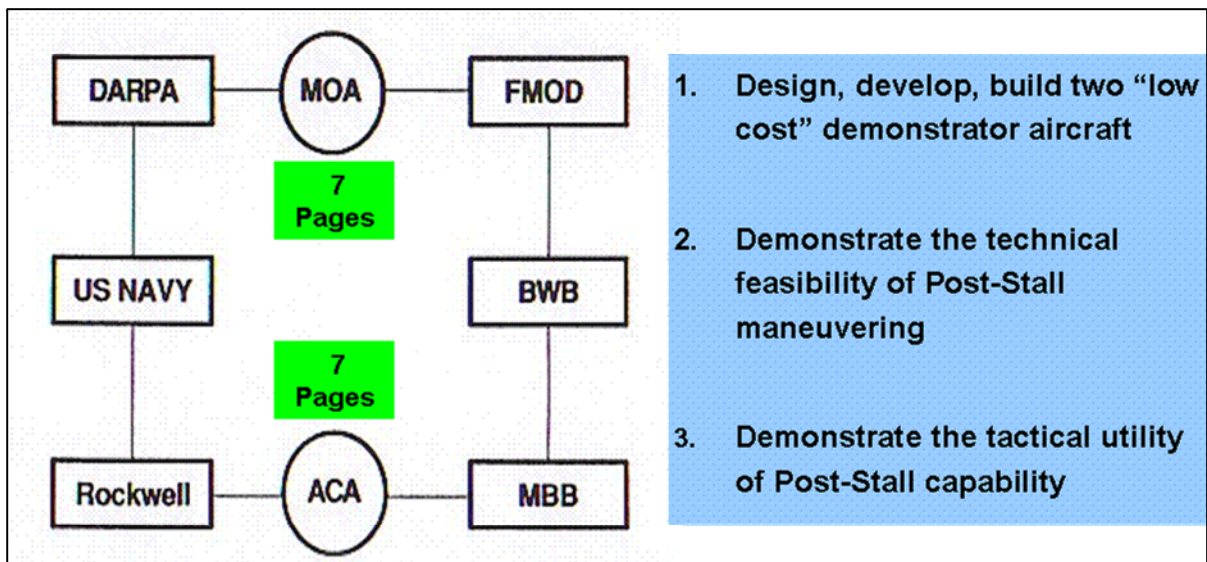


Fig. 4.4-10 Government / Industry Organization & X-31 Program Objectives

A 7 page Memorandum of Agreement was signed by DARPA and the German MOD, accompanied by an Associate Contractor Agreement (ACA) between MBB and Rockwell in 1986 and provided the framework for the X-31 program. It is important to note that the objectives (Fig. 4.4-10) were unchanged throughout the 10 year program, in spite of frequent changes of program managers on both sides and severe financing difficulties. A very important aspect for

the cooperative spirit and therefore the success of the program was the fact, that all the data, reports, results etc. generated (foreground rights), were available to both parties.

Since both companies had experience with variable sweep aircraft (Tornado and B-1) and also canarded configurations (TKF/J-90 studies and HIMAT) and were not competing in the fighter market, the configuration selection was quickly achieved. Based MMB's extensive design and analysis work a scaled down J-90 delta canard configuration with a single engine was selected (Fig. 4.4-11 and Fig. 4.4-12).

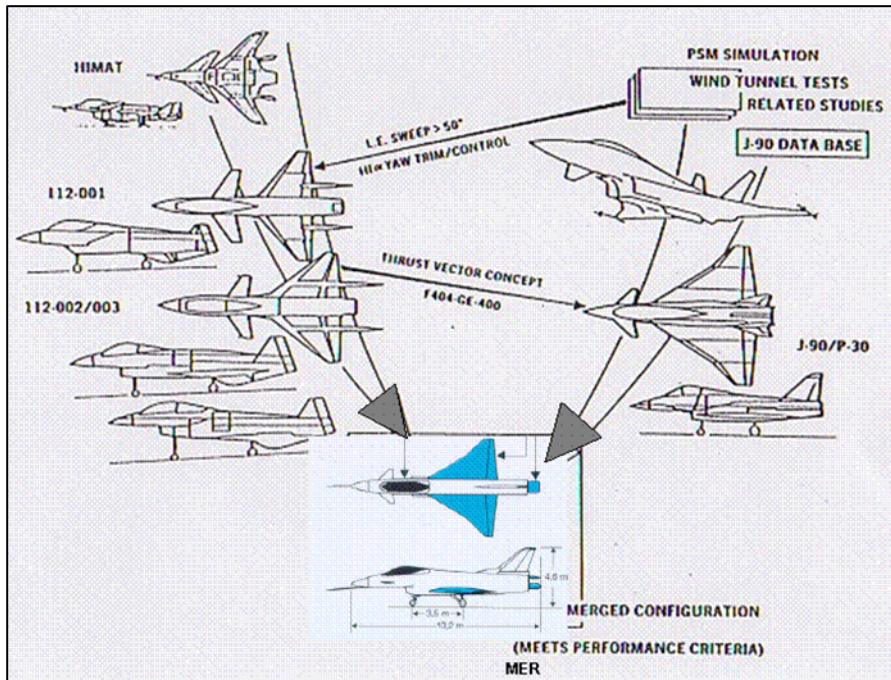


Fig. 4.4-11 Configuration Selection Process

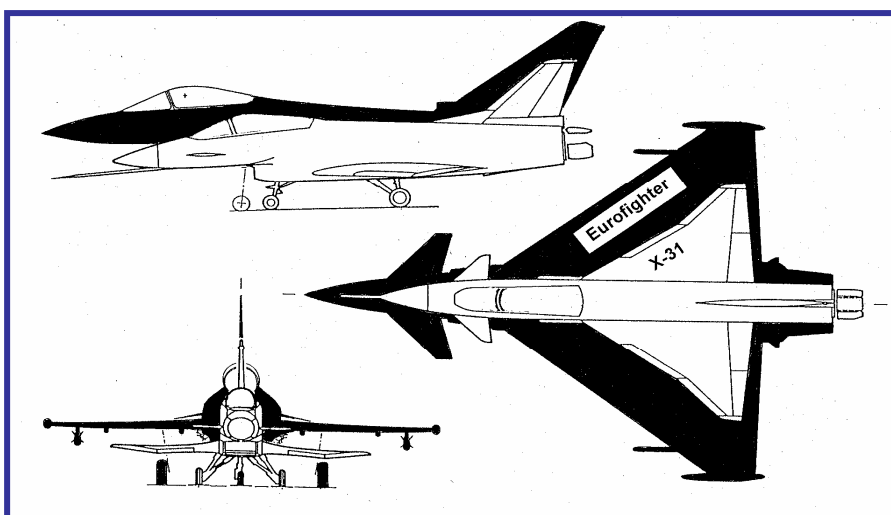


Fig. 4.4-12 Size Comparison of X-31 and Eurofighter

The US side accepted the initial work performed by MBB between 1975 and 1985 as a significant contribution to the program and the cost share of the joint program was agreed to be

25% German and 75% for the US side. This is also reflected in the work share. Nevertheless MBB got very important and challenging work packages (**Fig. 4.4-13**).

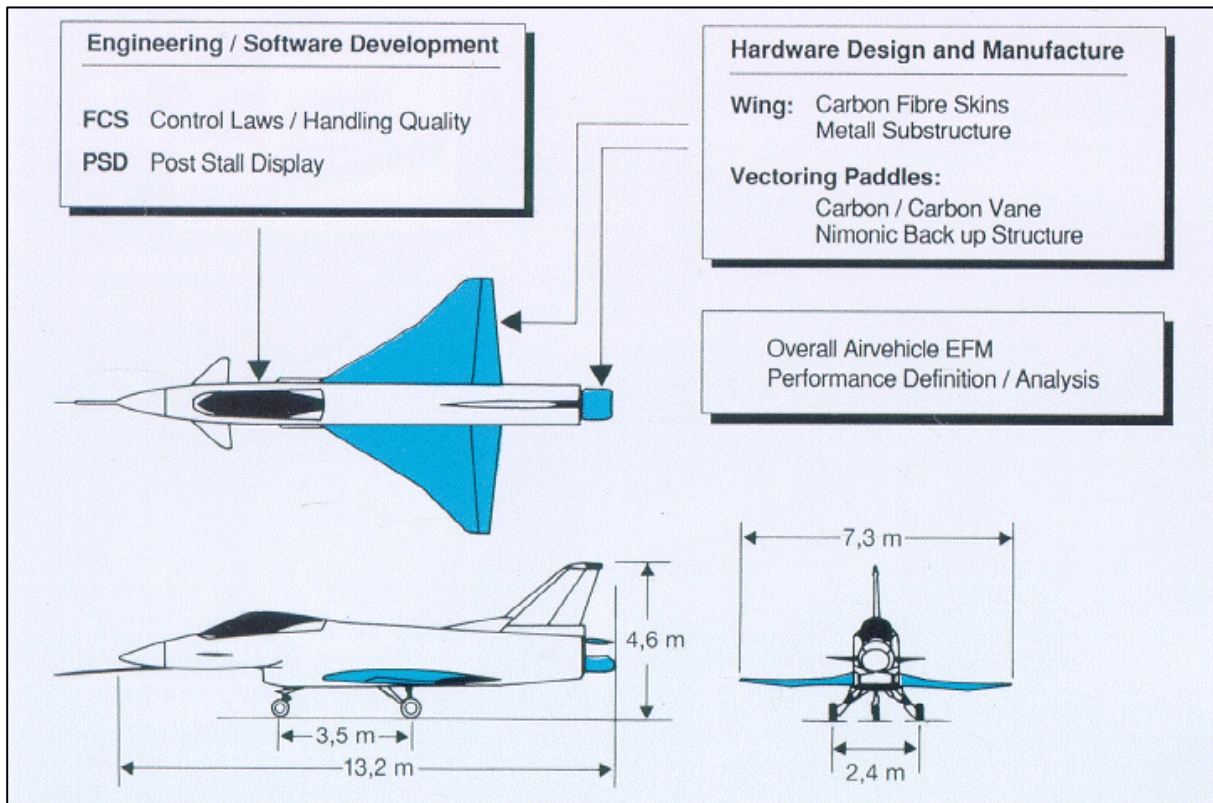


Fig. 4.4-13 Primary MBB Work Share

Design and manufacturing of the wing, with carbon fibre skins and a metallic substructure, was a challenge, because MBB had not build a wing since the VJ-101 and the carbon fibre/resin to be used was a new system planned for the Eurofighter. Material data and manufacturing processes needed to be generated, confirmed and established. The experience gained within the X-31 program was very valuable for the Eurofighter production.

The US Navy had tested a (metal) spoon like jet deflection vane on the F-14. The geometry was adapted to the F-404 engine and the decision was made to build the vanes from Carbon/Carbon rather than steel, to save weight. An arrangement with three vanes with 120 degree separation was selected. Wind tunnel and full scale tests behind an F-18 were performed to determine the side forces by deflecting the vanes **Fig. 4.4-14**. The resultant force diagram is shown in **Fig. 4.4-15**.

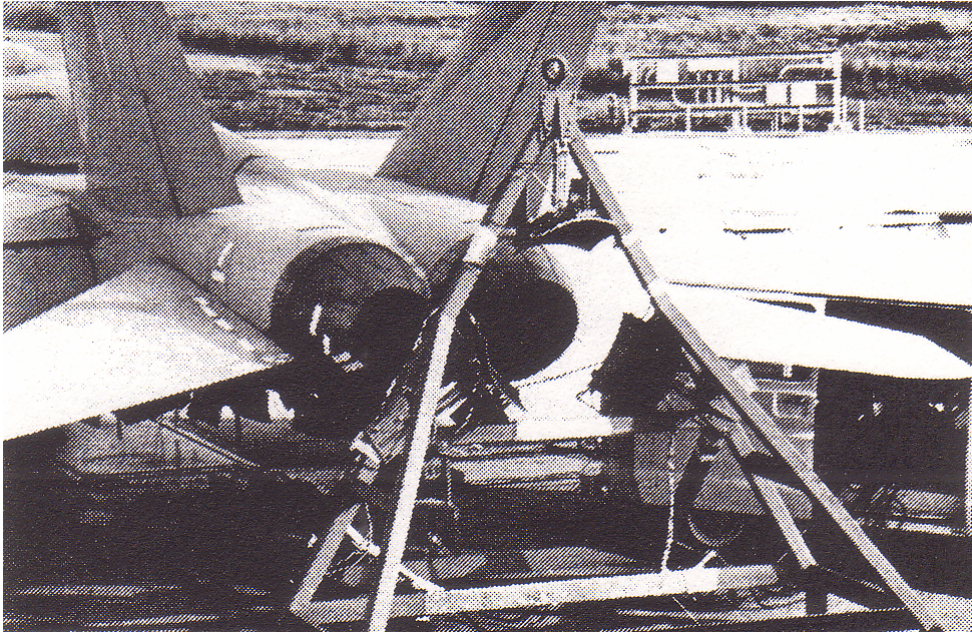


Fig. 4.4-14 Thrust Vectoring Tests behind an F-18

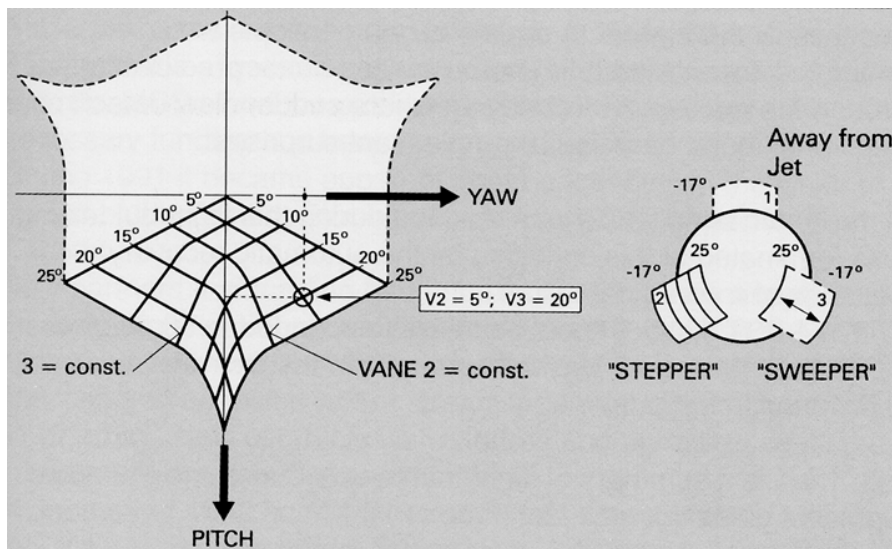


Fig. 4.4-15 Side force generation with the vane system

Only two companies in Europe were candidates for the manufacturing of the vanes. The French one had experience in aerospace products and was five times as expensive as the German company SIGRI (now SGL Carbon). We decided for SIGRI and had a close cooperation with the military certification agency ML from the outset, to jointly establish the manufacturing and certification procedures. SIGRI had never before manufactured a flight article. Very little design data were available, and certainly no experience with the vibration and acoustic loads to be expected. All 10 vanes manufactured had delaminations (**Fig. 4.4-16**) during the first cycles but all could be cured by improved tools and manufacturing processes. The fabrication cycle time for the vane was 9 month! The ground tests were successful and we never had any problem with the C/C structure. They look like new, even today. Metal parts from the supporting attachment structure had to be exchanged because of the wear by vibration loads.

The overall arrangement of the vanes at the aft end is shown in **Fig. 4.4-17** in comparison to a triple metal vane arrangement with external actuators and significant ballast in the nose of the NASA F-18 HARV (High AoA Research Vehicle), which resulted in high moments of inertia in pitch and yaw.

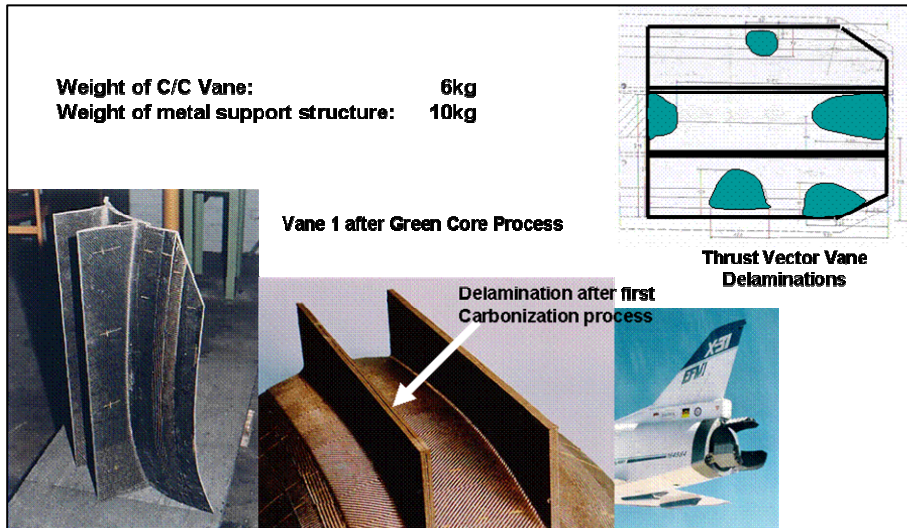


Fig. 4.4-16 Vane with delaminations after first curing cycle



Fig. 4.4-17 General arrangement of TV vanes at X-31 and F-18 HARV

Control power for trailing edge, canard and rudder has a strong dependency with angle of attack; see **Fig. 4-18** through **Fig. 4-20**. The configuration is designed to be recoverable by pure aerodynamic control, even at 70 degree angle of attack. Note that the pitch down power of the trailing edge flaps at that point is almost zero, while the canard is still working properly, another reason for the long coupled canard arrangement. The rudder is losing its control power around 25° and above 40° AoA it has no efficiency left.

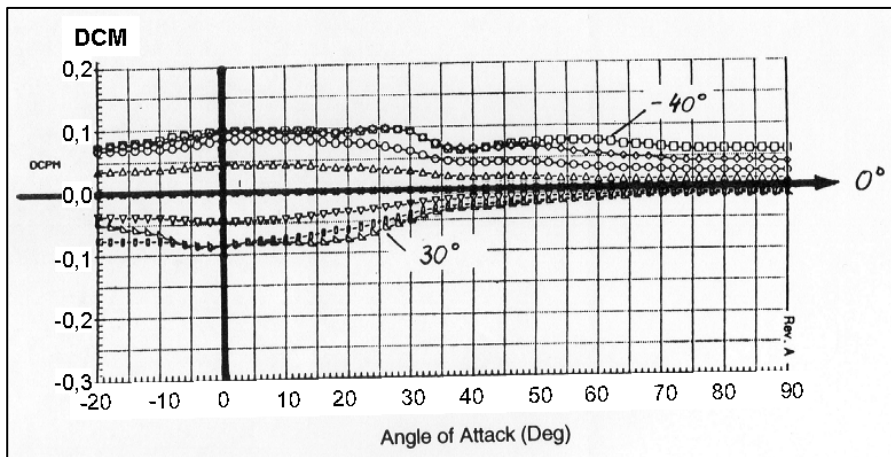


Fig. 4.4-18 Trailing edge pitch power vs. angle of attack

Roll manoeuvres at high AoA must be performed around the velocity vector rather than the body axis to prevent critical sideslip angles. Therefore thrust vectoring around the body yaw axis is essential for Post-Stall manoeuvres. The available acceleration in pitch and yaw resulting from aerodynamic surfaces and thrust vectoring is summarized in **Fig. 4.4-21**.

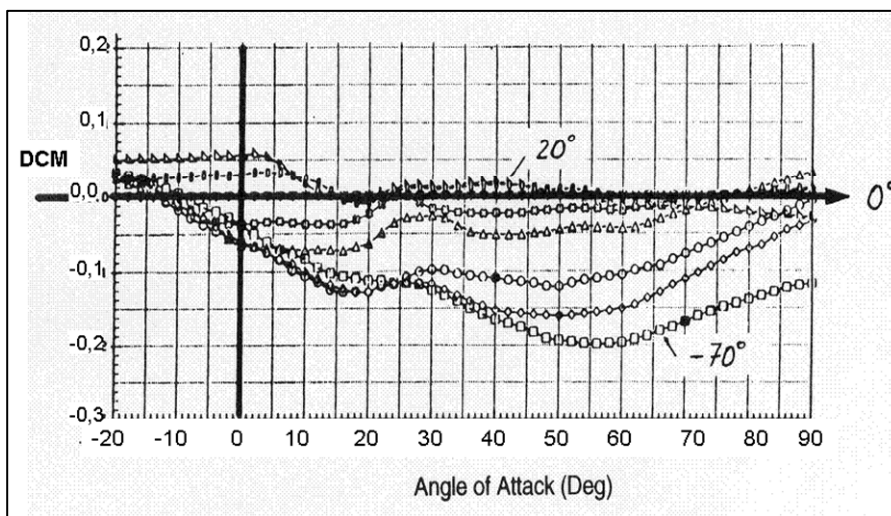


Fig. 4.4-19 Canard pitch power vs. angle of attack

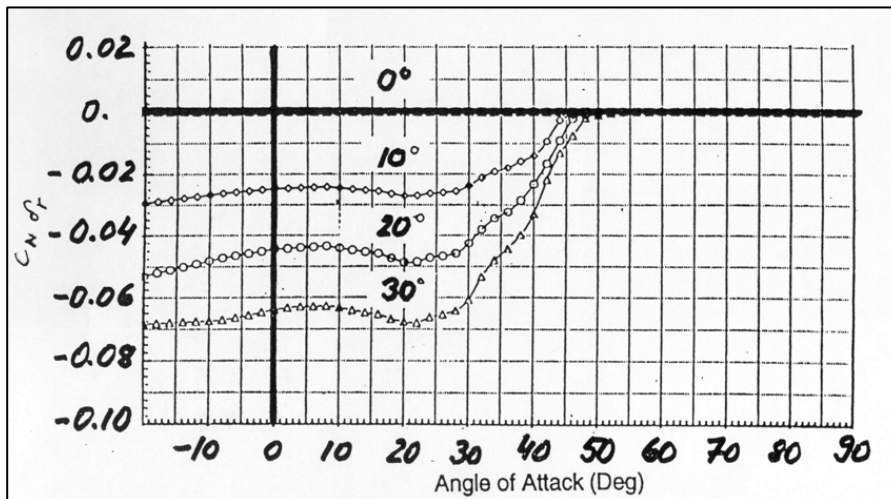


Fig. 4.4-20 Rudder power vs. angle of attack

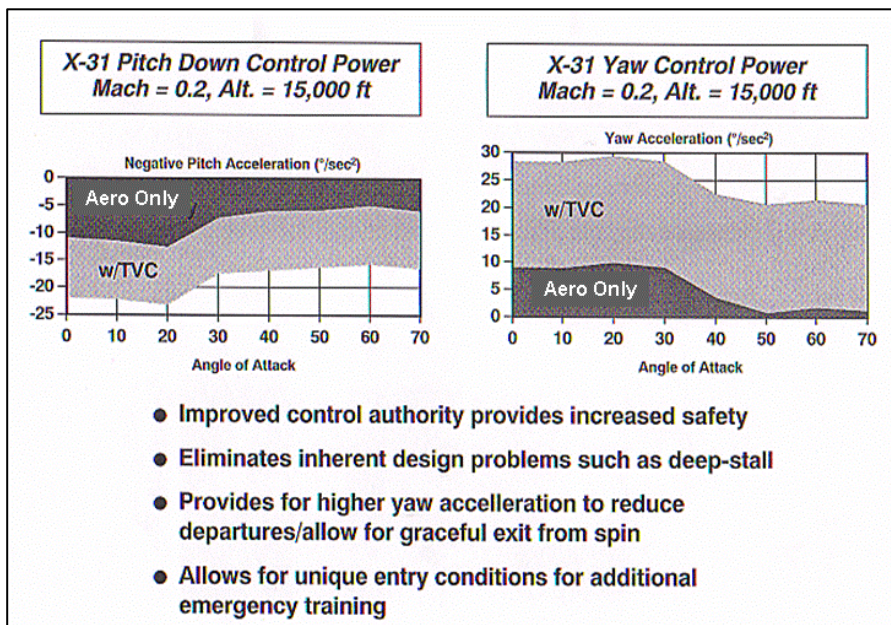


Fig. 4.4-21 Total Control Power, Aero and Thrust Vectoring

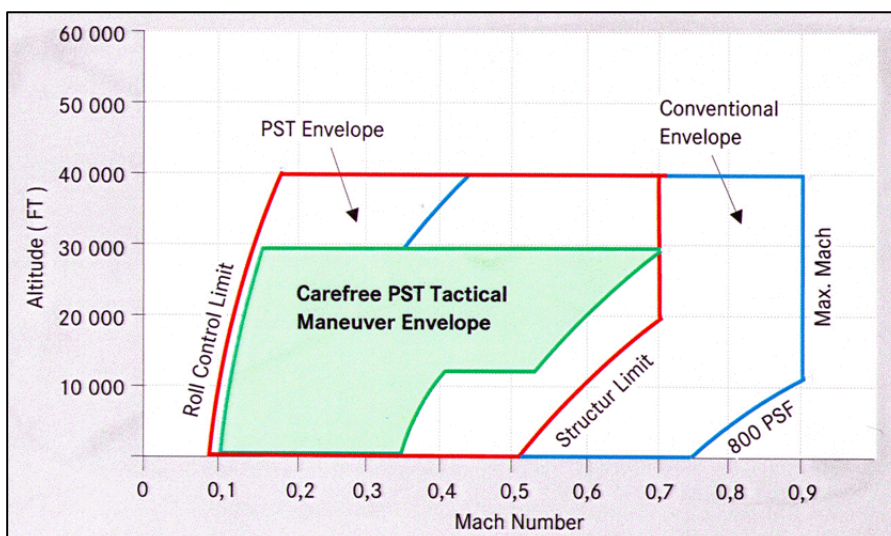


Fig. 4.4-22 X-31 conventional and PST flight envelope

The conventional and Post Stall envelope of the X-31 is presented in **Fig. 4.4-22**. Though the primary objective of the program was to test the aircraft at high AoA no spin testing was performed, because the thrust vectoring system should allow to always prevent an uncontrolled flight and recover the aircraft. A prerequisite was that the engine would be operational throughout the envelope. Thanks to the drooping lip at the inlet and good engine characteristics (F-404) we never had any engine problem during the program.

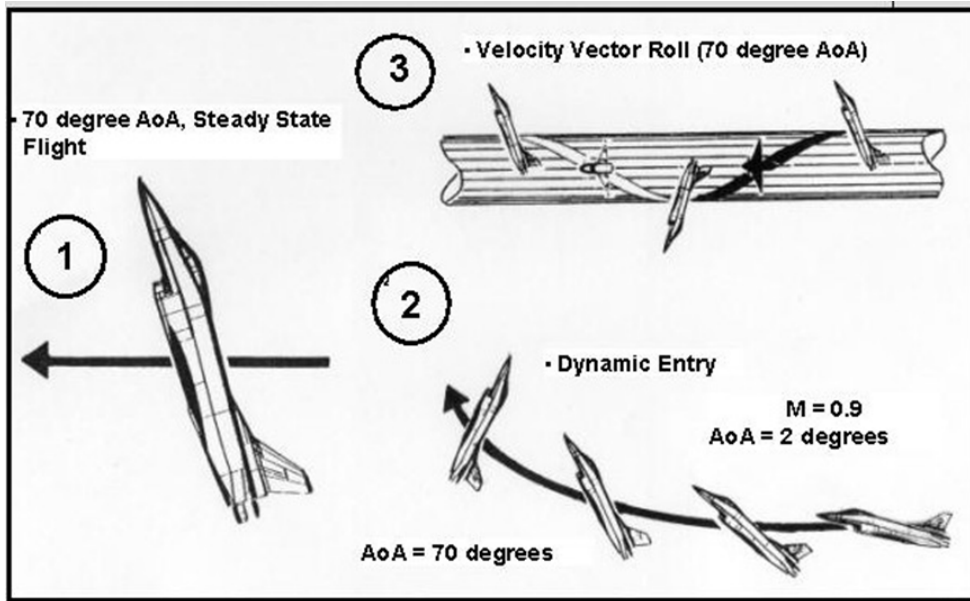


Fig. 4.4-23 Post-Stall Test Milestones

After the conventional envelope was cleared the feasibility of high AoA manoeuvres was demonstrated in an incremental approach by three milestones: steady state flight a 70° AoA, dynamic entry into the Post-Stall arena and velocity vector rolls up to 70° AoA, **Fig. 4.4-23**. These test resulted in only two changes to the external geometry of the aircraft and is an indication of the design skill of the engineers.

Initial wind tunnel tests were performed with booms at the aft fuselage housing the thrust vectoring vane attachment and actuation. In the detail design phase these were integrated into the aft fuselage structure. However the pitch-down contribution of these booms was missing in the data set and had to be reinstated by two boards, which were bolted onto the aft fuselage (**Fig. 4.4-24**). This reduced the pitch trim deflection of the trailing edge flaps and provided enough roll control power for the coordinated velocity vector rolls (there is no other roll power control surface than the trailing edge flaps!).

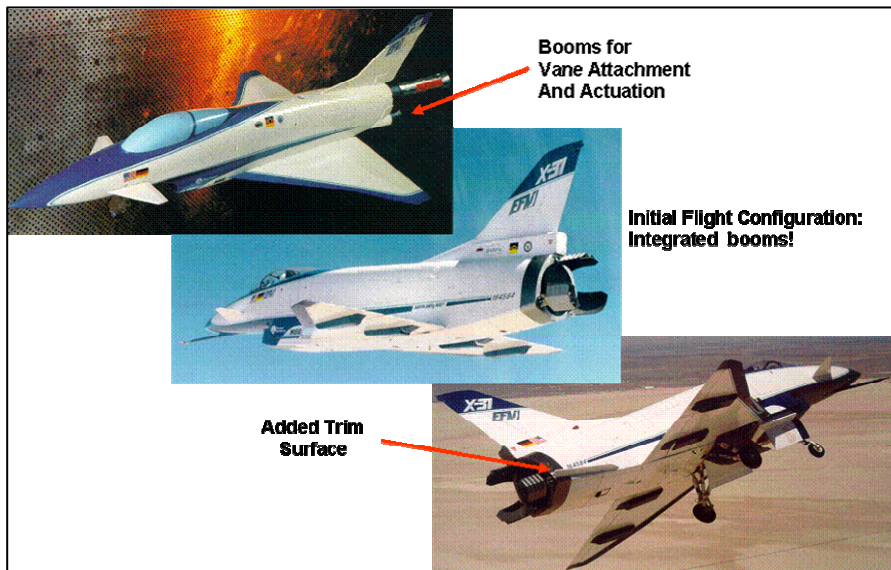


Fig. 4.4-24 Trim surface bolted on to aft fuselage

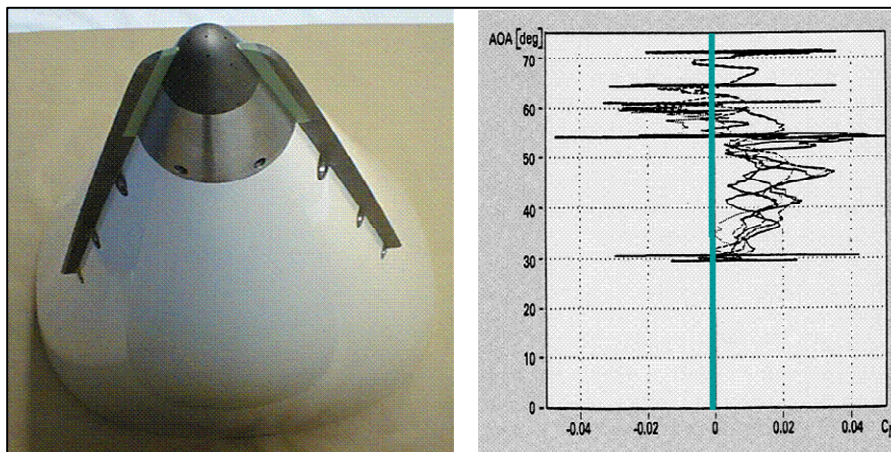


Fig. 4.4-25 Addition of nose strakes

The second configuration change was the addition of two nose cone strakes to eliminate uncontrolled vortex separation resulting in strong yawing moments, **Fig. 4.4-25**. One of these tests resulted in the one and only spin entry which was quickly recovered.

The aircraft was then cleared for tactical flight testing. Close in Combat (CIC) engagements were flown primarily against the F-18 available at NASA Dryden, but also against F-14, F-15, and F-16. Simulated gun and missiles were used to conduct the tactical performance evaluation. The results were even better than found in the simulator (**Fig. 4.4-26**).

At the end of the tactical flight tests one aircraft was lost due to icing in the pitot-static tube. The pilot ejected safely. An accident evaluation board was established and an in-depth accident report was prepared. Since the technical reason for the crash was known after a day, design changes to the sensor system and the flight control system were worked out and implemented, to prepare the aircraft for the extension of the Post-Stall envelope to sea level. This was required to demonstrate the Post-Stall capabilities at low altitude. An Air Show Routine

was developed and practiced by the pilots. The aircraft was shipped to Europe in a C-5A with one wing removed, reassembled in Manching and flown to Paris. It very successfully demonstrated Post-Stall manoeuvring at the Paris Air Show in 1995, **Fig. 4.4-27**. All objectives of the EFM program have been met.

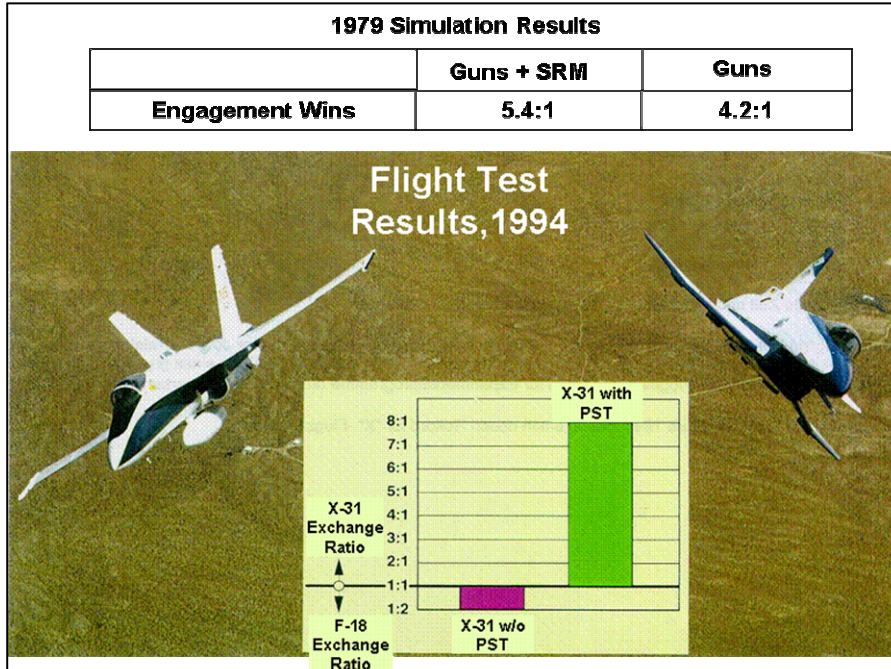


Fig. 4.4-26 Close in Combat effectiveness: Simulation vs. Flight Test

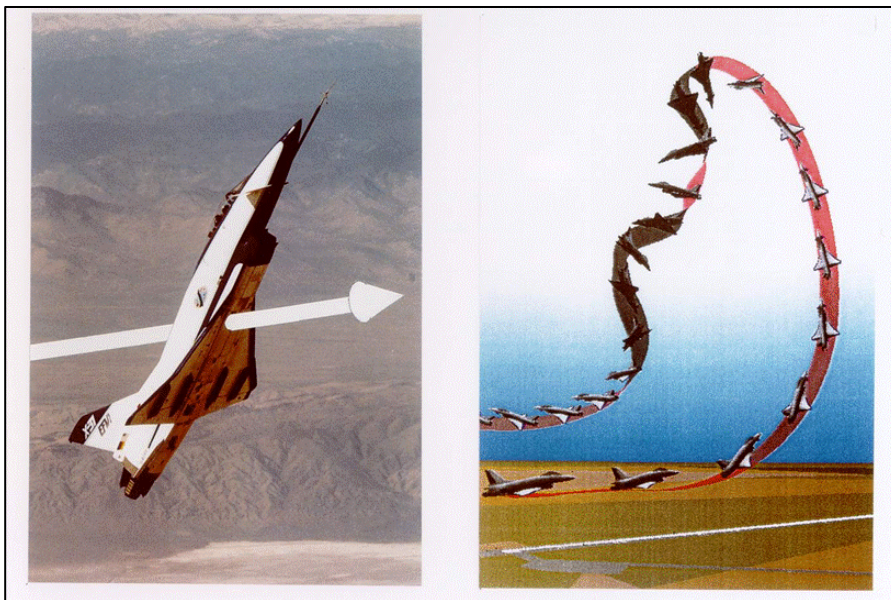


Fig. 4.4-27 Post-Stall Manoeuvre

4.4.2 The VECTOR Program

A second program using the X-31 aircraft was started in 1999. Participants were the US Navy, the German MOD, EADS (former MBB) and Boeing (former Rockwell). The objectives are listed in **Fig. 4.4-28**. The primary objective was to land the aircraft at higher AoA thereby reducing the approach speed with beneficial effects on wheels, brake and tires. The ESTOL concept (= Extremely Short Take-off and Landing) was in particular interesting for the US Navy. And also to use thrust vectoring for early rotation during take-off, **Fig. 4.4-29**.



Fig. 4.4-28 Vector Program Elements

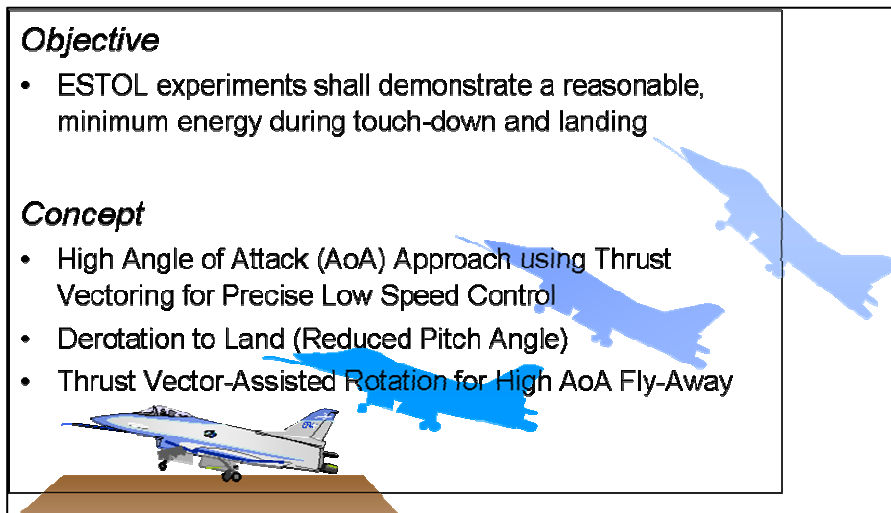


Fig. 4.4-29 Extremely Short Take-off and Landing (ESTOL)

The X-31 EFM program was flown with a conventional noose boom mounted air-data system to provide adequate air data, in particular in the high angle of attack regime. The Advanced Air Data System (AADS) was designed to have similarly good characteristics as a boom system, because it is located at the most forward and least disturbed part of the aircraft and –since

it is flush mounted – eliminate the signature of the ADS. The tail-less operation was to demonstrate, that even a fighter with a reduced or tailless configuration could be controlled with thrust vectoring, thus reducing the radar cross-section. The thrust vectoring system was required to perform the fully automated ESTOL landing and of course to provide yaw and pitch power for a tail-less aircraft.

The aircraft required several changes in the soft- and computer hardware. In particular the accuracy of the navigation system relative to the runway was significantly improved using a special differential GPS to a "centimetre" level to allow the precise initiation and conduct of the derotation manoeuvre. This whole landing procedure was fully automated, however, the pilot could watch on a TV screen the manoeuvre with the option to take over and start a go around, **Fig. 4.4-30**. A picture of a landing with 24 degrees AoA is shown in **Fig. 4.4-31**. Derotation is initiated when the lowest point of the aircraft is about 2 feet off the ground. The approach speed was reduced from 160 kts to 120 kts resulting in significantly shorter ground roll.

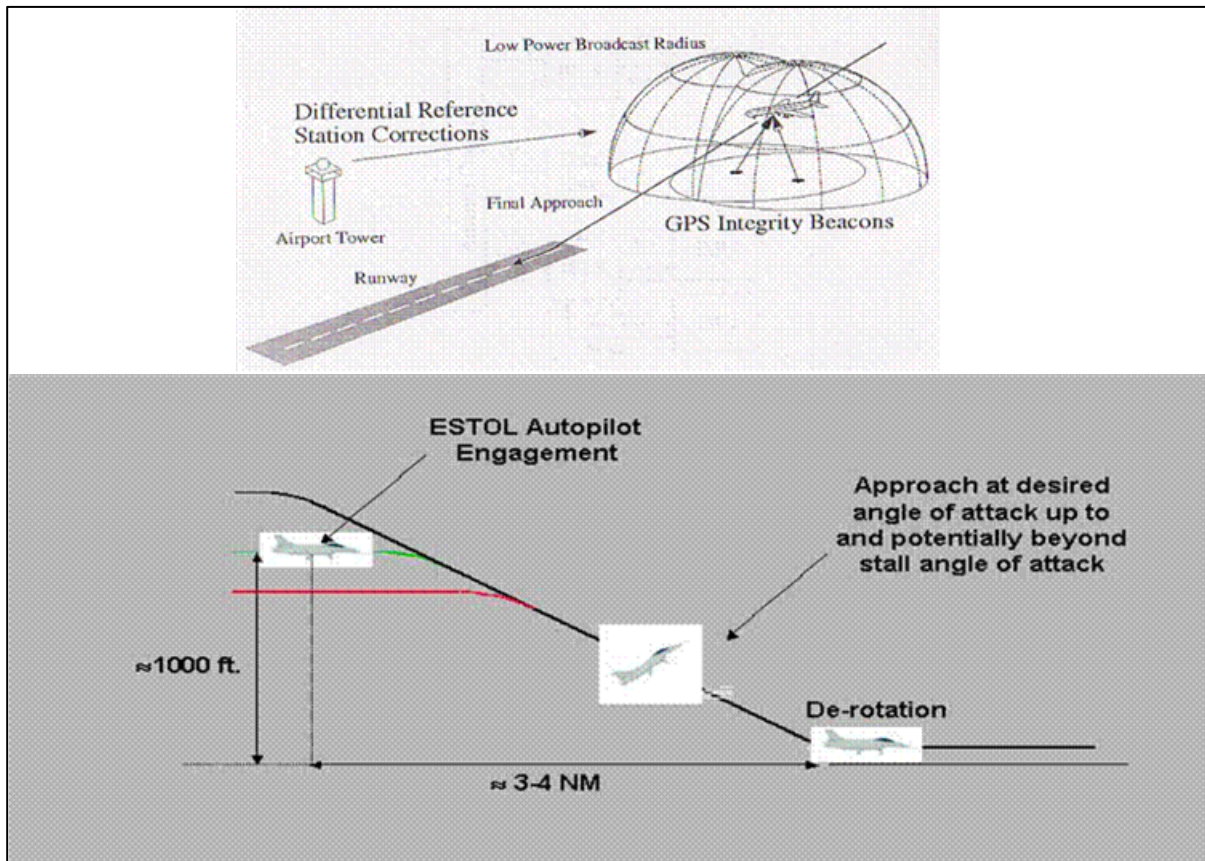


Fig. 4.4-30 ESTOL automated landing procedure



Fig. 4.4-31 Landing attitude at 24° approach, just before derotation

The flush air data system was flown in parallel to the conventional nose boom system, which had to be relocated to the upper side of the nose cone to not disturb the airflow; it was not used as the primary ADS for the flight control system.

Due to shortage of program funding the tailless aircraft was not tested in flight. Wind tunnel tests were performed and the new aerodynamic data set was integrated into the flight control system and the evaluation was successfully completed on a simulator.



Fig. 4.4-32 Thrust Vectoring is a reality and used on operational aircraft of the US and Russia

Thrust vectoring has not really been considered for commercial aircraft yet. The reasons why it is so difficult are the low thrust/weight ratio, the small moment arms for pitch and yaw with

wing mounted engines, and the fact, that there is no variable nozzle mechanism which could be used for deflection, **Fig. 4.4-33**.

Model flight tests have been performed in Israel using a Boeing 727 type configuration. Future configurations may offer new opportunities.

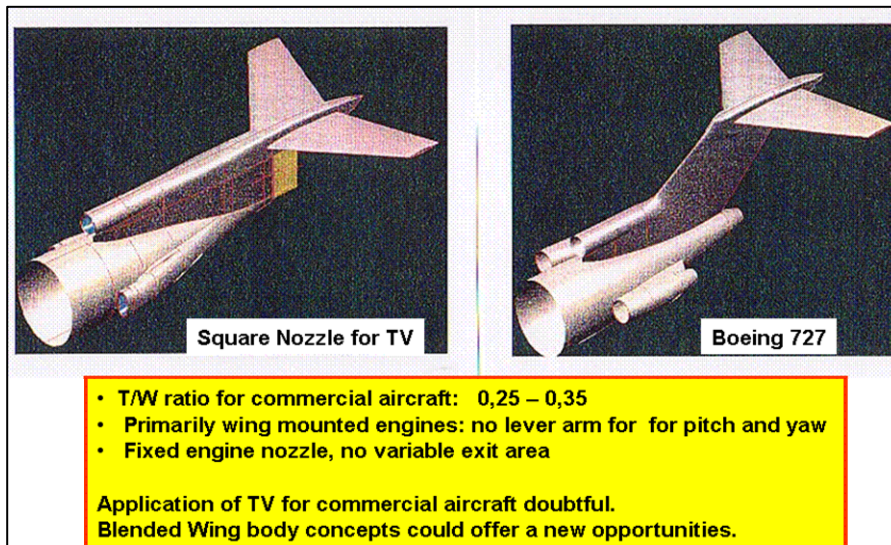


Fig. 4.4-33 Thrust vectoring is difficult to implement on commercial aircraft

The program took 3 years including the transfer of the aircraft from Dryden to the Naval Test Site in Patuxent River at the East coast and the reactivation of the aircraft after a 4 year period in "flyable storage".

The initial goal of MBB, to use thrust vectoring on the Eurofighter, has not (yet) been achieved. Provisions for TV have been made in the Eurofighter; this is currently an option for later upgrades using the TV-nozzle for the Eurojet engine developed by ITP (Spain). However, other US and Russian aircraft are already using thrust vectoring system in their operational aircraft, **Fig. 4.4-27**.

The X-31 aircraft is currently on display in the Deutsches Museum in Oberschleißheim.

4.5 Aircraft Signature

The signature of an air vehicle includes visual, radar, infrared and audible emissions. All of these can be detected, tracked and used to identify the location of the vehicle and even its type.

During WW I the famous "Red Baron", Manfred von Richthofen, painted his aircraft in bright red colour so the opponent would know already from the distance who was coming, **Fig. 4.5-1**. Later the camouflage principle, known from other military actions throughout the past centuries, was applied and the aircraft were painted like tanks and other vehicles, **Fig. 4.5-2**. Optical reflections (e.g. sun light) can be very strong and seen from quite a distance (**Fig. 4.5-3**).

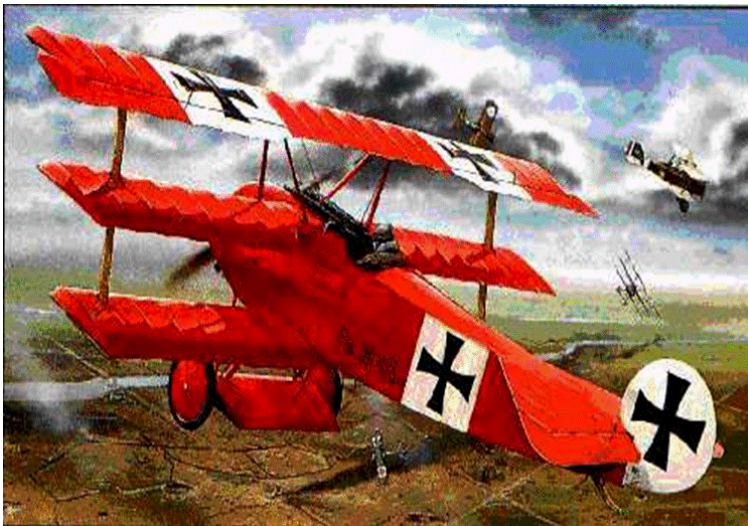


Fig. 4.5-1 Intentionally High Signature Aircraft: the "Red Baron"



Fig. 4.5-2 Optical Signature Reduction by Camouflage Paint

With the invention of other sensors for different frequencies it became more and more difficult to hide. It is important to know that each frequency/wavelength radiated by a vehicle (or a human being) can be detected and used to determine its location, i.e. direction and distance. The emissions used can be visible, electromagnetic, infrared or acoustic. The latter is a very important signal in the submarine environment. In the aeronautical world it did play a role during WW II.

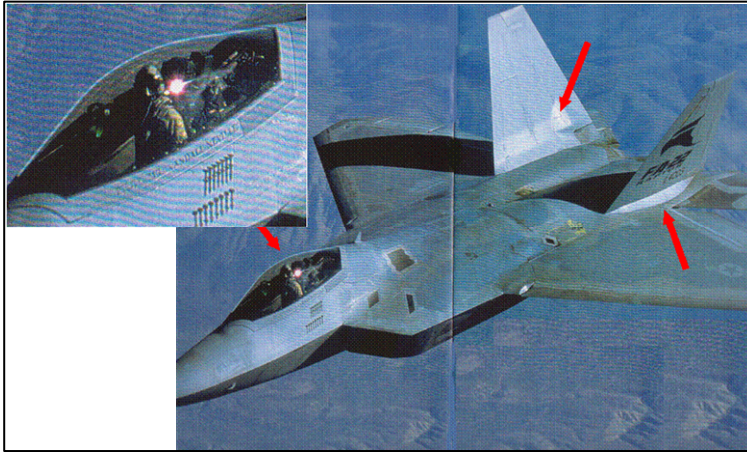


Fig. 4.5-3 Sun Reflection on Canopy and Structure

Radar signature got very important when radar systems allowed tracking the enemy from the far distance and in bad weather. But it was not until the late 60ies when the Russian Pjotr Ufimtsev published an article about "Methods of Edge Waves in the Physical Theory of Diffraction" that the radar cross-section could become a design parameter. The article was read by American engineers. It provided the mathematical tool to compute the signature of a body when illuminated with a radar beam and allowed to do trade studies.

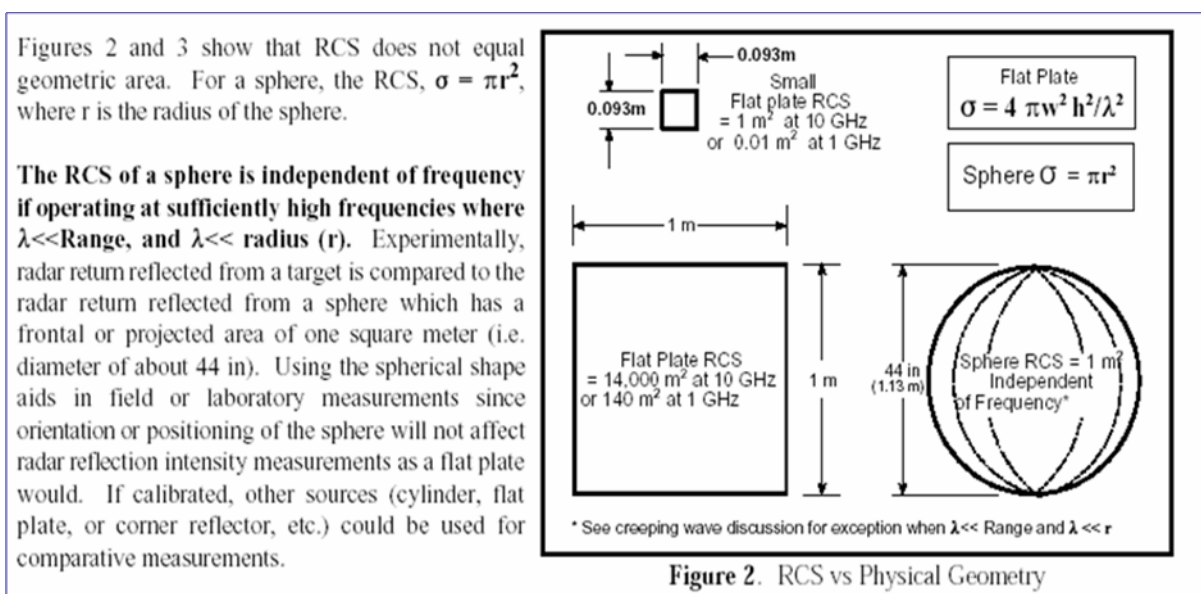


Fig. 4.5-4 Radar Cross-Section Definition

The definition of Radar cross section is given in **Fig. 4.5-4**. The energy radiated back from a body/vehicle is related to the energy reflected by a sphere with a cross-section/projected frontal area of 1m^2 ($\sim 1,13\text{ m}$ diameter). The radar return is a function of frequency, the higher the frequency, the higher the radar cross-section. Relative magnitude and direction of the radar cross-section are shown in **Fig. 4.5-5** for different body shapes. Obviously the radar return of a flat plate is high, however, but it is focused perpendicular to the plate's surface. There is almost no return in other directions. This is the reason why the initial stealth aircraft were designed with flat plate surfaces. A comparison of a sphere and a cube clearly identifies this characteristic **Fig. 4.5-6**.

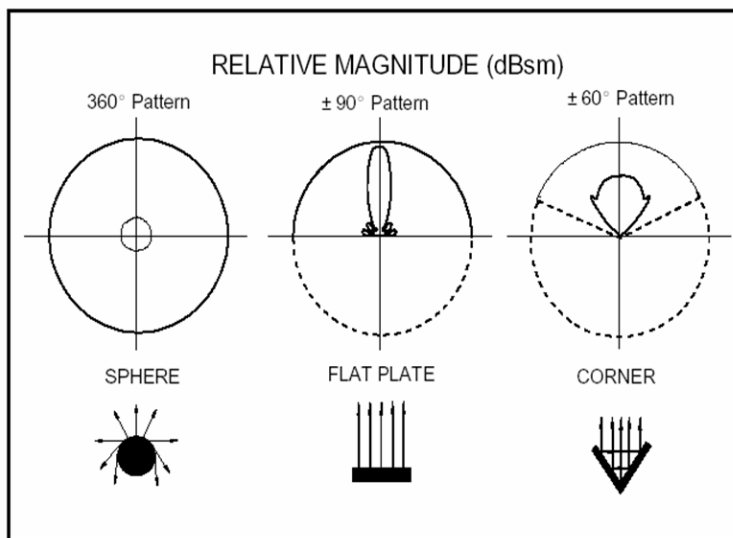


Fig. 4.5-5 Relative magnitude of Radar reflection for different body shapes

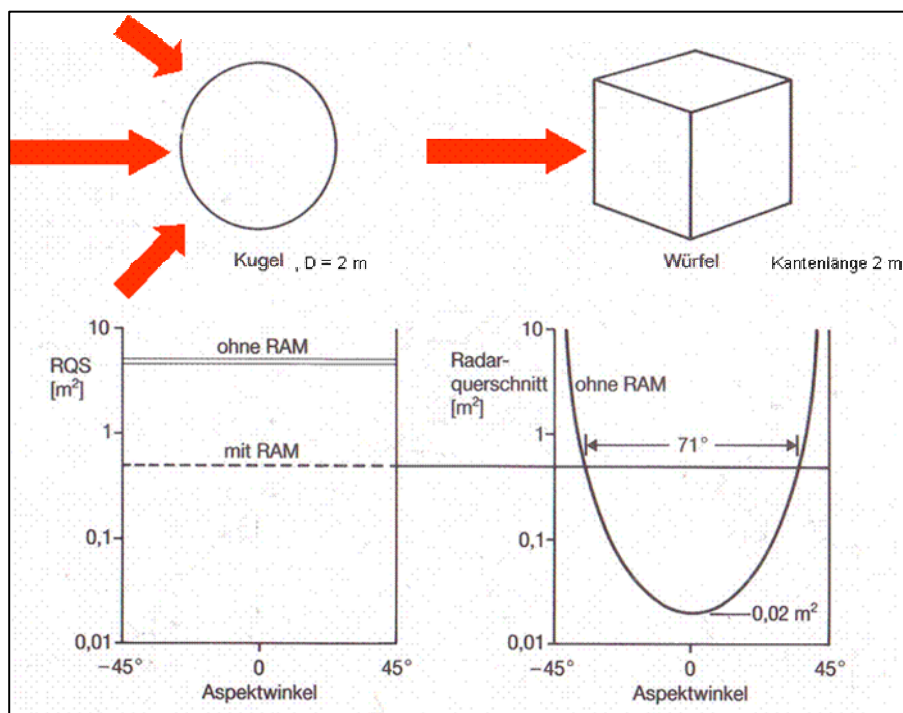


Fig. 4.5-6 Comparison: radar reflection of sphere and cube

Main contributors to radar cross-section (RCS) are identified in **Fig. 4.5-7**. The desired radar cross-section and its effect on the aircraft geometry is illustrated in **Fig. 4.5-8**, measures to reduce the radar cross-section are listed in **Fig. 4.5-9**.

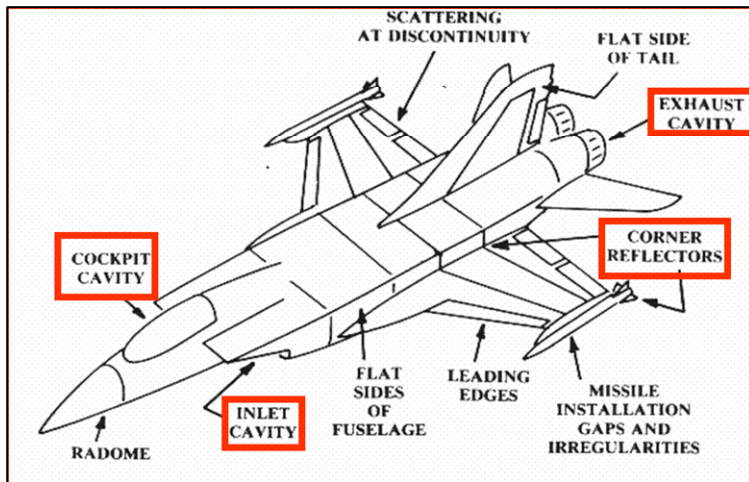


Fig. 4.5-7 Major contributors to radar cross section

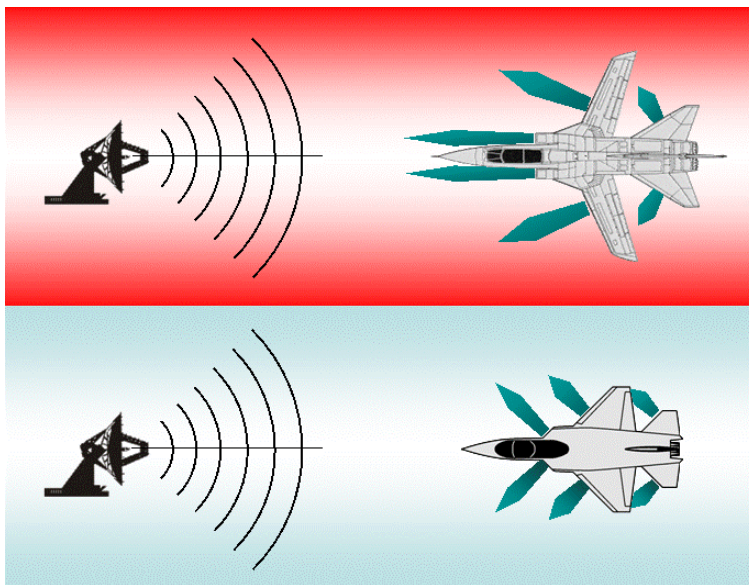


Fig. 4.5-7 Desired radar beam reflection

- Proper Aircraft Shaping
- Stealthy Radomes and Antennas
- Goldplated Cockpit
- Internal Weapon Carriage
- Absorbing Structures
- Treated Engine Inlet
- Signature avionics

Fig. 4.5-9 Measures to reduce radar reflections

The first US stealth demonstrator (code name Have Blue, **Fig. 4.5-10**) was built in 1977. Both prototypes were lost during the test flights. However, the signature was very low. Based on these tests about 60 F-117 aircraft (**Fig. 4.5-11**) were produced. There are rumors that the aircraft will be already phased out by the end of 2008 and replaced by F-22 fighters (**Fig. 4.5-12**). Like all stealth the F-117 has an internal weapon bay which can be used for missiles and bombs.



Fig. 4.5-10 First "Stealth" aircraft, code name "Have Blue", Lockheed Skunk Works



Fig. 4.5-11 First operational low signature aircraft: F-117, Lockheed

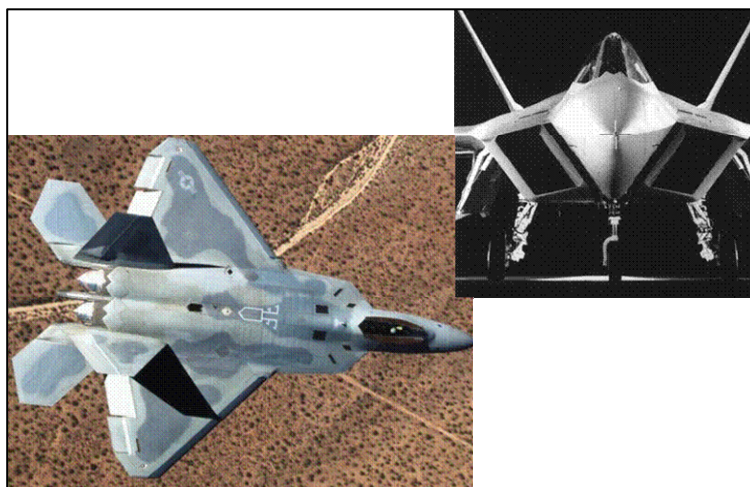


Fig. 4.5-12 F-22 air superiority fighter to replace F-117 !?

The most extreme stealth aircraft in service is the high altitude B-2 bomber, **Fig. 4.5-13**. With its internal bomb bay, no horizontal and no vertical tail, engine inlet and exit on top of the wing, and only two directions for the borderlines of the wing, it has a very low radar cross-section from below.



Fig. 4.5-13 B-2 Bomber, Northrop-Grumman

Under the direction of Dr. Wolfgang Herbst **MBB** did develop the low signature aircraft Lampyridae (latin: Glühwürmchen) in the early eighties, **Fig. 4.5-14**. The concept involved even less surface panels than the F-117. A wooden model with a metallic surface was built for RCS testing, **Fig. 4.5-15**. A second flight worthy model was manufactured and was tested in the German/Nederland Low speed wind-tunnel (DNW) flown by a pilot in a tethered mode **Fig. 4.5-16**. It was planned to tow the aircraft to an altitude of 4-5 km and than explore it's RCS in an unpowered flight mode.

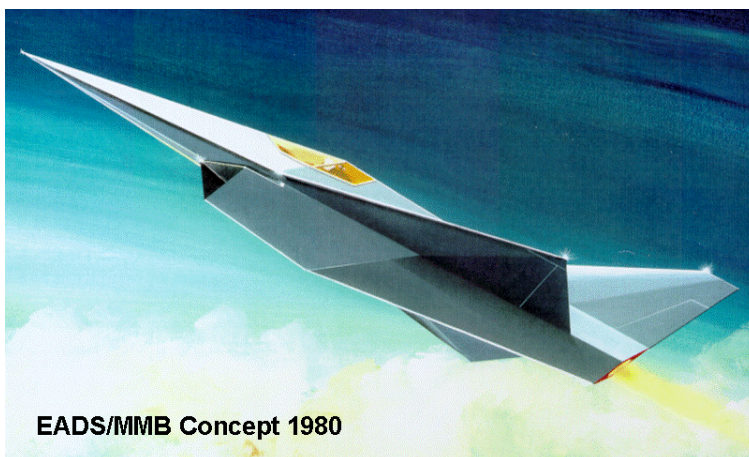


Fig. 4.5-14 The MBB developed Lampyridae (Glühwürmchen)

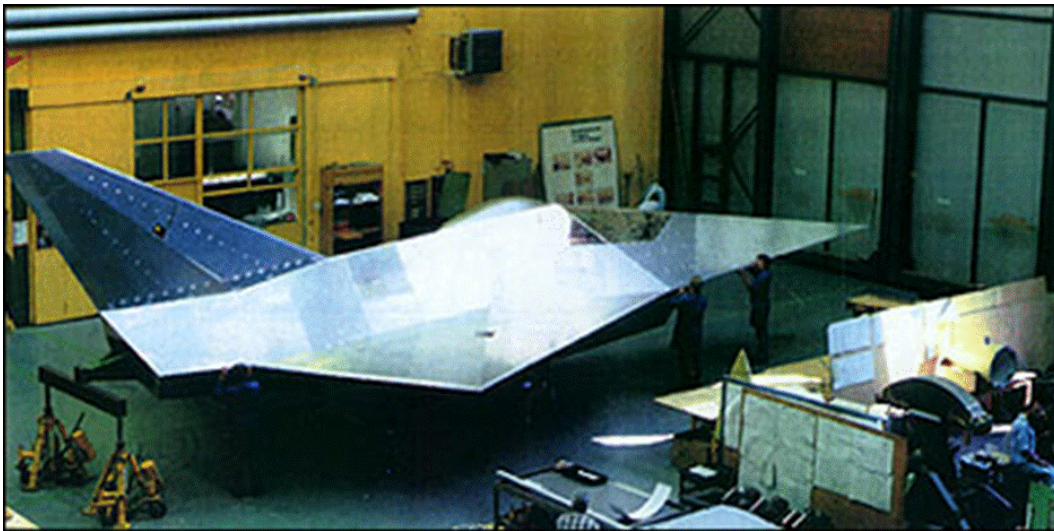


Fig. 4.5-15 Metal mock-up for RCS testing

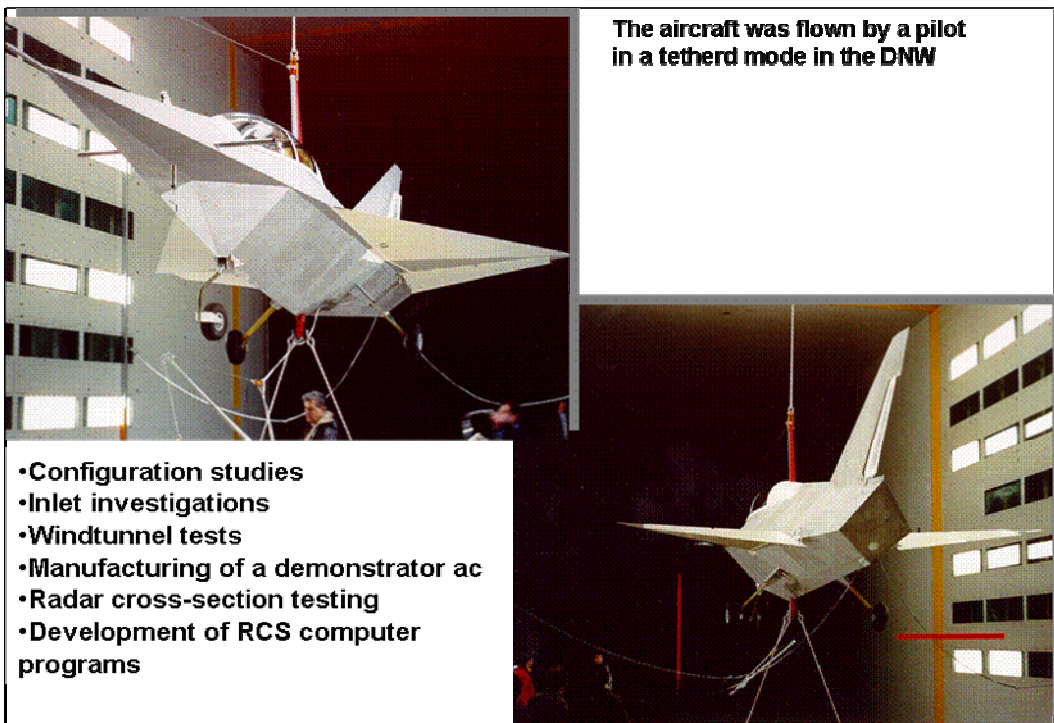


Fig. 4.5-16 "Flight Test" of Lamyridae in the DNW Wind Tunnel

The Horten Ho IX/Gotha Go 229 was flown in 1945 and was to have transatlantic range. It exhibited many characteristics of the B-2, **Fig. 4.5-17**.

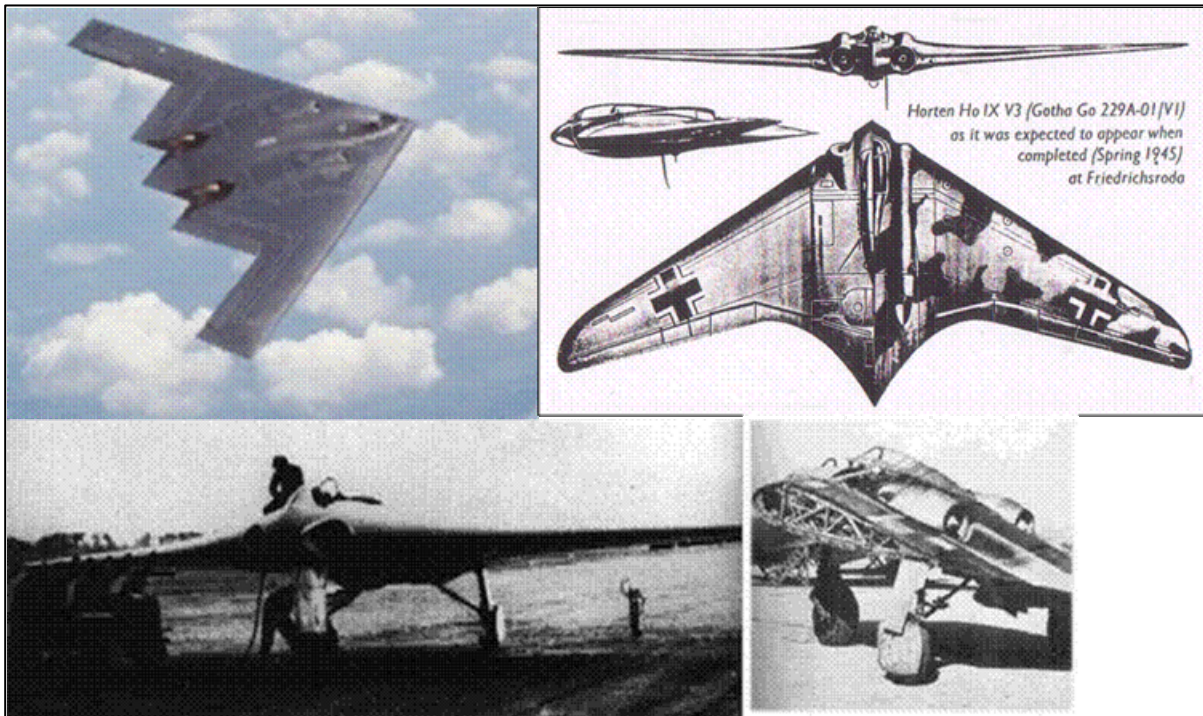


Fig. 4.5-17 Horten Ho IX/Gotha Go 229, First Flight January 1945

There are little known stealth activities outside the US in the time period between 1980 and the late 90ies. BAe built and tested the RCS of a fighter type configuration 1 (code name Replica, non flying model), **Fig. 5.4-18**.



Fig. 4.5-18 British Aerospace RCS Model, code name "Replica", 1994-1999

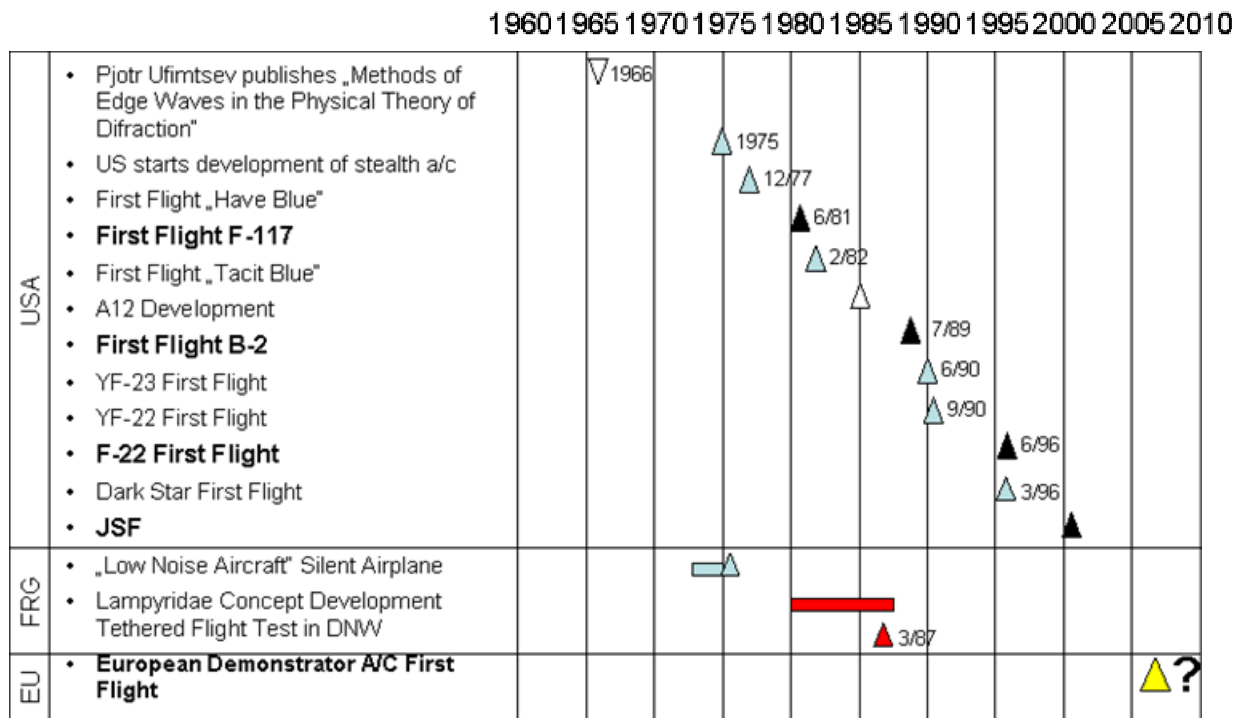


Fig. 4.5-19 Stealth aircraft development

A time history of the stealth technology evolution is shown in **Fig. 4.5-19**. The US has about 30 years of low signature ac development experience and 4 stealthy aircraft in series production. A summary of US build and tested stealth aircraft is collected in **Fig. 5.4-20**.



Fig. 4.5-20 US developed and flight tested stealth aircraft

EADS test facilities in Germany are identified in **Fig. 4.5-21** and **Fig. 4.5-22**.

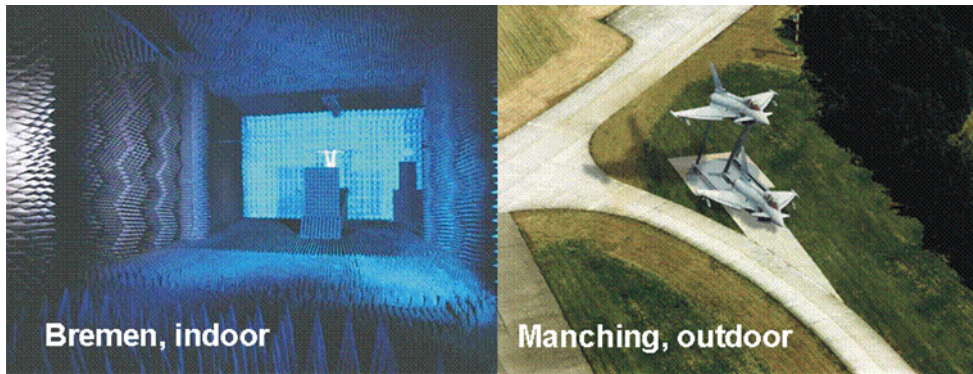


Fig. 4.5-21 EADS RCS test facilities



Fig. 4.5-22 Tornado RCS Tests, Manching

As usual, one measure will trigger the development of a countermeasure. Anti-Stealth technologies are being worked on and include passive radar systems which use the direct signal from a known emitter and its signal reflected by a target. If the location of the emitter is known, the time difference can be used to determine the location of a target. Potential emitters used include space based radars, but also radio or TV stations. This method needs a lot of computing capability.

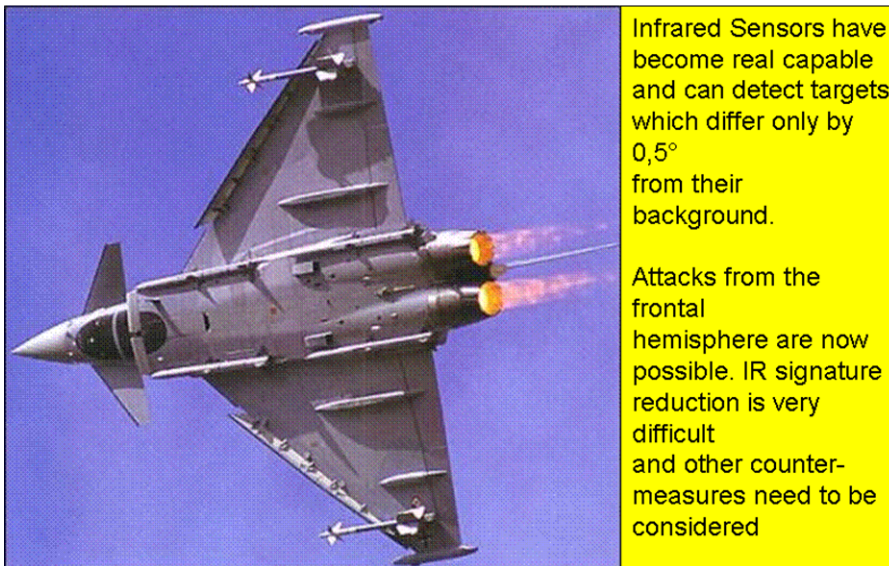


Fig. 4.5-23 Infrared Signature is very difficult to reduce

There are a lot of options to reduce the RCS of a vehicle. However, it seems to be more critical to reduce the infrared (IR) signature. The reason is simple: As long as the air vehicle is propelled by a fossil fuel burning engine, the exhaust temperatures are very high and difficult to hide, **Fig. 4.5-23**. Current sensor technologies allow the detection of surfaces which differ only by 0,5 degrees from their background temperature. Therefore aircraft can be even detected from the front hemisphere without the exhaust system being visible. Missiles and guided bombs with modern infrared sensors are increasingly difficult to fool by older flares, because they now analyse the flare spectrum and compared it to the known one of the target. Modern flares must now offer a very precise copy of an air vehicle's IR signature to be effective, **Fig. 5.4-24**.

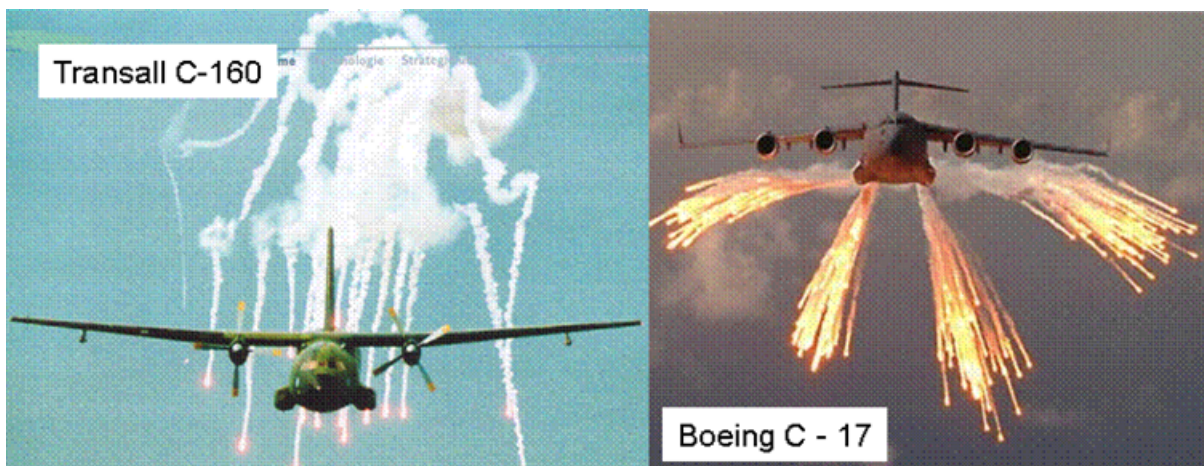


Fig. 4.5-24 Flare dispensing

Low signature aircraft become very visible when looking at their price tag. Because they are so expensive only a small number is being manufactured, which of course increases the price again. Less than 60 F-117 (130 Mio \$/copy), 20 B-2's (> 1 Billion \$/copy) have been built. None of the European or Russian build aircraft have (as of 2007) a full stealth capability included. Stealth technology is very closely guarded by the US and even the UK, as a prime

partner in the development of the Joint Strike Fighter, is still negotiating with the US to get access to certain aspects of stealth. Realistically there is a technology gap between the US and the rest of the world in this area of more than 10 years, **Fig. 4.5-25**.

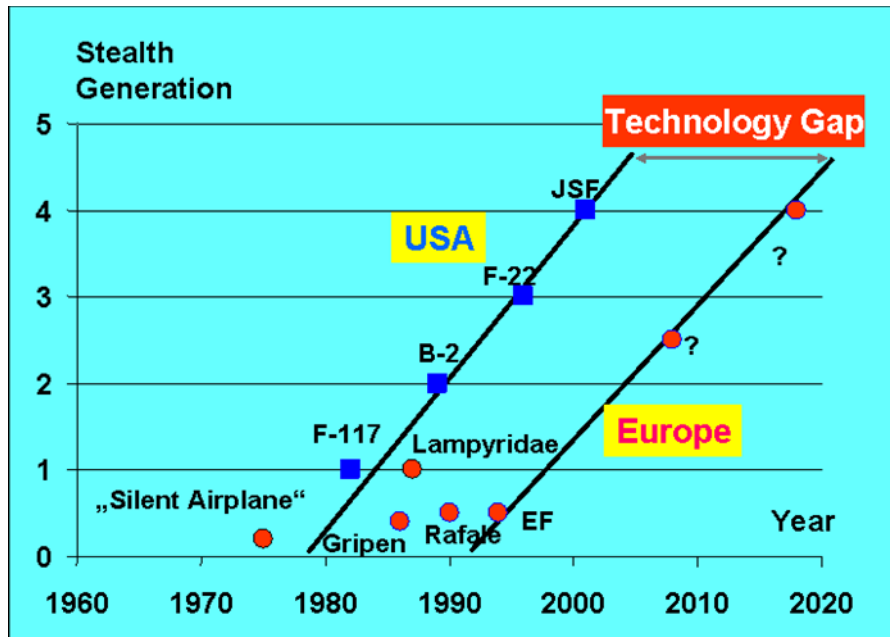


Fig. 4.5-25 Stealth Technology Gap between the US and Europe

5 Unmanned Vehicles

RPV's (Remotely Piloted Vehicles), UAV's (Unmanned Air Vehicles), or UAS's (Unmanned Aerial Systems) as they are now called, have been around for more than 50 years, **Fig. 5-1**. Early versions developed in Germany were "one way" systems; later versions developed in the US were recoverable and could be used more than one mission.

A different attitude to human losses, improvements in technologies, and different scenarios led to strong activities in this field in the last 15 to 20 years, and also the hope, to save money with these systems, **Fig. 5-2**. Another argument which could be used is, that in "class one" accidents (definition: loss of human life and/or very costly damage of the vehicles involved) in about 75% of the cases the crew was a factor in the mishap, **Fig. 5-3**.

UAVs are not brand new systems

- Unmanned vehicles and required technologies (remote/autonomous control, data link, navigation systems etc.) were already developed in Germany during WW II and in operational use



- The US have used unmanned remotely controlled aircraft as air targets and for reconnaissance missions in Vietnam and the Gulf war, e.g. Firebee (3435 Sorties), Pioneer (520+ sorties in the Gulf)



Fig. 5-1 Unmanned Aerial Vehicles (UAV) are more than 50 years old

1. Prevent pilot/crew loss
2. Mission duration exceeds human capabilities
3. New technologies available
4. (Hope to) reduce system cost

Fig. 5-2 Why do we want UAV's?

GAO Human Error Was Contributing Factor in High Percentage of Flight Mishaps

- During fiscal years 1994-95, human error was a factor in
 - 71 percent of Air Force mishaps
 - 76 percent of Army mishaps
 - 74 percent of Navy/USMC mishaps

Fig. 5-3 Involvement of Crew members in accidents

An UAV system does consist of all the elements required by a manned system for the same mission (exception crew support, rescue) but also needs some additional features like (ground or airborne) control station, data links, special sensors (see and avoid for flight in controlled air space), emergency systems to prevent damage in case of problems etc., **Fig. 5-4**.



Fig. 5-4 UAV System Elements

The well known classification of UAV missions (Dull, dirty, dangerous) allows to also classify UAV vehicle types, **Fig. 5-5**. Basically they are the same types as manned vehicles, except that the mission capabilities are somewhat different: there are reconnaissance vehicles for different altitudes and durations, and attack vehicles for different targets, **Fig. 5-6**. Currently the prime development emphasis is on reconnaissance systems. The challenges in developing reconnaissance systems are listed in **Fig. 5-7**.

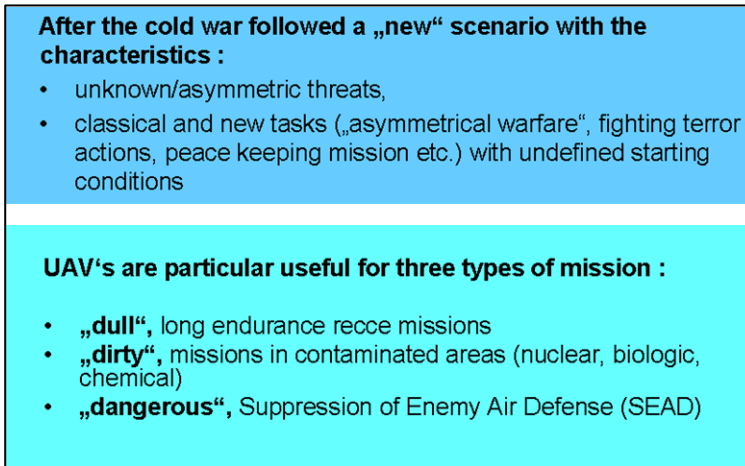


Fig. 5-5 UAV utilization in "d,d,d" missions

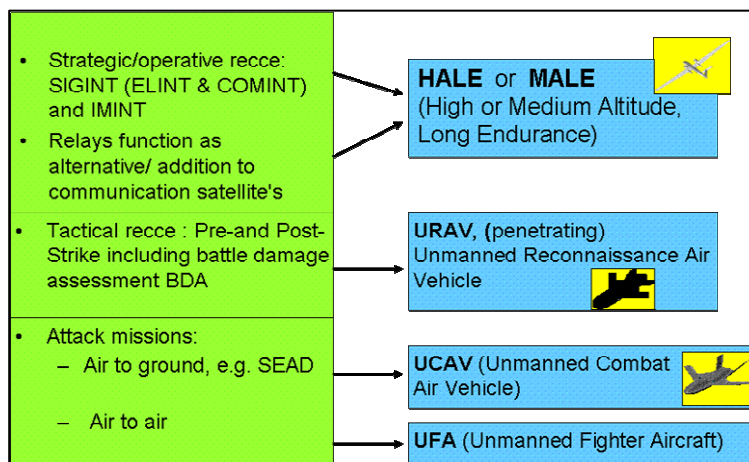


Fig. 5-6 UAV missions and vehicle types

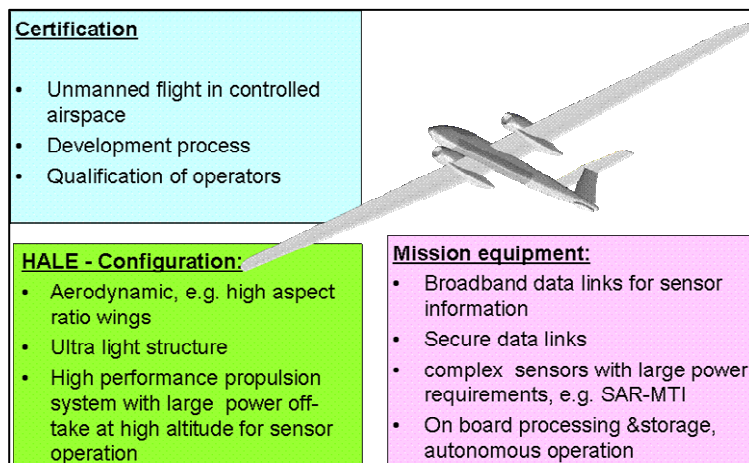


Fig. 5-7 Technical Challenges for Reconnaissance UAV's

The hope to save a substantial amount of life cycle cost has not come true (yet) with the current systems for the reasons summarized in Fig. 5-8. But the comparison is difficult, since conventional/manned systems can not fly/will not be flown in the same missions. Analytical studies for air to ground missions have shown significant savings, however, these systems are not yet available.

No large cost savings for the vehicle because

- High tech characteristics required: configuration, signature, sensor, software, antenna, etc.
- Limited production numbers, in particular for recce aircraft (HALE / MALE)
- Higher reliability required: 75% of UAV losses due to problems in propulsion, flight control, operator training)

Savings expected by

- Reduced flight hours in peace time operation
- Reduced training cost for operators, control of more than one system through one ground station/operator
- reduced peace time operating cost through flyable storage concept

Fig. 5-8 Cost considerations

There is a whole range of UAV's available or under development from a Micro UAV (weighing about 100g) to the (currently) biggest HALE (Global Hawk) weighing about 12 to. They can be classified by range, payload, operational altitude and endurance (**Fig. 5-9, 5-10**). The number of systems developed and in operation for countries with more than 5 systems is given in **Fig. 5-11**, the number of vehicles per category in **Fig. 5-12**.

UAV Categories	Acronym	Range (kilometers)	Flight Alt. (meters)	Endurance (hours)	Take-Off Mass (kilograms)	Currently Flying
Micro	μ (Micro)	< 10	250	1	< 5	◆
Miniature	Mini	< 10	150 ^b to 300 ^a	< 2	< 30 (150 ^b)	◆
Close Range	CR	10 to 30	3.000	2 to 4	150	◆
Short Range	SR	30 to 70	3.000	3 to 6	200	◆
Medium Range	MR	70 to 200	5.000	6 to 10	1.250	◆
Medium Range Endurance	MRE	> 500	8.000	10 to 18	1.250	◆
Low Altitude Deep Penetration	LADP	> 250	50 to 9.000	0,5 to 1	350	◆
Low Altitude Long Endurance ^a	LALE	> 500	3.000	> 24	< 30	◆
Medium Altitude Long Endurance	MALE	> 500	14.000	24 to 48	1.500	◆
High Altitude Long Endurance	HALE	> 2000	20.000	24 to 48	(4.500 ^c)12.000	◆
Special Purpose UAVs:						

Fig. 5-9 UAV Categories, Characteristics

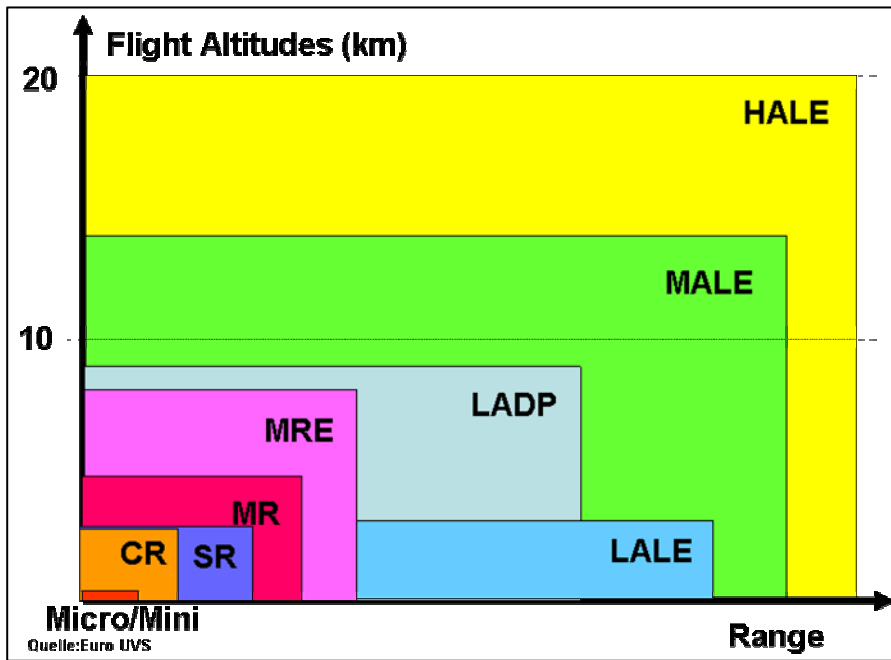


Fig. 5-10 UAV Categories, Altitude and Range

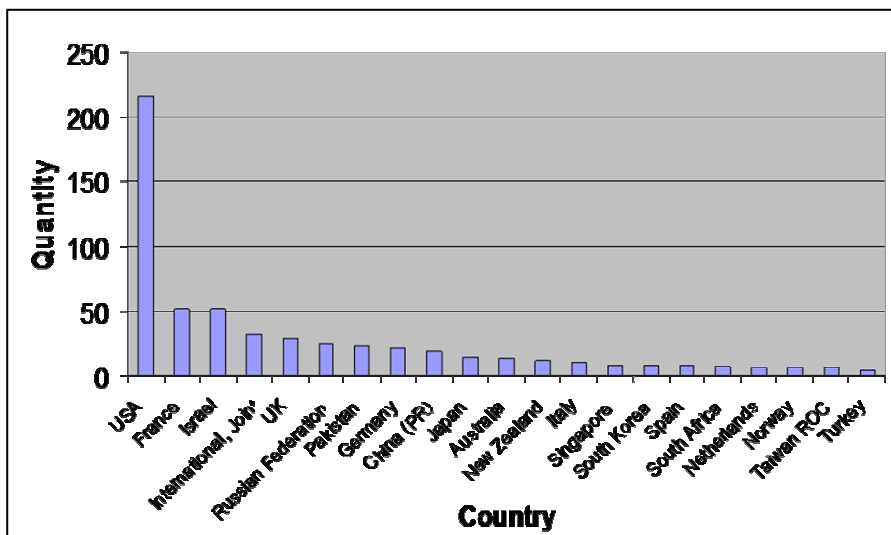


Fig. 5-11 Quantity of UAV types developed and procured per country (only >5 considered)

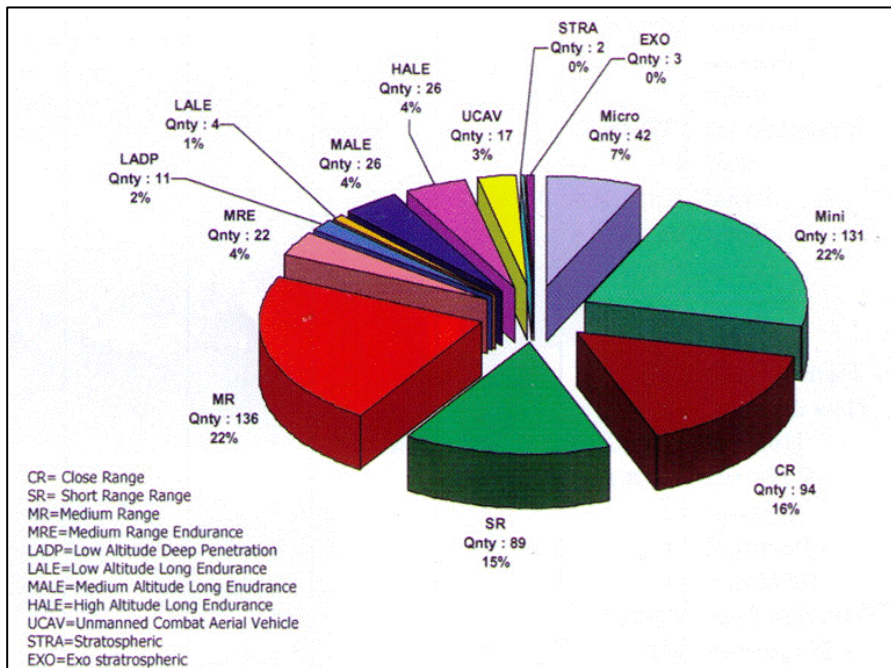


Fig. 5-12 Number of vehicles per category (source Euro UAV)

One of the big questions, which is answered differently by different users and for various systems, is how much autonomy a UAV should have, **Fig. 5-13**. The more autonomy it has, the less control options remain for the human operator. More autonomy reduces also the data link requirements for vehicle control and transmission of sensor information and therefore may allow one operator to monitor more than one system. If target information can be generated and reduced to type/location/speed/direction by onboard processing, even real time information would be possible by small data bursts. However, that is still not possible with the necessary quality. Currently the autonomy is considered critical for any attack missions by UAV's and usually requires a man in the loop.

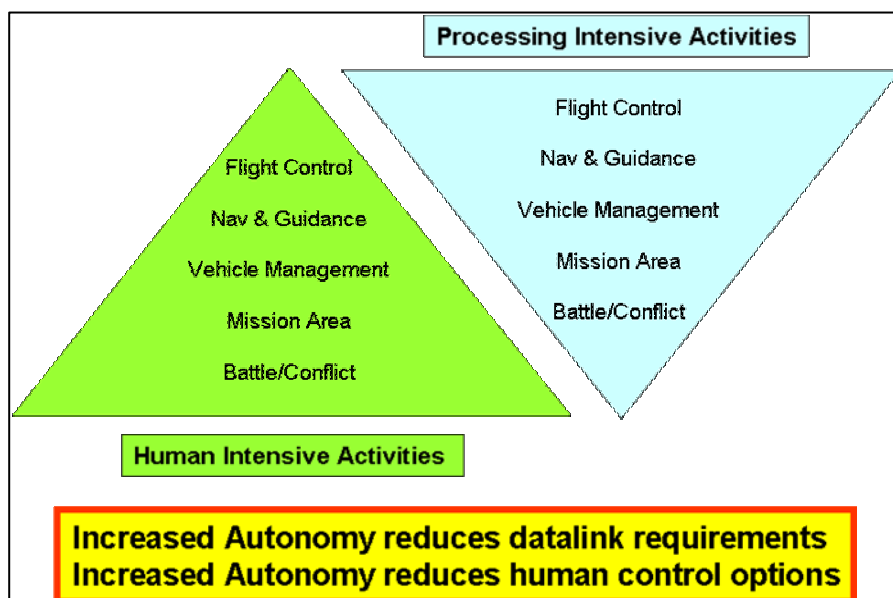


Fig. 5-13 Conflicting Autonomy Requirements

Systems currently in operational use in Germany (Luna and CL 289) for tactical reconnaissance and Euro-Hawk (under development, based on the Northrop Grumman Global Hawk) for strategic reconnaissance, are shown in **Fig. 5-14**. The Global Hawk is a very capable system with flight altitudes close to 20km and time on station up to 36 hours. It has been flown from the west coast of the USA to Australia and also to Germany and performed test flights from Nordholz over the North Sea with German manufactured SIGINT equipment. The German MOD has decided to acquire the "green" airframe and develop a national reconnaissance system for it, because the availability of that kind of information in the Balkan conflict -even between NATO members- was unsatisfactory, **Fig.5-15**. The German industry would be perfectly capable of developing such a vehicle, however, the number of systems required (<10 for Germany) do not justify the development cost.



Fig. 5-14 Range of UAV's in use or planned for the German forces.

Development Contract for a Euro Hawk Demonstrator:

GMOD->Euro Hawk GmbH

- Modification of a „green“ Global-Hawk aircraft
- Integration of a German SIGINT System (Comint/Elint)
- Test of the system starting 2010
- Four more SIGINT Euro Hawk's to be delivered by 2014
- Basing tbd
- 430 Mio € for Demonstrator including test
- Acquisition for IMINT mission tbd

Source: Luft und Raumfahrt 3/2007

Fig. 5-15 GMOD Plan for Euro-Hawk

Acquisition cost of Global Hawk systems has steadily grown because of the desire of the military users to increase its sensor capability, **Fig. 5-16 and -17**. One of the critical items is the availability of sufficient electrical power for the imaging sensors, SAR in particular, at high altitude. The latest US version has therefore a larger wing and a bigger engine.

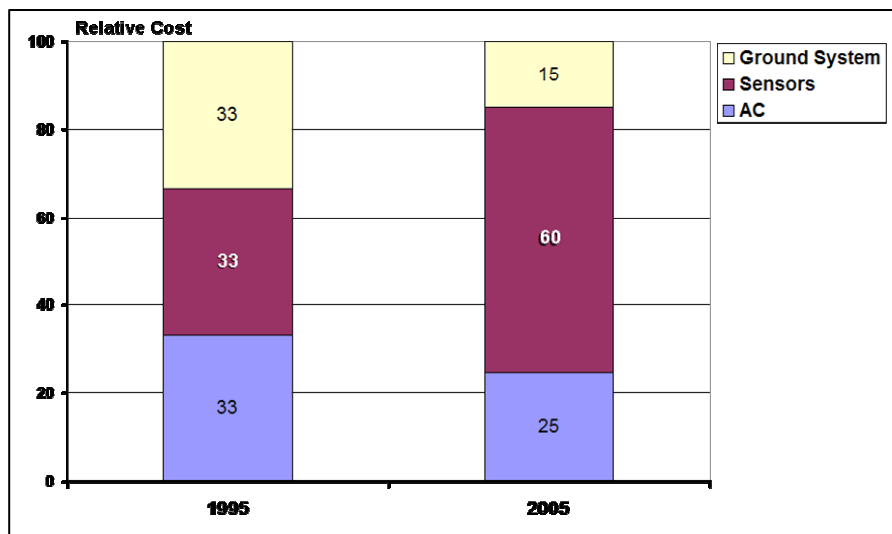


Fig. 5-17 Global Hawk acquisition cost changes

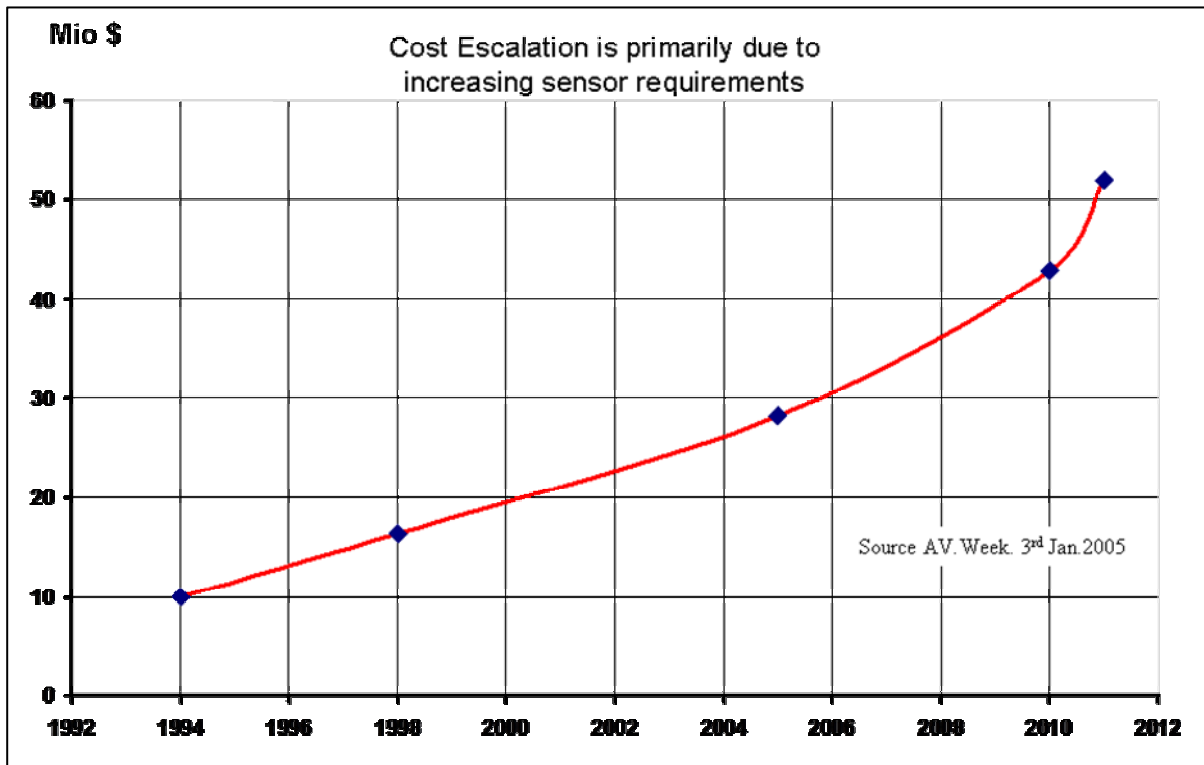


Fig. 5-18 Global Hawk cost escalation

Sufficient air space (restricted to general aviation) for test and development flights of UAV's is available in the US. Only a few areas in Europe are available for this purpose, because of the high density of population and commercial traffic. No country has currently a fully established and approved procedure to fly UAV's in controlled air space. The current baseline concept asks for the same procedures for manned and unmanned aircraft. I.e. any unmanned aircraft must have a "controller" available for the air traffic control system to communicate any desired or required change of the flight path.

A flight test program was conducted in Germany using the DLR ATTAS aircraft as a "simulated" unmanned vehicle (with a safety crew aboard) to define the consequences for hard- and software and the operational procedures to be executed in a failure situation, **Fig. 5-18 and -19**. The results show the feasibility of this concept, but there is no approved procedure yet.

The question, how a UAV could detect and avoid other non-cooperative aircraft, is also still to be resolved. The NASA conducted "ACCES" Study addressed similar topics which need a standardised solution, **Fig. 5-21**.



Fig. 5-19 Simulated Unmanned Vehicle ATTAS in controlled German air space

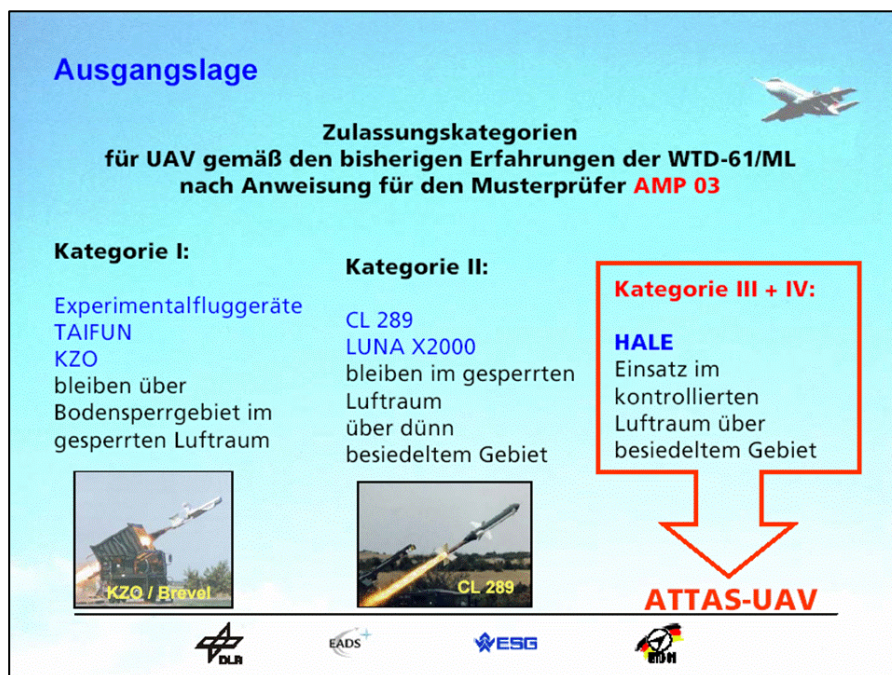


Fig. 5-20 Current Certification classes for UAV's in Germany

Results from US Study „ACCESS 5“, Feb. 2006

Open Questions:

- Minimum technical and operational UAS Airworthiness Standards
- Sense and Avoid Standards
- Frequency Spectrum
- Pilot qualifications and Medical Standards
- Separation Issues
- System Safety analysis and appropriate Level of Safety need to be defined and agreed before UAV's/UAS's can routinely operate in controlled airspace together with manned vehicles.

Fig. 5-21 Open Questions from NASA "ACCESS" Study

It is expected, that the UAV development will continue from surveillance and reconnaissance aircraft to ground attack vehicles around 2020 and potentially fighter type vehicles around 2030, **Fig. 5-22**.

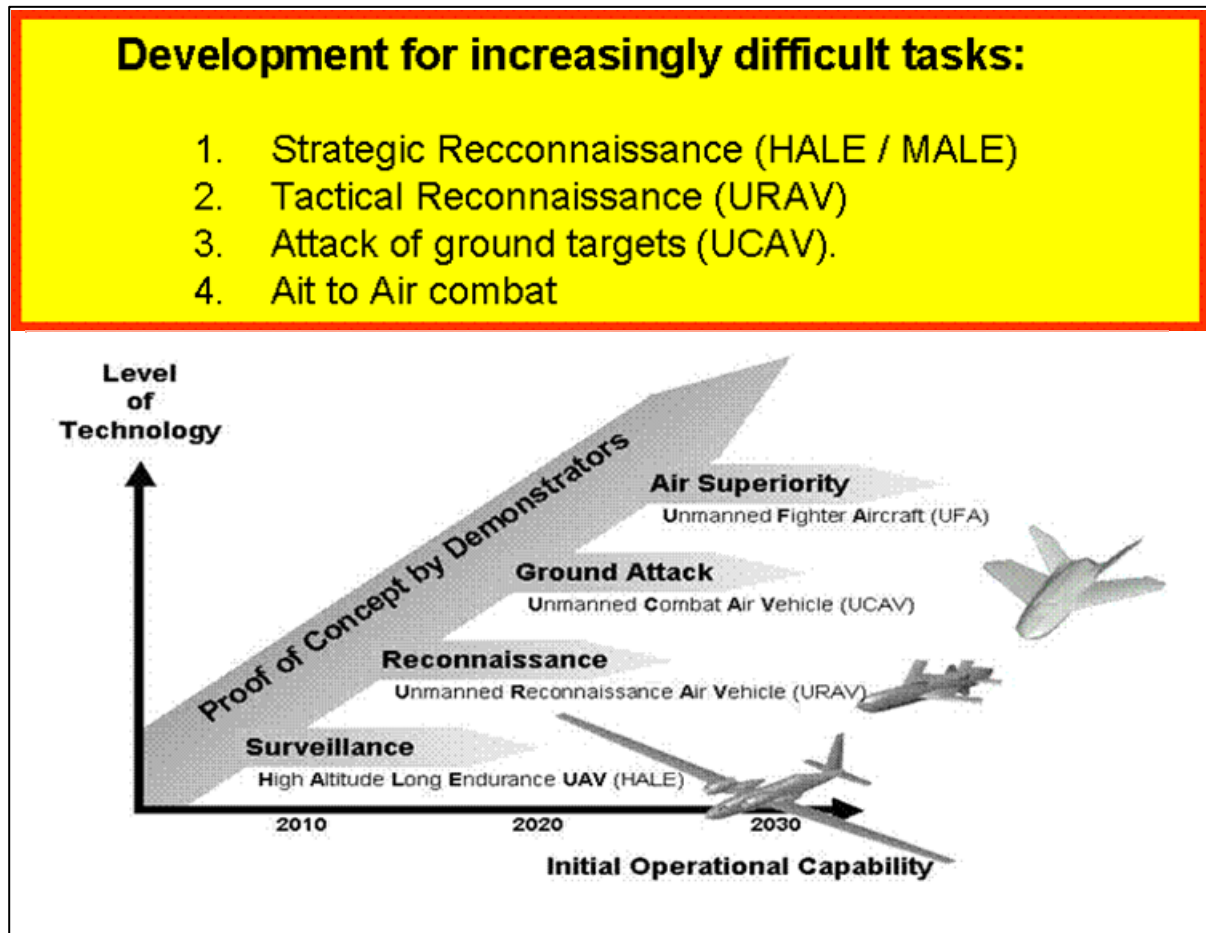


Fig. 5-22 Expected UAV development sequence

In the US there is no longer a joint approach between the services for combat UAV's after the DARPA UCAV program was cancelled. In Europe we have an even more splintered approach since every Nation is trying to establish a good position for its industry in the expected UAV development programs, **Fig. 5-23**



Fig. 5-23 Example of European cooperation

The German situation is summarized below:

- Smaller unmanned vehicles have been developed, built and are tested/operated in Germany (CL 289, Taifun, Luna, KZO, Brevel)
- After the successful utilization of UAV's during the Kosovo conflict the need for UAV's is accepted by the European air-forces.
- There is a primary requirement for reconnaissance systems. An overall reconnaissance concept for all services (Army, Navy, Air-force) is still to be defined for Germany.
- The German MOD has decided to acquire a Euro Hawk System for the SIGINT mission. Solution for a strategic IMINT system is still tbd. The German army is already using smaller UAV's for tactical recce missions.

A common European approach for reconnaissance (e.g. through EDA) is not yet defined. The US has a number of strategic reconnaissance UAV systems in operation, attack UAV's are under development.

There is no new manned fighter aircraft program on the horizon for a considerable time, just upgrades of the recently introduced Gripen, Rafale, and Eurofighter. So the hope of the industry rests on UAV's to keep their teams employed and to maintain their skill.

6 Future Aspects

If one looks at the number of aircraft developed in the US per ten year interval during the last 50 years, there is an alarming signal: How do we maintain teams which have the skill to develop an aircraft system and to put it into production, **Fig. 6-1**? European numbers show a similar picture. The turnover of the aeronautical industry is still increasing, however, the number of people employed is diminishing, **Fig. 6-2**.

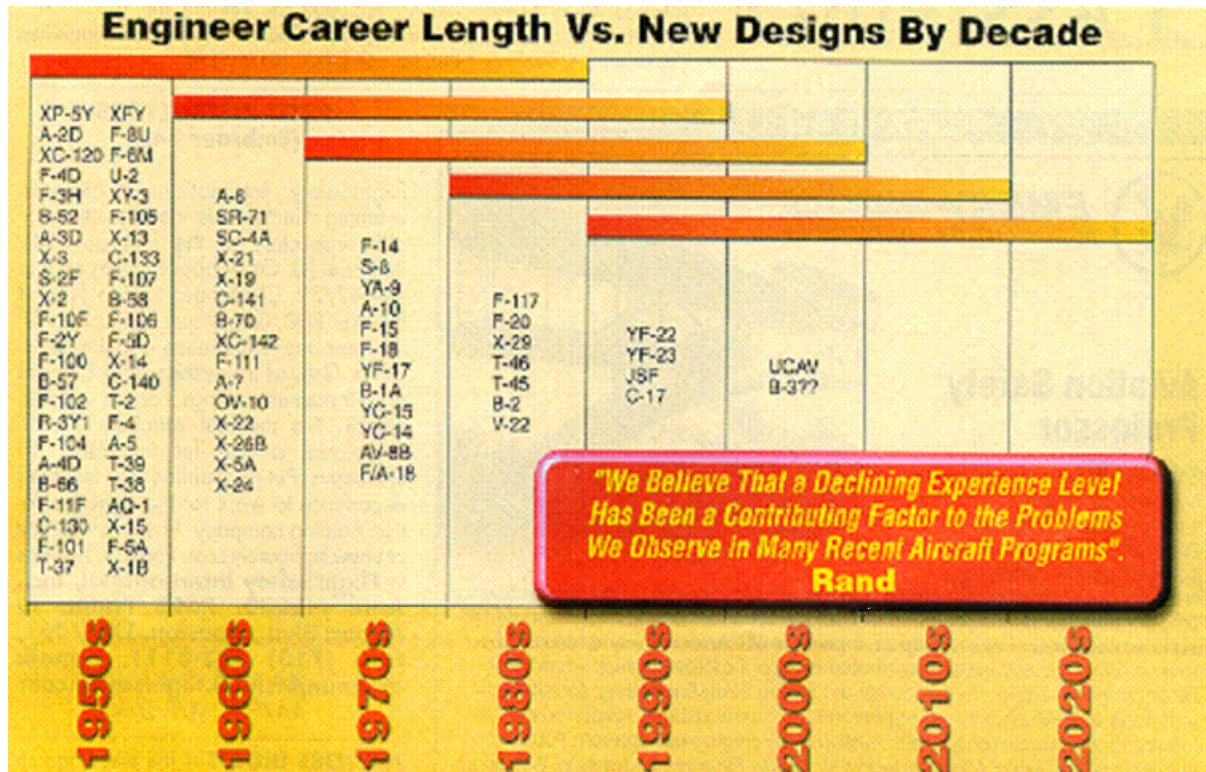


Fig. 6-1 How do we maintain the knowledge base of the development and production team?

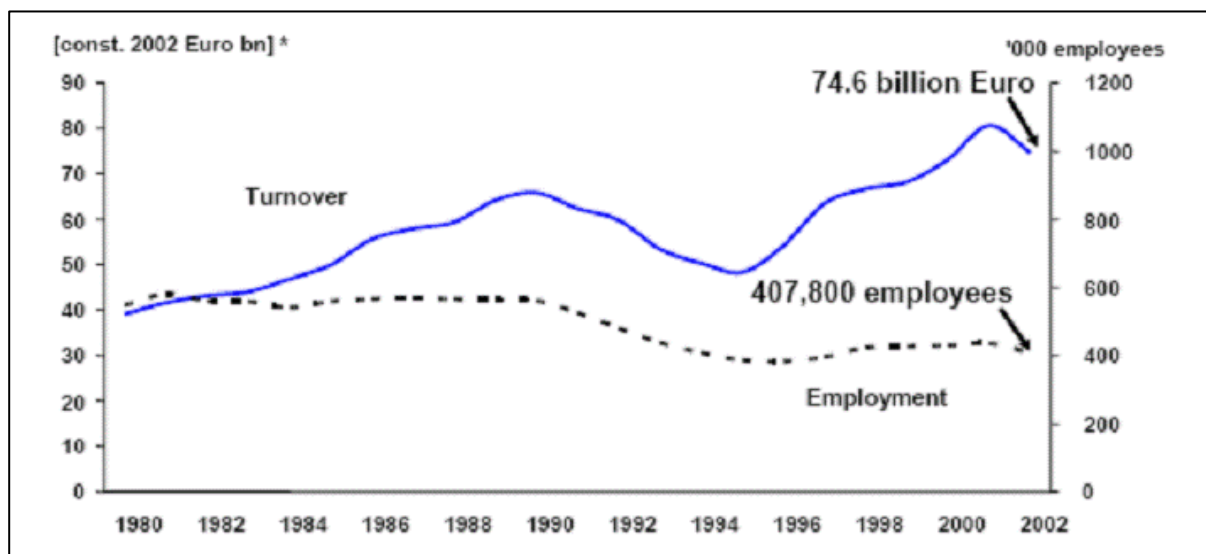


Fig. 6-2 Aerospace industries turnover and employment

One of the side effects of the declining number of programs was, that many famous aircraft companies quit to exist: There was not enough business in the market to keep all the companies alive and maintain their competitive position. Many companies merged with others or were bought with the effect, that many design teams had to look for different work. Currently there are but three major companies in the US with the capability to develop a high technology aircraft system: Lockheed Martin, Boeing and Northrop Grumman (with more emphasis in the electronic system side).

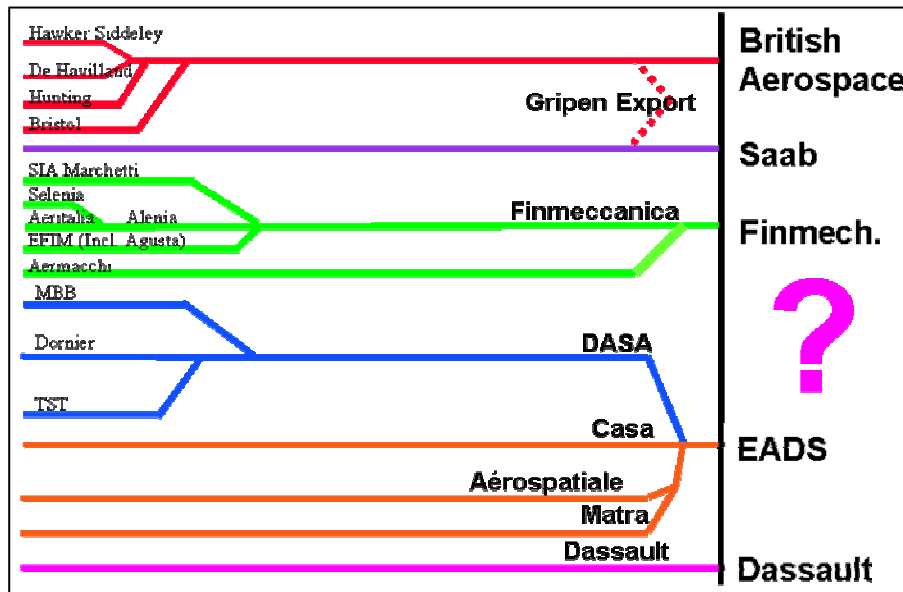


Fig. 6-3 National company consolidation

The very same situation evolved in Europe. In Germany (**Fig. 6-3**) many well known companies are no longer in the market. However, in Europe we still have six countries with a significant industrial capacity in the military field: France, Germany, Italy, Spain, Sweden, and the UK. And other countries (e.g. Greece, Turkey) are trying to establish new national capabilities to participate in the few programs around. The competition for fighter aircraft with Gripen, Rafale and Eurofighter developed in parallel has already been mentioned in Chapter 1. And the fact, that national policies and economic interest still play a very vital role and currently do prevent a joint European solution, is evident in the UAV field.

EADS, representing all Airbus activities but also military and civil helicopter as well as the German Military Air Systems activity, is a 49 % share holder of Dassault, however, has no control and little insight into the French national programs and activities.

BAE-Systems, the biggest remaining British company, has bought many companies in the US and is one of the ten biggest companies providing military equipment to the Pentagon. It got out of the commercial aircraft market altogether. SAAB in Sweden gave up the development and manufacturing of commercial aircraft and is trying to participate in Airbus products and

military aircraft development. In Italy Finmeccanica with Alenia as the main military company has strong ties to the US, through their transport aircraft activities (C-27, and participation in Boeings commercial aircraft programs). So, it is currently not quite clear, how the European companies will share the military pie. Dassault has a good chance to take the lead.

One of the reason for the shrinking military market – at least as far as the number of aircraft manufactured is concerned, since the price tag per copy has certainly gone up considerably– is of course the threat scenario, which has considerably changed. A big change occurred when the wall came down in 1989. The trend from an all out war to smaller conflicts including guerrilla warfare and terrorists action continues, **Fig. 6-4**. Asymmetric force situations are the norm and require new and different solutions.

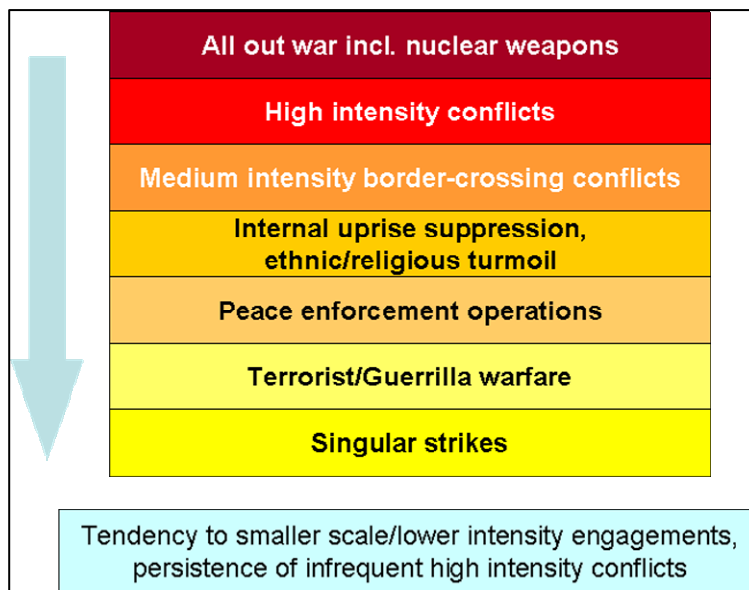


Fig. 6-4 Scenario change since 1940: From all out war to singular strikes

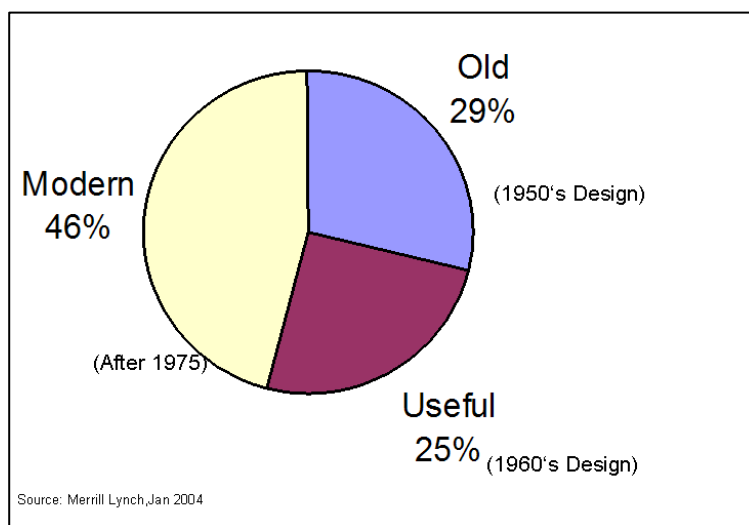


Fig. 6-5 World fighter inventory

Less than half of the fighter inventory has been manufactured after 1975, **Fig. 6-5**. That would suggest that the other half need replacement. Fact is that the inventories of all Nations are

steadily decreasing, i.e. old aircraft will be phased out and not necessarily be replaced, or at least not in the same quantity.

Looking at the distribution of the total inventory by quantity (**Fig. 6-6**) the PR of China has the second largest fleet of fighter aircraft but only a very small percentage are modern aircraft. In contrast, Saudi Arabia has only modern aircraft, with a bigger quantity than China. With still many F-4's in the inventory, Germany will show only red colour when the F-4's will be replaced by Eurofighter's, however, the total number of aircraft will go down to about half by 2015, **Fig. 6-7** due to the reduction of Tornado aircraft.

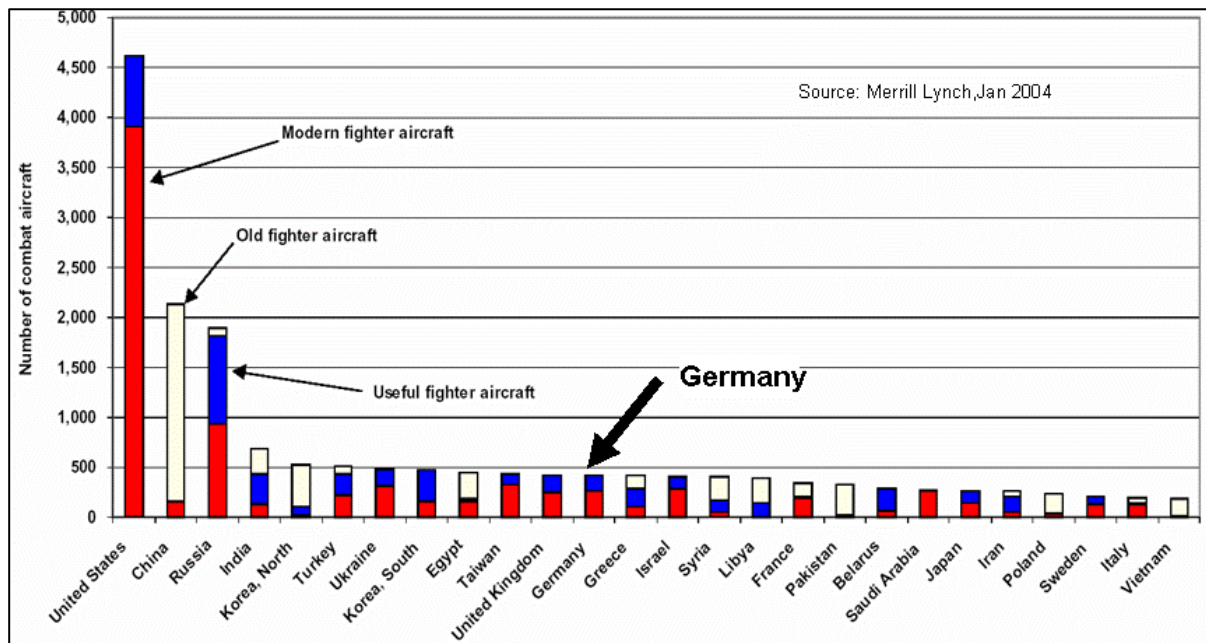


Fig. 6-6 Distribution of fighter inventory

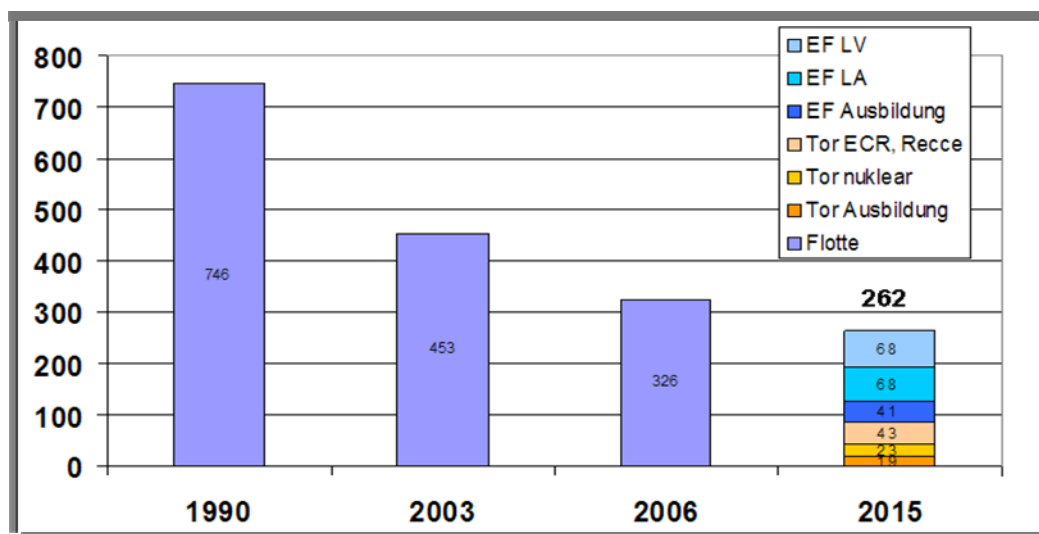


Fig. 6-7 German Fighter Inventory Planning, Status 2003

The inventory of the 6 countries in Europe with an own military aircraft industry is continuously shrinking since 1970, **Fig. 6-8**, i.e. it follows the world wide trend. Since the air defence capability is being renewed with the introduction of Gripen, Rafale and Eurofighter, the next logical task will be the replacement of the air/ground capability. The options, which are being studied, include new manned systems and/or unmanned systems, **Fig. 6-9**.

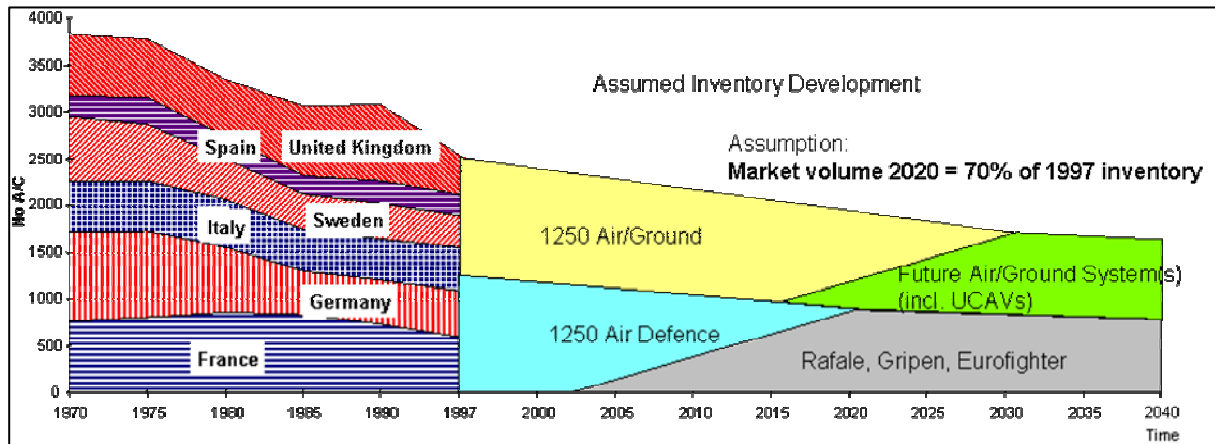


Fig. 6-8 European fighter inventory

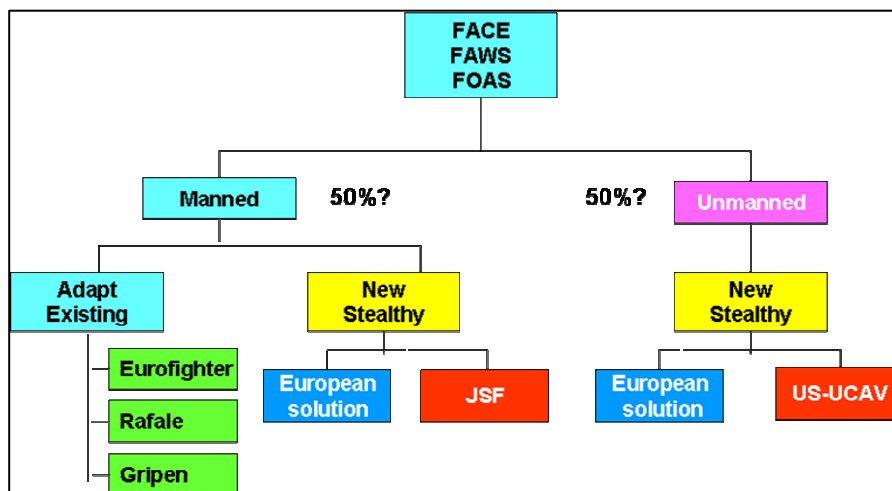


Fig. 6-9 European options for a new Future Airborne Weapon System (FAWS)

Part of this task will be taken care off by the new air defence systems, which have a dual/multi role capability and will be further upgraded. Only a remaining portion will have to be replaced by other systems. It is very unlikely that a brand new manned system will be developed in the next 10-15 years, even considering the stealth aspect. However, the development of unmanned combat aircraft as a supplement to manned systems has a high probability. One of the key questions will be:

- How much stealth technology will be included?
- Will the European nations be willing to cooperatively develop such a system (as proposed by Dassault, which has taken the lead in a multinational European study) or whether a

number of nations will buy American? The UK is most likely a candidate for a transatlantic solution.

Most fighter aircraft developed in the last 40 years have production runs below 1000 aircraft. F-15, F16 and the Russian Mig-29 are exemptions, **Fig. 6-10**. The next generation US fighter, the Joint Strike Fighter (Lightning II) is intended to be another exemption. From the very beginning it was planned to develop and build an aircraft which should fulfil the needs of the Air-Force, the Navy and the Marines.

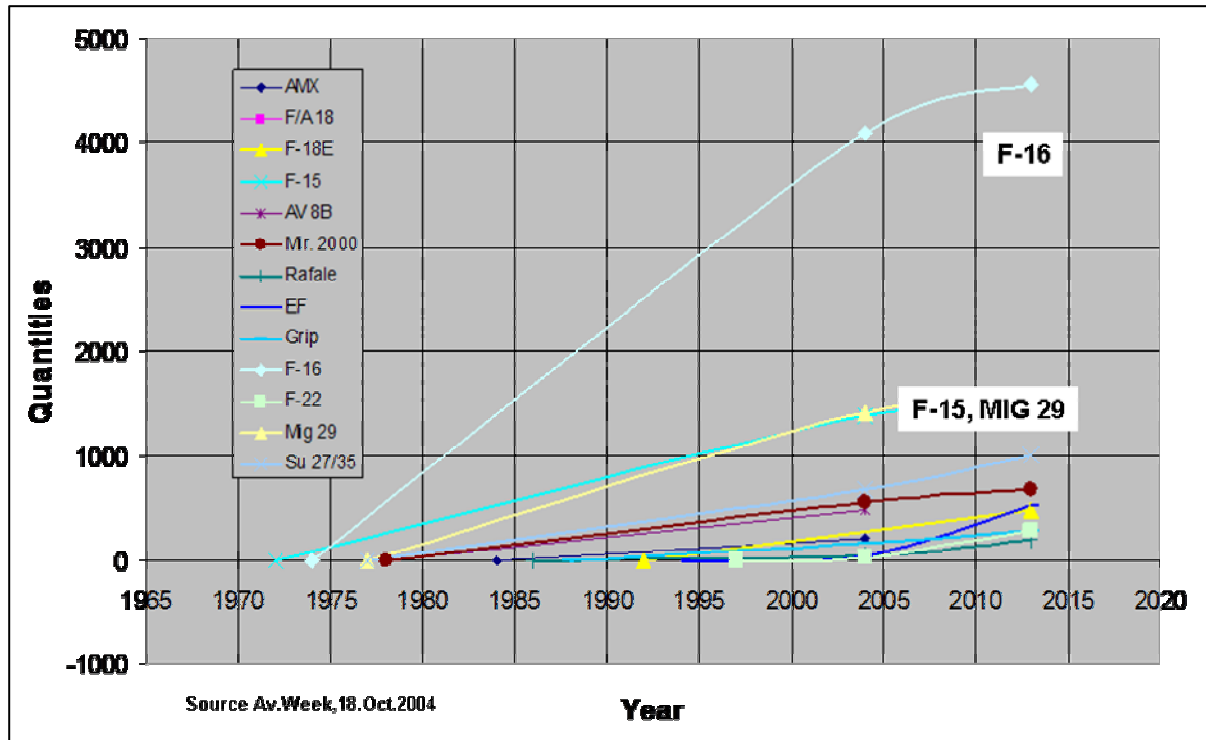


Fig. 6-10 Fighter aircraft production quantities

Never before in the US aircraft history did a joint project get off the ground. The F-111 was a last unsuccessful try. To make the challenge even bigger, the UK, in need of a Harrier replacement, joined the program as a level 1 partner and brought its requirement to the table. Other nations were also invited to join the team already during the development phase, **Fig. 6-11**. However, there is a major difference between the multinational development programs in Europe: Tornado and Eurofighter were developed with every nation being a partner. The JSF has but one major contractor, Lockheed Martin. That makes decisions and responsibilities much easier.

It is quite obvious, that a significant share of the next generation combat aircraft market in Europe will be taken by the US. And that is true even for countries with a national aircraft industry such as the UK and Italy, which have been partners of the Tornado and Eurofighter program.

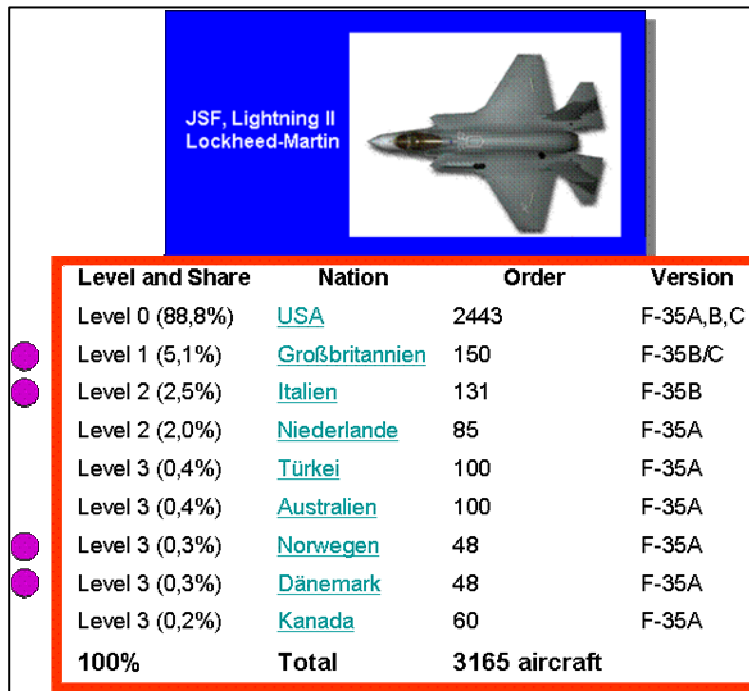


Fig. 6-11 The Lockheed Martin Joint Strike Fighter, the "Blue Threat"

The Joint Strike Fighter is to be built with a quoted commonality of 80% in three different versions: the (lightest) land version for the Air-Force, a carrier version with a larger wing for the Navy, and a third version, which can land vertically, for the Marines. Initial projections to buy 3000 aircraft alone for the US have not materialized. The initial fly away cost of around 35 Million US \$ has steadily increased and program delays and technical problems led to speculations, that the price tag may be as high as 100 Mio US \$ per copy.

The relation of the home market between Europe and the US is about 1 to 3 (**Fig. 6-12**), and that figure includes already all European nations. It clearly indicates that a single nation will have a hard time to sell its aircraft on the international market at a competitive price since it has to bear all development cost and has a limited home market. This is for example true for the French Rafale and the Swedish Gripen.

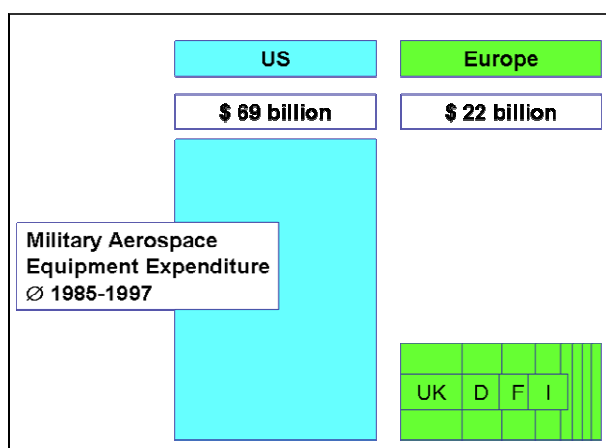


Fig. 6-12 Home Market Relations, Annual Volume

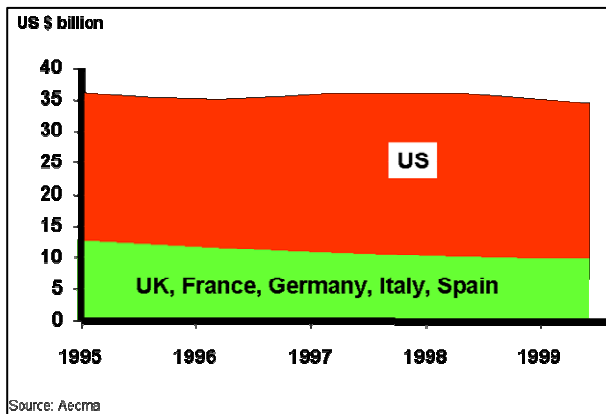


Fig. 6-13 R&D Expenditure, 1995 – 1999

About the same ratio (1:3) exists for the expenditures in research and development, **Fig. 6-13**. Europe can not match the American funding, leave alone a single nation. Yet there is not yet a real pooling of the national resources into a common fund to support the European needs. The European Technology Acquisition Program (ETAP) was a start (about 1999) but has not made great progress. But at least the technologies which are of common interest have been defined, **Fig. 6-14**.

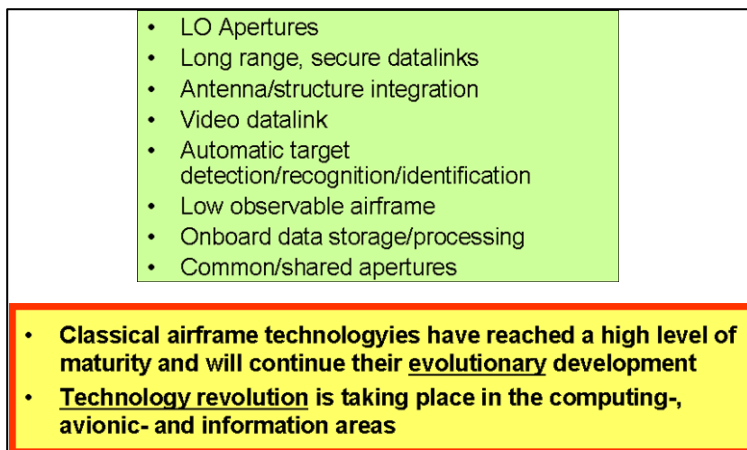


Fig. 6-14 High Priority Technologies for Europe

The options for new systems to be developed in the next 10 to 15 years are very small, **Fig. 6-15**. There is a need for new trainer aircraft, since the pilots of tomorrow are today trained with yesterday's aircraft (which have received some upgrade in the cockpit electronics). Some European nations are training their pilots in the US (Shepard AFB) on upgraded T-38's, some do it national with their own aircraft (UK-Hawk, France-Alpha Jet). A common European centre for basic and advanced training and operational aircraft like the Eurofighter would certainly allow significant overall cost reductions, however, with some national cut-backs.

In addition to the ongoing upgrades of the new manned fighter aircraft there is only one project on the horizon: the unmanned combat air vehicle (UCAV) for air to ground missions, that

is in competition with the manned Joint Strike Fighter and other unmanned UCAV programs under development in the US by Navy and Air-Force (X-45, X47).

Trainer:	Eurotrainer (Mako,, Alpha Jet +, Hawk, AM 346) 200 Stück Europ?. Common trainings Centre?
Fighter:	Manned: Upgrades EF, Rafale, Gripen Unmanned: UCAV
Recce:	Manned: Breguet Atlantique Successor?! Unmanned: HALE (EH), MALE (50 units for Europe?) URAV (unmanned penetrating reconnaissance) Air Ground Surveillance System (~10 units for EU/Nato?)
Transport:	A 400 M, ~195 units

Fig. 6-15 Potential new systems in Europe

In the Recce area Germany has opted for a German version of the US HALE Global Hawk = Euro-Hawk, while other nations are looking at a lower altitude range MALE aircraft. The Gap until the Euro-Hawk can fly with a German SIGINT system is to be closed by the Lockheed Orian, which was bought from the Netherlands to replace the Breguet Atlantique. The UK is acquiring the ASTOR, a system using a business jet and primarily US equipment.

These solutions are all pursued on a national basis. No project for a low(er) level penetrating system (URAV) has been officially announced yet. The A400M military transport aircraft is under development and may find additional export customers.

The outlook for new development programmes to be started in the next 10 to 15 years is not that bright. The American competition is strong and clearly ahead of the Europeans. Europeans do have sales opportunities in many countries which – for political reasons – do not want to buy American products. However, to maintain competitiveness over the long run, the European countries and companies must get closer together and get rid of national priorities, **Fig. 6-14.**

1. Europe needs a common foreign and security policy (→GASP) i.e. European forces with common equipment, to be defined by a European MOD (EDA? = European Defense Agency) 2. EU needs a common acquisition office →OCCAR?! 3. EU need a joint research and military technology funding agency (EDA?)
<ul style="list-style-type: none"> • European political objectives have to be defined • National goals have to become secondary priority This process has started, but will still take one or two more generations to become a reality

Fig. 6-16 Europe must grow together!

Dieter Scholz

References
(from Chapters 5, 7, 9)

References ¹

- Abbott 1959** ABBOTT, I.H.; DOENHOFF, A.E.: *Theory of Wing Sections*, New York : Dover, 1959
- Anderson 1989** ANDERSON, J.D.: *Introduction to Flight*, New York : McGraw-Hill, 1989
- Anderson 1991** ANDERSON, J.D.: *Fundamentals of Aerodynamics*, New York : McGraw-Hill, 1991
- Brüning 1993** BRÜNING, G.; HAFFER, X.; SACHS, G.: *Flugleistungen - Grundlagen, Flugzustände, Flugabschnitte*, Berlin : Springer, 1993
- DATCOM 1978** HOAK, D.E.: *USAF Stability and Control Datcom*, Wright-Patterson Air Force Base, Air Force Flight Dynamics Laboratory, Flight Control Division, Ohio, 1978. - Sale: NTIS
- Dubs 1987** DUBS, F.: *Aerodynamik der reinen Unterschallströmung*, Basel : Birkhäuser, 1987
- FAR 1** U.S. DEPARTMENT FOR TRANSPORTATION, FEDERAL AVIATION ADMINISTRATION: *Federal Aviation Regulations, Part 1, Definitions and Abbreviations*, Washington, D.C.
- FAR 23** U.S. DEPARTMENT FOR TRANSPORTATION, FEDERAL AVIATION ADMINISTRATION: *Federal Aviation Regulations, Part 23, Normal, Utility, Aerobatic and Commuter Category Airplanes*
- FAR 25** U.S. DEPARTMENT FOR TRANSPORTATION, FEDERAL AVIATION ADMINISTRATION: *Federal Aviation Regulations, Part 25, Transport Category Airplanes*
- CS 23** JOINT AVIATION AUTHORITIES: *Joint Aviation Requirements, JAR-23, Normal, Utility, Aerobatic and Commuter Category Aeroplanes*
- CS 25** JOINT AVIATION AUTHORITIES: *Joint Aviation Requirements, JAR-25, Large Aeroplanes*

¹ Sources quoted in Section 5, 7, and 9

- Jenkinson 1999** JENKINSON, L. R., SIMPKIN, P., RHODES, D.: *Civil Jet Aircraft Design*. London : Arnold, 1999
- Kallmeyer 1999** KALLMEYER, J.: *Anpassung von Statistik-Gleichungen des Flugzeugentwurfs an neue Flugzeugtypen*. Project, Hamburg University of Applied Sciences, 1999
- Lambert 1993** LAMBERT, M.: *Jane's all the World's Aircraft*, 1997. - Published annually, Jane's Information Group, 163 Brighton Road, Coulsdon, Surrey CR5 2NH, UK
- Loftin 1980** LOFTIN, L.K.: *Subsonic Aircraft: Evolution and the Matching of size to Performance*, NASA Reference Publication 1060, 1980
- Marckwardt 1998a** MARCKWARDT, K.: *Unterlagen zur Vorlesung Flugzeugentwurf*, Fachhochschule Hamburg, Fachbereich Fahrzeugtechnik, 1998
- Obert 1997** OBERT, E.: *Aircraft Design and Aircraft Operation*, Short Course Notes, Linköping Technical University, 1997
- Raymer 1989** RAYMER, D.P.: *Aircraft Design: A Conceptual Approach*, AIAA Education Series, Washington D.C. : AIAA, 1989
- Roskam I** ROSKAM, J.: *Airplane Design*. Vol. 1 : *Preliminary Sizing of Airplanes*, Ottawa, Kansas, 1989. - Sale: Analysis and Research Corporation, 120 East Ninth Street, Suite 2, Lawrence, Kansas, 66044, USA
- Roskam II** ROSKAM, J.: *Airplane Design*. Vol. 2 : *Preliminary Configuration Design and Integration of the Propulsion System*, Ottawa, Kansas, 1989
- Roskam III** ROSKAM, J.: *Airplane Design*. Vol. 3 : *Layout Design of Cockpit, fuselage, Wing and Empenage: Cutaways and Inboard Profiles*, Ottawa, Kansas, 1989
- Roskam IV** ROSKAM, J.: *Airplane Design*. Vol. 4 : *Layout Design of Landing Gear and Systems*, Ottawa, Kansas, 1989
- Roskam V** ROSKAM, J.: *Airplane Design*. Vol. 5 : *Component Weight Estimation*, Ottawa, Kansas, 1989

- Roskam VI** ROSKAM, J.: *Airplane Design. Vol. 6 : Preliminary Calculation of Aerodynamic, Thrust and Power Characteristics*, Ottawa, Kansas, 1990
- Roskam VII** ROSKAM, J.: *Airplane Design. Vol. 7 : Determination of Stability, Control and Performance Characteristics: FAR and Military Requirements*, Ottawa, Kansas, 1991
- Roskam VIII** ROSKAM, J.: *Airplane Design. Vol. 8 : Airplane Cost Estimation: Design, Development, Manufacturing and Operation*, Ottawa, Kansas, 1990
- Schmitt 1998** SCHMITT, D.: *Luftfahrttechnik, Flugzeugentwurf*, Technische Universität München, Lehrstuhl für Luftfahrttechnik, Skript zur Vorlesung, 1988
- Scholz 1995** SCHOLZ, D.; CIORNEI, S.: Mach number, relative thickness, sweep and lift coefficient of the wing - An empirical investigation of parameters and equations, (Deutscher Luft- und Raumfahrtkongreß, Friedrichshafen, 26. - 29. September 2005). In: BRANDT, P. (Ed.): *Jahrbuch 2005*. Bonn : Deutsche Gesellschaft für Luft- und Raumfahrt, 2005. - Paper: DGLR-2005-122, ISSN 0070-4083. Download: <http://paper.ProfScholz.de>
- Torenbeek 1988** TORENBEEK, E.: *Synthesis of Subsonic Airplane Design*, Delft : Delft University Press, 1988

Dieter Scholz

Appendix

Deutscher Luft- und Raumfahrtkongress 2007

**First CEAS European Air and Space Conference
Century Perspectives**

DGLR Short Course Aircraft Design

Berlin, Germany, 11 – 14 September 2007

Evaluation

Part 1 - Numerical Evaluation

Numerical evaluation scale explanation:

Please indicate your satisfaction by giving points from 1 to 5:

- | | |
|---|----------------------------|
| 1 | needs a lot of improvement |
| 2 | needs some improvement |
| 3 | ok |
| 4 | I am satisfied |
| 5 | I am very satisfied |

Alternatively you may indicate "NA" (not applicable).



Application:

- 1.) General Information provided on the short course
- 2.) Assistance during application phase.

Permanent Information:

- 3.) Lecture notes, physical quality
- 4.) Lecture notes, content: Hannes Ross
- 5.) Lecture notes, content: Erhard Rumpler
- 6.) Lecture notes, content: Dieter Schmitt
- 7.) Lecture notes, content: Dieter Scholz
- 8.) Lecture notes, content: Jürgen Thorbeck
- 9.) Additional information on the Internet

Lecturing:

- 10.) Hannes Ross
- 11.) Erhard Rumpler
- 12.) Dieter Schmitt
- 13.) Dieter Scholz
- 14.) Jürgen Thorbeck

Additional learning/networking activities:

- 15.) CEAS conference programme (plenary session)
- 16.) Tuesday: Parliamentary evening
- 17.) Wednesday: Conference dinner
- 18.) Thursday: Public lecture

Learning environment:

- 19.) Overall course organisation
- 20.) Lecture room
- 21.) Coffee break service
- 22.) Lunch arrangements (apart from payment)

Part 2 - Written Evaluation

a) In addition to the above, I would like to add:

b) Particularly I liked:

c) I did not like:

d) Imagining I would be responsible to organise the short course, I would do differently:



DEUTSCHE GESELLSCHAFT FÜR LUFT- UND RAUMFAHRT – LILIENTHAL OBERTH E.V.
Wissenschaftlich-Technische Vereinigung

in cooperation with
Hamburg University of Applied Sciences (HAW Hamburg)

Certificate of Attendance

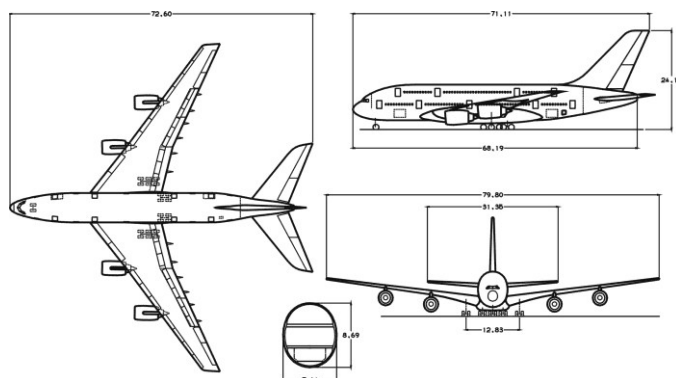
This is to certify that

XYZ

attended the Short Course

Aircraft Design

11 – 14 September 2007
Berlin, Germany



Prof. Dr.-Ing. Joachim Szodruch
President of DGLR
DLR - Executive Committee
Aviation and Energy

Prof. Dr.-Ing. Dieter Scholz, MSME
Department of
Automotive and Aeronautical Engineering
Hamburg University of Applied Sciences